



Waterford Institute *of* Technology  
INSTITIÚID TEICNEOLAÍOCHTA PHORT LÁIRGE

# An Investigation into the Bioaccumulation of Chromium by Macroalgae

A thesis submitted to  
Waterford Institute of Technology by  
Catherine Murphy  
in partial fulfilment of the requirements  
for a Degree of Doctor of Philosophy

Supervised by Helen Hughes, Peter McLoughlin and Orla O'Donovan

September 2016

# Declaration

This thesis is a presentation of my original research work, of which no element has been previously submitted for a degree at this or any other research institute.

Wherever contributions of others are involved, every effort is made to indicate this clearly, with due reference to the literature, and acknowledgement of collaborative research and discussions.

Signed: \_\_\_\_\_

Date: \_\_\_\_\_

# Acknowledgements

This research was funded by the Environmental Protection Agency (EPA) (Reference no. 2006-S-ET-11). The Newfoundland biomonitoring study was funded by the Ireland Newfoundland partnership project. The SEM-EDX was funded by the Tyndall National Institute under the National Access Program (NAP) (Reference 284).

I would like to thank the following people:

My supervisors Dr Peter Mc Loughlin, Dr. Orla O'Donovan and Dr. Helen Hughes for their advice, patience and encouragement.

Brian Murphy for his help with sampling, and with any other queries I had along the way.

Joseph O'Mahony for his enthusiasm, time and support in the use of the AFM.

Vince Lodge and Paul Roseingrave in the Tyndall National Institute for carrying out the SEM and EDX analysis presented in this work.

Jim Stack for his help with statistical analysis.

Wade Bowers and Dean Strickland from Sir Wilfred Grenfell College, Memorial University and Bob Hooper from the Bonne Bay Marine Station, Memorial University, Newfoundland, as well as the staff and technicians for their support while sampling in Newfoundland.

The other postgraduate students for their help and support, especially those in my lab; Adil Bakir and Siobhan Ryan.

My family and my partner John for their understanding, and constant support.

# Table of Contents

<b>Declaration .....</b>	<b>I</b>
<b>Acknowledgements .....</b>	<b>II</b>
<b>Table of Contents.....</b>	<b>III</b>
<b>Abbreviations.....</b>	<b>VIII</b>
<b>List of Figures .....</b>	<b>X</b>
<b>List of Tables.....</b>	<b>XV</b>
<b>Abstract .....</b>	<b>XVII</b>
<b>Chapter 1: Introduction and Literature Review .....</b>	<b>1</b>
<b>1.1 Introduction: Metals and Algae .....</b>	<b>2</b>
<b>1.2 Seaweed Classification and Structure.....</b>	<b>2</b>
1.2.1 Classification .....	2
1.2.2 Structure.....	3
1.2.3 Brown Seaweeds.....	4
1.2.4 Green Seaweeds.....	8
1.2.5 Red Seaweeds .....	10
<b>1.3 Heavy Metals.....</b>	<b>12</b>
1.3.1 Heavy Metals in the Environment .....	12
1.3.2 Metals in the Marine Environment .....	14
1.3.2.1 Chromium .....	14
1.3.2.2 Cadmium.....	17
1.3.2.3 Cobalt.....	17
1.3.2.4 Copper.....	18
1.3.2.5 Iron.....	18
1.3.2.6 Lead .....	18
1.3.2.7 Manganese .....	19
1.3.2.8 Mercury.....	19
1.3.2.9 Nickel.....	19
1.3.2.10 Zinc .....	19
<b>1.4 Heavy Metal Binding Groups.....</b>	<b>20</b>
1.4.1 Proteins and Peptides .....	20
1.4.2 Carbohydrates .....	22
1.4.2.1 Alginate.....	22
1.4.2.2 Fucoidans .....	23
1.4.2.3 Cellulose .....	24
1.4.2.4 Carrageenans .....	25
1.4.2.5 Agars .....	25
1.4.2.6 Xylans .....	26
1.4.2.7 Ulvans .....	26
1.4.2.8 Laminarans.....	27
1.4.2.9 Floridean starch.....	28
1.4.3 Phlorotannins and Other Polyphenols .....	29
1.4.4 Mechanisms of Binding .....	30
1.4.4.1 Surface Interactions.....	31
1.4.4.2 Intracellular Mechanisms .....	32
1.3.4. Production of Metal Chelating Agents.....	33
<b>1.5 Algal Biofilms.....</b>	<b>34</b>
1.5.1 Introduction.....	34
1.5.2 Biofilm Development .....	34
1.5.3 Biofilms, Metals and Algae .....	35

<b>1.6 Scientific and Technological Applications of Seaweed .....</b>	<b>37</b>
1.6.1 Traditional Commercial Uses of Seaweeds .....	37
1.6.1.1 Biofunctional Seaweeds and Extracts .....	37
1.6.2 Seaweeds as Biosorbents .....	38
1.6.3 Seaweeds as Biomonitorers .....	39
<b>1.7A Review of Bioaccumulation and Biosorption in the Literature .....</b>	<b>49</b>
1.7.1 Seasonal Effects in Metal Bioaccumulation .....	49
1.7.2 The Seaweed Surface: Potential for Epiphytes and Biofilms to Accumulate Metals and the Role of Surface Shedding of Cells .....	50
1.7.3 Species Specific Responses to Bioaccumulation .....	51
1.7.4 Effect of Water Composition and Physico-Chemical Parameters.....	51
1.7.4.1 Effect of Nutrients.....	51
1.7.4.2 Importance of Salinity.....	52
1.7.4.3 Effect of Temperature .....	54
1.7.4.3 Importance of pH .....	55
1.7.5 Influence of Exudates .....	56
1.7.6 Toxicity of Metal Bioaccumulation: Oxidative Stress and Photosynthesis .....	57
1.7.7 Behaviour of Chromium in Solution.....	58
<b>1.8 Objectives of Research .....</b>	<b>68</b>
<b>Chapter 2: Seaweed Characterisation .....</b>	<b>69</b>
<b>2.1 Introduction .....</b>	<b>70</b>
2.1.1 Phosphorus and Sulphur Determination by ICP-OES.....	70
2.1.2 Protein Content by the Kjeldahl Method .....	71
2.1.3 Functional Group Determination by Fourier Transform Infrared Spectroscopy.....	72
2.1.5 Objectives .....	74
<b>2.2 Experimental.....</b>	<b>76</b>
2.2.1 Sampling, Storage and Drying .....	76
2.2.2 Phosphorus and Sulphur by ICP-OES .....	76
2.2.2.1 Microwave Digestion.....	76
2.2.2.2 ICP Analysis .....	76
2.2.3 Protein Content by the Kjeldahl Method .....	77
2.2.3.1 Digestion .....	77
2.2.3.2 Distillation and Titration .....	77
2.2.4 Functional Group Determination by FTIR.....	78
<b>2.3 Results and discussion .....</b>	<b>79</b>
2.3.1 Phosphorus and Sulphur by ICP-OES .....	79
2.3.1.1 Validation.....	79
2.3.2 Protein Content by the Kjeldahl Method .....	83
2.3.3 Functional Group Characterisation by FTIR Analysis.....	86
2.3.3.1 <i>Fucus vesiculosus</i> .....	86
2.3.3.2 <i>Palmaria palmata</i> .....	88
2.3.3.3 <i>Ulva lactuca</i> .....	91
<b>2.4 Conclusions .....</b>	<b>94</b>
<b>Chapter 3. Biomonitoring and the Use of Metal Pollution Indices.....</b>	<b>96</b>
<b>3.1 Introduction .....</b>	<b>97</b>
3.1.1 Environmental Monitoring and Biomonitoring .....	97
3.1.2 Metal Pollution Indices .....	99
3.1.3 Objectives .....	100
<b>3.2 Experimental.....</b>	<b>101</b>
3.2.1 Site Locations .....	101
3.2.1.1 Bonne Bay.....	101
3.2.1.2 Humber Arm .....	103
3.2.1.3 Suir Estuary.....	104
3.2.2 Sampling, Storage and Drying .....	106
3.2.3 Metal Analysis by ICP-OES .....	107
3.2.4 Calculation of Metal Pollution Indices .....	107
<b>3.3 Results and Discussion .....</b>	<b>108</b>

3.3.1 Seawater Analysis .....	108
3.3.2 Seaweed Analysis .....	111
3.3.2.1 Cadmium .....	113
3.3.2.2 Cobalt .....	114
3.3.2.3 Chromium .....	116
3.3.2.4 Copper .....	117
3.3.2.5 Manganese .....	120
3.3.2.6 Nickel .....	121
3.3.2.7 Zinc .....	122
3.3.2.8 Comparison of Results and Application of Metal Pollution Indexes .....	123
<b>3.3 Conclusions .....</b>	<b>126</b>
<b>Chapter 4: Bioaccumulation of Chromium by <i>F. vesiculosus</i>, <i>P. palmata</i> and <i>U. lactuca</i> .....</b>	<b>127</b>
<b>4.1 Introduction .....</b>	<b>128</b>
<b>4.2 Experimental .....</b>	<b>130</b>
4.2.1 Sampling and Storage .....	130
4.2.2 Preliminary Metal Uptake Experiment .....	131
4.2.3 Metal Exposure Experiments .....	131
4.2.4 Microwave Digestion .....	132
4.2.5 ICP Analysis .....	132
4.2.6 Fourier Transform Infrared Analysis .....	133
4.2.7 Statistical Analysis .....	133
<b>4.3 Results and Discussion .....</b>	<b>134</b>
4.3.1 Method Validation .....	134
4.3.2 Preliminary Metal Uptake Data .....	136
4.3.3 Temperature study of Cr Uptake by <i>Ulva lactuca</i> , <i>Fucus vesiculosus</i> and <i>Palmaria palmata</i> .....	140
4.3.3.1 Site results .....	140
4.3.3.2 Analysis of Seawater Controls .....	141
4.3.3.3 Chromium Uptake by <i>Fucus vesiculosus</i> .....	146
4.3.3.4 Chromium Uptake by <i>Palmaria palmata</i> .....	153
4.3.3.5 Chromium Uptake by <i>Ulva lactuca</i> .....	159
4.3.3.6 Relationship Between Metal Uptake and Temperature .....	163
4.3.4 FTIR .....	165
4.3.4.1 FTIR Spectra of Raw and Metal loaded <i>Fucus vesiculosus</i> Sampled in Feb/Mar .....	165
4.3.4.2 FTIR Spectra of Raw and Metal loaded <i>P. palmata</i> Sampled in Feb/Mar .....	170
4.3.4.3 FTIR Spectra of Raw and Metal loaded <i>Ulva lactuca</i> Sampled in Feb/Mar .....	172
<b>4.4 Conclusions .....</b>	<b>175</b>
<b>Chapter 5: Microscopic and Bacteriological Examination of the Seaweed Surface .....</b>	<b>179</b>
<b>5.1 Introduction .....</b>	<b>180</b>
5.1.1 Atomic Force Microscopy .....	180
5.1.1.1 Application of AFM in the Imaging of Seaweed .....	181
5.1.2 Scanning Electron Microscopy/Energy Dispersive X-Ray Analysis .....	186
5.1.3 Total Viable Counts of Surface Bacteria .....	186
5.1.4 Aims .....	187
<b>5.2 Experimental .....</b>	<b>188</b>
5.2.1 Metal Exposure .....	188
5.2.2 Method for Removal of Biofilm .....	188
5.2.3 Microscopy .....	188
5.2.3.1 Optical Microscopy .....	188
5.2.3.2 Scanning Force Microscopy .....	188
5.2.3.3 Scanning Electron Microscopy and Electron Dispersive X-Ray Analysis .....	189
5.2.4 Total Viable Counts .....	189
<b>5.3 Results and Discussion .....</b>	<b>190</b>

5.3.1	Characterisation of Raw <i>Ulva lactuca</i> and Biofilm .....	190
5.3.2	Time Course Analysis of the Effect of Cr(III) on the Surface of <i>U. lactuca</i> .....	194
5.3.2.1	Surface at t = 1.5 min .....	195
5.3.2.2	Surface at t = 5 min .....	196
5.3.2.3	Surface at t = 10 min .....	197
5.3.2.4	Surface at t = 30 min .....	198
5.3.2.5	Surface at t = 60 min .....	200
5.3.2.6	Surface at t = 120 min .....	201
5.3.2.7	Surface at t = 240 min .....	202
5.3.2.7	Trends in Surface Area and Roughness .....	202
5.3.4	Analysis of raw and metal loaded samples of <i>F. vesiculosus</i> , <i>P. palmata</i> and <i>U. lactuca</i> .....	204
5.3.4.1	<i>Fucus vesiculosus</i> .....	205
5.3.4.2	<i>Palmaria palmata</i> .....	212
5.3.4.3	<i>Ulva lactuca</i> .....	219
5.3.5	EDX Analysis of Surface .....	227
5.3.6	Total Viable Counts .....	230
<b>5.4</b>	<b>Conclusions .....</b>	<b>232</b>
<b>Chapter 6: Conclusions and Future Work.....</b>		<b>234</b>
<b>6.1</b>	<b>Conclusions .....</b>	<b>235</b>
<b>6.2</b>	<b>Future Work .....</b>	<b>238</b>
6.2.1	Experimental Conditions .....	238
6.2.2	Determine the toxicity of Cr .....	238
6.2.3	Studying the seaweed surface .....	239
<b>References .....</b>		<b>240</b>
<b>Appendix 1: Research Outputs .....</b>		<b>263</b>
<b>Appendix 2: EDX Scans.....</b>		<b>266</b>



# Abbreviations

AFM	Atomic Force Microscopy
AN	<i>Ascophyllum nodosum</i>
AP	Ascorbate Peroxidase
ATR	Attenuated Total Reflectance
CAT	Catalase
CRM	Certified Reference Material
DHAR	Dehydroascorbate Reductase
DTGS	Deuterated Triglycine Sulfate
EDX	Energy Dispersive X-ray Spectroscopy
EPA	Environmental Protection Agency
FTIR	Fourier Transform Infrared Spectroscopy
FV	<i>Fucus vesiculosus</i>
GR	Glutathione Reductase
ICA	Irish Countrywomen's Association
ICP-OES	Inductively Coupled Plasma-Optical Emission Spectroscopy
LOD	Limit of Detection
LOQ	Limit of Quantitation
LOX	Lipoxygenase
meq	milliequivalents
RMS	Roughness Mean Squared
ROS	Reactive Oxygen Species
SEM	Scanning Electron Microscopy
SFM	Scanning Force Microscopy
SOD	Superoxide dismutases
SRM	Standard Reference Material
TBARS	Thiobarbituric Acid Reactive Substances
TEM	Transmission Electron Microscopy
TVC	Total Viable Counts
UNESCO	United Nations Educational, Scientific and Cultural Organization
UKCIP	UK Climate Impacts Programme
V	Volt
WFD	Water Framework Directive
‰	Salinity

# List of Figures

Figure 1.1: Typical cell wall structure of brown seaweeds (Davis <i>et al.</i> 2003).....	4
Figure 1.2: Thallus of <i>Ascophyllum nodosum</i> (Åberg 1996).....	6
Figure 1.3: <i>Ascophyllum nodosum</i> , © Michael Guiry (Algaebase 2016).....	6
Figure 1.4: <i>Fucus spiralis</i> , © Michael Guiry (Algaebase 2016). ....	7
Figure 1.5: <i>Fucus vesiculosus</i> , © Michael Guiry (Algaebase 2016). ....	7
Figure 1.6: <i>Ulva intestinalis</i> , © Michael Guiry (Algaebase 2016).....	8
Figure 1.7: <i>Ulva linza</i> , © Michael Guiry (Algaebase 2016). ....	9
Figure 1.8: <i>Ulva compressa</i> , © Michael Guiry (Algaebase 2016). ....	9
Figure 1.9: <i>Ulva lactuca</i> , © Katrin Oesterlund (Algaebase 2016). ....	10
Figure 1.10: <i>Palmaria palmata</i> , © Michael Guiry (Algaebase 2016).....	11
Figure 1.11: <i>Vertebrata lanosa</i> , © Michael Guiry (Algaebase 2016). ....	11
Figure 1.12: Processes which effect metal availability in the environment (Reeder, Schoonen, and Lanzirrotti 2006).....	13
Figure 1.13: A Pourbaix diagram of Cr speciation in aqueous systems, without the influence of complexing agents other than H <sub>2</sub> O and OH <sup>-</sup> . The dashed lines shows the pH range of natural waters (Kotaš & Stasicka 2000). ....	16
Figure 1.14: Cr(VI) speciation in aqueous solution (Alvarado <i>et al.</i> 2009). ....	16
Figure 1.15: Cr(III) speciation in aqueous solution (taken from Fahim <i>et al.</i> 2006). ....	17
Figure 1.16: Metal binding amino acids and peptides; (a) cysteine, (b) phytochelatin (Clemens 2006), and (c) glutathione.....	21
Figure 1.17: Copper bonding to two cysteine molecules (Baker & Czarnecki-Maulden 1987).....	21
Figure 1.18: Structure of alginate, (a) structural monomers, (b) alginate polymer and (c) alginate polymer sequence (Smidsrød & Draget 1996). ....	22
Figure 1.19: ‘Egg box’ binding of polyguluronic carbohydrate chains with Ca <sup>2+</sup> .....	23
Figure 1.20: Fucoidan (Davis <i>et al.</i> 2003).....	24
Figure 1.21: Cellulose structure (Phelps 1972). ....	24
Fig. 1.22: Repeat disaccharide unit for <i>ι</i> -carrageenan (Gunning <i>et al.</i> 1998).....	25
Figure 1.23: Agarose (Usov, 1998). ....	26
Figure 1.24: Xylan from <i>Palmaria palmata</i> (Elicityl-Oligotech 2012).....	26
Figure 1.25: Main repeating disaccharide unit in ulvan, ulvanobiouronic acid (Lahaye & Robic 2007). ....	27
Figure 1.26: Laminarin (laminaran) showing either M chains (a), which contain mannitol at the reducing end, or G chains (b), which have glucose at the reducing end (Davis <i>et al.</i> 2003).....	28
Figure 1.27: Floridean starch (Usov 2011).....	28
Figure 1.28: Phloroglucinol (a), and a phlorotannin molecule, dieckol (b) (from PubChem 2012).....	29
Figure 1.29: Routes of metal uptake in the algal cell (adapted from Stokes 1983). ....	31
Figure 1.30: Fate of chromate in the cell (Kaim & Schwederski 1994). ....	33
Figure 1.31: Biofilm development (Latasa <i>et al.</i> 2006).....	35
Figure 1.32: Biosorption columns. Diagram of process and columns operating in industry (BV Sorbex 2013). ....	39
Figure 1.33: Uptake isotherms of seasonal differences in Cu uptake (18 °C, 24 h exposure time, fully illuminated (Vasconcelos & Leal 2001).....	49
Figure 1.34: Uptake of metal by <i>Elodea canadensis</i> (black) and <i>Potamogeton natans</i> (white) at 3 temperatures (Fritioff <i>et al.</i> 2005). ....	54
Figure 2.1: Variation in phosphorus content with season.....	81
Figure 2.2: Variation in sulphur content with season. ....	82
Figure 2.3: Variation in total protein (% dry weight) with season. ....	83
Figure 2.4: Proposed mechanism of reduction of Cr(VI) by brown seaweed biomass (Park <i>et al.</i> 2005). ....	85
Figure 2.5: Representative FTIR scans of <i>F. vesiculosus</i> sampled in May/June (top) and Feb/Mar (bottom), taken from triplicate analysis.....	86
Figure 2.6: Representative FTIR scans of <i>P. palmata</i> sampled in May/June (top) and Feb/Mar (bottom), taken from triplicate analysis. ....	89
Figure 2.7: Representative FTIR scans of <i>U. lactuca</i> sampled in May/June (top) and Feb/Mar (bottom), taken from triplicate analysis. ....	91
Figure 3.1: Bonne Bay Sites in Newfoundland, Canada (1-5). ....	103
Figure 3.2: Humber Arm Sites in Newfoundland, Canada (6-10).....	104
Figure 3.3: Suir estuary sites in Waterford, Ireland (11-14).....	106
Figure 3.3: Cadmium concentration in <i>A. nodosum</i> (AN) and <i>F. vesiculosus</i> (FV) at all sites. (An * indicates that value is below LOQ but above LOD).....	114

Figure 3.4: Cobalt concentration in <i>A. nodosum</i> (AN) and <i>F. vesiculosus</i> (FV) at all sites. ....	115
Figure 3.5: Chromium concentration in <i>A. nodosum</i> (AN) and <i>F. vesiculosus</i> (FV) at all sites. (An * indicates that value is below LOQ but above LOD).....	117
Figure 3.6: Copper concentration in <i>A. nodosum</i> (AN) and <i>F. vesiculosus</i> (FV) at all sites, inset at a smaller concentration scale to show lower concentration sites. ....	119
Figure 3.7: Manganese concentration in <i>A. nodosum</i> (AN) and <i>F. vesiculosus</i> (FV) at all sites.....	120
Figure 3.8: Nickel concentration in <i>A. nodosum</i> (AN) and <i>F. vesiculosus</i> (FV) at all sites. (An * indicates that value is below LOQ but above LOD).....	121
Figure 3.9: Zinc concentration in <i>A. nodosum</i> (AN) and <i>F. vesiculosus</i> (FV) at all sites. ....	122
Figure 4.1: Location map and picture of Baginbun. ....	130
Figure 4.2: Results of preliminary Cr (III) uptake experiment over 240 min for six seaweed species. Errors based on standard deviation of samples from three replicate plants (n=3). ....	136
Figure 4.3: Cr(III) binding over time for biomass from six seaweed species. Conditions were as follows: Initial metal concentration = 1 mM, biomass concentration = 2 mg/mL, pH = 4.5 (Murphy <i>et al.</i> 2008). ....	137
Figure 4.4: Correlation between light ion content (Na, Ca, Mg, K) and chromium uptake (n=3). ....	138
Figure 4.5: Mean monthly precipitation (1961-2000) from UKCIP data for January (left) and July (right) in mm/month (Semmler <i>et al.</i> 2006). ....	141
Figure 4.6: Changes in pH of control seawater samples. 0 min sample taken after the metal solution was prepared and allowed to equilibrate (n=3). ....	142
Figure 4.7: Changes in the concentration of total and soluble Cr <sup>3+</sup> (n=3). ....	143
Figure 4.8: Changes in the concentration of total and soluble CrO <sub>4</sub> <sup>2-</sup> (n=3). ....	143
Figure 4.9: Charts showing amount of Cr soluble in seawater controls at both the start (0 min) and end (360 min) of the experiment. ....	144
Figure 4.10: Uptake of Cr <sup>3+</sup> (a) and CrO <sub>4</sub> <sup>2-</sup> (b) by <i>F. vesiculosus</i> (sampled May/Jun): Total and soluble Cr in seawater (n=3). ....	146
Figure 4.11: Uptake of Cr <sup>3+</sup> / Cr(III) (a) and CrO <sub>4</sub> <sup>2-</sup> / Cr(VI) (b) by <i>F. vesiculosus</i> (sampled May/Jun) (n=3). ....	147
Figure 4.12: Forecast of Cr(VI) / CrO <sub>4</sub> <sup>2-</sup> uptake by <i>F. vesiculosus</i> (sampled May/Jun) at 14 days (20160 min). ....	148
Figure 4.13: Seasonal variation in baseline chromium levels in <i>F. vesiculosus</i> (n=3). ....	150
Figure 4.14: Seasonal variation in Cr uptake in <i>F. vesiculosus</i> (n=3). ....	151
Figure 4.15: Total Cr, and intracellular Cr in <i>F. vesiculosus</i> sampled in May/Jun (a) and Feb/Mar (b) (n=3). ....	152
Figure 4.16 Uptake of Cr <sup>3+</sup> / Cr(III) (a) and CrO <sub>4</sub> <sup>2-</sup> / Cr(VI) (b) by <i>P. palmata</i> : Total and soluble Cr in seawater (n=3). ....	153
Figure 4.17: Uptake of Cr <sup>3+</sup> / Cr(III) (a) and CrO <sub>4</sub> <sup>2-</sup> / Cr(VI) (b) by <i>P. palmata</i> (n=3). ....	154
Figure 4.18: Forecast of Cr(VI) uptake by <i>P. palmata</i> (sampled May/Jun) at 14 days (20160 min). ..	155
Figure 4.19: Seasonal variation in baseline Cr levels in <i>P. palmata</i> (n=3). ....	156
Figure 4.20: Seasonal variation in Cr uptake in <i>P. palmata</i> (n=3). ....	157
Figure 4.21: Total Cr, and intracellular Cr in <i>P. palmata</i> sampled in May/June (a) and Feb/Mar (b) (n=3). ....	158
Figure 4.22: Uptake of Cr <sup>3+</sup> / Cr(III) (a) and CrO <sub>4</sub> <sup>2-</sup> / Cr(VI) (b) by <i>U. lactuca</i> : Total and soluble Cr in seawater (n=3). ....	159
Figure 4.23: Uptake of Cr <sup>3+</sup> / Cr(III) (a) and CrO <sub>4</sub> <sup>2-</sup> / Cr(VI) (b) by <i>U. lactuca</i> . ....	160
Figure 4.24: Seasonal variation in baseline Cr levels in <i>U. lactuca</i> (n=3). ....	161
Figure 4.25: Seasonal variation in Cr uptake in <i>U. lactuca</i> . ....	162
Figure 4.26: Total Cr, and intracellular Cr in <i>U. lactuca</i> sampled in May/June (a) and Feb/Mar (b) (n=3). ....	163
Figure 4.27: ATR FTIR spectra of raw <i>F. vesiculosus</i> (top), Cr(VI) loaded <i>F. vesiculosus</i> at 7 and 16 °C (middle), and Cr(III) loaded <i>F. vesiculosus</i> at 7 and 16 °C (bottom) (resolution-4 cm <sup>-1</sup> , number of scans-64, representative shown from n=3). ....	167
Figure 4.28: Mechanisms for metal uptake by seaweed (Park <i>et al.</i> 2005).....	168
Figure 4.29: Carboxyl chelates (Nakamoto 1997).....	169
Figure 4.30: Spectrum of protonated <i>F. vesiculosus</i> (resolution-4 cm <sup>-1</sup> , number of scans-64, representative shown from n=3). ....	170
Figure 4.31: ATR FTIR Spectra of raw <i>P. palmata</i> (top), Cr(VI) loaded <i>P. palmata</i> at 7 and 16 °C (middle), and Cr(III) loaded <i>P. palmata</i> at 7 and 16 °C (bottom) (resolution-4 cm <sup>-1</sup> , number of scans-64, representative shown from n=3). ....	171

Figure 4.32: Spectrum of protonated <i>P. palmata</i> (resolution-4 cm <sup>-1</sup> , number of scans-64, representative shown from n=3).	172
Figure 4.33: ATR FTIR Spectra of raw <i>U. lactuca</i> (top), Cr(III) loaded <i>U. lactuca</i> at 7 °C (middle), and Cr(III) loaded <i>U. lactuca</i> at 16 °C (bottom) ((resolution-4 cm <sup>-1</sup> , number of scans-64, representative shown from n=3).	173
Figure 4.34: Spectrum of protonated <i>U. lactuca</i> (resolution-4 cm <sup>-1</sup> , number of scans-64, representative shown from n=3).	174
Figure 5.1: Topographic image (a) and line profile (b) showing height and depth measurements	180
Figure 5.2: Acquisition of topographic data by SFM (Heaton <i>et al.</i> 2004).	181
Figure 5.3: Iota-carrageenan imaged by AFM. Image (a) was taken in the absence of added salts, (b) shows the effect of K <sup>+</sup> , (c) shows the effect of Ca <sup>2+</sup> (Images 1µm x 1µm) (Funami <i>et al.</i> 2007).	181
Figure 5.4: Alginate imaged by AFM. (a) + (b) Lower concentrations of Ca <sup>2+</sup> used to gel the alginate, (c) and (d) higher concentrations of Ca <sup>2+</sup> used to gel the alginate (Liao <i>et al.</i> 2015).	182
Figure 5.5: Alginate imaged by AFM (500nm x 500nm), p: the polymer chain, k: kinks in the polymer chain (Decho 1999).	183
Figure 5.6: EPS isolated from a biofilm of the marine algal associated bacterium <i>Bacillus licheniformis</i> (Singh <i>et al.</i> 2011).	183
Figure 5.7: Native cell wall of <i>Ventricaria ventricosa</i> imaged by AFM. Long open head arrows point to coiling fibrillar structures; short dotted arrows pointing to ‘draping’ of the fibrillar meshwork (Scale bar: 1 µm) (Eslick <i>et al.</i> 2014).	184
Figure 5.8: Enzyme treated cell wall of <i>Ventricaria ventricosa</i> imaged by AFM. Thin fibril-like structure (long arrows) and cross-linking structures (short arrows) can be seen. The directions of underlying fibrils can also be seen (double headed dashed arrow) (Scale bar: 0.5 µm) (Eslick <i>et al.</i> 2014).	184
Figure 5.9: <i>E. maxima</i> , (a) raw, (b) ‘activated’ by CaCl <sub>2</sub> treatment and (c) ‘regenerated’ by NaCl treatment post CaCl <sub>2</sub> treatment and metal binding, showing changes in surface height (Feng & Aldrich 2004).	185
Figure 5.10: <i>U. lactuca</i> (1) Raw, (2) 1 µg/L Cu(II) and (3) 50 µg/L Cu(II), highlighting polysaccharide fibrils (Murphy 2007).	186
Figure 5.11 (a), (b) and (c): Raw <i>Ulva lactuca</i> images, all 80 µm x 80 µm.	191
Figure 5.12: Raw <i>U. lactuca</i> . Image (a) is an 11µm scan from image 5.11 (b) above. Image (b) is a 2µm scan from image 5.12 (a).	192
Figure 5.13: Cleaning method results; (a) Rinsed with seawater only, (b) rinsed with seawater and scraped and (c) rinsed with 10% ethanol and scraped (all 50 µm x 50 µm).	193
Figure 5.14: Cleaning method results obtained by optical microscope (magnification-40x); (a) Rinsed with seawater only, (b) rinsed with 10% Ethanol and scraped.	194
Figure 5.15: Concentration of Cr at time points ranging from 0 (raw) to 240 min (n=3).	195
Figure 5.16: <i>U. lactuca</i> exposed to 200 µg/L Cr <sup>3+</sup> at t=1.5 min, 80µm scan (a) and zoom to 20µm (b) on features marked.	196
Figure 5.17. <i>U. lactuca</i> exposed to 200 µg/L Cr <sup>3+</sup> at t=5 min, 80 µm (a) and zoom in to 20 µm (b).	196
Figure 5.18: <i>U. lactuca</i> exposed to 200 µg/L Cr <sup>3+</sup> at t=10 min, 80 µm scan.	197
Figure 5.19: <i>U. lactuca</i> exposed to 200 µg/L Cr <sup>3+</sup> at t=10 min, 50 µm scan (a) showing fibre bundles and 10 µm (b) with arrow showing surface detail of cuticle shedding	198
Figure 5.20: SEM image of the surface of <i>Chondrus crispus</i> showing removal of biofilm (c), clean algal surface (a) and bacterial biofilm (b), bar-10µm (Sieburth & Tootle 1981).	198
Figure 5.21: Two surface topographies seen in <i>U. lactuca</i> exposed to 200 µg/L Cr <sup>3+</sup> at t=30 min, 80 µm scans.	199
Figure 5.22: (a) 10 µm detail of Figure 5.21 (a), and (b) 20 µm detail of Figure 5.21 (b).	199
Figure 5.23: SEM image of a sheet like EPS layer on <i>Osmundaria serrata</i> (Barreto & Meyer 2007).	200
Figure 5.24: <i>U. lactuca</i> exposed to 200 µg/L Cr <sup>3+</sup> at t=60 min, 80 µm scan.	200
Figure 5.25: Zoom to 20 µm of above t=60 min scan, showing detail of seaweed outer cell wall (a) and 10 µm highlighting detail of remnants of bacterial biofilm (b).	201
Figure 5.26: <i>U. lactuca</i> exposed to 200 µg/L Cr <sup>3+</sup> at t=120 min, 80 µm and 20 µm scan.	201
Figure 5.27: <i>U. lactuca</i> exposed to 200 µg/L Cr <sup>3+</sup> at t=240 min. 80 µm <sup>2</sup> (a) showing cells and and zoom to 40 µm <sup>2</sup> (b) showing crystal deposits.	202
Figure 5.28: Surface area of <i>U. lactuca</i> at each time point. Error bars, where shown, refer to the average value ± one standard deviation based on at least two scans.	203
Figure 5.29: Roughness (RMS) of <i>U. lactuca</i> at each time point. Error bars, where shown, refer to the average value ± one standard deviation based on at least two scans.	203

Figure 5.30: AFM images of blank and metal loaded <i>F. vesiculosus</i> , under conditions described left-hand column. All 50 $\mu\text{m}^2$ . Three replicates attempted at each condition. ....	206
Figure 5.31: Surface area of blank (B, raw) and Cr bound <i>F. vesiculosus</i> at 7 and 16°C. Error bars show confidence intervals of 3 replicates. No data indicates sample could not be imaged. ....	206
Figure 5.32: Roughness mean squared (RMS) of blank (B, raw) and Cr bound <i>F. vesiculosus</i> at 7 and 16°C. Error bars show confidence intervals of 3 replicates. No data indicates sample could not be imaged. ....	207
Figure 5.33: Blank (raw) <i>F. vesiculosus</i> SEM scans, conditions as labelled in diagram.....	208
Figure 5.34: Cr(VI) exposed <i>F. vesiculosus</i> SEM scans, conditions as labelled in diagram. ....	209
Figure 5.35: Cr(III) exposed <i>F. vesiculosus</i> SEM scans, conditions as labelled in diagram. ....	210
Figure 5.36: SEM image of <i>F. vesiculosus</i> showing algal cells and bacterial biofilm, scale bar is 5 $\mu\text{m}$ (Wahl <i>et al.</i> 2012).....	211
Figure 5.37: AFM images of blank and metal loaded <i>P. palmata</i> , under conditions described left-hand column. All 50 $\mu\text{m}^2$ . Three replicates were attempted at each condition, but could not be completed. ....	212
Figure 5.38: Surface area of blank (B, raw) and Cr bound <i>P. palmata</i> at 7 and 16°C. Error bars show confidence intervals of 2 replicates. No data indicates sample could not be imaged. ....	213
Figure 5.39: Roughness mean squared (RMS) of blank (B, raw) and Cr bound <i>P. palmata</i> at 7 and 16°C. Error bars show confidence intervals of 2 replicates. No data indicates sample could not be imaged. ....	214
Figure 5.40: Blank (raw) <i>P. palmata</i> SEM scans, conditions as labelled in diagram.....	215
Figure 5.41: Cr(VI) exposed <i>P. palmata</i> SEM scans, conditions as labelled in diagram. ....	216
Figure 5.42: Cr(III) exposed <i>P. palmata</i> SEM scans, conditions as labelled in diagram. ....	217
Figure 5.43: Raw <i>P. palmata</i> dead biomass (a) exposed to 2000 mg/L Cr(III) (b) and 2000 mg/L Cr(VI) (c) (Murphy, Tofail, <i>et al.</i> 2009).....	218
Figure 5.44: AFM images of blank and metal loaded <i>U. lactuca</i> , under conditions described left-hand column. All 50 $\mu\text{m}^2$ . Three replicates attempted at each condition. ....	220
Figure 5.45: Surface area (per 625 $\mu\text{m}^2$ projected area) of blank (B, raw) and Cr bound <i>U. lactuca</i> at 7 and 16°C. Error bars show confidence intervals of 3 replicates. ....	221
Figure 5.46: Roughness mean squared (RMS) of blank (B, raw) and Cr bound <i>U. lactuca</i> at 7 and 16°C. Error bars show confidence intervals of 3 replicates. ....	221
Figure 5.47: Images showing agreement in features between SEM (B/W) and SFM (Orange) scans. All are blank seaweeds, samples in Feb/Mar.....	222
Figure 5.48: Raw <i>U. lactuca</i> SEM scans, conditions as labelled in diagram. ....	223
Figure 5.49: SEM scans of Cr(VI) exposed <i>U. lactuca</i> , conditions as labelled in diagram. ....	224
Figure 5.50: SEM scans of Cr(III) exposed <i>U. lactuca</i> , conditions as labelled in diagram. ....	225
Figure 5.51: Raw <i>U. lactuca</i> dead biomass (a) exposed to 2000 mg/L Cr(III) (b) and 2000 mg/L Cr(VI) (c) (Murphy, Tofail, <i>et al.</i> 2009). ....	226
Figure 5.52: EDX spectrum of <i>F. vesiculosus</i> biomass exposed to 2000 mg/L Cr(III) (Murphy, Tofail, <i>et al.</i> 2009).....	227
Figure 5.53: Blank <i>F. vesiculosus</i> 16 °C. ....	228
Figure 5.54: Blank <i>P. palmata</i> 16 °C. ....	228
Figure 5.55: Blank <i>U. lactuca</i> 16 °C. ....	229
Figure 5.56: Total viable count of bacteria present on the surface of <i>F. vesiculosus</i> quoted as $\log_{10}$ (n=3). Error bars show confidence intervals. ....	230
Figure 5.57: Total viable count of bacteria present on the surface of <i>P. palmata</i> quoted as $\log_{10}$ (n=3). Error bars show confidence intervals. ....	230
Figure 5.58: Total viable count of bacteria present on the surface of <i>U. lactuca</i> quoted as $\log_{10}$ (n=3). Error bars show confidence intervals. ....	231

# List of Tables



Table 1.1: Main photosynthetic pigments, storage products and cell wall polysaccharides for phaeophyta, chlorophyta and rhodophyta (Graham & Wilcox 2000). .....	3
Table 1.2: Summary of functional groups which may be involved in metal binding. ....	30
Table 1.3: Seaweed Polysaccharides of Commercial Importance (Holdt & Kraan 2011).....	37
Table 1.4: Comparison Of Removal Efficiencies of Seaweed Biomass and Commercial Resins (Kratochvil & Volesky 1998).....	38
Table 1.5: A summary of biomonitoring studies. ....	41
Table 1.6: A summary of relevant bioaccumulation studies. ....	59
Table 2.1: Protein content of some species of seaweed.....	72
Table 2.2: Main functional groups occurring in seaweeds and their associated infrared absorption bands. ....	73
Table 2.3: Microwave digestion program. ....	76
Table 2.4: ICP instrument settings for seaweed digests. ....	77
Table 2.5: Instrument settings for IR analysis. ....	78
Table 2.6: LOD and LOQ for Phosphorus and Sulphur Analysis .....	79
Table 2.7: Comparison of certified / indicative values for P and S and those found by analysis .....	80
Table 2.8: Comparison of certified / indicative values for N and those found by analysis (all in % dry weight) .....	83
Table 2.9: Peak table for <i>F. vesiculosus</i> . Resolution-2 cm <sup>-1</sup> , sensitivity-1, scan number-64. Values based on triplicate analysis, 95 % confidence intervals are shown. References for assignments are given in text to improve clarity of the table. ....	86
Table 2.10: Peak table for <i>P. palmata</i> . Resolution-2 cm <sup>-1</sup> , sensitivity-1, scan number-64. Values based on triplicate analysis, 95 % confidence intervals are shown. References for assignments are given in text to improve clarity of the table. ....	89
Table 2.11: Peak table for <i>U. lactuca</i> . Resolution-2 cm <sup>-1</sup> , sensitivity-1, scan number-64. Values based on triplicate analysis, 95 % confidence intervals are shown. References for assignments are given in text to improve clarity of the table. ....	91
Table 3.1: Assessment criteria for metals in seawater used to classify good and less than good status of water bodies as compiled by the Marine Institute (Marine Institute 2010). ....	98
Table 3.2: Assessment criteria for metals in shellfish used to classify good and less than good status as compiled by the Marine Institute (Marine Institute 2010).....	98
Table 3.1: GPS coordinates of sites. Sites 1-5 Bonne Bay, 6-10 Humber Arm and 11-14 Suir Estuary .....	101
Table 3.2: Conductivity, pH and Temperature readings for all sites. Readings taken in triplicate. Site 1-5 refers to Bonne Bay, 6-10 Bay of Islands and 11-14 the Suir Estuary. ....	108
Table 3.3: LOD and LOQ for metal analysis in seawater. ....	109
Table 3.6: Heavy metal limits in tidal waters (Clenaghan <i>et al.</i> 2006) .....	111
Table 3.7: LOD and LOQ for seaweed analysis, units are µg/L. ....	111
Table 3.9: A summary of metal contents of <i>F. vesiculosus</i> and <i>A. nodosum</i> . ....	123
Table 3.10: MPI and PLI values for <i>F. vesiculosus</i> and <i>A. nodosum</i> . ....	124
Table 4.1: Average monthly sea temperatures at the Met Eireann M5 Buoy, off the south coast of Co. Wexford. Data from 2004-2015 (Met Eireann 2016). ....	128
Table 5.1: SEM/EDX settings .....	189
Table 5.2: Marine Agar Composition.....	189

# Abstract

Heavy metals in industrial effluents are of particular concern because of their ability to bioaccumulate in the food chain, making it possible for toxic levels to reach higher animals and plants. Chromium is widely used in processes such as leather tanning, electroplating, pigmentation and in corrosion inhibitors. Trivalent and hexavalent are the most common species used in industry, with hexavalent being widely understood to be the most toxic. It is important, therefore, to understand the mechanisms of how chromium and other metals accumulate in the environment.

The aim of this project was to investigate metal, and in particular chromium uptake, by live seaweeds. This was done by characterising the seaweed (ICP-OES, Kjeldahl, FTIR), using the seaweed as a biomonitor, and looking at the surface morphology of the seaweed (AFM, SEM-EDX). A set of bioaccumulation experiments under many different conditions was carried out in order to determine the effect of seaweed species (*Fucus vesiculosus*, *Palmaria palmata*, *Ulva lactuca*), metal species (Cr(III) vs. Cr(VI)), season (May/June versus Feb/Mar), and temperature (7 °C vs. 16 °C) on metal uptake. To the author's knowledge, this was the first study to look at bioaccumulation by live seaweed of these two chromium species.

Characterisation confirmed the presence of sulphate, carboxylate, amide, and phosphorus containing groups. Seasonal and inter-species differences in seaweed composition were also identified.

A biomonitoring study, carried out on *F. vesiculosus* and *A. nodosum* sampled in Ireland and Newfoundland, showed that both seaweeds are suitable biomonitors. Metal contents reflected the levels of pollution which were likely to be present in the sampling areas.

Surface microscopy showed that a biofilm was present on the surface of *U. lactuca*. A time course study on Cr(III) binding showed that the biofilm was disrupted and reduced as metal exposure continued. Further experiments using AFM, SEM-EDX and total viable surface counts did not show differences between blank and metal loaded seaweeds. This was likely to be because the experimental conditions were slightly different, with a lower final metal concentration. To the author's knowledge, this was the first time the removal and disruption of a seaweed biofilm was shown by AFM, and the first time metal uptake in these three species was studied using AFM.

The following general trends were observed for Cr accumulation: *U. lactuca* > *P. palmata* > *F. vesiculosus*; Cr(III) > Cr(VI); 16 °C > 7 °C; Feb/Mar > May/Jun; intracellular uptake ~ 100%. Seasonal and inter-species differences were found to be attributable to difference in composition e.g. greater levels of P or N for a particular species, or a particular season. Greater binding at higher temperatures, could be because of greater cell membrane fluidity, increased metabolism and increased protein synthesis.

# Chapter 1: Introduction and Literature Review

## **1.1 Introduction: Metals and Algae**

Defining algae is a difficult task because of the large diversity in morphological, ultrastructural, ecological, biochemical and physiological traits (www.seaweed.ie 2016). A general definition of the term is a large group of organisms that are aquatic, photosynthetic autotrophs (Graham & Wilcox 2000). Marine macroalgae (or seaweed) discussed in this thesis are plant like organisms, normally attached to a substrate such as rock by a holdfast (www.seaweed.ie 2016).

Algae may accumulate metals from the environment in its tissues. This gives rise to the use of algae as biomonitors. The algae may be analysed to determine the amount of biologically relevant or bioavailable metal in the environment (Rainbow 1995). This is preferable to analysis of sediments or water, which give total, rather than bioavailable metal. Often concentrations of metals are very low in sediments and water, so it is also convenient that algae concentrate the metal to levels which are easier to detect (Rainbow 1995). Bioaccumulation is defined as the uptake of metals by live seaweed. This is distinct from biosorption, which is defined as uptake of metals by dead seaweed biomass, which may be dried and/or chemically treated for this purpose (Volesky 2007). It is the bioaccumulation of metals by seaweeds which is studied in this thesis.

## **1.2 Seaweed Classification and Structure**

### **1.2.1 Classification**

The term algae refers to a large group of organisms that are aquatic, photosynthetic autotrophs which are frequently smaller and morphologically less complex than land plants (Graham & Wilcox 2000). This statement is general and has many exceptions as the group is highly diverse. One of the methods for defining algae would be the use of ribosomal RNA gene sequences which provides evidence for the following eight major groups; glaucophyta, euglenophyta, cryptophyta, haptophyta, dinophyta, ochrophyta (includes brown algae), rhodophyta and chlorophyta. As more rRNA based information is made available it is possible that relationships between and in algal groups may change but, in general, it appears to confirm existing information based on other methods of defining algae such as nutrition, means of reproduction etc. (Graham & Wilcox 2000). The classification of marine algae has traditionally been based primarily on their pigmentation. This gives three groups: phaeophyta or brown

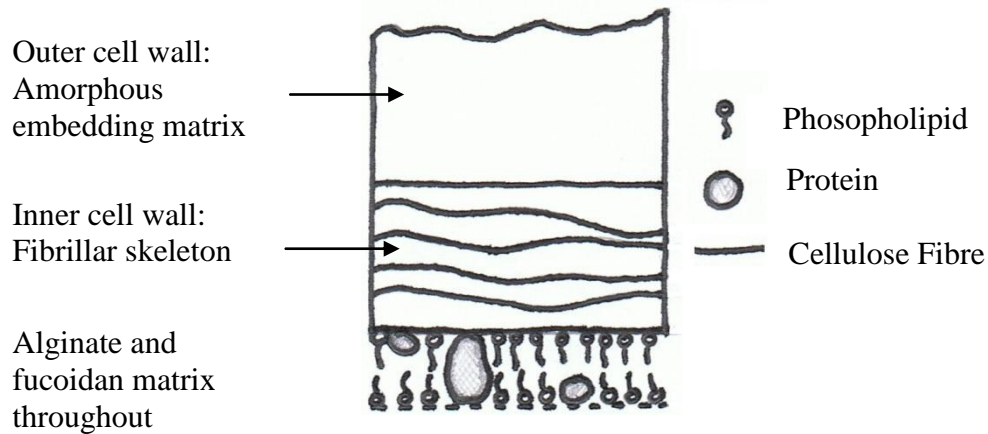
seaweed, chlorophyta or green seaweed, and rhodophyta or red seaweed. Other criteria for classification include their morphology e.g. unicellular or filamentous, or their main storage polysaccharides such as starch or laminaran (Dring 1992). A summary of these characteristics is given in Table 1.1 (Graham & Wilcox 2000).

**Table 1.1: Main photosynthetic pigments, storage products and cell wall polysaccharides for phaeophyta, chlorophyta and rhodophyta (Graham & Wilcox 2000).**

<b>Algal Group</b>	<b>Photosynthetic pigments</b>	<b>Storage products</b>	<b>Cell wall polysaccharides</b>
Phaeophyta Brown seaweed	chlorophyll <i>a</i>	Laminaran	Cellulose
	chlorophyll <i>c</i>		Alginates
	$\beta$ -carotene		Sulphated
	xanthophylls		polysaccharides
Chlorophyta Green seaweed	chlorophyll <i>a</i>	Starch	Cellulose
	chlorophyll <i>b</i>		(and different polymers
	$\beta$ -carotene		in some)
Rhodophyta Red seaweed	chlorophyll <i>a</i>	Floridean starch	Cellulose
	$\beta$ -carotene		Sulphated polygalactans
	phycoerythrin		May be impregnated with CaCO <sub>3</sub>

### 1.2.2 Structure

Marine algae may be microscopic or macroscopic in size. Macroscopic algae are referred to as macroalgae or seaweed (Graham & Wilcox 2000). The three main types of macroalgae of interest in this study are; phaeophyta (brown seaweed), chlorophyta (green seaweed) and rhodophyta (red seaweed). The body of the seaweed is known as the thallus, which generally consists of a holdfast, stipe and blade. Shown in Figure 1.1 is the typical cell wall structure of brown seaweed (Davis *et al.* 2003).



**Figure 1.1: Typical cell wall structure of brown seaweeds (Davis *et al.* 2003).**

The red and green seaweeds also have an inner cellulose layer. In some species of green seaweeds it may be cellulose with other polysaccharides, such as ulvan (Lahaye & Robic 2007). Red seaweeds contain polysaccharides called carrageenans, agars and porphyrans (Usov 1998). These polysaccharides will be discussed in more detail in Section 1.4.2.

In this study seven seaweeds were used; the brown seaweeds, *Fucus spiralis*, *Fucus vesiculosus*, and *Ascophyllum nodosum* the green seaweeds, *Ulva spp.* and *Ulva lactuca* and the red species, *Palmaria palmata* and *Polysiphonia lanosa*. These seaweeds were selected because of their high metal uptake capacity and their availability in the southeast of Ireland, which was established by previous work carried out by the Eco-Innovation Research Centre (EIRC), WIT (Murphy 2007). These are discussed in further detail below in their respective groups.

### 1.2.3 Brown Seaweeds

Brown algal photosynthetic pigments consist of chlorophyll *a*, chlorophyll *c* and  $\beta$ -carotene, as well as xanthophylls such as fucoxanthin, which gives them their brown colour. The main polysaccharides associated with brown seaweeds are alginate, fucoidan, cellulose, and laminaran (Graham & Wilcox 2000).

Alginic Acid is a polymer of mannuronic and guluronic acids and their  $\text{Na}^+$ ,  $\text{K}^+$ ,  $\text{Mg}^+$  and  $\text{Ca}^+$  salts. It gives flexibility to the thallus as well as preventing desiccation and having a role in ion exchange. It is the primary component of the thallus and can make

up about 35% of the thallus dry weight. Alginate is located primarily in the intercellular matrix (Graham & Wilcox 2000).

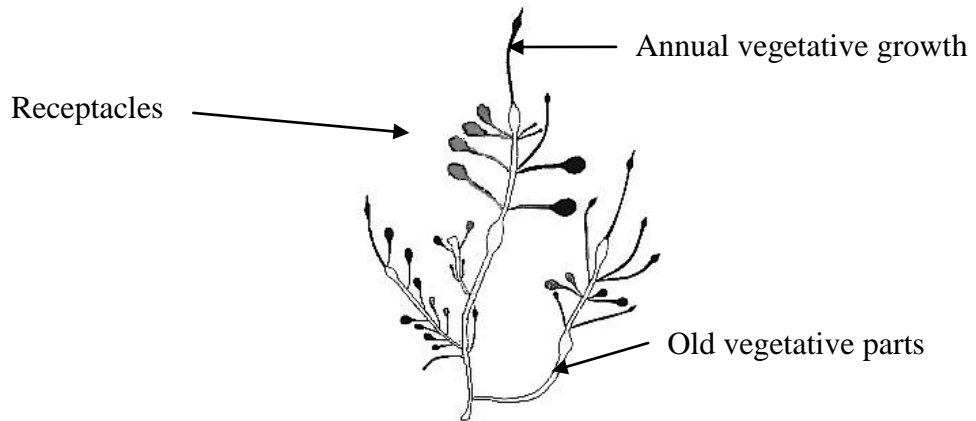
Cellulose provides structural support to the cell wall. It is usually a minor component and makes up about 1-10% of the dry weight of the thallus. It occurs as ribbon-like microfibrils which are generated by terminal complexes embedded in the cell membrane that are believed to contain cellulose synthesising enzymes (Graham & Wilcox 2000).

Fucans, fucoidans and ascophyllans, are sulphated polymers of L-fucose (Graham & Wilcox 2000). They vary greatly in their complexity and composition between seaweed species (Lobban & Harrison 1996). The structures of important seaweed polysaccharides are given in Section 1.4.2.

*Fucus spiralis* and *Fucus vesiculosus* were the brown seaweeds used in metal uptake experiments in this work. *Ascophyllum nodosum* was also used during biomonitoring studies. *Fucus* species are large brown seaweeds which grow abundantly on rocks in the upper regions of the intertidal zone of the seashore. They are attached to rocks by a disc shaped holdfast. They are easily recognised by their colour and by the presence of large receptacles (Lee & Webster 1986). Receptacles are enlarged ends of branches covered with conceptacles which produce eggs and sperm (Bold & Wynne 1978).

In *Ascophyllum nodosum* receptacles originate from pits and are shed each year after gametes have been released (Åberg 1996), see Figure 1.2 and 1.3 below. *Ascophyllum nodosum* is a brown fucoid species commonly known as yellow tang, knotted wrack, knobbed wrack, Asco, sea whistle or egg wrack. (Algaebase 2016). The fronds are long, with bladders which are formed annually. The plant generally regenerates new fronds from the base when one of the larger fronds are damaged or cut. Reproduction takes place in yellow receptacles in spring. These start to develop in response to short days in the autumn, mature during the winter, and are at their most prolific in spring (Algaebase 2016). Fronds vary in colour from yellow to dark olive green. Growth is slowest in winter, and faster for the rest of the year depending on conditions such as salinity and sun exposure (Gibb 1957; Stengel & Dring 1997).





**Figure 1.2: Thallus of *Ascophyllum nodosum* (Åberg 1996).**



**Figure 1.3: *Ascophyllum nodosum*, © Michael Guiry (Algaebase 2016).**

*Fucus spiralis* (Figure 1.4) has olive or yellow-green coloured flattened fronds with a prominent midrib and are twisted. Receptacles are present at the tips and have a distinctive winged appearance. The fronds may reach a length of 15-45 cm. As they are located in the upper intertidal zone, and are only covered with water for a few hours each day, they are resistant to drying out (Lee & Webster 1986).



**Figure 1.4:** *Fucus spiralis*, © Michael Guiry (Algaebase 2016).

*Fucus vesiculosus*, commonly known as bladderwrack, is a brown fucoid species. It grows in the middle region of the intertidal zone. It can be recognised by a prominent midrib, flattened fronds and the presence of air bladders, whose function is to keep the plant afloat, aiding photosynthesis. Its receptacles are not winged, allowing it to be differentiated from *Fucus spiralis* easily (Lee & Webster 1986). See Figure 1.5 below.



**Figure 1.5:** *Fucus vesiculosus*, © Michael Guiry (Algaebase 2016).

### 1.2.4 Green Seaweeds

Green algae contain chlorophyll *a*, *b* and  $\beta$ -carotene. Less is known about green algal polysaccharides because of their complexity and the fact that there is not as much commercial interest in them when compared to the hydrocolloid polysaccharides such as carrageenan and alginate used in the food and pharmaceutical industries. They typically produce highly sulphated heteropolysaccharides made up of glucuronic acid, xylose, rhamnose, arabinose and galactose (Lobban & Harrison 1996), and are known as ulvans. *Ulva* species can tolerate wide variations in salinity and are also resistant to pollution, specifically eutrophication (Lobban & Harrison 1996; Blomster *et al.* 1998). *Ulva* spp. and *Ulva lactuca* were used in this study.

*Ulva* spp. are comprised of *Ulva intestinalis*, *Ulva linza* and *Ulva compressa*, shown in Figures 1.6-1.8. Separating these species was not attempted because of their similarity (Lee & Webster 1986). *Ulva linza* is a flattened, narrow green blade that becomes hollow towards the base of the plant; it may grow up to 30 cm long. It grows on rocks in the upper intertidal zone. *Ulva intestinalis* is narrower than *linza* and hollow throughout the length of the plant. It is commonly seen in the lower intertidal and sublittoral zones of the shore (Lee & Webster 1986). *Ulva compressa* is considered a sub species of *intestinalis* and is found on lower littoral positions and tends to be branched more than *intestinalis* (Burrows 1991).



**Figure 1.6:** *Ulva intestinalis*, © Michael Guiry (Algaebase 2016).



**Figure 1.7: *Ulva linza*, © Michael Guiry (Algaebase 2016).**



**Figure 1.8: *Ulva compressa*, © Michael Guiry (Algaebase 2016).**

*Ulva lactuca* (Figure 1.9), also known as sea lettuce, is a thin membrane only two cells thick and is broader than *intestinalis*, *linza* and *compressa*. It may grow in long or rounded sheets and is attached to rocks by a small disc holdfast. It grows in the lower intertidal portion of the shore and in rock pools (Lee & Webster 1986).



**Figure 1.9: *Ulva lactuca*, © Katrin Oesterlund (Algaebase 2016).**

### 1.2.5 Red Seaweeds

Red algae also contain chlorophyll *a*,  $\beta$ -carotene and additionally, phycoerythrin. The cell wall of red algae, as seen in various other groups, is composed of cellulose microfibrils associated with an amorphous matrix material. In red algae this amorphous matrix makes up a higher proportion of the extracellular material. Cellulose microfibrils may be replaced by xylose in some species. This matrix material is made up of hydrophilic sulphated polygalactans, mucalages and cellulose. These sulphated polygalactans are mainly made up of carageenan and agar (Graham & Wilcox 2000).

*Palmaria palmata* is an edible seaweed also known as dulse. It is dark red in colour, branched and has a small disc shaped holdfast at its base (see Figure 1.10). It commonly grows in the sublittoral zone (Lee & Webster 1986).



**Figure 1.10: *Palmaria palmata*, © Michael Guiry (Algaebase 2016).**

*Vertebrata lanosa*, also known as *Polysiphonia lanosa*, has a very fine branched structure. It is an obligate epiphyte, meaning that it can only survive attached to a host seaweed. It commonly grows on *Ascophyllum nodosum* which is found in the intertidal zone (Lee & Webster 1986), see Figure 1.11.



**Figure 1.11: *Vertebrata lanosa*, © Michael Guiry (Algaebase 2016).**

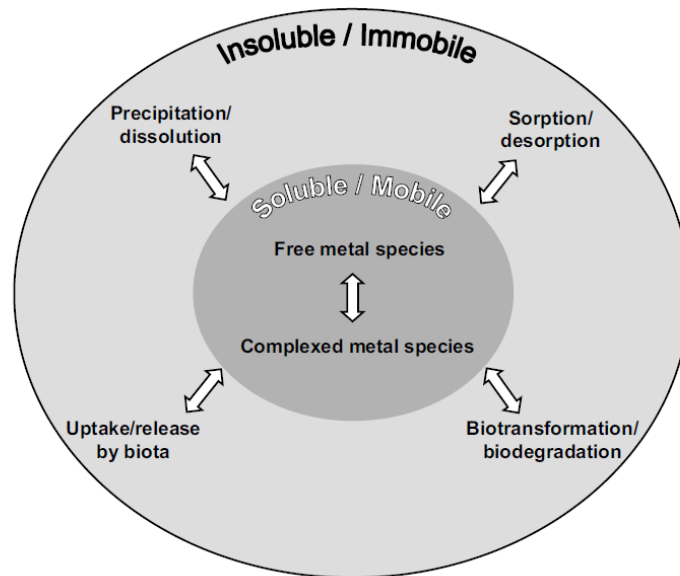
### 1.3 Heavy Metals

#### 1.3.1 Heavy Metals in the Environment

Heavy metals are of particular importance environmentally because of their ability to bioaccumulate in the food chain and the fact that unlike organic pollutants, they will not degrade. Although some metals are beneficial for animals and plants at trace levels, e.g., copper and selenium, they may become toxic, even at low levels. The most environmentally significant heavy metals of concern in Ireland are arsenic (As), mercury (Hg), chromium (Cr), copper (Cu), lead (Pb), nickel (Ni) and zinc (Zn) (Lucey 2007). An example of how aquatic heavy metal pollution may directly affect people is the consumption of bivalves. Bivalves are filter feeders that have the ability to concentrate pollutants and for this reason are widely used as indicators of pollution. The latest report on water quality in Ireland was published by the EPA in 2015, and covers the years 2010-2012. The monitoring of shellfish waters has shown that the levels of metals are below EU limits (arsenic, cadmium, chromium, copper, lead, nickel, silver and zinc analysed). In addition, all Water Framework Directive (WFD) water bodies were sampled in 2012 for copper, arsenic, zinc and chromium. The annual average metal concentrations complied with the national standards set in SI 272 of 2009, and the Environmental Quality Standard for chromium VI (EPA 2015).

Heavy metals may occur in the environment in two ways; naturally and related to human activity. They may enter aqueous systems naturally through slow leaching of soil or rock. This usually occurs at very low levels and is not damaging to human health (Zhou *et al.* 2008). However, heavy metals are used widely in industry in metallurgy, paints, electronic components, batteries, piping, catalysts, plastics, and as fuel additives. They may be introduced into the environment in a number of ways including power generation, transportation, metal industries and incineration amongst others (Lucey 2007).

Some of the pathways which control the mobility of metals in the environment are given in Figure 1.12. Metal speciation is of great importance when discussing the bioavailability of metals. These processes may involve reduction/oxidation depending on the process and conditions (Reeder *et al.* 2006).



**Figure 1.12: Processes which effect metal availability in the environment (Reeder, Schoonen, and Lanzirotti 2006).**

There are a number of European agreements in place to limit or reduce metal pollution in the marine environment. The WFD aims for all water bodies in Europe to achieve the level of good or higher status by 2015, and that water use is sustainable throughout Europe (Lucey 2007). A report by the EPA and the EU indicates that this aim was not achieved, although a final report does not appear to be available. However, the WFD has been successful in improving water quality throughout Europe (EPA 2015; European Commission 2015). The high priority metals of arsenic, mercury, chromium, copper, lead, nickel and zinc are selected because of international concern, based on the Oslo-Paris Commission for the Protection of the Marine Environment of the North East Atlantic (OSPARCOM), and also because of their likely presence in Ireland (Lucey 2007). The United Nations Economic Commission for Europe 1998 Aarhus Protocol is also in effect which targets mercury, cadmium and lead. This protocol calls for the reduction in emissions of these metals to 1990 levels within eight years for existing sources, and two years for new sources (United Nations Economic Commission for Europe 1998). Ireland signed the legislation in 1998, and it was ratified in 2012 (United Nations Economic Commission for Europe 2012).



### **1.3.2 Metals in the Marine Environment**

Seawater is made up of major, minor and trace constituents. The concentrations of the major elements, chloride, sodium, sulphate, magnesium, calcium, potassium and bicarbonate, stays close to constant throughout the world's oceans. The minor and trace elements, on the other hand, can be affected by both natural and anthropogenic activities. Minor elements such as strontium, bromide, boron, fluoride and lithium will be present in  $\mu\text{g}$ – $\text{mg/L}$  concentrations. Trace elements are present in  $\text{ng}$ – $\text{mg/L}$  concentrations and are heavily influenced by human or anthropogenic activities. These trace elements may have toxic effects on marine biota, and through bioaccumulation, on humans and other animals (Sadiq 1992). Natural sources include weathering of rocks, geothermal discharges, and volcanic activity. Anthropogenic sources include industrial discharge, sewage, and the shipping industry (De Filippis & Pallaghy 1994).

Adsorption of these trace elements in seawater can occur through a number of different mechanisms, which normally involve colloidal particles. These may be clays, iron (Fe) or manganese (Mn) oxides or hydroxides, calcium carbonates or organic matter (Sadiq 1992). Clays are basically negatively charged silicate materials and can therefore adsorb positively charged ions in seawater. In freshwater, these negatively charged sites are mostly occupied by calcium (Ca). When they are transported to seawater the Ca can be replaced by magnesium (Mg), sodium (Na) or potassium (K) and the Ca is then released into the sea. Trace metals can also be adsorbed in this way by filling any remaining negatively charged sites (Sadiq 1992).

Trace metals can also be adsorbed on biological calcium carbonate particles. These are produced in the marine environment by calcifying organisms such as algae and plankton. The binding of metals to particles of biological origin is most important at the surface of the sea, where biological processes are at a maximum (Sadiq 1992). Some of the metals discussed in this thesis are introduced here. Chromium will be discussed in more detail as it is the subject of this thesis.

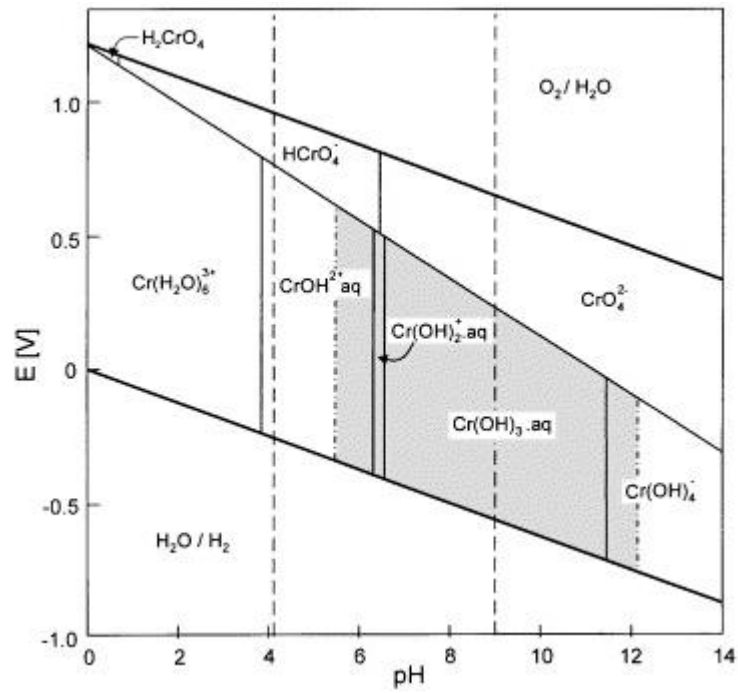
#### ***1.3.2.1 Chromium***

Chromium is used in steel manufacturing, production of ferrous and nonferrous alloys, electroplating, leather tanning and in the production of pigments such as lead

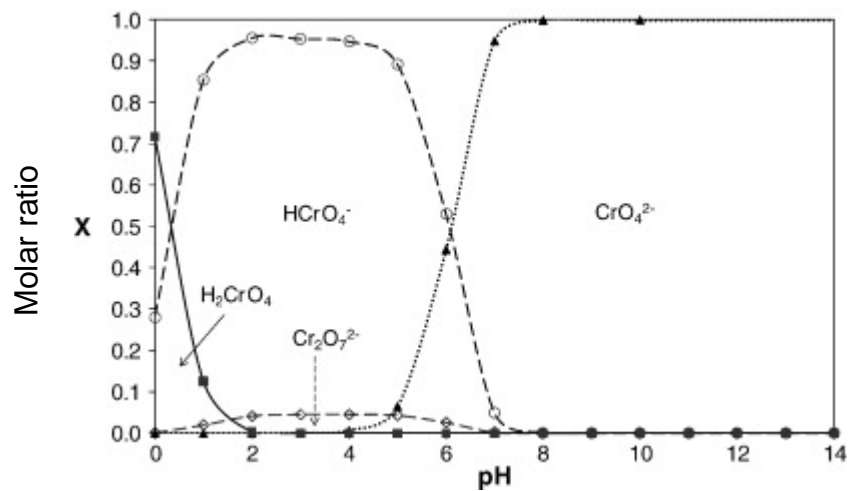
chromate, zinc chromate and iron chromate. Cr (VI) compounds are in general more soluble, mobile and more bioavailable than Cr (III) compounds. The toxicity of chromium is related to its speciation. Cr (VI) compounds are more toxic than Cr (III) compounds. Exposure to hexavalent chromium compounds leads skin, respiratory tract and kidney damage. It also leads to an increased risk of lung cancer (Cornelis *et al.* 2005). The toxic properties of hexavalent chromates arise from the possibility of free diffusion across cell membranes and strong oxidative potential. Cr(VI) is an oxidising material, and once inside the cell, this oxidation can cause damage by the generation of free radicals. Once the Cr(VI) has been oxidised to Cr(III), this then has the potential to bind to organic compounds causing the inhibition of some metalloenzyme systems (Kotaś & Stasicka 2000). Seawater has been reported to have total chromium levels of 0.1-16 nM (0.005-0.831 µg/L) (Eisler 2000; Kotaś & Stasicka 2000), but this can be much higher in polluted waters.

Cr can exist in several chemical forms with oxidation numbers from 0 to VI. Cr in the environment is stable only in Cr (III) and Cr (VI) oxidation states. Cr(IV) and Cr(V) form unstable intermediates in reactions of trivalent and hexavalent oxidation states with oxidizing and reducing agents, respectively. Cr(II) is readily oxidized to Cr(III). In fact, Cr(II) species are stable only in the absence of an oxidant (ie in anaerobic conditions) (Kotaś & Stasicka 2000).

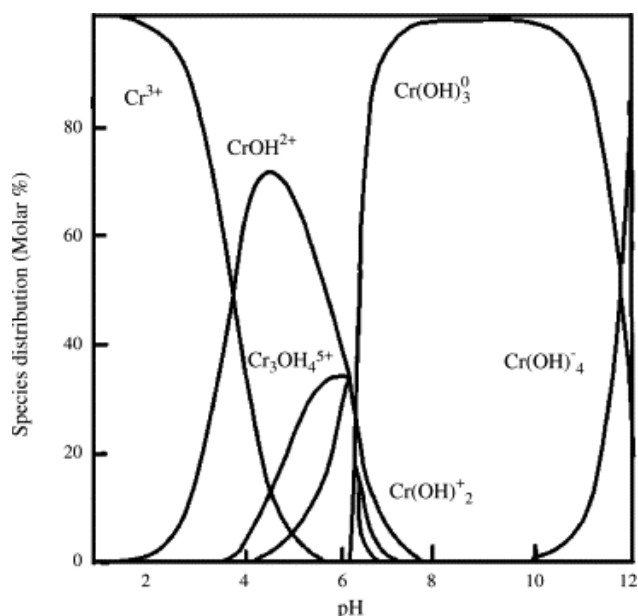
A Pourbaix diagram (Figure 1.13) can be useful to determine the environmentally stable speciation of a metal. It is a diagram of potential versus pH. The reduction potential of surface seawater is taken to be about 0.4 V (Silver 1991; Baas Becking *et al.* 1960), and the pH is about 8. Cr(III) is present as  $\text{CrOH}^{2+}$ ,  $\text{Cr(OH)}_2^+$ ,  $\text{Cr(OH)}_3$  and  $\text{Cr(OH)}_4^-$ . It can also form complexes with organic and inorganic ligands. Cr(VI) occurs as the chromate ( $\text{CrO}_4^{2-}$ ), or dichromate anion ( $\text{Cr}_2\text{O}_7^{2-}$ ) (Reeder *et al.* 2006). Speciation diagrams are also useful to find the likely forms of Cr at a given pH, see Figure 1.14 and 1.15.



**Figure 1.13:** A Pourbaix diagram of Cr speciation in aqueous systems, without the influence of complexing agents other than  $\text{H}_2\text{O}$  and  $\text{OH}^-$ . The dashed lines shows the pH range of natural waters (Kotaš & Stasicka 2000).



**Figure 1.14:** Cr(VI) speciation in aqueous solution (Alvarado *et al.* 2009).



**Figure 1.15: Cr(III) speciation in aqueous solution (taken from Fahim *et al.* 2006).**

It is important to note however that this diagram refers to natural speciation of chromium in the environment, and does not take into account kinetics, the presence of other complexing agents, or when Cr is introduced into the natural environment. In these cases its actual form may differ from that predicted by the diagram (Kotaš & Stasicka 2000).

### **1.3.2.2 Cadmium**

Cadmium (Cd) may be found in phosphate fertilisers and also in sewerage sludge (Satarug *et al.* 2003). Its other industrial sources include use in batteries, pigments and alloys. Cadmium compounds are highly toxic with no known physiological role and they affect many organs including the kidneys, bones and lungs (Cornelis *et al.* 2005). Background concentrations of 5-26 ng/L have been found in European estuarine and coastal waters, but this figure may be elevated in polluted areas (Green *et al.* 2003).

### **1.3.2.3 Cobalt**

Natural sources of cobalt (Co) in the environment include erosion, weathering, volcanoes, forest fires and biogenic emissions, while anthropogenic sources include the mining and processing of cobalt containing ores, processing of alloys, fossil fuels, sewage sludge, phosphate fertilisers and use in industry. Exposure to elevated concentrations of cobalt can lead to respiratory diseases, dermal sensitisation, and

interstitial lung disease, as well as being a suspected mutagen (Kim *et al.* 2006). Cobalt concentrations in seawater are under 10 µg/L (Ryan *et al.* 2012; Kim *et al.* 2006).

#### **1.3.2.4 Copper**

Copper (Cu) is widely used industrially as conductors and circuits, for corrosion resistance, machinery parts, alloys and in chemical manufacture, notably fungicides, algacides and pigments. Copper mining is damaging to the environment creating mine tailings which can often lead to more widespread contamination. It also occurs naturally in the environment. Copper concentration in water can range from 0.001-0.1mg/L in unpolluted sites. It is an essential trace nutrient and takes part in many biochemical processes. Chronic toxicity mainly affects the gastrointestinal tract and liver, leading to cirrhosis of the liver and liver failure (Cornelis *et al.* 2005).

#### **1.3.2.5 Iron**

Iron (Fe) is the fourth most abundant element in the earth's crust. It is of importance in many human activities and anthropogenic input to the environment, via activities such as mining and fertilisers, greatly exceeds natural deposition. Iron is an essential nutrient, used in oxygen transfer and energy production in the body, and in the production of chlorophyll in plants (US EPA 1978). Iron concentrations range from 9-40 µg/L in unpolluted estuaries (Martin *et al.* 1993; Byrne *et al.* 2011).

#### **1.3.2.6 Lead**

The use of lead (Pb) industrially has decreased in recent years due to increased concern about its adverse affects on health and the environment. It was very common in household and marine antifouling paints, in petrol as an antiknock additive, as a catalyst and in flame retardants. Most of these uses have lessened considerably. Chronic lead overdoses lead to symptoms such as tiredness, abdominal discomfort, irritability anaemia, nervous and reproductive system dysfunction, and a possible link to cancer (Cornelis *et al.* 2005). Natural levels of lead in European estuarine waters have been found to be about 100 ng/L (Green *et al.* 2003).

### **1.3.2.7 Manganese**

Manganese (Mn) is an essential trace nutrient. It can be found naturally through erosion and leaching from plant tissues. Its anthropogenic sources include wastewater and sewage sludge discharge, mining, production of alloys, steel and iron manufacture, combustion of fossil fuels and fuel additives (Howe *et al.* 2004). Natural concentrations of manganese in seawater are about 0.1 µg/L (Bender *et al.* 1977).

### **1.3.2.8 Mercury**

Mercury (Hg) is used industrially in the preparation of chlorine and caustic soda, and in fungicide and bactericide manufacture. It is also introduced into the environment by natural weathering of rock (Klein & Goldberg 1970). Mercury is toxic to the central nervous system and kidneys. It is also embryotoxic to humans, and may readily pass the placental barrier. Exposure to mercury has been linked to reduced mental development in children. Background levels of mercury in European estuarine waters have been found to be about 20 ng/L (Green *et al.* 2003).

### **1.3.2.9 Nickel**

Natural sources of nickel (Ni) are the erosion of soils and rock. Anthropogenic sources include mining and refining, production of steel and alloys, fossil fuel combustion, sewerage sludge, battery manufacture and catalysts. It is an essential element for some plant and animal species at low levels. The main toxic effects relate to respiratory conditions (Cornelis *et al.* 2005). Levels in seawater are about 0.1-0.5 µg/L (Cempel & Nikel 2006).

### **1.3.2.10 Zinc**

Zinc (Zn) is an essential trace element. It is widely used as a protective coating for other metals. It is also used in alloys, batteries and dental and medical applications. Its main source in the environment is natural, through erosion of rock. It may also be found due to corrosion, mining, combustion of fuel and waste incineration. Background levels of zinc in seawater may range from 0.001–0.1 µg/L (WHO 2001).

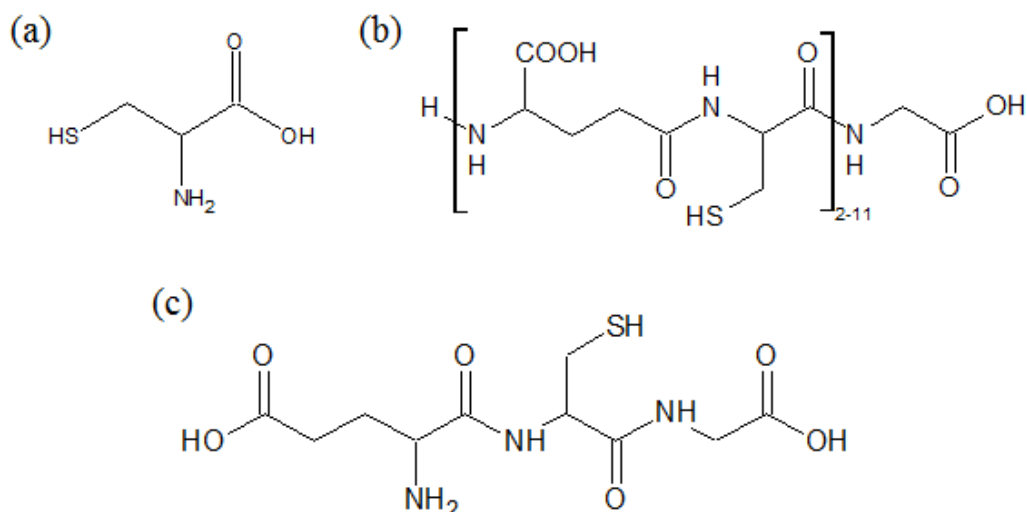
## 1.4 Heavy Metal Binding Groups

This section will review the components of seaweed which are involved in heavy metal binding, namely proteinaceous compounds, carbohydrates and phlorotannins.

### 1.4.1 Proteins and Peptides

Proteins and peptides are found both intracellularly, and as part of the cell wall in algae. The cell walls of algae can contain significant amounts of protein. Ranges reported by Siegel and Siegel (1973) are 10-69, 37-50 and 16-27 %, for green, red and brown algae, respectively (Siegel & Siegel 1973). Eight amino acids were found in the cell walls of *Chlorella* and *Scenedesmus*; aspartic acid, glutamic acid, glycine, alanine, serine, valine, leucine and isoleucine. These were present as peptides rather than proteins. In addition the walls sometimes contained proline, hydroxyproline and amino sugars (Punnett & Derrenbacker 1966). The cell walls of *Lobochlamys seignis*, a unicellular green algae, were found to be composed of a glycoprotein rich in hydroxyproline. The hydroxyproline was linked glycosidically to a mixture of heterooligosaccharides composed of arabinose and galactose. The glycoprotein complex accounted for 32% of the cell wall mass (Miller *et al.* 1974). Cell walls isolated from the red seaweed *Phyllophora crispera* was found to contain 36 % protein, which made protein the major constituent of the cell wall (Meichik *et al.* 2011).

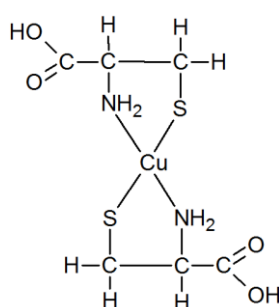
Phytochelatin is a low molecular weight peptide which has the ability to bind metals. They are synthesised from glutathione, with the molecular formula of  $(\gamma\text{GluCys})_n\text{Gly}$ ,  $n=2-11$  (Pawlik-Skowrońska *et al.* 2007). They have a high cysteine content. See Figure 1.16 for structures of cysteine, glutathione, and a general phytochelatin.



**Figure 1.16: Metal binding amino acids and peptides; (a) cysteine, (b) phytochelatin (Clemens 2006), and (c) glutathione.**

These proteins and peptides give rise to nitrogenous groups on the surface of the seaweed, and inside the algal cells. These give amide, and primary and secondary amine and carboxyl functional groups at the end of the protein/peptide chains, and sulphhydryl or thiol groups where cysteine is present as a residue.

It has been found that exposure to metals increases phytochelatin production in algal cells (Le Faucheur *et al.* 2006). An example of metal binding to cysteine is shown in Figure 1.17. Its binding of trivalent Cr has also been shown (Tewari 2002).



**Figure 1.17: Copper bonding to two cysteine molecules (Baker & Czarnecki-Maulden 1987).**

Hexavalent Cr has been shown to bind thiol (sulphur containing) groups in cysteine containing molecules such as glutathione (Brauer & Wetterhahn 1991; Brauer *et al.* 1996). A study by Armas (2004) showed the bonding of Cr(III) to glutathione was

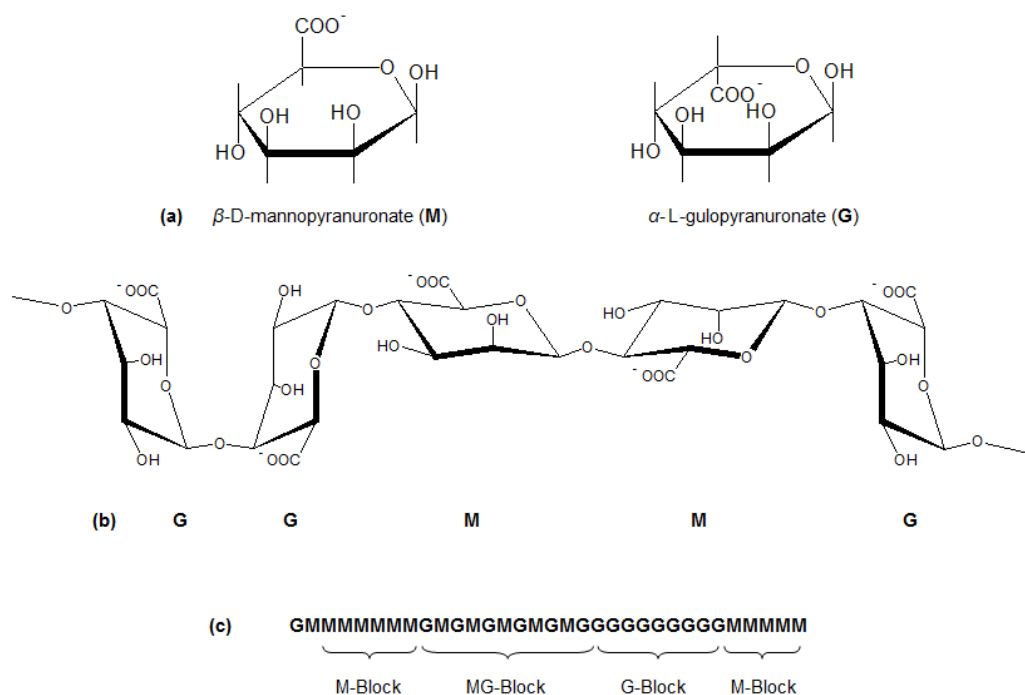


likely through coordination to thiol (S), amine ( $\text{NH}^{3+}$ ), amide (CONH) and carboxylate groups ( $\text{COO}^-$ ) groups (Armas *et al.* 2004).

## 1.4.2 Carbohydrates

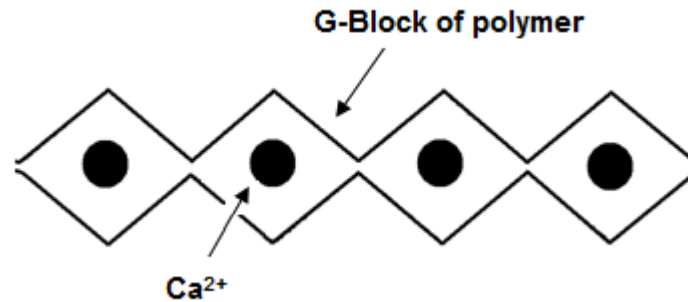
### 1.4.2.1 Alginate

Alginate is commercially important and is used as a food thickener, in cosmetic and pharmaceutical products. It is made up of  $\beta$ -(1 $\rightarrow$ 4)-bonded D-mannuronic ( $\beta$ -D-mannopyranuronate) and  $\alpha$ -(1 $\rightarrow$ 4)-bonded L-guluronic ( $\alpha$ -L-gulopyranuronate) acid units which are arranged in blocks (Figure 1.18) (Lobban & Harrison 1996).



**Figure 1.18: Structure of alginate, (a) structural monomers, (b) alginate polymer and (c) alginate polymer sequence (Smidsrød & Draget 1996).**

In the presence of calcium ions very strong gels are formed with the pairing of L-guluronic acid sections by coordination around the metal ions (Collins & Ferrier 1996). The zig zag conformation of polyguluronic acid allows  $\text{Ca}^{2+}$  to fit into the spaces formed (called ‘egg box’ model, Figure 1.19). D-mannuronic rich alginates are much more elastic as it’s conformation is not as favourable to calcium binding (Lobban & Harrison 1996).



**Figure 1.19: 'Egg box' binding of polyguluronic carbohydrate chains with Ca<sup>2+</sup>.**

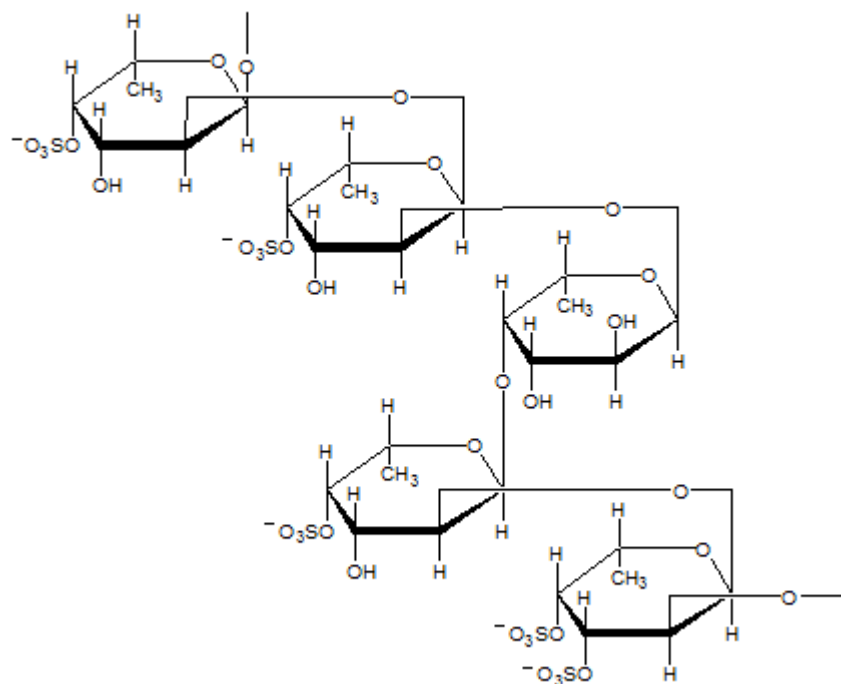
This model explains the relationship of increased uptake of divalent metal ions (Pb<sup>2+</sup>, Cu<sup>2+</sup>, Cd<sup>2+</sup> and Zn<sup>2+</sup>) by alginates that are rich in L-guluronic acid. This is also seen in seaweeds that have a high content of L-guluronic acid (Davis *et al.*, 2003).

*Ascophyllum nodosum* is a particularly good source of alginate (McHugh 2003b).

*Fucus* spp. also contain the carbohydrate, albeit in lower amounts and quality, and is therefore rarely used in industry for alginate production (McHugh 2003b; Rioux *et al.* 2007). Alginate has been shown to bind Ca, Cd, Cr, Zn, Cu and Pb (Fourest & Volesky 1997; Ibáñez & Umetsu 2004; Davis *et al.* 2004)

#### **1.4.2.2 Fucoïdians**

Fucoïdians refer to a large group of polysaccharides of which fucose is the main monomer. The simplest is fucan which consists entirely of fucose. The more complex fucoïdians may contain uronic acids, xylose and galactose. Fucan (Figure 1.20) is a complex molecule consisting of  $\alpha$ -(1→2) and  $\alpha$ -(1→4) linked fucose units, with  $\alpha$ -(1→3) branches and sulphation of hydroxyl groups to varying degrees (Lobban and Harrison, 1997).

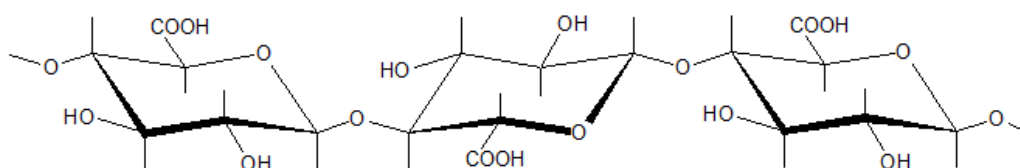


**Figure 1.20: Fucoidan (Davis *et al.* 2003).**

They are found in brown seaweeds, such as *Fucus* spp. and *Ascophyllum nodosum* (Holtkamp 2009). Only one study has determined the metal binding of fucoidan in isolation (and not part of a seaweed matrix), where it was found to effectively bind Ca and Pb (Paskins-Hurlburt *et al.* 1978). The sulphonate and hydroxyl groups in their structure however, are well established as taking part in metal binding.

#### 1.4.2.3 Cellulose

Cellulose is a linear, unbranched polysaccharide consisting of  $\beta$ -(1 $\rightarrow$ 4) bonded D-glucose units (see Figure 1.21). They occur as ordered fibres, mostly in the inner cell wall (Davis *et al.* 2003). Hydrogen bonding between polysaccharide chains, which may be composed of up to 3000 monomers, gives the fibres their strength.

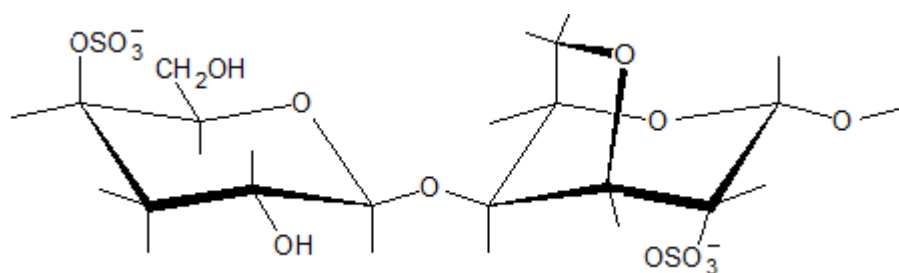


**Figure 1.21: Cellulose structure (Phelps 1972).**

All seaweeds in this study contain varying amounts of cellulose. Cellulose has been shown to bind many metal cations ( $\text{Al}^{3+}$ ,  $\text{Be}^{2+}$ ,  $\text{Cd}^{2+}$ ,  $\text{Cr}^{3+}$ ,  $\text{Fe}^{3+}$ ,  $\text{Pb}^{3+}$ ,  $\text{Zn}^{2+}$ ) (Burba & Willmer 1983), but research in this area has concentrated on the use of modified cellulose to increase the uptake capacity (O'Connell *et al.* 2008).

#### 1.4.2.4 Carrageenans

Carrageenan refers to a group of polysaccharides from red algae which are all linear sulphated galactans. They are very important industrially because of their gelling capability. Carrageenans are mostly composed of  $\alpha$ -(1 $\rightarrow$ 3) and  $\beta$ -(1 $\rightarrow$ 4) alternately linked D-galactopyranose. They may vary in their degree of sulphation and the presence or absence of 3,6-anhydrogalactose. The most common types are referred to as  $\iota$  (iota),  $\kappa$  (kappa) and  $\lambda$  (lambda) carrageenan (Van de Velde 2008). Iota-carrageenan is shown here in Figure 1.22.

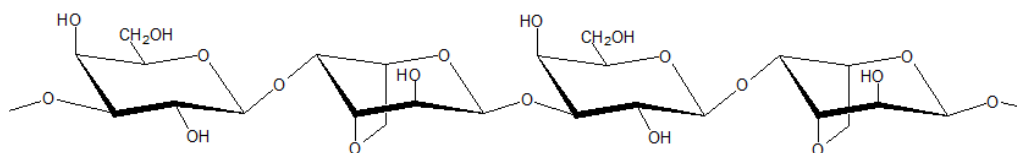


**Fig. 1.22: Repeat disaccharide unit for  $\iota$ -carrageenan (Gunning *et al.* 1998).**

Their binding to alkali earth metals is well known (McHugh 2003c), and their affinity for Pb, Hg and Cu has been shown (Son *et al.* 2004).

#### 1.4.2.5 Agars

Agars are also important gelling agents found in red seaweeds. They consist of alternating  $\beta$ -D-galactose and  $\alpha$ -L-galactose which are not highly sulphated. Shown in Figure 1.23 is the simplest agar, agarose, which has almost no sulphation (Lobban & Harrison 1996).

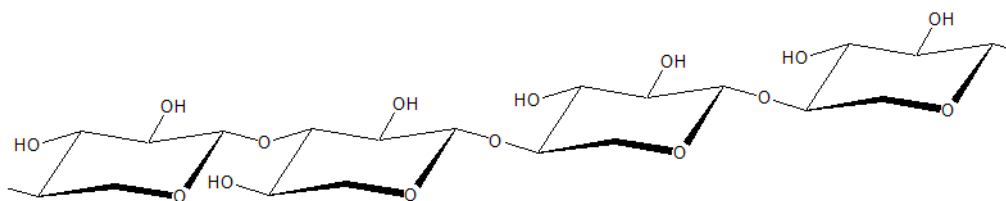


**Figure 1.23: Agarose (Usov, 1998).**

Agar's ability to bind Zn, Ni, Al and Sb (antimony) has been shown (Bakir *et al.* 2010).

#### 1.4.2.6 Xylans

Xylans (Figure 1.24) occur in the cell wall of *Palmaria palmata* and are composed of mixed linked  $\beta$ -(1,3)/  $\beta$ -(1,4)-D-xylans with varying amounts of sulphate and phosphate. It's structure is still being studied and the position of sulphate and phosphate groups is still to be elucidated (Deniaud, Quemener, *et al.* 2003; Deniaud, Fleurence, *et al.* 2003).

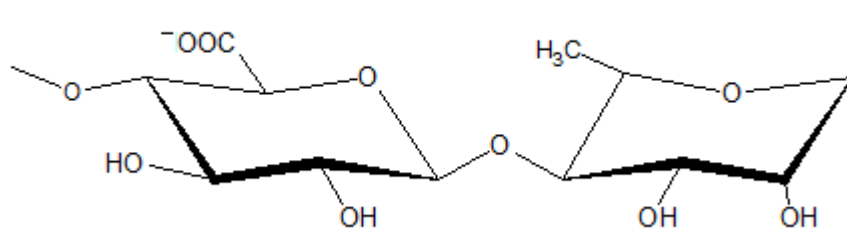


**Figure 1.24: Xylan from *Palmaria palmata* (Elicityl-Oligotech 2012).**

These hydroxyl, sulphate and phosphate groups are capable of metal binding, although this has not been studied using the isolated polysaccharide yet.

#### 1.4.2.7 Ulvans

Ulvans (Figure 1.25) are a generic name given to a type of sulphated seaweed polysaccharide found in green seaweeds. It typically comprises 8-29 % of the algal dry weight. It is composed mainly of sulphate, rhamnose, xylose, glucuronic acid and iduronic acid (Lahaye & Robic 2007).

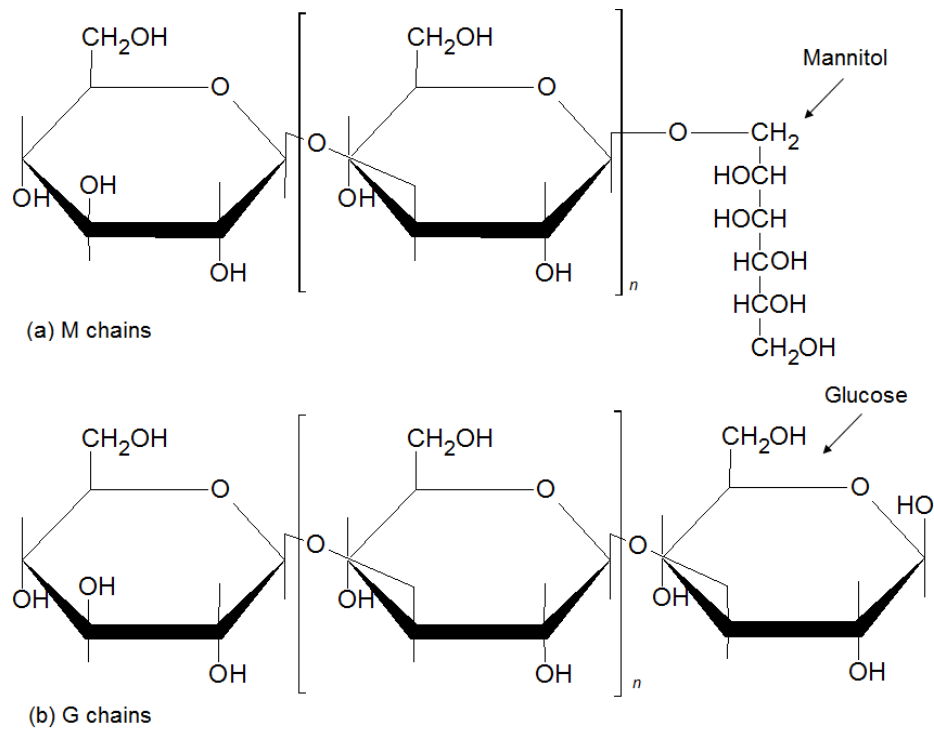


**Figure 1.25: Main repeating disaccharide unit in ulvan, ulvanobiouronic acid (Lahaye & Robic 2007).**

The ability of ulvan to bind metal has not yet been determined in the purified polysaccharide, probably as its structure and activity is an area of current research (Robic *et al.* 2009; Tako *et al.* 2015). However, the presence of hydroxyl, carboxylic, and sulphate groups indicates the capacity for metal binding.

#### ***1.4.2.8 Laminarans***

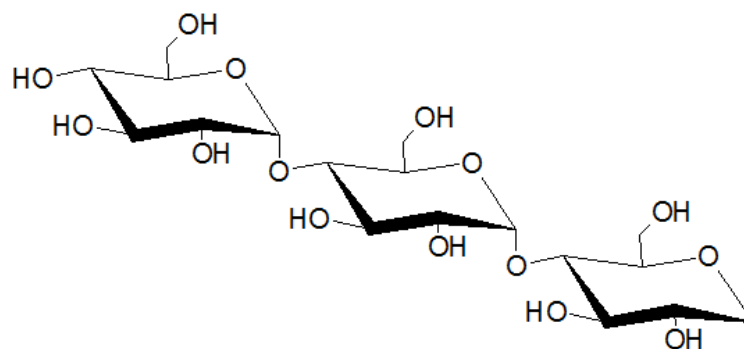
Laminaran (occasionally called laminarin) is a polysaccharide found in brown seaweeds. These are glucans, mainly with  $\beta(1-3)$  linkages (as shown in Figure 1.26), but  $\beta(1-6)$  linkages have also been observed (Davis *et al.* 2003). They are composed mostly of glucose with a small amount of uronic acids (Rioux *et al.* 2007). The functional groups present which may take part in binding are therefore hydroxyl and carboxyl.



**Figure 1.26: Laminarin (laminaran) showing either M chains (a), which contain mannitol at the reducing end, or G chains (b), which have glucose at the reducing end (Davis *et al.* 2003).**

#### 1.4.2.9 Floridean starch

Floridean starch is the major storage polysaccharide in red algae (Graham & Wilcox 2000), although it is not present in *Palmaria palmata* to any great extent (Rødde *et al.* 2004). The polymer is composed of  $\alpha(1-4)$  linked glucose with some  $\alpha(1-6)$  linked branches (Yu *et al.* 2002). The unbranched form is shown in Figure 1.27.

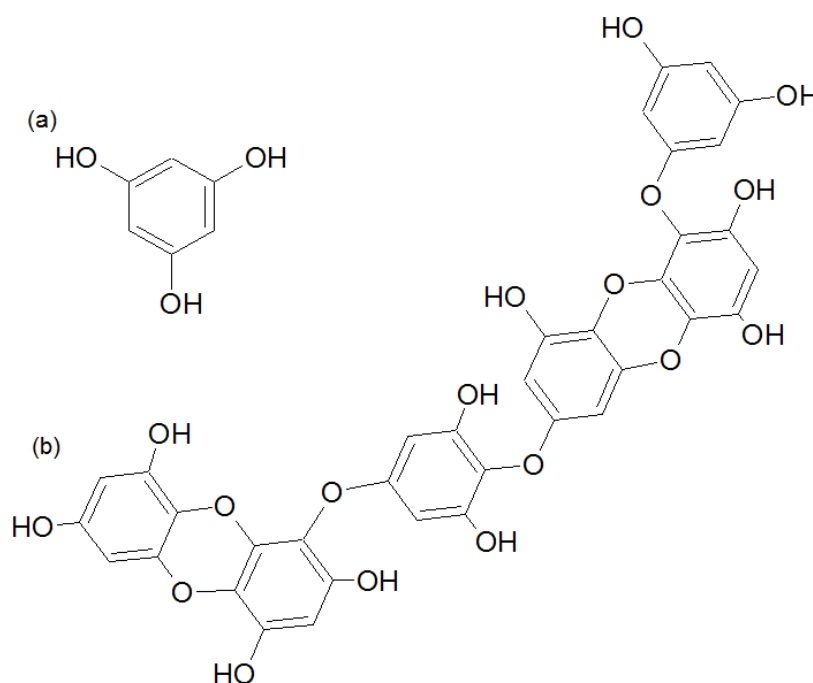


**Figure 1.27: Floridean starch (Usov 2011).**

Phosphate has been shown to be present in small amounts (Yu *et al.* 2002), giving floridean starch phosphate and hydroxyl functional groups for metal bonding.

### 1.4.3 Phlorotannins and Other Polyphenols

Phlorotannins are oligomers and polymers of phloroglucinol that are found in brown algae. There is a wide molecular weight range of phlorotannins isolated from *Ascophyllum nodosum* (0.32 - 400 kDa), with the majority being about 10 kDa (Ragan & Glombitza 1986). They may be divided into soluble and insoluble tannins. Soluble tannins may be low molecular weight tannins or oligomeric proanthocyanidins. They are found in physodes, which are vesicles within the cells (Schoenwaelder 2008). Insoluble tannins are high molecular weight tannins, or tannins that are bound to proteins or cell wall polysaccharides (Serrano *et al.* 2009). Phlorotannins are known to bind to metals and proteins (Ragan & Glombitza 1986). A phlorotannin molecule and the monomer from which they are composed are shown in Figure 1.28. Polyphenol levels are lower in the red and green seaweeds and are predominantly a mixture of catechins, gallate catechins and gallic acid (Yoshie *et al.* 2000; Rodríguez-Bernaldo de Quirós *et al.* 2010).



**Figure 1.28: Phloroglucinol (a), and a phlorotannin molecule, dieckol (b) (from PubChem 2012).**



Phlorotannin binding to copper has been shown. Purified phenolics from *Ascophyllum nodosum* were found to contain Cu, as well as Zn, Cd and Cr (Connan & Stengel 2011b).

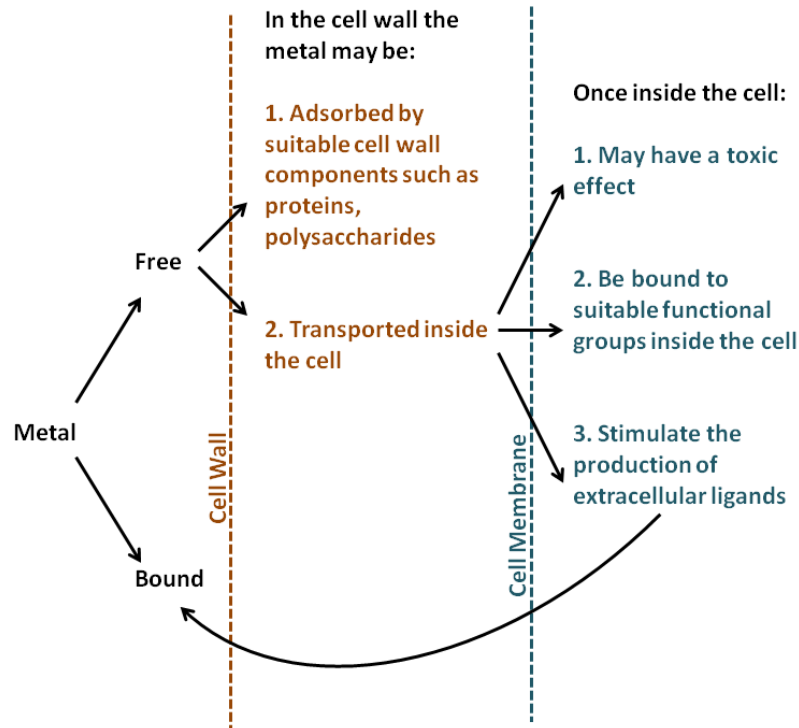
In Table 1.2, the functional groups discussed in this section have been summarised.

**Table 1.2: Summary of functional groups which may be involved in metal binding.**

Functional Group		Macromolecular source
Carboxyl	R-COOH	Carbohydrates, peptides/proteins
Hydroxyl	R-OH	Carbohydrates, phlorotannins
Amide	R-CO-NH-R	Peptides/proteins
Primary amine	R-NH <sub>2</sub>	Peptides/proteins
Secondary amine	R-NH-R	Peptides/proteins
Sulphate	R-SO <sub>4</sub>	Carbohydrates
Phosphate	R-PO <sub>4</sub>	Carbohydrates
Thiol	R-SH	Peptides/Proteins

#### 1.4.4 Mechanisms of Binding

The diagram shown in Figure 1.29 gives an overview of the main mechanisms of metal uptake which can take place in the algal cell. Note that they are both active and passive. The active form of metal uptake refers to metabolically mediated routes, such as transportation through the cell membrane. Passive uptake refers to biosorption, which is passive uptake of the metal by the algae's cell wall polysaccharides. Bioaccumulation refers to a combination of all the mechanisms of metal uptake, which will take place in live seaweed (Stokes 1983).



**Figure 1.29: Routes of metal uptake in the algal cell (adapted from Stokes 1983).**

#### 1.4.4.1 Surface Interactions

Functional groups present on the surface of a seaweed play a key role in the biosorption of metals. Common functional groups found include carboxyl, amide hydroxyl and sulphonate. Seaweeds which have large concentration of these groups normally display excellent metal uptake abilities. The concentrations of these groups may be determined by titration (Davis *et al.* 2000).

Ion exchange is considered to be an important mechanism of metal uptake by seaweeds. It is part of the mechanism of detoxification shown in the cell wall (number 1 in Figure 1.29). Here the metal is bound to functional groups on the cell surface with light metal release (Ca, Mg, K naturally found in seaweed). In a study by Figueira *et al.* (2000) it was found that presaturation of brown seaweed with light metal ions and subsequent binding with cadmium led to the release of these ions from the seaweed (Figueira *et al.* 2000).

The cell wall of fucoids will typically be composed of cellulose filaments, surrounded by a cellulose/alginate/fucoidan mucilage (Graham & Wilcox 2000). Cellulose and

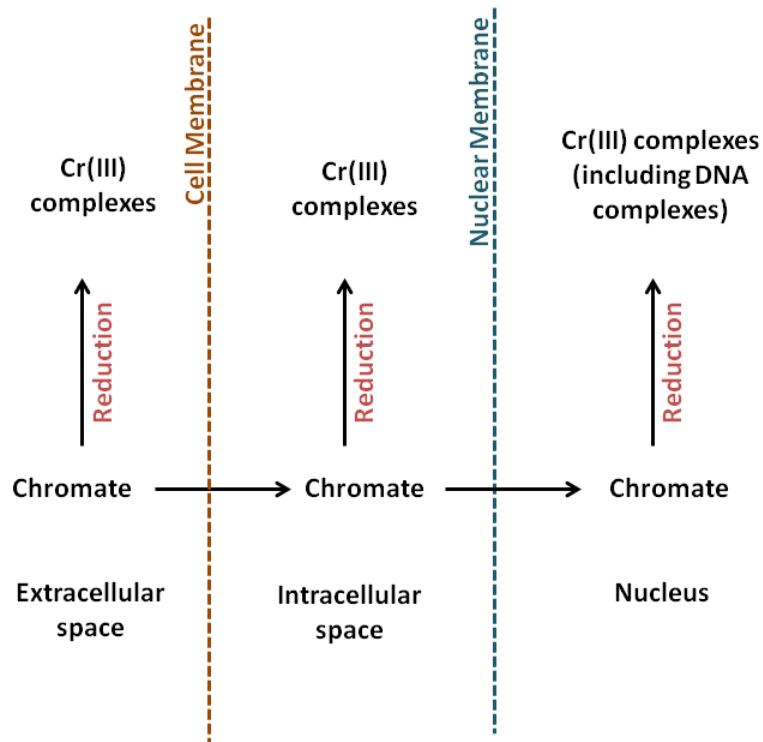
alginate both provide carboxyl and hydroxyl functional groups for binding. Fucoidan isolated from *F. vesiculosus* was shown to be composed of fucose primarily, with trace amounts of galactose and xylose (Patankar *et al.* 1993). Fucoidan provides sulphate and hydroxyl groups for metal binding. (Structures shown in Figure 1.18-1.27).

#### **1.4.4.2 Intracellular Mechanisms**

An important active mechanism of metal tolerance in live seaweed is the binding of the metal once it is in the cell in order to reduce its toxicity. Sequestering of metals by binding and transport to vacuoles has also been observed. In a study by Talarico *et al.* (2002), a red algae exposed to metals formed electron opaque deposits, that when analysed by transmission electron microscopy, were found to aggregate in the cytoplasm of the cell and was then transported to the vacuoles (Talarico 2002).

In brown seaweeds metals may be detoxified internally in physodes, which are vesicles containing polyphenolics called phlorotannins (Figure 1.28). These may be involved in the sequestration of heavy metals once they enter the cell (Pawlik-Skowrońska *et al.* 2007). Intracellular phytochelatins have also been found to be correlated to total metal content in red and brown, but not green algae. The authors stated that other mechanisms such as cell wall binding may be more important in green algae (Pawlik-Skowrońska *et al.* 2007).

Chromate ( $\text{CrO}_4^{2-}$ ) is known for its ability to enter cells because of its similarity in structure to sulphate ( $\text{SO}_4^{2-}$ ). Once inside the cell, reduction to Cr(III) leads to the formation of radicals which can attack DNA. Further to this, the resultant Cr(III) produced may bind to phosphate in DNA or nucleotides and also affect genetic function (Figure 1.30) (Kaim & Schwederski 1994).



**Figure 1.30: Fate of chromate in the cell (Kaim & Schwederski 1994).**

#### ***1.3.4. Production of Metal Chelating Agents***

Exposure of algae to a metal may cause the production of metal chelating agents by the seaweed which are then released into its surroundings. Gledhill *et al.* (1999) studied *Fucus vesiculosus* germlings grown in a copper containing media. It was found that Cu chelating agents were produced and increased Cu concentration led to increased ligand concentration in the culture medium. It was not known, however, if the ligand was released already complexed to the metal or if the complexation was extracellular (Gledhill *et al.*, 1999). The microalgae *Emiliania huxleyi* was found to release copper complexing ligands on exposure to Cu (Leal *et al.* 1999). In several species of macro and micro algae, these ligands were found to be rich in cysteine and glutathione-like thiols (Figure 1.16) (Vasconcelos *et al.*, 2002).

## 1.5 Algal Biofilms

### 1.5.1 Introduction

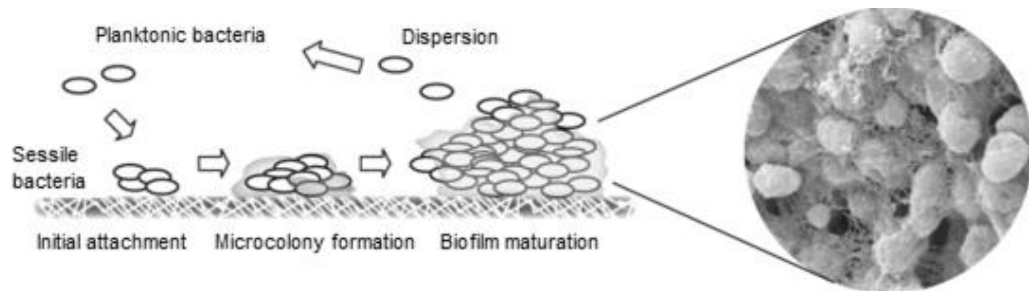
Biofilms are very common in aqueous environments and often occur on the surface of macroalgae (Egan *et al.* 2012). It is now known that bacteria are more likely to live in biofilms than as planktonic cells (Lindsay & Von Holy 2006). A biofilm may be defined as highly diverse, heterogeneous colonies which may contain bacteria, fungi, microalgae, protozoa and viruses although bacterial biofilms are the most studied and best understood. They produce extracellular polymeric substances (EPS) and behave differently from planktonic microorganisms showing a different phenotype and by interacting with each other. They are of increasing importance in microbiology as they are more resistant to antibiotics than planktonic bacteria which are studied in the lab. In fact they cause most infections related to medical and dental devices (i.e., pacemakers and catheters) as well as being the cause of most chronic infections (Lindsay & Von Holy 2006). They have also been studied widely in relation to biofouling of pipes, machinery and membranes (Flemming *et al.* 1996).

### 1.5.2 Biofilm Development

Shown in Figure 1.31 is the development of a biofilm on a surface. The stages of biofilm development are surface conditioning, primary adhesion, secondary adhesion, maturation and dispersion (Dunne 2002).

Surface conditioning occurs when the surface is modified in some way to make microorganism attachment more favourable. Note that it does not always occur in biofilm development. In general, it can be described as the deposition of some substance from the environmental media which favours biofilm development (Latasa *et al.* 2006). Primary adhesion, also known as docking or initial attachment, may be achieved by electrostatic and hydrophobic interactions, steric hindrance, van der Waals forces, temperature, and hydrodynamic forces. The interactions responsible vary depending on the microorganism species, the surface being colonised and the environmental conditions. Secondary adhesion, also known as locking or irreversible attachment, occurs when the production of extracellular polymeric substances (EPS) permanently anchor the microorganisms to the surface. Once the microorganisms are irreversibly attached microcolony formation and biofilm maturation occurs. The microorganisms begin to multiply and produce EPS. Dispersion occurs at the

outermost layer of the biofilm when cells on the surface become planktonic rather than sessile and move on to colonise other surfaces (Dunne 2002).



**Figure 1.31: Biofilm development (Latasa *et al.* 2006).**

### 1.5.3 Biofilms, Metals and Algae

A biofilm is therefore a community of microorganisms with an associated EPS layer. These biofilms have been shown to be beneficial to macroalgae, providing nutrients such as CO<sub>2</sub>, and prevent the settlement of harmful fouling epibiota such as polychaetes or other harmful microorganisms (Egan *et al.* 2012).

Biofilms may be important in metal binding to seaweeds as both the microorganisms and the EPS will have their own metal binding abilities, distinct from that of the macroalgae. Algal biofilm and metal interactions have not been studied widely, probably because of the difficulty in quantifying the amount of metal absorbed by the algae in relation to that absorbed by the biofilm. Biosorption and bioaccumulation of metals in standard microorganism cultures (rather than biofilms) has already been studied in some detail, so the ability of microorganisms to bind metals is already well known (Perales-Vela *et al.* 2006; Cervantes *et al.* 2001; Dohnalkova *et al.* 2006). The impact of biofilms on metal accumulation in seaweeds, however, has not been studied to date. They have, however, been studied on artificial substrates such as filter papers and glass slides in order to better understand the fate of metals in the aqueous environment. These biofilms have been shown to bind metals such as Mn, Fe, Ni, Cd, Pb and Cu (Dong *et al.* 2000; Ferris *et al.* 1989). A bacterial biofilm was shown to reduce Cr(VI) to Cr(III) (Nancharaiah *et al.* 2010). Biofilms cultivated in polluted

waters were shown to accumulate very high levels of metals compared to reference sites (Mages *et al.* 2004).

There have been some non-metal related studies of macroalgal biofilms. Sieburth and Tootle studied the seasonal variation in biofilms in brown and red seaweeds qualitatively using SEM. They found an overall decline in microbial coverage for all four species studied between April and May which corresponded to an increase in water temperature. They also suggested peeling of the upper layer of the alga surface and possibly algal antibiosis as mechanisms for biofilm control (Sieburth & Tootle 1981). Macroalgae have been shown to produce chemicals which both inhibit and encourage specific types of biofilm development. These are very diverse and some which have been studied to date have included compounds which are protein, polysaccharide and fatty acid in nature (Steinberg & De Nys 2002).

## 1.6 Scientific and Technological Applications of Seaweed

### 1.6.1 Traditional Commercial Uses of Seaweeds

Seaweed has traditionally been used as food, fodder and as a fertiliser, although its use as a fertiliser has lessened considerably in the Western world. It can be used directly as a food source e.g. the red alga *Porphyra* or indirectly, supporting the aquaculture of aquatic animals. The worldwide seaweed industry is worth about US\$ 6 billion, of which about US\$ 5 billion is attributed to human consumption (McHugh 2003a). The hydrocolloids industry, which refers to the production of agars, alginates and carrageenans, accounted for about US\$ 1.018 billion in 2009 (Bixler & Porse 2011). Shown in Table 1.3 below are the most commercially valuable polysaccharides which are extracted from seaweeds and their applications.

**Table 1.3: Seaweed Polysaccharides of Commercial Importance (Holdt & Kraan 2011).**

<b>Polysaccharide</b>	<b>Application in Order of Decreasing Commercial Value</b>
<b>Agars</b>	Confectionary, water gels, baking, retail (gel powder), meat, other food (dairy etc.), microbial culture medium /pharmaceutical/ agarose production (for gel electrophoresis/immunoassays etc.
<b>Alginates</b>	Technical/industrial grades, food/pharmaceutical, animal feed, PGA (propylene glycol alginate)
<b>Carrageenans</b>	Meat, dairy, pet food, water gels, toothpaste

#### ***1.6.1.1 Biofunctional Seaweeds and Extracts***

This is an extension of the traditional food use of seaweeds as hydrocolloids. Here the focus is on bioactive components rather than the texture-modifying and gelling properties of seaweeds. Seaweeds have been consumed in Asia and parts of Europe for centuries. The benefits of eating seaweed were first seen as epidemiological effects. Studies have noted the low prevalence of diseases such as coronary heart disease and dietary cancers in countries with high intakes of seaweed such as Japan and China (Yuan 2008). This has led people to study the nutritional benefits of seaweed. Seaweed is an excellent source of bioactive chemicals. They are produced naturally by seaweeds in response to the harsh environment they live in, with



fluctuating levels of salinity, temperature, light, and herbivory (Maschek & Baker 2008). The use of seaweed extracts as plant and animal nutritional supplements, functional food additives, flavours, and colours is starting to attract commercial attention. Examples of such molecules include carbohydrates, proteins and peptides, polyphenols, lipids and small molecules such as carotenoids (Hurst 2006; Holdt & Kraan 2011; Cardoso *et al.* 2015). Since seaweeds are not in general palatable to western consumers, there is some interest in the extraction of these components (or bioactives) from algae for medicinal or nutraceutical use.

### 1.6.2 Seaweeds as Biosorbents

The low cost, abundance, and efficiency of seaweed biomass are its main advantages over conventional remediation technologies as well as other types of biosorbents. The difference between biosorption and bioaccumulation is important. Biosorption is passive binding of metals to dead biomass. Bioaccumulation is an active process where the metal is metabolised by the live seaweed (Davis *et al.* 2003). This is true for all types of biomass e.g. fungal, microbial and microalgae as well as seaweed.

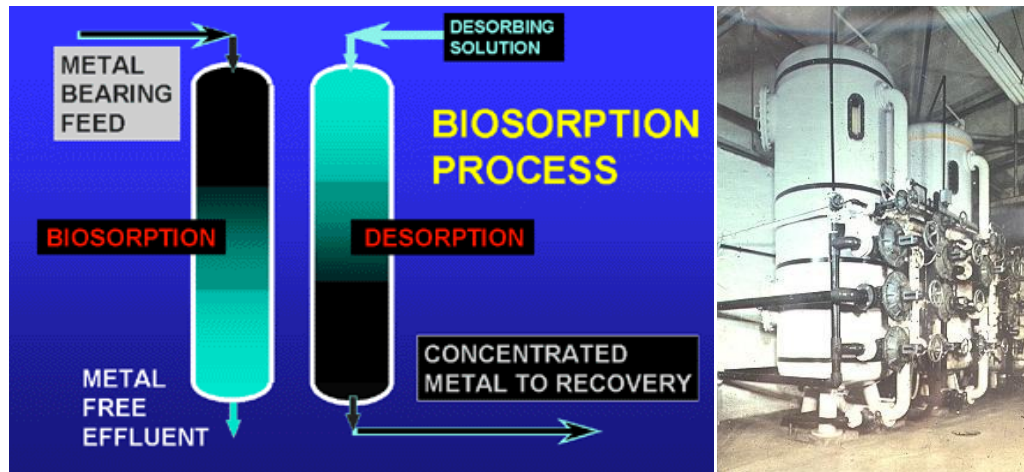
There is a huge potential market for biosorbents. Conventional remediation technologies that are commonly used for the removal of metal from solution include ion exchange and precipitation. When comparing directly to ion exchange technologies, seaweed biosorbents are suitable replacements in a lot of cases. Their capacity and applicability compare favourably with conventional technologies and they are one tenth of the cost based on estimates (Table 1.4). Their only disadvantage is that they cannot be regenerated and reused as often (Volesky 2007).

**Table 1.4: Comparison Of Removal Efficiencies of Seaweed Biomass and Commercial Resins (Kratochvil & Volesky 1998).**

Sorbant	Capacity (meq/g)
<i>Ascophyllum sp.</i>	2.0–2.5
<i>Sargassum sp.</i>	2.0–2.3
Commercial resins	0.35–5.0

meq: milliequivalents

In practice biosorbents are used in columns (see Figure 1.32). The metal bearing waste is pumped through and when it is at capacity a desorbing solution is pumped through. This yields a concentrated metal solution. Using the columns in pairs means there is no down time while a column is being desorbed of metal (Volesky 2007).



**Figure 1.32: Biosorption columns. Diagram of process and columns operating in industry (BV Sorbex 2013).**

### 1.6.3 Seaweeds as Biomonitors

Direct chemical analysis of environmental matrices such as sediment and water gives an overall picture of the concentration of a pollutant in the environment. However, it does not give information on the bioavailability and toxicity of the pollutant. The use of biomonitors is gaining popularity as a method that can achieve this. A biomonitor species can be defined as an organism which accumulates pollutants in its tissues which will relate to the fraction of pollutant present in the environment which is bioavailable, i.e., of toxicological relevance. Suitable organisms include filter feeders such as oysters, mussels and barnacles (Ruelas-Inzunza & Páez-Osuna 2000), mosses and lichens (Giordano *et al.* 2013) and macroalgae (Ryan *et al.* 2012). Algae are becoming important biomonitors of aquatic systems. They concentrate metals in their tissues, are tolerant to metal pollution, are easy to sample, and if the correct species is chosen, such as *Ascophyllum* or *Fucus*, they are easy for the non-expert to identify (Zhou *et al.* 2008).

Here, studies which look at the amount of metal found in the native seaweed are discussed. A table is presented (Table 1.5) with bioaccumulation studies, showing the seaweed and the metals studied, along with a summary of the main findings. Chromium has been highlighted in red where it has been studied, and the seaweed species have been colour coded as red, green and brown. *Sargassum*, *Fucus*, *Ascophyllum*, *Laminaria*, and *Ulva* have been abbreviated to *S.*, *F.*, *A.*, *L.* and *U.*, respectively. Brown seaweeds have been most widely studied, especially in temperate climates (R Villares *et al.* 2013; Ryan *et al.* 2012; Varma *et al.* 2011; Viana *et al.* 2010). The importance of a consistent sampling technique has been emphasised as different plant parts tend to contain different concentrations of metal (Sáez *et al.* 2012; Stengel *et al.* 2005). Seasonal changes in metal content have been found, and it is necessary to sample seaweeds at the same time to obtain results which enable comparison. For example, the metal content of a seaweed sampled in winter of one year can be compared with one sampled in winter the next year, but not with one sampled in summer (Viana *et al.* 2010; Morrison *et al.* 2008; Stengel *et al.* 2005; Favero & Frigo 2002). This is because metabolic, physico-chemical (e.g. more rainfall in winter in an estuarine environment), and growth factors will all impact metal content. Some studies have suggested that metal containing sediment attached to the macroalgae may cause an overestimation of metal content (Barreiro *et al.* 2002; Varma *et al.* 2011). Later studies which report intracellular metal content, have found that most metal is internalised in the cell (Ryan *et al.* 2012). This suggests that contamination from sediment is negligible for most metals. Exceptions may be Fe and Al which are contained in high concentration in sediments (Nassar *et al.* 2003). In recent years work has begun to assess the impact of metals on the level of oxidative stress in the macroalgae. This has mostly been assessed through bioaccumulation studies (Table 1.6) but there is some work in biomonitoring by comparing the oxidative stress biomarkers of seaweed present in polluted versus non-polluted areas (Gaete Olivares *et al.* 2016) (see Table 1.5). Overall, the suitability of seaweeds as biomonitor/bioindicator species has been shown, as they concentrate the bioavailable portion of the metal in the water, are easy to sample and identify if the correct species are chosen, and reflect the level of pollution in the area.

**Table 1.5: A summary of biomonitoring studies.**

Metals	Seaweed	Summary of Findings
<b>Reference</b>		
Fe Cu Cr Cd Mo Zn	<i>Scytosiphon lomentaria</i> , <i>U. rigida</i>	Location: Northern Chile. Sampled: September 2011. No relationship between water and algae metal content was observed. Correlation between metal content and increased oxidative stress biomarkers for 2 sites, which would be considered polluted in <i>S. lomentaria</i> only. Some correlation seen for <i>U. rigida</i> between oxidative stress markers and polluted sites (not all oxidative stress markers appeared to be present).
Gaete Olivares <i>et al.</i> 2016)		
Cd Cu Fe Ni Pb Zn	<i>Cystoseira sp.</i> , <i>Gelidium crinale</i> , <i>Laurencia obtusa</i> , <i>Gracilaria verrucosa</i> , <i>Jania rubens</i> , <i>U. compressa</i>	Location: Egyptian Coast. Sampled: Autumn 2009-Summer 2010. Seagrasses also sampled. Levels found: Cd 0.21-1.34, Cu 3.26-65.72, Fe 73.48-3865.96, Ni 3.15-52.56, Pb 13.94-159.39, Zn 4.95-111.70 mg/kg. MPI values 11.73-26.62. Found that seagrasses accumulated more metal, and recommended them for use as biomonitors in these areas.
Khaled <i>et al.</i> 2014		
Cd Cr Cu Mn Ni Pb Zn	<i>Caulerpa racemosa</i> , <i>U. lactuca</i> Linn., <i>U. Compressa</i> , <i>Ulva spp.</i> , <i>Caulerpa scalpeliformis</i> , <i>Lola capillaries</i> , <i>Lola sp.</i> , <i>Padina gymnospora</i> , <i>Dictyota bartayresiana</i> , <i>Dictyota dichotoma</i> , <i>Fucus spp.</i> , <i>Gracilaria verrucosa</i> , <i>Acanthophora spicifera</i> , <i>Acanthophora delilei</i> , <i>Hypnea sp.</i>	Location: Western India. Sampled: April, May, June 2011. Sediments and seawater also sampled. Levels found: Cd 0.05-3.23, Cr 0.6-6.2, Cu 1.1-21.5, Fe 124-1439, Mn 2.8-26.7, Ni 0.02-3.8, Pb 0.02-6.9, Zn 6.1-282 mg/kg. Site and seaweed specific levels, green and brown tended to have higher levels. In general, linear correlation found between seaweed and seawater metal content (per species). Levels found comparable to literature values for industrialised sites.
Chakraborty <i>et al.</i> 2014		
Cd Cr Cu Fe Mn Zn	<i>F. spiralis</i>	Location: Northwest coast of Portugal. Sampled: April 2013. Seawater also sampled. In general, seaweed tissues reflected water metal concentration. Contaminated sites could be identified versus 'reference sites'. Levels found: Cd 0-3.5, Cr 0.05-0.9, Cu 1-17, Fe 30-600, Mn 50-400, Zn 25-200 mg/kg.
Reis <i>et al.</i> 2014		
Cd Cu Pb	<i>Caulerpa sertularioides</i> , <i>Halimeda opuntia</i> , <i>Dictyota dichotoma</i> , <i>Galaxaura obtusata</i>	Location: Southern Gulf of Mexico. Sampled: July/Sept (Early/late rainy season, respectively) 2008. All benthic algae. In general, higher levels found during late rainy season, indicating greater fluvial inputs to be one of the main sources of metal contamination from anthropogenic sources.
Horta-Puga <i>et al.</i> 2013		

Li Be Na Mg Al P K Ca Sc Ti V Cr Mn Fe Ni Cu Zn Ga Co As Se Rb Sr Y Zr Mo Rh Pd Ag Cd Sn Sb Cs Ba La Ce Nd Ta W Au Hg Tl Pb Bi Th U	<i>F. vesiculosus</i>	Location: South west Greenland. Sampled: Yearly 2004-2011. Tips only sampled. Mine in operation 2005-2009. Increased metal loading seen after mining commenced for Cr and Ni for site closest to the mine, decreased after shut down. Cr increased 7 fold to 2.6 mg/kg; Ni increased 2 fold to 5.6 mg/kg.
Sondergaard 2013		
Fe Mn Cu Zn + macronutrients N, P, K	<i>Ascophyllum nodosum, F. vesiculosus, F. spiralis</i>	Location: North west Spain. Sampled: May 2008. Apical portions only. N varied seasonally for all three species (low seen approx May till October). Similar trend for K. P peak for <i>F. vesiculosus</i> late winter/spring. No clear seasonal trends observed for other macro or micro nutrients.
Villares <i>et al.</i> 2013		
Fe Cr Cu Zn Mn Pb Cd Ni Al	<i>Lessonia trabeculata</i>	Location: Chile. Sampled: Jan 2009 (Summer). Divided into holdfast, stipe and centre of blade. Concentration of all metals except Cd were higher in polluted site than pristine site. Metal concentration varied between plant parts sampled.
Sáez <i>et al.</i> 2012		
Pb Zn As Cd Co Cr Cu Mn Ni	<i>Polysiphonia lanosa, A. nodosum, F. vesiculosus, Ulva sp.</i>	Location: South east of Ireland. Sampled: May 2008. Biomonitoring of seaweeds, sediment and water in at a clean site. Highest metal level was intracellular, highest accumulator of metal was <i>P. lanosa</i> .
Ryan <i>et al.</i> 2012		
Al Cu Fe Mn Zn	<i>F. ceranoides</i>	Location: South-west of England. Sampled: Sep-Nov 2010. Sediments also studied. Advantage using <i>F. ceranoides</i> because of its ability to live in a variety of salinities, therefore allowing the monitoring of an estuarine environment.
Varma <i>et al.</i> 2011		
Zn Cu Sn	<i>Saccharina latissima</i>	Location: South west England. Sampled: Aug to Sep 2007. Epibiota fouling of <i>Saccharina latissima</i> was increased in marinas compared to reference locations. Much higher concentrations of metals associated with anti-fouling paints found in algae associated with marinas.
Johnston <i>et al.</i> 2011		
Fe Zn Pb Cu Cr Cd Hg Akcali & Kucuksezgin 2011	<i>Cystoseira sp., Ulva sp., Enteromorpha sp.</i>	Location: Western Turkey. Sampled: Feb, Apr, Jul and Oct 2006. Biomonitoring at several sites, plus sediment and water. High levels of metals could be connected to high industrial/domestic activity. Concentration factors of seaweed metal load/seawater metal load showed a high ability to concentrate several metals. Lowest concentration factors for Pb. All seaweeds studied showed potential as biomonitors.
Al Cd Co Cr Cu Fe Hg Mn Ni Pb V Zn	<i>F. spiralis, F. vesiculosus, F. ceranoides</i>	Location: North west Spain. Sampled: Jul 1990–2007. Lower 3 cm of plant sampled. Found that contamination by particulate material (i.e. sediment) around 4 %. Concentrations were lower in 2001 than 1990, after 2001 no significant lowering of metal content.
Viana <i>et al.</i> 2010		
Cl K Ca Ti Fe Br Sr I Ba	<i>U. lactuca</i>	Location: North west Turkey. Sampled: No date specified. Used (energy-dispersive X-ray fluorescence spectrometry) EDXRF, rather than digestion. No SRM analysed, likely that only surface metals were detected?
Apaydm <i>et al.</i> 2010		

Co Cu Mn Zn	<i>Padina durvillaei</i>	Location: Western Mexico. Sampled: May, Aug 2004, June 2005. Polluted site. High loading of Co, Cu, Mn and Zn, probably related to mining activities.
Rodríguez-Figueroa <i>et al.</i> 2009		
Cr Co Cd Pb	<i>A. nodosum</i>	Location: West, south west and east Ireland. Sampled: Feb 1999-Jul 2000. Plant tips only sampled, and washed in 10% EtOH. Co concentration higher in Winter than spring, no other strong seasonal differences.
Morrison <i>et al.</i> 2008		
Cd Cr Pb	<i>U. lactuca</i>	Location: South east India. Sampled: Sep 2004–April 2005. Biomonitoring at several sites, polluted area. No significant correlation in the concentration of metals in <i>U. lactuca</i> , water or sediment samples.
Kamala-Kannan <i>et al.</i> 2008		
Co Cu Fe Mn Ni Pb Zn	<i>U. lactuca</i> , <i>Chondracanthus squarrulosus</i> , <i>S. sinicola</i> , <i>Gracilariopsis lemaneiformis</i>	Location: Western Mexico. Sampled: Jun, 1999, Mar, 2000. No significant differences in Co, Cu, Fe, Ni and Zn metal concentrations were found among the different seaweed species, but spatial differences were found.
Huerta-Diaz <i>et al.</i> 2007		
Cr Mn Co Ni Cu Pb As Zn	<i>F. vesiculosus</i> , <i>F. distichus</i> , <i>U. lactuca</i> , <i>Enteromorpha intestinalis</i> , <i>Gracilaria tikvahiae</i>	Location: Eastern US. Sampled: Mar 2006. Low contamination site. Suggests the use of metal pollution index (MPI) and pollution load index (PLI) as useful comparative outputs of monitoring.
Chaudhuri <i>et al.</i> 2007		
Fe Mn As B Ti Zn Hg	<i>Plocamium corallorhiza</i>	Location: East South Africa. Sampled: Jun 2002 to May 2003. No overall seasonal trends were detected which applied to all sites.
Misheer <i>et al.</i> 2006		
Total As /inorganic As Pb Cd	112 samples of seaweed preparations (edible)	Various locations. For all the contaminants analysed there were failures to comply with legislated values.
Almela <i>et al.</i> 2006		
Cu Fe Mn	<i>A. nodosum</i> , <i>F. vesiculosus</i> , <i>Laminaria digitata</i>	Location: Western Ireland. Sampled: For temporal study seaweed was sampled fortnightly from Oct 2003-Feb 2004. For spatial and inter-thallus variation, sampled in Oct 2003 (except <i>L. digitata</i> , Feb 2003). Tips and whole plants sampled. In <i>A. nodosum</i> , Cu decreased from Oct-Feb, whereas Fe increased. Spatial and inter-thallus variation was observed.
Stengel <i>et al.</i> 2005		
Al Cd Cr Cu Fe Mn Ni Pb Zn	<i>Padina gymnospora</i>	Location: Eastern Brazil. Sampled: Jun 2002 to May 2003. One clean and one polluted site. Used a cleaning treatment to remove sediment from seaweed. Fe and Al concentrations were reduced by 78% and 50% respectively. Higher Fe, Al, Cu content at polluted site after cleaning.
Nassar <i>et al.</i> 2003		
Zn Cu Cd Pb Fe Ag Mn	<i>F. vesiculosus</i>	Location: South-east England. Sampled: Aug 2001. 2cm section of older frond, rather than whole plant was sampled. Increased contamination due to point sources of pollution discussed. In general sites were 'cleaner' than 1980's.
Rainbow <i>et al.</i> 2002		
Cd Hg Zn Mn Al	<i>Macrocystis pyrifera</i>	Location: Western Mexico. Sampled: Jan to Oct (except Mar) of 1985. Upper frond sampled. High Cd concentration related to upwelling (upwelling inferred through high seawater phosphate).
M Lucila Lares <i>et al.</i> 2002		

Cd Cu Zn Fe Mn	<i>U. lactuca</i> , <i>Gelidium pulchellum</i> , <i>F. spiralis</i> , <i>Bifurcaria bifurcata</i>	Location: North west Morocco. Sampled: Physico-chemical water parameters, May–Jun 1995, but not specified if seaweed sampled at the same time. Metal content was species specific, and found to be generally low when compared to literature results.
Kaimoussi <i>et al.</i> 2002		
Al Mn Fe Cu Zn Cr Co Ni Cd	<i>U. laetevirens</i> , <i>Enteromorpha intestinalis</i> , <i>Gracilaria verrucosa</i> , <i>S. muticum</i>	Location: North east Italy. Sampled: Jun 1994, Sep 1994, Jan 1995 and May 1995 though sampling not complete for all species/all seasons. Trends: Apices and basal portion of plant were separated for <i>S. muticum</i> . In <i>S. muticum</i> higher concentrations found in the older plant parts. <i>U. laetevirens</i> : Cd higher in winter time. <i>E. intestinalis</i> : Al, Fe, Cr and Pb higher in spring. Lower metal concentrations found in sites far from built up areas with a higher water turnover.
Favero & Frigo 2002		
Fe Zn Cu Cd Ni Pb Cr As	<i>U. rigida</i> , <i>Gracilaria gracilis</i> , <i>Porphyra leucosticta</i> , <i>Grateloupia doryphora</i> , <i>Undaria pinnatifida</i> , <i>F. virsoides</i> , <i>Cystoseira barbata</i>	Location: North east Italy. Sampled: Spring and autumn 1999, though sampling not complete for all species/all seasons. Metal concentrations comparable to other polluted areas. <i>U. rigida</i> had the highest concentration of Fe, Cu, Pb, Cr, and along with <i>F. virsoides</i> the highest concentration of Cd and Ni. Decrease in metals in the last 5 years when compared to literature.
Caliceti <i>et al.</i> 2002		
Cu Cr Mn Zn Fe Al	<i>F. vesiculosus</i> , <i>F. ceranoides</i>	Location: North west Spain. Estuary received inputs of chromium from a tannery. Contamination of seaweed Cr, Fe, and Al levels by sediment was suggested.
Barreiro <i>et al.</i> 2002		
As/inorganic As Pb Cd Hg	<i>Undaria pinnatifida</i> , <i>L. japonica</i> , <i>Hizikia fusiforme</i> , <i>Eisenia bicyclis</i> , <i>Porphyra sp.</i> , <i>Palmaria palmata</i> , <i>U. pertusa</i> .	Packaged products from various locations. Cd and inorganic As levels higher than those permitted by legislation in some countries were discovered (no regulation in the country of study, Spain).
Almela <i>et al.</i> 2002		
Al As Br Cd Fe La Mn Ni Hg V Zn	<i>Polycavernosa dentata</i> , <i>Gigartina acicularis</i> , <i>Centroceras clavulatum</i> , <i>Bryocladia thysigera</i> , <i>Jania rubens</i> , <i>Hypnea musciformis</i>	Location: South Ghanian coast. Sampled: Jun 1996 to Aug 1998. Instrumental Neutron Activation Analysis (INAA) validated by SRM. Baseline data, high interspecies variability.
Serfor-Armah <i>et al.</i> 2001		
Cu Mn Ni Zn Cd Pb	Red, brown and green	Location: Eastern Greece and south east islands. Sampled: Not specified. Notes geology of area is important in determining whether seaweed metal content is natural or anthropogenic.
Sawidis <i>et al.</i> 2001		
Rb Cs Ca Sr Ba Sc Cr Fe Co Ni Zn Se As Sb Th U Br Hf Ta Zr Ag	<i>Codium cuneatum</i> , <i>S. sinicola</i> , <i>Padina durvillaei</i> , <i>L. papillosa</i> , <i>Laurencia johnstonii</i> , <i>Gracilaria pachidermatica</i> , <i>Hypnea pannosa</i>	Location: Eastern Mexico. Sampled: Apr and Jul 1997. In general brown seaweeds had the highest levels of metals. A significant correlation between seaweed metal content and north pacific metal concentration was found.
Sánchez-Rodríguez <i>et al.</i> 2001		
Fe Mn Zn Cu Pb Ni Cr Cd Ag	<i>F. vesiculosus</i>	Location: North east England. Sampled: Winter 1997-1998. Lower 8-10 cm portion of frond tested. Used Metal Pollution Index (MPI) to calculate metal burden. Seaweed MPI was positively correlated with fine grained (63-180 µm) sediment MPI, but not pelite (<63 µm) MPI.
Giusti 2001		

Cu Fe	<i>A. nodosum</i>	Location: North east and north west Ireland. Sampled: Oct, Dec 1990, Feb 1991. Both tips and whole plants sampled. Concentration of both Fe and Cu in tips decreased from October to February. Showed epidermal shedding which may be important as metal maybe bound to surface cells/epibiota.
Stengel & M. Dring 2000		
As Cd Co Cr Cu Fe Hg Mn Ni Pb Zn	<i>F. vesiculosus, A. nodosum, L. longicruris, Palmaria palmata, U. lactuca, F. distichus</i>	Location: Quebec and New Brunswick, Eastern Canada. Sampled: Sep and Oct 1995. Metal concentrations were found to be low.
Phaneuf <i>et al.</i> 1999		
Cd Cu Pb Zn Na Ca Sc Cr Fe Co As Br Rb Sr Cs Ce	<i>F. vesiculosus, F. distichus, A. nodosum</i>	Location: West Greenland. Sampled: Summer 1980-1982. Tips only sampled. Should be relatively unpolluted due to lack of industry, found lower levels of metals than northern Europe.
Riget <i>et al.</i> 1997		
Cr Cu Fe Mn Zn	<i>U. lactuca, Chondrus crispus, Pelvetia canaliculata, F. serratus, F. vesiculosus</i>	Location: West Ireland. Sampled: May 1994. <i>U. lactuca</i> best accumulator of all metals bar Zn, of which <i>P. canaliculata</i> contained the most.
Leary & Breen 1997		
Sc Cr As Co Zn Se Ag Hg P V Mn Fe Cu Zn As Pb	<i>F. vesiculosus</i>	Location: North west Germany. Sampled: Bimonthly in 1993. Seaweed separated into tip, one year old, two year old and basal parts. Sc, V, Cr, Fe, and Pb maximum in late spring and a minimum in early winter. P, Cu, Zn, As, Ag, Cd, Hg: maximum in late winter/early spring and a minimum in summer months. Plant part had an effect on metal concentration.
Amer <i>et al.</i> 1997.		
Hg As Se Cd Pb Cu Na K S P Zn Mn Fe Sr Ca Ba Mg Tl Ni Co	<i>F. vesiculosus</i>	Location: North Germany. Sampled: Some observations from a 10 year sampling programme. Some trends of lowering metal content over time (Cd, Ni), as well as one increase (As).
Ostapczuk <i>et al.</i> 1997		
Zn Mn Fe Cu Pb Ni	<i>A. nodosum</i>	Location: South west Scotland. Sampled: Apr 1964-1994. Metal concentration could be correlated to mining and land reclamation activities in some cases.
Molloy & Hills 1996		
As Cd Co Cr Hf Ni Th U Zn Ce Eu Sm Tb Yb	<i>F. vesiculosus, S. filipendula, Ulva sp.</i>	North east and north west Germany: <i>F. vesiculosus</i> sampled bimonthly for a year and homogenised to make a composite sample. West Sri Lanka: <i>S. filipendula</i> sampled February 1992 and 1994. Higher concentrations of Ni, Cr and Co found in Germany, probably related to more industrialised nature of the site. Other differences related to geology of areas. Few differences found between 1992 and 1994 homogenates in Sri Lanka.
Jayasekera & Rossbach 1996		
Mo Pb Hg As U Ni Co Mn Ag Fe Cu Zn Vn Cd	<i>A. nodosum</i>	Location: Western Norway. Sampled: Oct, Nov, Feb, Mar 1976-1977. Section containing the four lower air bladders. Baseline study showing variation in many estuaries in the sampling area, related to freshwater input, the geological environment and previous mining activities.
Sharp 1995		
Zn Cd Cu Pb	<i>F. vesiculosus</i>	Location: West Greenland. Sampled: May 1987 to Sep 1990. Growing tips sampled. Summer lows consistent with growth observed, however other explanation could be valid, such as higher primary productivity in Summer.
Riget <i>et al.</i> 1995		



Al Fe Mn Co Cr Cu Ni Zn Pb	<i>F. ceranoides</i> , <i>F. spiralis</i> , <i>A. nodosum</i> , <i>Ulva sp.</i>	Location: North west Spain. Sampled: Sep/Oct 1990. Apices and thalli separated. Error due to sediment contamination of seaweed was estimated at <10% and so not corrected for in reported values.
Carral <i>et al.</i> 1995		
Cd Co Cr Cu Fe Ni Pb Zn	<i>F. serratus</i>	Location: Northern France. Sampled: Every 2 weeks for 13 months. Seasonal variation in Cd, Co, Cu, Fe, Ni and Zn concentration in <i>F. serratus</i> , maximum in Winter. Results indicated non-polluted area.
Miramand & Bentley 1992		
Cd Cu Pb Zn	<i>F. vesiculosus</i> , <i>F. distichus</i>	Location: West Greenland. Sampled: 1976-1988. Whole plants and tips sampled. Difference between tips and whole plants: Cu, Pb, Zn-yes, with less in the tips than whole plants, Cd-no. Elevated Pb and Zn levels within 30 km of mine.
Johansen <i>et al.</i> 1991		
Zn Mn Fe Cu	<i>F. vesiculosus</i>	Location: South west Finland. Sampled: May 1987 and Apr 1988. Investigating fish farm metal pollution. Transplantation experiment from unaffected area to farm area. Higher concentration of Fe and Cu in autumn and winter in plants transplanted to farm area.
Rönnberg <i>et al.</i> 1990		
Cd Cu Cr Pb Zn Fe Ni	<i>A. nodosum</i> , <i>Chondrus crispus</i> , <i>Furcellaria fastigiata</i> , <i>Palmaria palmata</i> , <i>Gigartina stellata</i> , <i>L. digitata</i> , <i>L. longicuris</i>	Location: South and west coast New Brunswick, south coast Prince Edward Island, south, east and west coast Nova Scotia, Canada. Sampled: Jun and Aug 1983. No significant impact of plant part sampled on metal concentration was found. Found levels of metal in general comparable with other polluted sites.
Sharp <i>et al.</i> 1988		
Al Cd Co Cr Cu Fe Mn Ni Pb V Zn	<i>F. vesiculosus</i>	Location: Eastern Sweden. Found <i>F. vesiculosus</i> to be a good indicator of metal pollution. A transplant experiment found an increase in metal content in plants transplanted close to a large city.
Forsberg <i>et al.</i> 1988		
Zn Mn Cu Cd Mg Fe	<i>Galaxaura lapidescens</i> , <i>Laurencia obtusa</i> , <i>Liagora turneri</i> , <i>Colpomenia sinusa</i> , <i>Padina pavonica</i> , <i>S. dentifolium</i> , <i>Turbinaria elatensis</i> , <i>Enteromorpha clathrata</i> , <i>Halimeda tuna</i> , <i>U. lactuca</i>	Location: South west Jordan (Red sea). Sampled: Mar-May 1983. Significant differences in metal concentration found between species, with red algae having the highest metal contents, and green and brown having similar metal contents. Baseline study which indicated an unpolluted sampling area when compared to other studies.
Wahbeh <i>et al.</i> 1985		
Cd Cr Cu Fe Mn Ni Pb Zn	<i>F. vesiculosus</i>	Location: North East England. Results indicated the location was a polluted estuary when compared to other contaminated and unpolluted sites.
Barnett & Ashcroft 1985		
Ag Cd Cu Pb Zn	<i>F. vesiculosus</i>	Location: England and Wales. Found increasing Cd concentration with decreasing salinity. High Zn concentrations were associated with lower Cd concentrations.
Bryan 1983		
Ag Cd Co Cr Ni Pb As Hg	<i>F. vesiculosus</i>	Location: Large number of estuaries in the west, south and east of the UK. Sampled: 1972-1982. Older plant parts sampled. Found sediment contamination to be significant for Pb and Cr (Method: assumed all Fe is due to sediment, analysed Fe in sediment, determine Fe:metal ratios in sediment, then applied the ratio to calculate other metals in seaweeds).
Bryan <i>et al.</i> 1983		

Cu Cd Mn Zn Woolston <i>et al.</i> 1982	<i>A. nodosum</i>	Location: North New Brunswick, Canada. Differences in concentration between sites. Could be related to sources of pollution.
Cu As Pb Zn Ag Cd Co Fe Mn Hg Luoma <i>et al.</i> 1982	<i>F. vesiculosus</i>	Location: South and west of England. Raised the possibility of sediment contamination on measurement of metal in seaweed. Concentrations of Cu, As, Pb, Zn and Ag (but not Cd, Co, Fe, Mn and Hg) correlated significantly with concentrations in sediment. Suggested method to account for possible sediment contamination (same as detailed in Bryan <i>et al.</i> 1983)
Fe Cu Co Cd Ni Cr Ag Pb Mn Zn Burdon-Jones <i>et al.</i> 1982	<i>Padina tenuis, Padina tetrastromatica</i>	Location: North east Australia. Sampled: Monthly from Feb 1976-77. Some correlation of metal content with seasonal changes in temperature/salinity was found, though none consistent as spatial variation found also. Highest Ag during winter; Mn, Zn was inversely correlated to salinity (except one site for Zn).
As Cu Cd Pb Se Zn Hg Sirota & Uthe 1979	<i>Palmaria palmata</i>	Location: 3 different areas (prob. Nova Scotia, Canada), and a holding tank. Concentration ranges ( $\mu\text{g/g}$ dry weight) were: As 5.50-7.50, Cu 3.90-6.34, Cd 0.97-2.65, Pb 0.688-3.5, Se 2.00-2.91, Zn 57.5-84.1, Hg < 0.02.
Cd Cu Fe Mn Ni Pb Zn Agadi <i>et al.</i> 1978	17 species, red, brown and green	Location: West India.
Zn Cu Pb Cd Melhuus <i>et al.</i> 1978	<i>A. nodosum, F. vesiculosus</i>	Location: Western Norway. Zn and Cd concentration was found to be essentially the same throughout the sampling area, Cu and Pb concentrations decreased towards the mouth of the estuary. Concentration factors for Cu, Pb and Cd are in good agreement with the previous literature, Zn concentrations were found to be higher.
Cu Pb Seeliger & Edwards 1977		Location: New York Coast. High correlation between water and seaweed metal concentrations found.
Cu Pb Romeril 1977	<i>Fucus sp</i>	Location: Jersey, UK. Related Cu and Pb pollution to effluent from a desalination plant.
Cd Co Cr Cu Fe Mn Ni Zn Ag Pb Bryan & Hummerstone 1977	<i>Fucus sp.</i>	Location: South west UK. Sampled: Dec 1975, Mar 1976. Some evidence of Ag, Pb and Cu contamination found when results were compared to other reported values. Metal concentrations fell towards the mouth of the estuary.
Zn Cu Cd Pb Cr Foster 1976	<i>A. nodosum, F. vesiculosus</i>	Location: North Wales, UK. Found no correlation between water and seaweed metal concentration in a polluted area.
Cd Cu Mn Zn Morris & Bale 1975	<i>F. vesiculosus</i>	Location: South Wales, UK. Found a correlation between water and seaweed metal concentration except for Mn, which appeared to be regulated.
Zn Cu Pb Cd Hg Haug <i>et al.</i> 1974	<i>A. nodosum</i>	Location: West Norway. Elevated levels of Zn, Cu, Pb, Hg, Cd were found up to 90 km from the point source of pollution.

Zn Cd Cu Mn Fe Co Ni Mo	<i>F. serratus, F. vesiculosus</i>	Location: West Wales. Seasonal variation in metal concentration was found. Concentration of Zn, Cd, Cu, Fe Ni, and Co was highest in the spring and lowest in the autumn. Spatial variation was observed for most metals studied.
Fuge & James 1973		
Cu Zn Pb Mn Fe	<i>F. vesiculosus</i>	Location: South west England, UK. Sampled: Jun 1969, Sept 1969, Jan 1970 and Aug 1970. Separated into thallus, stipe and tip. Used older parts of the thallus as concentration of metal was greater here. Indicated that time of sampling, and position on shore was important. Concentration factors of $10^3$ - $10^5$ ( $\mu\text{g/g}$ dry tissue / $\mu\text{g/mL}$ water) were seen.
Bryan & Hummerstone 1973		
Unknown	Unknown	Location: UK. Sampled: 1960-1970. Showed that metal pollution is unchanged since 1960, or in the case of Cd, lower.
Preston <i>et al.</i> 1972		
Zn Fe Cu Mn	<i>L. digitata</i>	Location: South west England. Sampled: Feb. Samples taken from growing regions of plants. Zn, Fe and Mn appear to increase in concentration with distance from tips. Cu does not show this trend. Conc. factors of $10^2$ - $10^3$ were seen ( $\mu\text{g/g}$ dry tissue / $\mu\text{g/mL}$ water).
Bryan 1969		
Cu Ba Sr Mn Co Ni Mo Fe Pb Sn Zn V Ti Cr Ag	<i>L. cloustoni, L. digitata, F. spiralis</i>	Location: West Scotland. Sampled: Oct 1947, Jul 1948, Jan, May 1949, Jun 1950. Reported seasonal and species variation in metal content. Conc factors up to $10^4$ seen (Ti), but most around $10^2$ (Ni, V, Cr).
Black & Mitchell 1952		

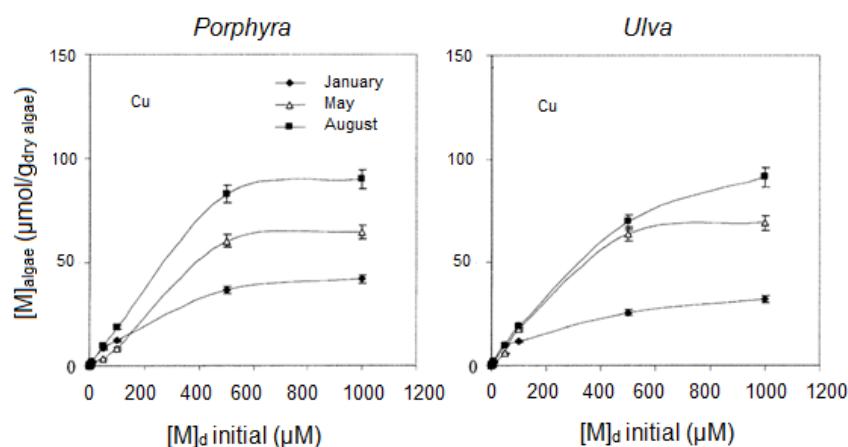
Chromium has been highlighted in red where it has been studied, and the seaweed species have been colour coded as red, green and brown. *Sargassum*, *Fucus*, *Ascophyllum*, *Laminaria*, and *Ulva* have been abbreviated to S. F. A. L. and U., respectively.

### 1.7A Review of Bioaccumulation and Biosorption in the Literature

Studies discussed here concern bioaccumulation experiments, where live seaweed are exposed to metals. This has been studied much less than biosorption, which is the binding of metals to dead biomass, and biomonitoring, where the seaweed is sampled *in situ* and analysed for metal content. Cr has been much less studied than other metals such as Zn, Cu or Cd. As this is the case, other plants and organisms besides algae have been discussed here where relevant, especially where studies of Cr accumulation have been carried out. Most metals studied are cationic (form positively charged ions). The chemical species used will be noted where this is possible, as not all papers supply this information (Table 1.6).

#### 1.7.1 Seasonal Effects in Metal Bioaccumulation

There has been only one study of the effect of season on metal uptake by macroalgae. The bioaccumulation of Cu, Hg, Pb and Cd by *Porphyra* spp and *Enteromorpha* spp. (now known as *Ulva* spp., as *Ulva* and *Enteromorpha* have been shown to be the same genera (Hayden *et al.* 2003)) was studied. The most definite seasonal trends were seen for Cu, with the greatest uptake seen in August, followed by May and then January for both species (Figure 1.33). Hg uptake is similar in August and May, and lower in January. Pb and Cd uptake was quite similar. It should also be noted that metal uptake was similar for both species (Vasconcelos & Leal 2001).



**Figure 1.33: Uptake isotherms of seasonal differences in Cu uptake (18 °C, 24 h exposure time, fully illuminated (Vasconcelos & Leal 2001).**

### 1.7.2 The Seaweed Surface: Potential for Epiphytes and Biofilms to Accumulate Metals and the Role of Surface Shedding of Cells

The influence of surface biofouling in seaweeds on metal uptake has not been widely studied. Scanning electron microscopy and X-ray microanalysis was used to study surface binding of Cu ( $\text{CuSO}_4 \cdot 2\text{H}_2\text{O}$ ,  $\text{Cu}^{2+}$ ) and Fe ( $\text{FeCl}_2$ ,  $\text{Fe}^{2+}$ ) in *Ascophyllum nodosum*. About 18 % of the total Cu was found to be located in the surface cells. These cells were found to undergo increased shedding during the experimental period. Fe was found to be located mostly in diatoms on the seaweed surface. This showed the effect that epiphytism may have on metal binding in seaweeds (Stengel & Dring 2000). In another study, the red seaweed *Audouinella saviana*, was exposed to Cd ( $\text{Cd}(\text{NO}_3)_2$ ,  $\text{Cd}^{2+}$ ), and ultrastructural changes were examined by SEM/TEM. The cell wall was found to thicken and become smoother after 10-15 days exposure at concentrations of 600-1000  $\mu\text{M}$  Cd. The author suggested that the cell wall changes were due to newly formed proteins and polysaccharides, and that these were part of the seaweeds response mechanism to Cd stress (Talarico 2002).

Two fungal strains associated with the marine seaweed *Eucheuma* sp. were found to accumulate Cr ( $\text{K}_2\text{Cr}_2\text{O}_7$ ,  $\text{Cr}_2\text{O}_7^{2-}$ ) from solution. Both species (*Aspergillus flavus* and *Aspergillus niger*) were found to be Cr tolerant as only a non-significant decrease in biomass was found under the experimental conditions (up to 100 mg/L Cr). Although the study discusses the use of fungal biomass as a biosorbant, it illustrates how microorganisms associated with seaweed may contribute to metal binding (Vala *et al.* 2004).

Gregory (2009) attempted to discover the influence of the quantity of bacteria in solution on metal uptake (Cd and Se) in the green alga, *Ulva lactuca*, but was unable to discover any trends because of experimental difficulties (lack of significant differences in bacterial numbers between control and test experiments) (Gregory 2009). It is reasonable to assume adding bacterial biomass to a metal solution will reduce algal uptake as competition will exist between the two types of biomass. It is also reasonable to assume that the lack of significant differences is real under the conditions studied, and that there was not enough bacteria in solution to effect metal uptake.

### 1.7.3 Species Specific Responses to Bioaccumulation

Species specific responses to metals have been found by many researchers, and there is difficulty in generalising trends to red, green and brown seaweeds. For example, phytochelatins were found to be induced by Cd ( $\text{Cd}(\text{NO}_3)_2$ ,  $\text{Cd}^{2+}$ ) in the brown seaweed *Fucus* spp., the red seaweed *Solieria chordalis* and the green seaweed *Rhizoclonium tortuosum*, but not in two other green seaweeds, *Ulva* spp. and *Codium fragile*. This implies a different detoxification mechanism, suggested to be uptake by polysaccharides or exclusion by thicker cell walls (Pawlik-Skowrońska *et al.* 2007). Two fucoid species (brown), *F. vesiculosus* and *A. nodosum* were found to have different responses to Cu ( $\text{CuSO}_4 \cdot 5\text{H}_2\text{O}$ ,  $\text{Cu}^{2+}$ ) exposure. At low salinity, Cu uptake decreased in *A. nodosum*, but increased on *F. vesiculosus*, indicating a species specific mechanism of uptake even in these two related species (Connan & Stengel 2011a).

A study of seven different seaweed species found that green and red generally accumulated more metal than brown seaweeds (metals studied:  $\text{CuCl}_2$  ( $\text{Cu}^{2+}$ ),  $\text{Pb}(\text{ClO}_4)_2$  ( $\text{Pb}^{2+}$ ),  $\text{ZnCl}_2$  ( $\text{Zn}^{2+}$ ),  $\text{K}_2\text{CrO}_4$ , ( $\text{CrO}_4^{2-}$ ),  $\text{CdCl}_2$  ( $\text{Cd}^{2+}$ )). An exception to this was the green seaweed *Cladophora rupestris*, which generally accumulated the least amount of metal in laboratory experiments (Baumann *et al.* 2009). These studies show the difficulty in generalising metal uptake patterns to other species of seaweed. Other factors clearly affect metal uptake besides colour, such as thallus form, cell wall thickness, and polysaccharide composition.

### 1.7.4 Effect of Water Composition and Physico-Chemical Parameters

#### 1.7.4.1 Effect of Nutrients

A study of metal uptake by a green seaweed, *Ulva crinita*, found that ammonium and nitrate enrichment significantly increased the accumulation of cadmium chloride ( $\text{CdCl}_2$  -  $\text{Cd}^{2+}$ ) and zinc chloride ( $\text{ZnCl}_2$  -  $\text{Zn}^{2+}$ ), but sodium dichromate ( $\text{Na}_2\text{Cr}_2\text{O}_7$  -  $\text{Cr}_2\text{O}_7^{2-}$ ) accumulation was unaffected. Phosphate addition did not increase uptake of any metals studied. The experiments were carried out over 48 h. The possibility of nitrogen enrichment enhancing the production of amino containing compounds, and enhancement of photosynthesis, which in turn enhanced carboxyl and carbonyl groups was suggested by the authors (Chan *et al.* 2003; Wang 2013). A direct assay of the nitrogen content of the seaweed, e.g. by Kjeldahl assay, which may confirm this, was not carried out, but this is a plausible explanation for the enhancement in Cd and Zn

uptake. Amino, carboxyl and carbonyl groups all act as effective chelators for metals (Davis *et al.* 2003; Cobbett & Goldsbrough 2002). Faster growth was another possible explanation for enhanced uptake of the essential metal, Zn. Chromium uptake may have been unaffected due to the formation of weaker ligand-metal complexes, and because of its cationic nature (Chan *et al.* 2003).

Cd and Zn, but not Cr accumulation in *Ulva fasciata* was also found to be enhanced by nitrate enrichment of the medium. Phosphate enrichment caused a small increase to Cr ( $\text{Na}_2\text{CrO}_4$ ,  $\text{CrO}_4^{2-}$ ) accumulation, but Se (Sodium selenite -  $\text{Na}_2(\text{SeO}_3)$ ,  $\text{SeO}_3^{2-}$ ) accumulation was markedly decreased. Cr(VI) and Se(IV), both anionic metals, were studied, but the difference in algal response suggests a different uptake mechanism for the metal. Cr and Se uptake was also significantly lower than the cationic metals Cd and Zn, showing the greater prevalence of functional groups capable of binding to these positively charged metals (Lee & Wang 2001).

#### 1.7.4.2 Importance of Salinity

Cd (cadmium sulphate -  $\text{CdSO}_4$ ,  $\text{Cd}^{2+}$ ) uptake by *Fucus vesiculosus* from a low salinity (Baltic Sea 5 psu) and full salinity (Irish Sea 35 psu) site were studied. *F. vesiculosus* from the full salinity site took up less Cd and had less acidic groups (determined by titration) than the same seaweed from the low salinity site (Brinza *et al.* 2009). The quantity of acidic sites give an indication of groups capable of metal binding in the biomass (Naja *et al.* 1999). This study demonstrates how site specific factors can have a big impact on metal uptake in the same species of seaweed, and demonstrates the difficulty in comparing metal uptakes between studies.

A pair of studies looked at how the uptake of Cu (copper sulphate -  $\text{CuSO}_4 \cdot 5\text{H}_2\text{O}$ ,  $\text{Cu}^{2+}$ ) by *F. vesiculosus* and *A. nodosum* was impacted by changing salinity (5, 15, 25, 35). An increase in salinity was found to decrease Cu accumulation by *F. vesiculosus*, but the opposite was true for *A. nodosum*. Growth and photosynthesis for both species was negatively affected by both low salinity and increasing Cu (Connan & Stengel 2011a). The differences in results between this study and that of Brinza *et al.* (2009), discussed above, may be because in Brinza's study the seaweed was sampled in a low salinity area, and the experiments carried out in low salinity water sampled at the growth site along with the seaweed. In Connan's study the seaweed was sampled from a full salinity site, and low salinity water was prepared artificially. It is possible that

the seaweed in Brinza's study has adapted to low salinity conditions biochemically, thus leading to different uptake trends. The second study focussed on the phenolic content of the seaweeds. Phlorotannin (a phenolic molecule) quantity was reduced due to reducing salinity in both seaweeds studied. Increased Cu concentration also reduced phenolic content, and more cell wall bound phenolics were found (Connan & Stengel 2011b).

In the freshwater plants *Elodea canadensis* (Michx.) and *Potamogeton natans* (L.), it was found that increasing salinity (0, 0.5, and 5 ‰) reduced metal uptake for Cu, Cd and Zn. Pb accumulation was enhanced, or stayed stable at higher salinity. This study was carried out over 48 h, so biomass quantity was unaffected. The difference in uptake at higher salinity was probably due to decreased metal availability due to the formation of metal complexes (e.g. chloride complexes), and because of competition with salt ions such as sodium and magnesium. Pb is less likely to form chloride complexes and has a high affinity towards biomass, and therefore an effect for salinity was not seen (Fritioff *et al.* 2005).

Increasing salinity (10, 15, 20, 28 ‰) was found to have a negative effect on the uptake of Cd, Zn, Cr ( $\text{Na}_2\text{CrO}_4$ ,  $\text{CrO}_4^{2-}$ ), and Se ( $\text{Na}_2(\text{SeO}_3)$ ,  $\text{SeO}_3^{2-}$ ) in *Ulva lactuca*. Cd and Zn chemical form was not specified, but the metals used were most likely divalent cations. This was also the case for *Gracilaria blodgettii* for Se and Cd, but only small non-significant differences were found for Zn and Cr in this seaweed. The reasons for this effect of salinity are probably similar to the study by Fritioff (2005), such as reduced metal availability due to the metal behaviour in solution, and biochemical effects, such as increased membrane permeability at lower salinities. Cd and Zn were most affected by the change in salinity (Wang & Dei 1999). A similar negative effect of increasing salinity was found for Cu, Zn, Mn and Cd uptake by *Chaetomorpha linum*, *Sargassum siliculosum* and *Gracilaria changii* at salinities of 20, 25, 30 and 35 ppt (Murugadas 1995).

The influence of salinity (Full (32), mid (16) and low (8)) on the uptake of Zn (zinc sulphate -  $\text{ZnSO}_4$ ,  $\text{Zn}^{2+}$ ), Mn (manganese chloride -  $\text{MnCl}_2$ ,  $\text{Mn}^{2+}$ ), and Co (cobalt chloride -  $\text{CoCl}_2$ ,  $\text{Co}^{2+}$ ) by the brown seaweed *F. vesiculosus* was studied. For Zn and



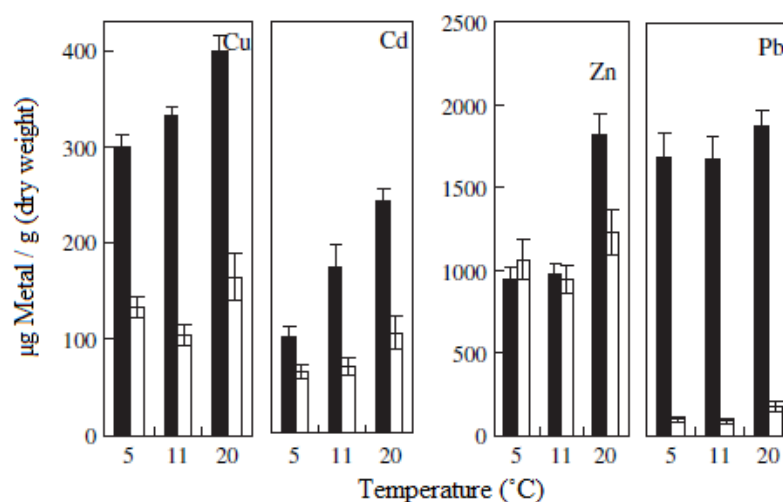
Mn, the greatest uptake was observed at lowest salinity. For Co, greatest uptake was observed at the mid salinity studied. No definitive reason could be found for this result, but this was probably due to changes in Co specific interactions between cell wall/membrane components in different salinity conditions. In general however, results were similar to other studies, with decreasing salinity having a positive effect on metal accumulation (Munda & Hudnik 1988).

In general, studies have found that decreasing salinity increases metal bioaccumulation, probably because of decreased competition from other ions present in sea water, such as Na, Mg, K, and Ca.

#### 1.7.4.3 Effect of Temperature

Few studies exist on the relationship between temperature and metal bioaccumulation, and it is therefore not well characterised at present. Some of the research that has explored this aspect of bioaccumulation is presented here.

Fritioff *et al.* (2005) found that increasing temperature generally increased metal accumulation for *Elodea canadensis* (Michx.) and *Potamogeton natans*. Note that aquatic plants are studied in this case. Several explanations for this behaviour were proposed including an increase in fluidity of the plasma membrane and increased metabolism, both of which may facilitate metal uptake (shown in Figure 1.34).



**Figure 1.34: Uptake of metal by *Elodea canadensis* (black) and *Potamogeton natans* (white) at 3 temperatures (Fritioff *et al.* 2005).**

The influence of two temperatures (5 and 15 °C) on Zn (ZnSO<sub>4</sub>, Zn<sup>2+</sup>), Mn (MnCl<sub>2</sub>, Mn<sup>2+</sup>), and Co (CoCl<sub>2</sub>, Co<sup>2+</sup>) uptake in *F. vesiculosus* was studied after a 21 day period of exposure. There was a small increase in Zn concentration at 15 °C, Mn accumulation was almost the same at the two temperatures studied, and Co accumulation decreased at 15 °C. This may be related to protein content, which was reduced on Co exposure at 15 °C. These nitrogenous protein compounds may have been involved in Co binding, and therefore a reduction in them may reduce Co binding at higher temperatures (no temperature related trends in protein content were observed for Zn or Mn) (Munda & Hudnik 1988). In an earlier study, both *F. virsoides* and *U. prolifera* were found to accumulate more Zn (ZnSO<sub>4</sub>, Zn<sup>2+</sup>) at 20 °C, than 5 and 10 °C, and the effect was more pronounced for the brown seaweed *F. virsoides* (Munda 1979).

#### 1.7.4.3 Importance of pH

The uptake of two neutral Cd complexes (Cd(DDC)<sub>2</sub><sup>0</sup> and Cd(XANT)<sub>2</sub><sup>0</sup>, diethyldithiocarbamate (DDC) and ethylxanthate (XANT) are the ligands in question) and free Cd<sup>2+</sup> by freshwater microalgae was examined at pH 5.5 and 7. For the alga *C. reinhardtii*, uptake of the neutral complexes was greater than that of Cd<sup>2+</sup>, and there was a decrease in uptake of the neutral complexes at pH 5.5, compared to pH 7. The difference in uptake at lower pH was negligible for Cd<sup>2+</sup>. The uptake of Cd(DDC)<sub>2</sub><sup>0</sup> was compared in all three algae (*C. fuscaga*, *C. reinhardtii*, and *P. subcapitata*) and again the rate of uptake was higher than for the free Cd<sup>2+</sup> ion, and the reduction in uptake on lowering the pH was observed again. These complexes are lipophilic and the evidence supports partitioning between the aqueous medium and the cell membrane, followed by diffusion through the cell membrane into the cytoplasm. The origin of the pH effect could not be fully elucidated, but it was suggested that protonation of the phospholipid head groups in the cell membrane led to tighter packing of these groups, and hence lower membrane permeability. This suggests that the lowering of pH effects the protonation of the cell membrane and, therefore, the metal cation transport mechanism in the cell (Boullemant *et al.* 2009).

Increasing pH (7.3 to 8.6) was found to increase metal uptake for *Ulva lactuca*, *Porphyra umbilicalis*, and *Laminaria agardi* (Gutknecht 1963). The change in pH was quite small, and is commonly seen in estuarine environments where freshwater

inputs may lower the pH. Therefore pH, and salinity of the sampling site is important while discussing metal accumulation. This is the opposite of the trend seen in biosorption, where dead biomass is used to bind metal. Here it is commonly seen that the lowering of pH, to below 5.5, increases the uptake of metals. This is because of metal stability, with most metals being more soluble below this pH (Murphy, Hughes, *et al.* 2009; Murphy *et al.* 2008). This shows how uptake by live seaweed is dependent not only on surface groups, but also by internal, metabolically controlled, mechanisms.

### 1.7.5 Influence of Exudates

Increasing Cu concentration was found to increase ligand exudation in *F. vesiculosus* germlings grown in culture. Cu content of the germlings was not studied here so it was unknown if the exudates affected Cu uptake (Gledhill *et al.* 1999). The researchers Vasconcelos and Leal have carried out several studies on the influence of algal exudates on metal accumulation. The production of exudates by *Emiliana huxleyi* (coccolithophore, phytoplankton) in response to Cu was studied. Thiols (see Section 1.4.1) were found to be the major ligand produced (Leal *et al.* 1999). In a later paper, the seaweeds *Porphyra* and *Enteromorpha*, were found to produce cysteine or glutathione ligands on exposure to Pb, Cd and Cu (Vasconcelos & Leal 2001). In another study, *Phaeodactylum tricornutum* was grown in cultures containing exudates from itself, *Emiliana huxleyi*, *Porphyra* spp. or *Enteromorpha* spp., and the effect on metal uptake and growth was studied. Growth was promoted by the presence of exudates, and metal uptake was also affected. In some cases metal uptake was increased by the presence of exudates. This shows that the metal-ligand complexes may be more bioavailable than the free metal ion (Vasconcelos & Leal 2008). Increasing Cu concentration increased phenolic exudation in the brown seaweeds *F. vesiculosus* and *A. nodosum*. Purified phenolic extracts from the seaweed *A. nodosum* were analysed for and found to contain Cu, Zn, Cd and Cr, indicating their ability to sequester heavy metals (Connan & Stengel 2011b).

### 1.7.6 Toxicity of Metal Bioaccumulation: Oxidative Stress and Photosynthesis

Some researchers have begun to look at the toxicity of metal bioaccumulation on macroalgae; either through measuring the effect of bioaccumulation on oxidative stress levels (for example Gaete Olivares *et al.* 2016; Babu *et al.* 2014; Contreras *et al.* 2009), or photosynthesis (for example Costa *et al.* 2016; Connan & Stengel 2011a; Vajpayee *et al.* 1999).

Oxidative stress is measured by quantifying the levels of oxidative stress biomarkers in the seaweed. The effect of metal uptake on oxidative stress biomarkers appears to be species and metal specific. Researchers have measured antioxidant stress in the following ways: quantified the activity of antioxidant enzymes, for example, superoxide dismutases (SOD), catalase (CAT), glutathione peroxidase (GP), ascorbate peroxidase (AP), dehydroascorbate reductase (DHAR) and glutathione reductase (GR) and the lipoxygenase (LOX); or measured reactive oxygen species (ROS), thiobarbituric acid reactive substances (TBARS) and photosynthetic pigments. In general, when seaweed is exposed to metals, quantity of photosynthetic pigments, phenolics and glutathione decreases (Sáez *et al.* 2015; Schiavon *et al.* 2012), ROS increases (Sáez *et al.* 2015; Ramesh *et al.* 2015; Schiavon *et al.* 2012; Contreras *et al.* 2009), and enzyme activity increases (Sáez *et al.* 2015; Babu *et al.* 2014; Schiavon *et al.* 2012; Contreras *et al.* 2009).

In general, authors have found impairment in photosynthetic activity with metal exposure, again this appears to be metal and species specific.

Bismuth (Bi(II)) caused a decline in photosynthetic capacity of the red algae *Chondrus crispus*, as measured by chlorophyll fluorescence. This only occurred at the higher levels studied, and no effect was seen at any of the studied concentrations for *U. lactuca* or *F. vesiculosus* (Kearns & Turner 2016). Quantification of photosynthetic pigments is also used to measure the likely effect of bioaccumulation on photosynthesis (Sáez *et al.* 2015). Schmidt found a reduction in chlorophyll fluorescence, but not in photosynthesis, which the author attributed to the red algae's tolerance mechanisms (Schmidt *et al.* 2015).

A review by Moenne *et al.* (2016) discusses the effects of bioaccumulation of Cu in particular on red and green algae.

### 1.7.7 Behaviour of Chromium in Solution

Vignati *et al* (2010) studied the toxicity of Cr(III) versus Cr(VI) towards freshwater algae (Vignati *et al.* 2010). This paper is included because it is the only study of Cr(III) behaviour in solution, which will be discussed in more detail later in this thesis. Most authors have studied hexavalent chromium, which is fully soluble in fresh and seawater, overcoming the problem of the low solubility of Cr(III) in these conditions (Baumann *et al.* 2009; Vala *et al.* 2004; Amoroso *et al.* 2001). It was found that the initial concentration of Cr(III) was reduced by 60-90% under the conditions studied (standard ISO medium and modified ISO medium prepared in ultrafiltered natural lake water). After taking account of the poor solubility, Cr(III) was found to be more toxic to the green microalgae studied than Cr(VI). Wang and Dei (1999) found that the accumulation of the anionic metals Se and Cr was much slower than Cd and Zn in the seaweeds. Although not studied in this paper, the authors suggest that uptake of these anionic metals takes place through phosphate and sulphate channels, due to the similarities of these to the metals in structure and charge (Wang & Dei 1999).

**Table 1.6: A summary of relevant bioaccumulation studies.**

Metals	Seaweed	Summary of Findings
<b>Reference</b>		
CdCl <sub>2</sub> (Cd <sup>2+</sup> )	<i>S. cymosum</i>	Apical portions exposed to 0.1, 0.2, 0.4, 0.8 mg/L for 14 days. Growth reduced, no effect on photosynthesis, increased chlorophyll and carotenoids, phenolics and flavanoids lowered, no significant differences in ultrastructure (SEM), TEM showed thickening of cell wall, disorganization of fibrils, increase in number of vacuole vesicles and physodes, which appeared to be in the process of fusion with cell wall.
Costa, Simioni, <i>et al.</i> 2016		
CuCl <sub>2</sub> (Cu <sup>2+</sup> ), PbCl <sub>2</sub> (Pb <sup>2+</sup> )	<i>S. cymosum</i>	Apical portions exposed to metals (10, 25, 50 μM separately and 10+10, 25+25, and 50+50 μM combined) for 7 days. Cu was accumulated more than Pb or Pb+Cu mixtures. Cu and Cu+Pb exposure reduced growth rates, Pb on its own did not. Cu and Cu+Pb inhibited photosynthesis as shown in ETR curves, Pb enhanced. Increased pigments, phenolics, radical scavenging ability, physodes on metal uptake compared to controls. SEM showed Cu at 10 and 25 μM increased roughness, no change at 50 μM. Pb and Cu+Pb decreased roughness. Suggested change in surface ultrastructure to facilitate uptake.
Costa <i>et al.</i> 2016		
Bi(II)	<i>U. lactuca</i> , <i>F. vesiculosus</i> , <i>Chondrus crispus</i>	<i>F. vesiculosus</i> and <i>C. crispus</i> tips, <i>U. lactuca</i> discs exposed to 0, 5, 10, 20, 40 and 50 ppb Bi. Literature review shows dominant species to be Bi(OH) <sub>3</sub> <sup>0</sup> , although Bi(O) <sup>+</sup> and Bi(OH) <sup>2+</sup> may be present. Chlorophyll fluorescence measured. Recovery of metal only approx 70%-possible loss on vessel walls. <i>C. crispus</i> at high conc had lowered photosynthetic capacity, others unaffected. Uptake <i>F. vesiculosus</i> > <i>C. crispus</i> > <i>U. lactuca</i> . Approx 10% metal internalised for <i>F. vesiculosus</i> , 30 % for <i>U. lactuca</i> and <i>C. crispus</i> .
Kearns & Turner 2016		
Cd(NO <sub>3</sub> ) <sub>2</sub> (Cd <sup>2+</sup> ), Zn(NO <sub>3</sub> ) <sub>2</sub> (Zn <sup>2+</sup> ), Pb(NO <sub>3</sub> ) <sub>2</sub> (Pb <sup>2+</sup> ), Ni(NO <sub>3</sub> ) <sub>2</sub> (Ni <sup>2+</sup> ), Cu(NO <sub>3</sub> ) <sub>2</sub> (Cu <sup>2+</sup> )	<i>U. lactuca</i> , <i>Agardhiella subulata</i>	Both species exposed to 10, 100, and 1000 μg/L of five metal mixtures for 48 h. <i>U. lactuca</i> was exposed to 10 and 100 μg/L metal individually for 48 h. When exposed to 10 μg/L a greater quantity of metal was accumulated than after exposure to 100 μg/L of individual metal. Author suggests this is due to down regulation of metal transport mechanisms at the higher concentrations. Concentrations in seaweeds exposed to metal individually was greater than those exposed as a mixture (even though the overall metal conc would be higher in the mixture). Suggests competition for binding sites as a cause. Uptake pattern similar for both seaweeds: Cu, Zn >> Pb, Ni, Cd. Decreased photosynthesis @ 48 h with increasing metal conc.
Jarvis & Bielmyer-Fraser 2015		
AgNO <sub>3</sub> (Ag <sup>+</sup> )	<i>F. ceranoides</i>	Increasing Ag and decreasing salinity inhibited growth and increased ROS and lipid peroxidation. Ag speciation was modelled, responses were associated with the greater bioavailability of toxic species of Ag (Ag <sup>+</sup> and AgCl <sup>0</sup> ) at reduced salinities (even though AgCl <sup>2-</sup> , AgCl <sub>3</sub> <sup>2-</sup> , AgCl <sub>4</sub> <sup>3-</sup> ) are the most abundant forms (>96%) according to modelling for all salinities).
Ramesh <i>et al.</i> 2015		

CuSO <sub>4</sub> ·5H <sub>2</sub> O (Cu <sup>2+</sup> )	<i>Ectocarpus siliculosus</i>	10 day exposure, strains from polluted and unpolluted sites studied. Plants from unpolluted areas had higher concentrations of H <sub>2</sub> O <sub>2</sub> , lower contents of photosynthetic pigments (chl <sub>a</sub> and chl <sub>c</sub> ), ascorbate, glutathione, and phenolic compounds, and less activity of CAT and SOD at low Cu exposure levels than the strains from polluted sites in UK and Chile. Author suggests seaweed from polluted sites is acclimatised to dealing with metal toxicity.
Sáez <i>et al.</i> 2015		
CdCl <sub>2</sub> (Cd <sup>2+</sup> )	<i>Pterocladia capillacea</i>	Apical portions exposed to Cd (0.17-0.70 ppm) for 7 days at a range of salinities (25, 35 and 45 psu). Reduction in floridean starch, chlorophyll fluorescence, protein on ↑ salinity and Cd, however no decrease in photosynthesis (which has been noted in other literature), authors attributed this to tolerance mechanisms. Concluded that toxic effects of Cd are increased by increasing salinity.
Schmidt <i>et al.</i> 2015		
CuCl <sub>2</sub> (Cu <sup>2+</sup> ), CdCl <sub>2</sub> (Cd <sup>2+</sup> )	<i>Acanthophora spicifera</i> , <i>Chaetomorpha antennina</i> , <i>U. reticulata</i>	Aim of the study was to determine antioxidant response and DNA damage caused by metal bioaccumulation. Metal was exposed at concentrations of 0.25, 0.50, 0.75, and 1.00 mg/L. Cu uptake significantly greater than Cd. Cu and Cd caused DNA damage (comet) and antioxidant response (increased antioxidant enzymes: SOD, GPX, CAT), effect more pronounced for Cu under long term stress, more pronounced for Cd under short term stress.
Babu <i>et al.</i> 2014		
CuCl <sub>2</sub> (Cu <sup>2+</sup> ), PbCl <sub>2</sub> (Pb <sup>2+</sup> )	<i>Gracilaria domingensis</i>	Whole plant sections exposed to metal at 5 and 10 ppm for 7 days. Growth reduced, could be observed visually on Cu exposure. Cu reduced floridean starch. TEM showed cell damage on metal uptake-chloroplasts disrupted, organelles destroyed, smaller cytoplasmic volume. Photosynthetic pigments decreased. Cu exposure reduced trans-β-carotene and lutein. Protein reduction on Cu but not Pb exposure. NADH dehydrogenase activity reduction on Cu and Pb exposure.
Gouveia <i>et al.</i> 2013		
Na <sub>2</sub> SeO <sub>4</sub>	<i>Ulva sp.</i>	Exposed to 0-100 μM for 10 days. Increase in ROS (H <sub>2</sub> O <sub>2</sub> ), SOD, CAT activity and phenolics. No ultrastructural changes observed by SEM.
Schiavon <i>et al.</i> 2012		
Cu Cd Pb	<i>Fucus ceranoides</i>	Uptake studied at several salinities-greater uptake seen at lower salinity. Exposed to 20 ppb metal for 120 h @15 °C. First order Cu, and pseudo first order for Cd and Pb. Species present were modelled, at low salinities more free ions were present, agreed with observation regarding greater uptake at lower salinities, as more free ions were available to complex.
Varma <i>et al.</i> 2013		
CuSO <sub>4</sub> ·5H <sub>2</sub> O (Cu <sup>2+</sup> )	<i>A. nodosum</i> , <i>F. vesiculosus</i>	Growth rates of <i>A. nodosum</i> decreased significantly with increasing Cu concentration and reducing salinity. Decreasing salinity reduced growth in <i>F. vesiculosus</i> , while Cu did not have an effect on growth. At low salinity Cu uptake decreased in <i>A. nodosum</i> , but increased on <i>F. vesiculosus</i> , suggesting a species specific regulation/uptake mechanism.
Connan & Stengel 2011a		
CuSO <sub>4</sub> ·5H <sub>2</sub> O (Cu <sup>2+</sup> ) plus phlorotannin bound Zn, Cd, Cr	<i>A. nodosum</i> , <i>F. vesiculosus</i>	Study of seaweed phlorotannin content and Cu binding, plus Cu binding of a purified phlorotannin. In both seaweeds studied, reducing salinity and increasing Cu decreased phlorotannin content, resulted in more cell wall bound phlorotannins, and increased phlorotannin exudation. A phlorotannin extract was found to contain Cu, Cd, Zn and Cr, and exposure of the extract to Cu caused a decrease in Cd and Zn, but not Cr content of the phlorotannin extract (extract was obtained from <i>A. nodosum</i> ).
Connan & Stengel 2011b		

Cr(NO <sub>3</sub> ) <sub>3</sub> (Cr <sup>3+</sup> ), K <sub>2</sub> Cr <sub>2</sub> O <sub>7</sub> (Cr <sub>2</sub> O <sub>7</sub> <sup>2-</sup> ), Na <sub>2</sub> CrO <sub>4</sub> (CrO <sub>4</sub> <sup>2-</sup> )	<i>Pseudokirchneriella subcapitata</i> , <i>Chlorella kessleri</i> (freshwater microalgae)	Discusses the precipitation of Cr(III) complexes in solution. Taking into account soluble Cr only (rather than total which included insoluble species) Cr(III) was found to be more toxic than Cr(VI).
Vignati <i>et al.</i> 2010		
CuCl <sub>2</sub> (Cu <sup>2+</sup> ), Pb(ClO <sub>4</sub> ) <sub>2</sub> (Pb <sup>2+</sup> ), ZnCl <sub>2</sub> (Zn <sup>2+</sup> ), K <sub>2</sub> CrO <sub>4</sub> , (CrO <sub>4</sub> <sup>2-</sup> ), CdCl <sub>2</sub> (Cd <sup>2+</sup> )	<i>A. nodosum</i> , <i>F. vesiculosus</i> ; <i>U. intestinalis</i> , <i>Cladophora rupestris</i> , <i>Chondrus crispus</i> , <i>Palmaria palmata</i> , <i>Polysiphonia lanosa</i>	Metal accumulation was generally found to vary between species with uptake occurring as follows: Cu > Pb > Zn > Cr > Cd. Species variation generally occurred in the following order, <i>U. intestinalis</i> > <i>Palmaria palmata</i> > <i>Chondrus crispus</i> > <i>Polysiphonia lanosa</i> > <i>A. nodosum</i> > <i>F. vesiculosus</i> > <i>Cladophora rupestris</i> . The relationship between metal accumulation and fluorescence, a measure of photosynthetic activity, was found to be algal species and metal-specific
Baumann <i>et al.</i> 2009		
Cd <sup>2+</sup> , Cd(L) <sub>2</sub> <sup>0</sup>	<i>Chlamydomonas reinhardtii</i> , <i>Chlorella fusca</i> , <i>Pseudokirchneriella subcapitata</i>	Uptake of lipophilic complexes of Cd (Cd(L) <sub>2</sub> <sup>0</sup> ) in unicellular freshwater algae was found to be dependent on pH, with higher uptakes seen at pH 7 than pH 5.5. It was suggested that at lower pH a greater proportion of the phospholipid head groups will be protonated, have a reduced charge, allow tighter packing of the phospholipids, leading to lower membrane fluidity and a lower metal uptake. This study emphasises that metal uptake is not only affected by the chemistry of the metal in question, but also by changes which may occur in the algae itself in different conditions such as pH.
Boullemant <i>et al.</i> 2009		
CdSO <sub>4</sub> (Cd <sup>2+</sup> )	<i>F. vesiculosus</i>	Spatial differences in Cd uptake were revealed. Seaweed from the Bothnian sea was more sensitive (photosynthesis was effected) to Cd exposure, and accumulated more metal. Results relate this to a higher number of binding sites revealed by titration, and lower salinity at the site.
Brinza <i>et al.</i> 2009		
Cd, Mg, Mn, Zn	<i>Cystoseira abies-marina</i>	A transplant experiment from a low metal to high metal site was used to study uptake in <i>Cystoseira abies-marina</i> . Increasing levels of Cd, Mg, and Mn were found in the seaweed and did not reach a maximum over the eight week study. Zn, on the other hand, remained the same throughout the study period.
Wallenstein <i>et al.</i> 2009		
CuCl <sub>2</sub> (Cu <sup>2+</sup> )	<i>Lessonia nigrescens</i> , <i>Scytosiphon lomentaria</i>	Exposed to metal @ 20, 40 and 100 mg/L for 96h. Determined ROS and enzyme activity: CAT, GP, AP, DHAR, GR and LOX. Morphological changes observed in <i>L. nigrescens</i> (retraction of the protoplast in cortical cells, blurred thylakoidal membranes) but not <i>S. lomentaria</i> . Both produced H <sub>2</sub> O <sub>2</sub> , only <i>L. Nigrescens</i> produced superoxide anions. <i>S. lomentaria</i> had a greater base enzyme activity, this increased in both seaweeds on metal exposure. Author suggested that <i>S. lomentaria</i> has better tolerance to metals, explaining why it found in polluted areas.
Contreras <i>et al.</i> 2009		
Cr <sub>2</sub> (SO <sub>4</sub> ) <sub>3</sub> (Cr <sup>3+</sup> ), Cr(VI)	<i>Phragmites australis</i> (Reed)	Real tannery wastewater used for experiments, nearly all Cr(III) with only trace amounts of Cr(VI). Cr(III) was supplemented to wastewater for phytoremediation trial. The wastewater inhibited germination. Rhizomes accumulated most Cr, although signs of toxicity were seen at high concentrations.
Calheiros <i>et al.</i> 2008		
Pb <sup>2+</sup>	<i>Chlorella</i> , <i>Chlamydomonas</i> ,	Microalgae. Found a reduction in Pb uptake by live microalgal cultures corresponding to the increasing toxic effect of the metal
Kumar & Goyal 2008	<i>Lyngbya sp.</i> (cyanobacteria)	



Cu, Ni, Cd, Fe, Zn, Mn	<i>Phaeodactylum tricornutum</i> and exudates from <i>Emiliania huxleyi</i> (coccolithophore), <i>Porphyra spp.</i> , <i>Enteromorpha spp</i>	Exudates were found to bind to Cu, but also promoted algal ( <i>Phaeodactylum tricornutum</i> , a diatom) uptake of Cu in the diatom. Effects were also seen for Ni, Cd, Fe, Zn and Mn. Production of exudates by <i>Phaeodactylum tricornutum</i> was also influenced by the presence of other algal exudates.
Vasconcelos & Leal 2008		
Cd(NO <sub>3</sub> ) <sub>2</sub> , (Cd <sup>2+</sup> ), Zn(NO <sub>3</sub> ) <sub>2</sub> , (Zn <sup>2+</sup> )	<i>Fucus spp. Solieria chordalis</i> <i>Rhizoclonium tortuosum, Ulva spp., Codium fragile</i>	The concentration of phytochelatins has been shown to be correlated to pollution at the site, and the amount of metal in the seaweed. In contrast to the brown and red seaweeds, the green seaweeds studied, <i>U. intestinalis</i> , <i>U. lactuca</i> and <i>Codium fragile</i> , did not produce detectable amount of phytochelatins even when exposed to high levels of Cd. An exception was <i>Rhizoclonium tortuosum</i> collected from a contaminated site
Pawlik- Skowrońska <i>et al.</i> 2007		
Cu, Zn, Cd, Pb	<i>Elodea canadensis</i> , <i>Potamogeton natans</i> (submersed plants)	Metal uptake (Cu, Zn, Cd) by submersed plants was found to increase with increasing temperature and decreasing salinity, with the exception of Pb which increased with increasing salinity
Fritioff <i>et al.</i> 2005		
K <sub>2</sub> Cr <sub>2</sub> O <sub>7</sub> (Cr <sub>2</sub> O <sub>7</sub> <sup>2-</sup> )	Strains of fungi associated with <i>Euchema Spp</i>	Marine seaweed associated bacteria, <i>Aspergillus flavus</i> and <i>Aspergillus niger</i> , were found to grow normally in cultures up to 100 ppm Cr(VI), with only non significant decreases in biomass found. This study showed the potential for epiphytic and biofilm material to accumulate metals. Uptake by both isolates was ~25% of Cr supplied.
Vala <i>et al.</i> 2004		
Cu, Cd	<i>Gracilaria lemaniformis</i>	Exposure to Cd and Cu lowered the growth rate, pigment content, and rate of photosynthesis in <i>Gracilaria lemaneiformis</i> . Cu was more toxic. This may be because Cd is non-essential and therefore excluded from the cells, where as the plants have a requirement for Cu. Actual uptake not shown, just results of exposure to metal.
Xia <i>et al.</i> 2004		
CdCl <sub>2</sub> (Cd <sup>2+</sup> ), ZnCl <sub>2</sub> (Zn <sup>2+</sup> ), Na <sub>2</sub> Cr <sub>2</sub> O <sub>7</sub> (Cr <sub>2</sub> O <sub>7</sub> <sup>2-</sup> )	<i>Enteromorpha crinita</i>	Ammonium and nitrate treatment which may increase the amount of amino, carboxyl and carbonyl groups either directly or through the enhancement of photosynthesis, had a significant effect on Cd and Zn uptake, but no significant effect on Cr uptake. Linear uptake of Cr was found over the study period 48 h. Also found that EDTA treatment removed little of the bound Cr (<3%), i.e. binding was mostly intracellular.
Chan <i>et al.</i> 2003		
Cd or Cd combined with Zn	<i>Padina gymnospora</i>	EDXA and ESI spectroscopy showed co-location of S with Cd and Zn, indicating the importance of sulphated polysaccharides in metal uptake. They were seen as crystalline deposits in the well walls.
De Andrade 2002		
Cd(NO <sub>3</sub> ) <sub>2</sub> , Cd <sup>2+</sup>	<i>Audouinella saviana</i>	Structural changes in the red algae on exposure to Cd were analysed by transmission electron microscopy. Ribosomes and Golgi bodies, which were not present to a significant degree in control plants, suggested enhanced protein and carbohydrate. This may be part of the algal defence mechanism. Cell walls which were grooved in control samples became smooth and thick. Electron opaque deposits were formed on exposure to Cd. They were found in the cytoplasm of the cell and were then transported to the vacuoles.
Talarico 2002		

Cu, Pb, Cd, Zn, Fe, Mn, Ni, Co	<i>Emiliania huxleyi</i> (coccolithophore) and exudates from <i>Phaeodactylum</i> <i>tricornutum</i> , <i>Porphyra spp.</i> , <i>Ulva</i> <i>spp</i>	The effect of exudates of all the named species on growth and metal uptake of <i>Emiliania huxleyi</i> was studied. It was found that its growth was improved by glutathione like compounds produced by <i>Ulva</i> , and inhibited by cysteine like compounds produced by <i>Phaeodactylum tricornutum</i> . The exudates also influenced metal uptake with ligands complexing metals, as well as <i>Emiliania huxleyi</i> .
Vasconcelos <i>et al.</i> 2002		
$\text{Na}_2\text{CrO}_4$ ( $\text{CrO}_4^{2-}$ )	<i>Streptomyces spp.</i> (bacteria)	Found that the vast majority of Cr was bound to the cell wall, authors suggest mechanism was reduction to Cr(III), although no speciation was studied. Only small amounts were found in the bacterial exopolymer, membrane and in the cell.
Amoroso <i>et al.</i> 2001		
Cr(III), Cr(VI)	Bacteria, algae, fungi, plants	Review on the interactions of chromium with plants and microorganisms. Cr(VI) is transported across the cell membrane in eukaryotes such as algae and plants; in contrast Cr(III) can form water insoluble compounds and therefore is not available to cells. In yeasts and bacteria, active transport of Cr(VI) by sulphate and phosphate channels has been shown. Studies in plants have shown that Cr(VI) is dependent on metabolism, whereas Cr(III) is not. To the authors knowledge, none of these have been shown in algae to date
Cervantes <i>et al.</i> 2001		
Cd, Zn, $\text{Na}_2\text{CrO}_4$ ( $\text{CrO}_4^{2-}$ ), $\text{Na}_2(\text{SeO}_3)$ ( $\text{SeO}_3^{2-}$ )	<i>U. fasciata</i>	The influence of nitrate, ammonium, and phosphate on the accumulation of Cd, Cr, Zn and Se over 8 h was studied. Increasing nitrate increased Cd uptake but had no influence on Cr, Zn or Se. Cd, Cr and Zn accumulation was not affected by ammonium. Increasing phosphate inhibited Se accumulation (competitive inhibition suggested). Cr uptake increased with increasing phosphate.
W.-Y. Lee & W.-X. Wang 2001		
Cu, Pb, Cd, Hg	<i>Porphyra spp.</i> , <i>Enteromorpha spp</i>	Titration with metal revealed that metal binding capacity did not vary significantly by season for Pb, Cd or Hg, but did for Cu (high in August, low in January). Exudates of cysteine and glutathione with a high Cu binding capacity were promoted by exposure to Cu, cysteine was promoted by Pb, and glutathione by Cd. Seasonal difference were found, with highs in uptake in January for Cu, Cd, and Pb for <i>Ulva</i> and <i>Porphyra</i> . Uptake of Pb did not appear to be seasonally dependent
Vasconcelos & Leal 2001		
$\text{Na}_2\text{CrO}_4$ ( $\text{CrO}_4^{2-}$ ), $\text{Na}_2(\text{SeO}_3)$ ( $\text{SeO}_3^{2-}$ )	<i>Thalassiosira</i> <i>pseudonana</i> , <i>Skeletonema</i> <i>costatum</i> , (Diatoms) and <i>Chlorella</i> <i>autotrophica</i>	Studied the influence of phosphate and silicate on Cr(VI) and Se(IV) accumulation in two diatoms and a unicellular algae. There was no relationship between Cr uptake and phosphate, and a decreasing relationship for Si for <i>Chlorella</i> . In general, decreasing Se uptake was related to increasing phosphate concentration. The authors therefore concluded that accumulation may take the same pathways as macronutrients. Note that the results were species and metal specific.
W.-X. Wang & Dei 2001		
$\text{CuSO}_4 \cdot 2\text{H}_2\text{O}$ ( $\text{Cu}^{2+}$ ), $\text{FeCl}_2$ , ( $\text{Fe}^{2+}$ )	<i>A. nodosum</i>	Uptake of Cu and Fe in the brown seaweed, <i>A. nodosum</i> , was studied with no statistically significant differences being found relating to thallus age. Fe was located mostly in diatoms on the surface, whereas Cu was accumulated in cells near the thallus surface. This study revealed that epidermis shedding may occur, leading to the loss of metals accumulated by the seaweed, or surface associated diatoms. This study highlighted the importance of shedding, and epiphytism in metal uptake.
Stengel & Dring 2000		
$\text{CuCl}_2$ ( $\text{Cu}^{2+}$ )	<i>A. nodosum</i>	It was found that the phlorotannin content of <i>A. nodosum</i> was not affected by Cu exposure, and although the seaweed accumulated Cu in its tissue, extracted phlorotannins were not bound to Cu to any large degree. Note that an earlier study had previously found that divalent ions chelated to a phlorotannin extract in acidic solution (Ragan <i>et al.</i> 1979).
Toth & Pavia 2000		

$K_2Cr_2O_7$ ( $Cr_2O_7^{2-}$ )	<i>Nymphaea alba</i> L. (Aquatic plant.)	Metal was accumulated in plant tissues, with the maximum being found in the roots. High amounts of accumulation caused a decrease in chlorophyll, nitrate assimilation and protein concentration.
Vajpayee <i>et al.</i> 2000		
$Cu^{2+}$	<i>F. vesiculosus</i>	<i>F. vesiculosus</i> germlings were found to release Cu complexing ligands, the concentration of which increased with increasing Cu concentration up to a maximum level. Growth rate was also reduced as time passed, and with increasing Cu concentration. It was not known if the ligands bound metal in solution, or internally detoxified Cu and were then released into solution.
Gledhill <i>et al.</i> 1999		
$CuCl_2$ ( $Cu^{2+}$ ), $K_2Cr_2O_7$ ( $Cr_2O_7^{2-}$ ), $NiCl_2$ ( $Ni^{2+}$ ), $ZnSO_4$ ( $Zn^{2+}$ )	<i>Chlorella vulgaris</i>	Uptake of Cu, Cr, Ni and Zn was studied in the unicellular algae <i>Chlorella vulgaris</i> . Intracellular uptake was determined by EDTA washing of the pellet, and Cr was found to have the greatest uptake. The majority of uptake occurred in the first 6-8 hours of treatment. There was a sharp rise in proline content after 4-8 hours, which then decreased sharply over the next few hours and slowly until the end of the experiment. At high concentrations proline production appeared to be inhibited. Cr and Cu caused lipid peroxidation, and loss of $K^+$ through the cell membrane. This study showed the role of proline in metal uptake by <i>Chlorella</i> .
Mehta & Gaur 1999		
Cd, Zn, Cr ( $Na_2CrO_4$ , $CrO_4^{2-}$ ), Se ( $Na_2(SeO_3)$ , $SeO_3^{2-}$ )	<i>U. lactuca</i> , <i>Gracilaria</i> <i>blodgettii</i>	This is the first study of Cr uptake by macroalgae. Uptake of Cr(VI) by <i>U. lactuca</i> , and <i>Gracilaria blodgettii</i> was found to be almost identical at around 0.15 $\mu\text{g/g}$ over 2 days when exposed to 0.5 $\mu\text{g/L}$ Cr. This increased to 1.8 and 4.8 $\mu\text{g/g}$ when exposed to 10 $\mu\text{g/L}$ , for <i>Ulva</i> and <i>Gracilaria</i> , respectively. They found that uptake was proportional to Cr content of the dissolved phase. Cr or Se uptake was unaffected by dark, whereas a decline was seen in Cd and Zn uptake. A linear pattern was seen over two days at low concentrations, but two phase uptake was seen at higher concentrations. This suggests an initial adsorption onto the cell walls, followed by a metabolically controlled second stage where the metal is taken into the cell. The authors suggested uptake of the anionic metals (Cr, Se) through the anionic channels analogous to phosphate and sulphate. They also found that Cr uptake was dependant on salinity for <i>Ulva</i> (decreasing uptake with decreasing salinity), but not for <i>Gracilaria</i> .
W.-X. Wang & Dei 1999		
$K_2Cr_2O_7$ ( $Cr_2O_7^{2-}$ )	<i>Eichhornia crassipes</i> (wetland plant)	Study of chromium binding by a live plant. When the plant was exposed to Cr(VI) it was shown that it was detoxified to the less toxic form, Cr(III). X-ray Absorption Near-Edge Structure (XANES) was used to determine the oxidation state of chromium present in the sample.
Mel Lytle <i>et al.</i> 1998		
$K_2Cr_2O_7$ ( $Cr_2O_7^{2-}$ ), $CrCl_3$ ( $Cr^{3+}$ )	Vegetable crops	In general Cr(VI) was found to be to be accumulated more than Cr(III) in most species. Most was found in the root, with little being transported to the shoots. In all cases Cr(VI) was found to be reduced to Cr(III) in the plants. The highest accumulation of both Cr(III) and (VI) occurred in the sulphur loving Brassica species. The similarity between sulphate and chromate ions partly explains the high uptake of Cr(VI), but not Cr(III), and points to the high ability of these species to accumulate metals in general
Zayed <i>et al.</i> 1998		

ZnSO <sub>4</sub> (Zn <sup>2+</sup> )	<i>U. lactuca</i> , <i>Enteromorpha flexuosa</i> , <i>Padina gymnospora</i> , <i>S. filipendula</i> , <i>Hypnea musciformis</i> , <i>Spyridia filamentosa</i>	Low level exposure to Zn was found to cause toxicity (decrease in growth rate) in seaweeds, with brown species being the most resistant. All species died at a concentration of 5000 µg/L, and 20µg/L was sufficient to cause growth inhibition. The brown seaweed <i>Padina gymnospora</i> accumulated the highest levels of Zn, and the red seaweed <i>Hypnea musciformis</i> the least. Therefore brown seaweeds were suggested as being better for biomonitoring of metals.
Amado Filho et al. 1997		
Cd	<i>Gracilaria tenuistipitata</i> , <i>U. pertusa</i> , <i>U. intestinalis</i> , <i>S. thunbergii</i> , <i>Gracilaria asiatica</i>	Found that a brown <i>Sargassum</i> accumulated more Cd than <i>Gracilaria</i> and <i>Ulva</i> spp.
Hu et al. 1996		
Cu, Zn, Mn, Cd	<i>Chaetomorpha linum</i> , <i>Padina tetrastomatica</i> , <i>S. baccularia</i> , <i>S. siliquosum</i> , <i>Gracilaria changii</i> , <i>Gracilaria edulis</i> , <i>Gracilaria salicornia</i>	Several different patterns of uptake emerged over a 24 h period for the seaweeds studied. <i>Pattern (1) An initial rapid uptake, followed by a gradual accumulation; (2) A continuous gradual accumulation pattern; (3) An initial rapid uptake, followed by a release-uptake pattern before a steady state concentration or gradual accumulation; (4) An alternating uptake-release pattern; (5) An initial net accumulative pattern, followed by a continuous regulatory discharge.</i> Decreasing salinity was found to increase metal uptake in a two hour study. Cd toxicity was found, measured by dry weight decrease and photosynthesis inhibition.
Murugadas 1995		
Cr(III), Cr(VI)	<i>Bacteria</i>	Reviewed the literature on bacterial reduction of Cr(VI) to Cr(III) and discussion of possible mechanisms. Possible electron donors for reduction were discussed; mainly polysaccharides and amino acids. Sulphydryl groups were also of importance. This is interesting, as many algae contain these groups in phytochelatin. Growth was not required for reduction to occur. Phenolic compounds and other metals were found to interfere with reduction. The presence of other electron accepting groups like sulphate and nitrate does not appear to affect reduction, but NaNO <sub>3</sub> and ZnSO <sub>4</sub> were found to reduce reduction.
Y.-T. Wang & Shen 1995		
Cu, Cd, Mn, Ni, Pb, Zn	<i>Neorhodomela larix</i> , <i>S. pallidum</i>	Study of uptake over 48 h was carried out. The red seaweed took up more of every metal bar Cd. They found that all the metals, except Ni were more strongly accumulated by the polysaccharide fraction of the cells. In the red seaweed the water soluble fraction was also found to contain significant amounts of metal.
Tropin & Zolotukhina 1994		
Cu, Cd, Ni, Zn, Mn, Pb	<i>Gracilaria tikvahiae</i> , <i>Gelidium pusillum</i> , <i>Agardhiella subulata</i> , <i>Chondrus crispus</i>	<i>Gracilaria tikvahiae</i> , accumulated the greatest amount of the metals studied. The accumulation of Pb was greater in living seaweed than in freeze dried seaweed. Except for <i>Agardhiella subulata</i> , freeze dried seaweed accumulated more Cu, Ni, and Zn. There was no difference in Cd uptake between living and freeze dried seaweed. There was no significant accumulation of Mn for any freeze dried or living seaweed at the concentration tested (0.5 mg/L) tested.
Burdin & Bird 1994		
Zn	<i>Padina gymnospora</i>	The absorption of Zn depended on exposure time and increased with increasing Zn concentration in the medium. It was found that insignificant amounts of Zn could be desorbed from <i>Padina</i> in experiments suggesting a high affinity of this metal towards the binding sites
Karez et al. 1994		

Cd, Cu	<i>Cystoseira barbata</i>	Following 24 days' exposure of <i>Cystoseira barbata</i> to Cd or Cu, Cd-binding proteins (Cd-BP) (15,000 Da and 9,000 Da) and Cu-binding proteins (Cu-BP) (9,500 Da) were isolated. This study suggests that induction of metal-binding proteins (M-BP) is regulated by the presence of metal. For high Cu concentrations, Cu is spread among all the protein fractions inhibiting the vital physiological processes.
Berail <i>et al.</i> 1992		
ZnSO <sub>4</sub> , (Zn <sup>2+</sup> ), MnCl <sub>2</sub> , (Mn <sup>2+</sup> ), CoCl <sub>2</sub> , (Co <sup>2+</sup> )	<i>F. vesiculosus</i>	The effect of temperature and salinity on the uptake of Zn, Mn and Co by <i>F. vesiculosus</i> was studied. In general decreasing salinity encouraged metal uptake. Interestingly, metal uptake at 5 and 15 °C were similar, or and in one case (Co) was even greater at 5 °C. Protein content was measured, but showed no definite trends.
Munda & Hudnik 1988		
Zn, Co, Mn	<i>Scytosiphon lomentaria</i> , <i>U. intestinalis</i>	Decreased salinity enhanced metal uptake. Metal uptake was highest for Zn, followed by Co and then Mn.
Munda 1984		
Fe, Mn, Zn, Cd, Rb	<i>U. fasciata</i>	Light level exerted a greater overall effect than nutrient level (nitrate/nitrogen) on metal uptake by <i>Ulva</i> grown in outdoor culture. Concentrations of cadmium and rubidium in the algae decreased as the specific growth rate increased, but the concentration of manganese increased as specific growth rate increased. Showed the importance of considering growth characteristics in biomonitoring studies.
Rice & Lapointe 1981		
Zn	<i>F. virsoides</i> , <i>U. prolifera</i>	One of the few to study the influence of temperature on bioaccumulation in seaweed. In both species metal uptake increases at higher temperature (20°C vs 5 and 10°C).
Munda 1979		
Cu	Diatoms	Reduction of growth rates was observed by the addition of 10, 25 and 400 µg/l of Cu ions, respectively for the three species investigated. At the higher levels of Cu addition (400 and 700 MS/l) cells of <i>P. tricornutum</i> in dialysis culture increased their Cu content to more than 200 times over those of the controls, the ratio of Cu to chlorophyll in the cells increasing 150 times.
Jensen <i>et al.</i> 1976		
Zn	Diatoms	50, 250 and 25,000 µg/l of Zn reduced the growth rate of the diatoms. One species showed a significant increase in Zn uptake at Zn levels which did not seem to influence the growth and development of the alga.
Jensen <i>et al.</i> 1974		
Zn, Cd, Cu, Mn	<i>L. digitata</i>	Rapidly growing <i>Laminaria</i> was found to take up more Zn from solution than slow growing weed. At very high concentration growth was inhibited (100 µg/L). Two processes were suggested, metabolically and non-metabolically controlled. At high concentrations of exposure, uptake was so high the authors concluded that non-metabolically controlled uptake must be dominant. Cu, Mn and Cd (20- 500 µg/L) slowed or stopped Zn uptake. Cu (200 µg/L) appeared to kill the seaweed.
Bryan 1969		
B, Mn, Zn, Sr, Rb, Li, I, Fe, Co, Br	<i>Porphyra tenera</i> (free living phase)	Requirements for B, Mn, Zn, Sr, Rb, Li, and I were demonstrated; the effective concentration range was narrow. Fe, Co, and Br seemed to be adequately supplied as impurities of the macro-nutrients.
Iwasaki 1967		
Zn	<i>Ulva</i> , <i>Laminaria</i> , <i>Porphyra</i>	Zn uptake was higher at higher pH (8.6 vs. 7.3) and higher in light than in dark. The authors conclude that due to the effect of pH, and the fact that uptake was found for dead cells, that uptake was non-metabolically controlled.
Gutknecht 1963		

Y, Sr	<i>F. serratus</i> , <i>Palmaria palmata</i> , <i>U. lactuca</i> , <i>Chodrus</i> <i>crispus</i> , <i>Mastocarpus</i> <i>stellatus</i> , <i>L. digitata</i>	First detailed study of metal uptake in seaweeds. A number of bioaccumulation experiments were performed and uptake of radioactive ytterbium, and to a lesser extent strontium (brown seaweed only, <i>F. serratus</i> , <i>A. nodosum</i> and <i>L. digitata</i> ) was found. Ytterbium was taken up by red ( <i>Rhodomenia</i> , <i>Chodrus</i> and <i>Gigartina</i> ) and green ( <i>Ulva</i> ) seaweeds, but much less so by brown seaweeds. Ion exchange is put forward as the mechanism of uptake, with adsorption also being important in red and green seaweeds.
Spooner 1949		

---

Chromium has been highlighted in red where it has been studied, and the seaweed species have been colour coded as red, green and brown. *Sargassum*, *Fucus*, *Ascophyllum*, *Laminaria*, and *Ulva* have been abbreviated to S. F. A. L. and U., respectively.

## 1.8 Objectives of Research

- To carry out a biomonitoring project comparing metal concentrations in seaweed in the Suir Estuary in Ireland and in Bonne Bay and the Bay of Islands in Newfoundland, Canada. This is to determine the extent of heavy metal pollution in both sites.
- To study the bioaccumulation of chromium by a variety of seaweed species. The seaweeds chosen for study were *Fucus vesiculosus* and *Fucus spiralis* (brown), *Ulva lactuca* and *Ulva spp* (green) and *Polysiphonia lanosa* and *Palmaria palmata* (red).
- To study the bioaccumulation of Cr(III) and Cr(VI) and to determine the difference between anionic and cationic metal uptake.
- To study bioaccumulation at two different temperatures to determine the effect of temperature on metal uptake.
- To further examine the types of functional groups on the surface of the seaweed by Fourier Transform Infrared Spectroscopy (FTIR). By examining the changes that occur in the spectra on metal binding, the importance of certain functional groups can be determined.
- To determine the effect of binding on the surface of the seaweed by Scanning Force Microscopy (SFM). The presence of a biofilm on the seaweed surface will be confirmed and changes that occur to it on exposure to chromium will also be examined. This is important as the role of biofilms in bioaccumulation or biosorption has not been studied.

# Chapter 2: Seaweed Characterisation



## 2.1 Introduction

Characterisation of the seaweeds is discussed in this chapter, with particular emphasis on functional groups which may be involved in metal binding. This was carried out by several methods, namely Inductively Coupled Plasma-Optical Emission Spectroscopy (ICP-OES) to quantify phosphorus and sulphur levels, Kjeldahl analysis to quantify protein levels and FTIR to determine functional groups present in the seaweed. The three main seaweeds studied in this thesis are; *Fucus vesiculosus* (brown), *Palmaria palmata* (red) and *Ulva lactuca* (green). As differences in uptake seasonally may be important, seaweeds were characterised in May/June and Feb/Mar and any differences found are discussed.

### 2.1.1 Phosphorus and Sulphur Determination by ICP-OES

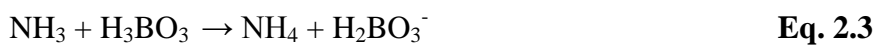
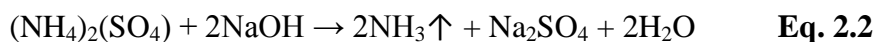
ICP-OES is used to determine the concentration of many elements simultaneously, often down to low  $\mu\text{g/L}$  levels. The atomisation of analyte in plasma occurs at temperatures of about 6000 K which reduces chemical interferences which may occur with flame techniques (Skoog *et al.* 2007). A sample is introduced into a plasma where the temperature is sufficient to produce excitation of the sample atoms. The atoms then decay to the lower states with the accompanying emission of light. The intensity of the light at specific wavelengths can then be measured in order to determine the concentration of the analyte of interest (Boss & Fredeen 1997). Many wavelengths can be measured simultaneously, allowing for the measurement of several elements. Of course, the analysis may be subject to interference as the number of emission lines increase (Boss & Fredeen 1997).

In this study, ICP-OES was used to measure metal concentration in seaweed digests and water samples. Phosphate and sulphate groups are important when talking about metal accumulation as these will form part of the most acidic functional groups on the seaweed surface. Examples of these are sulphated carbohydrates such as carrageenan, fucoidan, laminarin and ulvan (see Section 1.4.2 for structures). Seaweeds have also been shown to contain acidic phosphorylated carbohydrates or phosphorylated glycoproteins (Deniaud *et al.* 2003). These acidic functional groups will become deprotonated more easily than other less acidic functional groups, such as carboxyl, and will therefore have a greater impact on metal uptake. Sulphur containing

functional groups have been frequently determined by FTIR (Fourest & Volesky 1996; Murphy *et al.* 2007; Bakir *et al.* 2009) in biosorption studies, but the application of ICP-OES to quantify total S has not yet been shown. The method has been used, however, to quantify total S in seaweed polysaccharides (Rioux *et al.* 2007).

### 2.1.2 Protein Content by the Kjeldahl Method

The Kjeldahl method is used to determine the amount of nitrogen in a substance. The method consists of three different steps, digestion, distillation and titration. The aim of the digestion step is to break all nitrogen bonds in the sample and convert all of the nitrogen into ammonium ions. For this purpose, sulphuric acid is commonly used (Persson *et al.* 2008). This sample is then distilled in order to convert ammonium ( $\text{NH}_4^+$ ) into ammonia ( $\text{NH}_3$ ) by adding alkali (NaOH) and steam distilling the sample into a receiver flask containing boric acid with indicator. Quantitation is then achieved by titration (Persson *et al.* 2008). The relevant equations are given below in Eq. 2.1-2.4. A conversion factor is used to determine the amount of protein from the amount of N. For most foods a conversion factor of 6.25 is used as most proteins are 16 % N (Nielsen 2010). This conversion factor is commonly used for seaweeds (Galland-Irmouli *et al.* 1999; Dawczynski *et al.* 2007).



There are large differences in the protein content of seaweeds, depending on species, season and environmental conditions (Venugopal 2008). Typical contents from the literature are given in Table 2.1.

**Table 2.1: Protein content of some species of seaweed.**

Seaweed	Colour	% Protein (dry mass)
<i>Palmaria palmata</i>	Red	8-35 <sup>1</sup>
<i>Porphyra tenera</i>	Red	33-47 <sup>1</sup>
<i>Grateloupia turuturu</i>	Red	20 <sup>2</sup>
<i>Ulva lactuca</i>	Green	10-21 <sup>1</sup>
<i>Ulva pertusa</i>	Green	17.5 <sup>2</sup>
<i>Laminaria digitata</i>	Brown	8-15 <sup>1</sup>
<i>Fucus sp.</i>	Brown	3-11 <sup>1</sup>
<i>Ascophyllum nodosum</i>	Brown	3-15 <sup>1</sup>
<i>Analipus japonicus</i>	Brown	23.7 <sup>2</sup>
<i>Codium fragile</i>	Brown	15.6 <sup>2</sup>
<i>Eisenia bicyclis</i>	Brown	13.1 <sup>2</sup>
<i>Hizikia fusiforme</i>	Brown	11.06 <sup>3</sup>
<i>Laminaria japonica</i>	Brown	15.6 <sup>2</sup>
<i>Undaria pinnatifida</i>	Brown	12.5-19.8 <sup>2,3</sup>

<sup>1</sup>(Fleurence 1999), <sup>2</sup>(Galland-Irmouli *et al.* 1999), <sup>3</sup>(Dawczynski *et al.* 2007)

Red and green seaweeds contain 10-47 % protein. Brown seaweeds typically have a lower protein content of about 3-15 % dry weight of the seaweeds (Fleurence 1999). Proteins and peptide content can affect metal uptake as they are capable of becoming charged depending on the pH of the solution. There are also metal binding peptides called phytochelatins present in seaweeds which may contribute to intracellular metal binding (discussed in more detail in Section 1.3.1).

### 2.1.3 Functional Group Determination by Fourier Transform Infrared Spectroscopy

Fourier transform infrared spectroscopy (FTIR) can be used to investigate the structure of organic and inorganic materials. Vibrational absorption occurs in the infrared (IR) region of the electromagnetic spectrum. It is not sufficiently energetic to excite electrons to higher energy levels. An IR spectrum is, therefore, the series of absorbance bands observed from the transitions between various vibrational energy states. The range used for most analyses is between 4000–400cm<sup>-1</sup> (Atkins 1996).

Fourier transform spectrometers offer several advantages over traditional dispersive instruments. These include better sensitivity, resolution and faster data acquisition (ThermoNicolet Corporation 2001).

FTIR analysis can be used to determine the functional groups which take part in biosorption of metals on a seaweed surface. The occurrence of band shifts in the spectra of a protonated and metal loaded sample are studied to determine the functional groups involved in metal complexation. Band shifts may be caused by mass effects, steric interactions, resonance effects, inductive effects, dipole-dipole interactions and intermolecular interactions (Günzler & Gremlich 2002). IR spectra of seaweed biomass have been studied extensively (Murphy *et al.* 2007; Sheng *et al.* 2004; Park *et al.* 2005; Naja *et al.* 2005) and Table 2.2 lists the main functional groups occurring in seaweeds and their associated absorption bands.

**Table 2.2: Main functional groups occurring in seaweeds and their associated infrared absorption bands.**

Wavenumber ( $\text{cm}^{-1}$ )	Assignment	Reference
3350	Bonded hydroxy -NH stretching	D. Park <i>et al.</i> 2005 D. Park <i>et al.</i> 2005
2925-2800	Asymmetric and symmetric stretching of alkyl chains	Naja <i>et al.</i> 2005
1740	C=O stretch of COOH	D. Park <i>et al.</i> 2005
1650	C=O chelate stretching Amide I band	D. Park <i>et al.</i> 2005 D. Park <i>et al.</i> 2005
1530	Amide II	D. Park <i>et al.</i> 2005
1450	Symmetric carboxylate stretching	D. Park <i>et al.</i> 2005
1260-1220	S=O sulphate ester band	Gómez-Ordóñez & Rupérez 2011
1237	C-O stretch of COOH	Murphy <i>et al.</i> 2007
1205-1156	Sulphate group bands	Naja <i>et al.</i> 2005

1160	-CN stretching Symmetric -SO <sup>3</sup> stretching	D. Park <i>et al.</i> 2005 Murphy <i>et al.</i> 2007
1150 1030-1010	C-O and C-C stretches of polysaccharides	Gómez-Ordóñez & Rupérez 2011
1150	P=O	Y. S. Yun <i>et al.</i> 2001
1150-1030	P-O-C linkages of organic phosphate groups	Naja <i>et al.</i> 2005
1030	C-O stretch of an alcohol group	Murphy <i>et al.</i> 2007
1040-910	P-OH	Y. S. Yun <i>et al.</i> 2001
605-805	C-O-SO <sub>3</sub> stretches with actual wavenumber varying according to sulphate group substitution	Pereira <i>et al.</i> 2009
850	S=O	Y. S. Yun <i>et al.</i> 2001
817	S-O stretch	Murphy <i>et al.</i> 2007
620-590	Sulphate group bands	Naja <i>et al.</i> 2005

Potassium bromide methods have been the most commonly used, either by using diffuse reflectance (Sheng *et al.* 2004) or by making potassium bromide discs (Naja *et al.* 2005; Park *et al.* 2005). This study is the first to study seasonal changes in FTIR spectra. The fast analysis time achieved with FTIR is an advantage over other chemical analysis techniques used to determine seasonal changes (e.g. digestion and Kjeldahl and ICP).

### 2.1.5 Objectives

The objectives of the work in this chapter are to:

- Determine the amount of phosphorus and sulphur in *Fucus vesiculosus*, *Palamaria palmata* and *Ulva lactuca* using ICP-OES.
- Determine the amount of protein in *F. vesiculosus*, *P. palmata* and *U. lactuca* using the Kjeldahl method.
- Determine the types of functional groups present in *F. vesiculosus*, *P. palmata* and *U. lactuca* using FTIR.

- Determine any seasonal differences in seaweed composition. This is the only study which has been carried out detailing seasonal changes in functional groups by FTIR.
- Discuss the relevance of seaweed composition and seasonality to metal binding.

## 2.2 Experimental

### 2.2.1 Sampling, Storage and Drying

Seaweed was collected randomly by hand from Baginbun in Co. Wexford, Ireland (GPS coordinates: 52° 10.596' N, 6° 49.787' W) from late May to June 2009, and from the mid February to early March 2010. In text and diagrams these will be referred to as May/Jun and Feb/Mar. The seaweed was transported to the lab in cooler boxes. Three samples from 3 different plants for each species was taken and frozen for later analysis. The seaweeds were dried before analysis at 60 °C for 24 h, and ground using a mortar and pestle or mill, if necessary (Ryan *et al.* 2012) (see Section 2.2.4).

### 2.2.2 Phosphorus and Sulphur by ICP-OES

#### 2.2.2.1 Microwave Digestion

Seaweed samples were digested in a nitric acid (Sigma-Aldrich Fluka, 69 % puriss, Lennox, Ireland), hydrogen peroxide (Sigma-Aldrich Fluka, 30 % puriss, Lennox, Ireland) and water mixture (5:2:3) using a Mars 5 microwave (JVA Analytical, Ireland). The program is described in Table 2.3. About 300 mg of dried sample was used for each digestion. The accuracy of the analytical balance (Mettler-Toledo AT200, Mason Technology, Ireland) was checked on a regular basis by using calibration weights.

**Table 2.3: Microwave digestion program.**

Power (W)	Ramp time (min)	Temperature (°C)	Hold time (min)
600	5	120	2
1200	5	150	2
1200	5	180	10

#### 2.2.2.2 ICP Analysis

Digests were analyzed for S and P using a Varian 710-ES ICP-OES (JVA Analytical, Ireland) and the instrumental conditions given in Table 2.4. Standards were prepared in 2 % nitric acid using a custom standard obtained from Inorganic Ventures (JVA Analytical, Ireland). P and S were monitored at several wavelengths (P: 177.434, 178.222, 213.618, 214.914 nm; S: 180.669, 181.972, 182.562 nm) in a preliminary

analysis, and those showing no interferences and maximum recovery of the standard reference material were used. These are given in Table 2.4.

**Table 2.4: ICP instrument settings for seaweed digests.**

Analysis wavelength	P: 213.618 nm	Stabilization time	15 s
	S: 182.562 nm		
Power	1.15 kW	Sample uptake delay	30 s
Plasma flow	15.0 L/min	Rinse time	10 s
Auxiliary flow	1.50 L/min	Pump rate	15 rpm
Nebulizer pressure	200 kPa	Replicates	2
Replicate read time	5.0 s		

Standard reference materials sea lettuce (BCR 279), NIST SRM 1573a (Tomato leaves) and NIES CRM 9 (Sargasso) were digested and analyzed in the same way.

### 2.2.3 Protein Content by the Kjeldahl Method

#### 2.2.3.1 Digestion

The digestion unit (Büchi K-424 Digestion Unit, Mason Technology, Ireland) was preheated for about 15 min prior to adding samples. About 1.5 g of dried, ground seaweed was weighed accurately, and added to a clean digestion flask. Glass beads, one antifoam tablet (Lennox, Ireland), two Kjeltabs (Type S, Merck, Lennox, Ireland), and 20 ml concentrated sulphuric acid (AnalaR Grade, VWR, Ireland) were then added. Blanks were run at the same time, where the seaweed was omitted. The samples were then placed in the digestion unit and heated until they were clear, and then for a further 15 min. This took approximately 1 h in total. The flasks were then removed and allowed to cool.

#### 2.2.3.2 Distillation and Titration

A Büchi distillation unit was used (K-350, Mason Technology, Ireland). 75 mL of boric acid solution (40 g/L with BDH 4.5 indicator, VWR, Ireland) was added to a 250 mL conical flask and placed under the receiver tube on the right side of the unit. 80 mL of distilled water was then added to the flask. The flask was attached to the digestion unit and 100 mL of 30 % sodium hydroxide (ReactaPur, VWR, Ireland) was added to neutralize the solution. The distillation unit was then used to distill the



sample for 4 min. The solution was then titrated with 0.1 M hydrochloric acid (Riedel-de Haen, Lennox, Ireland) (Ryan 2010). A protein conversion factor of 6.25 (to convert % Nitrogen to % protein) was used (Galland-Irmouli *et al.* 1999; Rødde *et al.* 2004; Dawczynski *et al.* 2007).

#### 2.2.4 Functional Group Determination by FTIR

The seaweed was finely ground using a Retsch MM301 ball mill. A potassium bromide (KBr) disc method was used. A ratio of approximately 1:100 sample:KBr was used. A disc was made by using a press (Atlas T25, JVA Analytical, Ireland) and a 10 mm die (JVA Analytical, Ireland). 6 tonnes of pressure for a period of 2 min was used to compress the disc. The FTIR instrument parameters used are shown in Table 2.5. A DTGS detector was used. Samples were analysed in triplicate.

**Table 2.5: Instrument settings for IR analysis.**

<b>Speed</b>	25 kHz
<b>Electronic bypass</b>	17.4 kHz
<b>Interferogram sampling interval</b>	2
<b>Resolution</b>	2 cm <sup>-1</sup>
<b>Sensitivity</b>	1
<b>Scans</b>	64
<b>Scan range</b>	4000–400 cm <sup>-1</sup>
<b>Aperture</b>	open

## 2.3 Results and discussion

### 2.3.1 Phosphorus and Sulphur by ICP-OES

#### 2.3.1.1 Validation

The Limit of Detection (LOD) and Limit of Quantification (LOQ) are shown in Table 2.6. They were determined by the analysis of at least 3 blanks, prepared in the same way as the sample. The following calculation was used (Gustavo González & Ángeles Herrador 2007):

$$\text{LOD} = \text{Mean blank concentration} + (3 \times \text{Standard deviation of blank})$$

$$\text{LOQ} = \text{Mean blank concentration} + (10 \times \text{Standard deviation of blank})$$

**Table 2.6: LOD and LOQ for Phosphorus and Sulphur Analysis**

Element and Wavelength (nm)	LOD and LOQ in mg/L	
	LOD	LOQ
Phosphorus 213.618	0.45	0.52
Sulphur 182.562	8.66	8.89

The validity of the results was determined by analysis of certified reference materials, which were digested and analysed in the same way as samples. BCR 279 (Sea lettuce), NIST SRM 1573a (Tomato leaves) and NIES CRM 9 (Sargasso) were used for validation of the method. Phosphorus was certified for only one reference material, tomato leaves. In that case, and for indicative values given for sargasso and sea lettuce, excellent recovery was seen. Sulphur was not certified for any reference material, but the results were compared to indicative values where possible. Sulphur recovery was found to be high in both cases (120-130 % of the indicative value). Although not ideal, this was considered suitable for the identification of major trends or seasonal differences (Table 2.7).

**Table 2.7: Comparison of certified / indicative values for P and S and those found by analysis**

Certified material and units	P		S	
	Certified / Indicative value	Found	Certified / Indicative value	Found
Sea lettuce (mg/g)	1.78 ± 0.02 <sup>a</sup>	1.66 ± 0.00 <sup>b</sup>	–	3.47 ± 0.07
Tomato leaves (%)	0.216 ± 0.004	0.213 ± 0.006	0.96a	1.18 ± 0.03
Sargasso (%)	0.26 <sup>a</sup>	0.27 ± 0.02	1.20 <sup>a</sup>	1.51 ± 0.11

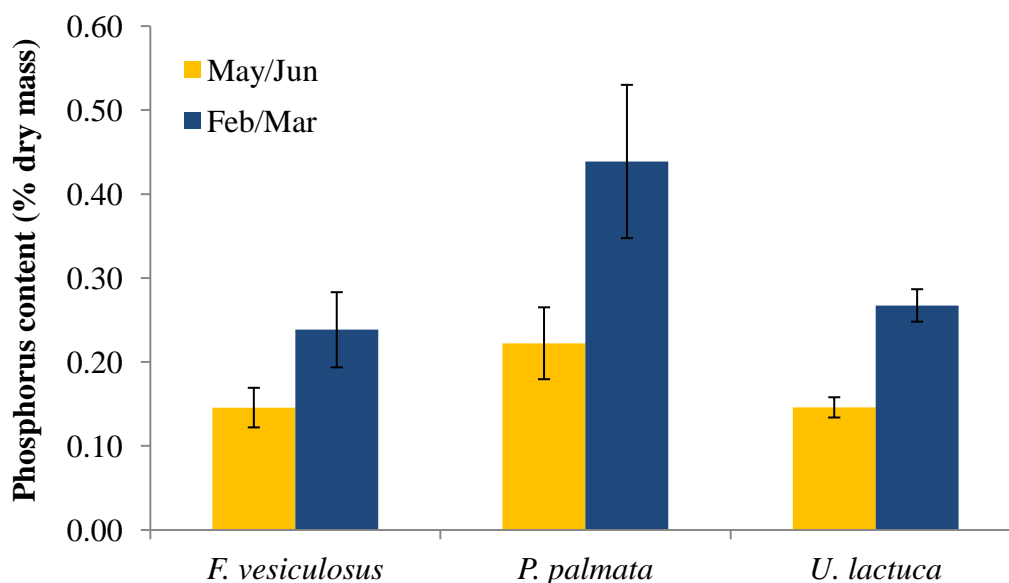
<sup>a</sup>These values are indicative

<sup>b</sup>Uncertainty calculated in the same way as for certified reference material if specified on certificate.

Sea lettuce and sargasso uncertainty was based on standard deviation. Tomato leaf error was based on 95 % confidence intervals. Some values had no error specified where on the certificate.

The results of P and S analysis of *Fucus vesiculosus*, *Palmaria palmata* and *Ulva lactuca* are given in Figure 2.1 and 2.2 below. *P. palmata* had the highest concentration of phosphorus (May/Jun 0.22 %, Feb/Mar 0.44 %), and *F. vesiculosus* (May/Jun 0.15 %, Feb/Mar 0.24 %) and *U. lactuca* (May/Jun 0.15 %, Feb/Mar 0.27 %) were approximately equal. Phosphorus content was consistently higher in Feb/Mar. This is in agreement with the trend found by Villares *et al.* (1999) for *Ulva* sp. in Spain (Villares *et al.* 1999), and by Martinez *et al.* (2002) for *P. palmata*, also in Spain (Martinez & Rico 2002). A recent study showed a similar trend, but higher results than those shown here for *F. vesiculosus* (varied from approximately 0.1-0.5 % throughout the year, probably showing that the variation of P is dependent on local water conditions (Villares *et al.* 2013).

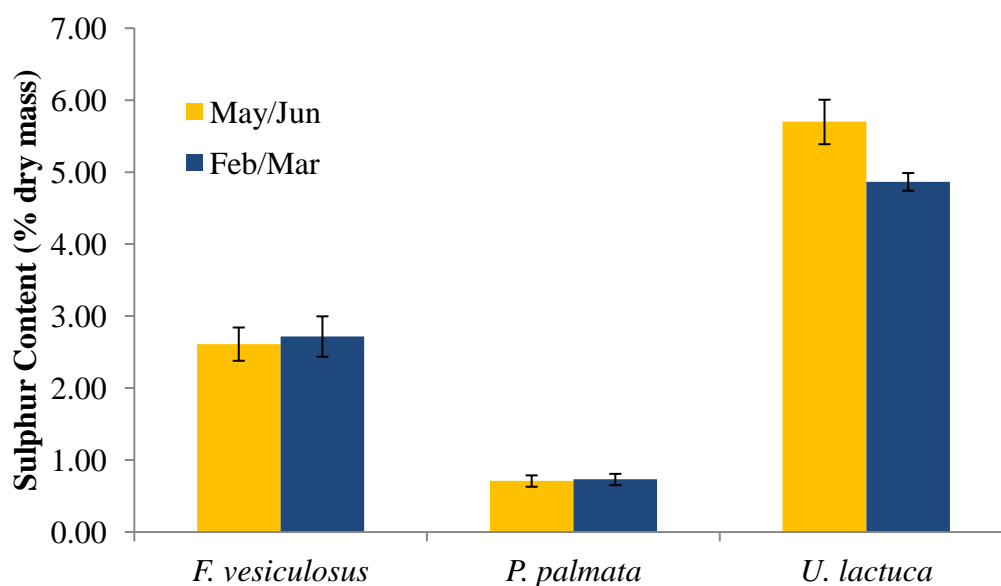
Deniaud's work (2003) on polysaccharide extracts from *P. palmata* showed evidence of acidic phosphorylated carbohydrates, although the possibility of the extracts having some contamination with phosphorylated proteins could not be excluded (Deniaud, Fleurence, *et al.* 2003). Another study confirmed the acidity of the xylans arose from linkages to proteins such as phosphorylated cell wall proteins (Deniaud, Quemener, *et al.* 2003). Phosphorylated carbohydrates or proteins are not very well described in the literature (Deniaud, Fleurence, *et al.* 2003), however their presence may well give rise to charged groups on the seaweed.



**Figure 2.1: Variation in phosphorus content with season.**

These charged phosphate groups may be capable of binding metal ions, or facilitating their transport into the cell if part of the lipid bilayer. The possibility of phosphate group interaction in bioaccumulation has rarely been discussed in the literature. One study looked at the accumulation of Cr(VI) (as potassium dichromate) on a mixed microbial biofilm. It was found that Cr(VI) was reduced to Cr(III) (XANES analysis), primarily as Cr(III)-phosphate. It is also interesting to note that Cr(VI) reduction by lyophilized (dead) biofilm was negligible, and indicating the involvement of active cell metabolism (Nancharaiah *et al.* 2010).

*U. lactuca* had the highest concentration of sulphur (May/Jun 5.70 %, Feb/Mar 4.87 %), followed by *F. vesiculosus* (May/Jun 2.61 %, Feb/Mar 2.72 %) and then *P. palmata* (May/Jun 0.71 %, Feb/Mar 0.73 %) (Figure 2.5). It was higher in May/Jun for *U. lactuca*, but *F. vesiculosus* and *P. palmata* showed no seasonal trend, with sulphur content being approximately equal in Feb/Mar and May/Jun. A study of sulphur content in *F. vesiculosus* (and *F. spiralis*) from Spain was carried out, which found results of 0.5-1.8 (mean 1.0 %) over a year of monthly analysis. No seasonal trend was found over the year. The difference in results may be analytical or spatial, but is most likely spatial as both this study and referenced work used standard reference materials to control analytical quality (Villares *et al.* 2013). To the authors knowledge, this is the only other study of seasonal variations in S content.



**Figure 2.2: Variation in sulphur content with season.**

*F. vesiculosus* contains fucoidan, a sulphated polysaccharide (Jiao *et al.* 2011).

Sulphur in *U. lactuca* comes from ulvan, a green seaweed polysaccharide with a high sulphate content (Lahaye *et al.* 1999). Sulphated polysaccharides are less well studied in *P. palmata*, but have been studied by Deniad *et al.* (2003) who found the presence of sulphated xylans (Deniaud, Quemener, *et al.* 2003). Sulphate content is also linked to sulphated proteins such as cysteine and ligands such as glutathione, which are found in seaweeds (Vasconcelos & Leal 2008; Vasconcelos *et al.* 2002; Vasconcelos & Leal 2001).

The impact of sulphate on metal accumulation has been much better studied than phosphate in the literature. Many authors have shown the participation of sulphate groups in metal binding in the context of biosorption, or surface uptake of metal. Sulphonate groups were shown to contribute to Cd, and especially Pb binding in the brown seaweed *Sargassum fluitans* (Fourest & Volesky 1996). Changes in the FTIR spectra of metal loaded seaweeds indicated sulphonate group participation in the binding of Cu by *F. vesiculosus* and *F. spiralis*, *Ulva* spp. *U. lactuca*, *P. palmata* and *Polysiphonia lanosa*. This was greatest for the green seaweeds *Ulva* spp. and *U. lactuca* (Murphy *et al.* 2007). The results observed in this work seem to support this, with *U. lactuca* having the greatest quantity of S.

Sulphur containing amino acids (namely cysteine) and glutathione have both been found to complex with metals (Vasconcelos & Leal 2008; Vasconcelos *et al.* 2002; Vasconcelos & Leal 2001). Of the species studied here, this binding has been shown for *Ulva* spp. (Vasconcelos *et al.* 2002), but not for *F. vesiculosus* or *P. palmata* to date. However, their presence and changes in concentration on metal binding has been shown for various species of red, brown and green algae (Pawlik-Skowrońska *et al.* 2007; Sáez *et al.* 2015; Vasconcelos & Leal 2008). The evidence shows that this is one of the detoxification/defence mechanisms used by seaweeds.

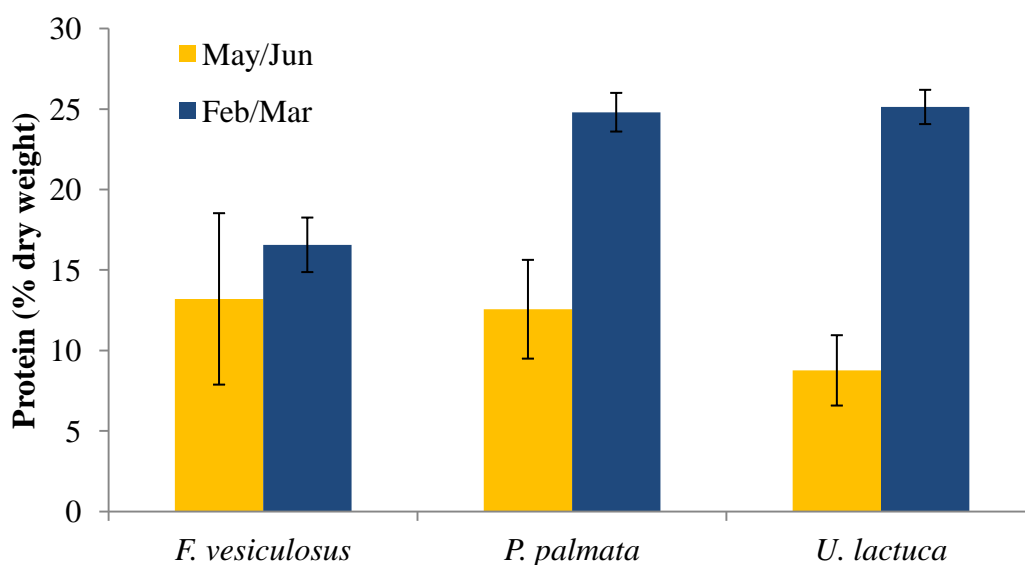
### 2.3.2 Protein Content by the Kjeldahl Method

The protein contents as determined by the Kjeldahl method are shown in Figure 2.3. The method was validated using NIST SRM 1573a (Tomato leaves). A comparison of the certified and determined values are shown in Table 2.8.

**Table 2.8: Comparison of certified / indicative values for N and those found by analysis (all in % dry weight)**

Certified material	Certified / Indicative value	Found
Tomato leaves	$3.03 \pm 0.15$	$2.91 \pm 0.02$

Uncertainty based on 95 % confidence intervals.

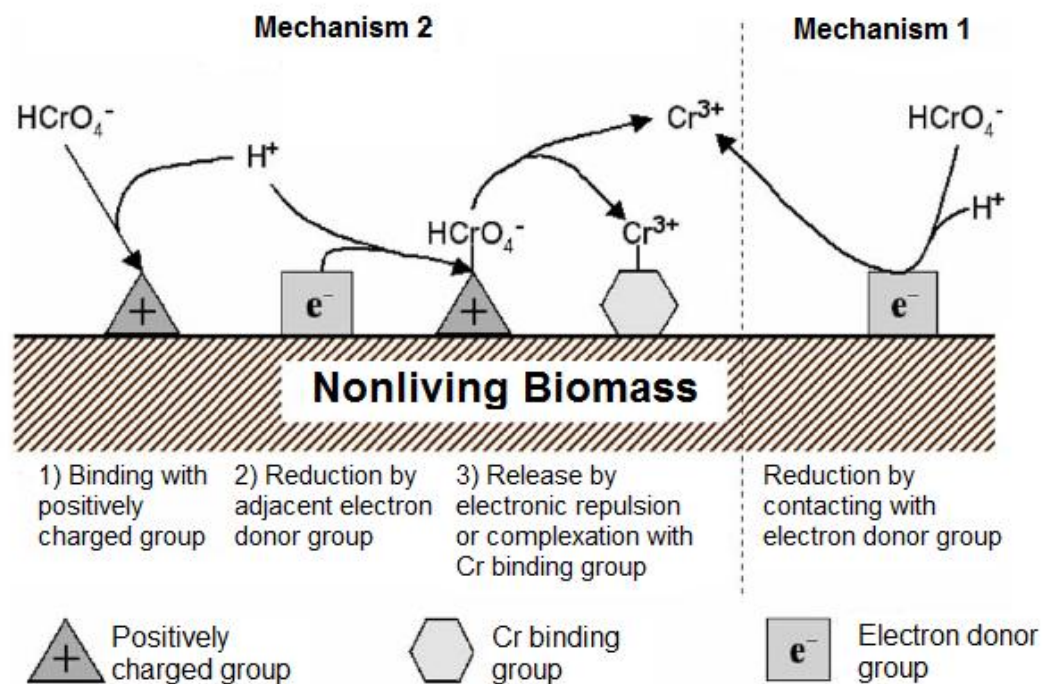


**Figure 2.3: Variation in total protein (% dry weight) with season.**

Protein content was higher in winter than in summer for *P. palmata* and *U. lactuca*, but not *F. vesiculosus*. Although the average protein content of *F. vesiculosus* was different for May/Jun (13.20 %) and Feb/Mar (16.56 %), there was no significant difference after taking the error into account. Most seaweeds have their lowest protein contents during the summer season. Nitrogen is accumulated from seawater during the winter and then is depleted during the growth season (Rosell & Srivastava 1985). In a review by Fleurence (1999), minimum and maximum protein levels in *U. lactuca*, *Fucus* sp. and *P. palmata* were found to be 10–21, 3–11 and 8–35 % dry weight, respectively (Fleurence 1999). The protein contents found in this study are in good agreement with this review except for *F. vesiculosus*, where the protein content was higher than the average expected for *Fucus* sp. It should be noted, however, that seaweeds will show geographical (as well as species and seasonal) variations in protein content (Rødde *et al.* 2004). Also, the review specifies *Fucus* sp. rather *F. vesiculosus* in particular. *F. vesiculosus* sampled in May from a site in the south-east of Ireland has been analysed for total protein with a result of 14.9 %, in agreement with the result seen here (Ryan 2010). This was the first time a seasonal study has been carried out on these seaweeds from the south east of Ireland.

Metals are known to bind with intracellular proteins and this may have a detoxifying effect (Malec *et al.* 2009). Cell wall proteins are also present (Cassab 1998), which can contribute to metal binding on the surface of the seaweed. Phytochelatin (a thiol containing peptide) concentration was found to be positively correlated with metal load in several red, green and brown seaweeds (Pawlik-Skowrońska *et al.* 2007). These phytochelatins are part of the algal detoxification process, and reduce the effect of heavy metals intracellularly, by binding the metal and sequestering it into vacuoles (Perales-Vela *et al.* 2006). The purified proteins, lysozyme, bovine serum albumin and ovalbumin were all found to be effective adsorbents of the precious metals Au and Pd over a wide pH range (maximum at pH 8 for Pd, and up to pH 7 for Au) (Maruyama *et al.* 2007). Protein is an integral part of the algal cell wall and may make up a significant proportion of it. Green algae has been shown to contain 10-69 % protein, brown 16-27 % protein, and red 35-50% protein (Siegel & Siegel 1973). The large amount of functional groups provided by these proteins undoubtedly affects

heavy metal accumulation in algae. In yeast, it was found that chemically blocking the amino groups of the isolated cell wall, significantly reduced  $\text{Cu}^{2+}$  biosorption, indicating their involvement in metal binding (Brady & Duncan 1994). In the biosorption of Cr(VI) by *Ecklonia* sp. it was shown that amination of carboxyl groups enhanced Cr(VI) removal, and reduced Cr(VI) to Cr(III). A mechanism was proposed whereby Cr(VI) was either reduced directly by electron donor groups on the surface (Figure 2.4, mechanism 1); or indirect reduction, where Cr(VI) was bound to positively charged sites on the biomass, reduced by an adjacent electron donor group, and then either released into solution, or bound (now as the reduced Cr(III)) to an adjacent negatively charged group (Figure 2.4, Mechanism 2) (Park *et al.* 2005). Amino groups from cell wall proteins are a rich source of positively charged groups on the seaweed surface.



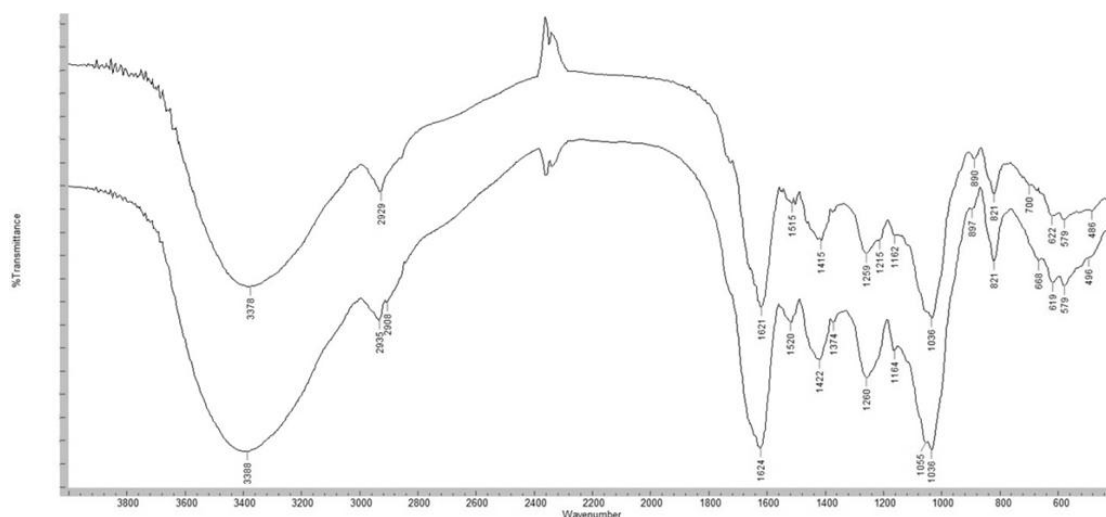
**Figure 2.4: Proposed mechanism of reduction of Cr(VI) by brown seaweed biomass (Park *et al.* 2005).**



### 2.3.3 Functional Group Characterisation by FTIR Analysis

#### 2.3.3.1 *Fucus vesiculosus*

Representative scans for *F. vesiculosus* samples in May/June and Feb/Mar are given in Figure 2.5. Specimens of *F. vesiculosus* from both seasons were similar. A peak table is shown in Table 2.9.



**Figure 2.5:** Representative FTIR scans of *F. vesiculosus* sampled in May/June (top) and Feb/Mar (bottom), taken from triplicate analysis.

**Table 2.9:** Peak table for *F. vesiculosus*. Resolution-2 cm<sup>-1</sup>, sensitivity-1, scan number-64. Values based on triplicate analysis, 95 % confidence intervals are shown. References for assignments are given in text to improve clarity of the table.

May/June (cm <sup>-1</sup> )	Feb/Mar (cm <sup>-1</sup> )	Assignment
3379.6 ± 2.7	3385.2 ± 4.5	-OH
2928.8 ± 1.7	2931.8 ± 2.7	Aliphatic chain stretches
2857.2 ± 1.8	2909.1 ± 1.9	Aliphatic chain stretches
1738.5 ± 1.9		C=O stretch of carboxylates
1658.6 ± 0.2	1658.0 ±	Asymmetric C=O chelate Amide I N-H stretch
1515.2 ± 0.7	1521.0 ± 1.6	Amide II stretch
1415.5 ± 0.4	1419.4 ± 2.9	Symmetrical carboxylate

1376.5 ± 0.8	1376.5 ± 4.6	Amide
1259.1 ± 1.3	1258.7 ± 1.3	C-O-C ether Sulphonate stretching
1161.0 ± 1.3	1164.2 ± 0.6	Sulphonate
1052.7 ± 1.8	1053.4 ± 2.1	C-O vibrations
1035.4 ± 0.4	1035.5 ± 0.4	Alcoholic C-O stretch
890.0 ± 2.2	893.8 ± 3.3	C-C-O and C-O-C
821.4 ± 0.6	821.0 ± 0.5	Characteristic mannuronic acid band
622.0 ± 0.6	619.1 ± 1.5	Sulphate

The first broad peak at ~ 3380 cm<sup>-1</sup> is attributable to hydroxyl groups arising from carbohydrates and amino groups from proteins and peptides (Park *et al.* 2004; Pons *et al.* 2004). The bands at ~ 2930 and ~ 2857 cm<sup>-1</sup> represented asymmetrical and symmetrical stretching of aliphatic hydrocarbon chains, respectively (Sheng *et al.* 2004).

The band at 1740 cm<sup>-1</sup>, seen as a shoulder in these spectra, corresponded to the C=O stretch of carboxylates (Naja *et al.* 1999). The band at 1650 cm<sup>-1</sup> showed the asymmetric C=O chelate stretch and the primary amide N-H stretch (Naja *et al.* 1999; Kapoor & Viraraghaven 1997). The band at 1520 cm<sup>-1</sup> corresponded to secondary amide stretching (Sheng *et al.* 2004). This peak is often very weak and may not be noticed in complex spectra of biologicals (Williams & Fleming 1995), but can be clearly seen here.

The peak at 1420 cm<sup>-1</sup> corresponded to symmetrical carboxylate stretching (Sheng *et al.* 2004). The peak at 1376 cm<sup>-1</sup> represented the presence of amide groups (Kapoor & Viraraghaven 1997). The band at ~ 1258 cm<sup>-1</sup> represented the C-O-C ether stretching found in all the seaweed polysaccharides (Pons *et al.* 2004). A band at ~1259 cm<sup>-1</sup> may also correspond to sulphonate stretching (Sheng *et al.* 2004; Fourest & Volesky 1996). The band at 1160 cm<sup>-1</sup> represented sulphonate groups associated with sulphated polysaccharides such as fucoidans in brown seaweeds (Murphy *et al.* 2007).

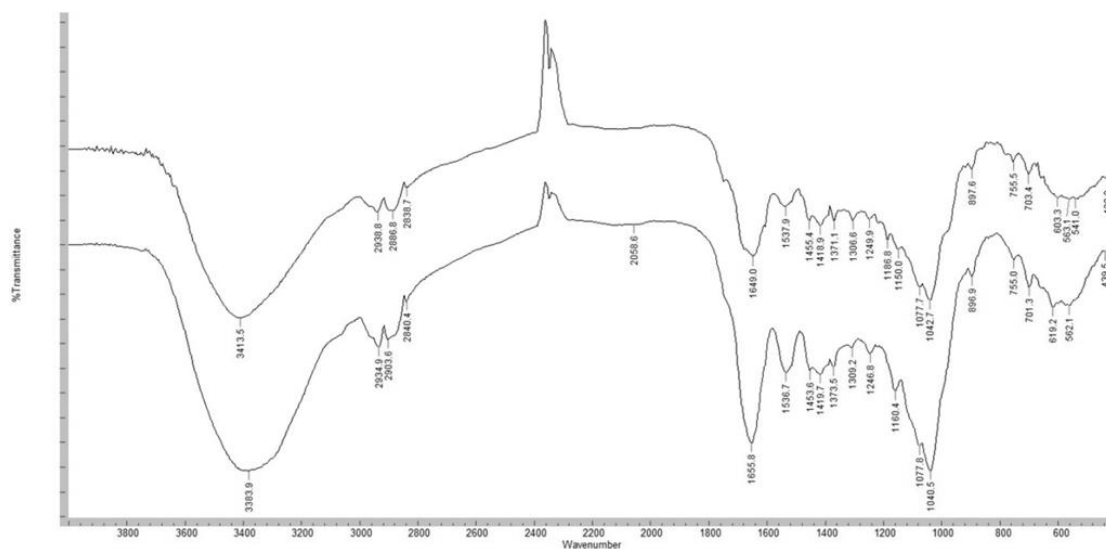
A very small shoulder, barely seen in the spectra at  $1075\text{ cm}^{-1}$  may refer to the P-O of the C-PO<sub>3</sub> moiety (Naja *et al.* 2005).

The slightly split peak at  $1055\text{ cm}^{-1}$  is due to C-O vibrations (Gaudenzi *et al.* 2003). Bands at  $1150$  and  $1030\text{-}1010\text{ cm}^{-1}$  represent C-O and C-C stretches common to polysaccharides (Gómez-Ordóñez & Rupérez 2011). The peak at  $1030\text{ cm}^{-1}$ , which was present in all spectra, corresponded to alcoholic C-O stretching (Murphy *et al.* 2007). The band at  $890\text{ cm}^{-1}$  can be assigned to C-C-O and C-O-C groups (Romero-González *et al.* 2003). The peak at about  $850\text{ cm}^{-1}$  was associated with S=O stretching (Fourest & Volesky 1996). The band at  $\sim 820\text{ cm}^{-1}$  seems to be characteristic of mannuronic acid residues, one of the building blocks of the brown seaweed polysaccharide, alginate (Leal *et al.* 2008). This peak was seen only in the spectrum of *F. vesiculosus*. The peak at  $619\text{ cm}^{-1}$  was due to sulphonate groups (Naja *et al.* 2005).

In summary, for *Fucus vesiculosus*, carboxyl, alcoholic, sulphonate and ether functionalities were observed. This agrees with the composition of *F. vesiculosus* found in earlier analysis (Section 2.3.1 and 2.3.2), and with the known structure of brown seaweed polysaccharides such as alginates, cellulose and fucoidan (Table 1.1 and Section 1.2.3). Amide functional groups were also observed, referring to the peptide and protein content of the seaweed.

### 2.3.3.2 *Palmaria palmata*

Spectra for May/June and Feb/Mar samples were quite similar, but some significant seasonal differences were found (Figure 2.6 and Table 2.10). Differences were deemed to be significant if there is still a difference after taking account of the error of three independent replicates and the resolution of the technique ( $2\text{ cm}^{-1}$ ).



**Figure 2.6: Representative FTIR scans of *P. palmata* sampled in May/June (top) and Feb/Mar (bottom), taken from triplicate analysis.**

**Table 2.10: Peak table for *P. palmata*. Resolution-2 cm<sup>-1</sup>, sensitivity-1, scan number-64. Values based on triplicate analysis, 95 % confidence intervals are shown. References for assignments are given in text to improve clarity of the table.**

May/June (cm <sup>-1</sup> )	Feb/Mar (cm <sup>-1</sup> )	Assignment
3399.3 ± 14.7	3382.6 ± 13.3	-OH
2936.5 ± 2.3	2934.9 ± 0.7	Aliphatic chain stretches
2897.8 ± 10.9	2904.0 ± 0.5	Aliphatic chain stretches
1649.6 ± 0.6	1654.8 ± 1.0	Asymmetric C=O chelate Amide I N-H stretch
1538.0 ± 0.1	1534.8 ± 2.5	Amide II stretch
1416.7 ± 2.1	1419.7 ± 0.6	Symmetrical carboxylate
1378.8 ± 14.1	1376.1 ± 2.7	Amide
1248.4 ± 1.6	1247.1 ± 0.3	Sulphonate stretch
1149.2 ± 0.8	1162.3 ± 3.0	Sulphonate
1043.4 ± 0.7	1042.2 ± 1.7	C-O vibrations
897.6 ± 0.1	896.6 ± 0.3	C-O-SO <sub>3</sub> stretching
607.2 ± 4.5	618.6 ± 1.1	Sulphate

The first peak was a broad peak at  $\sim 3380\text{ cm}^{-1}$ , which can be assigned to hydroxyl groups from carbohydrates and amino groups from proteins and peptides (Park *et al.* 2004; Pons *et al.* 2004). Alkyl chain stretching was seen from  $2930\text{-}2840\text{ cm}^{-1}$  (Naja *et al.* 2005). A weak band at  $\sim 1740\text{ cm}^{-1}$ , seen as a shoulder in these spectra, corresponded to the C=O stretch of carboxylates (Naja *et al.* 1999).

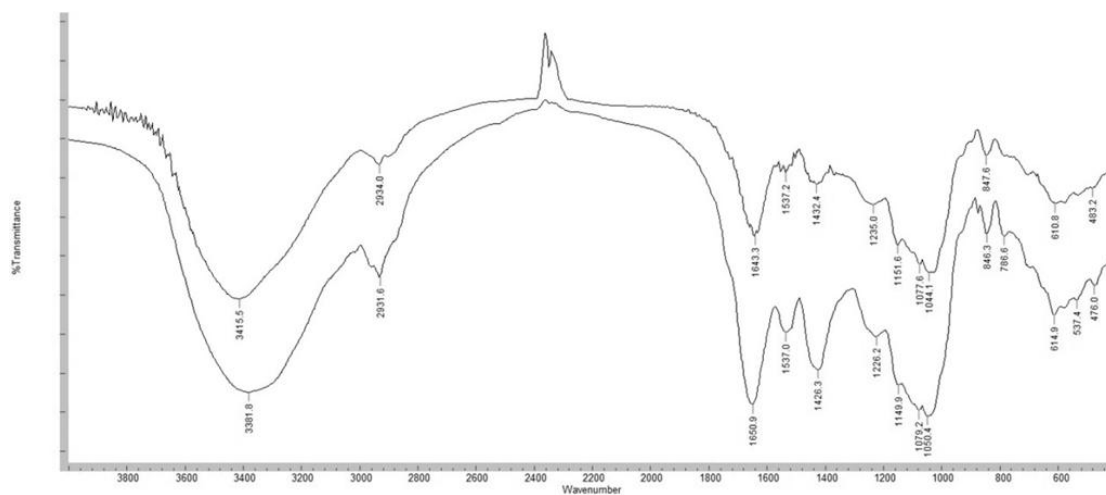
One of the main differences in the spectra was the peak which appeared at  $1649\text{ cm}^{-1}$  in the May/June spectrum and  $1654\text{ cm}^{-1}$  in the Feb/Mar spectrum. This was a primary/secondary amide bond, a result of the C=O stretching mode conjugated to the NH deformation mode (Kapoor & Viraraghavan 1997). The difference between the spectra, therefore, was probably due to the higher amount of protein found in *P. palmata* in winter. The band at  $\sim 1536\text{ cm}^{-1}$  corresponding to secondary amide stretching (Sheng *et al.* 2004), was bigger in the Feb/Mar spectrum also showing increased protein levels. The peak at  $1455\text{ cm}^{-1}$  referred to symmetrical carboxylate stretching (Sheng *et al.* 2004).

A broad band from  $1240\text{ to }1260\text{ cm}^{-1}$  was ascribed to the S=O stretching vibration of sulphated groups. This peak may be correlated to the sulphate content of the sample (Pereira *et al.* 2009), and it correlated well with the peak seen in *P. palmata* (0.7 % sulphur) being smaller than that seen for *F. vesiculosus* (2.76 % sulphur) or *U. lactuca* (5.7% sulphur). Peaks from  $905\text{-}805\text{ cm}^{-1}$  referred to C-O-SO<sub>3</sub> stretching of sulphate groups of polysaccharides (Pereira *et al.* 2009). The broad peak at  $560\text{ cm}^{-1}$  referred to sulphate groups (Naja *et al.* 2005).

In *P. palmata* carboxyl, alcoholic, sulphonate, ether and amide functionalities were observed. This agrees with the composition found in earlier analysis, confirming presence of sulphur as sulphonate, and nitrogen as amide (see Section 2.3.1 and 2.3.2). It also agrees with the known structure of red seaweed polysaccharides, such as sulphated xylans (Deniaud, Quemener, *et al.* 2003), and their protein content (Rødde *et al.* 2004).

2.3.3.3 *Ulva lactuca*

Again spectra for May/Jun and Feb/Mar samples were quite similar, but there were some significant seasonal differences (Figure 2.7 and Table 2.11).



**Figure 2.7: Representative FTIR scans of *U. lactuca* sampled in May/Jun (top) and Feb/Mar (bottom), taken from triplicate analysis.**

**Table 2.11: Peak table for *U. lactuca*. Resolution-2 cm<sup>-1</sup>, sensitivity-1, scan number-64. Values based on triplicate analysis, 95 % confidence intervals are shown. References for assignments are given in text to improve clarity of the table.**

May/Jun (cm <sup>-1</sup> )	Feb/Mar (cm <sup>-1</sup> )	Assignment
3417.8 ± 4.6	3384.7 ± 4.3	-OH
2936.8 ± 3.4	2934.1 ± 2.9	Aliphatic chain stretches
2901.8 ± 6.5		Aliphatic chain stretches
1643.0 ± 0.4	1651.2 ± 0.9	Asymmetric C=O chelate Amide I N-H stretch
1537.2 ± 0.4	1537.3 ± 0.3	Amide II stretch
1429.3 ± 3.0	1427.6 ± 1.4	Symmetrical carboxylate
1242.1 ± 16.0	1228.9 ± 2.6	S=O
1150.3 ± 1.5	1149.9 ± 0.1	Sulphonate
1049.3 ± 5.1	1051.5 ± 1.6	C-O vibrations

847.9 ± 0.5	846.6 ± 0.7	C-O-SO <sub>3</sub>
785.2 ± 2.7	788.0 ± 2.4	Typical ulvan bands

Similar differences were found in these spectra as those observed for *P. palmata*. The peak at 1643 cm<sup>-1</sup> in the May/Jun spectrum has again moved to 1651 cm<sup>-1</sup> in the Feb/Mar spectrum. This is a primary/secondary amide bond, a result of the C=O stretching mode conjugated to the NH deformation mode (Kapoor & Viraraghaven 1997). The difference between the spectra, therefore was probably due to the higher amount of protein found in *U. lactuca* in Feb/Mar (25.13 % dry weight) compared to May/Jun (8.76% dry weight). Also the peak at 1537 cm<sup>-1</sup>, which refers to the secondary amide stretch (Sheng *et al.* 2004), was bigger in the Feb/Mar spectrum.

The band at ~1428 cm<sup>-1</sup> refers to symmetrical carboxylate stretching (Sheng *et al.* 2004). The band at ~ 1240 cm<sup>-1</sup> was assigned to the S=O sulphate ester stretch (Gómez-Ordóñez & Rupérez 2011). This arose from the sulphated polysaccharides ulvan found in *Ulva* sp. (Lahaye & Robic 2007). Pereira *et al.* (2009) suggested that this peak may be correlated to the sulphate content of the sample, and this was in agreement with the fact that the peak seen in *U. lactuca* was bigger than that seen in *P. palmata* (0.7% vs 5.7% sulphur) (Pereira *et al.* 2009).

The band at 1160 cm<sup>-1</sup> represented sulphonate groups associated with fucoidans in brown seaweeds and carrageenans in red (Murphy *et al.* 2007). Green seaweed polysaccharides may also be highly sulphated (Lobban & Harrison 1996). Peaks from 905-805 cm<sup>-1</sup> referred to C-O-SO<sub>3</sub> stretching of sulphate groups of polysaccharides with different substitution patterns (Pereira *et al.* 2009). Note that the spectra showed the peaks seen in a typical ulvan spectra at ~ 850 and 790 cm<sup>-1</sup> (Robic *et al.* 2008) which are not present in the spectra of *F. vesiculosus* or *P. palmata*. This confirmed the presence of ulvan in these samples. The peak at about 610 cm<sup>-1</sup> may be assigned to the sulphate stretch (Naja *et al.* 2005).

In *U. lactuca* sulphate, carboxylate, hydroxyl, and ester groups were found, reflecting the ulvan content of the seaweed. Its high protein content was also observed by the

presence of the amide groups seen in the spectra. This is in agreement with total protein contents presented earlier in Section 2.3.2.



## 2.4 Conclusions

ICP-OES quantified the amount of sulphur and phosphorus in the seaweed biomass. Kjeldahl determination of protein gave the total protein present in the seaweed. Sulphur content was found to be unchanged seasonally, with *P. palmata* containing the least (0.71 and 0.73 % dry mass in May/Jun and Feb/Mar, respectively), followed by *F. vesiculosus* (2.61 and 2.72 % dry mass in May/Jun and Feb/Mar, respectively) and then *U. lactuca* (5.70 and 4.87 % dry mass in May/Jun and Feb/Mar, respectively). The sulphur content was linked to sulphated polysaccharides, present as sulphated xylans in *P. palmata* (Deniaud, Quemener, *et al.* 2003), fucoidans in *F. vesiculosus* (Gómez-Ordóñez & Rupérez 2011) and ulvans in *U. lactuca* (Lahaye & Robic 2007). The sulphur content is also linked to sulphur containing amino acids (namely cysteine) and glutathione. These have both been shown to form complexes with metals (Vasconcelos & Leal 2008; Vasconcelos *et al.* 2002; Vasconcelos & Leal 2001). Only one seasonal study on the sulphur content of seaweeds could be found in the literature. This study examined the brown seaweed *F. vesiculosus*, and it also concluded that there were no significant seasonal fluctuations, supporting the results found here (Villares *et al.* 2013).

Phosphorus content was found to change seasonally in agreement with the seasonal fluctuations seen by other authors (Villares *et al.* 1999; Martinez & Rico 2002). Higher levels were found in Feb/Mar and lower levels in May/Jun. *F. vesiculosus* (0.15 and 0.24 % dry mass in May/Jun and Feb/Mar, respectively) and *U. lactuca* (0.15 and 0.27 % dry mass in May/Jun and Feb/Mar, respectively) contained the least, and *P. palmata* contained the most (0.22 and 0.44 % dry mass in May/Jun and Feb/Mar, respectively). Interaction of P and metal has rarely been discussed in the literature. Interestingly, one study showed that Cr(VI) was bound to a mixed microbial biofilm as Cr(III)-Phosphate complex (Nancharaiah *et al.* 2010).

Protein content also showed a seasonal trend for *U. lactuca* and *P. palmata* with higher levels seen in Feb/Mar than in May/Jun. *U. lactuca* and *P. palmata* had the highest levels in Feb/Mar (25.1 and 24.8 % dry mass, respectively), which then fell to 8.8 and 12.6 %, respectively, in May/Jun. *F. vesiculosus* contained 13.2 and 16.56 %

protein in May/June and Feb/Mar, respectively, but the error seen suggested no real difference in protein content.

Both P and N (or protein) content has been shown to be connected to growth in seaweeds. A study of *Ulva* spp. in Spain showed maximums in winter and minimums in spring and summer for both elements. This is because the seaweed stores nutrients over the winter during low growth, which are then used in growth during spring and summer, causing the low in concentration (Villares *et al.* 1999). This has also been shown in *P. palmata* (Martinez & Rico 2002). In *F. vesiculosus*, no significant seasonal changes were found in N content (although a non-significant low in May/June was found). One year long study with monthly sampling did find a high in N in winter and low in summer for the two brown seaweeds, *F. vesiculosus* and *A. nodosum* (Villares *et al.* 2013). The lack of a significant difference may be due to the month of sampling.

These analyses gave quantitative information on the P, S and protein content of the seaweeds. FTIR then allowed the determination of the functional groups present. Differences in the FTIR spectra between the seaweed species could clearly be seen. Seasonal differences were found in the spectra of *P. palmata* and *U. lactuca* due to increased protein levels. Amide bands in both summer and winter spectra of *F. vesiculosus* remained the same, as did the total protein content found by Kjeldahl. This is the first time seasonal differences in the FTIR spectra of seaweed have been shown. No seasonal changes in sulphate stretching bands were seen. This would be expected as sulphur content remained unchanged seasonally according to ICP-OES determination.

Combining all the analysis, the functional groups shown to be present in the seaweed which can affect metal binding were ester sulphate groups, carboxylate and hydroxyl groups from polysaccharides. Amide groups from proteins were also seen. There was some evidence for the presence of phosphorus containing groups, such as phosphorus containing polysaccharides, or phosphorus containing glycoproteins.

Chapter 3. Biomonitoring  
and the Use of Metal  
Pollution Indices

### 3.1 Introduction

The use of living organisms as biomonitors is gaining popularity in recent years. It has many advantages over more traditional methods of directly analysing sediment, soil or water which will only give total pollutant content. The use of a biomonitor organism will give information on the concentration of the pollutant which is bioavailable (Zhou *et al.* 2008). Seaweeds have been used widely in biomonitoring studies. Morrison *et al.* (2008) carried out the first study of its kind in Ireland investigating polluted and unpolluted sites across the country. It was found that *Ascophyllum nodosum* was a suitable biomonitor for heavy metals (Morrison *et al.* 2008).

#### 3.1.1 Environmental Monitoring and Biomonitoring

The metals studied in this chapter are Cd, Cr, Co, Cu, Mn, Ni, and Zn. These metals and environmental directives associated with them are discussed in Section 1.3 in more detail. Chromium is of particular significance in the Suir Estuary due to a tannery operation located in Portlaw which operated from 1935 to 1985 (Portlaw I.C.A. 2012).

In 2010 the Irish Marine Institute published assessment criteria for metals in seawater in order to allow classification of pollution in water bodies (Table 3.1). These are based on a combination of Directives 2008/156/EC and SI 272. Directives for shellfish farming areas were used where there were gaps in the directives for certain metals. The standard for Cr(VI) is used as none exists for total Cr. The rationale for this is that Cr(VI) is the most abundant form of Cr present in seawater, and that total Cr, rather than Cr(VI) is routinely determined in seawater (Marine Institute 2010).

**Table 3.1: Assessment criteria for metals in seawater used to classify good and less than good status of water bodies as compiled by the Marine Institute (Marine Institute 2010).**

Metal	Annual Average ( $\mu\text{g/L}$ )	Maximum Allowable ( $\mu\text{g/L}$ )
Cd	0.2 <sup>a</sup>	5 <sup>c</sup>
Cr	0.6 <sup>b</sup>	32 <sup>b</sup>
Cu	5 <sup>b</sup>	10 <sup>c</sup>
Mn	-	-
Ni	20 <sup>a</sup>	50 <sup>c</sup>
Zn	40 <sup>b</sup>	200 <sup>c</sup>

<sup>a</sup> WFD Priority substance AA/MAC-QS Dir 2008/105/EC

<sup>b</sup> WFD Relevant pollutant .AA/MAC-QS SI 272 of 2009

<sup>c</sup> Shellfish Waters Imperative values (MAC- QS) SI 268 of 2006

There are no standards for maximum allowable levels of pollutants in seaweeds.

However, the Marine Institute has published assessment criteria for shellfish as this is a human health concern. These standards are given in Table 3.2.

**Table 3.2: Assessment criteria for metals in shellfish used to classify good and less than good status as compiled by the Marine Institute (Marine Institute 2010).**

Metal	Shellfish Type	Maximum Allowable (mg/kg dry weight)
Cd	Mussel	5
	Oyster	5
Cr	Mussel and oyster	8
Cu	Mussel	40
	Oyster	330
Mn	-	-
Ni	Mussel and oyster	5
Zn	Mussel	320
	Oyster	7070

Note: These are proposed values for the SWD (Shellfish Water Directive) and have no legislative basis at present.

The lack of directives for seaweed is a concern, as seaweed is increasingly being harvested for human consumption, as targeted by the Sea Change Strategy. This sets a target of increasing seaweed industry turnover from 18 to 30 million euro by 2020 (Walsh & Watson 2011). France is the only European country to have legislated for metal levels in seaweed. They are as follows: Pb 5 mg/kg, Cd 0.5 mg/kg, Hg 0.1 mg/kg and inorganic As 3 mg/kg dry weight (Besada *et al.* 2009). Coupled with the issue of consumption is the ease with which seaweed can be analysed for the bioavailable metal fraction in water, which makes biomonitoring of seaweed attractive from an environmental, as well as a human health viewpoint. Typical levels of metals found in seaweeds will be discussed in this chapter. This will act as a guide to levels of metal to be expected in unpolluted and polluted areas.

### 3.1.2 Metal Pollution Indices

The Metal Pollution Index or MPI is a useful method to compare total metal loads between sites in order to allow classification of sites as polluted or unpolluted (Giusti 2001; Chaudhuri *et al.* 2007). It was developed by Tomlinson and Wilson (1980) to facilitate useful interpretation of biomonitoring data (Tomlinson & Wilson 1980).

The Pollution Load Index (PLI) is a variation of the MPI which uses the lowest metal value found in the study as a baseline. Values vary from 0 (unpolluted) to 10 (highly polluted) and give an indication to the environmental state of the site (Chaudhuri *et al.* 2007; Zhang *et al.* 2011). The PLI calculated may be interpreted using the following guide. PLI values between 0 and 1 indicate an unpolluted area, 1-2 unpolluted to moderate pollution, 2-3 moderate pollution, 3-4 moderate to high pollution, 4-5 high pollution, >5 severely polluted (Zhang *et al.* 2011).

There are many examples of its application to soil and sediment biomonitoring in the literature (Cabrera *et al.* 1999; Chan *et al.* 2001; C. Zhang *et al.* 2011), but instances of its use in seaweed (and indeed any biota) are less common. The following papers give examples of use in plants and seaweeds (Sanchez *et al.* 1998; Giusti 2001; Chaudhuri *et al.* 2007).

The calculation of MPI and PLI values will be discussed in more detail in Section 3.2.4.

### 3.1.3 Objectives

The objectives of this chapter are to:

- Determine the levels of Cd, Co, Cu, Cr, Mn, Ni, and Zn in two brown seaweed species, *F. vesiculosus* and *A. nodosum*, in several sites with varying levels of industrialisation / population in Newfoundland and Ireland.
- Determine if these seaweeds can be used as model species to determine the state of pollution in the respective areas. Metal pollution indices which have not been commonly applied to seaweeds will be used and discussed.
- Compare these values to levels found by other researchers, and suggest the levels of these metals which may be of concern.

## 3.2 Experimental

### 3.2.1 Site Locations

Seaweed was sampled in Bonne Bay and the Humber Arm, Newfoundland, Canada (Figure 3.1 and 3.2), and in the Suir estuary in Ireland (Figure 3.3). These sites were chosen to represent varying levels of salinity (from freshwater mixing areas to fully saline environments) and pollution. GPS coordinates are given in Table 3.1.

**Table 3.1: GPS coordinates of sites. Sites 1-5 Bonne Bay, 6-10 Humber Arm and 11-14 Suir Estuary**

Site Number	Coordinates	
1	49° 34.205' N	57° 55.431' W
2	49° 29.182' N	57° 55.509' W
3	49° 30.690' N	57° 52.392' W
4	49° 30.282' N	57° 48.427' W
5	49° 28.965' N	57° 44.286' W
6	49° 06.229' N	58° 21.703' W
7	49° 02.174' N	58° 08.694' W
8	48° 58.457' N	58° 03.704' W
9	48° 57.920' N	58° 00.903' W
10	48° 47.898' N	57° 55.906' W
11	52° 15.606' N	07° 06.223' W
12	52° 15.479' N	07° 04.193' W
13	52° 16.303' N	06° 59.783' W
14	52° 14.417' N	06° 58.466' W

#### 3.2.1.1 Bonne Bay

Bonne Bay is located in the west of Newfoundland, in Gros Mourne National Park (see Figure 3.1). Gros Mourne is a Canadian national park and a UNESCO world heritage site. None of the rivers which flow into Bonne Bay pass major residential or industrial areas.



*Site 1: Salmon Point (near Rocky Cove)*

Rocky Cove is a series of residential areas located at the mouth of Bonne Bay, between Salmon Point in the south and Lobster Cove in the North. The population is about 1000, and fishing is the main activity in the area. The actual sampling site is on the south side of Salmon Point, away from the population centre. The substrate is rocky, and *Ascophyllum nodosum* grows abundantly here.

*Site 2: Winter House Brook (near Woody Point)*

Woody Point is small town consisting of Winter House Brook, Curzon Village, and Woody Point. It has population of 350. A fishing wharf is located here where fish are processed and boats are serviced. The seaweed was sampled directly adjacent to where this activity occurs.

*Site 3: Gadd's Harbour*

Gadd's Harbour is an uninhabited area, located across the water from Norris's Point, where the Bonne Bay Marine Station is located. It has a small sandy beach with rocky outcroppings. Ice scouring in 2006 severely reduced the seaweed population here, but the two brown seaweeds, *A. nodosum* and *F. vesiculosus* were available at the time of sampling.

*Site 4: Unnamed location, Bonne Bay*

This is a rocky site with no population centre or any other known local pollution source. The rocky substrate is covered with furoid beds, with abundant *A. nodosum* and *F. vesiculosus*.

*Site 5: Unnamed location (near Seal Cove)*

Seal Cove is an uninhabited area with no known current pollution source. However, a severe oil spillage occurred at this site in 1999, with 40,000 L of oil lost. Most of the *A. nodosum* at the site had to be removed to facilitate the clean up, and the population is still recovering from this damage.



**Figure 3.1: Bonne Bay Sites in Newfoundland, Canada (1-5).**

### ***3.2.1.2 Humber Arm***

The Humber Arm is located in Eastern Newfoundland. The river Humber flows into the Humber Arm Estuary and then on into the Gulf of St Lawrence. The river Humber passes the small towns of Pasadena, and Deer Lake, but the rest of its course has no major industrial or residential areas. Corner Brook located in the Humber Arm is the largest population centre (about 20,000). The outer area of the estuary is called the Bay of Islands.

#### *Site 6: Lark Harbour, Bay of Islands*

Lark Harbour is a low population fishing community located in the Bay of Islands.

#### *Site 7: Unnamed location, Humber Arm*

No known pollution source, and no area of high population in this region.

#### *Site 8: Cook's Cove*

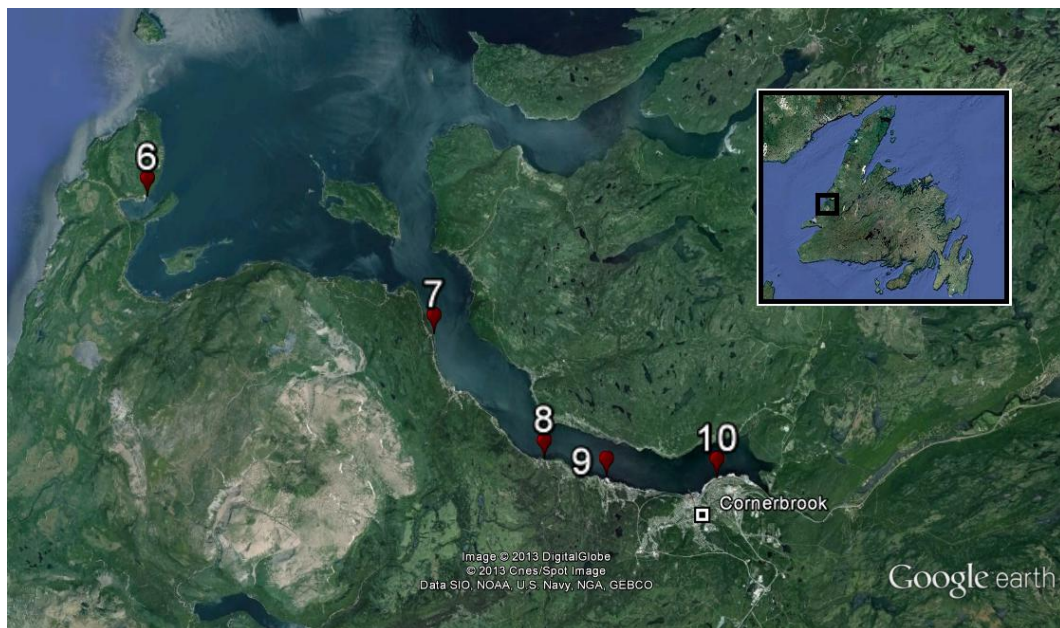
Cook's Cove is a sparsely populated area with no industrial activity.

#### *Site 9: Soper's*

Soper's is a sparsely populated community with no industrial activity.

*Site 10: Corner Brook*

Corner Brook is the major population and industrial centre in western Newfoundland (population 20,000). The major industry is a paper mill. Although paper mills commonly use Fe, Cu and Mn to catalyse hydrogen peroxide bleaching of pulp, Corner Brook mill appears to use a thermal mechanical method of pulping (NL Department of Environment and Conservation 2013). This is a low salinity site, due to the large influx of water from the Humber river close by.



**Figure 3.2: Humber Arm Sites in Newfoundland, Canada (6-10).**

*3.2.1.3 Suir Estuary*

The Suir Estuary is located in the south east of Ireland. The major population centre is Waterford (about 50,000). The river Suir flows through several other population centres, notably Clonmel (population: 16,000 / 47 km from Waterford) and Carrick on Suir (population: 6,000 / 32 km from Waterford). Additionally, just past Waterford city is the confluence of the Suir, the Nore and the Barrow. The river Nore runs through Kilkenny (population: 25,000 / 65 km from Waterford), and the Barrow flows through Athy (population: 10,000 / 110 km from Waterford), Carlow (population: 23,000 / 80 km from Waterford) and New Ross (population: 8000 / 28 km from Waterford).

*Site 11: St. John's River*

St John's river is a tributary of the river Suir and is located within the city centre. It has received waste from housing estates in the past, as well as hotels and other businesses. The Lisduggan stream of St. John's River has received effluent from Waterford Industrial estate. A scheme put in place in 2010 in partnership with the factories located here has reduced this contamination (Waterford City Council 2011). The seaweed present here has only man-made structures for substrate. Only *F. vesiculosus* could be sampled.

*Site 12: Ferrybank*

Ferrybank is a residential community on the north bank of the river Suir. The site itself was located outside of the main residential area.

*Site 13: Cheekpoint*

Cheekpoint is a village located near the confluence of the Suir, the Nore and the Barrow. It is located directly opposite the Great Island power station, which is an oil burning power station. The site was silty, and seaweeds used rocks and walls for holdfasts.

*Site 14: Passage east*

Passage east is a small village, which operates a car ferry to Ballyhack in Co. Wexford. The sampling site was adjacent to the car ferry ramp.



**Figure 3.3: Suir estuary sites in Waterford, Ireland (11-14).**

### 3.2.2 Sampling, Storage and Drying

Whole plant samples were collected randomly by hand and placed in resealable plastic bags and placed in a cool box for transportation to the lab. Sampling was carried out from the 3-16 October 2007 in Canada, and from 30-31 October 2007 in Ireland. *Fucus vesiculosus* and *Ascophyllum nodosum* were collected from all sites except site 10 in the Bay of Islands area and site 11 in the Suir Estuary, where only *Fucus vesiculosus* was present.

Water samples were collected in non-sterile nalgene bottles in Canada and in non-sterile polyethylene containers in Ireland. They were frozen at  $-20\text{ }^{\circ}\text{C}$  as soon as possible. Conductivity, pH and temperature readings were taken on site by lowering the probes a couple of centimetres below the water's surface. All readings were taken in triplicate. Where it was not possible to take a reading in triplicate, e.g., conductivity at a fresh water inlet, maximum and minimum readings were taken and the quoted value is the midpoint of these. All measurements and sampling were carried out approximately within an hour of low tide.

The seaweed was washed once with tap water and once with distilled water, making sure that all visible epiphytes were removed. Unhealthy specimens were discarded. Three samples from 3 different plants for each species was taken and frozen ( $-20\text{ }^{\circ}\text{C}$ )

for later analysis. Prior to analysis, the seaweeds were dried at 60 °C for 24 h, and ground using a mortar and pestle or mill, if necessary (Ryan *et al.* 2012).

### 3.2.3 Metal Analysis by ICP-OES

Seaweed samples were digested by microwave acid digestion using the procedure detailed in Section 2.2.2.1. Metals were analysed by ICP-OES using the procedure in Section 2.2.2.2, with the following modifications. Wavelengths for analysis were as follows: Cd 214.439, Co 238.892, Cu 327.395, Cr 267.716, Mn 257.610, Ni 231.604, and Zn 213.857 nm. Seawater analysis was verified by the use of LGC Estuarine Water Reference Material 6016. Seaweed analysis was verified by the use of Tomato Leaf Reference Material 1573a obtained from NIST.

### 3.2.4 Calculation of Metal Pollution Indices

The MPI (Metal Pollution Index) was calculated as follows (Giusti 2001; Chaudhuri *et al.* 2007):

$$\text{MPI} = (C_1 \times C_2 \times C_3 \dots \times C_n)^{1/n} \quad \text{Eq. 3.1}$$

where  $C$  is the concentration of metal  $n$  in mg/kg

The PLI (Pollution Load Index) is calculated as follows (Chaudhuri *et al.* 2007; Zhang *et al.* 2011)

$$\text{PLI} = (CF_1 \times CF_2 \times CF_3 \dots \times CF_n)^{1/n} \quad \text{Eq. 3.2}$$

where  $CF$  is the concentration of metal  $n$  in the seaweed divided by the baseline or lowest concentration of metal  $n$  found in the study (mg/kg).

### 3.3 Results and Discussion

#### 3.3.1 Seawater Analysis

Shown in Table 3.2 are the readings taken for conductivity, pH and temperature. The conductivity varied at fresh water input sites and is more constant in areas further out to sea. The pH was relatively constant and the conductivity dropped significantly only at site 10 which is the inlet to the river Lomond (Figure 3.1). The water temperature dropped significantly from earlier to the later dates in October at the Canadian sites. As expected, water temperatures in Ireland were higher.

**Table 3.2: Conductivity, pH and Temperature readings for all sites. Readings taken in triplicate. Site 1-5 refers to Bonne Bay, 6-10 Bay of Islands and 11-14 the Suir Estuary.**

Site Number	Date	Conductivity mS/cm	pH	Temperature °C
1	11/10/07	45.8	8.1	9.4
2	11/10/07	39.7	8.1	8.8
3	11/10/07	44.5	8.2	10.9
4	11/10/07	42.0	8.2	10.7
5	11/10/07	39.7	8.3	10.8
6	16/10/07	43.3	8.1	6.9
7	16/10/07	45.3	8.1	6.6
8	03/10/07	14.6	8.4	12.8
9	03/10/07	15.9	8.0	12.5
10	03/10/07	6.4	7.6	12.4
11	31/10/07	25.3	8.2	12.5
12	31/10/07	30.9	8.2	12.7
13	31/10/07	42.9	8.3	13.1
14	30/10/07	34.7	7.8	13.0

The limit of detection (LOD) and limit of quantitation (LOQ) for metals were calculated based on artificial seawater blanks using the following method (Gustavo González & Ángeles Herrador 2007) (Table 3.3).

LOD = Mean blank concentration + 3 x Standard deviation of blank

LOQ = Mean blank concentration + 10 x Standard deviation of blank

**Table 3.3: LOD and LOQ for metal analysis in seawater.**

Element and Wavelength (nm)	LOD and LOQ in µg/L	
	LOD	LOQ
Cd 214.439	0.38	1.12
Co 238.892	2.04	6.30
Cr 267.716	1.49	4.01
Cu 324.754	2.08	5.68
Mn 257.610	9.91	29.65
Ni 231.604	0.96	2.60
Zn 213.857	5.93	16.91

An estuarine water standard reference material containing all the metals studied at levels allowing their analysis using this ICP-OES method was not available. LGC 6016 had certified values of Cd, Cu, Mn, and Ni and an indicative value for Zn. Good recoveries were seen for all the certified values (93-101 %). Zn recovery was low at 73 % of the indicative value (Table 3.4).

**Table 3.4: Comparison of certified/indicative values for metals in seawater standard LGC 6016 and those found by analysis.**

Metal	Certified <sup>a</sup> / Indicative value <sup>b</sup> (µg/L)	Found (µg/L)
Cd	101 ± 2 <sup>a</sup>	102 ± 6
Cu	190 ± 4 <sup>a</sup>	178 ± 10
Mn	976 ± 31 <sup>a</sup>	904 ± 36
Ni	186 ± 3 <sup>a</sup>	185 ± 12
Zn	55 <sup>b</sup>	41 ± 4

Uncertainty calculated as 95 % confidence intervals. No errors were specified on certificate for indicative values.

All samples analysed were below the limit of quantitation, and most were below the limit of detection. Samples from Bonne Bay and Waterford were analysed first on the



hypothesis that these would be the least and most polluted sites, respectively. The results found are shown in Table 3.5.

**Table 3.5: Results of seawater analysis (all  $\mu\text{g/L}$ ).**

Site		Cd	Co	Cr	Cu	Mn	Ni	Zn
1	BB	<0.4	<2.0	<1.5	<2.1	<9.9	1.4 $\pm$ 0.6	<5.9
2	BB	0.5 $\pm$ 0.2	<2.0	<1.5	<2.1	<9.9	3.1 $\pm$ 0.7	<5.9
3	BB	0.5 $\pm$ 0.1	<2.0	<1.5	<2.1	<9.9	1.5 $\pm$ 1.0	<5.9
4	BB	0.5 $\pm$ 0.1	<2.0	<1.5	<2.1	<9.9	1.6 $\pm$ 1.3	<5.9
5	BB	0.4 $\pm$ 0.1	<2.0	<1.5	<2.1	<9.9	1.7 $\pm$ 0.5	<5.9
11	St J	0.5 $\pm$ 0.3	<2.0	<1.5	<2.1	<9.9	1.6 $\pm$ 1.6	<5.9
12	FB	0.5 $\pm$ 0.1	<2.0	<1.5	<2.1	<9.9	2.0 $\pm$ 0.6	<5.9
13	CP	0.5 $\pm$ 0.1	<2.0	<1.5	<2.1	<9.9	2.1 $\pm$ 1.7	<5.9
14	PE	0.5 $\pm$ 0.2	<2.0	<1.5	<2.1	<9.9	2.0 $\pm$ 0.3	<5.9
	LOD	0.4	2.0	1.5	2.1	9.9	0.9	5.9

As all the levels of heavy metals were low, and most metals did not give information beyond being below the limit of detection, it was decided not to analyse samples from Corner Brook.

Mean cobalt concentrations in seawater have been reported to be less than 1  $\mu\text{g/l}$  (Kim *et al.* 2006).

The limit for heavy metals in tidal waters according to the EU Commission's Advisory Scientific Committee on Toxicity, Ecotoxicity and the Environment (SCTEE) (Clenaghan *et al.* 2006) are given in Table 3.6.

**Table 3.6: Heavy metal limits in tidal waters (Clenaghan *et al.* 2006)**

<b>Metal</b>	<b>Limit in <math>\mu\text{g/L}</math> in tidal waters</b>
Arsenic	20
Chromium	15
Copper	5
Lead	5
Nickel	25
Zinc	40

The results found in this study are in agreement with the outcome of monitoring by the Irish EPA. Of 17 sites monitored in the Waterford and Wexford area by the EPA none were found to be non compliant with this standard. These sites include rivers, lakes and tidal waters. In Ireland as a whole most areas were found to be compliant with these standards. The areas that were non compliant were mostly attributed to either past industrial sources such as mines or tanneries or natural, geological sources (Clenaghan *et al.* 2006).

### 3.3.2 Seaweed Analysis

The limit of detection and limit of quantitation were calculated based on blank digestions as in Section 3.3.1. They are shown in Table 3.7.

**Table 3.7: LOD and LOQ for seaweed analysis, units are  $\mu\text{g/L}$ .**

<b>Metal and wavelength</b>	<b>LOD</b>	<b>LOQ</b>
Cd 214.439	1.2	3.6
Co 238.892	1.11	3.71
Cr 267.716	7.3	13.5
Cu 327.395	3.8	9.6
Mn 257.610	2.5	4.1
Ni 231.604	5.6	13.9
Zn 213.857	18.3	52.5

Standard reference material recoveries are presented in Table 3.8. The average metal recovery was 83 %.

**Table 3.8: Comparison of certified values for metals in Tomato Leaf Standard NIST 1573a and those found by analysis.**

Metal	Certified value (mg/kg)	Found (mg/kg)
Cd	1.52 ± 0.04	1.25 ± 0.06
Co	0.57 ± 0.02	0.41 ± 0.09
Cu	4.70 ± 0.14	3.97 ± 0.08
Cr	1.99 ± 0.06	1.57 ± 0.08
Mn	246 ± 8	201 ± 6
Ni	1.59 ± 0.07	1.45 ± 0.29
Zn	30.9 ± 0.7	27.0 ± 0.7

Uncertainty calculated using 95 % confidence intervals.

Error bars are based on triplicate samples with 95% confidence intervals. In the graph legends of the biomonitoring results, AN refers to *Ascophyllum nodosum*, FV refers to *Fucus vesiculosus*.

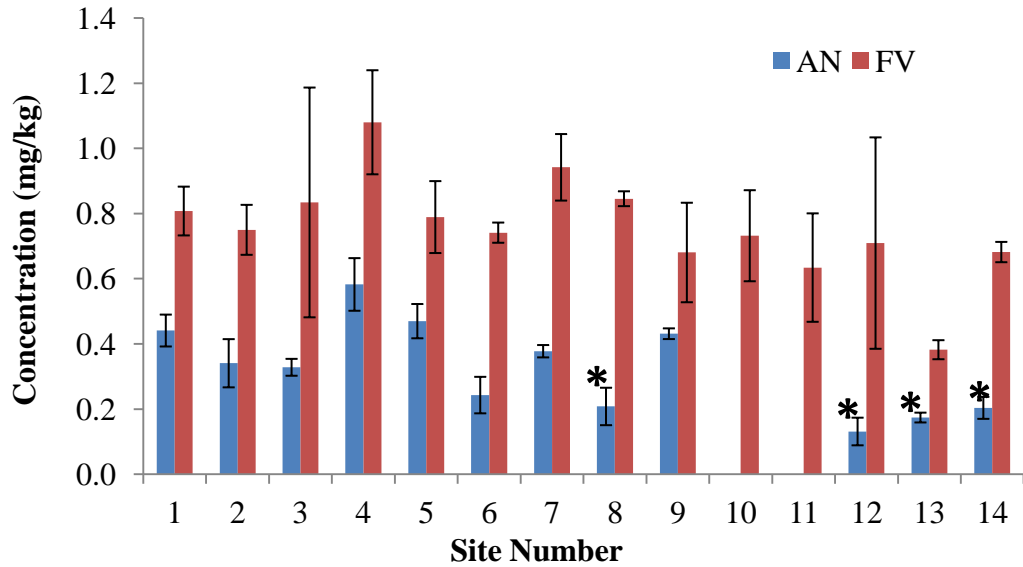
To choose suitable studies to compare results, the following reasoning was used. Studies which used whole plants were discussed where possible, as the growing tips of the plants have been exposed to seawater for what may be a significantly shorter period of time. This means that metal levels in whole plants may be significantly higher than the tips (Stengel *et al.* 2005). *Ascophyllum nodosum* and *Fucus vesiculosus* show seasonal growth, which is lowest in autumn and winter and highest in spring and summer (Sharp 1995). For this reason studies which specified sampling periods between September-February are most important in this discussion. In the present study sampling was conducted in October. Only four directly comparable studies were found. Four more studies which were conducted in a similar fashion, but at different time periods during the year, were used for discussion. Other studies were used for comparison purposes.

### 3.3.2.1 Cadmium

Results for the Cd content of *F. vesiculosus* and *A. nodosum* are shown in Figure 3.3. It was seen that both seaweeds significantly biomagnified the level of metal observed in seawater. Cd in seawater was found to be  $<0.5 \mu\text{g/L}$  at all sites. The range seen goes from  $0.13 \text{ mg/kg}$  (below LOQ) in *A. nodosum* sampled from site 12 in Waterford, to  $1.08 \text{ mg/kg}$  in *F. vesiculosus* sampled at site 4 in Bonne Bay.

Cd is present as  $\text{Cd}^{2+}$  in seawater, and the concentration of the free ion is related to salinity as Cd forms chloride complexes in saline conditions (Engel & Fowler 1979). No relationship with salinity was found here. *F. vesiculosus* accumulated significantly higher concentrations of Cd than samples of *A. nodosum* from the same site. This may be due to a higher affinity of *F. vesiculosus* biomass towards  $\text{Cd}^{2+}$  ions.

Using the same sampling technique, Phaneuf *et al.* (1999) found an average of  $0.46 \pm 0.14$  and  $1.40 \pm 0.69 \text{ mg/kg}$  in *F. vesiculosus* and *A. nodosum*, respectively, sampled from 10 sites along the St Lawrence River and the Gulf of St. Lawrence (Phaneuf *et al.* 1999). These levels indicate that the estuaries studied here were slightly less polluted than the St Lawrence River and the Gulf of St Lawrence. Riget *et al.* (1995) studied Cd in *F. vesiculosus* from unpolluted Arctic waters in Greenland by sampling the growing tips only. Much higher levels of Cd were found ( $2.5 \text{ mg/kg}$  low in August and  $5 \text{ mg/kg}$  high in January) (Riget *et al.* 1995). An explanation may be the slow growing nature of seaweeds in Arctic water, allowing more time for the accumulation of metals, the existence of a pollution source not known to the authors, or the existence of high Cd levels in the geology of the area.



**Figure 3.3: Cadmium concentration in *A. nodosum* (AN) and *F. vesiculosus* (FV) at all sites. (An \* indicates that value is below LOQ but above LOD).**

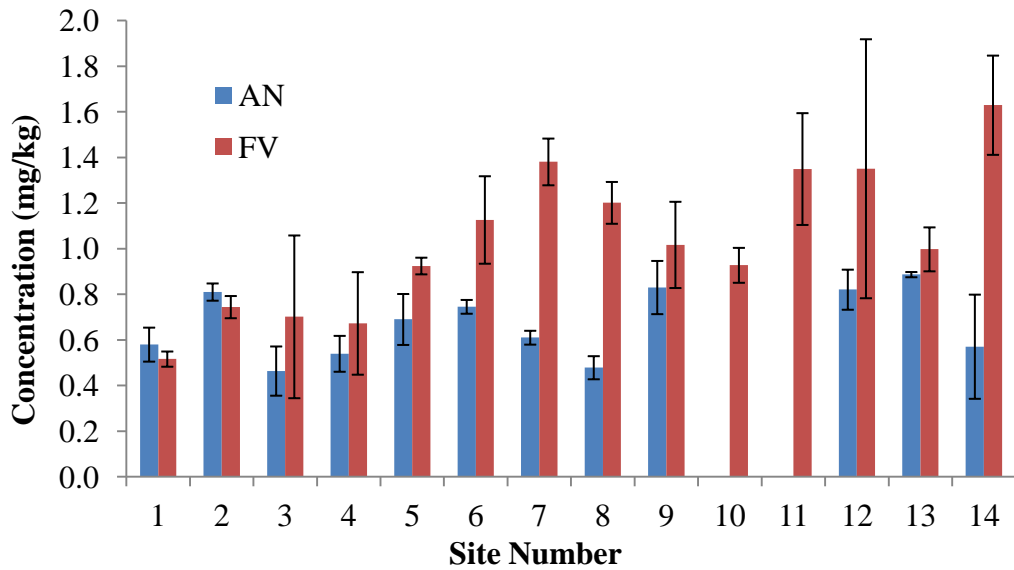
Morrison *et al.* (2008) found levels of 0.1-0.6 mg/kg in *A. nodosum* from several sites located across Ireland, which were chosen to include industrialised and pristine environments (Morrison *et al.* 2008). That is the same as the range found in this study, although it should be noted that only younger parts of the plant were sampled, and should therefore give a lower level of metal. This indicates that the sites analysed by Morrison *et al.* (2008) were probably slightly more polluted than those studied here.

### 3.3.2.2 Cobalt

The Co content of *F. vesiculosus* and *A. nodosum* from the various sites sampled is shown in Figure 3.4. The concentration of Co in the seawater tested was shown to be less than 2.0 µg/L in every case (Table 3.5), so a significant biomagnification of metal can be seen in the seaweeds.

In many cases *A. nodosum* and *F. vesiculosus* appeared to accumulate around the same amount of Co. There were a number of sites, however, where *F. vesiculosus* contained more Co. The main species of cobalt in seawater are cobalt carbonate ( $\text{CoCO}_3$ ) and free cobalt ion ( $\text{Co}^{2+}$ ) (Kim *et al.* 2006). *F. vesiculosus* appears to have a slightly higher affinity towards this divalent ion. Co is an essential metal and part of vitamin B12 structure. A vitamin B12 requirement has been shown in some brown

seaweed (Pedersén 1969), and it is possible that *F. vesiculosus* has a higher requirement for this, leading to greater Co uptake.



**Figure 3.4: Cobalt concentration in *A. nodosum* (AN) and *F. vesiculosus* (FV) at all sites.**

Using the same sampling technique used here, Phaneuf (1999) found an average of  $1.50 \pm 0.90$  mg/kg in *F. vesiculosus*, and  $0.69 \pm 0.36$  mg/kg in *A. nodosum* in the Gulf of St. Lawrence. This reflects the same pattern seen here, with slightly more metal accumulated by *F. vesiculosus*, and indicated a similar level of pollution in both estuaries (Phaneuf *et al.* 1999). Black (1952) found 0.70 mg/kg in *Fucus vesiculosus*, which was again similar to that seen in this study and indicated a low level of Co pollution at the site in Atlantic Bridge, Scotland (Black & Mitchell 1952).

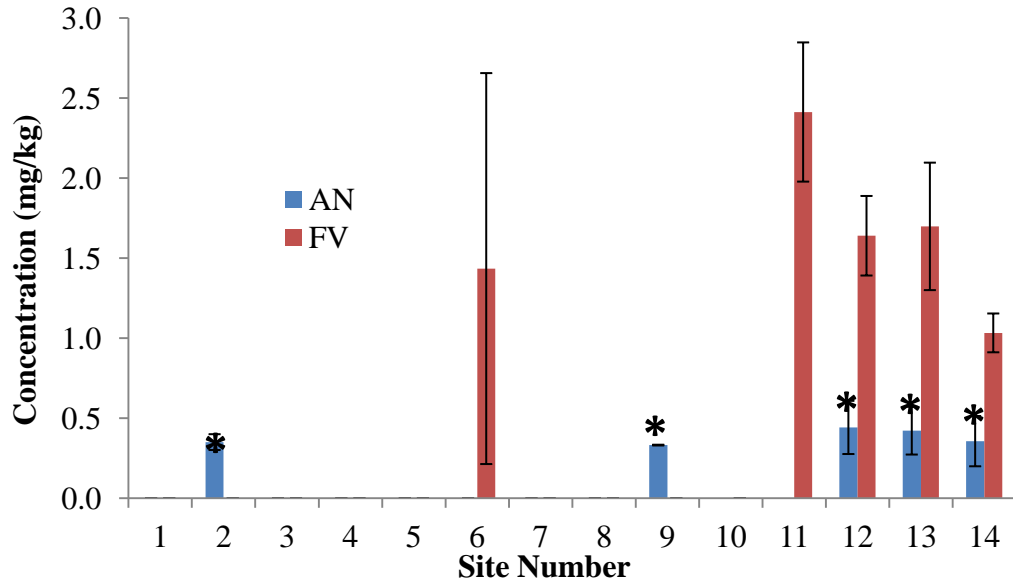
Levels of approximately 1.8 and 2.0 mg/kg were found in *F. vesiculosus* sampled from the North Sea and Baltic Sea, respectively. These whole plant samples were collected at two monthly intervals and homogenised to yield a composite sample. Higher metal concentrations were expected here, especially in the Baltic sea, due to higher anthropogenic inputs of metal (Jayasekera & Rossbach 1996).

### 3.3.2.3 Chromium

Chromium levels were mostly below the limit of detection (Figure 3.5). Significant biomagnification of metal in the seaweeds when compared to levels in seawater was again seen here, which were shown to be under 1.5 µg/L (Table 3.5).

*F. vesiculosus* accumulated significantly more Cr than *A. nodosum* in nearly all the sites where it could be detected. Cr in seawater is mostly present as  $\text{CrO}_4^{2-}$ . It is highly toxic and bioavailable due to its ability to cross biological membranes (Kotaś & Stasicka 2000).

The most significant finding here was the higher levels observed in the Waterford area (sites 11-14). This can be attributed to a historical point source of Cr pollution. A tannery operation located in Portlaw, located about 20 km upstream from Waterford city, closed in 1985 after 50 years of operation (Portlaw I.C.A. 2012). A reduction in Cr content can also be seen in the outermost sampling site (site 14). Site 2 in Bonne Bay is a boat service area which may explain the higher concentrations of chromium found in this area. The higher levels found in site 6 in the Bay of Islands area could not be readily explained. Although this was a much more industrialised area than Bonne Bay, this site on the outskirts of the sampling area was the furthest away from industrial or port activity. Elevated levels at site 9 in the Bonne Bay area were probably due to a paper mill located at this site. Dyes and pigments or the use of treated wood in production may have lead to the higher concentration found here (Clenaghan *et al.* 2006).



**Figure 3.5: Chromium concentration in *A. nodosum* (AN) and *F. vesiculosus* (FV) at all sites. (An \* indicates that value is below LOQ but above LOD).**

Levels of  $1.20 \pm 1.20$  and  $0.86 \pm 0.51$  mg/kg were found in *F. vesiculosus* and *A. nodosum* respectively, from the Gulf of St. Lawrence in Canada (Phaneuf *et al.* 1999). This result indicated the presence of several sites with Cr contamination levels similar to those seen here. Black (1952) found a concentration of 0.70 mg/kg in *F. vesiculosus* from a rural Scottish site (Black & Mitchell 1952).

The mean concentration of chromium found by Morrison *et al.* (2008) using *A. nodosum* across sites in Ireland, ranged from 0.054 to 1.071  $\mu\text{g/g}$  (different sampling method used). This indicated some sites with high Cr levels. These levels were thought to be related to the geology of the area rather than anthropogenic loading, due to the remote location of some of the sites in question (Morrison *et al.* 2008).

Comparing the levels of Cr found in Waterford with those found by other researchers indicated that levels of Cr pollution were not significantly elevated, but the identification of an historical pollution source was possible.

#### 3.3.2.4 Copper

Cu concentrations in *F. vesiculosus* and *A. nodosum* are shown in Figure 3.6. An inset graph is also presented to allow lower concentration sites to be more easily seen. The



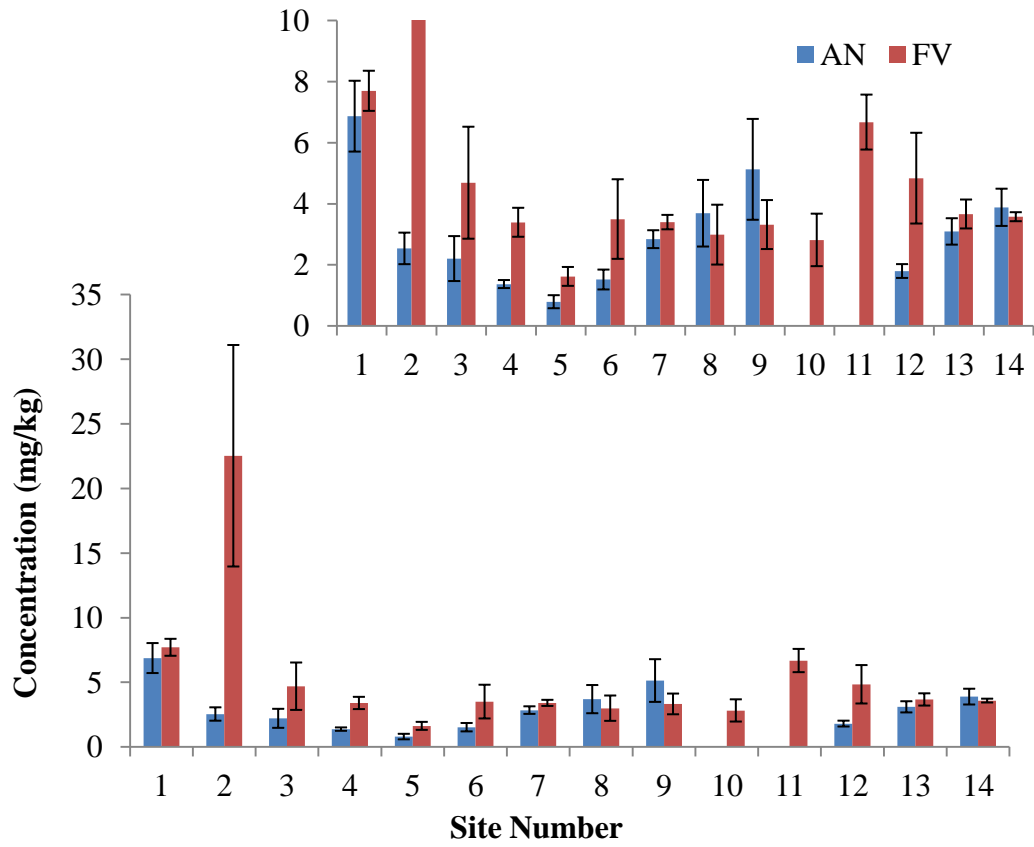
seaweeds significantly biomagnified Cu levels from seawater, where levels less than 1.5 µg/L were observed (Table 3.5).

The difference in uptake between *F. vesiculosus* and *A. nodosum* did not appear to be significant in most cases, with the notable exception of Site 2 in Bonne Bay, where *F. vesiculosus* contained significantly more.

Cu is present in seawater as Cu<sup>2+</sup> ions and ligands (Kozelka & Bruland 1998). Copper is widely used in algicides and paints which are used on boats. Mining is another key anthropogenic source (Cornelis *et al.* 2005). None of the sites here are affected by mining, but most are located in the vicinity of ports and jetties. Site 2 in Bonne Bay is a boat service area which explains the very high concentration of copper found in this area. The lower concentration at site 5 in Bonne Bay probably reflects the fact that the lowest amount of boating activity occurred in this area.

The results of Stengel (2005) add evidence with the assertion that Cu levels are related to boating activity (study using whole plants). In that study, 1.3 and 3.5 mg/kg were found in *F. vesiculosus* in a unpolluted and polluted Irish site, respectively, and 1.0 and 7.0 mg/kg in *A. nodosum* in a unpolluted and polluted site, respectively (Stengel *et al.* 2005).

Riget *et al.* (1995) studied Cu concentration in the growing tips of *F. vesiculosus* from an unpolluted site in Greenland. A 1.5 mg/kg low in August and 2.8 mg/kg high in January was observed (Riget *et al.* 1995). This result is lower than seen in this study, and probably reflected an increase in Cu pollution at sites in Bonne Bay, Cornerbrook and Waterford compared to this site in Greenland. Note however that only growing tips were sampled in Riget's study, which should give a lower metal value, due to lower water contact time than older plant parts.

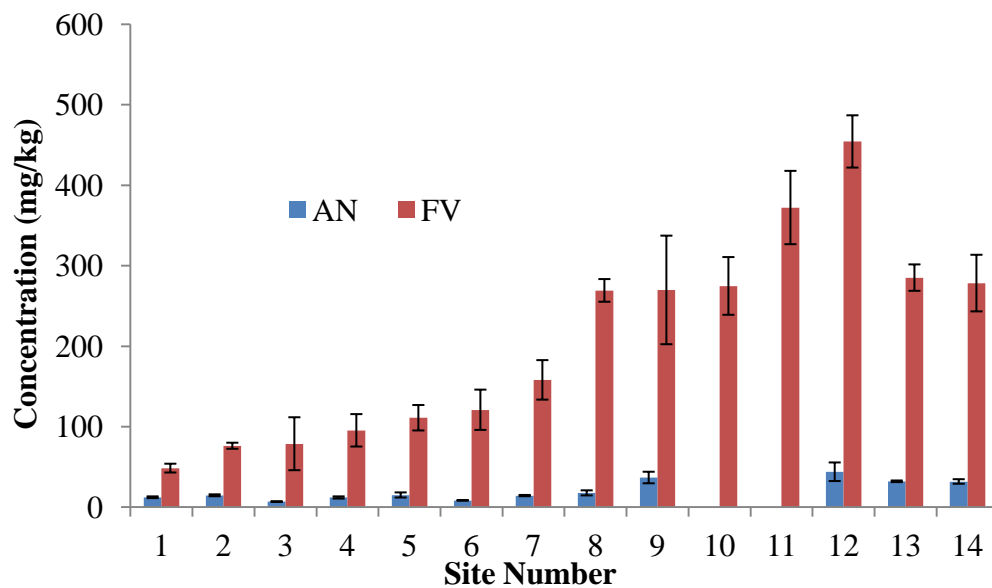


**Figure 3.6: Copper concentration in *A. nodosum* (AN) and *F. vesiculosus* (FV) at all sites, inset at a smaller concentration scale to show lower concentration sites.**

### 3.3.2.5 Manganese

The concentration of Mn in *F. vesiculosus* and *A. nodosum* is shown in Figure 3.7. Significant biomagnification of seawater Mn levels was seen (Table 3.5). *F. vesiculosus* accumulated significantly more Mn than *A. nodosum*.

Mn is an essential trace nutrient for seaweeds, and it has been found at concentrations of 130 to 735 mg/kg in unpolluted areas (Howe *et al.* 2004). All of the sites studied fell within this range. Its anthropogenic sources include wastewater, sewage sludge, the burning of fossil fuels and fuel additives. All of these are related to population and industrialisation. A relationship between urbanisation of an area and concentration can be seen in Figure 3.7, with Bonne Bay having lower metal loadings, Humber Arm loadings increasing with decreasing distance to the centre of population (Corner Brook), and Waterford concentrations being highest in the two most populated sites.



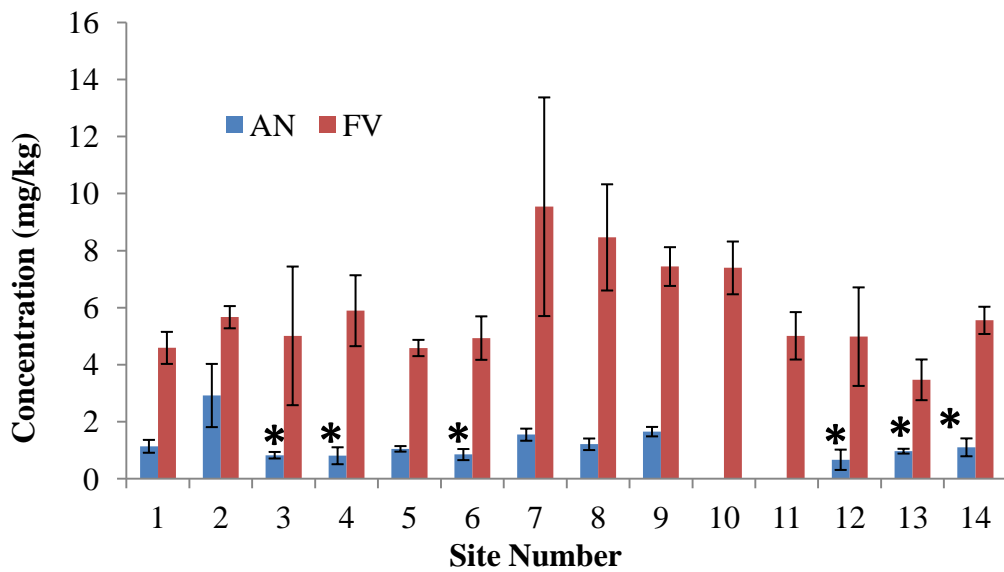
**Figure 3.7: Manganese concentration in *A. nodosum* (AN) and *F. vesiculosus* (FV) at all sites.**

Phaneuf (1999) found an average of  $158 \pm 101$  mg/kg in *F. vesiculosus*, and  $19.1 \pm 8.3$  mg/kg in *A. nodosum* across 10 sites in the Gulf of St. Lawrence. (Phaneuf *et al.* 1999). These results are higher than most of the Bonne Bay sites, but lower than most of the sites in the Humber arm and Waterford. This probably reflects the level of population in the sampling areas.

### 3.3.2.6 Nickel

The biomagnification of Ni levels by the seaweeds was significant, with seawater containing a maximum level of 3.1  $\mu\text{g/L}$  (Table 3.5). In the marine environment Ni is present as  $\text{Ni}^{2+}$ . *F. vesiculosus* was found to accumulate more Ni than *A. nodosum* (Figure 3.8), indicating that *F. vesiculosus* had a higher affinity for this ion.

In a highly polluted area (the Severn Estuary in the UK), nickel concentrations in *Fucus serratus* were found to range from 20 - 90  $\mu\text{g/g}$  (Martin *et al.* 1997). Although *F. serratus* is similar to *F. vesiculosus* a direct comparison cannot be made. Mature thalli were used in this study, which would make the study reasonably comparable to the present one. This would indicate that the sites studied here were generally less polluted than the Severn Estuary.



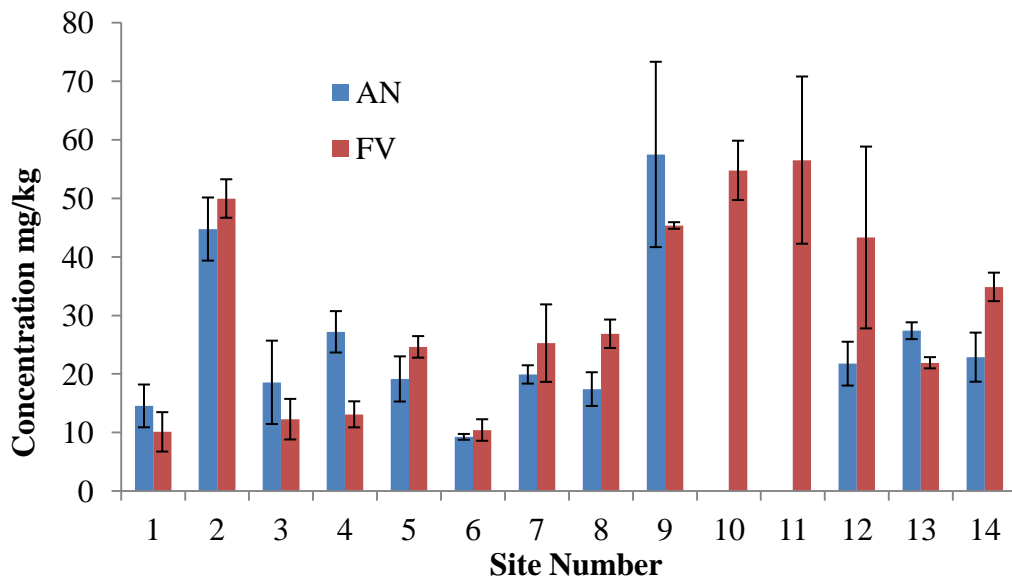
**Figure 3.8: Nickel concentration in *A. nodosum* (AN) and *F. vesiculosus* (FV) at all sites. (AN \* indicates that value is below LOQ but above LOD).**

Phaneuf (1999) found  $5.6 \pm 1.8$  and  $1.59 \pm 0.54$  mg/kg in *F. vesiculosus* and *A. nodosum* from the Gulf of St Lawrence in Canada (Phaneuf *et al.* 1999). This indicated a similar or slightly lower level of pollution to that seen here.

### 3.3.2.7 Zinc

The concentration of Zn found in *A. nodosum* and *F. vesiculosus* is shown in Figure 3.9. A significant biomagnification of Zn levels was seen compared to Zn levels in seawater (Table 3.5). There was no significant difference in Zn concentrations between the two seaweeds.

Zn is an essential element and therefore is expected to occur at small concentrations at all sites. Boating activity can be a source of zinc pollution, as it can be used in an anti corrosion capacity as sacrificial anodes on boats (Matthiessen *et al.* 1999). This explained the higher concentration found in site 2 (boat service site) in Bonne Bay, in the sites closer to port area in the Bay of Islands and in the Waterford sites.



**Figure 3.9: Zinc concentration in *A. nodosum* (AN) and *F. vesiculosus* (FV) at all sites.**

Phaneuf (1999) also found no difference between levels in *A. nodosum* ( $35.6 \pm 16.1$  mg/kg) and *F. vesiculosus* ( $32.6 \pm 16.9$  mg/kg), in agreement with the result found here. The results found by Phaneuf were lower than many of the results found here, and this difference was probably due to boating and port activity (Phaneuf *et al.* 1999).

Riget *et al.* (1997) found baseline levels of zinc in Greenland to be 7.2 - 10.2  $\mu\text{g/g}$  in *Fucus vesiculosus* and 6.6 - 10.7  $\mu\text{g/g}$  in *Ascophyllum nodosum* (Riget *et al.* 1997).

The 10 fold difference in concentration that was observed here can almost certainly be attributed to anthropogenic sources, namely boating activity.

### 3.3.2.8 Comparison of Results and Application of Metal Pollution Indexes

A summary of the results found in this study is given in Table 3.9.

**Table 3.9: A summary of metal contents of *F. vesiculosus* and *A. nodosum* (all mg/kg).**

	Cd		Co		Cu		Cr		Mn		Ni		Zn	
	FV	AN	FV	AN	FV	AN	FV	AN	FV	AN	FV	AN	FV	AN
<b>1</b>	0.8	0.4	0.5	0.6	7.7	6.9	<	<	48.4	12.2	4.6	1.1	10.1	14.5
<b>2</b>	0.8	0.3	0.7	0.8	22.5	2.5	<	0.4	76.2	14.6	5.7	2.9	50.0	44.7
<b>3</b>	0.8	0.3	0.7	0.5	4.7	2.2	<	<	78.7	6.8	5.0	0.8	12.3	18.6
<b>4</b>	1.1	0.6	0.7	0.5	3.4	1.4	<	<	95.3	11.9	5.9	0.8	13.1	27.2
<b>5</b>	0.8	0.5	0.9	0.7	1.6	0.8	<	<	111.0	15.0	4.6	1.1	24.6	19.1
<b>6</b>	0.7	0.2	1.1	0.7	3.5	1.5	1.4	<	120.9	8.3	4.9	0.8	10.4	9.3
<b>7</b>	0.9	0.4	1.4	0.6	3.4	2.8	<	<	158.0	14.2	9.5	1.5	25.3	19.9
<b>8</b>	0.8	0.2	1.2	0.5	3.0	3.7	<	<	269.2	17.6	8.5	1.2	26.9	17.4
<b>9</b>	0.7	0.4	1.0	0.8	3.3	5.1	<	0.3	269.8	36.7	7.4	1.7	45.4	57.5
<b>10</b>	0.7	ND	0.9	ND	2.8	ND	<	ND	274.8	ND	7.4	ND	54.8	ND
<b>11</b>	0.6	ND	1.3	ND	6.7	ND	2.4	ND	372.2	ND	5.0	ND	56.5	ND
<b>12</b>	0.7	0.1	1.4	0.8	4.8	1.8	1.6	0.4	454.3	43.8	5.0	0.7	43.3	21.8
<b>13</b>	0.4	0.2	1.0	0.9	3.7	3.1	1.7	0.4	285.1	32.0	3.5	1.0	21.9	27.4
<b>14</b>	0.7	0.2	1.6	0.6	3.6	3.9	1.0	0.4	278.3	31.8	5.6	1.1	34.9	22.9

<: below LOQ

MPI and PLI values for all the sites studied were calculated based on Zn, Cd, Co, Cu, Mn, and Ni values (shown in Table 3.9). Cr was not included as some of the values for Cr were below the limit of detection, and therefore no numerical value of Cr was available for calculations. The values for MPI and PLI are shown in Table 3.10.

**Table 3.10: MPI and PLI values for *F. vesiculosus* and *A. nodosum*.**

Site No	Site Description	<i>Fucus Vesiculosus</i>		<i>Ascophyllum nodosum</i>	
		MPI	PLI	MPI	PLI
1	Bonne Bay 1, NL, CA	4.4	1.5	2.7	2.4
2	Bonne Bay 2, NF, CA	8.0	2.8	3.3	3.0
3	Bonne Bay 3, NF, CA	4.9	1.7	1.8	1.6
4	Bonne Bay 4, NF, CA	5.1	1.8	2.2	2.0
5	Bonne Bay 5, NF, CA	5.0	1.7	2.1	1.8
6	Corner Brook 1, NF, CA	5.1	1.8	1.6	1.4
7	Corner Brook 2, NF, CA	7.4	2.6	2.6	2.3
8	Corner Brook 3, NF, CA	7.6	2.6	2.3	2.0
9	Corner Brook 4, NF, CA	7.7	2.7	4.3	3.8
10	Corner Brook 5, NF, CA	7.7	2.7	nd	nd
11	St Johns River, IE	9.2	3.2	nd	nd
12	Ferrybank, IE	8.8	3.1	2.2	2.0
13	Cheekpoint, IE	5.6	2.0	2.7	2.4
14	Passage East, IE	7.7	2.7	2.7	2.4

MPI values should only be compared for a single species as they depend on the species specific uptake. The ranking of uptake can however be compared. For example *F. vesiculosus* was found to accumulate more metal than *A. nodosum* in this study in some cases. Therefore, MPI values for *F. vesiculosus* were greater than for *A. nodosum*. PLI values have been normalized to the baseline or lowest value found in the study, and therefore should be comparable across species.

Some of the lowest MPI values for *F. vesiculosus* are found in Bonne Bay, and the outermost site in Corner Brook. These sites are not thought to be significantly affected by pollution. An exception to this is site 2 in Bonne Bay. The metal load values for this site have been positively influenced by high levels of Zn and Cu. This is very likely to be due to the site being a boat servicing area, leading to localized pollution associated with this activity. Cu is very widely used in anti-fouling paints and the highest Cu value was found in the study at this site (22.5 mg/kg) (Johnston *et al.* 2011). Zn is commonly used as a sacrificial anode in marine environments to delay rusting of iron and steel structures and boats (Bird & Comber 1996). The MPI values found here for *F. vesiculosus* tend to support the assertion that the most polluted areas were in the South-East of Ireland, with the top two MPIs being found in site 11 and 12

both located in the city of Waterford. MPI results found for *A. nodosum* somewhat support the overall ranking of polluted and non-polluted sites.

The PLI is useful to determine the level of pollution at a site in comparison to the others studied. None of the sites studied here were severely polluted (PLI >5). Zhang (2011) used the following categories after applying PLI calculation: 0 and 1 indicate an unpolluted area, 1-2 unpolluted to moderate pollution, 2-3 moderate pollution, 3-4 moderate to high pollution, 4-5 high pollution, >5 severely polluted (Zhang *et al.* 2011). Similarly low values were found by Chadhuri (2007) in the east coast of America (PLI 1.3-1.6) using *Ulva lactuca* and *F. vesiculosus* (Chaudhuri *et al.* 2007). No other study using this index in seaweed could be found by the author.

Pollution indexes have been successfully applied in biomonitoring programs using bivalves (see for example Usero *et al.* 1996), and its application to seaweed biomonitoring may be useful to enable comparisons between data sets.

Using the Pearson correlation coefficient to determine the relationship between the ranking of MPI/PLI loadings between *A. nodosum* and *F. vesiculosus* gives a moderate correlation of  $r = 0.5$ . However the relationship was found to be non-significant ( $p = 0.1$ ). This indicates the importance of using more than one biomonitor species, as a single species may not give a good indication of the level of pollution at a site.



### 3.3 Conclusions

Every metal was significantly biomagnified by the seaweeds, when compared to levels found in seawater. This reinforces the value of studying metal levels in biota as part of environmental monitoring studies. Another advantage is that the level of metal contained in the seaweed is related to the biologically relevant portion of metal in the environment.

*F. vesiculosus*, in general, accumulated more metals than *A. nodosum*. It was also easily available at most of these sites making it a good choice as a biomonitor species. Differences in metal concentrations could be attributed to activities/industries located at the sites in most cases. Although the Bonne Bay sites were located in a national park it was found that it was not necessarily a clean site, probably due to the fishing industry located there. In general the sites studied here were found to have low levels of pollution. An exception to this was Zn, which was present at levels higher than those found at unpolluted sites in Greenland. The low-polluted nature of the sites was confirmed by their PLI (pollution load index). No sites were severely polluted. The highest PLI value found was 3.8, indicating a polluted site. Most PLI levels were 2-3, which indicates moderate pollution (Zhang *et al.* 2011).

Chapter 4: Bioaccumulation  
of Chromium by *F.*  
*vesiculosus*, *P. palmata* and  
*U. lactuca*

#### 4.1 Introduction

The biosorption of metals by seaweed is relatively well quantified (He & Chen 2014), but bioaccumulation by live seaweeds is not as well understood. Many different variables affect this. The variables common to live and dead seaweed uptake include: seaweed composition, temperature, pH, and seaweed/solution ratio. The other factors which affect live seaweed accumulation, include seaweed metabolism and the exudation of chemicals, which is affected by season.

A preliminary study was carried out to study live seaweed accumulation of chromium. The aim was to compare the differences in metal uptake by six live seaweeds; two red, two brown and two green. After this step, three species were chosen for further study based on the results observed. The effects of temperature and chromium speciation in these species were also studied. Temperature has not been widely studied in the literature, but is known to affect the uptake of metals by both algae and plants (Fritioff *et al.* 2005; Munda 1979). In fact Munda (1979, 1988) has published the only studies relating to temperature and metal uptake in seaweed (Munda 1979; Munda & Hudnik 1988). Vasconcelos *et al.* (2001) studied seasonal differences in bioaccumulation of Cu, Pb and Cd for the red seaweed *Porphyra* and the green seaweed *Ulva* (Vasconcelos & Leal 2001).

The temperatures were chosen to reflect the highs and lows which are likely to occur in Ireland (Table 4.1), but these temperatures are common to many areas in the world (e.g. parts of UK, US, Canada, China, Argentina, Chile, and New Zealand) (National Oceanographic Data Center 2012).

**Table 4.1: Average monthly sea temperatures at the Met Eireann M5 Buoy, off the south coast of Co. Wexford. Data from 2004-2015 (Met Eireann 2016).**

Month	Jan	Feb	Mar	Apr	May	Jun	Jul	Aug	Sep	Oct	Nov	Dec
Temp (°C)	9.8	9.0	8.8	9.8	11.4	14.1	15.8	15.9	15.2	14.2	12.8	11.1

The aims of this chapter were to:

- Determine the differences in chromium uptake between seaweed species
- Determine the effect of chromium speciation on metal uptake

- Determine the effect of temperature on metal uptake
- Determine the effect of seasonality on metal uptake
- To determine if seasonal differences in metal uptake are related to water temperature or to differences in seaweed biochemistry/composition

## 4.2 Experimental

### 4.2.1 Sampling and Storage

Seaweed was collected randomly by hand from Baginbun in Co. Wexford, Ireland (GPS coordinates: 52° 10.596' N, 6° 49.787' W, see Figure 4.1) from late May to June 2009, and from mid February to early March 2010. In text and diagrams these will be referred to as May/Jun and Feb/Mar. Seaweed for the preliminary experiment was sampled in October 2007. For the preliminary metal uptake experiment, *F. vesiculosus*, *F. spiralis*, *Ulva* spp., *U. lactuca*, *P. lanosa*, and *P. palmata* were used. For further metal exposure experiments *F. vesiculosus*, *U. lactuca*, and *P. palmata* were used.



**Figure 4.1: Location map and picture of Baginbun.**

Seawater was also collected from the same site. Temperature, conductivity and pH were monitored at the site. The seaweed was transported to the lab in cooler boxes and stored in aerated tanks in a cold room set to the appropriate temperature (16 or 7 °C). A light:dark cycle of 16:8 h was used during the summer sampling season and 8:16 h during the winter sampling season. Seawater was immediately placed in a 4 °C cold room for storage and used within 1 week. Seawater was removed from 4 °C storage and allowed to equilibrate to experimental temperature (either 16 or 7 °C) and

filtered (Whatman® qualitative filter paper, Grade 1) to remove sand and debris before use.

#### 4.2.2 Preliminary Metal Uptake Experiment

The live seaweed was exposed to a Cr(III) metal solution at a concentration of approximately 60 g seaweed per L of metal solution. The 200 µg/L metal solution was prepared by adding a stock Cr(III) solution (in the form of  $\text{Cr}(\text{NO}_3)_3$ , obtained from Sigma-Aldrich, Ireland) to seawater. The experiment was carried out at 4 °C. Samples were taken at time intervals of 0, 1.5, 5, 10, 30, 60, 120 and 240 min and frozen immediately. They were then oven dried at 60 °C for 24 h and ground using a mortar and pestle and liquid nitrogen if necessary. The samples were microwave digested and analysed for Cr content by ICP-OES, as described in Section 4.2.5.

#### 4.2.3 Metal Exposure Experiments

200 µg/L seawater chromium solutions were prepared by diluting a standard solution appropriately (Cr(III) in the form of  $\text{Cr}(\text{NO}_3)_3$  and Cr(VI) in the form of  $(\text{NH}_4)_2\text{Cr}_2\text{O}_7$  obtained from Sigma-Aldrich, Ireland). The seawater metal solution was then allowed to equilibrate at 7 or 16 °C overnight.

For baseline metal content the seaweed was simply washed with distilled water and dried. An experiment was carried out to determine the effect of washing the seaweed with water and no effect on metal concentration was seen (results not given here). Triplicate samples from three different seaweed plants were used in each case.

In May/June a detailed time course experiment was carried out. The live seaweed was exposed to the metal solution at a concentration of 5 g (fresh weight of seaweed) per 150 mL of metal solution. Both seaweed and seawater samples were taken at time intervals of 0, 15, 30, 60, 120, 240 and 360 min, and the seaweed was rinsed immediately with deionized water. In Feb/Mar, only baseline and  $t = 360$  samples were taken.

Samples taken at  $t = 0$  and  $t = 360$  min were washed with a 5mM EDTA solution to determine the intracellular metal concentration. The EDTA was prepared from Titriplex® salt (Sigma-Aldrich, Ireland) and adjusted to a pH of 8. The samples were

then washed for 10 min at a concentration of 30 g / 200 mL, and rinsed with deionized water (García-Ríos *et al.* 2007). All seaweed samples were oven dried at 60 °C for 24 h. EDTA washing was only carried out to remove metals in the cationic form.

A portion of the seawater samples were filtered through a 0.45 µm disc to determine soluble chromium (Sadiq 1992). Then all the water samples were acidified to pH < 2 and stored at 4 °C for analysis by ICP. Water temperature, conductivity and pH were monitored throughout the experiment.

#### **4.2.4 Microwave Digestion**

Seaweed samples for the preliminary metal uptake experiment are described in Section 2.2.2.1, with the following exception. For the preliminary metal uptake experiment a HNO<sub>3</sub>, H<sub>2</sub>O<sub>2</sub> and H<sub>2</sub>O ratio of (5:1:3) was used. This procedure was improved upon in subsequent experiments by doubling the amount of hydrogen peroxide to obtain clear, colourless digestions, as described in Section 2.2.2.1.

#### **4.2.5 ICP Analysis**

Digests were analyzed for chromium content using a Varian 710-ES ICP-OES (JVA Analytical, Ireland) using the conditions given in Section 2.2.2.2, with the following changes: Samples from the preliminary metal uptake experiment described in Section 4.2.2 were analysed using a power of 1.10 kW, but this was increased to 1.15 kW in all subsequent experiments to increase the intensity of peaks. Seawater sample rinse times were increased from 10 to 15 s to ensure all salts were washed out from the system before the next sample was introduced.

ICP performance was monitored through the use of a certified constant value standard (Trace metals by AA 1, LGC, UK). This was an ampoule which was made to volume in distilled water. Standard reference materials sea lettuce (BCR 279), NIST SRM 1573a (Tomato leaves) and NIES CRM 9 (Sargasso) were digested and analyzed in the same way. Standards for analysis of seawater samples were prepared in synthetic seawater. Analysis was verified by the use of trace metal by AA 1 constant value ampoules which are diluted to volume in a certified salt water matrix modifier obtained from LGC, UK.

#### 4.2.6 Fourier Transform Infrared Analysis

Fourier transform infrared spectroscopy (Varian, 660-IR Spectrometer and 610-IR Microscope with Ge ATR attachment and MCT detector) was used to determine the functional groups available for binding. A resolution of  $4\text{ cm}^{-1}$  was used, and 64 scans were collected. Whole pieces of dried seaweed were analysed. ‘Metal loaded’ is used when discussing the results to indicate a sample taken at the longest time point (i.e.  $t = 360\text{ min}$ ).

Protonated samples were prepared according to Murphy *et al.* 2007. Biomass particles were washed with 250 mL of 0.1M HCl for 6 h. The biomass was filtered under vacuum and washed with distilled water until a constant conductance reading was obtained for the filtrate. The resultant biomass was then oven-dried at  $60\text{ }^{\circ}\text{C}$  for 24 h and stored in polyethylene bottles at room temperature.

#### 4.2.7 Statistical Analysis

Linear regression was used to model the relationship between time and metal uptake. The correlation coefficient ( $R^2$ ) was used to determine the fit of the data to the model. Paired, two-tailed t-tests were used to determine statistically significant differences between sample means. A statistically significant result was a P-value of less than 0.05.



## 4.3 Results and Discussion

### 4.3.1 Method Validation

ICP performance was monitored by the use of the certified constant value standard solution (AA1). For digest analysis, a value of  $75.95 \pm 1.36 \mu\text{g/L}$  ( $n = 24$ ) was obtained, compared to the certified value of  $71.70 \pm 5.38 \mu\text{g/L}$  (errors based on standard deviation). A seawater CRM containing Cr was not available at the appropriate concentration, so the trace metals AA1 standard (made in seawater) was used for both verification of the method and as a reference material. Typical values found were  $70.74 \pm 4.14 \mu\text{g/L}$  ( $n = 26$ ), compared to the certified value of  $71.70 \pm 5.38 \mu\text{g/L}$ . Typical relative standard deviations (% RSD) between replicates for both digest and seawater analyses were less than 5 % (and normally  $< 1$  %).

The limit of detection (LOD) and limit of quantitation (LOQ) were calculated based on blank digests or artificial seawater blanks. Typical LOD and LOQs achieved are shown below in Table 4.2.

**Table 4.2: LOD and LOQ for Chromium Analysis.**

Matrix, Element and Wavelength (nm)	LOD and LOQ in $\mu\text{g/L}$	
	LOD	LOQ
Digests, chromium, 267.716	6	8
Seawater, chromium, 267.716	5	15

Recovery of chromium by the digestion method was determined by analysis of certified reference materials which were digested and analysed in the same way as samples. BCR 279 (sea lettuce), NIST SRM 1573a (tomato leaves) and NIES CRM 9 (sargasso) were used.

Results for chromium content of standard reference materials agreed satisfactorily with certified or indicative values (Table 4.3 below). Sea lettuce and Sargasso standards were within the indicative range. There was no seaweed matrix available with a certified chromium content. The tomato leaf standard is certified for chromium, and was analysed as an additional check in the absence of a certified seaweed material. Although the recovery was not in the certified range, there is a difference in

the matrix, and analysis still gave a recovery of above 80 % (taking average values). This SRM (standard reference material) did not digest fully even though the seaweed samples did. The digests had a white or yellow colour with a large amount of sediment. The seaweed samples yielded clear digests with very little or no sediment. It is, therefore, probable that the Cr recovery was higher in the actual seaweed samples.

**Table 4.3: Comparison of certified / indicative values for Cr and those found by analysis (all in mg/kg).**

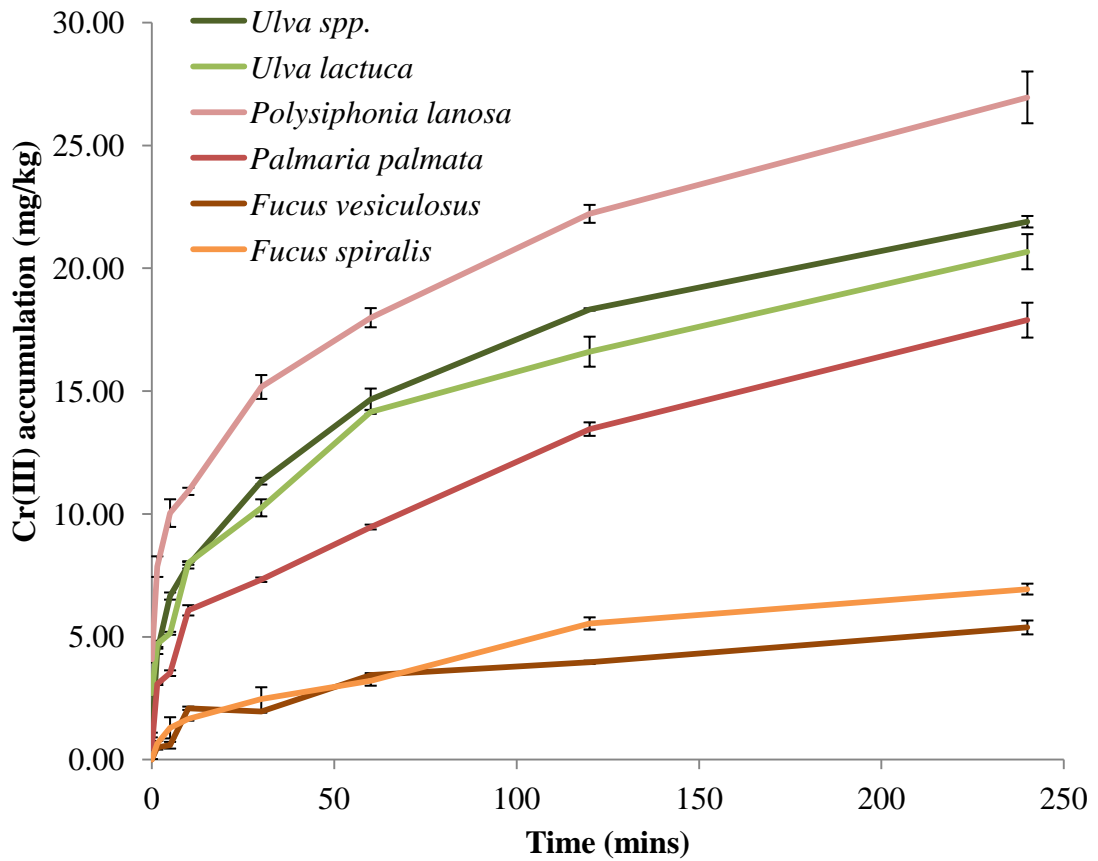
Certified material	Certified / Indicative value	Determined
Sea lettuce	$9.7 \pm 0.9^a$	$8.7 \pm 0.2^b$
Tomato leaves	$1.99 \pm 0.06$	$1.67 \pm 0.13$
Sargasso	$0.2^a$	$0.2 \pm 0.0$

<sup>a</sup> Indicative (uncertified) values

<sup>b</sup> Uncertainty calculated in the same way as for certified reference material if specified on certificate. Sea lettuce and sargasso uncertainty was based on one standard deviation. Tomato leaf error was based on 95 % confidence intervals.

### 4.3.2 Preliminary Metal Uptake Data

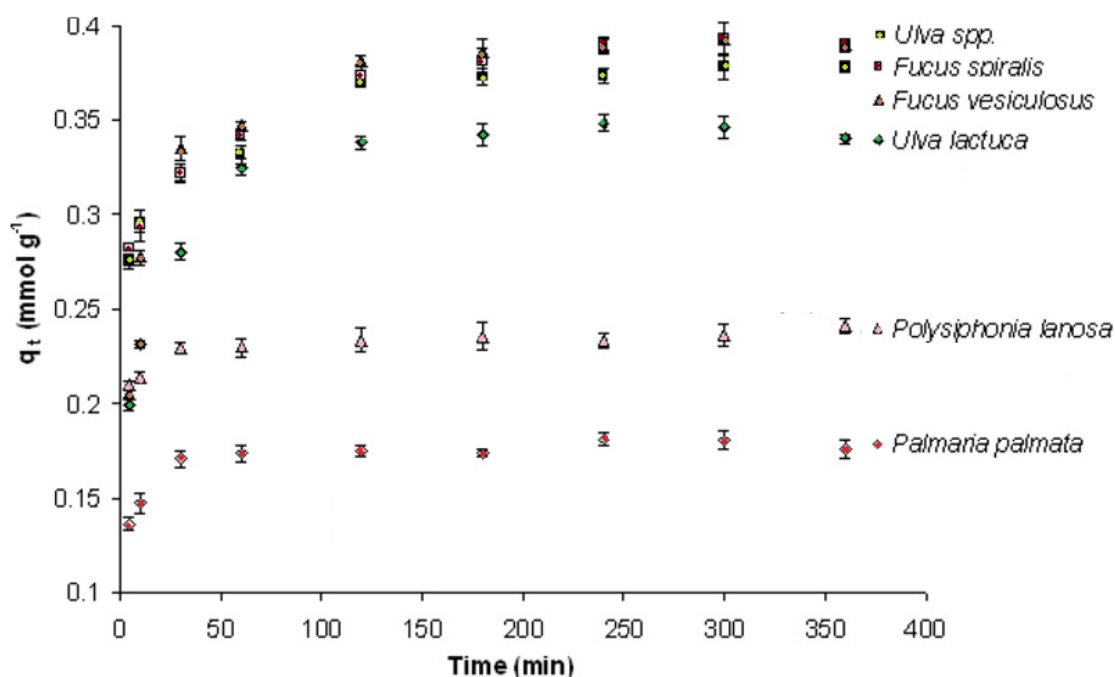
The preliminary uptake experiment, performed at 4 °C was carried out to determine the main trends in uptake for each species (Figure 4.2).



**Figure 4.2: Results of preliminary Cr (III) uptake experiment over 240 min for six seaweed species. Errors based on standard deviation of samples from three replicate plants (n=3).**

Brown seaweeds have been found to outperform green and red as biosorbants (dead seaweed biomass) (Hashim & Chu 2004; Murphy *et al.* 2008) but this was not found to be true for live seaweed bioaccumulation. In fact, over 240 min, the red and green seaweeds had a higher Cr(III) uptake than browns. The paper by Murphy *et al.* is particularly interesting as it studied biosorption of Cr(III) by the same seaweed species, but as dead protonated biomass, rather than live seaweed as used here (results shown in Figure 4.3). As seen in Figure 4.3, *F. vesiculosus*, *F. spiralis* and *Ulva spp.* performed similarly well. *U. lactuca* followed these, with the red seaweeds *P. lanosa*, and especially *P. palmata*, performing significantly worse. Comparing the uptake by

brown seaweeds in Figures 4.2 and 4.3, it can be seen that the trend in brown seaweed accumulation has reversed, from best when using dead seaweed biomass to worst when using live seaweed. Another notable comparison is *P. lanosa* being one of the worst accumulators as a dead biomass, but the best as live seaweed. This indicates a change in uptake mechanism. The change was probably not pH related, as changing the pH from 2-7 affected the amount of uptake, but not the ranking of the seaweeds by metal uptake efficiencies (Murphy *et al.* 2008). The change in uptake mechanism may be related to metabolically active internal Vs external uptake mechanisms. This will be discussed later in this chapter as results for internal metal content will be presented.



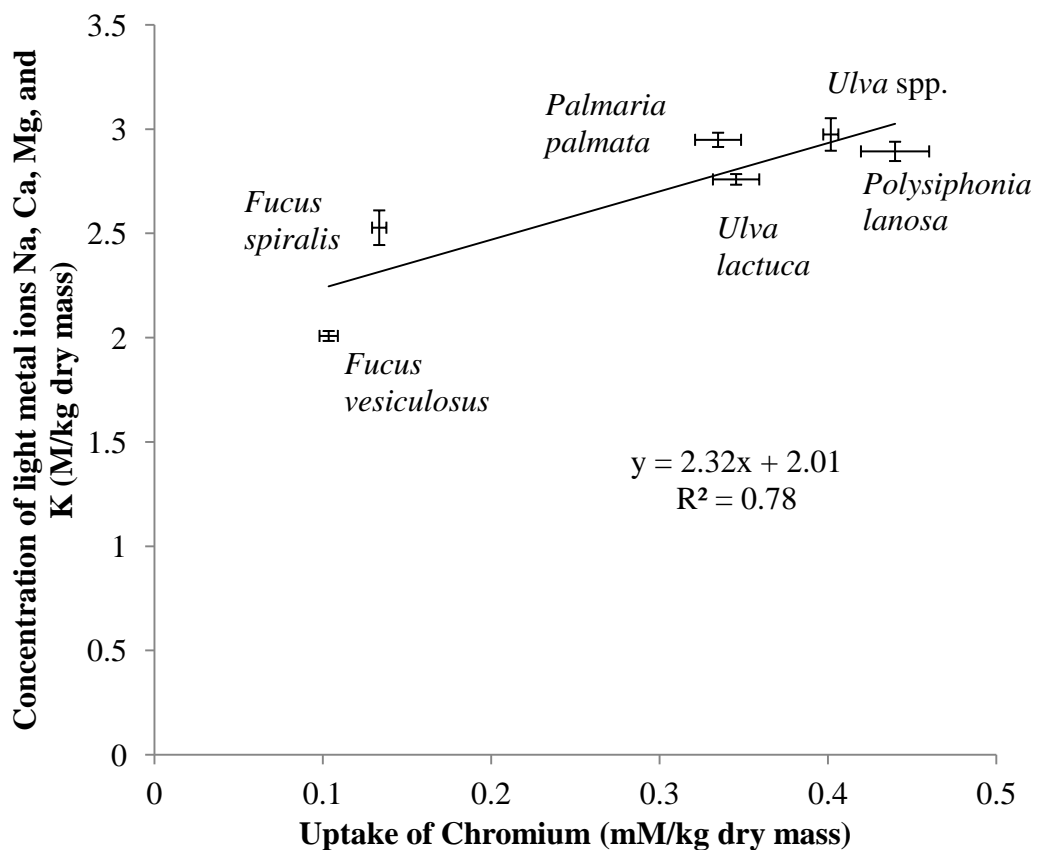
**Figure 4.3: Cr(III) binding over time for biomass from six seaweed species. Conditions were as follows: Initial metal concentration = 1 mM, biomass concentration = 2 mg/mL, pH = 4.5 (Murphy *et al.* 2008).**

Light ions may serve as exchangers for metal ions. The relationship between light metal ion and chromium concentration was studied by determining the concentration of Ca, Mg, K and Na in the seaweed. These cations are present in the seaweed as salts of Ca<sup>2+</sup>, Mg<sup>2+</sup>, K<sup>+</sup> and Na<sup>+</sup>. The results are given in Table 4.4. This was converted to moles and then compared to molar Cr uptake. As seen in Figure 4.4, there was some relationship between total light ion content and metal uptake ( $R^2 = 0.78$ ). This relationship was based mostly on Na<sup>+</sup> content ( $R^2 = 0.74$ , graph not shown here). This

is probably because  $\text{Na}^+$  is the salt with the highest concentration in the seaweeds in general, meaning it is more available for exchange.

**Table 4.4: Concentration of light metal ions in seaweed (% dry mass) (n=3).**

	Ca	Mg	K	Na
<i>Ulva</i> spp.	1.03±0.03	1.14±0.03	1.18±0.02	4.46±0.12
<i>Ulva lactuca</i>	0.39±0.01	0.48±0.00	4.25±0.03	3.16±0.04
<i>Polysiphonia lanosa</i>	0.43±0.00	0.75±0.00	2.45±0.07	4.24±0.06
<i>Palmaria palmata</i>	0.42±0.01	0.51±0.01	4.54±0.02	3.37±0.06
<i>Fucus vesiculosus</i>	0.85±0.01	0.65±0.01	1.76±0.03	2.47±0.02
<i>Fucus spiralis</i>	1.16±0.04	0.79±0.01	2.28±0.12	3.05±0.08



**Figure 4.4: Correlation between light ion content (Na, Ca, Mg, K) and chromium uptake (n=3).**

The correlation between light metal content and Cr uptake suggested ion exchange as a possible mechanism for metal uptake. Williams and Edyvean (1997) studied the uptake of  $\text{Ni}^+$  by seaweed based biomass (de-alginated seaweed waste and alginate fiber). Release of Ca was found to occur on  $\text{Ni}^+$  uptake. A control experiment with no metal found little release of Ca, so it was concluded that this was due to the presence of  $\text{Ni}^+$  (Williams & Edyvean 1997). A strong relationship with Ca was not found here ( $R^2 = 0.31$ ), but other ions may have the same effect (Mg, Na, K). Also note that these were biosorption experiments using dead algal biomass and  $\text{pH} < 7$ . The work presented in this thesis used live seaweed at natural seawater pH conditions (approximately pH 8).

For biomass of the brown seaweed *Sargassum flutans* it was found that protons displaced light metal ions in the following order  $\text{Ca}^{2+} < \text{Mg}^{2+} < \text{K}^+ \leq \text{Na}^+$  as the pH increased, meaning that  $\text{Na}^+$  and  $\text{K}^+$  had less affinity to bind with the biomass than the other ions (Lee & Volesky 1997). This is in agreement with the results seen here, with seaweeds containing higher amounts of Na taking up the most  $\text{Cr}^{3+}$  ( $R^2 = 0.74$ , Figure 4.4). This behaviour was confirmed by da Costa *et al.* (2001) in *Sargassum* sp. with Na and K being released first on Zn exposure during a continuous biosorption experiment (da Costa *et al.* 2001). To the author's knowledge, this is the first time the correlation between total Na content and  $\text{Cr}^{3+}$  has been shown.

Amado Filho *et al.* (1997) also carried out a species comparative bioaccumulation study of Zn with two brown, two green and two red (live) seaweeds over a period of 3 weeks. The trends in Zn uptake stayed the same regardless of Zn exposure concentration and time. The red seaweed *Hypnea musciformis* and the two species of green, *U. lactuca* and *U. flexuosa*, had the lowest uptakes. The highest bioaccumulators were the brown seaweed *Sargassum*, the red *Spyridea*, and the brown *Padina* (Amado Filho *et al.* 1997). This is in contrast to the results seen here, and points to the fact that metal accumulation may be highly metal and species dependent.

Vasconcelos *et al.*, (2001) found similar uptakes of metal (Cu, Pb, Cd, all similar with about 200 nmol/g dry algae) calculated on a molar basis for winter samples of the red seaweed, *Porphyra*, and the green seaweed, *Ulva*, over 25 h. As this is a seasonal

study the results will be discussed in more detail in the next section (Vasconcelos & Leal 2001).

The findings from the Baumann *et al.* (2009) study was interesting as they also studied anionic chromate ( $\text{CrO}_4^{2-}$ ) uptake in a variety of red, green and brown seaweed species over 14 days (Baumann *et al.* 2009). At a concentration in the range of that studied here, 1  $\mu\text{mol/L}$  (52  $\mu\text{g/L}$ ), uptake was similar for *P. palmata* (red), *C. crispus* (red), *F. vesiculosus* (brown), *A. nodosum* (brown), and *Cladophora rupestris* (green), at about 0.15  $\mu\text{mol/g}$  (8 mg/kg). *P. lanosa* (red) and *U. intestinalis* (green) had higher uptakes of about 0.23  $\mu\text{mol/g}$  (12 mg/kg) (Baumann *et al.* 2009). Uptake by *P. lanosa* and *Ulva* spp. were also found to be highest in this study (27 and 22 mg/kg, respectively), with a lower uptake found for the *F. vesiculosus* (5 mg/kg). *Palmaria palmata* was found to be higher (18 mg/kg) than reported by Baumann *et al.*, (2009). Experimental conditions of exposure time (14 days versus 6 h) and metal concentration (52 versus 200  $\mu\text{g/L}$ ) are very different in this study, and were probably the reason for the differences seen.

Of the six species originally studied, three species were chosen for further study, taking into account these results, availability, and ease of sampling. These species were *U. lactuca*, *P. palmata* and *F. vesiculosus*.

### **4.3.3 Temperature study of Cr Uptake by *Ulva lactuca*, *Fucus vesiculosus* and *Palmaria palmata***

For this experiment, seaweed sampled in summer was exposed to 200  $\mu\text{g/L}$   $\text{Cr}^{3+}$  and  $\text{CrO}_4^{2-}$  at temperatures of 7 and 16 °C. These temperatures were chosen to be similar to temperatures found off the south eastern coast of Ireland (Table 3.7).

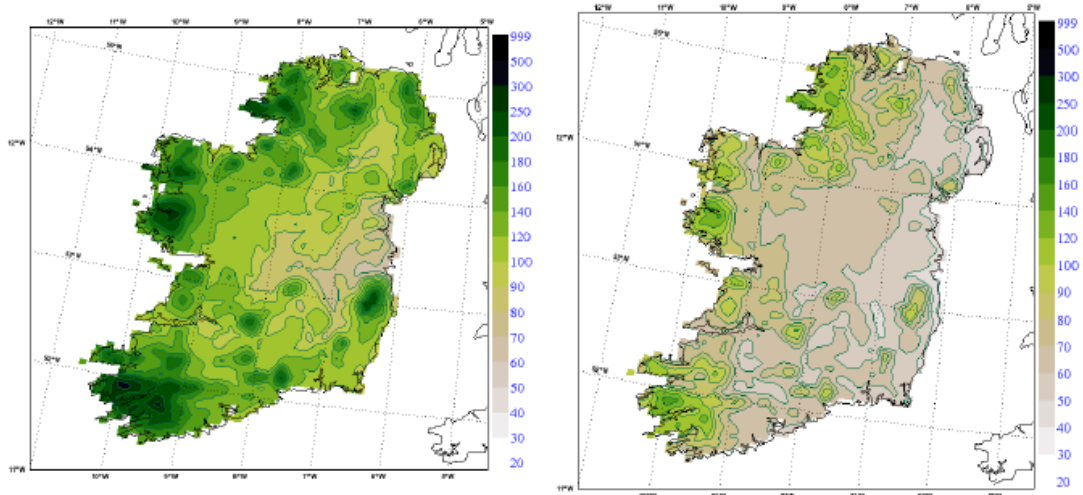
#### **4.3.3.1 Site results**

Conductivity, pH and temperature were taken at the site on each sampling trip and are given in Table 4.5. For this section, only seaweed sampled in the winter was used.

**Table 4.5: Site conditions at sampling times (n=3)**

Season	Sea Temperature	pH	Conductivity	Sampling time
May/June	16.9 ± 2.2 °C	8.5 ± 0.1	52.7 ± 0.5 mS/cm	low tide
Feb/Mar	7.9 ± 1.6 °C	8.2 ± 0.1	49.9 ± 0.3 mS/cm	low tide

Water temperature was close to the temperatures chosen here for experiments. The pH and conductivity may have been lower in winter because of fresh water input. Higher rainfall during winter months leads to a greater input of freshwater in estuarine areas in winter. This is due to run off from land and greater river input in winter months. Average rainfall data for Ireland is presented in Figure 4.5.



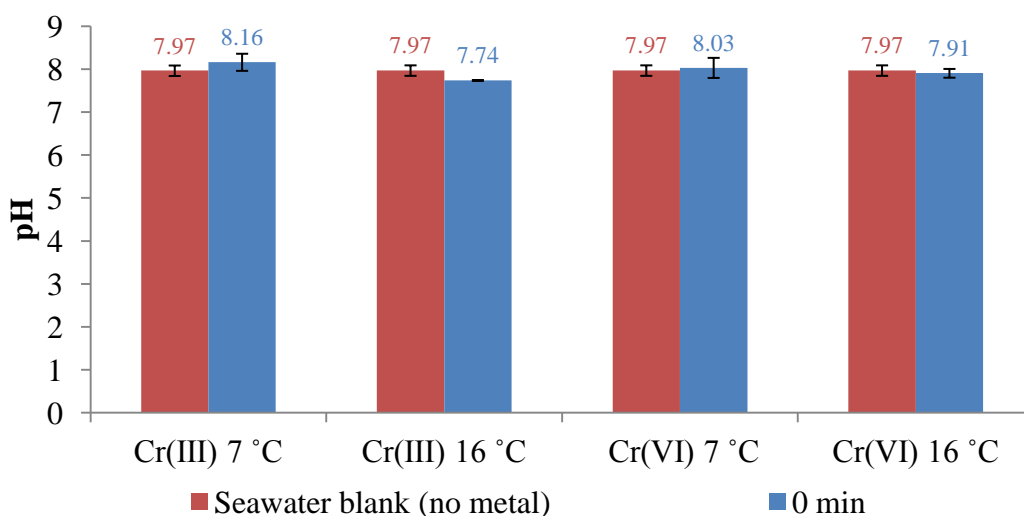
**Figure 4.5: Mean monthly precipitation (1961-2000) from UKCIP data for January (left) and July (right) in mm/month (Semmler *et al.* 2006).**

#### 4.3.3.2 Analysis of Seawater Controls

An investigation was carried out to determine if any changes in pH, temperature, metal content, and conductivity, occurred in seawater controls (without any seaweed added). The conductivity stayed constant ( $52.2 \pm 0.1$  mS/cm) throughout the experiments. Temperature remained within 1 °C of the desired experimental temperature.

Shown in Figure 4.6 are the changes in pH which occurred when metal was added to the fresh seawater for the experiments.

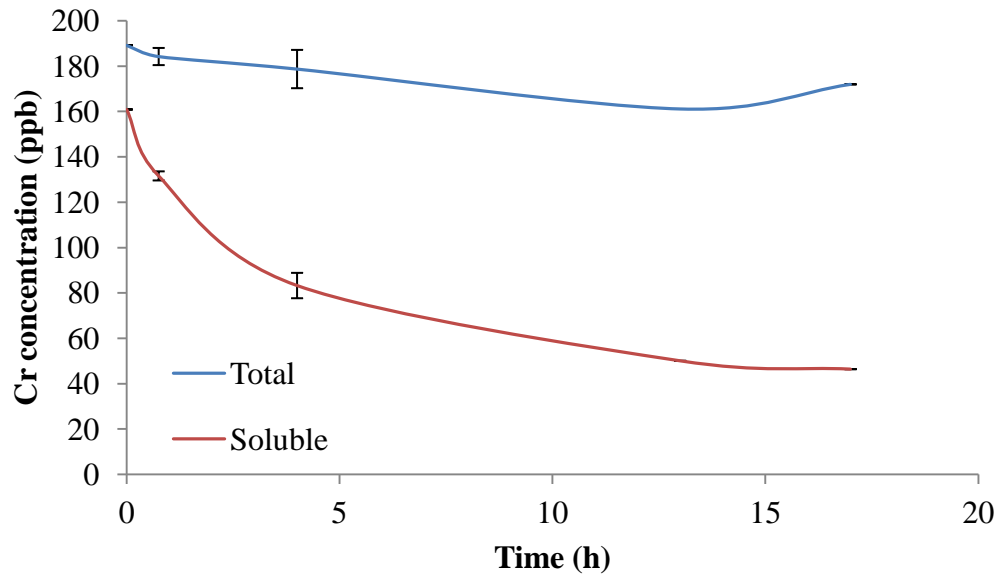




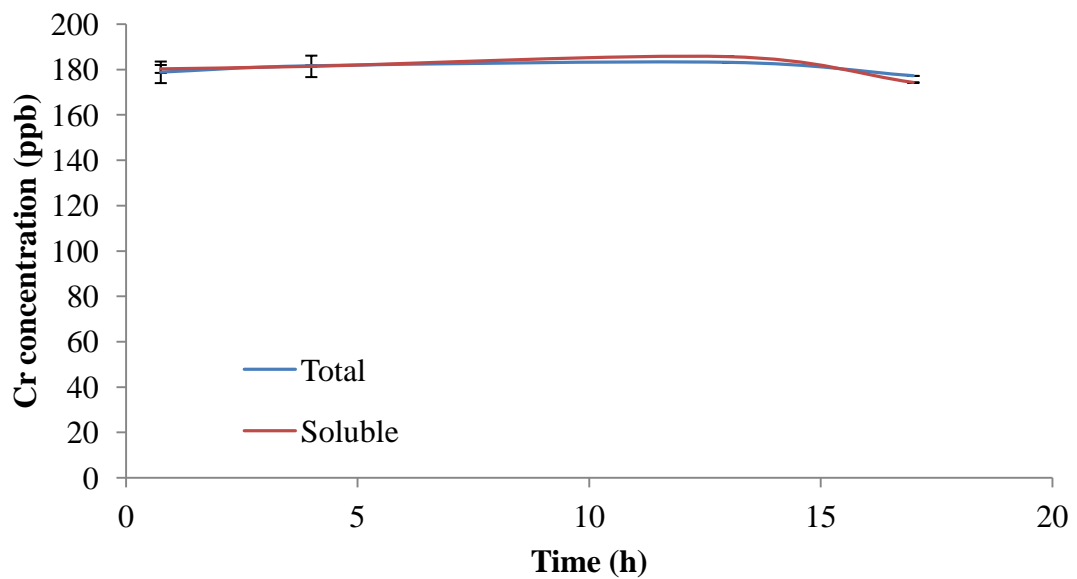
**Figure 4.6: Changes in pH of control seawater samples. 0 min sample taken after the metal solution was prepared and allowed to equilibrate (n=3).**

The red bar represents the average pH of the seawater taken from the beach and filtered to remove sand and debris. It is the same for all other metal and temperature conditions, and is shown for comparison purposes. According to t-test results (paired, 2-tailed), there were no significant differences in pH before and after the metal solutions were added. Therefore, there was no significant difference in pH between natural seawater and seawater with metal added. In further experiments, the pH of seawater with metal added can be considered equivalent to natural untreated seawater.

It is known that some metals in seawater bind to organic material and are insoluble in seawater conditions (Reeder *et al.* 2006). An experiment was carried out to determine the portion of total and soluble metal present in the seawater solution. The results of this experiment are given in Figures 4.7 and 4.8.



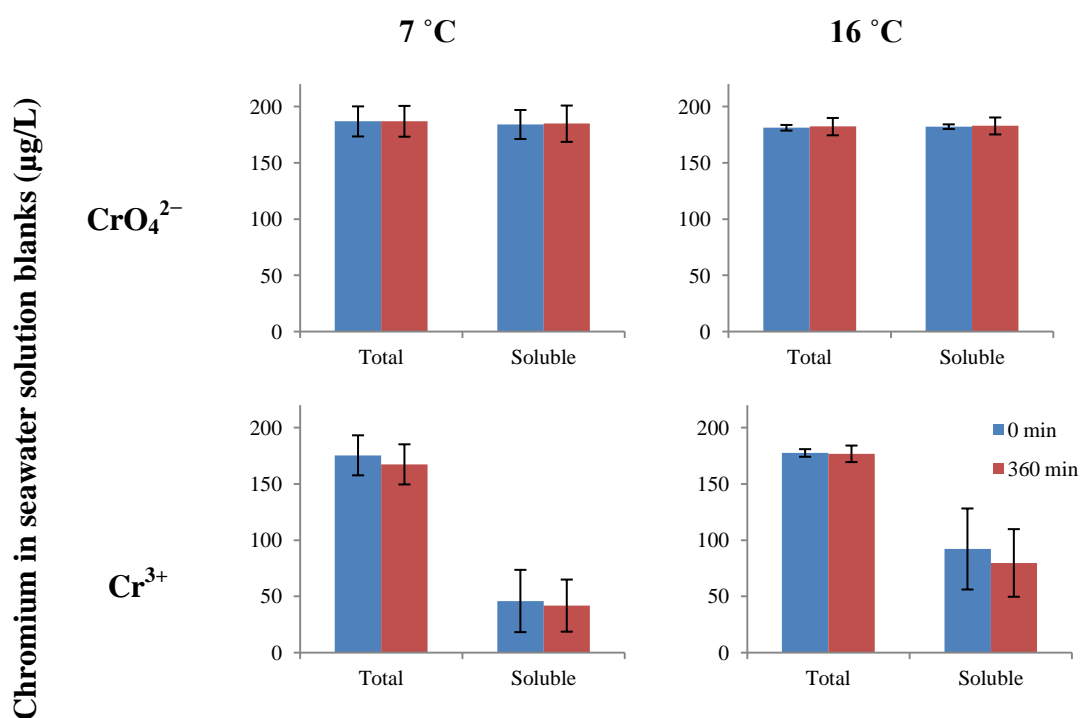
**Figure 4.7: Changes in the concentration of total and soluble Cr<sup>3+</sup> (n=3).**



**Figure 4.8: Changes in the concentration of total and soluble CrO<sub>4</sub><sup>2-</sup> (n=3).**

As seen in Figures 4.7 and 4.8 the amount of soluble Cr<sup>3+</sup> in the seawater solution changed over the 17 h tested, with the rate of change slowing after about 5 h. The total amount of Cr<sup>3+</sup> in the solution stayed constant after approximately 12 h. The amount of CrO<sub>4</sub><sup>2-</sup> in solution stayed constant throughout the test period. Therefore, for all the following experiments, metal solutions were made the night before the experiment. This ensured that the level of metal in the solution stayed constant throughout the experimental period, and any changes detected were due to the added seaweed.

As it was known from the previous experiment (Figure 4.7 and 4.8) that soluble Cr content could change over the experimental period, a seawater blank (with no seaweed added) was run alongside Cr uptake experiments at the temperatures to be studied. The results are as shown in Figure 4.9.



**Figure 4.9: Charts showing amount of Cr soluble in seawater controls at both the start (0 min) and end (360 min) of the experiment.**

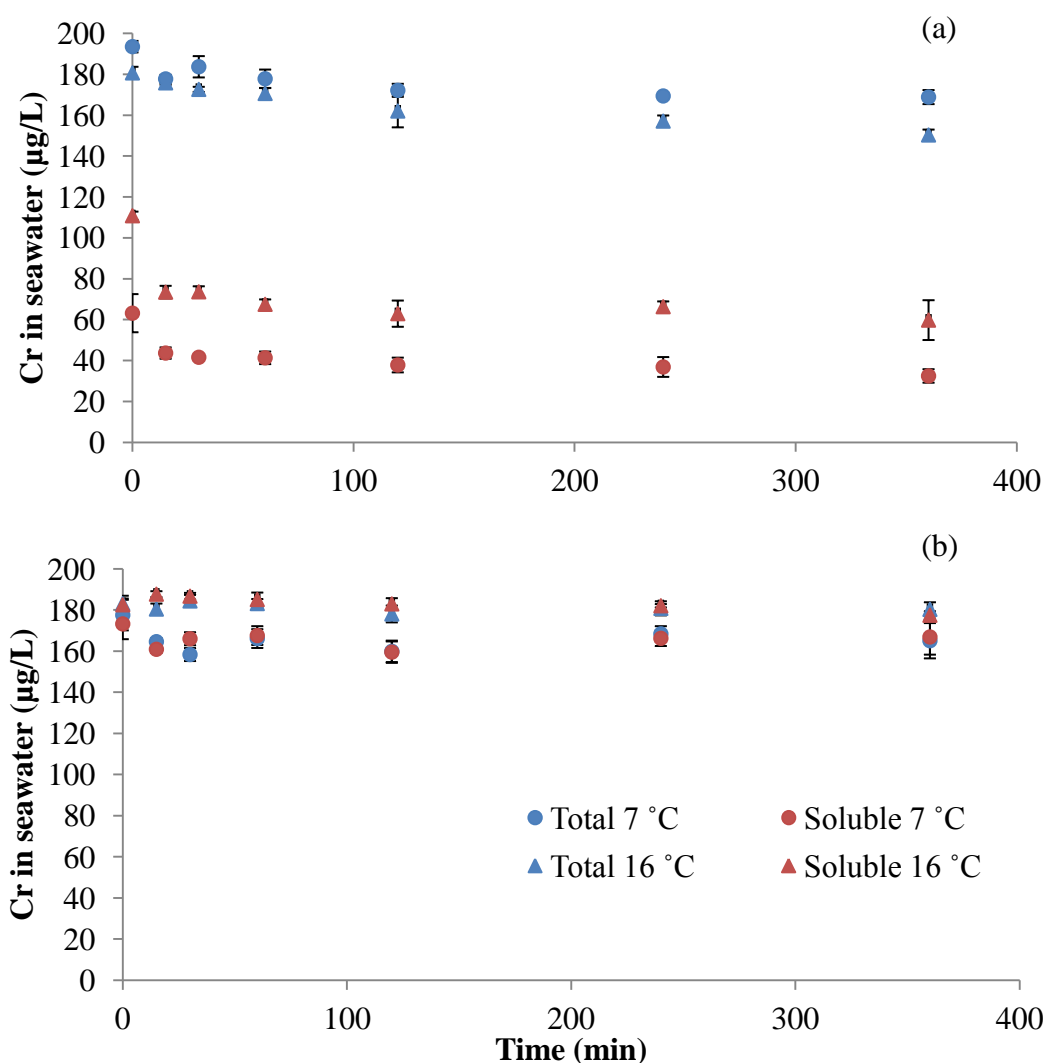
Soluble  $\text{CrO}_4^{2-}$  was virtually 100 % present in solution, throughout the experimental period. Soluble  $\text{Cr}^{3+}$  on the other hand was present at a concentration of 46 µg/L at 7 °C, and 92 µg/L at 16 °C. Some drop in solubility towards the end of the experimental period can be seen for  $\text{Cr}^{3+}$  containing blanks. Differences in concentration between  $t = 0$  and  $t = 360$  were not statistically different for any conditions except soluble Cr(III) at 16 °C ( $p = 0.006$ , student's t-test, paired, 2-tailed). Although the means differed significantly, the numerical difference is quite small (12 µg/L). Therefore, at the conditions studied, the concentration of both soluble and insoluble Cr(VI) and Cr(III) can be considered constant over the experimental period. Any change in total

and soluble Cr concentration in the experiments can therefore be attributed to the addition of seaweed.

The precipitation of  $\text{Cr}^{3+}$  from aqueous solution has been discussed by Vignati *et al.* (2010) Vignati observed a ~50 % loss in soluble  $\text{Cr}^{3+}$  after 24 h from a 430  $\mu\text{g/L}$  solution, while soluble  $\text{CrO}_4^{2-}$  remained essentially constant at 24 °C (Vignati *et al.* 2010). This is very much in agreement with the results seen here, where 52 % of Cr(III) was soluble after the 12 h equilibration period at 16 °C, and soluble  $\text{CrO}_4^{2-}$  content remained constant. The difference in  $\text{Cr}^{3+}$  solubility was even greater at 7 °C, with only 26 % remaining in soluble form. The increase in temperature from 7 to 16 °C was probably responsible for the increased solubility. This is important when discussing the uptake of metal as the bioavailable, soluble portion of the metal under study may be quite different from the total metal content. This was the case in this study, and the actual concentration of soluble  $\text{Cr}^{3+}$  the seaweed was exposed to was lower than the concentration of  $\text{CrO}_4^{2-}$  it was exposed to.

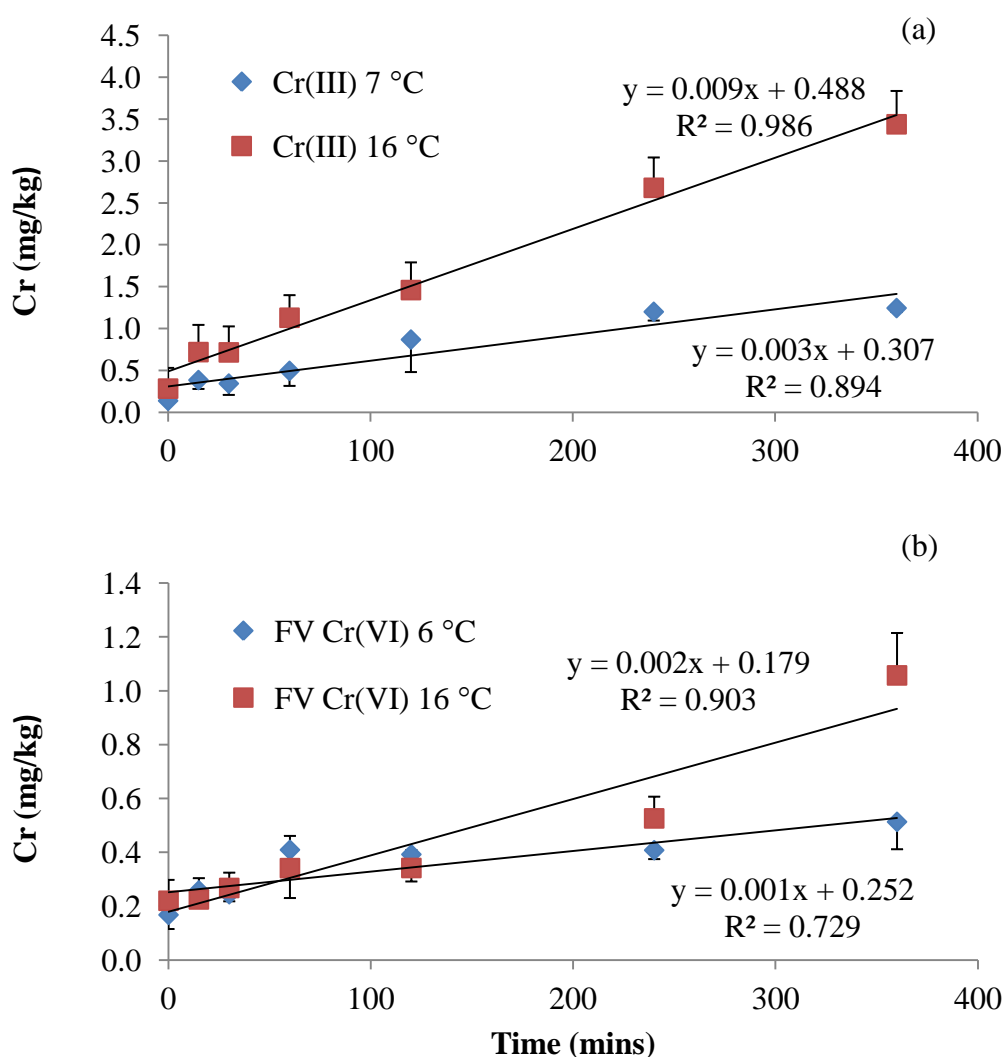
### 4.3.3.3 Chromium Uptake by *Fucus vesiculosus*

A detailed time course accumulation of Cr(III) and Cr(VI) from a seawater solution by *F. vesiculosus* sampled in May/June is shown in Figure 4.10.



**Figure 4.10: Uptake of Cr<sup>3+</sup> (a) and CrO<sub>4</sub><sup>2-</sup> (b) by *F. vesiculosus* (sampled May/June): Total and soluble Cr in seawater (n=3).**

The total concentration of CrO<sub>4</sub><sup>2-</sup> was equal to the soluble concentration at both 7 and 16 °C. The soluble concentration of Cr<sup>3+</sup> was significantly lower than the total concentration. Approximately 20 % of the total Cr<sup>3+</sup> was present in a soluble form at 7 °C, and 40 % at 16 °C. The total amount of Cr removed from the seawater solution was small, especially for CrO<sub>4</sub><sup>2-</sup>. The results can be more clearly seen in the Cr content of the digested seaweed samples shown in Figure 4.11.



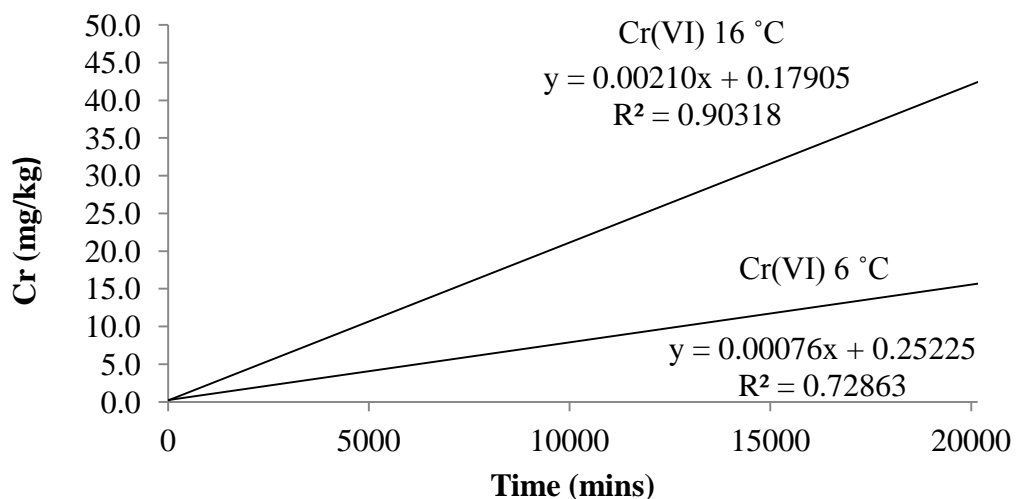
**Figure 4.11: Uptake of  $\text{Cr}^{3+}$  / Cr(III) (a) and  $\text{CrO}_4^{2-}$  / Cr(VI) (b) by *F. vesiculosus* (sampled May/Jun) (n=3).**

*F. vesiculosus* accumulated a maximum of 1.25 and 3.44 mg/kg of  $\text{Cr}^{3+}$  at 7 and 16 °C, respectively, and 0.51 and 1.06 mg/kg of  $\text{CrO}_4^{2-}$  at 7 and 16 °C, respectively. Uptake of  $\text{Cr}^{3+}$  was greater than uptake of  $\text{CrO}_4^{2-}$ , and uptake at 16 °C was higher than at 7 °C. Although the soluble, bioavailable portion of  $\text{CrO}_4^{2-}$  was much higher than  $\text{Cr}^{3+}$ , it can be seen from the results that  $\text{Cr}^{3+}$  was actually accumulated to a far greater amount than  $\text{CrO}_4^{2-}$ . More than 3 times the amount of Cr was found in *F. vesiculosus* at 360 min at 16 °C, and 2.5 times the amount at 7 °C when exposed to  $\text{Cr}^{3+}$  rather than  $\text{CrO}_4^{2-}$ . Taking into account the fact that soluble  $\text{CrO}_4^{2-}$  was present at concentrations 2.5 times greater than soluble  $\text{Cr}^{3+}$  at 16 °C and 5 times greater at 7 °C, it can be seen that *F. vesiculosus* has a much greater affinity for  $\text{Cr}^{3+}$  than  $\text{CrO}_4^{2-}$ .

The reasons for this are probably related to the functional group composition of the seaweed. This is discussed in more detail in Section 4.3.4.1.

Lower temperatures inhibited the uptake of both  $\text{Cr}^{3+}$  and  $\text{CrO}_4^{2-}$ .  $\text{CrO}_4^{2-}$  was 100 % soluble at both temperatures studied, yet the uptake of  $\text{CrO}_4^{2-}$  at 7 °C was reduced to half over the time period studied compared to at 16 °C. The amount of Cr(III) present as soluble (bioavailable) was half at 7 °C when compared to 16 °C, and this was certainly responsible for some reduction in  $\text{Cr}^{3+}$  uptake at 7 °C.

Bioaccumulation of metal by *F. vesiculosus* has not been widely studied. The only other work in the literature is that of Baumann *et al.* (2010), who studied the accumulation of Cr(VI) ( $\text{K}_2\text{CrO}_4$ ) by *F. vesiculosus*. After 14 days at 10 °C uptake of 7.8 mg/kg was found at an exposure concentration of 52 µg/L, and 26 mg/kg at an exposure concentration of 520 µg/L (Baumann *et al.* 2009). The exposure time in this study was much shorter (360 min), with an exposure concentration of 200 µg/L, explaining the lower concentrations seen here (Figure 4.11 (b)). The uptake of Cr by *F. vesiculosus* at all conditions displayed a linear pattern over the time period of the study ( $R^2=0.73-0.99$ , Figure 4.10). Projecting this linear uptake forward 14 days gives an uptake of 16 and 42 mg/kg at 7 and 16 °C, respectively (Figure 4.12).



**Figure 4.12: Forecast of Cr(VI) /  $\text{CrO}_4^{2-}$  uptake by *F. vesiculosus* (sampled May/Jun) at 14 days (20160 min).**

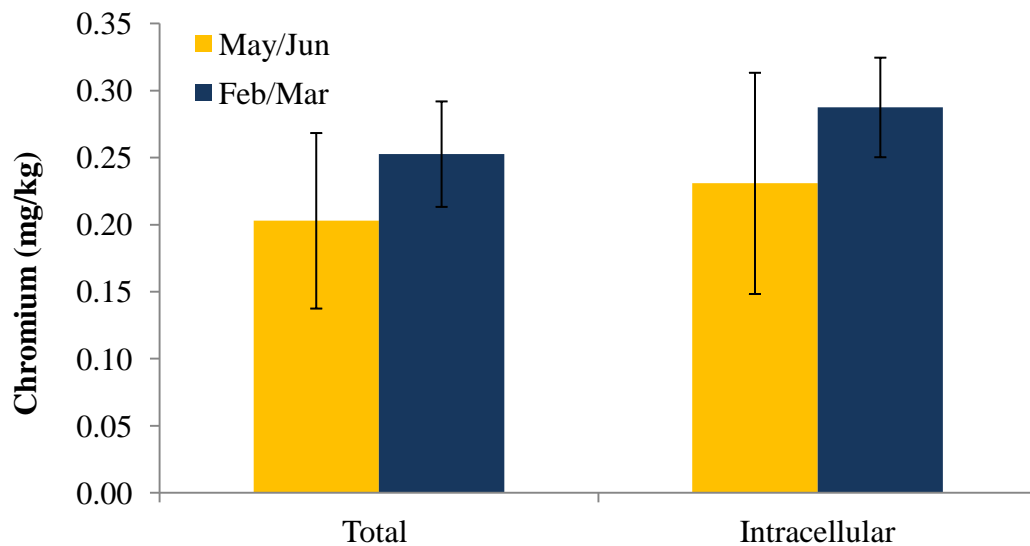
This is surprisingly close to the results found by Baumann *et al.* (2010), considering the differences in exposure conditions (seaweed to seawater ratio, light dark cycles), time and place of seaweed sampling, and the extended time period which was forecast. Linear uptake would also not continue indefinitely and a leveling off of the rate of uptake was likely to have occurred in this time. This supports the results found here, and also indicates that metal bioaccumulation in seaweeds is somewhat reproducible. To the authors knowledge, there are no other papers describing Cr accumulation in any other furoid species, including the rate of Cr bioaccumulation by *F. vesiculosus*, however there are studies on other macroalgal species. Cr(VI) ( $\text{Na}_2\text{Cr}_2\text{O}_7$ ) bioaccumulation by the green seaweed *Enteromorpha crinita* was shown to have a linear uptake pattern even after 2 days of exposure (0.9 mg/kg, exposed to 9.61 nM) (Chan *et al.* 2003). Wang and Dei (1999) also observed a linear pattern of Cr(VI) ( $\text{Na}_2\text{CrO}_4$ ) uptake for the red seaweed *Gracilaria blodgettii* and the green seaweed *U. lactuca* over 2 days (Wang & Dei 1999).

#### **4.3.3.3.1 Seasonal Chromium Uptake by *Fucus vesiculosus***

Another experiment using seaweed sampled in Feb/Mar was carried out. In this case samples were taken at  $t=0$  and  $t=360$  min. This was to determine the seasonal variation in metal uptake. The first graph (Figure 4.13) shows the difference in baseline levels of Cr in *F. vesiculosus* in May/June and Feb/Mar. Both total and intracellular levels are shown. Total and intracellular levels of Cr were equal within error (no significant difference,  $p > 0.05$ , student's t-test, paired, 2-tailed). This showed that all the Cr present in *F. vesiculosus* was internalized. Feb/Mar samples appeared to contain more Cr than May/June samples, although these differences were not statistically significant ( $p > 0.05$ , student's t-test, paired, 2-tailed). The levels found here were very much in agreement with a baseline study of *F. vesiculosus* from the same site in the south east of Ireland, which found 0.30 mg/kg Cr in May (Ryan *et al.* 2012). Baumann *et al.* (2009) also found a concentration of  $<0.5$  mg/kg Cr in *F. vesiculosus* sampled in Galway, Ireland (Baumann *et al.* 2009). This concentration of Cr is lower than what has been observed by other researchers, and probably reflects the relatively pristine nature of the site (Phaneuf *et al.* 1999 - 1.2 mg/kg, Sept/Oct; Chaudhuri *et al.* 2007 - 2.0-7.1 mg/kg, Mar, similar sampling methodology). Other studies have looked at baseline seasonal variation of metal in seaweeds. There are few



trends, with most papers reporting highs and lows specific to seaweed type and metal, or no observable trends at all (Villares *et al.* 2013; Morrison *et al.* 2008; Stengel *et al.* 2005). There are few studies which looked at seasonal baseline Cr levels. One found that Cr had maximum concentration in late spring, and minimum in early winter. However, there were several peaks in the data (Apr, May, Jun), and the peak location changed depending on the sampling site (all north sea coast Germany) (Amer *et al.* 1997). The idea that metal content will be lower in winter is plausible, as growth is also minimum at this time (Villares *et al.* 1999), but the relationship is complicated, and probably depends on many other factors, such as nutrient availability and local conditions.

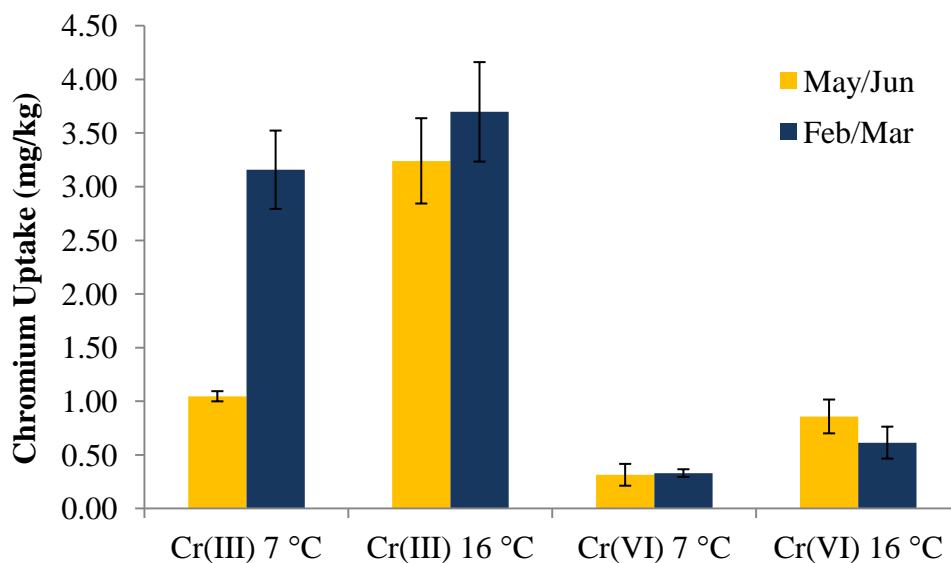


**Figure 4.13: Seasonal variation in baseline chromium levels in *F. vesiculosus* (n=3).**

The results found for the uptake of Cr by *F. vesiculosus* in both May/June and Feb/Mar is shown in Figure 4.14. The results presented are minus the baseline levels shown in Figure 4.13. Therefore the graphs exclusively represent metal uptake which occurred during the metal exposure experiments. Uptake of  $\text{CrO}_4^{2-}$  was found to be almost the same in May/June and in Feb/Mar. For  $\text{Cr}^{3+}$ , levels of uptake were higher in Feb/Mar samples than with May/June samples, especially at 7 °C. The differences in uptake were found to be significant ( $\text{Cr}^{3+}$  7 °C,  $p = 0.009$ ,  $\text{Cr}^{3+}$  16 °C,  $p = 0.015$ ). This indicates that seasonality may be important for  $\text{Cr}^{3+}$ , but not for  $\text{CrO}_4^{2-}$  uptake in *F.*

*vesiculosus*. Uptake of  $\text{Cr}^{3+}$  was also much higher than  $\text{CrO}_4^{2-}$ , giving evidence that uptake mechanisms of  $\text{Cr}^{3+}$  and  $\text{CrO}_4^{2-}$  are different.

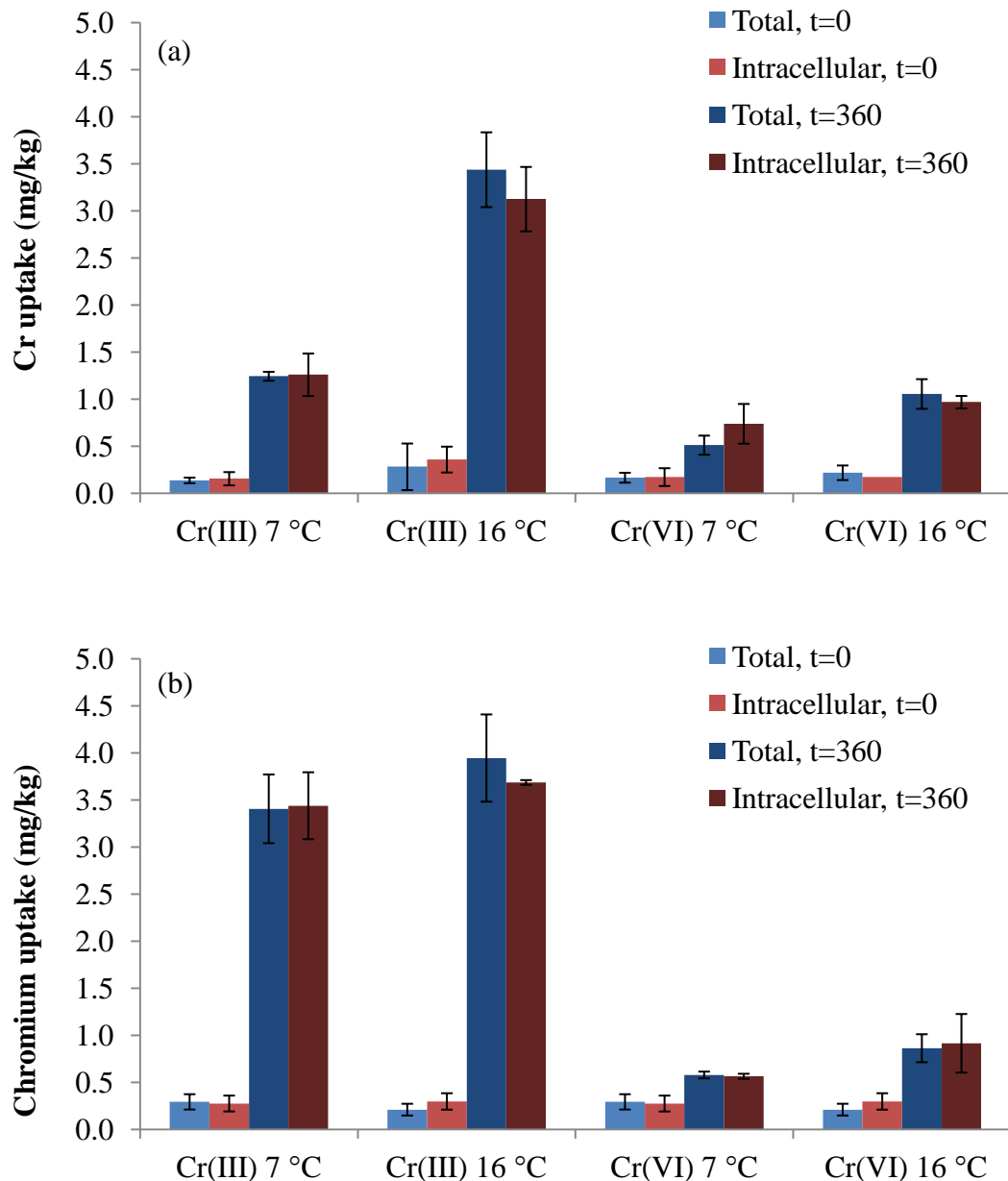
Vasconcelos (2001) was the only researcher to look at seasonal changes in bioaccumulation (*Porphyra* and *Ulva* spp.). Pb, Cd and Hg uptake was found to be similar in Jan, May and Aug, but Cu uptake, was highest in Jan, medium in May and lowest in Aug (Vasconcelos & Leal 2001). There is some evidence in Figure 4.14 that the same may be true for  $\text{Cr}^{3+}$ , but not  $\text{CrO}_4^{2-}$  uptake as higher uptake was seen in the *F. vesiculosus* samples from Feb/Mar. The reason for higher uptake in the Feb/Mar is probably due to either seaweed metabolism or compositional changes, which enhanced the seaweeds uptake ability during this time for cationic species such as  $\text{Cr}^{3+}$  but not anionic species such as  $\text{CrO}_4^{2-}$ . In this work, *F. vesiculosus* was shown to have a greater P content during Feb/Mar. P is used in the cell membrane and greater quantities may facilitate intracellular diffusion of  $\text{Cr}^{3+}$ . This has not been shown in the literature to date and this warrants further research.



**Figure 4.14: Seasonal variation in Cr uptake in *F. vesiculosus* (n=3).**

The results of EDTA washing of the seaweed surface to remove metals is shown in Figure 4.15. The results show that no metal was removed from the seaweed surface, indicating that the majority of the metal appears to have been accumulated by the seaweed by an intracellular route. Indeed, the differences between total and

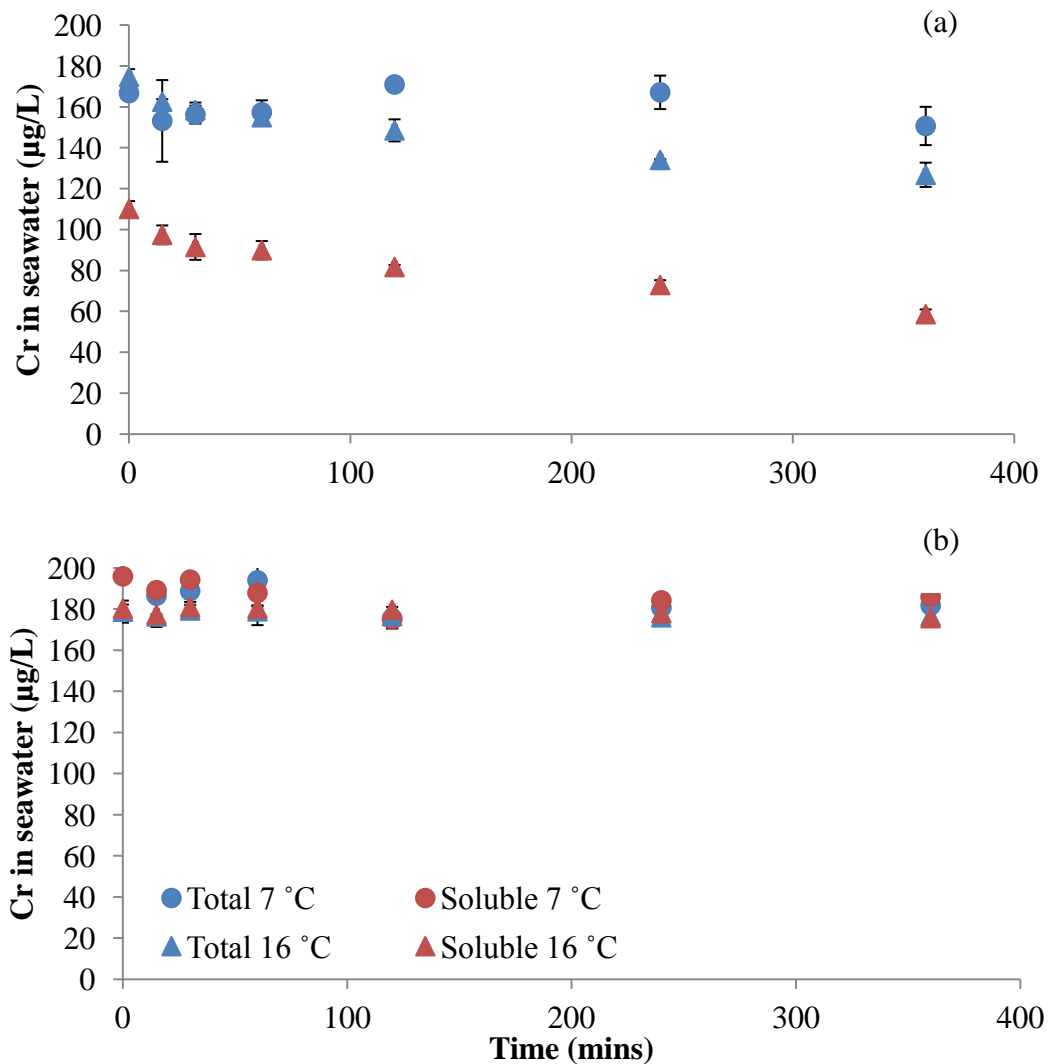
intracellular metal accumulation were not statistically significant in any case ( $p > 0.05$ ). This is in agreement with the results of Chan *et al.* (2003), who found that Cr(VI) uptake by the green seaweed *Ulva crinita* was mostly intracellular (>97 %). A similar pattern was seen in the unicellular freshwater algae, *Chlorella vulgaris* (approx. 85 % internalization of Cr (VI)) (S. Mehta & Gaur 1999). The present study showed that intracellular uptake is the dominant form of uptake in *F. vesiculosus*.



**Figure 4.15: Total Cr, and intracellular Cr in *F. vesiculosus* sampled in May/June (a) and Feb/Mar (b) (n=3).**

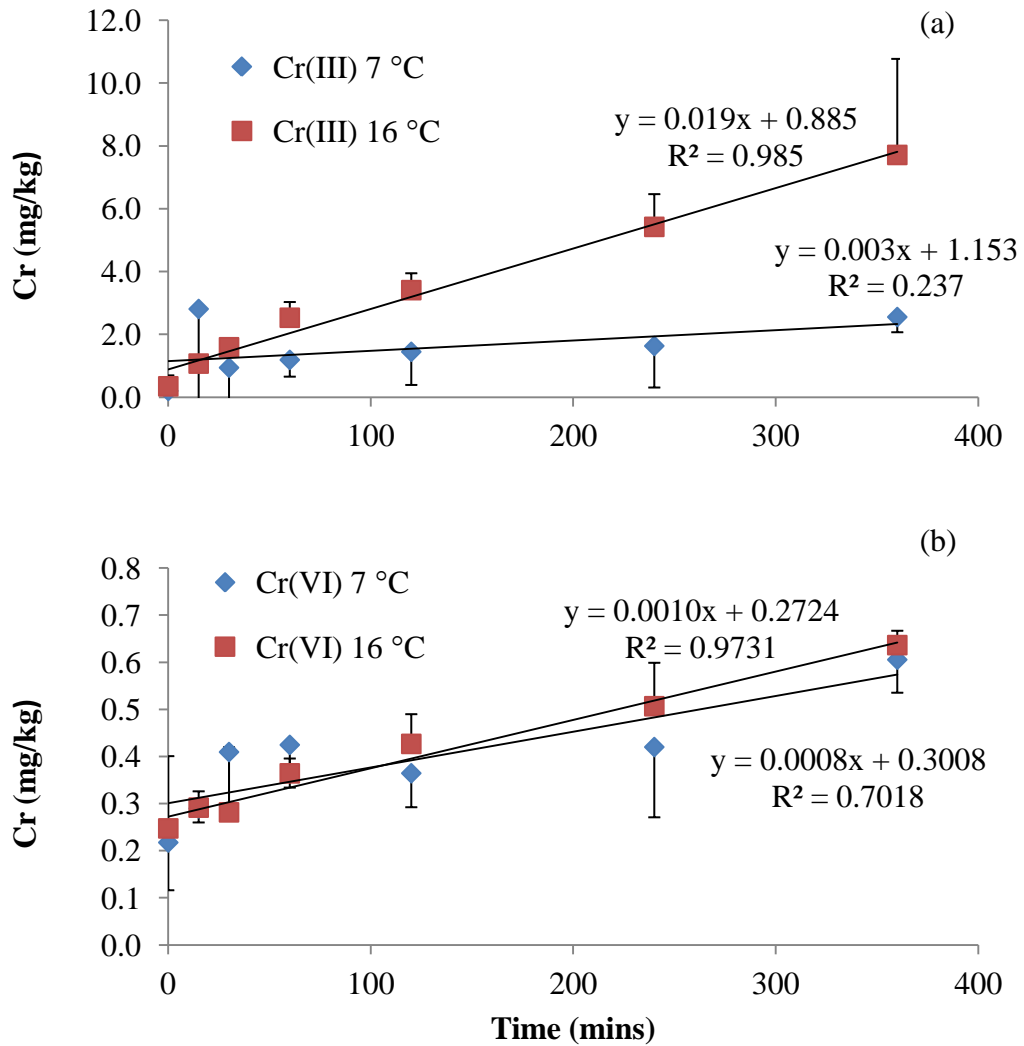
#### 4.3.3.4 Chromium Uptake by *Palmaria palmata*

Shown in Figure 4.16 is the uptake of  $\text{Cr}^{3+}$  and  $\text{CrO}_4^{2-}$  from a seawater solution by *P. palmata*. Note there was no result obtained for the soluble  $\text{Cr}^{3+}$  at 7 °C as the sample was acidified before filtration could be carried out in error.



**Figure 4.16 Uptake of  $\text{Cr}^{3+}$  / Cr(III) (a) and  $\text{CrO}_4^{2-}$  / Cr(VI) (b) by *P. palmata*: Total and soluble Cr in seawater (n=3).**

As seen for *F. vesiculosus*, the total amount of Cr removed from the seawater solution was small, but the downward trend for  $\text{Cr}^{3+}$  accumulation can be seen. The results can be more clearly seen in the Cr content of the digested seaweed samples, shown in Figure 4.17.

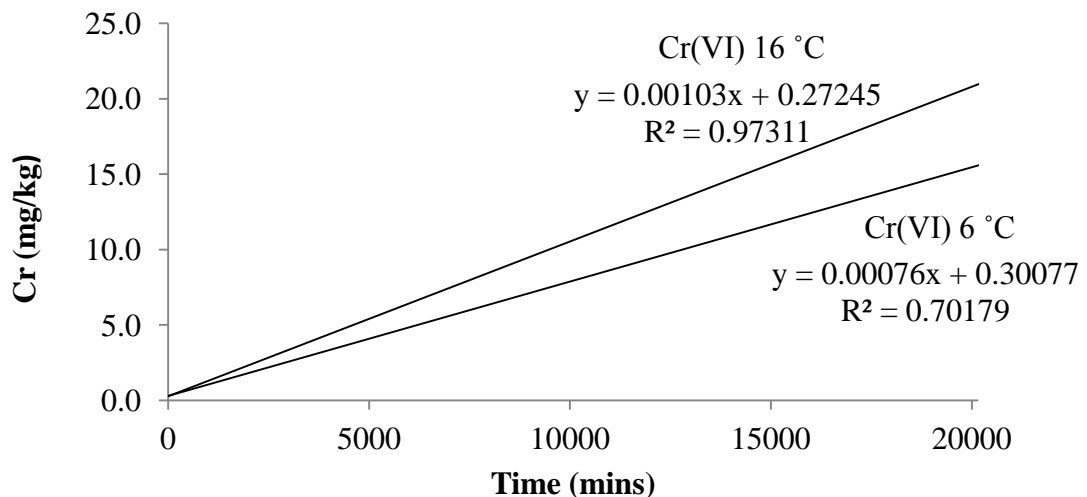


**Figure 4.17: Uptake of  $\text{Cr}^{3+}$  / Cr(III) (a) and  $\text{CrO}_4^{2-}$  / Cr(VI) (b) by *P. palmata* (n=3).**

*Palmaria palmata* accumulated a maximum of 2.55 and 7.71 mg/kg of  $\text{Cr}^{3+}$  at 7 and 16 °C, respectively, and 0.61 and 0.64 mg/kg of  $\text{CrO}_4^{2-}$  at 7 and 16 °C, respectively. Uptake of  $\text{Cr}^{3+}$  was greater than uptake of  $\text{CrO}_4^{2-}$ . Uptake of  $\text{Cr}^{3+}$  was higher at 16 °C than at 7 °C, but uptake of  $\text{CrO}_4^{2-}$  did not appear to change with temperature.

To the author's knowledge, the bioaccumulation of Cr by *P. palmata* has only been studied by Baumann *et al.* (2009). In a 14 day study, the uptake of Cr(VI) ( $\text{K}_2\text{CrO}_4$ ) was found to be 7.8 mg/kg at an exposure concentration of 52  $\mu\text{g/L}$ , and 57.2 mg/kg at an exposure concentration of 520  $\mu\text{g/L}$  (Baumann *et al.* 2009). The exposure time was shorter (360 min) here, with an exposure concentration of 200  $\mu\text{g/L}$ , explaining the lower concentrations seen here (Figure 4.17 (b)). The uptake of  $\text{CrO}_4^{2-}$  by *P.*

*palmata* at all conditions displayed a linear pattern over the time period of the study ( $R^2=0.70-0.99$ , Figure 4.17). Forecasting this linear uptake forward 14 days gives a  $\text{CrO}_4^{2-}$  uptake of 16 and 21 mg/kg at 7 and 16 °C, respectively (Figure 4.18). As was the case with *F. vesiculosus*, the forecasted results were relatively close to those found by Baumann *et al.* (2009), taking into account experimental differences. Again, there has been no study of the rate of Cr uptake by *P. palmata*, but this linear pattern has been observed for  $\text{CrO}_4^{2-}$  uptake by other macroalgal species (Chan *et al.* 2003), including the red algae *Gracilaria blodgettii*. The authors suggest that the linear uptake pattern showed that metal uptake proceeded by passive diffusion and facilitated transport across the cell membrane. The evidence for this was that the metals used in their study, which have a better binding affinity to proteins and therefore greater possibility of binding to protein ligands for transport across the cell membrane, were accumulated to a greater degree by the seaweed (Wang & Dei 1999).

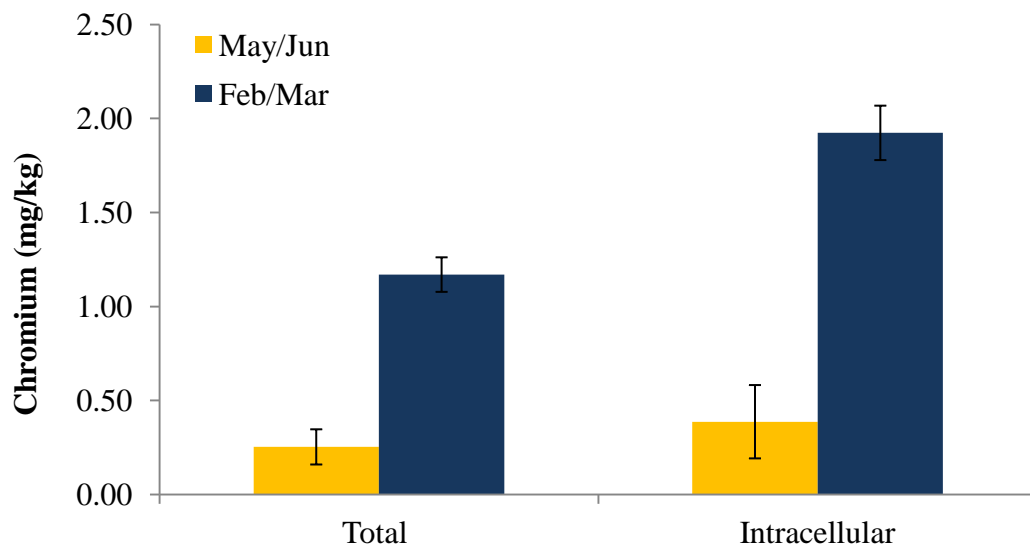


**Figure 4.18: Forecast of Cr(VI) uptake by *P. palmata* (sampled May/Jun) at 14 days (20160 min).**

#### 4.3.3.4.1 Seasonal Chromium Uptake by *P. palmata*

Another set of experiments using seaweed sampled in Feb/Mar was carried out in order to determine the seasonal variation in metal uptake. In this case samples were taken at  $t=0$  and  $t=360$  min. Figure 4.19 shows the difference in baseline levels of Cr in *P. palmata* in May/Jun and Feb/Mar. Both total and intracellular levels are shown. As for *F. vesiculosus*, the Cr was found to be intracellular. However, in Feb/Mar the

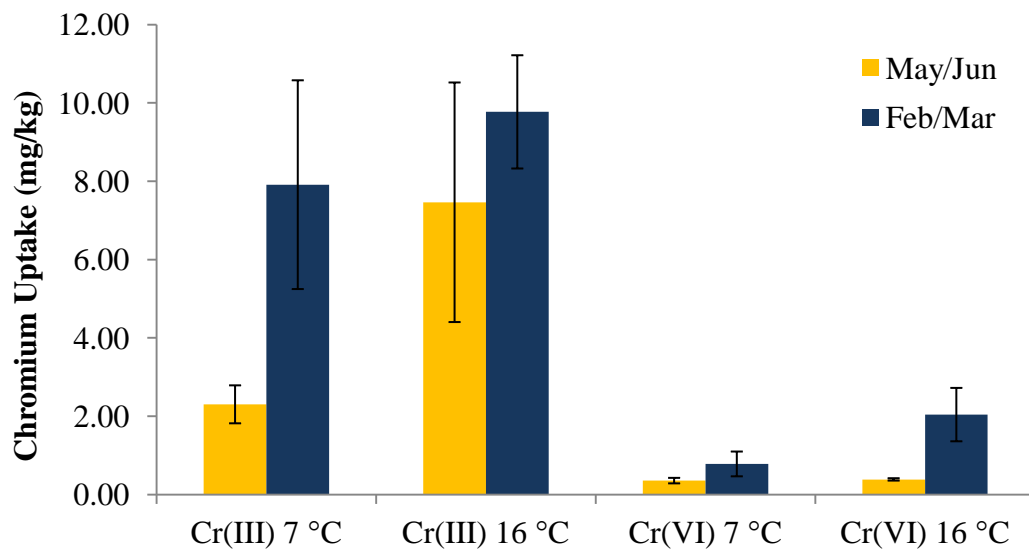
intracellular level of Cr was found to be higher than the total level of Cr ( $p < 0.01$ ). The reason for this was not known, and researchers using this common technique have not reported this problem previously (Ryan *et al.* 2012; García-Ríos *et al.* 2007; S. Mehta & Gaur 1999). It is possible that samples of *P. palmata* were less robust to the action of EDTA, which caused breakdown of the seaweed, and therefore loss of mass. This means that metal levels would be higher than expected as the mass the seaweed results are calculated from was lower. A significant increase in Cr content was observed in Feb/Mar ( $p < 0.01$ ). This result is based on total Cr content, not intracellular data. The baseline levels of total Cr in *P. palmata* sampled from Galway in the west of Ireland was found to be 1 mg/kg (Baumann *et al.* 2009). This is comparable to the results found here. These results also support the hypothesis that baseline Cr levels in some seaweeds are higher in Feb/Mar than in May/Jun (discussion in Section 4.3.3.3.1).



**Figure 4.19: Seasonal variation in baseline Cr levels in *P. palmata* (n=3).**

The seasonal variation in uptake is shown in Figure 4.20. As for *F. vesiculosus*, this data was zeroed using baseline values, so uptake only is shown in the figure. There was a consistent increase in uptake in Feb/Mar compared to May/Jun. This was non-significant except for  $\text{CrO}_4^{2-}$  at 16 °C ( $p = 0.04$ ), probably due to the large confidence intervals associated with the results. (Note  $\text{Cr}^{3+}$  at 7 °C had marginal significance with  $p = 0.047$ ). An indication that seasonal differences exist for metal uptake in seaweeds has been found in the only other published account (discussed previously in Section

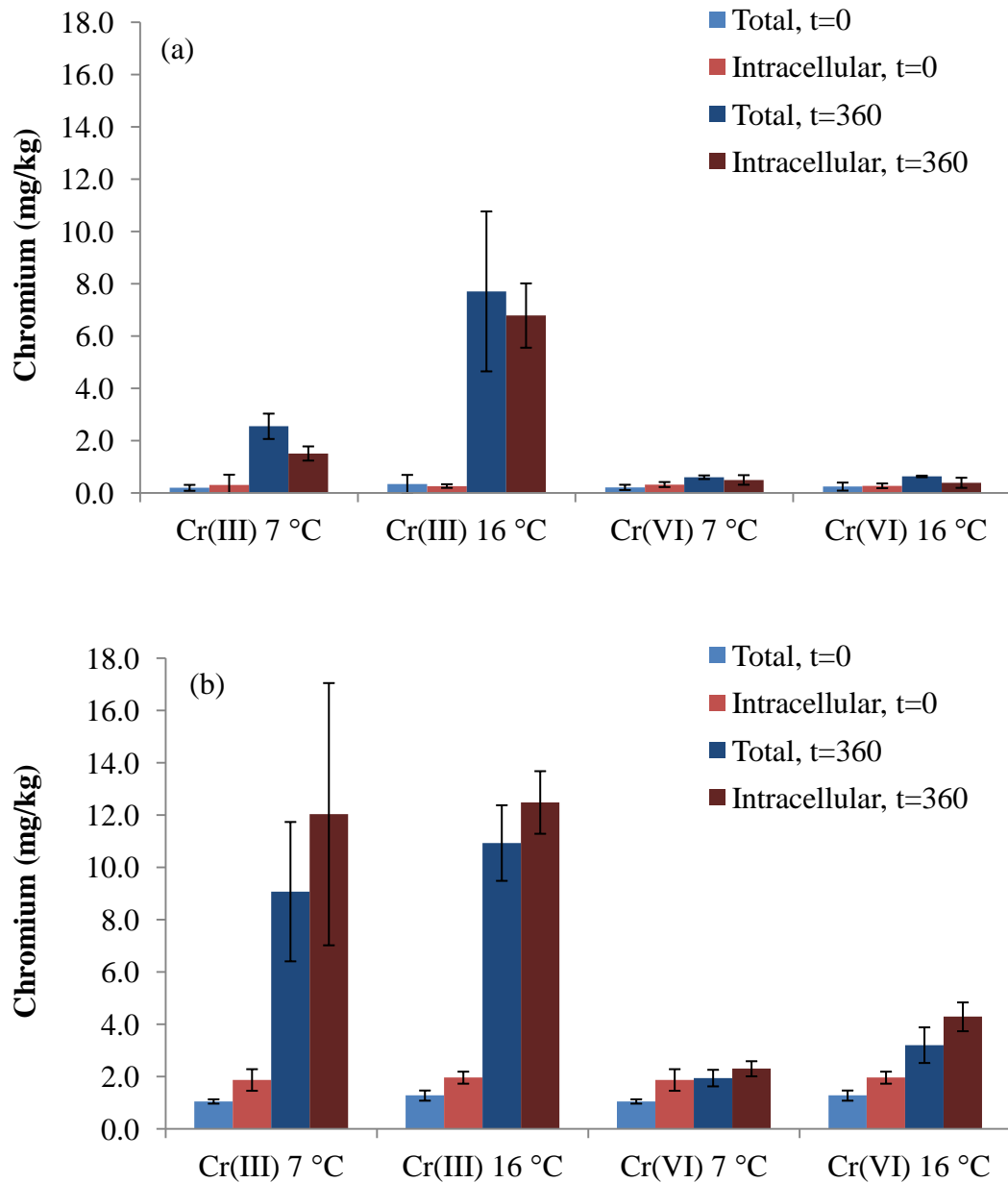
4.3.3.3.1, Vasconcelos & Leal 2001). Although the results were statistically non-significant, the consistency of the findings, plus the results of the published study by Vasconcelos and Leal (2001), add weight to the results found here. The reason for the seasonal difference is most likely related to the seasonal compositional differences in the seaweed. *P. palmata* contains more N in Feb/Mar (see Chapter 2: Characterisation). N is related to protein content. A greater concentration of protein ligands may well enhance metal binding and uptake across the cell membrane (Wang & Dei 1999; Leal *et al.* 1999; Vasconcelos *et al.* 2002; Vasconcelos & Leal 2008).



**Figure 4.20: Seasonal variation in Cr uptake in *P. palmata* (n=3).**

The results of EDTA washing of the surface of *P. palmata* to remove metals is shown in Figure 4.21.



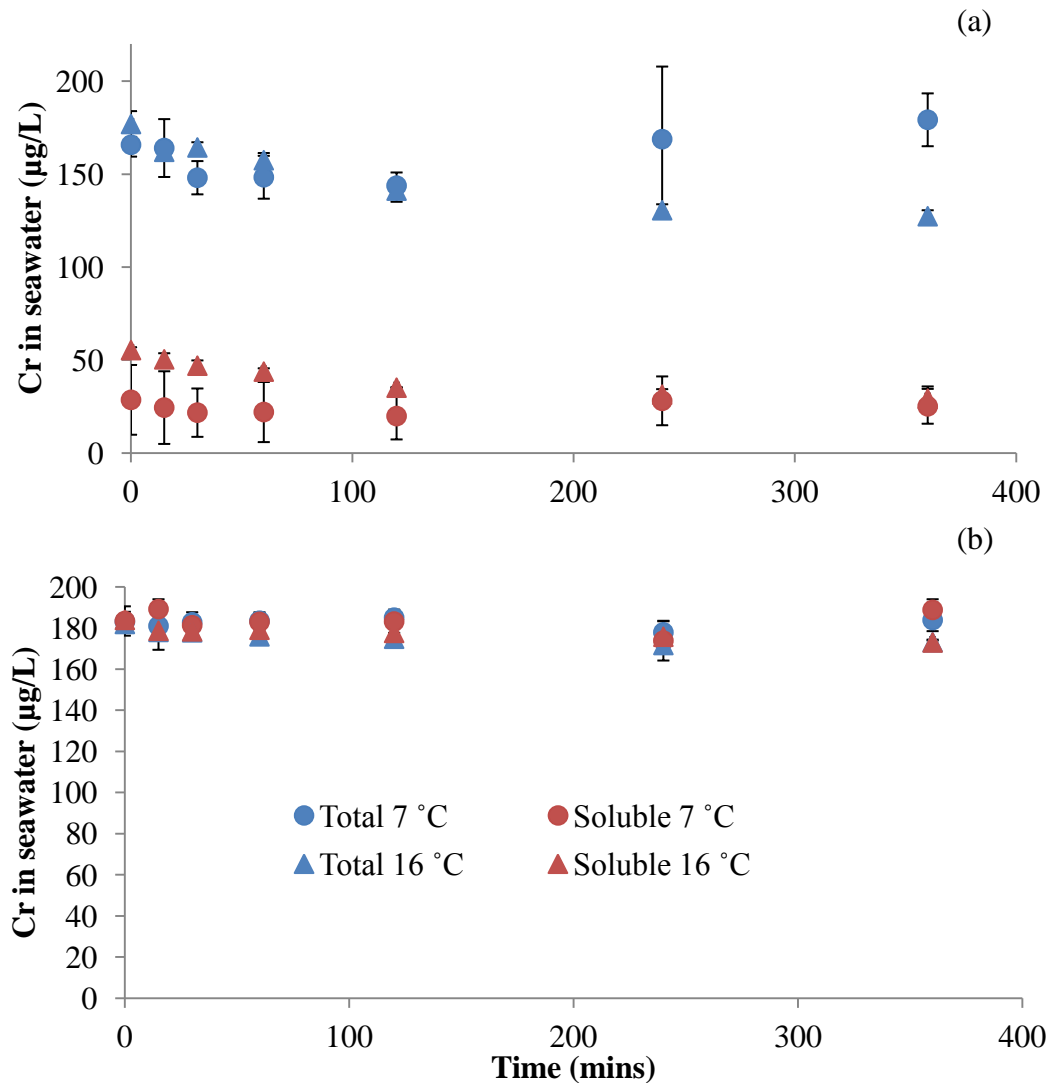


**Figure 4.21: Total Cr, and intracellular Cr in *P. palmata* sampled in May/June (a) and Feb/Mar (b) (n=3).**

As found for *F. vesiculosus*, the majority of uptake for *P. palmata* was intracellular; there were no statistically significant differences between total and intracellular bioaccumulation for any conditions except the uptake of Cr(III) at 7 °C in May/June ( $p = 0.002$ , student's t-test, paired, 2-tailed). The difference was very small, but this indicates that some of the Cr<sup>3+</sup> under these conditions was accumulated extracellularly, or bound to the cell wall.

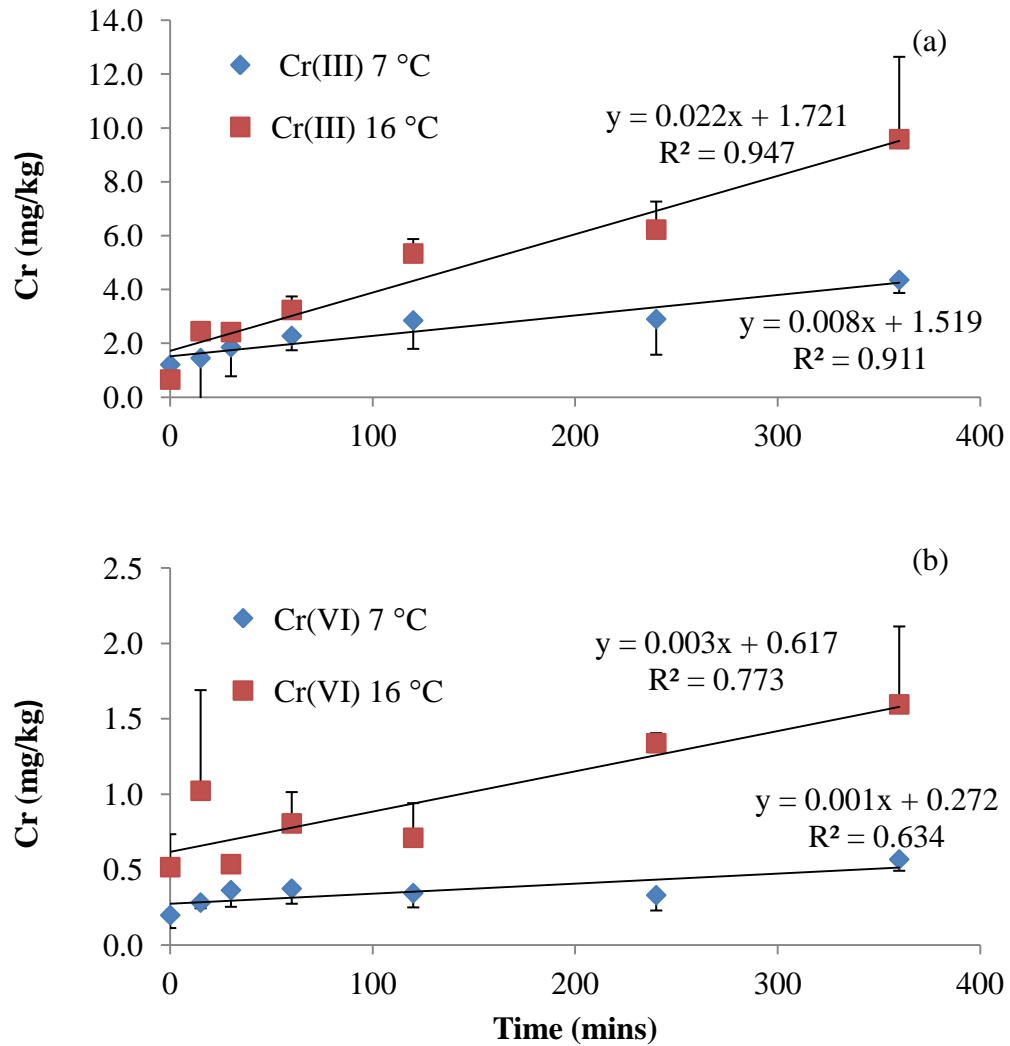
#### 4.3.3.5 Chromium Uptake by *Ulva lactuca*

Shown in Figure 4.22 is the uptake of Cr(III) and Cr(VI) from a seawater solution by *U. lactuca*.



**Figure 4.22: Uptake of  $\text{Cr}^{3+}$  / Cr(III) (a) and  $\text{CrO}_4^{2-}$  / Cr(VI) (b) by *U. lactuca*: Total and soluble Cr in seawater (n=3).**

As seen for *F. vesiculosus* and *P. palmata*, the total amount of Cr removed from the seawater solution was small, but the downward trend for  $\text{Cr}^{3+}$  accumulation especially can be seen. The results can be more clearly seen in the Cr content of the digested seaweed samples, shown in Figure 4.23.



**Figure 4.23: Uptake of  $\text{Cr}^{3+}$  / Cr(III) (a) and  $\text{CrO}_4^{2-}$  / Cr(VI) (b) by *U. lactuca*.**

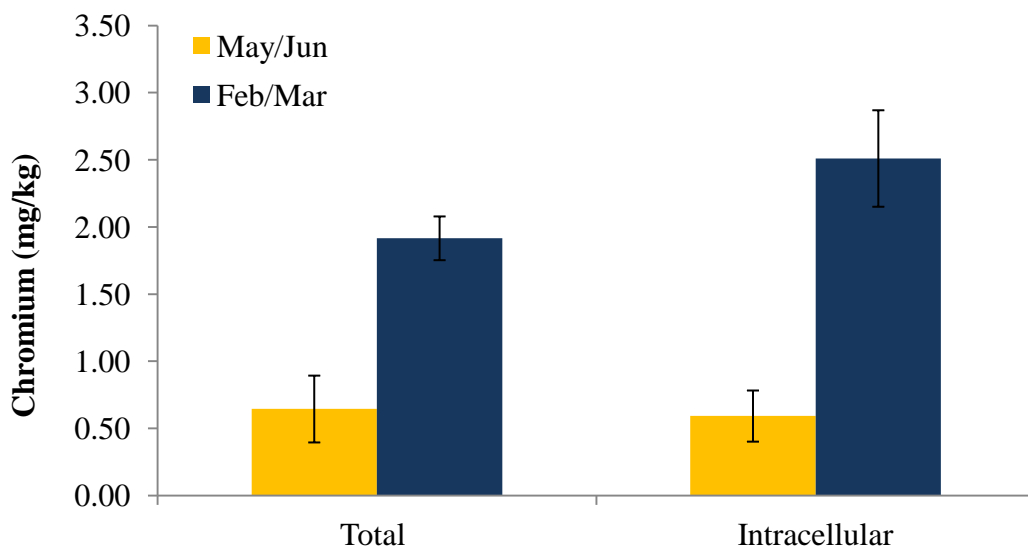
*U. lactuca* accumulated a maximum of 4.36 and 9.53 mg/kg of  $\text{Cr}^{3+}$  at 7 and 16 °C, respectively, and 0.57 and 1.60 mg/kg of Cr(VI) at 7 and 16 °C, respectively. Uptake of  $\text{Cr}^{3+}$  was greater than uptake of  $\text{CrO}_4^{2-}$ , and uptake at 16 °C was higher than at 7 °C. This is the same general pattern as seen for *F. vesiculosus*, and *P. palmata*.

Wang and Dei (1999) have studied  $\text{CrO}_4^{2-}$  uptake by *U. lactuca*. There are no studies detailing  $\text{Cr}^{3+}$  bioaccumulation. After 6 h, *U. lactuca* uptake of  $\text{CrO}_4^{2-}$  was 0.03 and 0.8 mg/kg at exposure concentrations of 0.5 and 10  $\mu\text{g/L}$ , respectively, at a temperature of 18 °C (Wang & Dei 1999). This was lower than the uptake of  $\text{CrO}_4^{2-}$  found in this experiment (1.6 mg/kg), but there were significant experimental differences (200  $\mu\text{g/L}$  vs. 0.5 and 10  $\mu\text{g/L}$ ). Uptake of  $\text{CrO}_4^{2-}$  by *U. lactuca* was found to be linear ( $R^2 = 0.6-0.8$ ), as was the case for *F. vesiculosus* and *P. palmata*. Wang

and Dei (1999) also found a linear pattern of uptake over a 2 day period, supporting these results, and indicating that saturation of binding sites had not occurred at the concentrations studied (Wang & Dei 1999). Uptake of  $\text{Cr}^{3+}$  also had a linear pattern over the 360 min period studied here ( $R^2 = >0.90$ ).

#### 4.3.3.5.1 Seasonal Chromium Uptake by *U. lactuca*

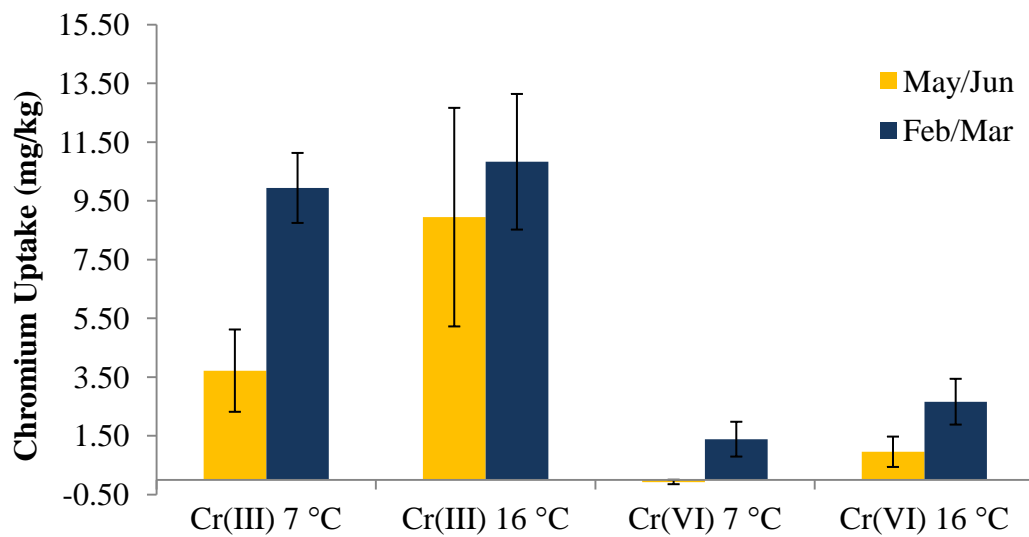
The experimental results using seaweed sampled in Feb/Mar, as well as May/Jun, are presented in this section. First, the baseline levels of Cr in *U. lactuca* in May/Jun and Feb/Mar are shown in Figure 4.24. Both total and intracellular levels are shown. Similarly to both *F. vesiculosus* and *P. palmata*, the Cr was found to be internalised. There was significantly more Cr found in *U. lactuca* sampled in Feb/Mar, than in May/Jun ( $p < 0.01$ ). These results confirmed the seasonal trend in baseline levels of Cr seen for *F. vesiculosus* and *P. palmata*, which indicate that levels of Cr are consistently lower in May/Jun than Feb/Mar.



**Figure 4.24: Seasonal variation in baseline Cr levels in *U. lactuca* (n=3).**

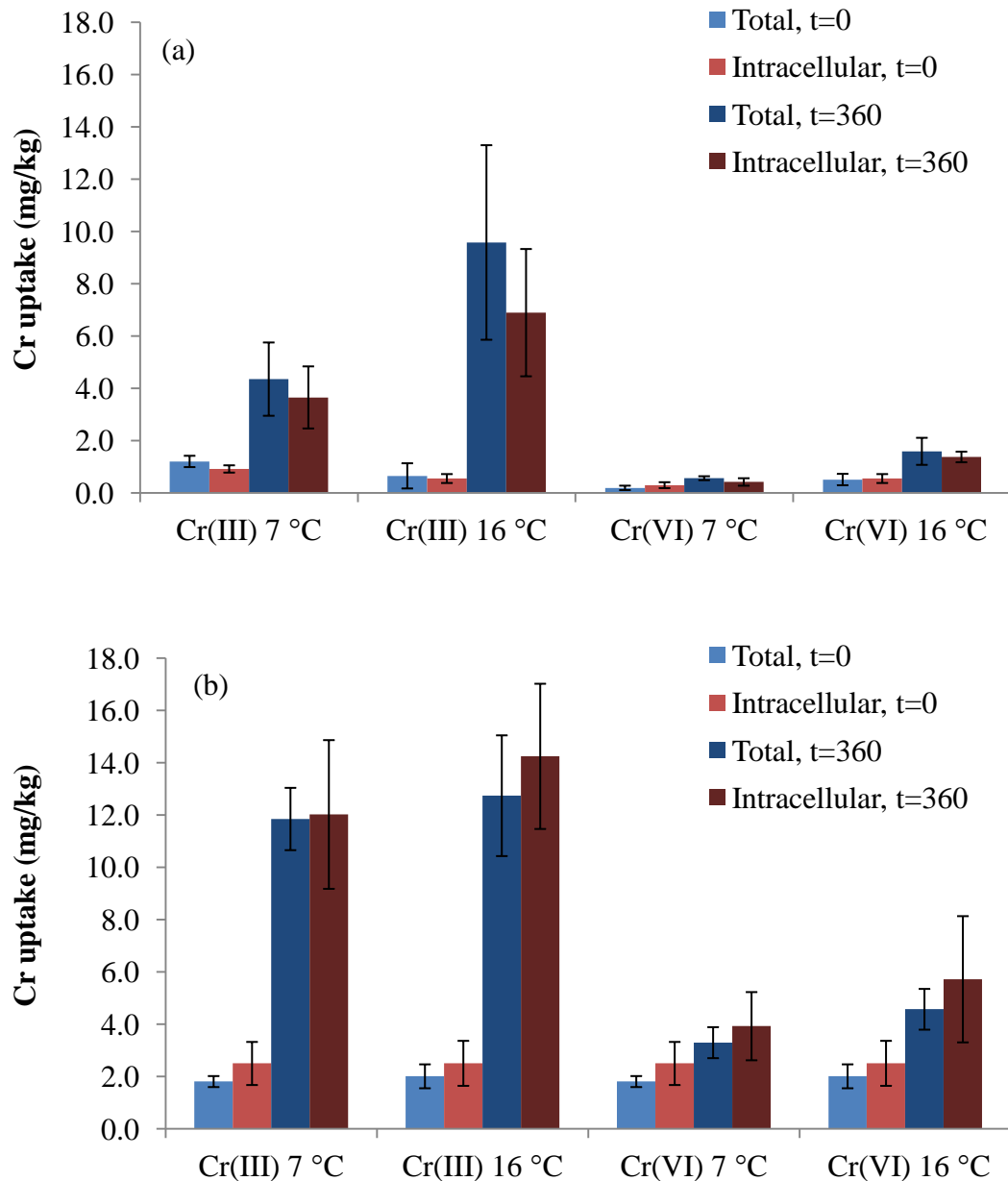
The seasonal variation in uptake of Cr by *U. lactuca* is shown in Figure 4.25. The Cr concentrations in samples taken at the end of the uptake experiment are presented here. The baseline levels shown in Figure 4.24 have been taken away from the total Cr result so that only Cr uptake is shown. *U. lactuca* sampled in Feb/Mar was consistently found to take up more Cr than seaweed sampled in May/Jun. There was zero  $\text{CrO}_4^{2-}$  uptake over the 360 min period at 7 °C. The difference in uptake was

significant ( $p < 0.05$ ), except for  $\text{Cr}^{3+}$  at 16 °C. Taking the results for all the seaweed together, there is a general, consistent trend for higher uptakes with seaweed sampled in Feb/Mar. As discussed for *P. palmata* above, the reason is probably because of seaweed compositional differences between the seasons. There is significantly more N during Feb/Mar, which means that there is more protein containing ligands available for binding, leading to greater uptake. The importance of metal binding ligands in seaweeds has been shown in various articles. These cysteine and glutathione ligands were shown to be produced by algae and to bind to Cu, Pb, Cd, Zn, Fe, Mn, Ni and Co (Leal *et al.* 1999; Vasconcelos *et al.* 2002; Vasconcelos & Leal 2008).



**Figure 4.25: Seasonal variation in Cr uptake in *U. lactuca*.**

The results of an EDTA wash of the seaweed surface to remove bound metals are shown in Figure 4.26. The EDTA wash removes cationic metals from the surface of the seaweed and allows the determination of intracellular metal. It is a common method used for seaweeds to determine intracellular metal content (Ryan *et al.* 2012; García-Ríos *et al.* 2007).



**Figure 4.26: Total Cr, and intracellular Cr in *U. lactuca* sampled in May/June (a) and Feb/Mar (b) (n=3).**

As seen for both *F. vesiculosus* and *P. palmata*, the majority of uptake was intracellular. There were no statistically significant differences between total and intracellular bioaccumulation under any conditions, indicating that uptake was almost entirely intracellular in nature.

#### 4.3.3.6 Relationship Between Metal Uptake and Temperature

The relationship of temperature to metal uptake is two-fold. First is the relationship between metal solubility and uptake.  $\text{Cr}^{3+}$  was less soluble, and therefore less

available at 7 °C. This has certainly contributed to the lower level of metal uptake at 7 °C than at 16 °C. However, there is also a relationship between temperature and metal uptake, which is independent of metal solubility. This can be seen in metal uptake results for  $\text{CrO}_4^{2-}$ , where solubility was not affected by temperature.  $\text{CrO}_4^{2-}$  was 100 % soluble no matter what temperature was studied. This can be clearly seen in Figures 4.11, 4.17 and 4.23, where uptake at 7 °C was lower than uptake at 16 °C. This indicates a physical/biochemical effect in the seaweed which affects uptake. This has not been shown in seaweeds to date. This has been discussed by Fritioff *et al.* (2005), who studied the effect of temperature on metal uptake in two submerged aquatic plants, *Elodea canadensis* and *Potamogeton natans*. It was found that, in general, the uptake of Cu, Cd, Zn, and Pb increased with increasing temperature from 5–20 °C over 48 h (Fritioff *et al.* 2005). One factor for this was a change in chemical equilibrium between cell wall functional groups and the metal, leading to greater extracellular uptake. Intracellular uptake could also be affected for reasons such as greater fluidity of the cell membrane, increased metabolism and increased protein synthesis (Fritioff *et al.* 2005). The effect of temperature may be explained by the ease of movement into the cell. At higher temperatures, cell membranes tend to allow easier access for substances to pass through. The membranes, composed of fatty acid chains behave as solids at lower temperatures, with a small space between the chains. As the temperature increases, they become liquid and the spaces between chains increase in size (Metzler 1997). This may facilitate chromium entry into the cell. This is especially relevant to anionic  $\text{CrO}_4^{2-}$  which can enter the cell through the sulfate ion channels (Ksheminska *et al.* 2005). Once inside the cells, *F. vesiculosus* is known to contain physodes, which are vesicles containing polyphenolics, terpenes and fucoidans. These may be involved in the sequestration of heavy metals once they enter the cell (Graham & Wilcox 2000).

Further study, controlling the levels of soluble metal present at various temperatures, would allow the elucidation of the relationship between temperature and metal uptake in live seaweeds.

#### 4.3.4 FTIR

ATR FTIR spectra of the three seaweed species studied were analysed to determine if there were any changes on metal binding. The ATR technique allows the analysis of the surface of the seaweed, as the whole seaweed piece is brought into contact with the crystal surface through which the IR beam is reflected. Samples from the Feb/Mar sampling season were studied in this section. As seen in Sections 4.3.3.3-4.3.3.5, in general more metal was accumulated by the seaweeds sampled during this period. Therefore any change in the FTIR spectrum as a result of metal binding would be more noticeable.

The raw seaweed spectra, as well as the  $\text{Cr}^{3+}$  and  $\text{CrO}_4^{2-}$  loaded spectra, are influenced by metal binding in general, as the functional groups are bound to salt ions, as well as heavy metals present at baseline levels (see Chapter 3 for further information on baseline metal contents). This makes band shifts and differences between spectra difficult to study. For this reason, literature and experimental spectra of protonated seaweeds are also discussed here. Protonated seaweeds are prepared by acid washing and rinsing the seaweed with deionised water. This replaces salt and metals with hydrogen ions (hence 'protonating').

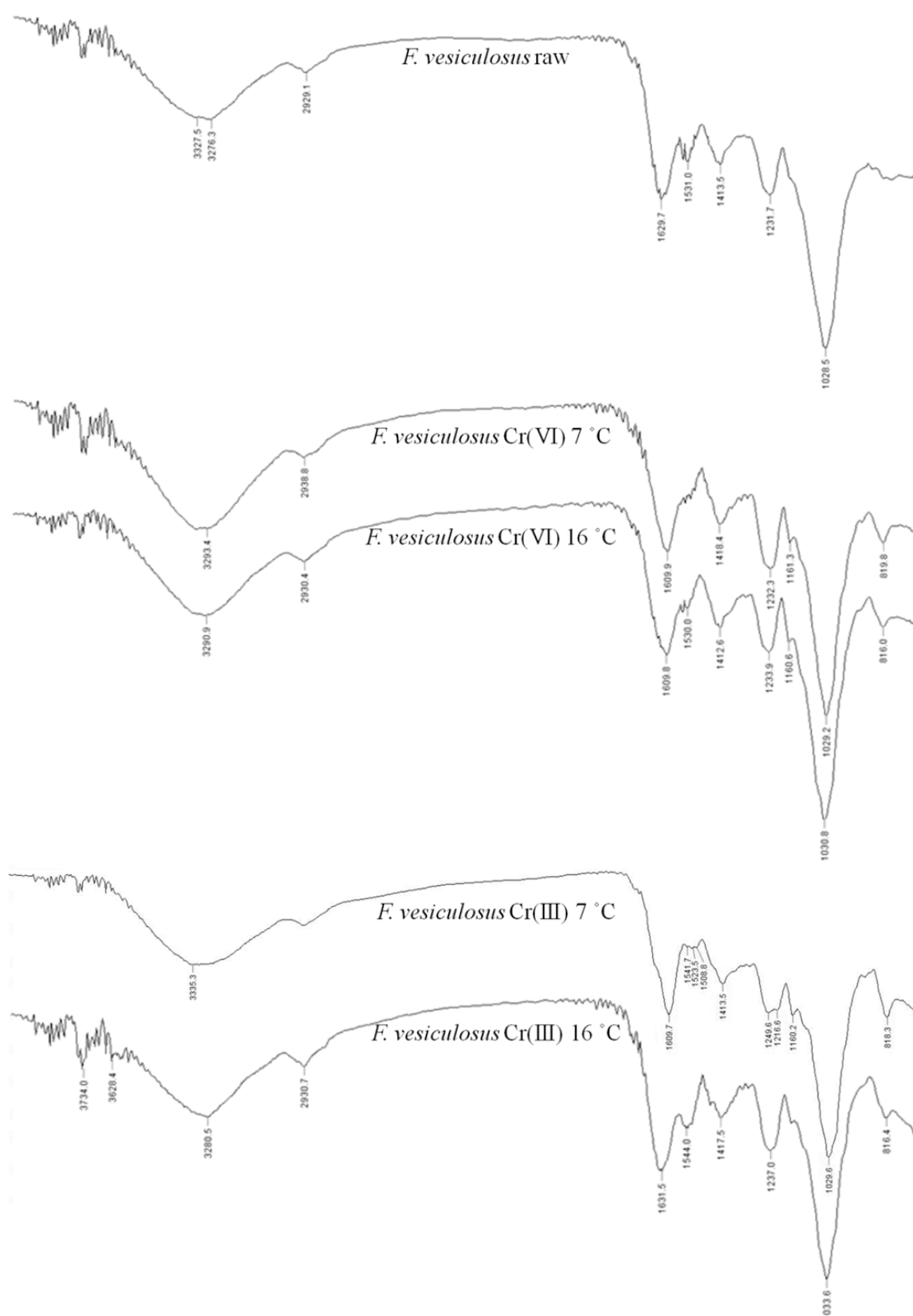
For characterization of the seaweed biomass by FTIR please see Chapter 2, Section 2.3.3. This section will only deal with possible mechanisms of metal binding, as evidenced by FTIR.

##### ***4.3.4.1 FTIR Spectra of Raw and Metal loaded *Fucus vesiculosus* Sampled in Feb/Mar***

Representative spectra are shown in Figure 4.27. The wavenumbers quoted are the average from three spectra  $\pm$  95% confidence intervals. The FTIR spectra below show the main functional groups which may be involved in metal binding. The bands at 1240 and 1160  $\text{cm}^{-1}$  showed the presence of sulphonate groups. The presence of carboxyl groups can be seen by the bands at approximately 1630 and 1413  $\text{cm}^{-1}$ . Both carboxyl ( $\text{pK}_a \approx 4$ ) and sulphonate ( $\text{pK}_a \approx 1$ ) groups will be negatively charged at a pH of 8 (Segel 1976). This means that positively charged Cr(III) (added as  $\text{Cr}(\text{NO}_3)_3 - \text{Cr}^{3+}$ ) ions will be attracted to the negatively charged groups. On the other hand

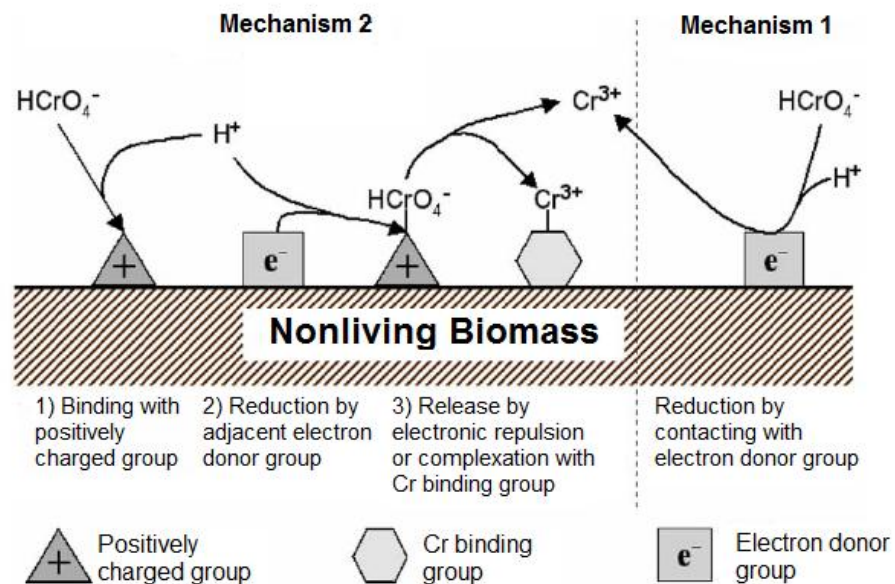


negatively charged Cr(VI) (added as  $(\text{NH}_4)_2\text{Cr}_2\text{O}_7$  -  $\text{Cr}_2\text{O}_7^{2-}$  -  $\text{CrO}_4^{2-}$ ) will have little interaction with these negatively charged groups. The presence of amide groups can be seen at about  $1412\text{ cm}^{-1}$  in these spectra. The NH group of amides will be protonated to  $\text{NH}_3^+$  under these conditions ( $\text{pK}_a \approx 10$ ). This gives the possibility of binding with the negatively charged  $\text{CrO}_4^{2-}$  ions. The relatively low concentration of amide groups on the seaweed surface (compared to carboxyl for example) explains why  $\text{CrO}_4^{2-}$  uptake was lower than  $\text{Cr}^{3+}$  uptake. The balance of the seaweeds composition will be mostly carbohydrate, which provides negatively charged functionalities, such as carboxyl and sulphonate.



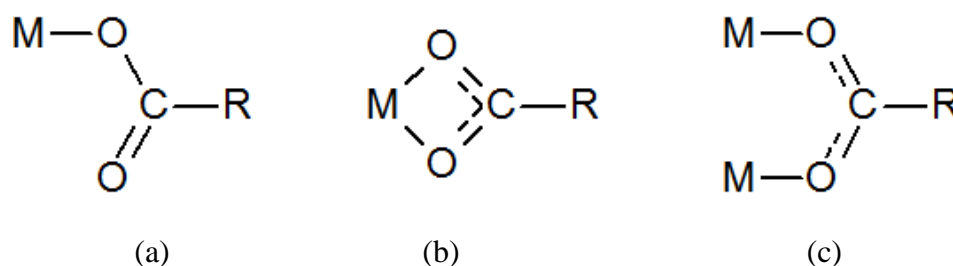
**Figure 4.27:** ATR FTIR spectra of raw *F. vesiculosus* (top), Cr(VI) loaded *F. vesiculosus* at 7 and 16 °C (middle), and Cr(III) loaded *F. vesiculosus* at 7 and 16 °C (bottom) (resolution-4  $\text{cm}^{-1}$ , number of scans-64, representative shown from  $n=3$ ).

Park *et al.* (2005) has suggested several mechanisms whereby seaweed biomass may deal with  $\text{CrO}_4^{2-}$  metal (shown in Figure 4.28). In mechanism I,  $\text{CrO}_4^{2-}$  will be reduced to  $\text{Cr}^{3+}$  by an electron donor group. It may then bind to another, positively charged group, or be released into solution. In mechanism II, it may bind with a positively charged functional group, be reduced subsequently by an electron donor group and then be either released into solution or bound to a negatively charged group (Park *et al.* 2005). The reduction of  $\text{CrO}_4^{2-}$  to  $\text{Cr}^{3+}$  has been shown many times in biosorbants, but is yet to be shown in live seaweed bioaccumulation (Park *et al.* 2005; Park *et al.* 2007; Murphy, Tofail, *et al.* 2009).



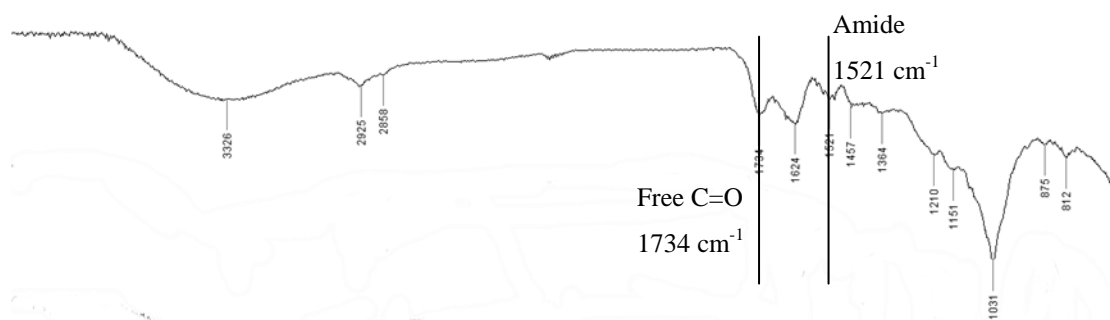
**Figure 4.28: Mechanisms for metal uptake by seaweed (Park *et al.* 2005)**

Free and chelate carboxyl bands are present at about  $1630$  and  $1413\text{ cm}^{-1}$ , respectively, in the spectra shown in Figure 4.27. Carboxyl groups may complex with metals in the ways shown in Figure 4.29 (Nakamoto 1997).



**Figure 4.29: Carboxyl chelates (Nakamoto 1997)**

If the carboxyl group is free this is referred to as protonated, i.e. a hydrogen is bound to the functional group. Metal binding may be studied using the difference between the ‘free’ and the ‘chelate’ FTIR bands. Unidentate complexes shown in Figure 4.29 (a) have differences greater than the protonated form. Bidentate or chelating complexes shown in Figure 4.29 (b) have differences lower than in the protonated form. Bridging complexes shown in Figure 4.29 (c) have differences greater than bidentate complexes and closer to values seen in the protonated form (Nakamoto 1997). In the spectra of *F. vesiculosus* there is little change in the difference between the ‘free’ and ‘chelate’ bands in all the spectra (all  $220 \pm 2 \text{ cm}^{-1}$ ). This may mean either (i) that carboxyl groups are not involved in binding or (ii) the raw seaweed is already bound to salts and metals naturally present in seawater which effectively hide the Cr binding effect. A protonated spectrum of *F. vesiculosus* is shown in Figure 4.30. Note that this seaweed was sampled during October 2008, and it was finely ground, not analysed as a whole piece. The most noticeable difference between the protonated spectrum and the raw and metal loaded spectra is the presence of the free C=O band seen at  $1734 \text{ cm}^{-1}$ . There is no free C=O band in the raw and metal loaded seaweeds, showing that carboxyl binding does occur in *F. vesiculosus*. The difference between the free and chelate carboxyl bands in the protonated spectrum was  $167 \text{ cm}^{-1}$ , smaller than the  $220 \pm 2 \text{ cm}^{-1}$  seen for the raw and metal loaded seaweeds. This indicates the formation of bidentate or bridged chelates shown in Figure 4.29 (b) and (c). The amide band at  $1521 \text{ cm}^{-1}$  in the protonated spectrum was also much smaller or absent in raw and metal loaded spectrum showing that amide groups take part in metal binding.

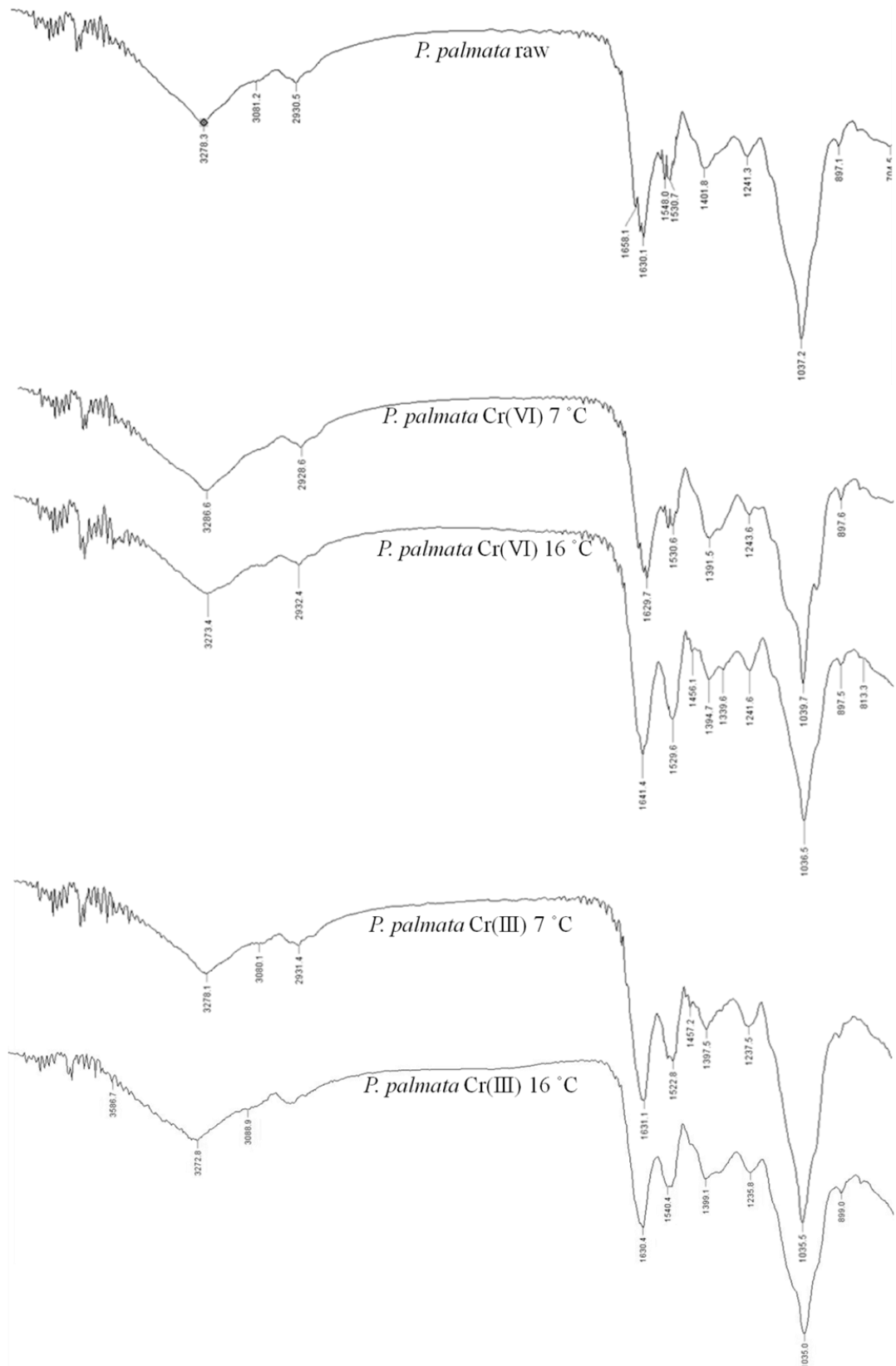


**Figure 4.30: Spectrum of protonated *F. vesiculosus* (resolution-4 cm<sup>-1</sup>, number of scans-64, representative shown from n=3).**

There are few significant differences between the raw and metal loaded spectra shown in Figure 4.27. The main change is in the band at approximately 820 cm<sup>-1</sup> which is characteristic of the presence of alginate, the main polysaccharide present in *F. vesiculosus*. The band is specifically characteristic of the mannuronic acid residues present in alginate. (Leal *et al.* 2008). The band became sharper in spectra of metal loaded seaweeds. This implies that alginate may be involved in the binding of Cr in *F. vesiculosus*.

#### 4.3.4.2 FTIR Spectra of Raw and Metal loaded *P. palmata* Sampled in Feb/Mar

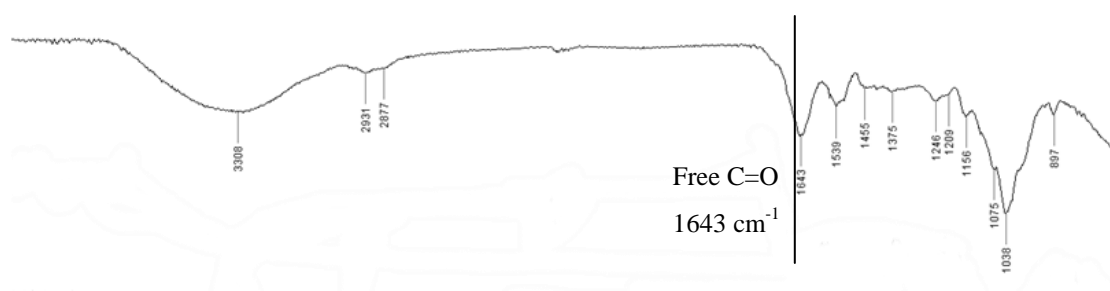
Representative spectra are shown in Figure 4.31. The presence of the sulphate groups can be seen at about 1240 cm<sup>-1</sup>, and carboxyl groups can be seen at about 1630 and 1400 cm<sup>-1</sup>. Both these groups are positively charged at pH conditions in seawater (pH ≈ 8). Therefore these groups will be available to bind with positively charged Cr<sup>3+</sup> ions, but will be unable to bind to negatively charged CrO<sub>4</sub><sup>2-</sup> ions. Amide groups can be seen at about 1530 cm<sup>-1</sup> in these spectra. The NH group of amides will be protonated to NH<sub>3</sub><sup>+</sup> under these conditions. These positively charged groups may interact with negatively charged CrO<sub>4</sub><sup>2-</sup> ions in the manner discussed in Figure 4.28, which will lead to CrO<sub>4</sub><sup>2-</sup> being mostly reduced to Cr<sup>3+</sup>. These factors explain why Cr<sup>3+</sup> is accumulated much more than CrO<sub>4</sub><sup>2-</sup> in *P. palmata*, as mostly positively charged groups are present.



**Figure 4.31:** ATR FTIR Spectra of raw *P. palmata* (top), Cr(VI) loaded *P. palmata* at 7 and 16 °C (middle), and Cr(III) loaded *P. palmata* at 7 and 16 °C (bottom) (resolution-4 cm<sup>-1</sup>, number of scans-64, representative shown from n=3).

There did not appear to be any significant shifts on binding to either  $\text{Cr}^{3+}$  or  $\text{CrO}_4^{2-}$  at 7 or 16 °C. There was a small change in the band located at  $1241 \pm 0 \text{ cm}^{-1}$  in the raw spectrum. It moved  $1235 \pm 1 \text{ cm}^{-1}$  in the sample exposed to  $\text{Cr}^{3+}$  at 16 °C. This frequency is associated with the sulphonate functional group, probably present due to sulphated polysaccharide content on the seaweed surface (Pereira *et al.* 2009). However, there was no similar shift in the sample exposed to  $\text{Cr}^{3+}$  at 7 °C, which contained a similar concentration of Cr. It is possible that different mechanisms are involved at different temperatures; however it was not possible to make a conclusion on whether this signifies involvement of this group on Cr binding.

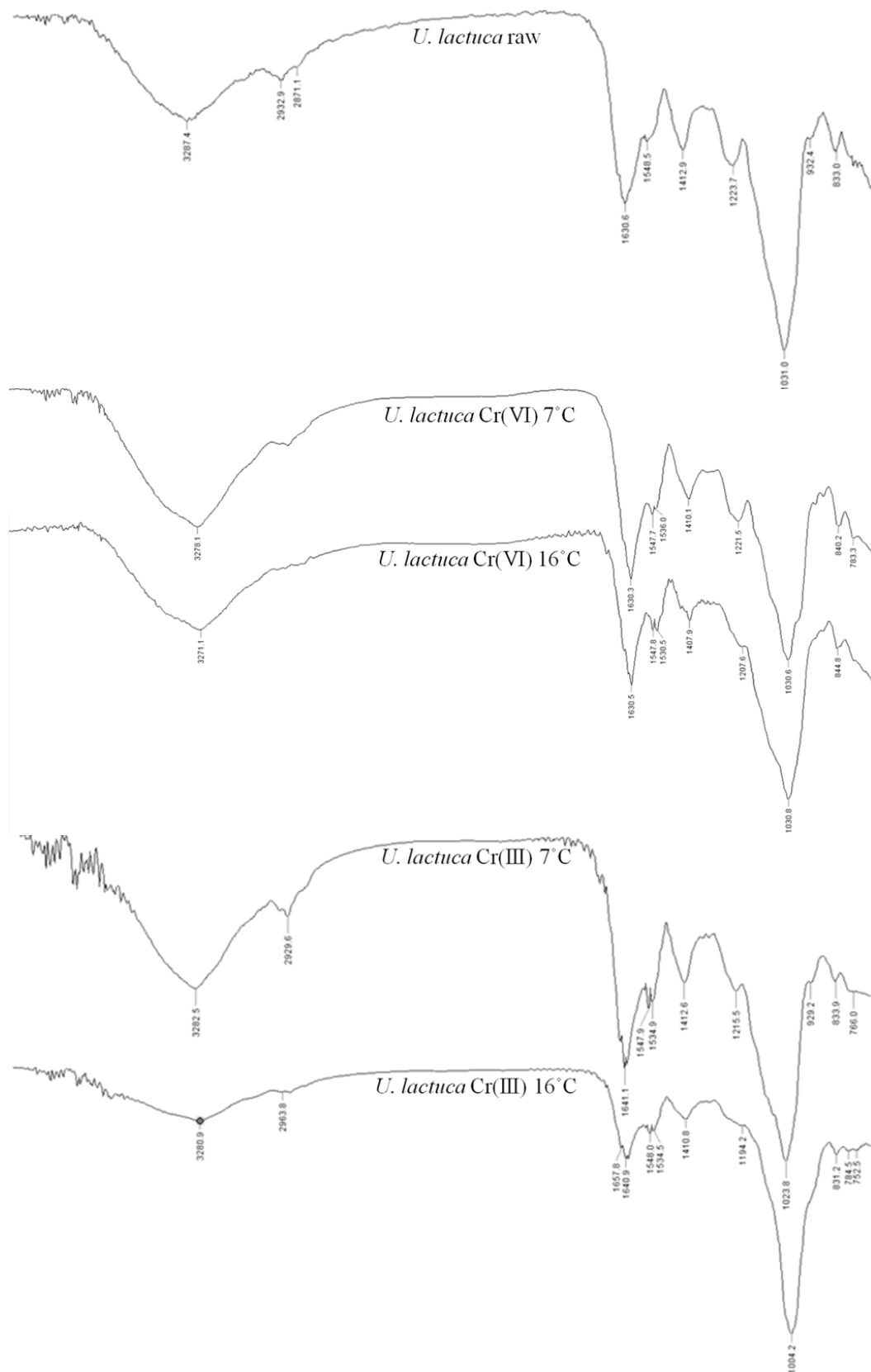
The FTIR spectrum of protonated *P. palmata* is shown in Figure 4.32. The free carboxyl band may be seen at  $1643 \text{ cm}^{-1}$  in this spectra, but the chelate band, which is usually present at about  $1400 \text{ cm}^{-1}$  was not visible. It is clearly visible, however in the raw and metal loaded spectra shown in Figure 4.31 indicating that carboxyl groups are involved in metal binding.



**Figure 4.32: Spectrum of protonated *P. palmata* (resolution- $4 \text{ cm}^{-1}$ , number of scans-64, representative shown from  $n=3$ ).**

#### 4.3.4.3 FTIR Spectra of Raw and Metal loaded *Ulva lactuca* Sampled in Feb/Mar

Representative spectra are shown in Figure 4.33. Carboxyl (approximately  $1630$  and  $1410 \text{ cm}^{-1}$ ) and sulphonate (approximately  $1220 \text{ cm}^{-1}$ ) functionalities are present in the spectra. These are negatively charged in natural seawater conditions, which allows the binding of positively charged  $\text{Cr}^{3+}$  ions. An amide band may be seen at approximately  $1530 \text{ cm}^{-1}$ , which acts as a positively charged group in these conditions. These groups may bind and reduce  $\text{CrO}_4^{2-}$  to  $\text{Cr}^{3+}$  as described in Figure 4.28.



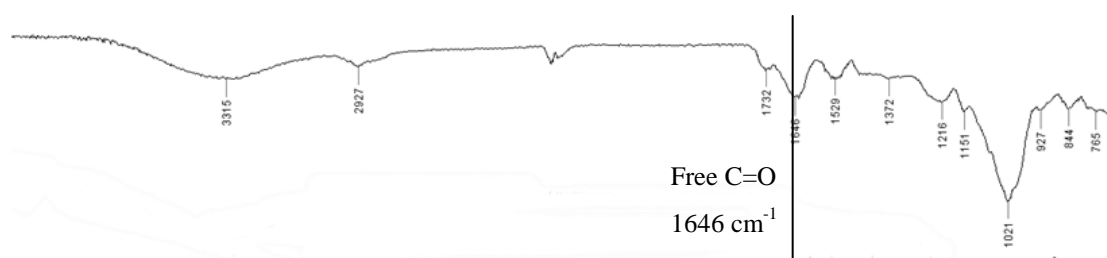
**Figure 4.33: ATR FTIR Spectra of raw *U. lactuca* (top), Cr(III) loaded *U. lactuca* at 7 °C (middle), and Cr(III) loaded *U. lactuca* at 16 °C (bottom) ((resolution-4  $\text{cm}^{-1}$ , number of scans-64, representative shown from n=3).**



There were some changes between the raw and metal loaded FTIR spectra of *U. lactuca*. A shift occurs in the band located at  $1032 \pm 1 \text{ cm}^{-1}$  in the raw spectrum. This moved to  $1010 \pm 8$  and  $1023 \pm 5 \text{ cm}^{-1}$  when exposed to  $\text{Cr}^{3+}$  at 7 and 16 °C, respectively. There is no significant shift on binding with  $\text{CrO}_4^{2-}$ . Note that the magnitude of the shift appears to reflect the concentration of Cr in the sample. This band at  $1030\text{-}1010 \text{ cm}^{-1}$  represents the alcoholic C-O stretches which occur in all polysaccharides (Murphy *et al.* 2007; Gómez-Ordóñez & Rupérez 2011). The shift in the wavelength of this band at higher metal concentrations indicate that it may have a role in metal binding, i.e. as the chromium coordinates to alcoholic groups, there is a change in the frequency at which the C-O bond vibrates.

The second change may be seen in the band located at  $1229 \pm 6 \text{ cm}^{-1}$  in the raw seaweed. The wavelength of the band shifted to a smaller wavelength and the peak itself appeared smaller on metal binding. When exposed to  $\text{CrO}_4^{2-}$  this band reduced in wavelength to  $1219 \pm 4$  and  $1205 \pm 4 \text{ cm}^{-1}$  at 7 and 16 °C, respectively. An even greater shift occurred on exposure to  $\text{Cr}^{3+}$ , to  $1217 \pm 2 \text{ cm}^{-1}$  and approx  $1194 \text{ cm}^{-1}$  at 7 and 16 °C, respectively. An error cannot be quoted for  $\text{Cr}^{3+}$  at 16 °C as the peak had almost entirely disappeared. This indicated the involvement of sulphonate groups to the binding of Cr to *U. lactuca* (Pereira *et al.* 2009).

The spectrum of protonated *U. lactuca* is shown in Figure 4.34. The free carboxyl group was present at  $1646 \text{ cm}^{-1}$ , but the chelate band, normally present at about  $1400 \text{ cm}^{-1}$  was not visible. The chelate bands are clearly visible in the raw and metal loaded spectra shown in Figure 4.33. This shows that carboxyl groups take part in metal binding.



**Figure 4.34: Spectrum of protonated *U. lactuca* (resolution- $4 \text{ cm}^{-1}$ , number of scans-64, representative shown from  $n=3$ ).**

#### 4.4 Conclusions

There were seasonal differences in Cr accumulation by *F. vesiculosus*, *P. palmata* and *U. lactuca*. The differences in seasonal uptake appear to be a combination of effects. The evidence found in this thesis shows that temperature and time of sampling (season) effects seaweed uptake. Differences in seaweed composition between ‘winter’ and ‘summer’ are noted in the literature, and confirmed in this thesis (see Chapter 2). The results found here demonstrated that ‘winter’ seaweed takes up more metal due to these differences. This is exemplified in the baseline Cr contents in all the species studied. Before any uptake experiment was carried out the seaweed in general had more Cr in ‘winter’. When subsequent uptake experiments were carried out the seaweeds sampled in ‘winter’ in general took up more metal than those sampled in ‘summer’. In the literature, some studies have found that certain metals are highly seasonally dependent, and some show no significant effect of season on metal content (Leal *et al.* 1997; Morrison *et al.* 2008). It has been suggested that seasonality in metal accumulation is due to a dilution effect, i.e., that metal concentrations in the seaweed are diluted during growth (Morrison *et al.* 2008). *P. palmata*, *U. lactuca* and *F. vesiculosus* all show maximum growth rates during the summer (Faes & Viejo 2003; Geertz-Hansen & Sand-Jensen 1992; Morrison *et al.* 2008). The other factor, besides composition, to take into account is temperature. Increasing temperature was shown to increase metal uptake, no matter when the seaweed was sampled. This suggests that increased sea temperature will increase metal uptake. However ‘summer’ seaweed contains less Cr than ‘winter’ seaweed. Therefore it can be concluded that compositional differences in the seaweed between ‘winter’ and ‘summer’ are the main driving force behind differences in Cr uptake. The compositional differences between the seaweeds have been discussed in Chapter 2.

Higher metal uptakes were seen for *F. vesiculosus* for  $\text{Cr}^{3+}$  in Feb/Mar and for *P. palmata* and *U. lactuca* for both  $\text{Cr}^{3+}$  and  $\text{CrO}_4^{2-}$  in Feb/Mar. The reason for higher uptake in the Feb/Mar is probably due to compositional changes, which enhanced the seaweeds uptake ability. In this work, *F. vesiculosus*, *P. palmata* and *U. lactuca* were shown to have a greater P content during Feb/Mar. P is used in the cell membrane and greater quantities may facilitate intracellular diffusion of  $\text{Cr}^{3+}$ . This has not been

shown in the literature, and requires more evidence to prove the hypothesis. *P. palmata* and *U. lactuca* were also shown to have seasonal highs in N content in Feb/Mar. This may be connected to their ability to accumulate more  $\text{Cr}^{3+}$  and  $\text{CrO}_4^{2-}$  in Feb/Mar through protein containing ligands. The production of ligands and their ability to bind metals has been shown in the literature (Leal *et al.* 1999; Vasconcelos *et al.* 2002; Vasconcelos & Leal 2008).

Warmer temperatures increased metal uptake, so higher concentrations of chromium would be expected during the summer season when water temperatures are at a maximum. Therefore, if all other factors are constant, an increased concentration of metal seen during the summer season is a result of increased water temperature. If, on the other hand, a decreased metal content occurs during the summer or growth season this is because the increased bioaccumulation rate is lower than the dilution effect of seaweed growth. Differences in bioaccumulation between winter and summer months are not entirely related to the seasonal 'dilution effect' but are also influenced by temperature. A combination of these two factors probably account for the majority of seasonal differences.

Live seaweed did not show any pattern in metal uptake regarding species colour. Bioaccumulation was species specific. This is contrary to dead biomass uptake where browns have the best biosorption ability, followed by green and then red (Hashim & Chu 2004; Murphy *et al.* 2008).

The importance of intracellular binding has been shown, as seen in Figures 4.15, 4.21, and 4.26. The seaweed was washed with EDTA to remove cationic metals. There were few significant changes between EDTA washed and metal loaded seaweeds. This indicated that the majority of metal binding was intracellular. Anions are able to move more freely into the cell (Metzler, 1977). Cr(VI) can be transported easily through cellular membranes because of its similarity to the sulphate anion ( $\text{SO}_4^-$ ). Once inside the cell, the metal may be bound to cytoplasmic ligands or sequestered in vacuoles, reducing its toxicity. If it crosses the nuclear membrane it may bind to DNA or proteins. Most of these mechanisms involve reduction to  $\text{Cr}^{3+}$  which may cause oxidative stress (Kaim & Schwederski 1994). Movement into the cell may be affected

by charge. Positively charged ions will bind to the negatively charged cell wall functional groups, inhibiting their entry into the cell.

The functional groups present in the seaweeds may be readily seen in the FTIR spectra. The main groups are carboxyl, sulphonate and amide. These relate to the protein and carbohydrate composition of the seaweeds (see Chapter 2 for more information on seaweed composition). The uptake behaviour of the seaweeds with regards to functional groups and metal species may be explained by the ionization behaviour of functional groups present in seaweeds, which can be predicted using the Henderson-Hasselbalch equation.

$$\text{Log} \frac{\text{deprotonated}}{\text{protonated}} = \text{pH} - \text{pKa}$$

Weaker acids like alcohols ( $\text{pK}_a \approx 15$ ) will be almost completely unionized at pH 8. Stronger acids such as carboxylic ( $\text{pK}_a \approx 4$ ) and sulphonate ( $\text{pK}_a \approx 1$ ) and phosphate ( $\text{pK}_a \approx 2$ ) groups will be negatively charged at this pH (Segel 1976). The N-H groups of amides ( $\text{pK}_a \approx 10$ ) will be protonated at this pH, giving them a positive charge. Note that all  $\text{pK}_a$ 's are approximate and only the first  $\text{pK}_a$  for polyprotic groups is given. As  $\text{CrO}_4^{2-}$  is negatively charged it was expected to interact mainly with amino groups. The relatively low concentration of amino groups on the seaweed surface (compared to carboxyl for example) explains why  $\text{CrO}_4^{2-}$  uptake was lower than  $\text{Cr}^{3+}$  uptake. The balance of the seaweeds composition will be mostly carbohydrate, which provides negatively charged functionalities, such as carboxyl and sulphonate. The composition of the seaweeds can be seen Chapter 2. In this study  $\text{Cr}^{3+}$  is cationic and  $\text{CrO}_4^{2-}$  is anionic.  $\text{Cr}^{3+}$  uptake is expected to be higher due to the greater abundance of negatively charged functional groups. This may also be explained by a biosorption mechanism proposed by Park *et al.* (2007), where chromate anions will be reduced to  $\text{Cr}^{3+}$  by electron donor groups on the seaweed (e.g., amino groups). The  $\text{Cr}^{3+}$  cations may then complex with negatively charged groups, or be released into the solution. It is therefore expected that  $\text{CrO}_4^{2-}$  was reduced to some degree to  $\text{Cr}^{3+}$  (Park *et al.* 2007).

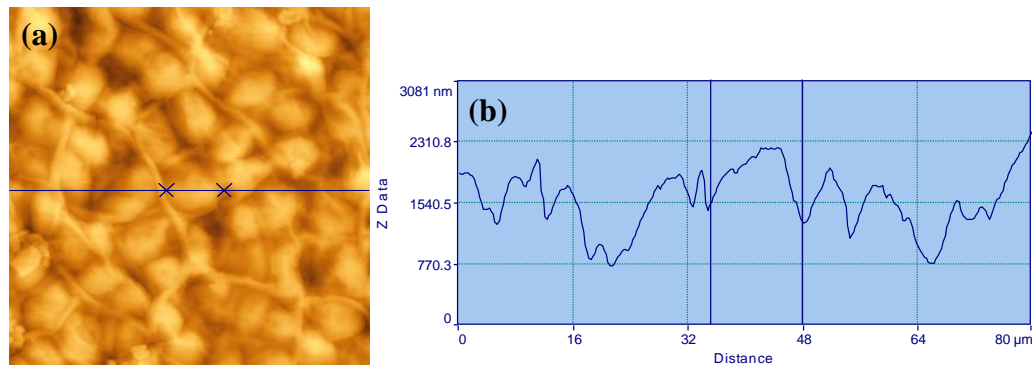
Overall there were few changes in the FTIR spectra of raw and metal bound seaweeds. This is likely to be due to two reasons. First the raw seaweed naturally contains light metal counter-ions. On the seaweed surface the seaweed accumulates metal either by coordination with functional groups or ion-exchange. The removal of a light metal counter ion and its replacement with a Cr ion may show only small changes or shifts in spectra, as the seaweed already has many metal ions bound to its surface. For this reason protonated spectra are also shown as they give the bands which are present on a 'clean', protonated seaweed. The second reason for the lack of band shifts or changes in the spectra is because the levels of metal the seaweed was exposed to are very low; the concentration used in this study was 200 ug/L. The presence of the shifts, especially seen in *U. lactuca*, does indicate that this is one method which could be used to study the mechanisms of bioaccumulation. In future work, an experiment may be designed to look at increasing concentrations of Cr, which may further elucidate IR spectra changes, without causing damage to the seaweed.

**Chapter 5: Microscopic and  
Bacteriological Examination  
of the Seaweed Surface**

## 5.1 Introduction

### 5.1.1 Atomic Force Microscopy

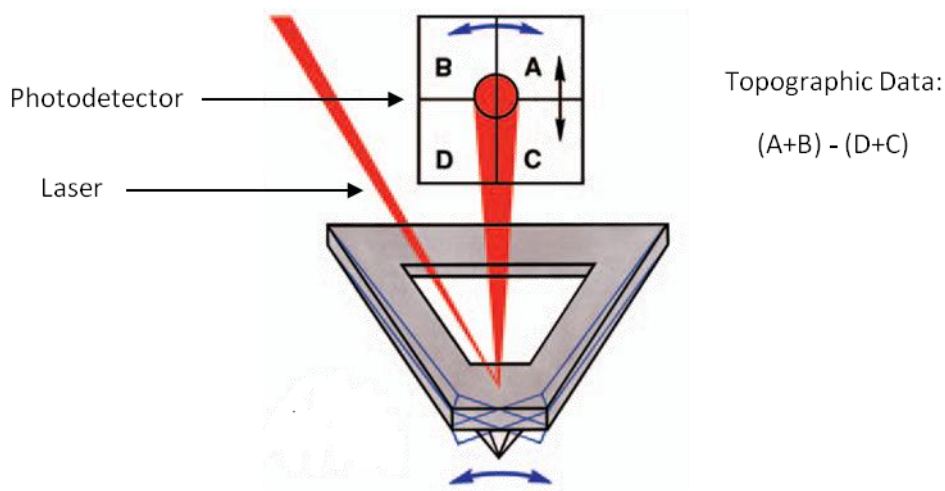
Atomic force microscopy (AFM), also known as Scanning Force Microscopy (SFM) may be used to investigate surface morphology including factors such as surface roughness. SFM allows high resolution imaging of non-conductive specimens by taking advantage of short range forces such as Van der Waals interactions. It allows imaging of biologicals in ambient conditions without use of coatings and without surface damage which may occur while using Scanning Electron Microscopy (SEM). It also provides a three dimensional image of the surface allowing measurements of feature depth, size and roughness (see Figure 5.1 for example).



**Figure 5.1: Topographic image (a) and line profile (b) showing height and depth measurements**

An image containing topographic information is obtained as follows (Figure 5.2).

Lateral force microscopy, also called LFM, is a measure of the frictional forces of a sample. As the tip scans over the surface, relative differences in the frictional forces in different areas can be mapped. Therefore, differences in composition that may not be evident in topographic scans can be seen (Jalili 2004).

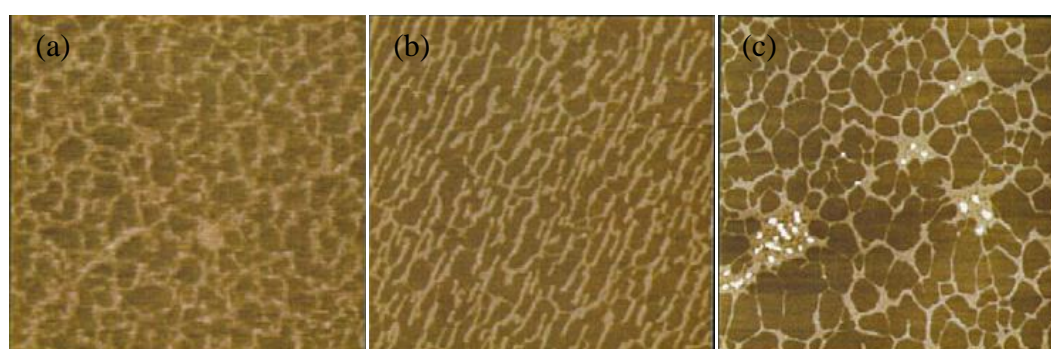


**Figure 5.2: Acquisition of topographic data by SFM (Heaton *et al.* 2004).**

### 5.1.1.1 Application of AFM in the Imaging of Seaweed

#### 5.1.1.1.1 Application of AFM in Imaging Seaweed Polysaccharides

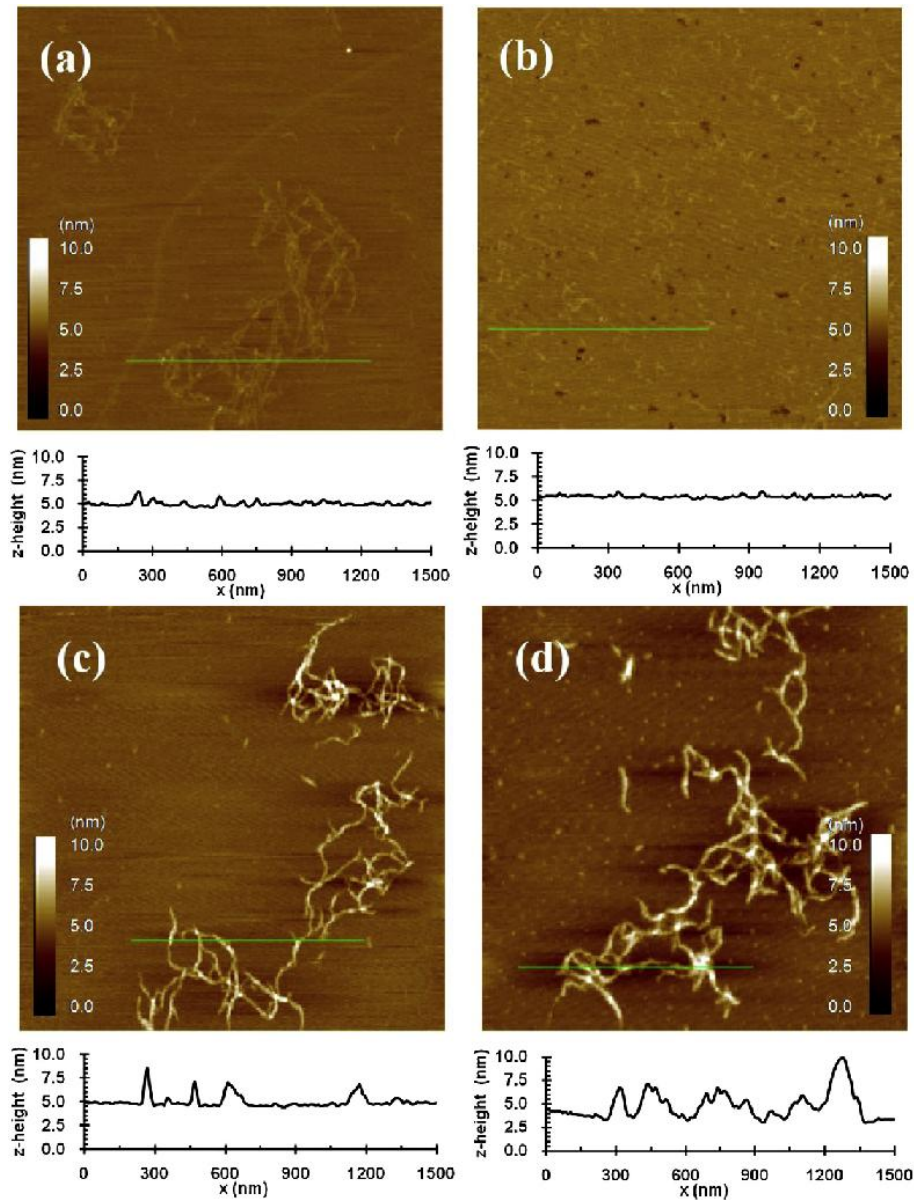
SFM has been successfully applied to the imaging of seaweed polysaccharides such as alginates and carrageenans. Funami *et al.* (2007) investigated the super molecular structural changes of carrageenan in the presence of cations ( $K^+$ ,  $Ca^{2+}$ ). The images shown in Figure 5.3 show the difference in structure between iota-carrageenan exposed to KCl and  $CaCl_2$ . Using AFM allowed the height of the carrageenan strands to be measured, which indicated the degree of aggregation of macromolecular strands (Funami *et al.* 2007).



**Figure 5.3: Iota-carrageenan imaged by AFM. Image (a) was taken in the absence of added salts, (b) shows the effect of  $K^+$ , (c) shows the effect of  $Ca^{2+}$  (Images  $1\mu m \times 1\mu m$ ) (Funami *et al.* 2007).**

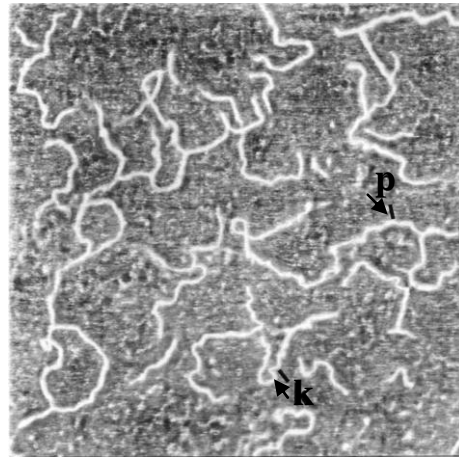


Liao *et al.* (2015) studied the  $\text{Ca}^{2+}$  induced gelation of alginate and studied the resultant polymers by AFM. Alginate gelled with higher  $\text{Ca}^{2+}$  concentrations (Figure 5.4 (c) and (d)) exhibited much thicker and elongated structures, compared with those observed in alginate gelled with lower  $\text{Ca}^{2+}$  concentrations (Figure 5.4 (a) and (b)). This showed the tendency for lateral aggregation of alginate polymers at higher  $\text{Ca}^{2+}$  concentrations (Liao *et al.* 2015).



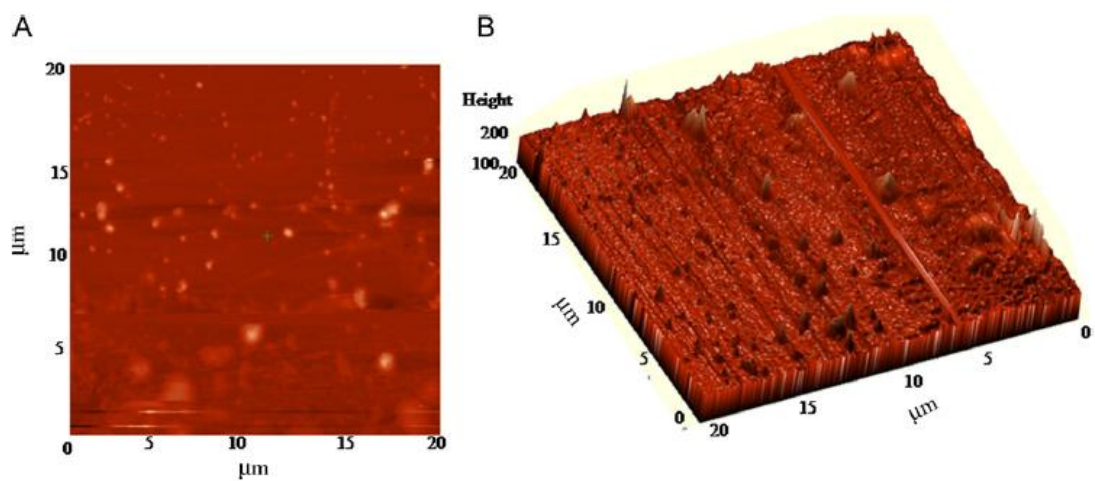
**Figure 5.4: Alginate imaged by AFM. (a) + (b) Lower concentrations of  $\text{Ca}^{2+}$  used to gel the alginate, (c) and (d) higher concentrations of  $\text{Ca}^{2+}$  used to gel the alginate (Liao *et al.* 2015).**

Decho (1999) studied the conformation of alginate polymers (shown in Figure 5.5). It was proposed that the ‘kinks’ (k) highlighted in the polymer chain (p) correspond to the locations where there are linkages between mannuronic and guluronic monomer chains of alginate and, therefore, a corresponding change in molecular orientation (Decho 1999).



**Figure 5.5: Alginate imaged by AFM (500nm x 500nm), p: the polymer chain, k: kinks in the polymer chain (Decho 1999).**

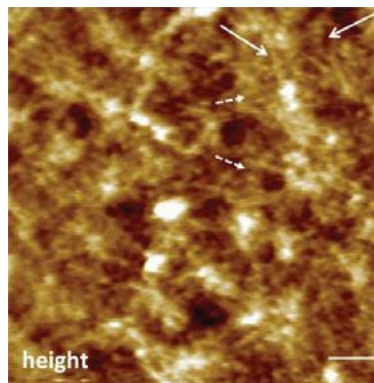
AFM was applied to the imaging of Extracellular Polysaccharides (EPS) isolated by solvent precipitation from a biofilm of the bacterium *Bacillus licheniformis*, which was present on the red seaweed *Gracilaria dura* (Singh *et al.* 2011). This is shown in Figure 5.6 and shows the application of AFM for imaging of EPS.



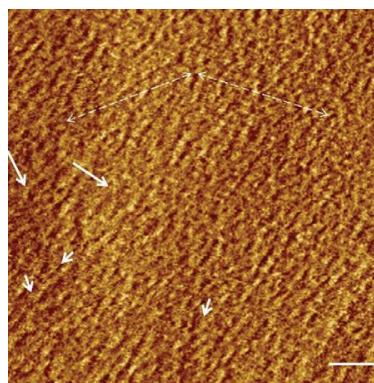
**Figure 5.6: EPS isolated from a biofilm of the marine algal associated bacterium *Bacillus licheniformis* (Singh *et al.* 2011).**

### 5.1.1.1.2 Application of AFM in Visualising Algal Surface Morphology

AFM has previously been used to analyse the ultrastructure of an alga. The cell wall of the unicellular algae *Ventricaria ventricosa* has been analysed. This alga is one of the largest single celled organisms, having cell diameters of up to 4 cm. In this study the cells were subjected to an enzyme (cellulose) treatment to remove surface mucilage. The study showed the presence of some mucilage areas (despite the enzyme treatment), but also areas where the underlying cellulose microfibril network could be observed. The network consisted of more ordered fibrils, along with coiling fibrils, Figure 5.7 (native) and Figure 5.8 (enzyme treated). This was the first published study of the native algal cell wall using AFM (Eslick *et al.* 2014).

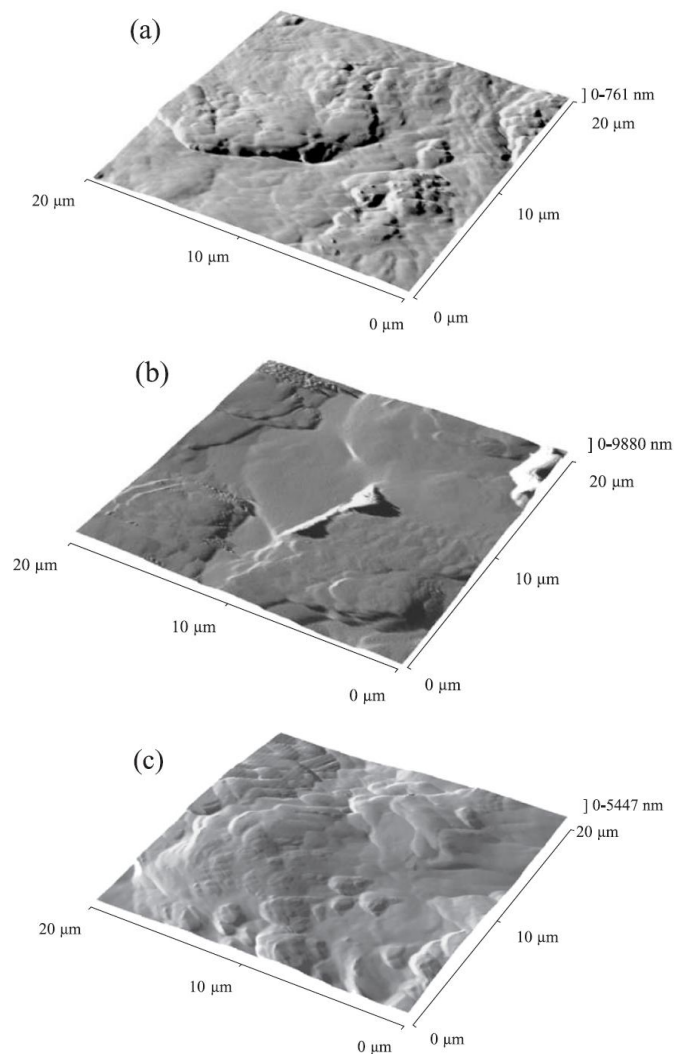


**Figure 5.7:** Native cell wall of *Ventricaria ventricosa* imaged by AFM. Long open head arrows point to coiling fibrillar structures; short dotted arrows pointing to ‘draping’ of the fibrillar meshwork (Scale bar: 1  $\mu\text{m}$ ) (Eslick *et al.* 2014).



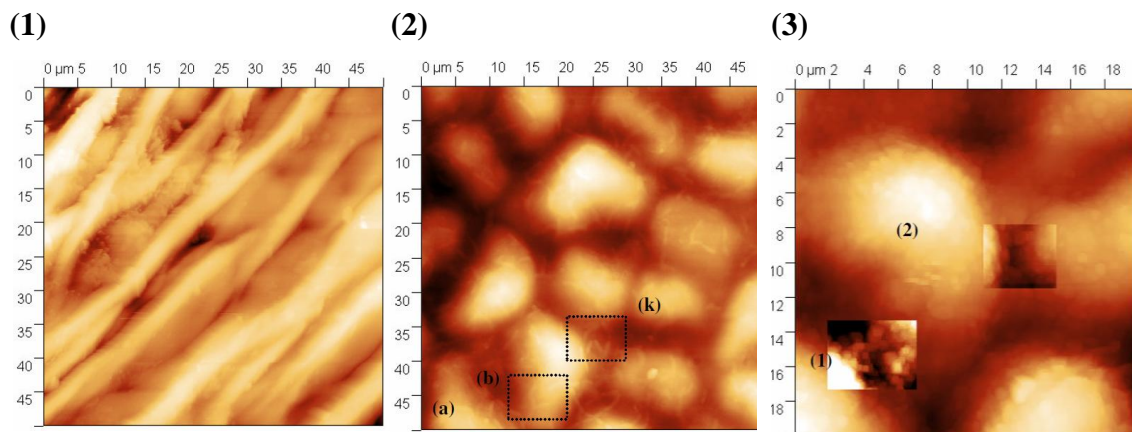
**Figure 5.8:** Enzyme treated cell wall of *Ventricaria ventricosa* imaged by AFM. Thin fibril-like structure (long arrows) and cross-linking structures (short arrows) can be seen. The directions of underlying fibrils can also be seen (double headed dashed arrow) (Scale bar: 0.5  $\mu\text{m}$ ) (Eslick *et al.* 2014).

Feng *et al.* (2004) looked at dried, ‘activated’ (CaCl<sub>2</sub> treatment), and ‘regenerated’ (NaCl treatment) *Ecklonia maxima* (brown seaweed) using SFM. Regenerated seaweed received NaCl treatment after metal binding in order to remove the bound metal. They found the surface of the regenerated seaweed had flattened compared to activated seaweed (either Cu<sup>2+</sup>, Pb<sup>2+</sup> and Cd<sup>2+</sup>; the metal the seaweed was exposed to prior to regeneration was not specified). They suggested that this could be due to the loss of alginate from the seaweed surface. Figure 5.9 shows the SFM images (Feng & Aldrich 2004). Clearly, the images show changes in surface height, but it appears no replication was carried out, so the level of variation in these measurements was not determined.



**Figure 5.9: *E. maxima*, (a) raw, (b) ‘activated’ by CaCl<sub>2</sub> treatment and (c) ‘regenerated’ by NaCl treatment post CaCl<sub>2</sub> treatment and metal binding, showing changes in surface height (Feng & Aldrich 2004).**

Previous work in Waterford Institute of Technology demonstrated that SFM could be applied to the study of topological changes in seaweed. This preliminary study showed the ultrastructural changes which occurred on Cu(II) binding to dead *U. lactuca* pieces (Figure 5.10). Significant surface reorganization was observed. At low concentrations of Cu(II) the surface was disrupted, with fibrils being observed, possibly because of Ca(II) being replaced by Cu(II) in the cell wall polysaccharide network. A higher concentration of Cu(II) appeared to cause the agglomeration of these fibrils (Murphy 2007). This work showed the potential of SFM for studying metal seaweed interactions.



**Figure 5.10: *U. lactuca* (1) Raw, (2) 1 µg/L Cu(II) and (3) 50 µg/L Cu(II), highlighting polysaccharide fibrils (Murphy 2007).**

### 5.1.2 Scanning Electron Microscopy/Energy Dispersive X-Ray Analysis

Scanning electron microscopy (SEM) was carried out to gain a representative view of the seaweed surface before and after metal binding. It was also used to confirm what was seen in scanning force microscope images. Energy dispersive X-ray (EDX) analysis was used to determine the elemental make up of the seaweed.

### 5.1.3 Total Viable Counts of Surface Bacteria

Preliminary studies by SFM clearly showed a biofilm on the seaweed surface. It is well known that seaweeds often have these biofilm layers (Egan *et al.* 2012). It is also well known that micro-organisms have the ability to accumulate heavy metals (Godlewska-Zyłkiewicz 2006). The seaweed biofilm is a complex community of bacteria, diatoms, dinoflagellates, ciliates, amoebae and fungi, but research indicates that bacteria are the most dominant micro-organism in this community. There are

species, spatial, and temporal shifts in the genera found but *Alphaproteobacteria*, *Gammaproteobacteria*, *Bacteroidetes*, and *Cyanobacteria* are commonly found (Egan *et al.* 2012). While SEM and AFM could be used to qualitatively determine changes to the seaweed surface, it was important to consider if there were quantitative changes to the bacterial count as a result of metal binding. This was done in this thesis by determining the total viable counts from the seaweed surface. Only a small percentage of the bacteria on the surface may be cultured by this method because of the differences between the growth culture and natural environment (Gregory 2009). However, even with these disadvantages the method provides a convenient comparison across seaweed species and treatments. The influence of metal binding on total viable counts of bacteria on the seaweed surface has not been studied widely. To the author's knowledge, this is the first attempt to study the effect of metal uptake on both the seaweed, and the associated biofilm, by AFM.

#### 5.1.4 Aims

The aims of this chapter were as follows:

- To carry out a detailed time course study of changes in the surface morphology of *Ulva lactuca* during metal binding.
- To confirm the existence of a biofilm on the seaweed surface.
- To characterize the morphology of the seaweed surface in order to determine if any changes occurred post metal binding; both SEM and AFM measurements were used to determine consistency in the methods. A comparison of SFM and SEM images in seaweed has not been carried out before.
- To determine if SFM measurements could be used to determine differences (1) between seaweed species, (2) post metal binding within species. A range of measurements were taken, including roughness, and surface area.
- To determine if there was a difference in viable bacterial counts before and after metal treatment. This would reveal if metal uptake has an effect on the viability of bacterial biofilms on the seaweed surface.
- To determine if EDX measurements could be used to determine Cr (and other metals) on the seaweed surface. Seaweed pre and post exposure was compared.

## 5.2 Experimental

### 5.2.1 Metal Exposure

As described in Section 4.2.3.

### 5.2.2 Method for Removal of Biofilm

Samples were cleaned using a method described in Gledhill *et al.* (1998). Synthetic seawater was prepared by a method described by Leal *et al.* (1999). The method is described here. A 10% ethanol (HPLC grade) in seawater solution was prepared. A small amount (approximately 5 mL) was dropped on the surface of the seaweed and scraped gently using a plastic implement (a PTFE sampling loop). The sample was then rinsed with artificial seawater. Two control samples were prepared. One was rinsed with seawater. The other was scraped gently using a plastic implement using only seawater and rinsed.

### 5.2.3 Microscopy

#### 5.2.3.1 Optical Microscopy

For optical microscope images, samples were viewed at 10x and 40x magnification using an Olympus CH20 microscope.

#### 5.2.3.2 Scanning Force Microscopy

A ThermoMicroscopes Explorer AFM was used to acquire all AFM images. Both contact and non-contact tips were used (contact tips: 1650-00, antimony doped silicon, and non contact tips: MLCT-EXMT-A, silicon nitride, Veeco). A sample of about 2-3 mm<sup>2</sup> was cut from the seaweed. Double sided tape was fixed to the sample stub and the seaweed sample was fixed on this. Alternatively, a drop of glutaraldehyde (photographic grade, 50% solution) was placed on the surface, the sample placed on top and allowed to dry overnight at room temperature. Debris was then removed from the surface with nitrogen and the sample was stored in a Petri dish sealed with parafilm at room temperature.

Set point, proportional, integral and derivative settings were determined experimentally. The scan rate was set to twice the scan range or less. A resolution of 400 pixels was used. If the surface was too rough a non contact tip was used in

contact mode as the cantilever stub is a smaller size and less likely to come into contact with high features on the sample.

### 5.2.3.3 Scanning Electron Microscopy and Electron Dispersive X-Ray Analysis

Pieces about 5 mm<sup>2</sup> were attached to stainless steel sample stubs using carbon tabs (Agar Scientific, UK). It was not necessary to coat the samples with a conductive substance. They were then analysed using a Jeol JXA-8600 Superprobe instrument. Settings used were as shown in Table 5.1.

**Table 5.1: SEM/EDX settings**

	Imaging	X-ray analysis
Accelerating Voltage	15 kV	15 kv
Probe current	13 A	6 A
Acquisition time	–	100 s (Mag: 350x)

### 5.2.4 Total Viable Counts

Marine agar plates were prepared as described in Table 5.2. Nystatin was added to retard fungal growth. Samples were exposed to metal as described in Section 4.2.3. They were then washed in sterile artificial seawater (Instant Ocean) to remove bacteria present in the seawater. Each sample was placed in a stomacher bag and 9 times the sample weight in sterile seawater was added to make the initial 1 in 10 dilution (about 10 g of seaweed and 90 mL of water was used). The samples were homogenised in a stomacher for 4 min. Dilutions were then carried out from the initial 10<sup>-1</sup> to 10<sup>-4/-5</sup>. The maximum dilution was informed by previous work in the EIRC. 100 µL of the dilutions were spread plated onto marine agar plates in duplicate. Control plates were prepared by stomaching sterile seawater and plating 100 µL. The plates were incubated for 6 days at 28 °C. Plates with 30-300 colonies were chosen as they are within a suitable range to be counted.

**Table 5.2: Marine Agar Composition**

0.5 %	Peptone
0.1 %	Yeast extract
3.33 %	Instant ocean
0.01 %	Ferric citrate
1.5 %	Agar
After autoclaving: 1mL/200 mL agar	Nystatin



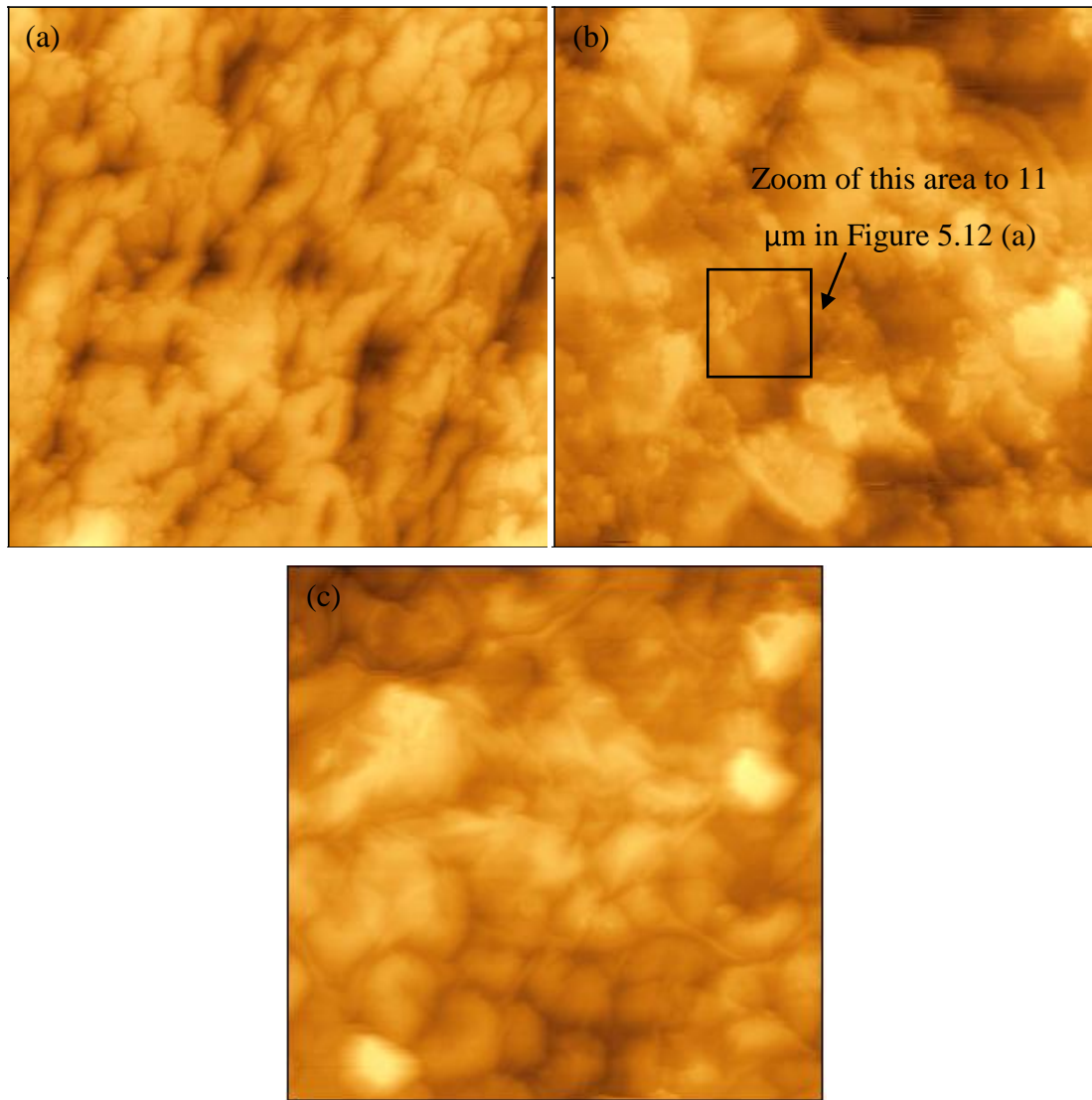
### 5.3 Results and Discussion

#### 5.3.1 Characterisation of Raw *Ulva lactuca* and Biofilm

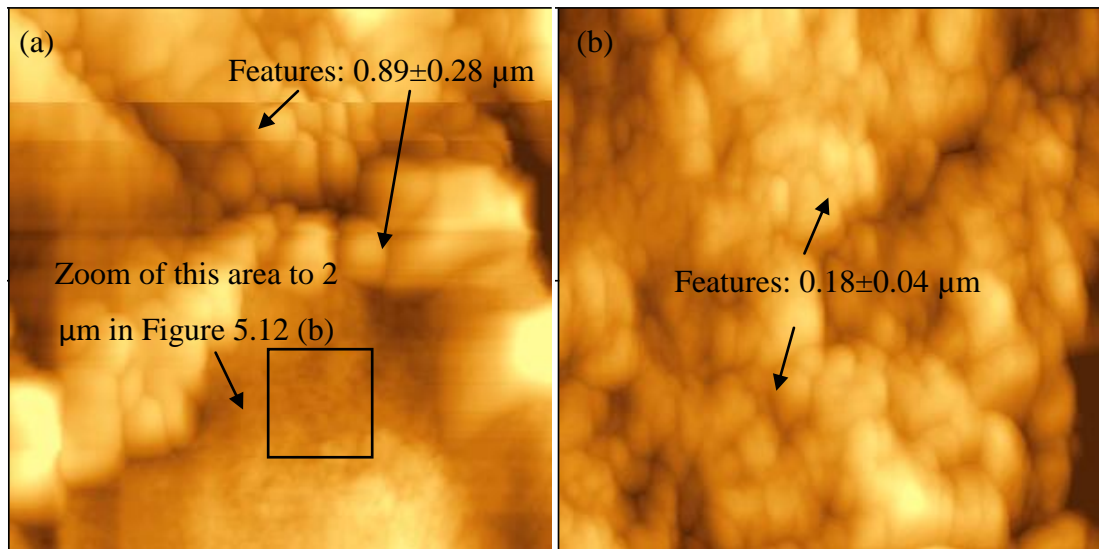
All images presented are based on triplicate analysis with representative images shown here. A minimum of processing was carried out on the sample images. They were all levelled, which removes tilt from the image. Some were filtered to remove lines which may be caused by debris on the surface; colour was adjusted on some to improve the appearance of the image.

Measurements of feature sizes were based on ten measurements unless otherwise stated and quoted as the average  $\pm$  one standard deviation. Measurements based on the full images, such as surface area or roughness, were taken in triplicate where possible. This was not possible in some cases due to bad image quality (streaking or image falling out of range of the z scanner) which would have affected the values.

The raw seaweed surface was variable as shown in Figure 5.11 (a), (b) and (c). The cellular surface was just visible in some instances, (Figure 5.11 (c)), but it was mostly obscured by a film or layer on the surface. It was concluded that a biofilm was present on the surface of the seaweed. The variability in the surface may be explained by the fact that a biofilm will not be continuous and may be made up of different microorganisms in different population densities at any point (Lindsay & Von Holy 2006). It was proposed that the surface of the seaweed is not visible in these images, and that what was seen here is actually a biofilm which covers the surface. The size of the structures observed supports this. The features marked in Figure 5.12 (a) are approximately  $0.89 \pm 0.28 \mu\text{m}$  in size. Features in Figure 5.12 (b) are  $0.18 \pm 0.04 \mu\text{m}$  in size. Although bacterial cell size varies widely, they are generally smaller than algal cells. It is reasonable to propose that the smaller features seen here are microorganisms in a biofilm on the algal surface. These were most likely to be areas of bacterial coverage on the seaweed surface which along with other microorganisms and extracellular polymeric substances (EPS) make up a biofilm.

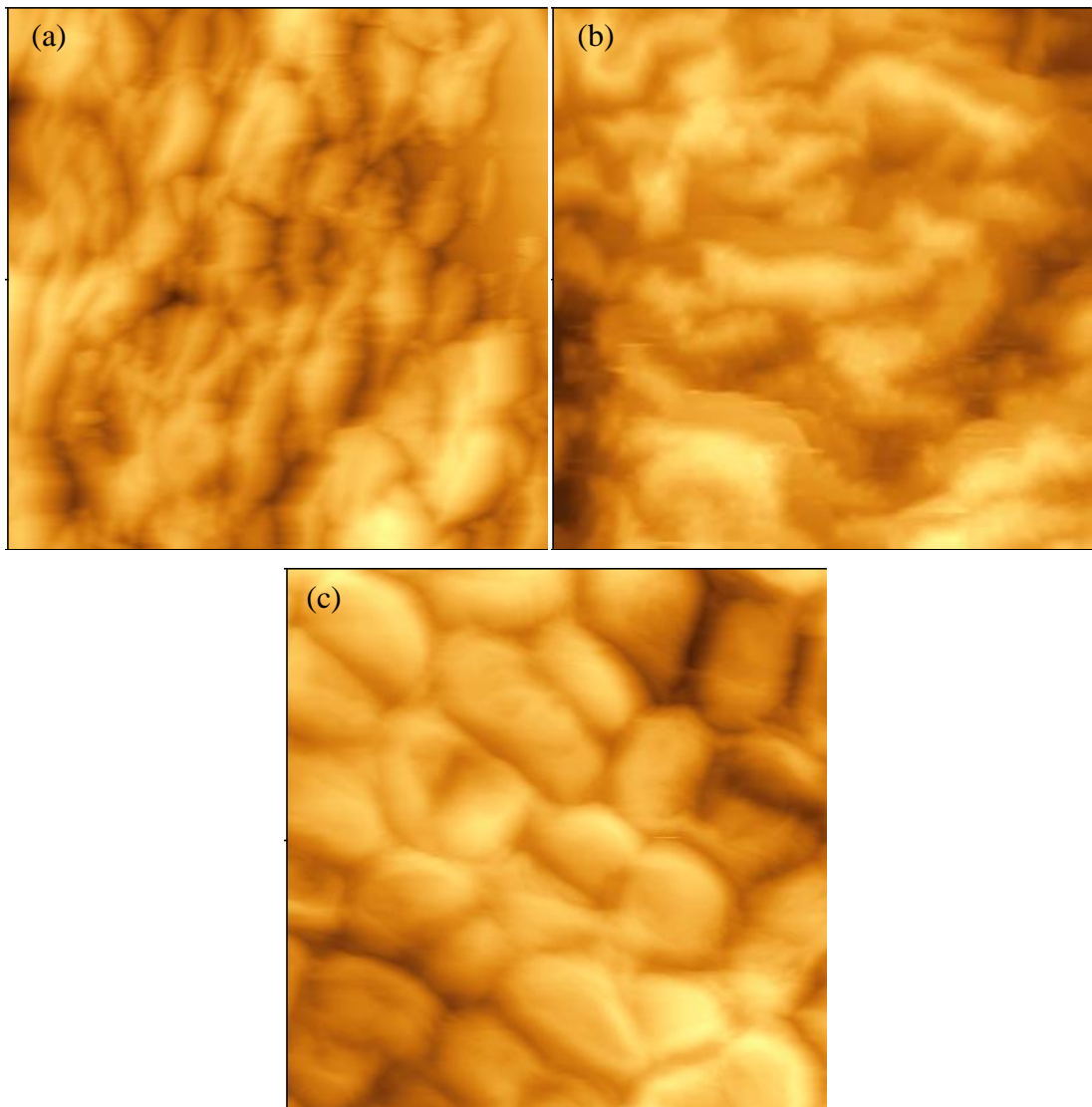


**Figure 5.11 (a), (b) and (c): Raw *Ulva lactuca* images, all 80  $\mu\text{m}$  x 80  $\mu\text{m}$ .**



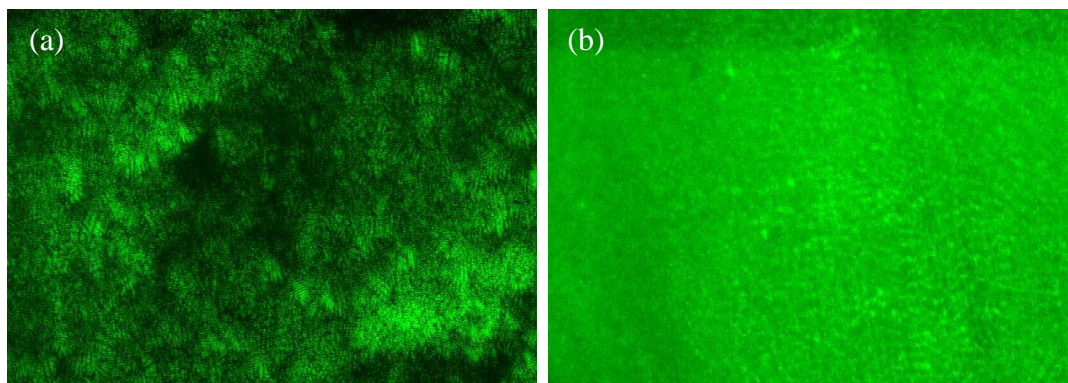
**Figure 5.12: Raw *U. lactuca*. Image (a) is an 11µm scan from image 5.11 (b) above. Image (b) is a 2µm scan from image 5.12 (a).**

To confirm this, a study was undertaken to attempt to remove this biofilm to reveal the underlying algal cells. The method described in Section 5.2.2 was used to remove the biofilm layer. The results are shown in Figure 5.13. The only successful method was the use of ethanol and seawater with scraping, as shown in Figure 5.13 (c). Algal cells shown were  $9.36 \pm 1.38 \mu\text{m}$  in size. Rinsing with seawater only gave a surface similar to that seen in Figure 5.11, as expected. Scraping the surface of the seaweed with seawater again resulted in a surface similar to the raw untreated but it was noted at the time of analysis that the surface was ‘stickier’ giving the streaks seen in Figure 5.13 (b). This indicated that the surface layer was disrupted to some extent, but not sufficiently to remove it.



**Figure 5.13: Cleaning method results; (a) Rinsed with seawater only, (b) rinsed with seawater and scraped and (c) rinsed with 10% ethanol and scraped (all 50  $\mu\text{m}$  x 50  $\mu\text{m}$ ).**

Optical microscopy results are shown in Figure 5.14. By comparing the surfaces it was seen that the cleaning of the seaweed led to a more uniform, smoother surface when compared to the raw seaweed control.

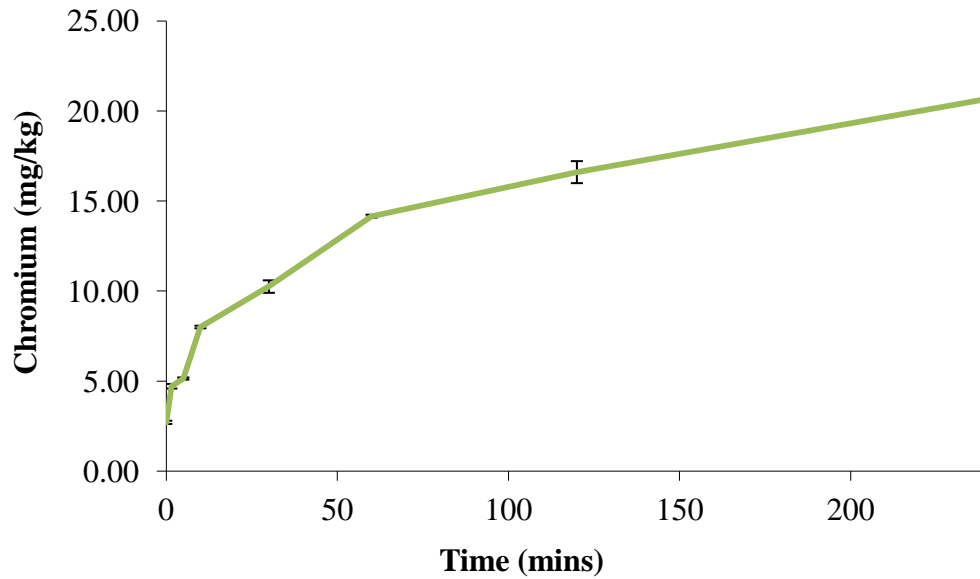


**Figure 5.14: Cleaning method results obtained by optical microscope (magnification-40x); (a) Rinsed with seawater only, (b) rinsed with 10% Ethanol and scraped.**

The limitation of this technique was that as a solvent had been used it is likely that extracellular matrix polysaccharides were removed from the surface as well as the biofilm layer. This makes the method unsuitable to study the effect of metal binding on the seaweed surface. It is possible that a seaweed cultivated in the lab in a medium spiked with bacteria to promote biofilm growth may be studied in the future to assess the effect of biofilm coverage when the seaweed is exposed to metal.

### **5.3.2 Time Course Analysis of the Effect of Cr(III) on the Surface of *U. lactuca***

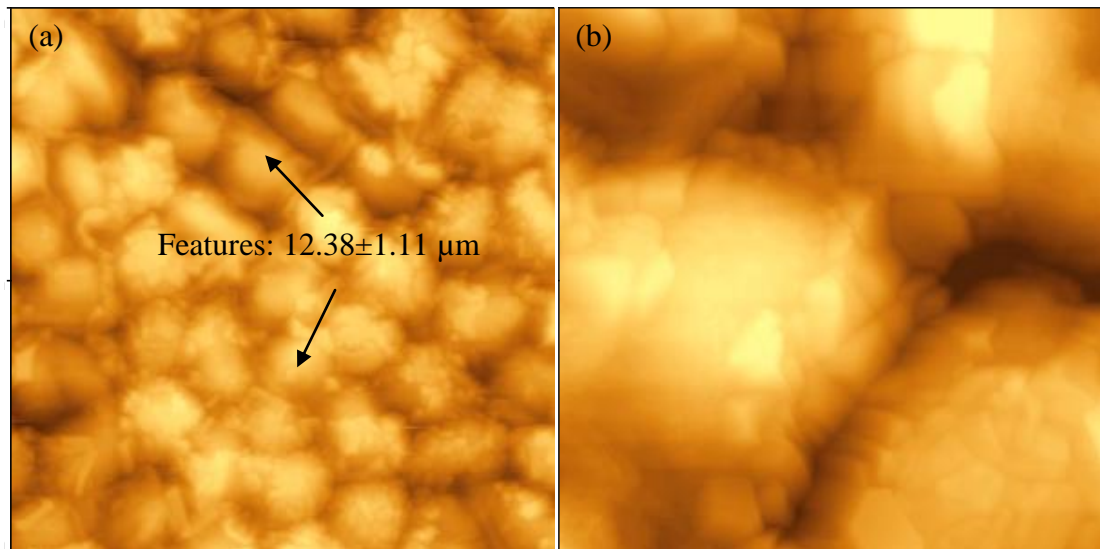
With this information about the cell surface biofilm, a time course study was carried out to determine the effect of  $\text{Cr}^{3+}$ /Cr(III) exposure on the surface morphology of *U. lactuca* over a 240 min exposure period. The seaweed used for this study was *U. lactuca* sampled in October 2007, which was exposed to 200  $\mu\text{g/L}$  Cr(III) over 240 min at 4 °C as described in Section 4.2.2. The concentration of Cr(III) in the samples was as shown in Section 4.3.2 and repeated here for convenience in Figure 5.15.



**Figure 5.15: Concentration of Cr at time points ranging from 0 (raw) to 240 min (n=3).**

#### **5.3.2.1 Surface at $t = 1.5$ min**

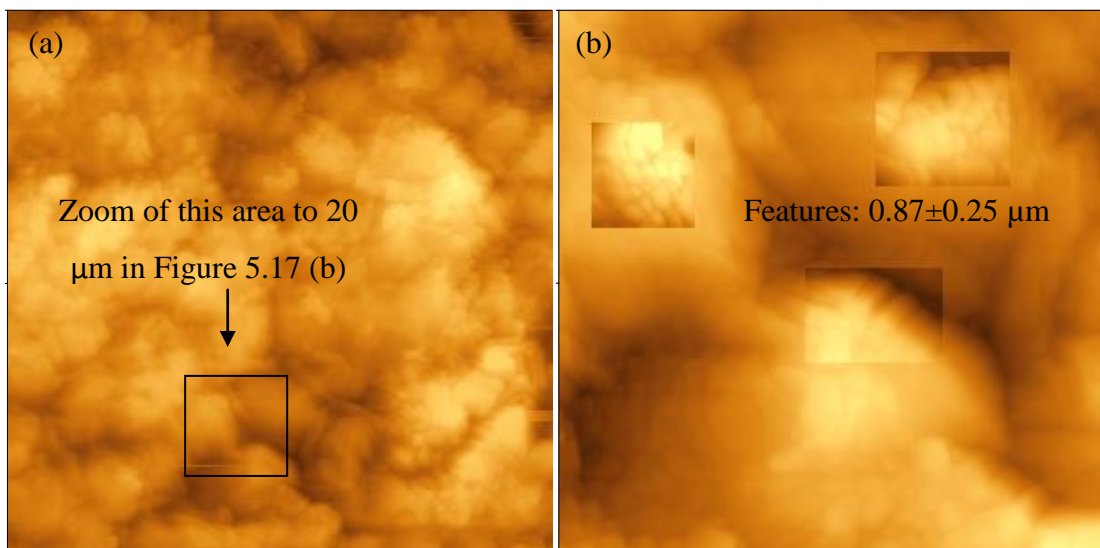
Exposing the seaweed to the 200  $\mu\text{g/L}$  solution of chromium appeared to have a rapid effect on the surface of the seaweed as seen in Figure 5.16 (a) and (b) which shows the surface of the seaweed after 1.5 min of contact. Features marked in Figure 5.16 (a) were  $12.38 \pm 1.11$   $\mu\text{m}$  in size. This appeared to be the underlying cellular structure of the seaweed. The size agrees reasonably well with the size of the cells seen after cleaning the seaweed surface ( $9.36 \pm 1.38$   $\mu\text{m}$ ).



**Figure 5.16:** *U. lactuca* exposed to 200 μg/L Cr<sup>3+</sup> at t=1.5 min, 80μm scan (a) and zoom to 20μm (b) on features marked.

### 5.3.2.2 Surface at t = 5 min

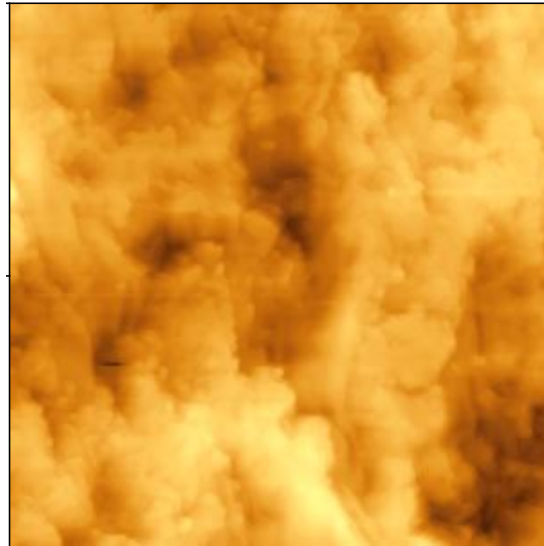
After 5 min of exposure the surface became rougher. Features highlighted in Figure 5.17 (b) were  $0.87\pm 0.25$  μm in size, corresponding well to bacterial cell size seen in the raw and t = 1.5 min scans.



**Figure 5.17.** *U. lactuca* exposed to 200 μg/L Cr<sup>3+</sup> at t=5 min, 80 μm (a) and zoom in to 20 μm (b).

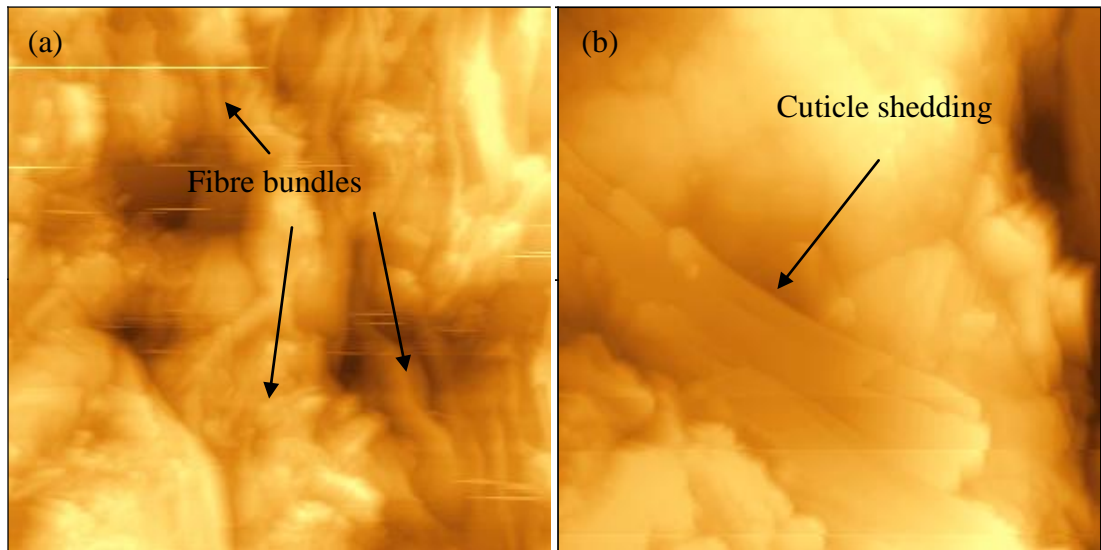
### 5.3.2.3 Surface at $t = 10$ min

After 10 min exposure there was again an increase in roughness of the surface (Figure 5.18). Two important differences between this and earlier time point scans, appeared to be the formation of fibres, which may be bundles of polysaccharides of  $2.01 \pm 0.22$   $\mu\text{m}$  in size (shown in Figure 5.19 (a)). These were not visible in earlier scans. Fig 5.19 (b) shows what appears to be an outer ‘cuticle’ shedding from the surface. Sieburth and Tootle (1981) showed that seaweed may shed its outer cuticle in order to control microorganism’s growth on the surface (Figure 5.19). The occurrence of this was observed on *Chondrus crispus*, a red macroalgae, using Scanning Electron Microscopy (SEM) (Sieburth & Tootle 1981, Figure 5.20).

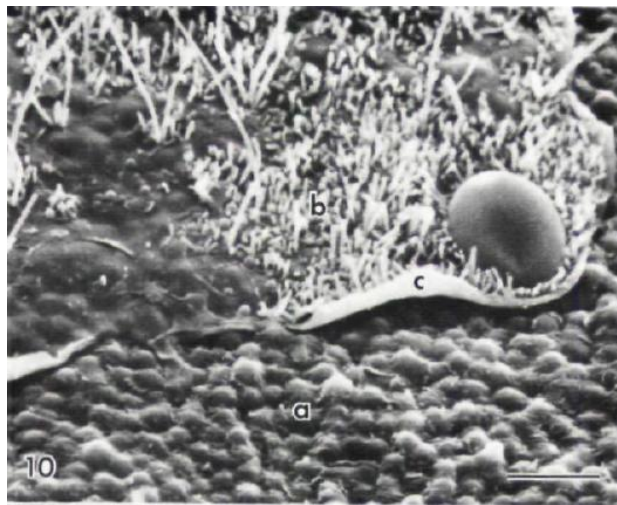


**Figure 5.18:** *U. lactuca* exposed to 200  $\mu\text{g/L}$   $\text{Cr}^{3+}$  at  $t=10$  min, 80  $\mu\text{m}$  scan.





**Figure 5.19:** *U. lactuca* exposed to 200  $\mu\text{g/L}$   $\text{Cr}^{3+}$  at  $t=10$  min, 50  $\mu\text{m}$  scan (a) showing fibre bundles and 10  $\mu\text{m}$  (b) with arrow showing surface detail of cuticle shedding.

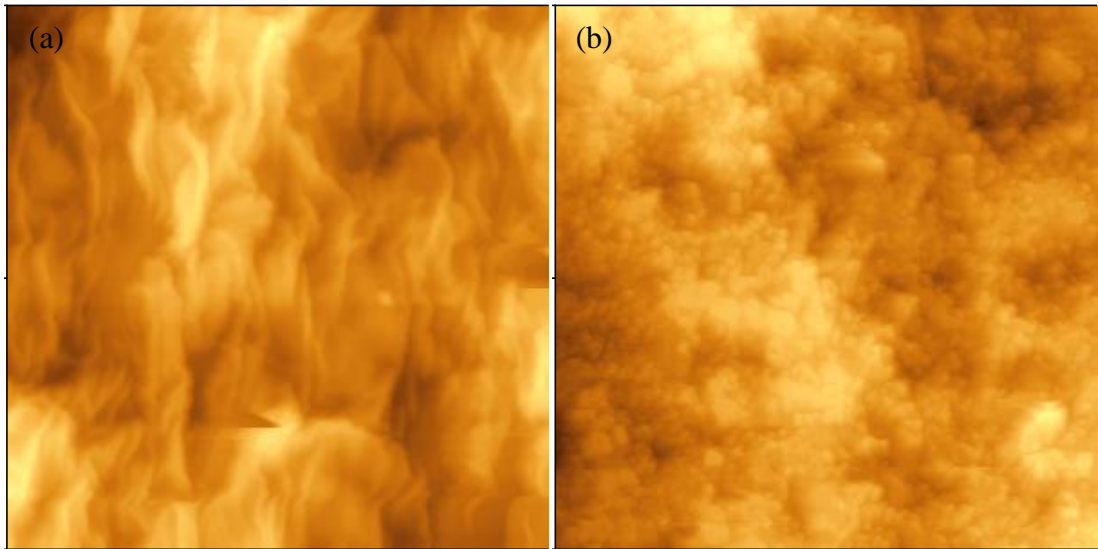


**Figure 5.20:** SEM image of the surface of *Chondrus crispus* showing removal of biofilm (c), clean algal surface (a) and bacterial biofilm (b), bar-10 $\mu\text{m}$  (Sieburth & Tootle 1981).

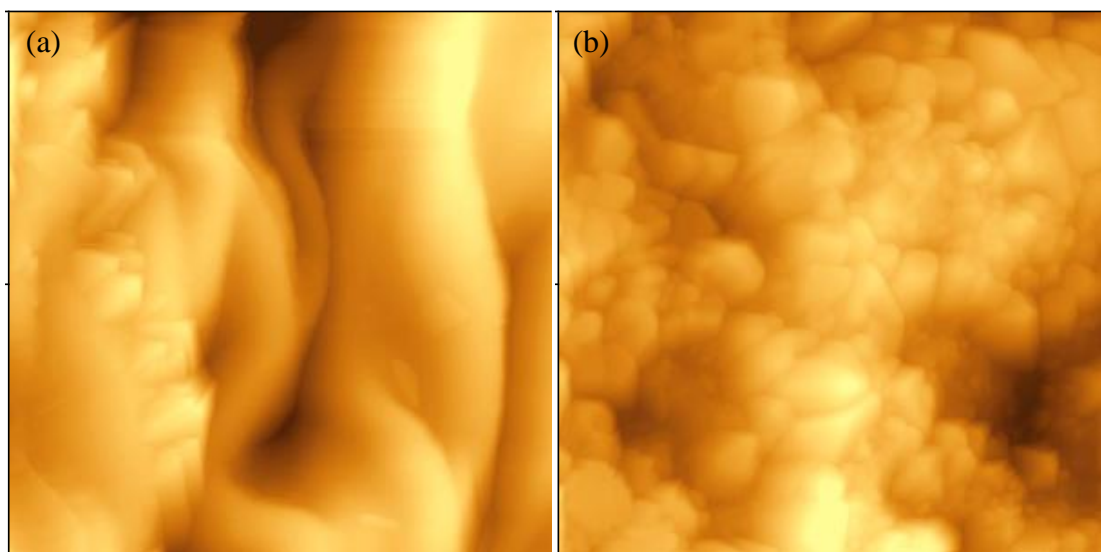
#### 5.3.2.4 Surface at $t = 30$ min

At  $t=30$  min there seemed to be two repeatable surface morphologies. In Figure 5.21 (a), there was a ‘folded’ effect surface layer. The substance this layer was composed of appeared smooth under higher magnification (Figure 5.22 (a)). This is similar to a

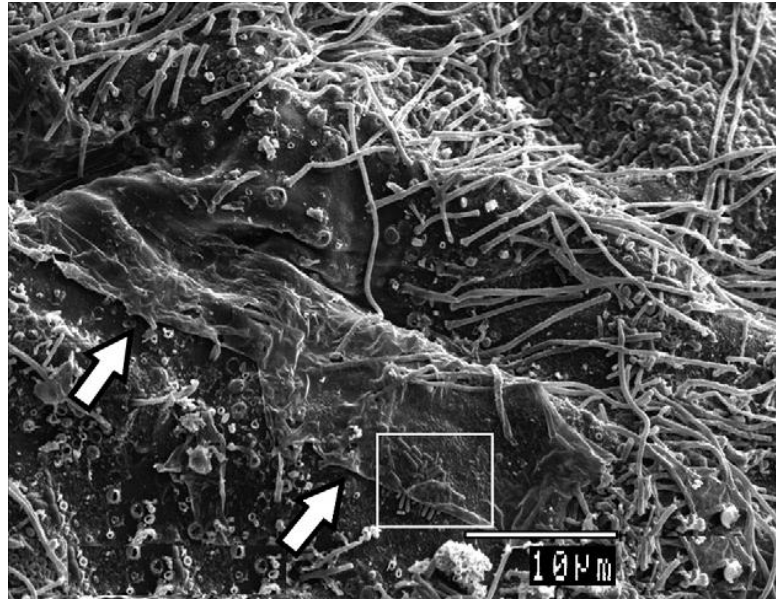
sheet like layer of EPS (extracellular polymeric substance) which is produced by bacteria in a biofilm environment. This was seen by Barreto and Mayer (2007) using SEM on the surface of *Osmundaria serrata* as shown in Figure 5.23 (Barreto & Meyer 2007). The second image shown in Figure 5.21 (b) had a much more complex structure when magnified which seemed to be a complete covering of bacteria (Figure 5.22 (b)).



**Figure 5.21: Two surface topographies seen in *U. lactuca* exposed to 200  $\mu\text{g/L}$   $\text{Cr}^{3+}$  at  $t=30$  min, 80  $\mu\text{m}$  scans.**



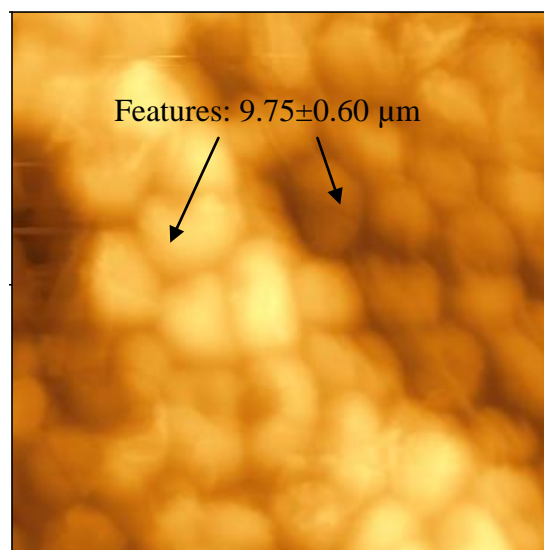
**Figure 5.22: (a) 10  $\mu\text{m}$  detail of Figure 5.21 (a), and (b) 20  $\mu\text{m}$  detail of Figure 5.21 (b).**



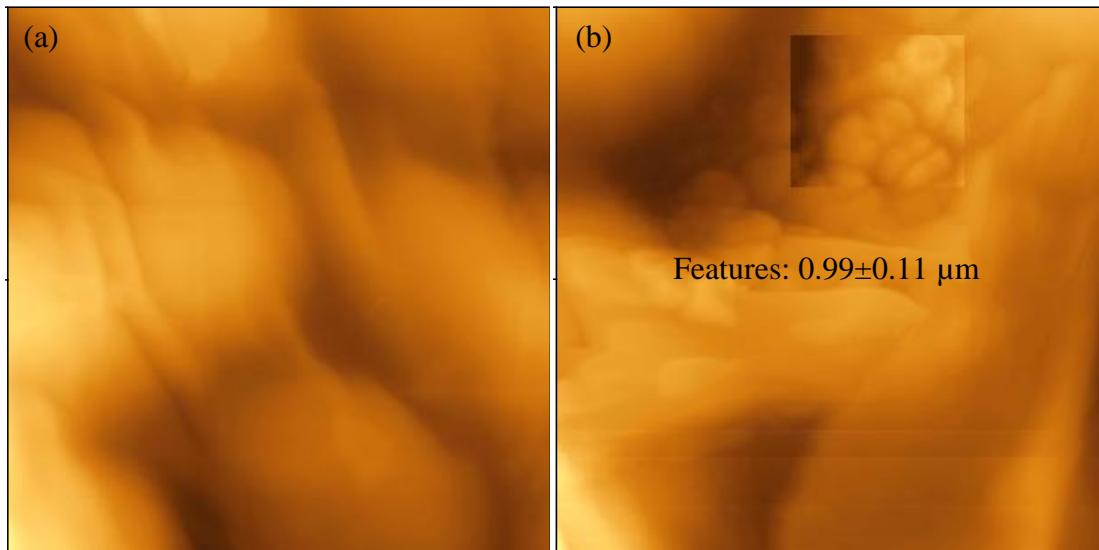
**Figure 5.23: SEM image of a sheet like EPS layer on *Osmundaria serrata* (Barreto & Meyer 2007).**

#### 5.3.2.5 Surface at $t = 60 \text{ min}$

After 60 mins exposure there was a decrease in the visual roughness of the surface, as shown in Figure 5.24. The algal cells were now visible but appear to be covered in a fine EPS layer (Figure 5.25 (b)). The cells are marked with arrows in Figure 5.24 were  $9.75 \pm 0.60 \mu\text{m}$  in size. There were only small areas of bacterial coverage remaining. Bacterial cells highlighted here in Figure 5.25 (b) were  $0.99 \pm 0.11 \mu\text{m}$  in size.



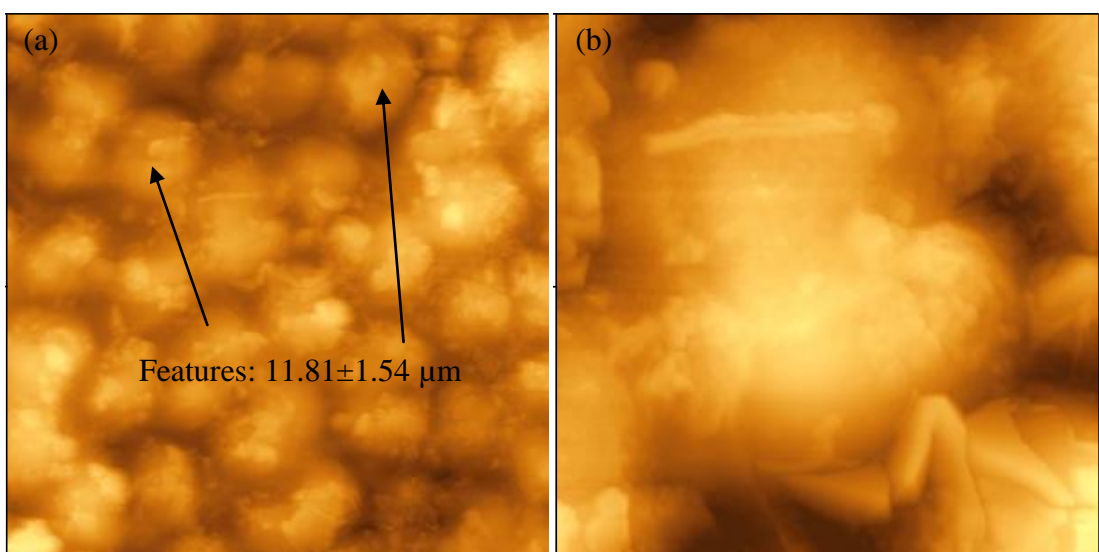
**Figure 5.24: *U. lactuca* exposed to  $200 \mu\text{g/L Cr}^{3+}$  at  $t=60 \text{ min}$ ,  $80 \mu\text{m}$  scan.**



**Figure 5.25: Zoom to 20  $\mu\text{m}$  of above  $t=60$  min scan, showing detail of seaweed outer cell wall (a) and 10  $\mu\text{m}$  highlighting detail of remnants of bacterial biofilm (b).**

#### 5.3.2.6 Surface at $t = 120$ min

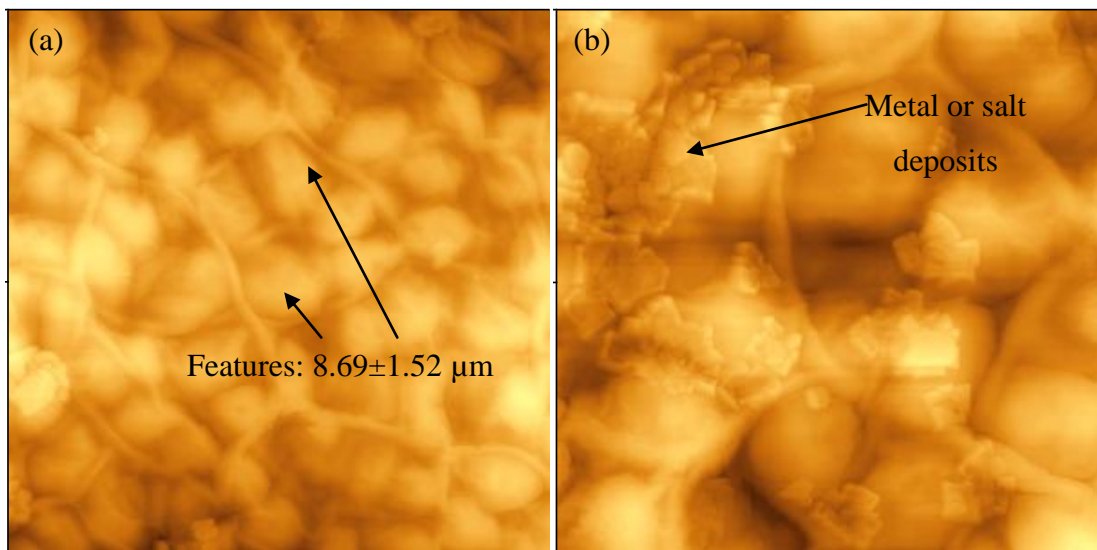
At 120 min there was now a large amount of debris on the surface of the seaweed. The algal cells, however, were still clearly visible. They are marked with arrows in Figure 5.26 and were measured as  $11.81 \pm 1.54 \mu\text{m}$  (Figure 5.26 (a)). The surface debris in Figure 5.26 (b) cannot be conclusively identified but it would appear to be the breakup of the EPS layer.



**Figure 5.26: *U. lactuca* exposed to 200  $\mu\text{g/L}$   $\text{Cr}^{3+}$  at  $t=120$  min, 80  $\mu\text{m}$  and 20  $\mu\text{m}$  scan.**

### 5.3.2.7 Surface at $t = 240$ min

The seaweed surface was now almost completely clear besides isolated areas of crystal like material, magnified in Figure 5.27 (b). These may be metal or sea salt deposits. No bacterial colonies were observed. Cells marked in Figure 5.27 (a) were  $8.69 \pm 1.52 \mu\text{m}$  in size. Fibres seen clearly in the same image were  $2.10 \pm 0.27 \mu\text{m}$ . They are similar in size to those seen in Fig 5.19 (a) but it is not known if they are the same structure.



**Figure 5.27: *U. lactuca* exposed to  $200 \mu\text{g/L Cr}^{3+}$  at  $t=240$  min.  $80 \mu\text{m}^2$  (a) showing cells and and zoom to  $40 \mu\text{m}^2$  (b) showing crystal deposits.**

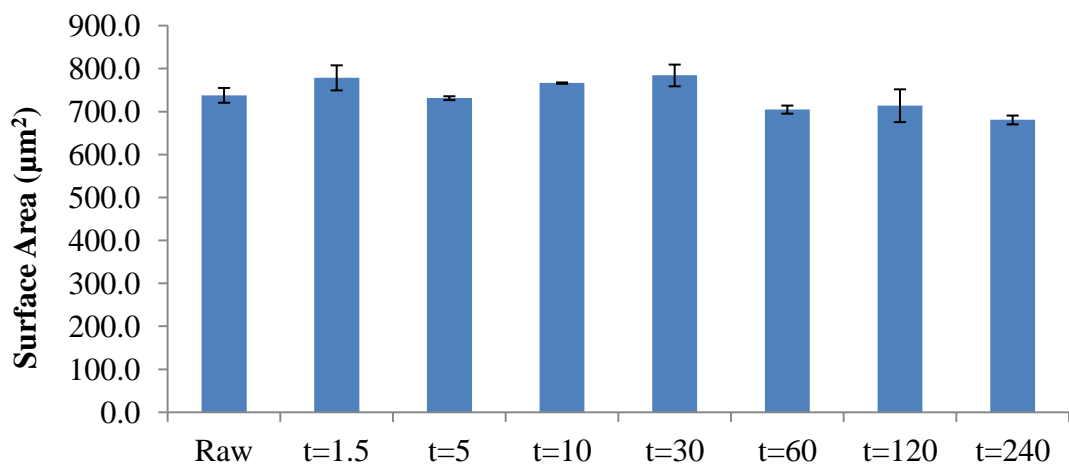
The later time point scans ( $t=60, 120, 240$  min, shown in Figure 5.24, 5.26 and 5.27, respectively) corresponded quite well to the surface cleaned image shown in Figure 5.13(c). This seemed to indicate that the biofilm on the surface of the seaweed was possibly disrupted and sloughed off as a result of  $\text{Cr}^{3+}$  exposure.

### 5.3.2.7 Trends in Surface Area and Roughness

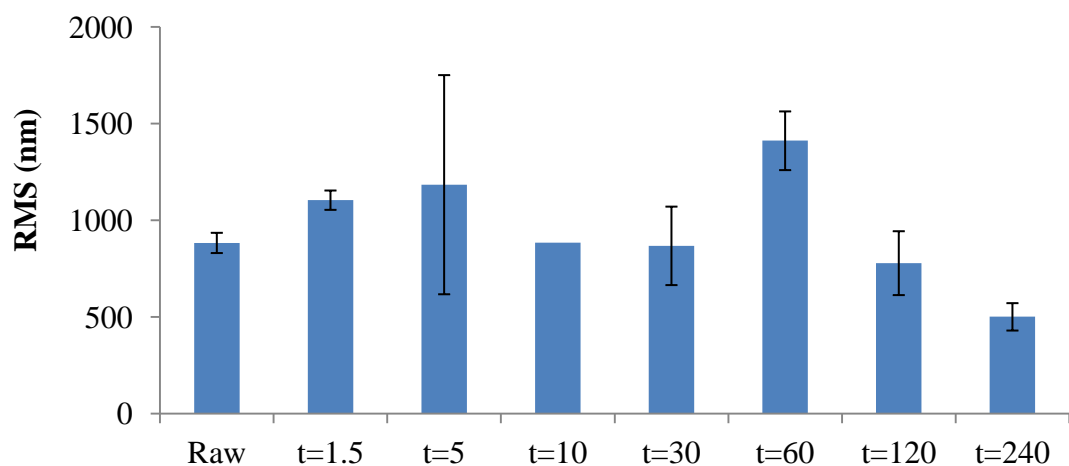
Preliminary trends in surface area and roughness mean squared (RMS, the standard deviation of the height for a given sample area) are given in Figure 5.28 and 5.29. Perfect scans are needed to accurately calculate roughness and RMS values. Some scans had imperfections such as streaking, and out of range areas, therefore some values are based on only one scan. However, there appeared to be a decline in roughness towards the final time points of 120 and 240 min. A  $t$ -test showed this to be non-significant ( $p > 0.05$ ). Only two values were available for calculations, so it is

possible that more data would clarify if the visual smoothing of the surface can be numerically proven.

This overall decline in surface area and roughness pointed to the disruption and breakup of the biofilm on the surface, leaving the algal cells which have a smoother surface morphology. This is the first time it has been attempted to relate AFM measurements to metal uptake in seaweeds. To the author's knowledge, there are no seaweed roughness or surface area measurements published in the literature.



**Figure 5.28: Surface area of *U. lactuca* at each time point. Error bars, where shown, refer to the average value  $\pm$  one standard deviation based on at least two scans.**



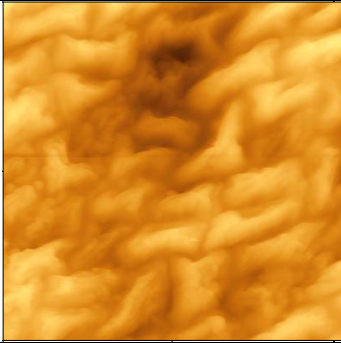
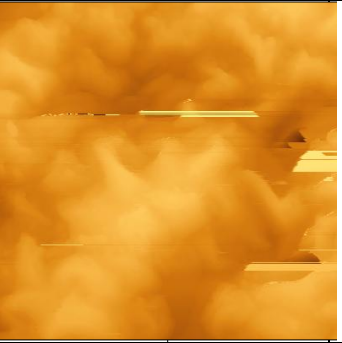
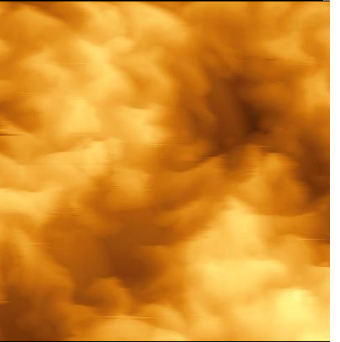
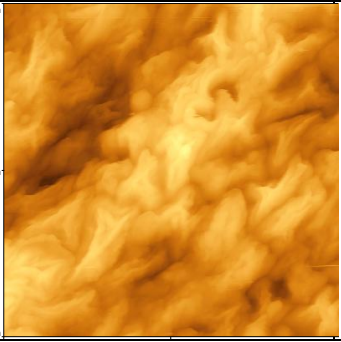
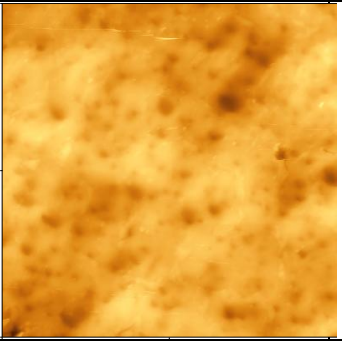
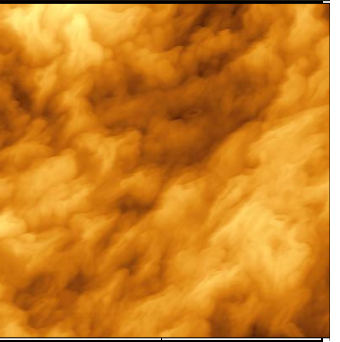
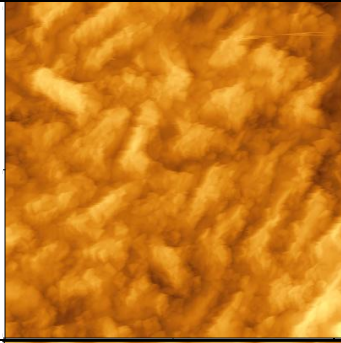
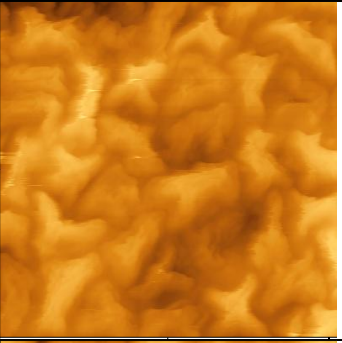
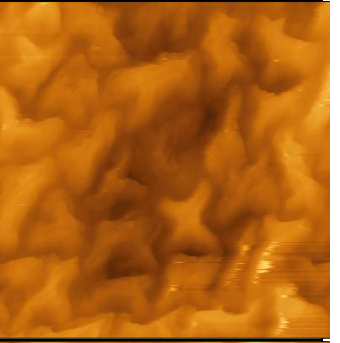
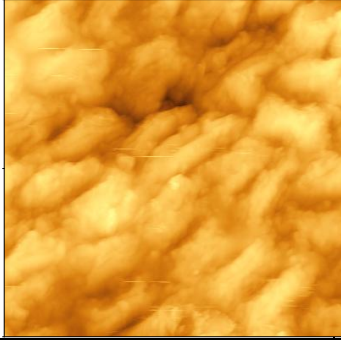
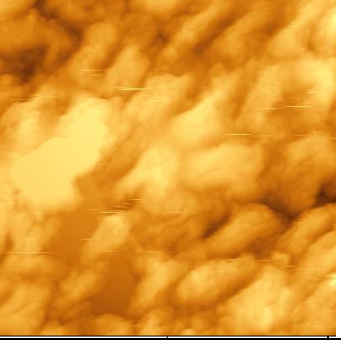
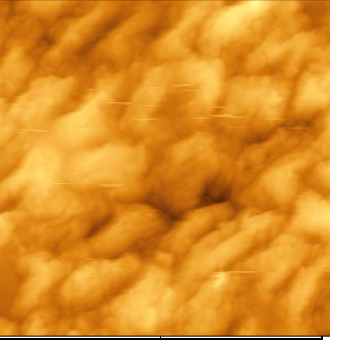
**Figure 5.29: Roughness (RMS) of *U. lactuca* at each time point. Error bars, where shown, refer to the average value  $\pm$  one standard deviation based on at least two scans.**

#### **5.3.4 Analysis of raw and metal loaded samples of *F. vesiculosus*, *P. palmata* and *U. lactuca***

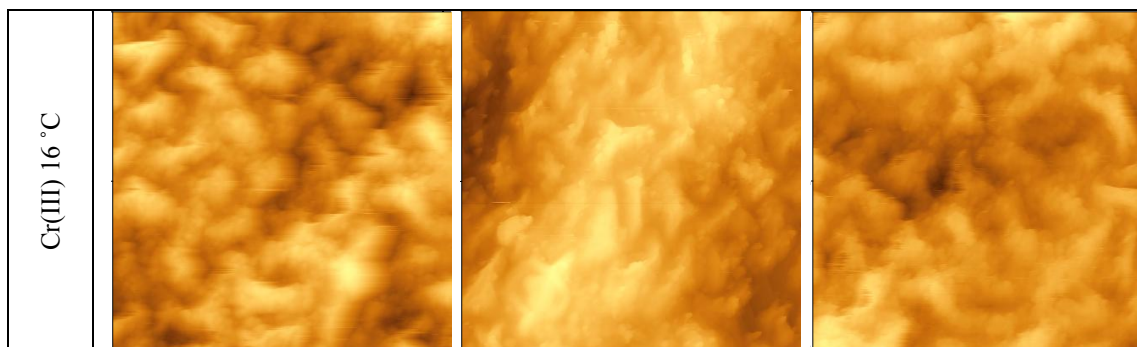
Given the results of this preliminary study it was decided to undertake a larger study with a greater amount of replication to understand if these results were repeatable. The study was extended to allow the analysis of Cr(VI) as well as Cr(III) bioaccumulation by *F. vesiculosus*, *P. palmata* and *U. lactuca*. SEM-EDX was also carried out to enable the rapid screening of many samples for changes in surface morphology (SEM) and to determine if Cr was present on the seaweed surface (EDX).

The samples analysed were as follows. Blanks were raw seaweed pieces which have had no treatment besides a rinse with filtered natural seawater to remove sand and other debris and drying at 60 °C for 24 h. Treatments consisted of 200 µg/L Cr(VI) or Cr(III) exposure at either 7 or 16 °C for 360 min as described in Section 4.2.3. Seaweeds were sampled in either May/June or Feb/Mar as described in Section 4.2.3. SEM-EDX analysis was carried out on all these samples. SFM was carried out on May/June samples only as it was more time consuming. It should be noted that each replicate refers to an entirely different plant subjected to the same treatment.

5.3.4.1 *Fucus vesiculosus*5.3.4.1.1 AFM images of *F. vesiculosus*

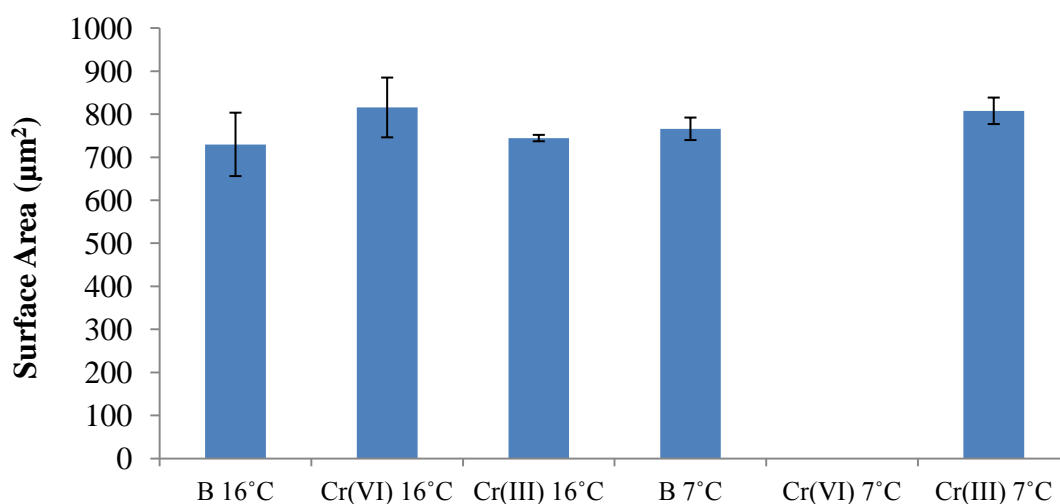
Rep	1	2	3
Blank 7 °C			
Blank 16 °C			
Cr(VI) 7 °C	Could not be imaged		
Cr(VI) 16 °C			
Cr(III) 7 °C			



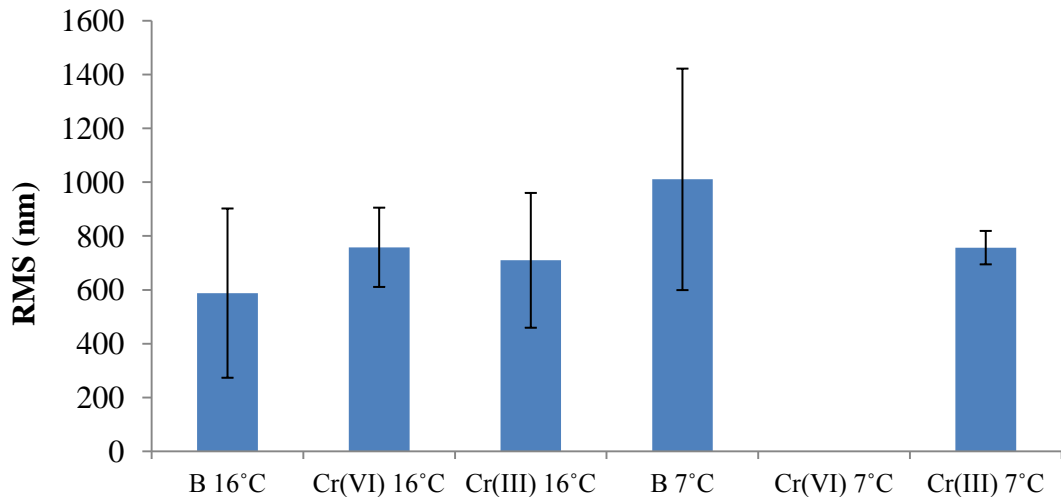


**Figure 5.30: AFM images of blank and metal loaded *F. vesiculosus*, under conditions described left-hand column. All  $50 \mu\text{m}^2$ . Three replicates attempted at each condition.**

The AFM images did not appear to show any visual differences due to either Cr(III) or Cr(VI) exposure. This could be due to the fact that *F. vesiculosus* accumulated the least amount of Cr in comparison to either *P. palmata* or *U. lactuca*. It is possible that the amount of Cr accumulated was too low to induce any visual change. The images appeared to show a continuous biofilm EPS layer shrouded over the underlying algal cellular surface. There are no AFM images of *F. vesiculosus* in the literature for comparison.



**Figure 5.31: Surface area of blank (B, raw) and Cr bound *F. vesiculosus* at 7 and 16°C. Error bars show confidence intervals of 3 replicates. No data indicates sample could not be imaged.**

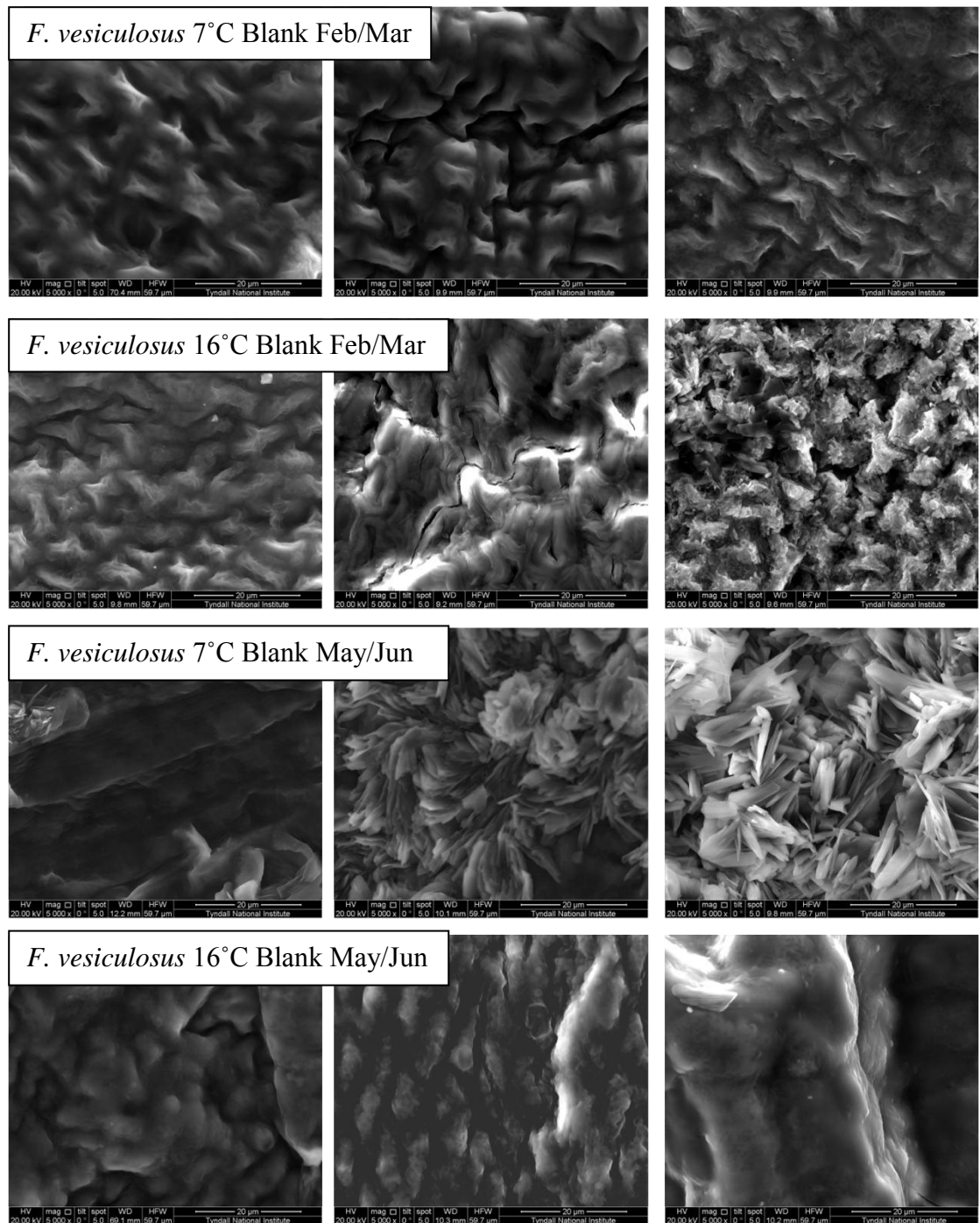


**Figure 5.32: Roughness mean squared (RMS) of blank (B, raw) and Cr bound *F. vesiculosus* at 7 and 16°C. Error bars show confidence intervals of 3 replicates. No data indicates sample could not be imaged.**

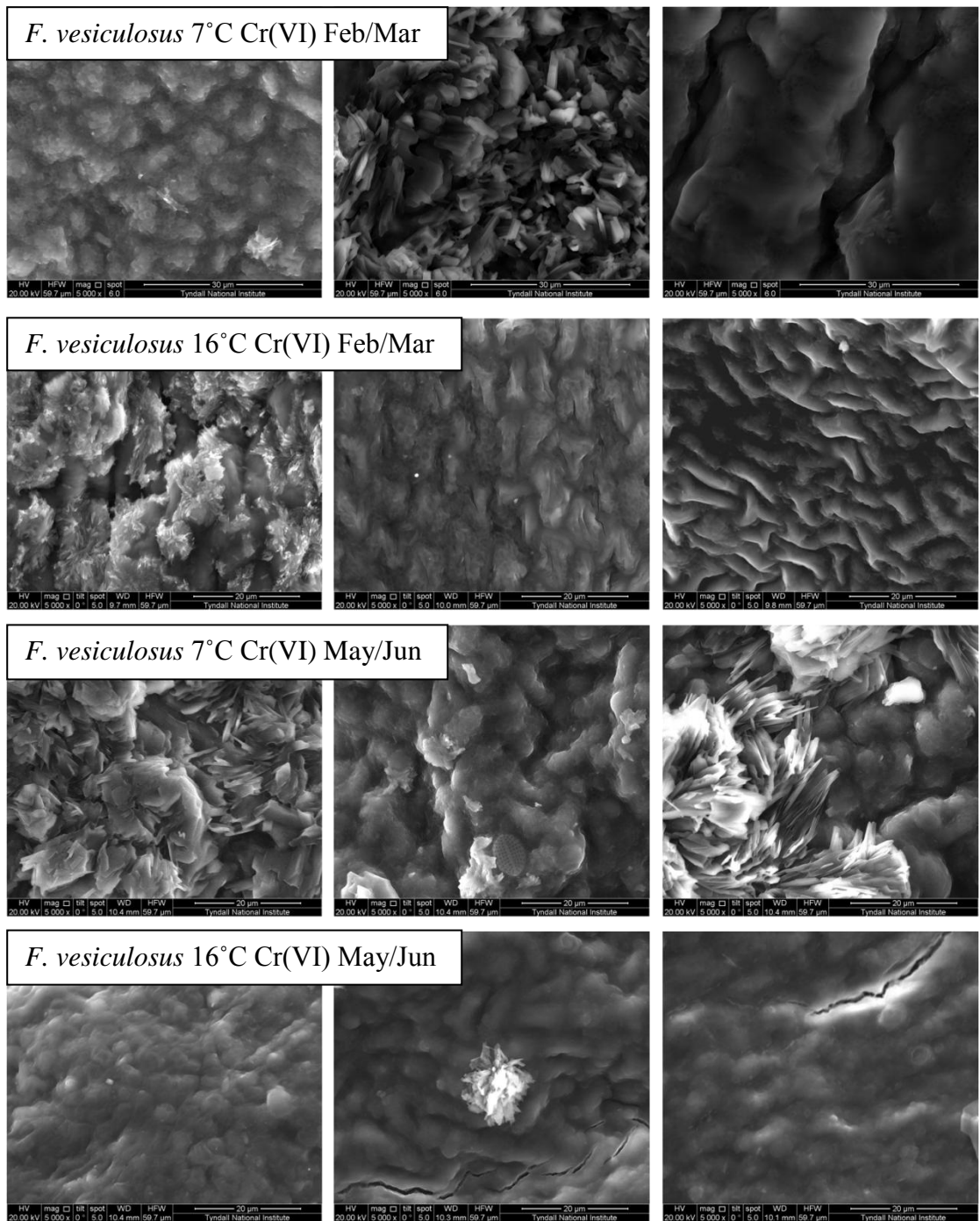
The surface area measurement was similar to that determined for *U. lactuca* in the previous study (Figure 5.28, average of 737  $\mu\text{m}^2$  vs. 773  $\mu\text{m}^2$ ). The RMS values were lower than those determined for *U. lactuca* in the previous study (Figure 5.29, 951 nm versus 764 nm). There were no apparent trends between metal exposure and either surface area or RMS.

#### 5.3.4.1.1 SEM images of *F. vesiculosus*

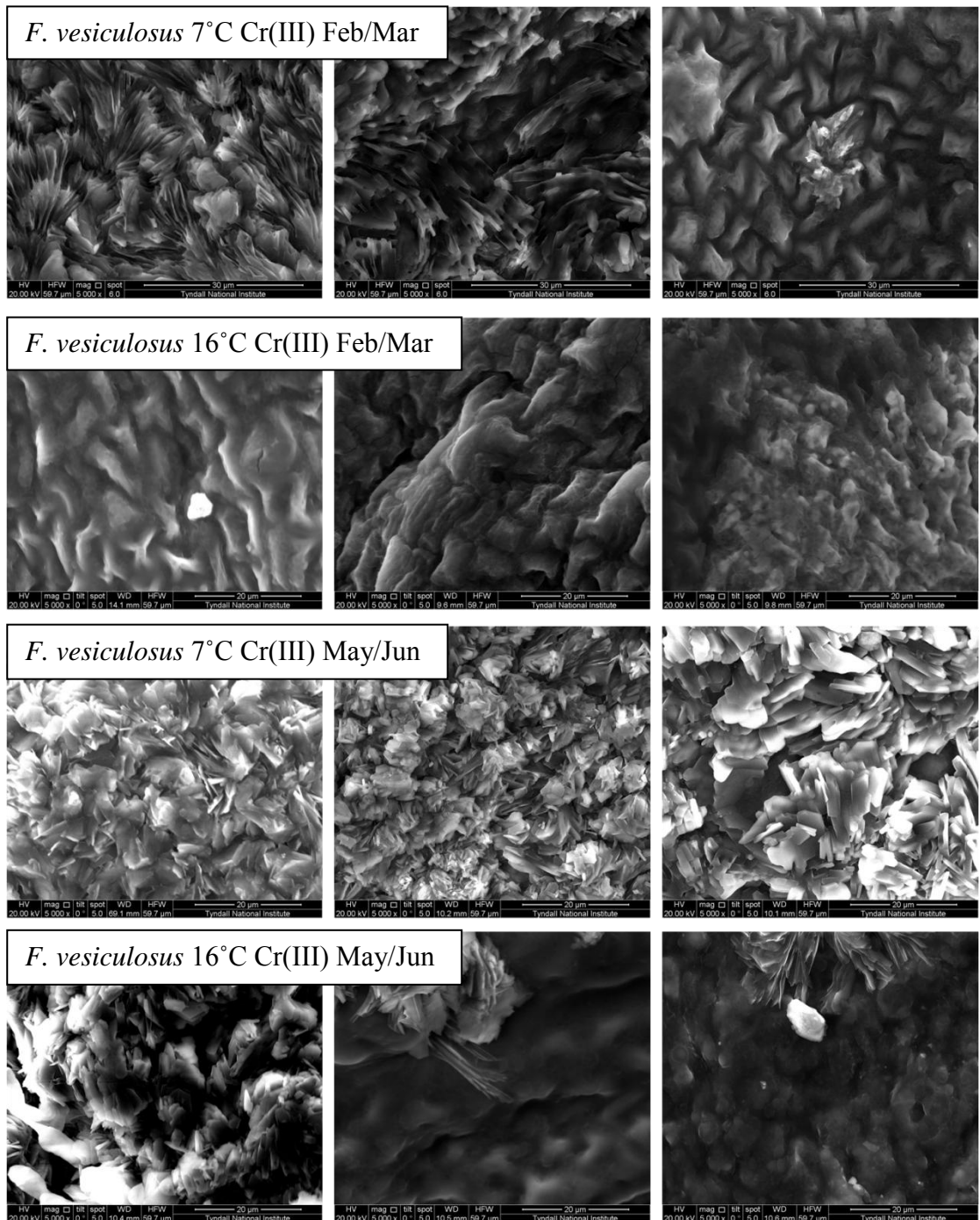
The AFM images appeared to show no differences between blank and metal exposed samples. In this section, SEM was used to determine the morphology of *F. vesiculosus* exposed to Cr(III) and Cr(VI) for 6 , both in Feb/Mar and May/Jun. This was to determine if there are any seasonal differences in the seaweed, or biofilm. The images are presented in Figure 5.33-5.35.



**Figure 5.33: Blank (raw) *F. vesiculosus* SEM scans, conditions as labelled in diagram.**



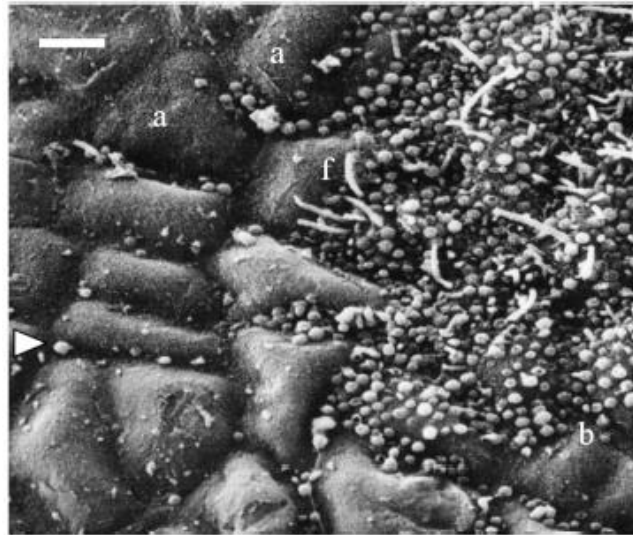
**Figure 5.34: Cr(VI) exposed *F. vesiculosus* SEM scans, conditions as labelled in diagram.**



**Figure 5.35: Cr(III) exposed *F. vesiculosus* SEM scans, conditions as labelled in diagram.**

The SEM images presented in Figure 5.33-5.35 appeared to show the surface of the seaweed shrouded in an EPS layer, with the algal cells visible underneath. Some images appeared to show salt crystals on the seaweed surface. The images were


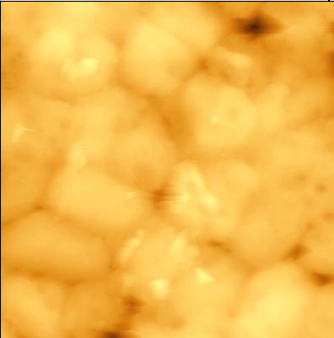
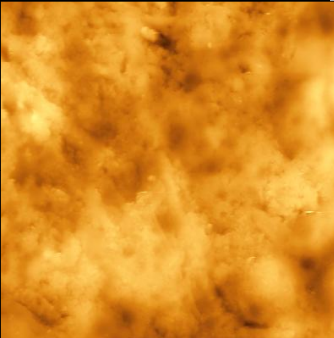
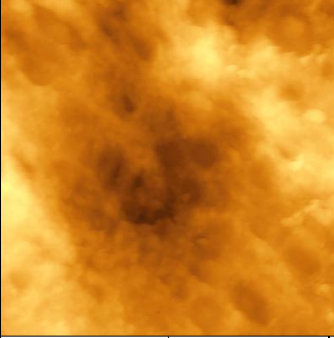
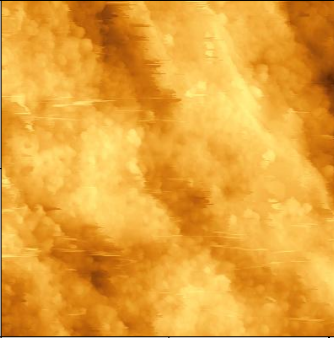
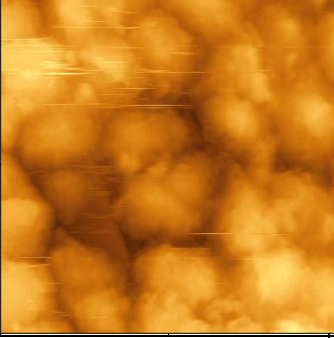
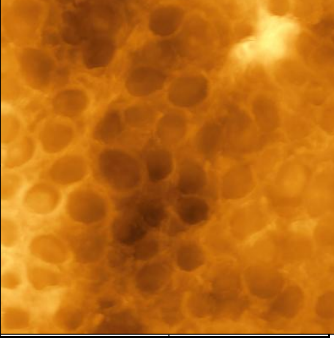
consistent with those seen in the AFM analysis (shown in Figure 5.30). An SEM image of *F. vesiculosus* is shown in Figure 5.36. The algal cells shown in this image were comparable to those seen in this thesis, both imaged by AFM and SEM. Bacterial cells were seen in Figure 5.36, which were not observed in either AFM (Figure 5.30) or SEM images (Figure 5.33-5.35).



**Figure 5.36: SEM image of *F. vesiculosus* showing algal cells and bacterial biofilm, scale bar is 5  $\mu\text{m}$  (Wahl *et al.* 2012).**

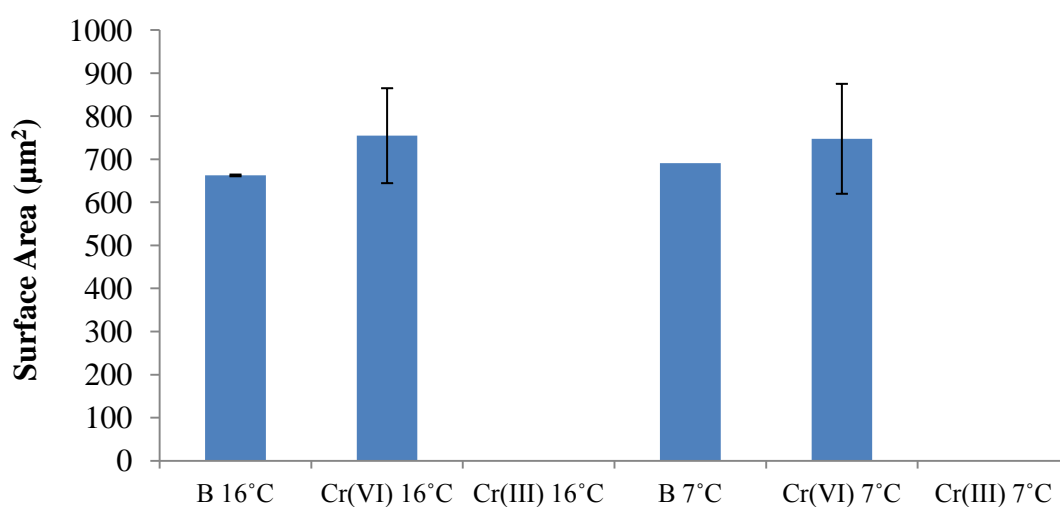
The difference between *U. lactuca* and *F. vesiculosus* could be seen in the images, with *U. lactuca* having rounder cells, and *F. vesiculosus* have more elongated cells (Figure 5.27 versus Figure 5.30).

5.3.4.2 *Palmaria palmata*5.3.4.2.1 AFM images of *P. palmata*

Rep	1	2
Blank 7 °C		Could not be imaged
Blank 16 °C		
Cr(VI) 7 °C		
Cr(VI) 16 °C		
Cr(III) 7 °C / Cr(III) 16 °C	Could not be imaged	Could not be imaged

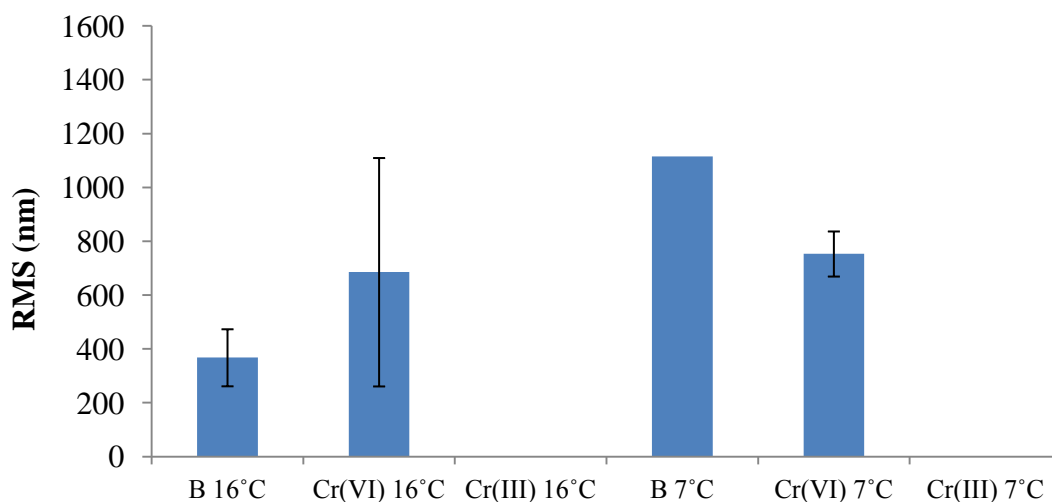
**Figure 5.37: AFM images of blank and metal loaded *P. palmata*, under conditions described left-hand column. All 50  $\mu\text{m}^2$ . Three replicates were attempted at each condition, but could not be completed.**

*P. palmata* proved very difficult to image by AFM. The surface was rough (macroscopically) and the scanner regularly fell out of range of the seaweed. It was also difficult to get the tip into contact with the sample, and tip breakages were frequent. For this reason, not all conditions could be imaged, and a maximum of 2 replicates at any given condition was possible. Little replication was possible so it was difficult to determine if any visual changes in the seaweed surface occurred. SEM was completed at these conditions and the results are presented in Section 5.3.4.2.2. Visual differences will be discussed more in this section. The author could find no AFM images of *P. palmata* in the literature to compare results to.



**Figure 5.38: Surface area of blank (B, raw) and Cr bound *P. palmata* at 7 and 16°C. Error bars show confidence intervals of 2 replicates. No data indicates sample could not be imaged.**



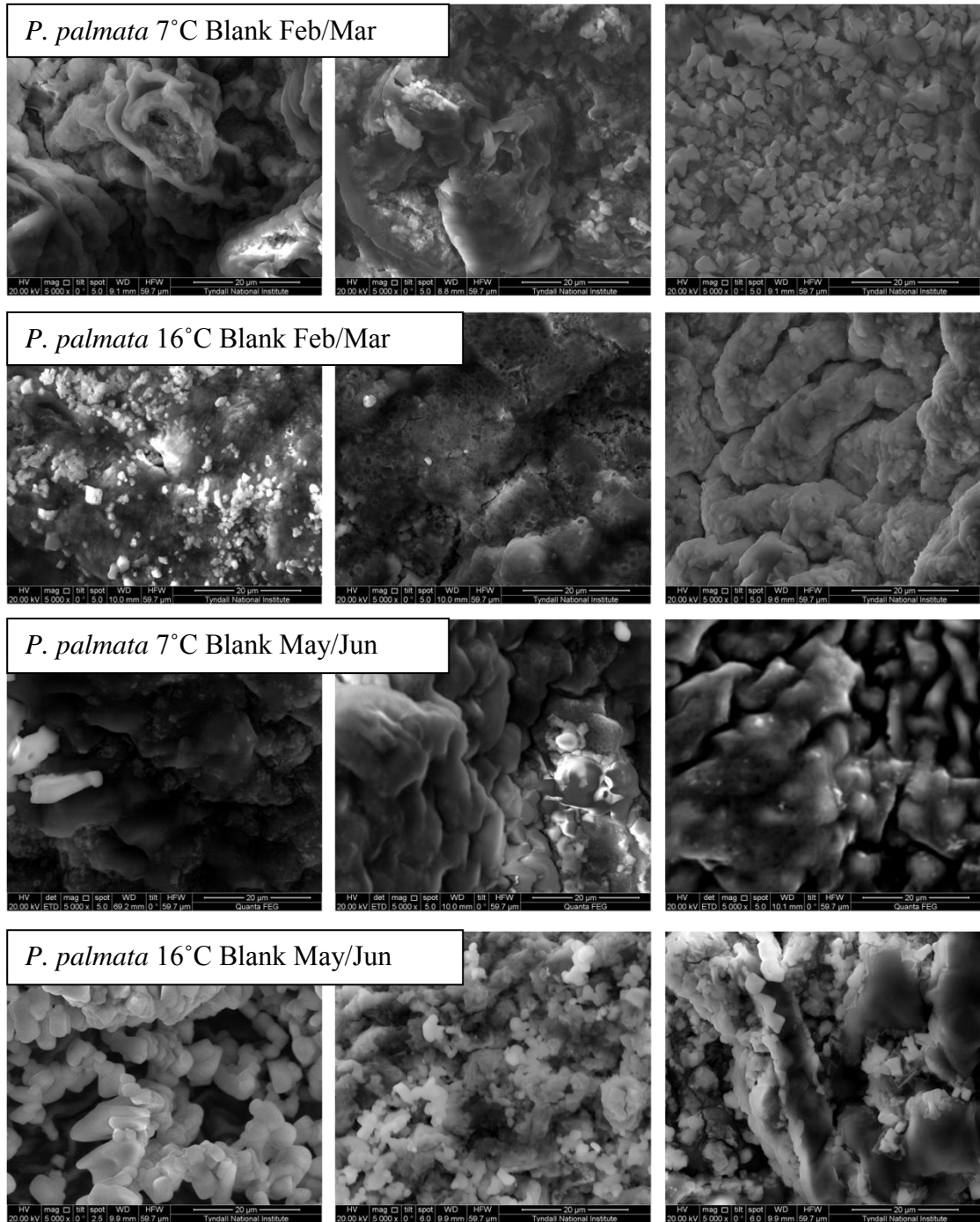


**Figure 5.39: Roughness mean squared (RMS) of blank (B, raw) and Cr bound *P. palmata* at 7 and 16°C. Error bars show confidence intervals of 2 replicates. No data indicates sample could not be imaged.**

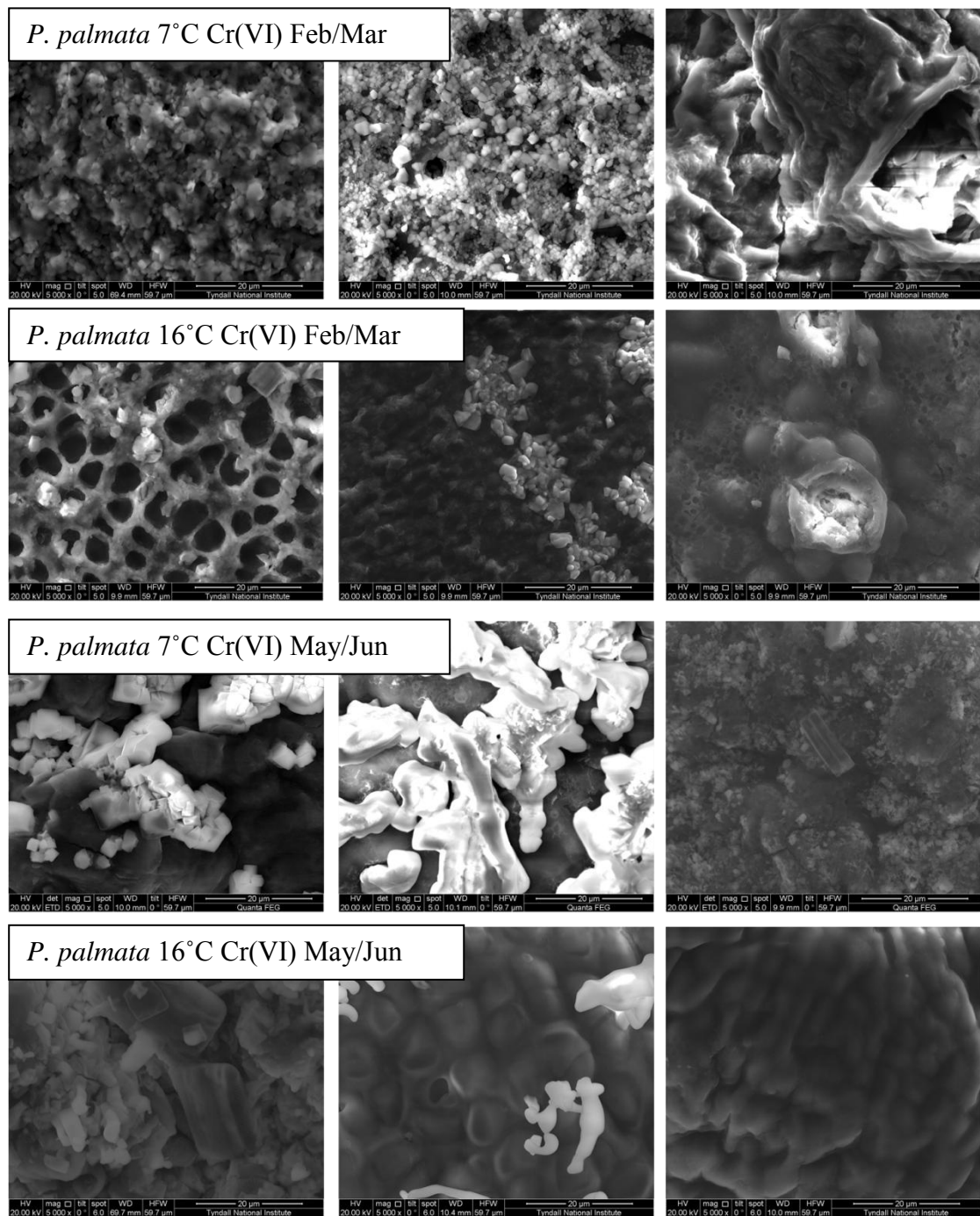
The surface area measurement was similar to that determined for *F. vesiculosus* (Figure 5.31, average of 773  $\mu\text{m}^2$  versus 713  $\mu\text{m}^2$ ). The RMS values were also similar to that determined for *F. vesiculosus* (Figure 5.32, 764 nm versus 730 nm). As the seaweed was difficult to image, there was little data to compare, and no determination could be made if there were any differences between blank and metal loaded samples.

### 5.3.4.2.2 SEM images of *P. palmata*

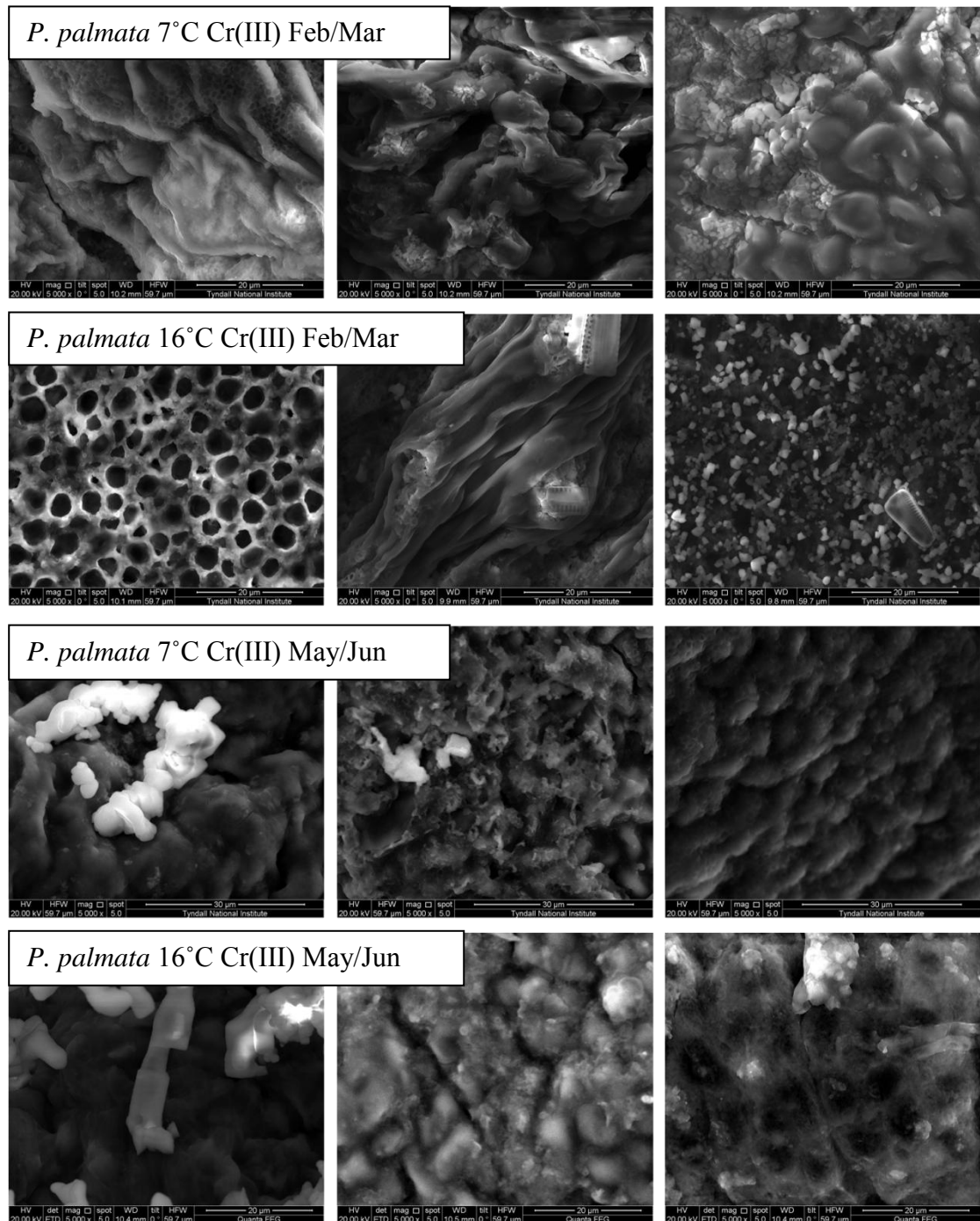
SEM imaging of *P. palmata* proved particularly important as imaging and replication of images by AFM was difficult. The results are presented in Figures 5.40-5.42.



**Figure 5.40: Blank (raw) *P. palmata* SEM scans, conditions as labelled in diagram.**



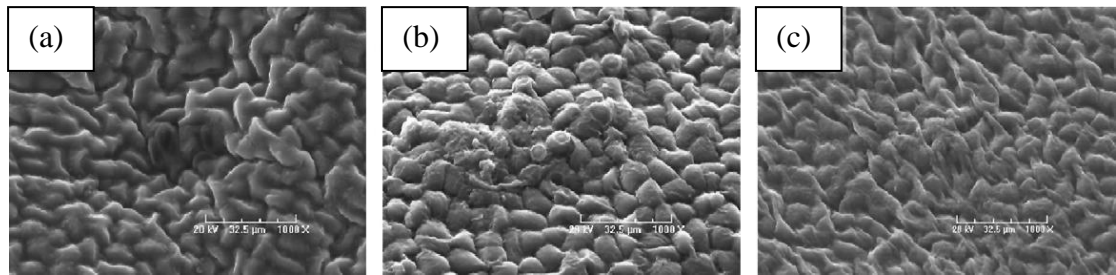
**Figure 5.41: Cr(VI) exposed *P. palmata* SEM scans, conditions as labelled in diagram.**



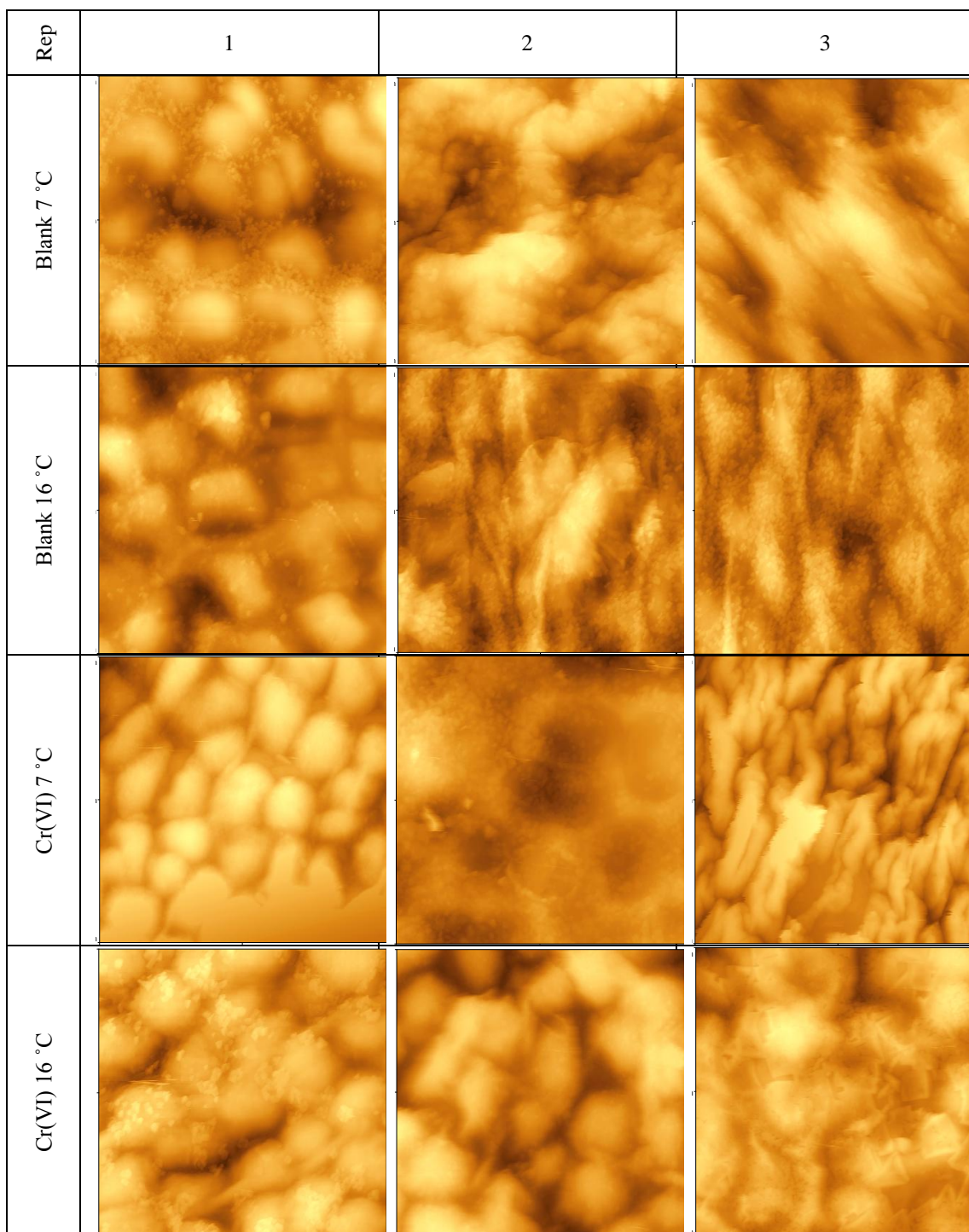
**Figure 5.42: Cr(III) exposed *P. palmata* SEM scans, conditions as labelled in diagram.**

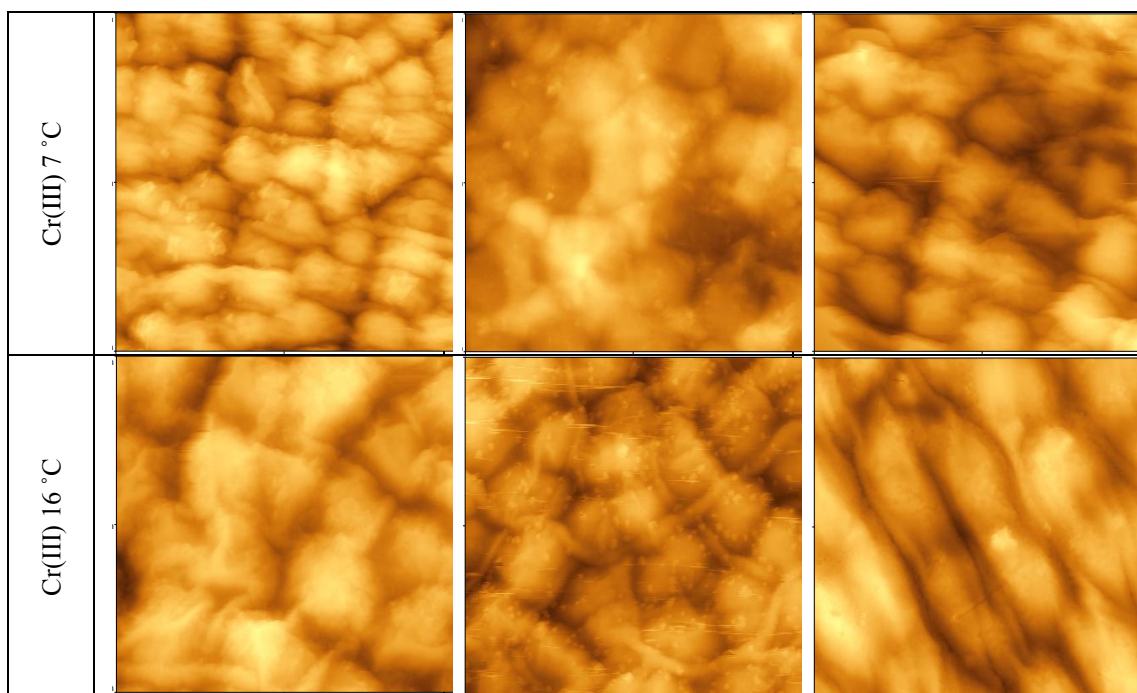
Although the number of AFM images were limited (Figure 5.37), there was good agreement seen between these and the SEM images presented in Figure 5.40-5.42. The images seemed to show a combination of EPS layer, with the algal cells just

visible underneath and bacterial biofilm. No consistent differences between blank and metal loaded samples were observed. No consistent differences between seasons were observed. It was possible that the concentration of metal *P. palmata* was exposed to was not sufficient to cause any morphological changes in the seaweed. Figure 5.43 shows dead *P. palmata* biomass exposed to 2000 mg/L Cr(III) and Cr(VI). The raw image appeared to agree with the images seen here in Figure 5.42. Metal exposure appeared to induce a visual change in the surface for Cr(III) exposure. The biofilm appeared to be removed, showing the algal cell surface. This was seen to a lesser degree with Cr(VI) exposure. 2000 mg/L was 10,000 times the concentration used in this study. Therefore, higher exposure concentrations, or longer exposure times may be necessary to see visual changes in the seaweed surface.



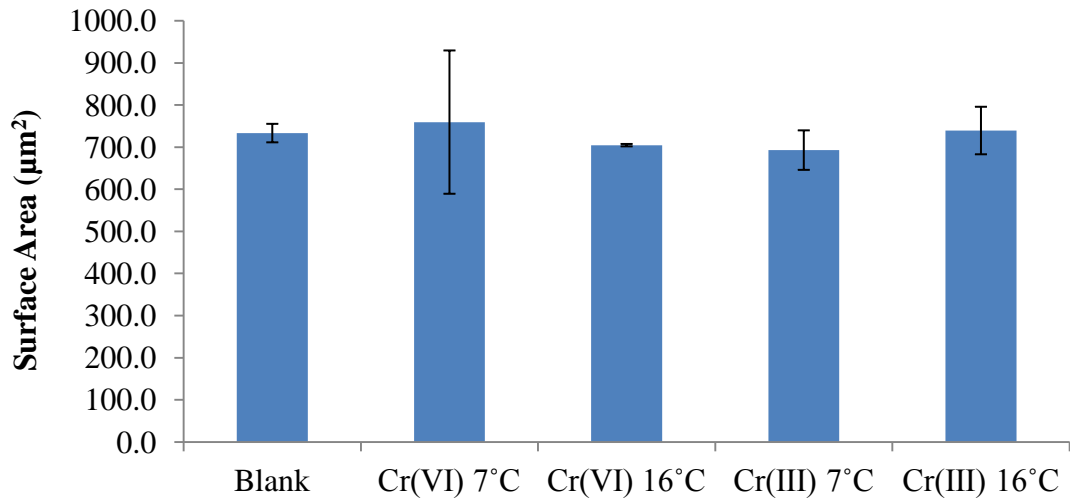
**Figure 5.43: Raw *P. palmata* dead biomass (a) exposed to 2000 mg/L Cr(III) (b) and 2000 mg/L Cr(VI) (c) (Murphy, Tofail, et al. 2009).**

5.3.4.3 *Ulva lactuca*5.3.4.3.1 AFM images of *U. lactuca*

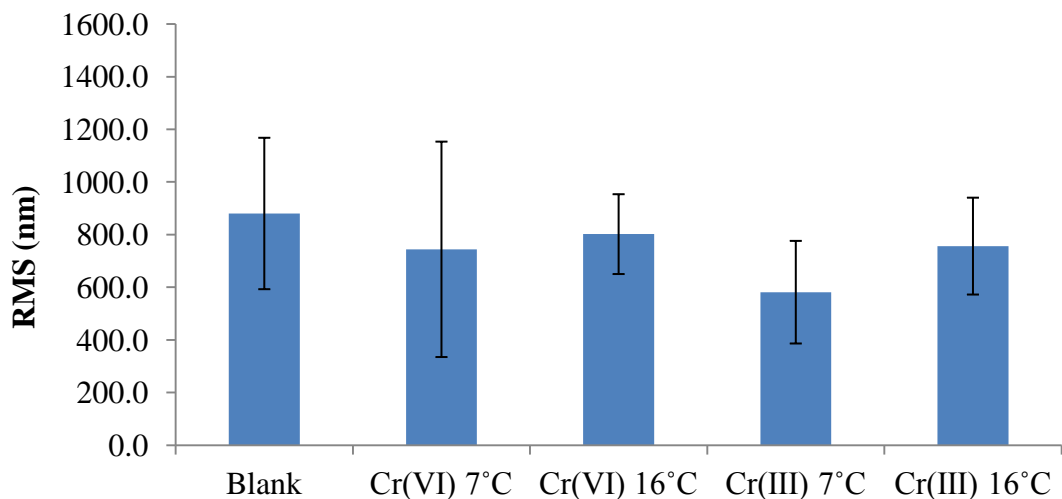


**Figure 5.44: AFM images of blank and metal loaded *U. lactuca*, under conditions described left-hand column. All 50  $\mu\text{m}^2$ . Three replicates attempted at each condition.**

The raw seaweed surface was highly variable with areas of complete biofilm coverage and areas where the seaweed cells could be observed. No great effect could be seen when exposed to Cr(VI) at 7 °C, but at 16 °C more of the seaweed surface could be seen. When exposed to Cr(III) at both 7 and 16 °C the underlying cellular structure of the seaweed could be observed in every case, although sometimes with biofilm debris or EPS film still visible. However, the trend was not as apparent as seen in the preliminary time course study for *U. lactuca* (Section 5.3.2). The reason for this may be due to the differences in experimental conditions, leading to the final concentration of Cr in the seaweeds being very different. Cr(III) exposure resulted in the accumulation of 10 mg/kg for Cr(III) exposure at 16 °C, and even less when exposing the seaweed to Cr(III) at 4 °C (4 mg/kg) versus 20 mg/kg accumulation found in the preliminary study. It is possible, therefore, that the seaweed was not exposed to enough metal to induce a significant change in morphology.



**Figure 5.45:** Surface area (per 625 µm<sup>2</sup> projected area) of blank (B, raw) and Cr bound *U. lactuca* at 7 and 16°C. Error bars show confidence intervals of 3 replicates.



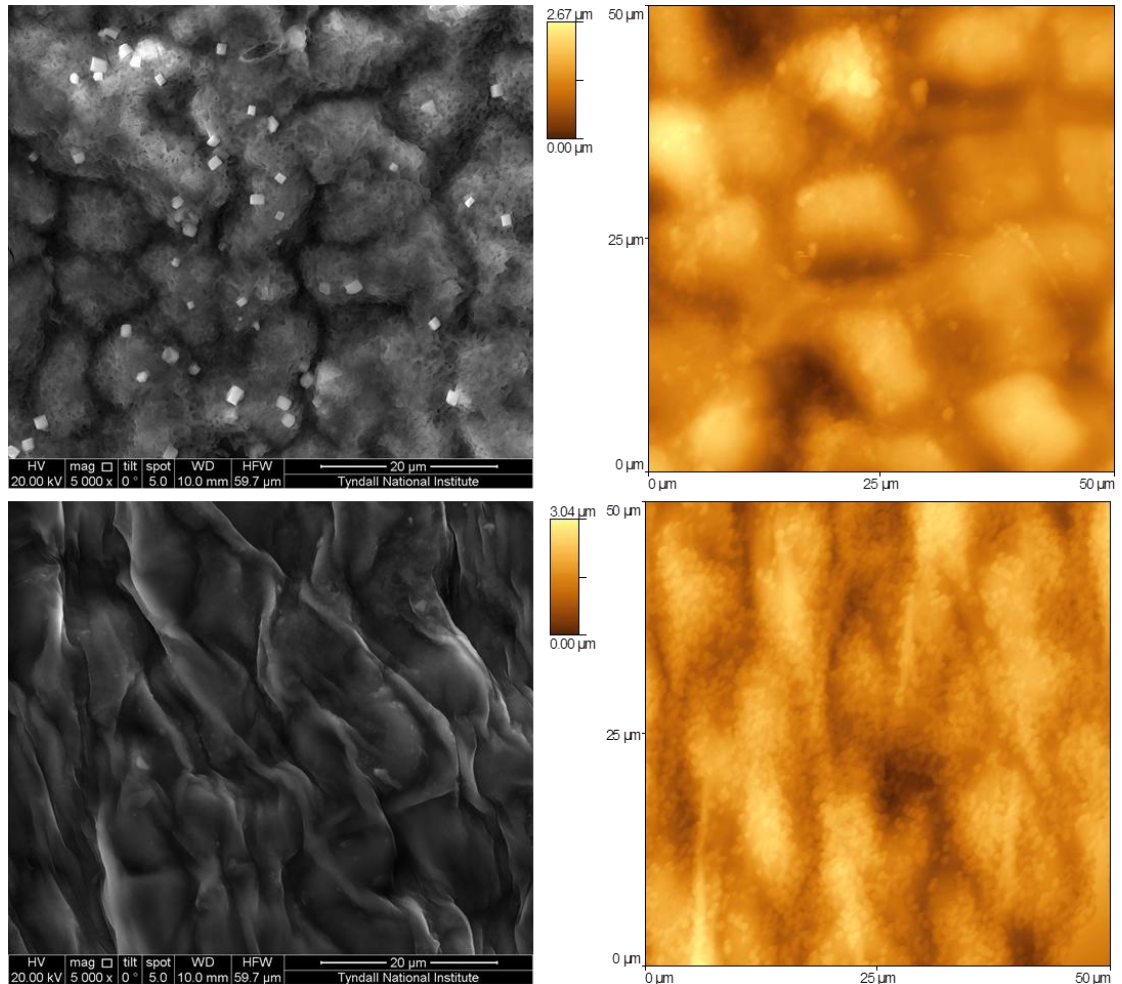
**Figure 5.46:** Roughness mean squared (RMS) of blank (B, raw) and Cr bound *U. lactuca* at 7 and 16°C. Error bars show confidence intervals of 3 replicates.

The surface area measurement was similar to that determined for *F. vesiculosus*, and *P. palmata* (Figure 5.31, 5.38, 5.45, giving an average of 773, 713, 726 µm<sup>2</sup>, respectively). No trend or differences were seen either between species or on metal exposure. This suggests that surface area measurements cannot be related to visual changes on the surface of the seaweed. The RMS values were also similar to both *F. vesiculosus* and *P. palmata* (Figure 5.32, 5.39, 5.46, giving an average 764, 730, 752 nm, respectively), suggesting that RMS data was also unsuitable for relating to morphological differences in metal uptake.



### 5.3.4.3.2 SEM images of *U. lactuca*

There was excellent agreement between the SFM and SEM images, showing that SFM gave a true representation of the seaweed surface.



**Figure 5.47: Images showing agreement in features between SEM (B/W) and SFM (Orange) scans. All are blank seaweeds, samples in Feb/Mar.**

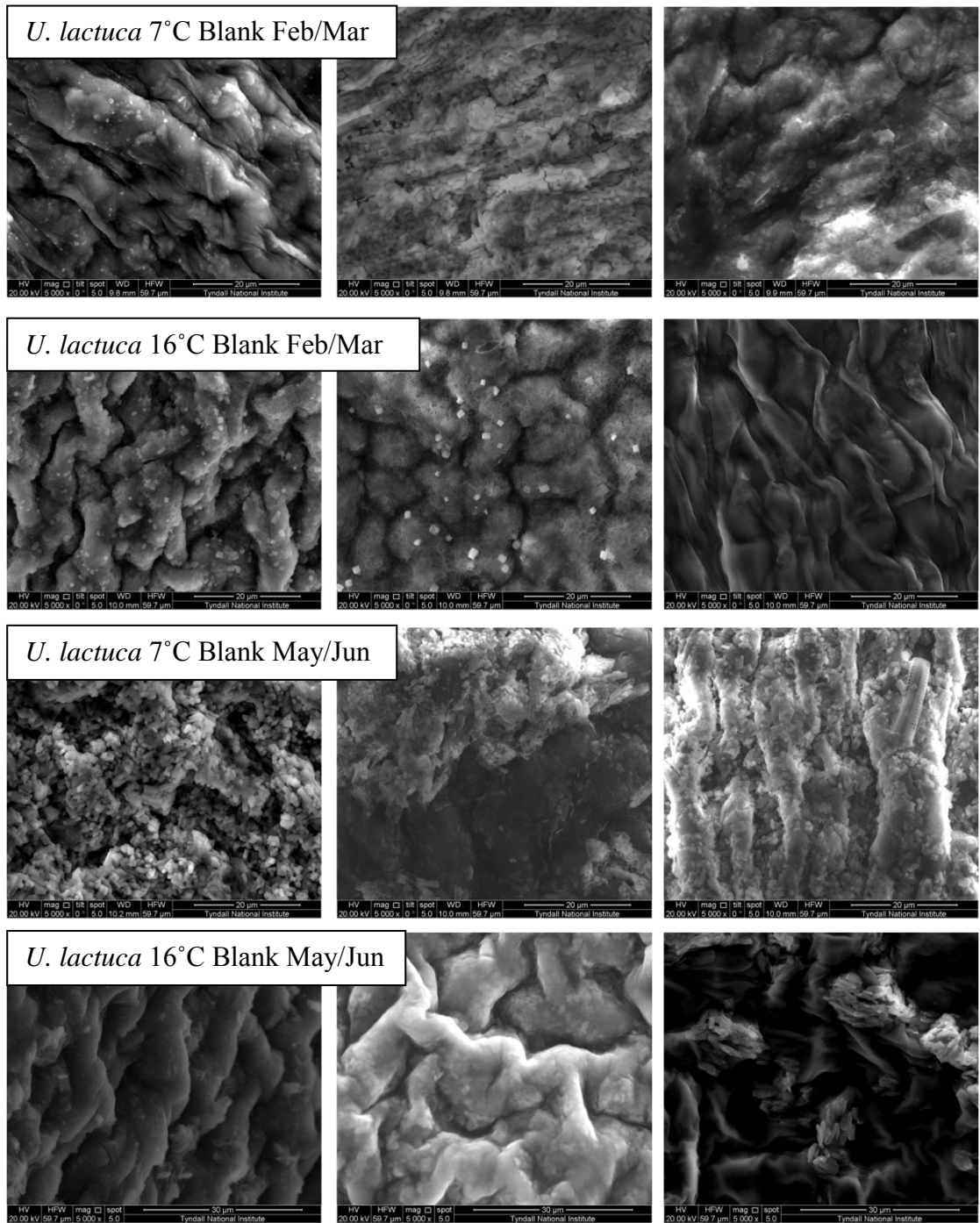
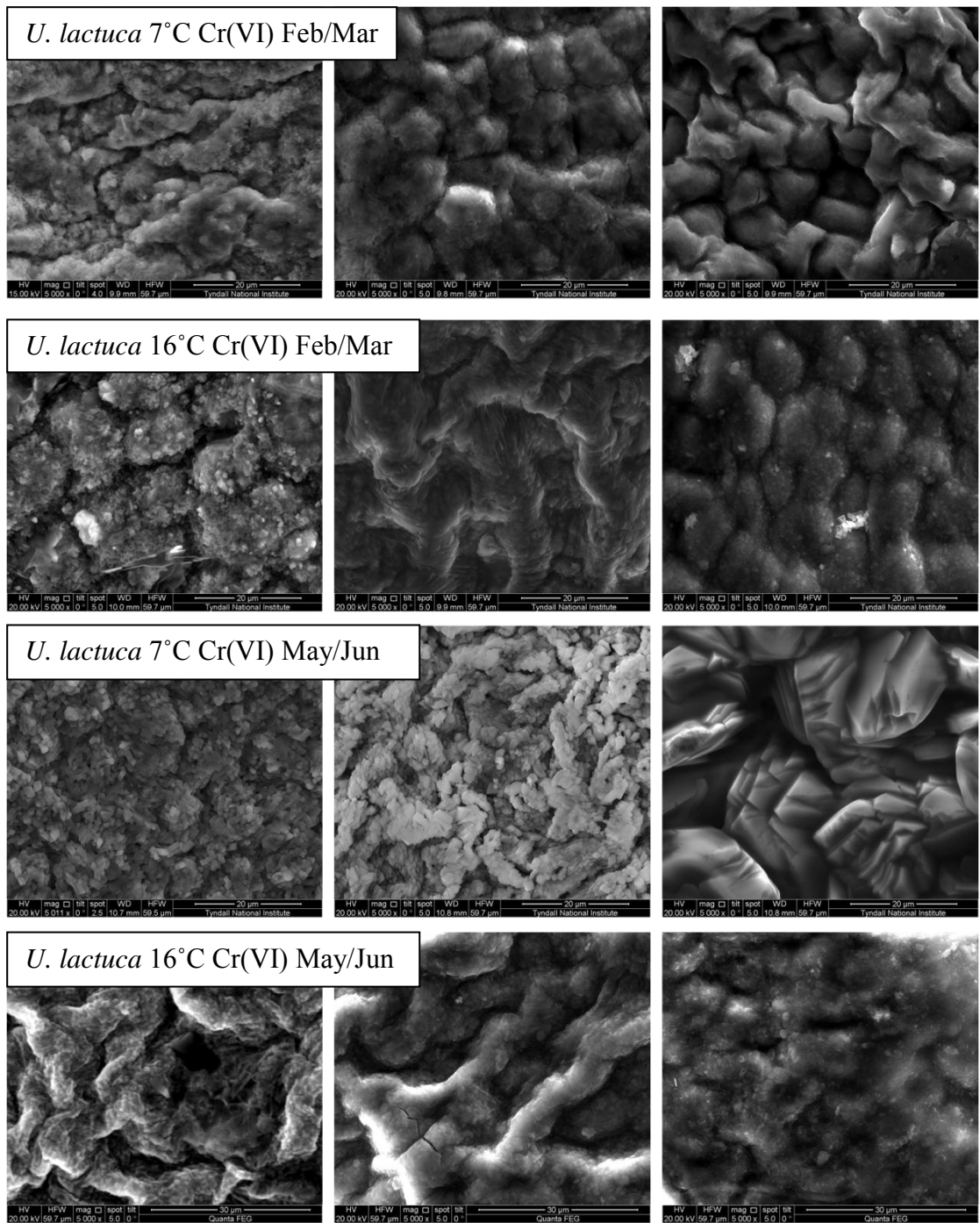
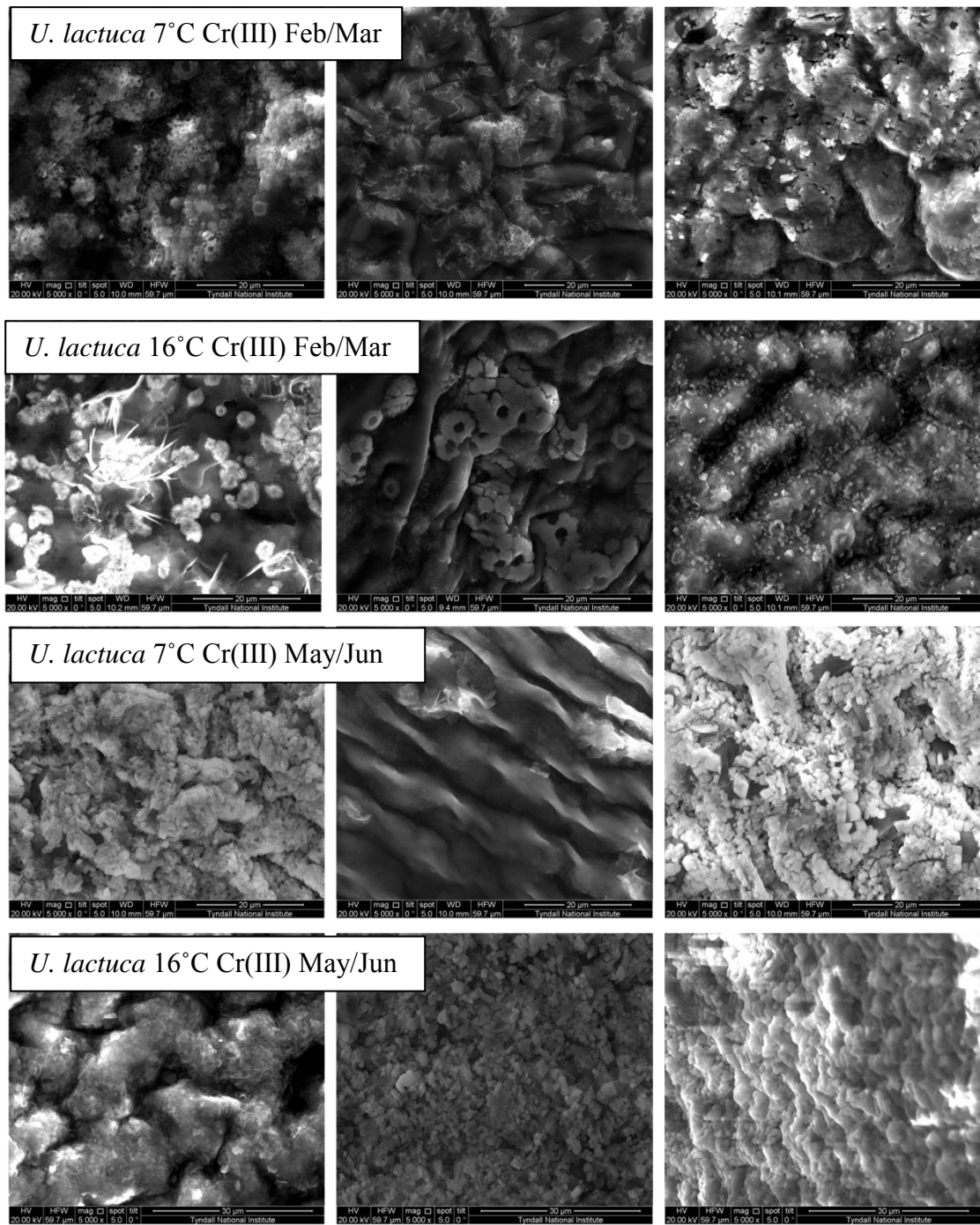


Figure 5.48: Raw *U. lactuca* SEM scans, conditions as labelled in diagram.



**Figure 5.49: SEM scans of Cr(VI) exposed *U. lactuca*, conditions as labelled in diagram.**

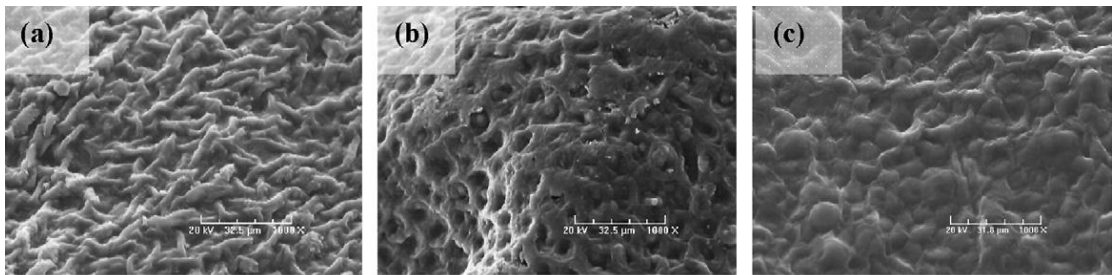


**Figure 5.50: SEM scans of Cr(III) exposed *U. lactuca*, conditions as labelled in diagram.**

The images seemed to show a combination of EPS layer, with algal cells just visible underneath, and bacterial biofilm. No consistent differences between blank and metal loaded samples were observed. This is in contrast to the preliminary study with *U.*

*lactuca* and possible reasons for the lack of difference are discussed in Section 5.3.4.3.1. There was possibly greater biofilm coverage in May/Jun. It has been shown that biofilm biomass reduces in winter (Chiu *et al.* 2006).

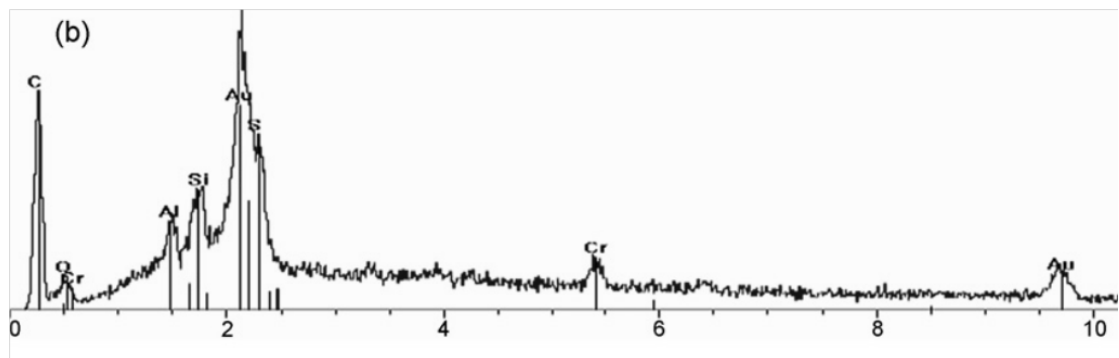
Figure 5.51 shows dead *U. lactuca* biomass exposed to 2000 mg/L Cr(III) and Cr(VI). The raw image appeared to agree with the SEM images in Figure 5.48. Metal exposure appeared to induce a visual change in the surface for both Cr(III) and Cr(VI) exposure (possible cuticle formation (Figure 5.51(b), and biofilm reduction (Figure 5.51(c)). 2000 mg/L was 10,000 times the concentration used in this study. This adds to the evidence that higher exposure concentrations, or longer exposure times, are necessary to see visual changes in the seaweed surface.



**Figure 5.51: Raw *U. lactuca* dead biomass (a) exposed to 2000 mg/L Cr(III) (b) and 2000 mg/L Cr(VI) (c) (Murphy, Tofail, *et al.* 2009).**

### 5.3.5 EDX Analysis of Surface

Cr binding could not be detected by EDX under any of the conditions or seaweeds studied. A peak would be expected at approximately 5.5 keV (Murphy, Tofail, *et al.* 2009). The scans may be seen in Appendix 2, and one scan is shown here for information (Figure 5.53-5.55). The reason that no Cr was detected is twofold. First, binding was shown to be intracellular (see Chapter 4). The results found by EDX analysis supports this finding. Secondly, it is possible that the limit of detection of the technique is not high enough to allow detection of Cr. One study exposed *F. vesiculosus* biomass to 2000 mg/L Cr(III) and Cr(VI). As seen in Figure 5.52, even at this elevated concentration, only a small peak was observed (Murphy, Tofail, *et al.* 2009). Levels 10,000 times less than that were used in this study, it is therefore likely that no peak would be observed.



**Figure 5.52: EDX spectrum of *F. vesiculosus* biomass exposed to 2000 mg/L Cr(III) (Murphy, Tofail, *et al.* 2009).**

Interestingly, the scans do show some inter-species differences, however, as they are non-quantitative, and no references were used, comparisons cannot be made directly between scans.

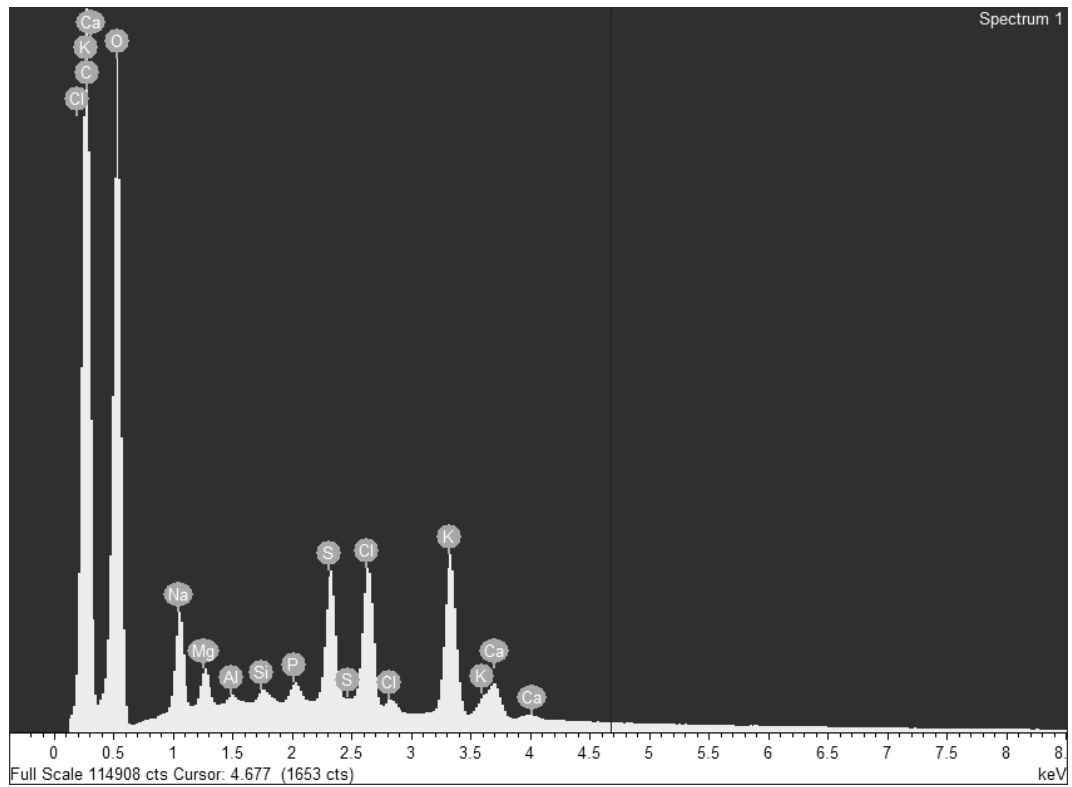


Figure 5.53: Blank *F. vesiculosus* 16 °C.

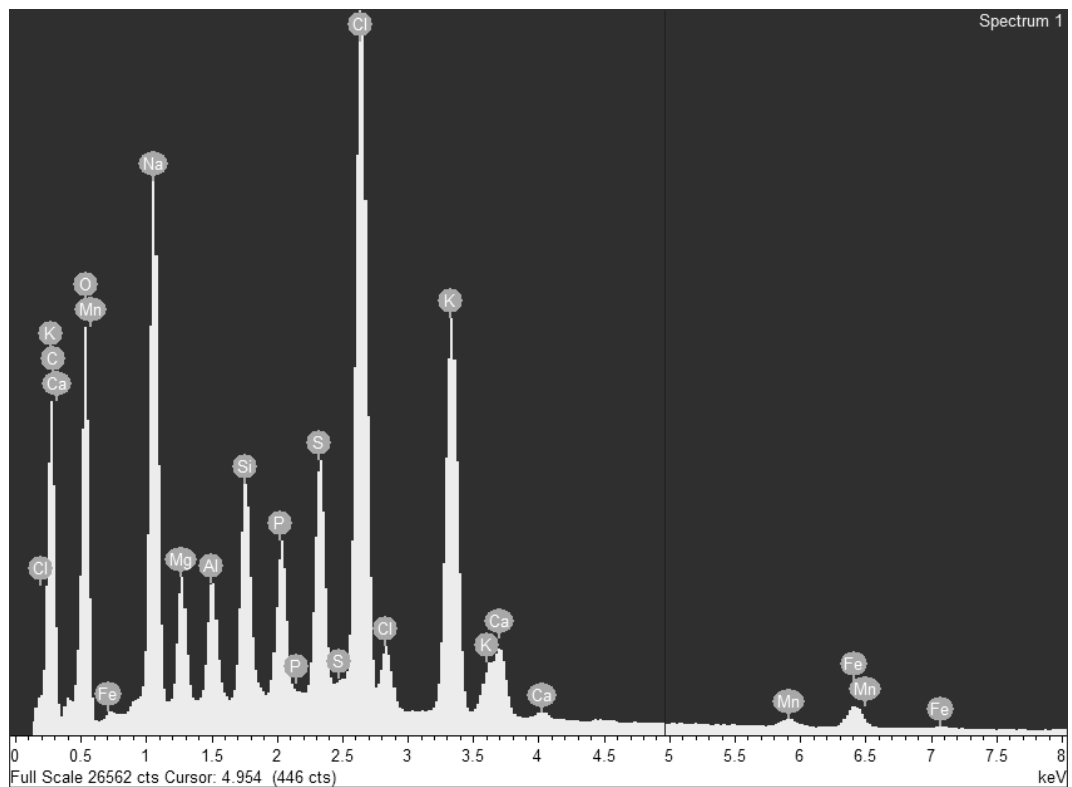


Figure 5.54: Blank *P. palmata* 16 °C.

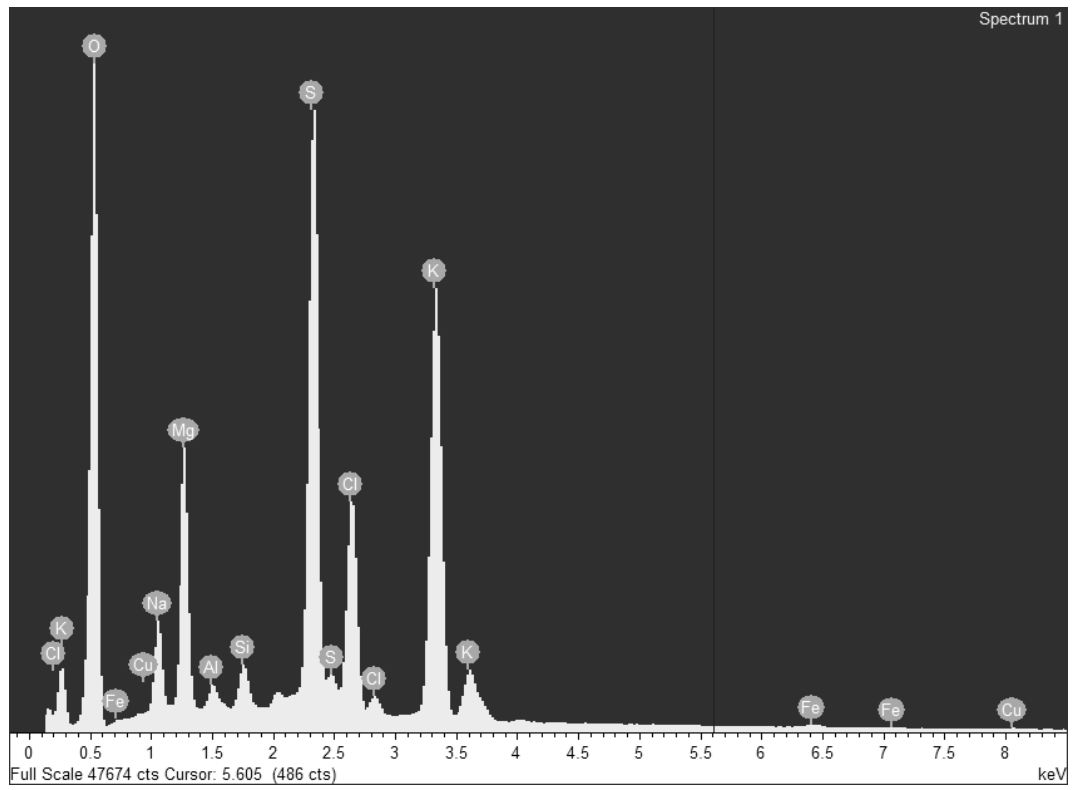
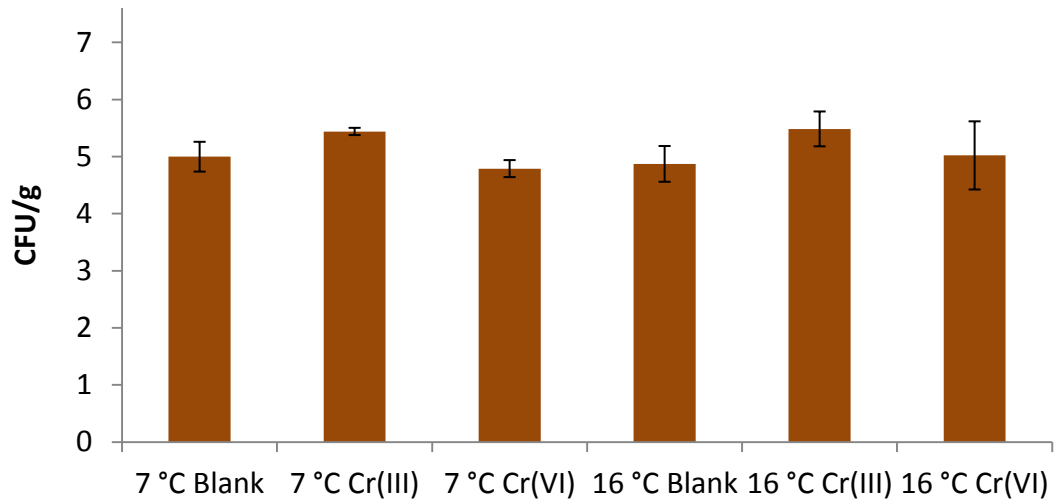


Figure 5.55: Blank *U. lactuca* 16 °C.



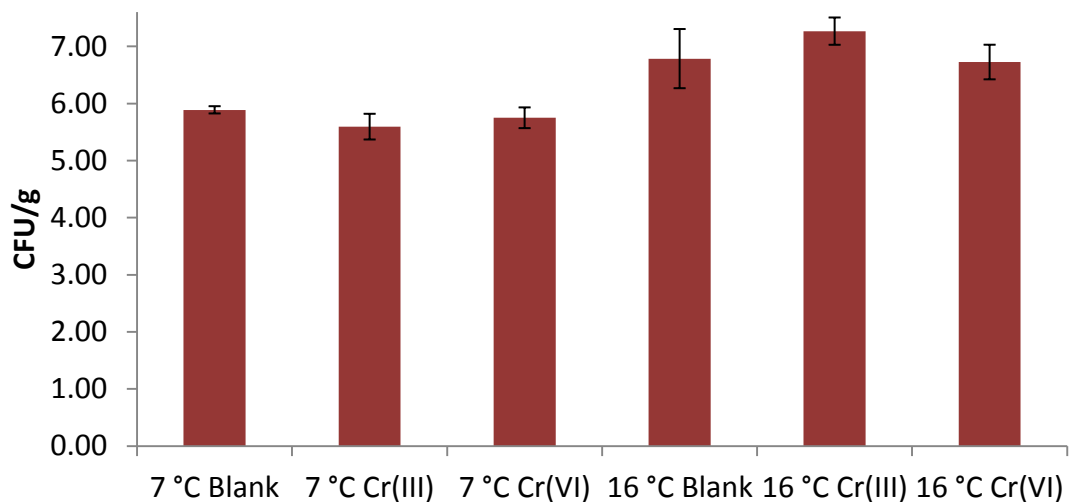
### 5.3.6 Total Viable Counts

As *U. lactuca* appeared to show a break up and reduction in surface biofilm (see Section 5.3.2), total viable counts were carried out to determine the quantity of culturable bacteria on the seaweeds surface before and after metal exposure. The results are shown in Figure 5.56-558.



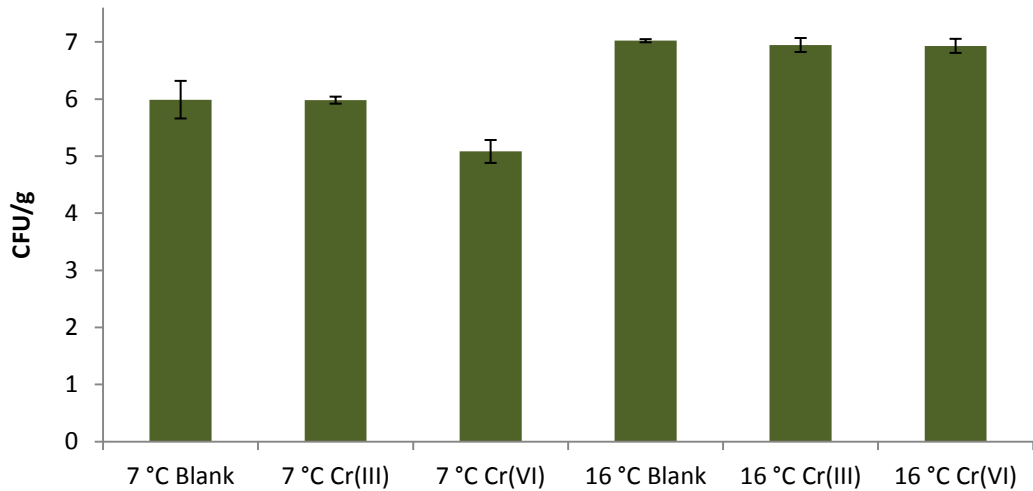
**Figure 5.56: Total viable count of bacteria present on the surface of *F. vesiculosus* quoted as log<sub>10</sub> (n=3). Error bars show confidence intervals.**

There were no apparent differences between any of the conditions studied for *F. vesiculosus*.



**Figure 5.57: Total viable count of bacteria present on the surface of *P. palmata* quoted as log<sub>10</sub> (n=3). Error bars show confidence intervals.**

There appeared to be a greater quantity of bacteria present from samples taken at 16 °C. However, Cr treatment did not appear to induce any change in bacterial numbers.



**Figure 5.58: Total viable count of bacteria present on the surface of *U. lactuca* quoted as  $\log_{10}$  (n=3). Error bars show confidence intervals.**

Similar to *P. palmata*, *U. lactuca* appeared to have a greater quantity of bacteria present at 16 °C. However, Cr treatment did not induce any change in bacterial numbers. Gregory (2009) attempted to discover the influence of the quantity of bacteria in solution on metal uptake (Cd and Se) in *U. lactuca*, but was unable to discover any trends because of experimental difficulties (lack of significant differences in bacterial numbers between control and test experiments) (Gregory 2009).

Considering the microscopy work in Section 5.3.4 also showed no or very little changes visually on the surface of the seaweed, this result is not surprising. However, others have found ultrastructural changes on metal binding.

Scanning electron microscopy and X-ray microanalysis was used to study surface binding of Cu and Fe in *Ascophyllum nodosum*. About 18 % of the total Cu was found in the surface cells, and the Fe was found on diatoms on the seaweed surface. These cells were found to undergo increased shedding during the experimental period. This showed the effect that epiphytism may have on metal binding in seaweeds, and the

surface changes (e.g. shedding) which may be induced by metal accumulation (Stengel & Dring 2000). The red seaweed *Audouinella saviana*, was exposed to Cd, and ultrastructural changes in the cross sections of cells were examined by TEM. The cell wall was found to thicken and become smoother after 10-15 days exposure at concentrations of 600-1000  $\mu\text{M}$  Cd. Increased ribosomes and golgi structures were also seen in the metal treated samples. The author suggested that the thickened cell walls, caused by newly formed polysaccharides and proteins, were part of the seaweeds response mechanism to Cd stress (Talarico 2002).

It is therefore reasonable to assume that some level of metal exposure does induce changes on the seaweed's surface. It would be beneficial to repeat experiments, using (for example) longer exposure times, and higher metal exposure concentrations.

#### **5.4 Conclusions**

Based on the information gathered in the preliminary time course experiment using *U. lactuca*, it was concluded that there was a biofilm on the surface of the seaweed. This biofilm was affected to a large extent by heavy metal binding, resulting in an apparent visual decrease in the number of microorganisms on the surface and the breakup of the EPS layer they produce. This EPS layer is composed mainly of polysaccharides with some proteins, which means that it can contribute suitable functional groups for metal binding in addition to the functional groups present on the surface of the seaweed. The uptake of metals by biofilms has not been taken into account in the literature when describing biosorption by dead seaweed. It has been shown here that there is a significant effect on the seaweed surface. Therefore the contribution of the biofilm to metal accumulation by seaweeds needs to be studied in greater detail.

Cleaning the seaweed with a 10 % solution of ethanol in seawater effectively removes the biofilm but may also remove the extracellular matrix polysaccharides of the seaweed. This makes it difficult to study the effect of metal binding on the live seaweed surface as it may be modified by this method of cleaning.

The AFM and SEM images showed excellent reproducibility across the two techniques. AFM was used to take several sets of surface measurements for surface

area ( $\mu\text{m}^2$ ) and roughness mean squared (RMS) (nm), and this data was used to determine if the visual smoothing resulted in any differences between time points of exposure. No statistically significant differences were found. More work, obtaining greater scan numbers, would enable more confidence in these results. However, between species variation in both surface area and RMS was also low, suggesting that these techniques may not be useful for indicating changes due to metal binding.

The experiments were extended to include *F. vesiculosus* and *P. palmata* (as well as *U. lactuca*) at a greater number of experimental conditions (7 °C, 16°C, Cr(III), Cr(VI), winter and summer samples). The samples were analysed by SEM, AFM, EDX and total viable counts were carried out. Unfortunately, no significant changes were found on the seaweed surface by any of these analysis techniques. There are likely to be three reasons for this.

- Firstly, there was no difference in ultrastructure shown by SEM and AFM images. This was likely to be because the metal concentration were not high enough to induce a change in the seaweed.
- Secondly, chromium binding was not seen on EDX analysis. EDX analysis was shown to be unable to detect Cr at the levels seen in this work. This supports the finding of Chapter 4, as binding was shown to be intra rather than intercellular. However, it was possible that the levels were below the limit of detection of this technique.
- Thirdly, as there was no ultrastructural changes shown by AFM or SEM, it makes sense that there would not be viable count changes between the different treatments.

Considering that changes on metal binding have been shown in the literature, it is reasonable to assume that changes do occur after a certain time, or when a certain metal concentration is reached. It is important to understand these changes, as they will help determine the mechanism whereby these seaweeds take up metal. In order to study Cr accumulation by these methods, this author would suggest repeating experiments, using longer exposure times, and higher metal exposure concentrations.

# Chapter 6: Conclusions and Future Work

## 6.1 Conclusions

It is well known that Cr(VI) is more toxic as it is less stable than Cr(III) and will be reduced to Cr(III) in natural environments. This reduction is coupled with oxidation which occurs in or on the cell, leading to oxidative stress. Many environmental regulations are based on this knowledge, with Cr(VI) inputs to the environment considered much more serious than Cr(III) inputs. However, this thesis has shown that Cr(III) has much more affinity for the algal cell, and is taken up in greater amounts. Therefore Cr(III), although less damaging to the cell, is more likely to be taken up in greater amounts. This has consequences for both environmental and food regulation.

A recent article has shown the toxicity of Cr(VI) versus Cr(III) in *Drosophila melanogaster*, an organism that was used as a model for neurotoxicity. Reduced neuronal cell numbers, reduced locomotor activity, and increased oxidative stress markers were observed (Singh & Chowdhuri 2016). However, there is also a question over the toxicity of Cr(III) versus Cr(VI) in algae (Vignati *et al.* 2010; Kováčik *et al.* 2015). Vignati (2010) looked at cell death in the freshwater algae *Pseudokirchneriella subcapitata* and *Chlorella kessleri*, and found that Cr(III) was more toxic (Vignati *et al.* 2010). Kováčik found increased ROS production on Cr(III) exposure, but decreased viability, chlorophyll and mitochondrial proteins on Cr(VI) exposure for the freshwater green alga *Scenedesmus quadricauda* (Kováčik *et al.* 2015). As seaweed becomes more and more popular as a healthy food, knowledge of metal uptake behaviour, and its possible consequences for human health is very important. Both Cr(III) and Cr(VI) uptake needs to be defined and safe levels in seawater defined. The greater toxicity of Cr(VI) needs to be balanced against the greater uptake of Cr(III) shown in this thesis.

The seaweeds (*F. vesiculosus*, *P. palmata* and *U. lactuca*) were characterised by ICP-OES, Kjeldahl, and FTIR. Combining the analysis allowed the functional groups present in the seaweed which can affect metal binding to be identified. Sulphate, carboxylate, amide, and phosphorus containing groups, arising from proteins and carbohydrates were found. Seasonal differences were identified. Higher P and protein was found in Feb/Mar than in May/Jun. Inter-species differences were also observed. *U. lactuca* contained the highest amount of S, followed by *F. vesiculosus* and then *P. palmata*. Both *U. lactuca* and *P. palmata* had similarly high levels of protein in

Feb/Mar, with *F. vesiculosus* being lower. They all had similar levels of protein in May/Jun, with *U. lactuca* and *P. palmata* protein content dropping significantly, and *F. vesiculosus* staying the same.

A biomonitoring study was carried out on *F. vesiculosus* and *A. nodosum* sampled in Ireland and Newfoundland. They both proved to be suitable biomonitor species for the areas. They were readily available at most sites and biomagnified the metals to levels which could be detected by ICP-OES. They also reflected the levels of pollution which were likely to be present, as determined by probable anthropogenic inputs in the areas from available site knowledge.

In general the following trends were observed for Cr uptake:

- *U. lactuca* > *P. palmata* > *F. vesiculosus*
- Cr(III) > Cr(VI)
- 16 °C > 7 °C
- Feb/Mar > May/Jun
- Intracellular uptake ~ 100%

The evidence from this thesis suggests the following reasons for these trends.

- Compositional changes, between seaweeds and between seasons.  
For example, in this work, *F. vesiculosus* was shown to have a greater metal uptake and greater P content during Feb/Mar. P is used in the cell membrane and greater quantities may facilitate intracellular diffusion of Cr<sup>3+</sup>. This has not been shown in the literature and, needs further work. *P. palmata* and *U. lactuca* were shown to have seasonal highs in N content in Feb/Mar. This may be enhancing their ability to bind Cr<sup>3+</sup> and CrO<sub>4</sub><sup>2-</sup> in Feb/Mar through protein containing ligands such as cysteine and glutathione.
- Physical differences in conditions, i.e. temperature.  
At higher temperatures, intracellular uptake could be increased because of greater cell membrane fluidity, increased metabolism and increased protein synthesis (Fritioff *et al.* 2005). Temperature may affect ease of movement into the cell. At higher temperatures, cell membranes tend to allow easier access for substances to pass through. Cell membranes are composed of fatty acid chains which behave as

solids at lower temperatures. As the temperature increases, they become liquid and the spaces between chains increase in size (Metzler 1997).

- The difference between Cr(III) and Cr(VI) needs more work to determine the mechanisms involved.

The literature suggests that Cr(VI) is more bioavailable and toxic in general (Cornelis *et al.* 2005). This was shown not to be the case as regards bioavailability for the species studied here. Future work on toxicity in seaweeds would clarify the effects of Cr(III) vs. Cr(VI). Work on freshwater algae has shown that Cr(VI) is not necessarily more toxic than Cr(III) (Vignati *et al.* 2010; Singh & Chowdhuri 2016).

AFM work showed a biofilm present on the surface of *U. lactuca*, which could be removed by ethanol washing. A time course study on Cr(III) binding showed that the biofilm was disrupted as metal exposure continued. There was excellent reproducibility found between AFM and SEM images. Further experiments using different conditions did not show the same changes, suggesting that it is important to use a high enough metal concentration at the exposure stage to induce changes.



## 6.2 Future Work

### 6.2.1 Experimental Conditions

As most bioaccumulation studies have used longer exposure times than used here, it would be interesting to use longer exposure times (upwards of 24 h). This would allow greater comparison with the literature. It would be beneficial to use artificial seawater culture medium, rather than natural filtered seawater, so that Cr speciation can be modelled (Ramesh *et al.* 2015; Varma *et al.* 2013).

Repeating microscopy and total viable counts with seaweeds which have had a greater exposure period may make any effects seen more pronounced, and using artificial seawater as culture medium, which can be sterilized, would reduce variation, and allow significant differences in biofilms to be seen.

As seen in the thesis, the seaweed and biofilm co-exist and both contribute to metal uptake. To understand this fully, it is necessary to separate the effect. It may be possible that a seaweed cultivated in the lab in a medium spiked with bacteria to promote biofilm growth could be studied in the future to assess the effect of biofilm coverage when the seaweed is exposed to metal.

### 6.2.2 Determine the toxicity of Cr

Given that the seaweed was shown to accumulate more Cr(III) than Cr(VI) it is important to determine the toxicity of Cr(III) vs. Cr(VI). This could be carried out by several methods.

- Analyse growth rates (Costa, de Felix, *et al.* 2016; Connan & Stengel 2011a)
- Determine the level of oxidative stress. This can be done by quantifying oxidative stress biomarkers (Jarvis & Bielmyer-Fraser 2015; Ramesh *et al.* 2015; Babu *et al.* 2014) and DNA damage (Babu *et al.* 2014)
- Quantify chlorophyll pigments (Costa, de Felix, *et al.* 2016) and level of photosynthesis (Jarvis & Bielmyer-Fraser 2015; Connan & Stengel 2011a).
- Quantify the level of phenolics (Connan & Stengel 2011b; Costa, de Felix, *et al.* 2016).

**6.2.3 Studying the seaweed surface**

- It may be possible to separate biofilm from seaweed uptake by using seaweed cultivated in the lab in a medium spiked with bacteria to promote biofilm growth.
- Carry out initial exposure experiments at a range of Cr concentrations to determine what concentration is necessary to observe changes to the seaweed surface, either to the seaweed itself, or to the biofilm on the seaweed surface. Measure surface bacteria using total viable counts and AFM/SEM-EDX to visualise and quantify these changes.

# References

- Åberg, P., 1996. Patterns of reproductive effort in the brown alga *Ascophyllum nodosum*. *Marine Ecology Progress Series*, 138, pp.199–207.
- Agadi, V., Bhosle, N. & Untawale, A., 1978. Metal concentration in some seaweeds of Goa (India). *Botanica Marina*, 21(4), pp.247–250.
- Akcali, I. & Kucuksezgin, F., 2011. A biomonitoring study: Heavy metals in macroalgae from eastern Aegean coastal areas. *Marine pollution bulletin*, 62(3), pp.637–45.
- Algaebase, 2016. Algaebase. Available at: [www.algaebase.org](http://www.algaebase.org) [Accessed March 3, 2012].
- Almela, C., Algora, S., Benito, V., Clemente, M.J., Devesa, V., Súañer, M. a, Vélez, D. & Montoro, R., 2002. Heavy metal, total arsenic, and inorganic arsenic contents of algae food products. *Journal of Agricultural and Food Chemistry*, 50(4), pp.918–23.
- Almela, C., Clemente, M., Vélez, D. & Montoro, R., 2006. Total arsenic, inorganic arsenic, lead and cadmium contents in edible seaweed sold in Spain. *Food and Chemical Toxicology*, 44(11), pp.1901–8.
- Alvarado, L., Ramírez, a. & Rodríguez-Torres, I., 2009. Cr(VI) removal by continuous electrodeionization: Study of its basic technologies. *Desalination*, 249(1), pp.423–428.
- Amado Filho, G.M., Karez, C.S., Andrade, L., Yoneshigue-Valentin, Y. & Pfeiffer, W.C., 1997. Effects on growth and accumulation of zinc in six seaweed species. *Ecotoxicology and environmental safety*, 37(3), pp.223–8.
- Amer, H., Emons, H. & Ostapczuk, P., 1997. Application of multielement techniques for the fingerprinting of elemental contents in *Fucus vesiculosus* from the North Sea. *Chemosphere*, 34(9/10), pp.2123–2131.
- Amoroso, M.J., Castro, G.R., Durán, A., Peraud, O., Oliver, G. & Hill, R.T., 2001. Chromium accumulation by two *Streptomyces* spp. isolated from riverine sediments. *Journal of industrial microbiology & biotechnology*, 26(4), pp.210–5.
- De Andrade, L., 2002. Role of *Padina gymnospora* (Dictyotales, Phaeophyceae) cell walls in cadmium accumulation. *Phycologia*, 41(1).
- Apaydın, G., Aylıkçı, V., Cengiz, E., Saydam, M., Küp, N. & Tıraşoğlu, E., 2010. Analysis of Metal Contents of Seaweed (*Ulva lactuca*) from Istanbul, Turkey by EDXRF. *Turkish Journal of Fisheries and Aquatic Sciences*, 10, pp.215–220.
- Armas, M., Mederos, A., Gili, P., Dominguez, S., Hernandez-Molina, R., Lorenzo, P., Araujo, M., Brito, F., Otero, A. & Castellanos, M., 2004. Speciation in the chromium (III)-glutathione system. *Chemical Speciation and Bioavailability*, 16(1/2), pp.45–52.
- Atkins, P.W., 1996. *The Elements of Physical Chemistry*, Oxford University Press.
- Baas Becking, L., Kaplan, I. & Moore, D., 1960. Limits of the natural environment in terms of pH and oxidation-reduction potentials. *The Journal of Geology*, 68(3), pp.243–284.
- Babu, M.Y., Palanikumar, L., Nagarani, N., Devi, V.J., Kumar, S.R., Ramakritinan, C.M. & Kumaraguru, A.K., 2014. Cadmium and copper toxicity in three marine

- macroalgae: Evaluation of the biochemical responses and DNA damage. *Environmental Science and Pollution Research*, 21(16), pp.9604–9616.
- Baker, D. & Czarnecki-Maulden, G., 1987. Pharmacologic role of cysteine in ameliorating or exacerbating mineral toxicities. *Journal of Nutrition*, 117(6), pp.1003–1010.
- Bakir, A., McLoughlin, P. & Fitzgerald, E., 2010. Regeneration and Reuse of a Seaweed-Based Biosorbent in Single and Multi-Metal Systems. *CLEAN - Soil, Air, Water*, 38(3), pp.257–262.
- Bakir, A., McLoughlin, P., Tofail, S. & Fitzgerald, E., 2009. Competitive Sorption of Antimony with Zinc, Nickel, and Aluminum in a Seaweed Based Fixed-bed Sorption Column. *CLEAN - Soil, Air, Water*, 37(9), pp.712–719.
- Barnett, B.E. & Ashcroft, C.R., 1985. Heavy metals in *Fucus vesiculosus* in the Humber Estuary. *Environmental Pollution Series B, Chemical and Physical*, 9(3), pp.193–213.
- Barreiro, R., Picado, L. & Real, C., 2002. Biomonitoring heavy metals in estuaries: a field comparison of two brown algae species inhabiting upper estuarine reaches. *Environmental monitoring and assessment*, 75(2), pp.121–34.
- Barreto, M. & Meyer, J., 2007. The preservation of biofilms on macroalgae by osmium vapour. *South African Journal of Botany*, 73(1), pp.64–69.
- Baumann, H., Morrison, L. & Stengel, D., 2009. Metal accumulation and toxicity measured by PAM--chlorophyll fluorescence in seven species of marine macroalgae. *Ecotoxicology and environmental safety*, 72(4), pp.1063–75.
- Bender, M., Klinkhammer, G. & Spencer, D., 1977. Manganese in seawater and the marine manganese balance. *Deep Sea Research*.
- Berail, G., Prudent, P., Massiani, C. & Pellegrini, M., 1992. Isolation of heavy metal-binding proteins from a brown seaweed *Cystoseira barbata* f. *repens* cultivated in copper or cadmium enriched seawater. *Science and technology letters*, pp.55–62.
- Besada, V., Andrade, J.M., Schultze, F. & González, J.J., 2009. Heavy metals in edible seaweeds commercialised for human consumption. *Journal of Marine Systems*, 75(1–2), pp.305–313.
- Bird, P. & Comber, S., 1996. Zinc inputs to coastal waters from sacrificial anodes. *Science of the Total Environment*, 181(3), pp.257–264.
- Bixler, H.J. & Porse, H., 2011. A decade of change in the seaweed hydrocolloids industry. *Journal of Applied Phycology*, 23, pp.321–335.
- Black, W. & Mitchell, R., 1952. Trace elements in the common brown algae and in sea water. *Journal of the Marine Biological Association of the United Kingdom*, 30(3), pp.575–584.
- Blomster, J., Maggs, C.A. & Stanhope, M.J., 1998. Molecular and morphological analysis of *Enteromorpha intestinalis* and *E. compressa* (Chlorophyta) in the British Isles. *Journal of Phycology*, 34(0), pp.319–340.
- Bold, H.C. & Wynne, M.J., 1978. *Introduction to the Algae: Structure and Reproduction*, Prentice Hall, Inc.
- Boss, C.B. & Fredeen, K.J., 1997. *Concepts, Instrumentation and Techniques in Inductively Coupled Plasma Optical Emission Spectrometry* 2nd ed., Perkin-

- Elmer Corporation.
- Boullemant, A., Lavoie, M., Fortin, C. & Campbell, P.G.C., 2009. Uptake of hydrophobic metal complexes by three freshwater algae: unexpected influence of pH. *Environmental Science & Technology*, 43(9), pp.3308–14.
- Brady, D. & Duncan, J.R., 1994. Binding of heavy metals by the cell walls of *Saccharomyces cerevisiae*. *Enzyme and Microbial Technology*, 16(7), pp.633–638.
- Brauer, S., Hneihen, A., McBride, J. & Wetterhahn, K., 1996. Chromium (VI) forms thiolate complexes with  $\gamma$ -glutamylcysteine, N-acetylcysteine, cysteine, and the methyl ester of N-acetylcysteine. *Inorganic Chemistry*, 35, pp.373–381.
- Brauer, S. & Wetterhahn, K., 1991. Chromium (VI) forms a thiolate complex with glutathione. *Journal of the American Chemical Society*, 113, pp.3001–3007.
- Brinza, L., Nygård, C. a, Dring, M.J., Gavrilescu, M. & Benning, L.G., 2009. Cadmium tolerance and adsorption by the marine brown alga *Fucus vesiculosus* from the Irish Sea and the Bothnian Sea. *Bioresource technology*, 100(5), pp.1727–33.
- Bryan, G.W., 1983. Brown seaweed, *Fucus vesiculosus*, and the gastropod, *Littorina littoralis*, as indicators of trace-metal availability in estuaries. *Science of the Total Environment*, 21(1–3), pp.91–104.
- Bryan, G.W., 1969. The absorption of zinc and other metals by the brown seaweed *Laminaria digitata*. *Journal of the Marine Biological Association of the United Kingdom*, 49, pp.225–243.
- Bryan, G.W. & Hummerstone, L.G., 1973. Brown Seaweed as an Indicator of Heavy Metals in Estuaries in South-West England. *Journal of the Marine Biological Association of the United Kingdom*, 53, pp.705–720.
- Bryan, G.W. & Hummerstone, L.G., 1977. Indicators of heavy-metal contamination in the Looe Estuary (Cornwall) with particular regard to silver and lead. *Journal of the Marine Biological Association of the United Kingdom*, 57, pp.75–92.
- Bryan, G.W., Langston, W.J., Hummerstone, L.G., Burt, G.R. & Ho, Y.B., 1983. An assessment of the gastropod, *Littorina littorea*, as an indicator of heavy-metal contamination in United Kingdom estuaries. *Journal of the Marine Biological Association of the United Kingdom*, 63, pp.327–345.
- Burba, P. & Willmer, P., 1983. Cellulose: a biopolymeric sorbent for heavy-metal traces in waters. *Talanta*, 30(5), pp.381–383.
- Burdin, K.S. & Bird, K.T., 1994. Heavy metal accumulation by carrageenan and agar producing algae. *Botanica Marina*, 37(5), pp.467–470.
- Burdon-Jones, C., Denton, G.R.W., Jones, G.B. & McPhie, K.A., 1982. Regional and seasonal variations of trace metals in tropical Phaeophyceae from North Queensland. *Marine Environmental Research*, 7, pp.13–30.
- Burrows, E.M., 1991. *Seaweeds of the British Isles. Volume 2: Chlorophyta*, Natural History Museum.
- BV Sorbex, 2013. BV Sorbex Process. Available at: <http://www.bvsorbex.net/sxProcess.htm>.
- Byrne, G., Worden, R., Hodgson, D., Polya, D., Lythgoe, P., Barrie, C. & Boyce, A.,

2011. Understanding the fate of iron in a modern temperate estuary: Leirárvogur, Iceland. *Applied Geochemistry*, 26, pp.S16–S19.
- Cabrera, F., Clemente, L., Díaz Barrientos, E., López, R. & Murillo, J.M., 1999. Heavy metal pollution of soils affected by the Guadiamar toxic flood. *The Science of the Total Environment*, 242(1–3), pp.117–29.
- Calheiros, C.S.C., Rangel, A.O.S.S. & Castro, P.M.L., 2008. The effects of tannery wastewater on the development of different plant species and chromium accumulation in *Phragmites australis*. *Archives of Environmental Contamination and Toxicology*, 55(3), pp.404–14.
- Caliceti, M., Argese, E., Sfriso, a & Pavoni, B., 2002. Heavy metal contamination in the seaweeds of the Venice lagoon. *Chemosphere*, 47(4), pp.443–54.
- Cardoso, S.M., Pereira, O.R., Seca, A.M.L., Pinto, D.C.G.A. & Silva, A.M.S., 2015. Seaweeds as preventive agents for cardiovascular diseases: From nutrients to functional foods. *Marine Drugs*, 13(11), pp.6838–6865.
- Carral, E., Puente, X., Villares, R. & Carballeira, A., 1995. Background heavy metal levels in estuarine sediments and organisms in Galicia (northwest Spain) as determined by modal analysis. *Science of The Total Environment*, 172(2–3), pp.175–188.
- Cassab, G.I., 1998. Plant Cell Wall Proteins. *Annual review of plant physiology and plant molecular biology*, 49, pp.281–309.
- Cempel, M. & Nikel, G., 2006. Nickel: A review of its sources and environmental toxicology. *Polish Journal of Environmental Studies*, 15(3), pp.375–382.
- Cervantes, C., Campos-García, J., Devars, S., Gutiérrez-Corona, F., Loza-Tavera, H., Torres-Guzmán, J.C. & Moreno-Sánchez, R., 2001. Interactions of chromium with microorganisms and plants. *FEMS microbiology reviews*, 25(3), pp.335–47.
- Chakraborty, S., Bhattacharya, T., Singh, G. & Maity, J.P., 2014. Benthic macroalgae as biological indicators of heavy metal pollution in the marine environments: A biomonitoring approach for pollution assessment. *Ecotoxicology and Environmental Safety*, 100(1), pp.61–68.
- Chan, L.S., Ng, S.L., Davis, A.M., Yim, W.W.S. & Yeung, C.H., 2001. Magnetic Properties and Heavy-metal Contents of Contaminated Seabed Sediments of Penny 's Bay, Hong Kong. *Marine Pollution Bulletin*, 42(7), pp.569–583.
- Chan, S., Wang, W.-X. & Ni, I.-H., 2003. The uptake of Cd, Cr, and Zn by the macroalga *Enteromorpha crinita* and subsequent transfer to the marine herbivorous rabbitfish, *Siganus canaliculatus*. *Archives of environmental contamination and toxicology*, 44(3), pp.298–306.
- Chaudhuri, A., Mitra, M., Havrilla, C., Waguespack, Y. & Schwarz, J., 2007. Heavy metal biomonitoring by seaweeds on the Delmarva Peninsula, east coast of the USA. *Botanica Marina*, 50(3), pp.151–158.
- Chiu, J.M.Y., Thiyagarajan, V., Tsoi, M.M.Y. & Qian, P.Y., 2006. Qualitative and quantitative changes in marine biofilms as a function of temperature and salinity in summer and winter. *Biofilms*, 2(3), p.183.
- Clemens, S., 2006. Evolution and function of phytochelatin synthases. *Journal of Plant Physiology*, 163(3), pp.319–32.
- Clenaghan, C., O'Neill, M. & Page, D., 2006. *DANGEROUS SUBSTANCES*

- REGULATIONS NATIONAL IMPLEMENTATION REPORT, 2005,*
- Cobbett, C. & Goldsbrough, P., 2002. Phytochelatins and metallothioneins: roles in heavy metal detoxification and homeostasis. *Annual review of plant biology*, 53, pp.159–82.
- Collins, P. & Ferrier, R., 1996. *Monosaccharides: their chemistry and their roles in natural products*, John Wiley & Sons Ltd.
- Connan, S. & Stengel, D., 2011a. Impacts of ambient salinity and copper on brown algae: 1. Interactive effects on photosynthesis, growth, and copper accumulation. *Aquatic toxicology*, 104, pp.94–107.
- Connan, S. & Stengel, D., 2011b. Impacts of ambient salinity and copper on brown algae: 2. Interactive effects on phenolic pool and assessment of metal binding capacity of phlorotannin. *Aquatic Toxicology*, 104(1–2), pp.1–13.
- Contreras, L., Mella, D., Moenne, A. & Correa, J. a, 2009. Differential responses to copper-induced oxidative stress in the marine macroalgae *Lessonia nigrescens* and *Scytosiphon lomentaria* (Phaeophyceae). *Aquatic toxicology (Amsterdam, Netherlands)*, 94(2), pp.94–102.
- Cornelis, R., Caruso, J., Crews, H. & Heumann, K., 2005. *Handbook of Elemental Speciation II: Species in the Environment, Food, Medicine and Occupational Health*, John Wiley & Sons Ltd.
- da Costa, A., Mora Tavares, A. & da Franca, F., 2001. The release of light metals from a brown seaweed (*Sargassum* sp.) during zinc biosorption in a continuous system. *Electronic Journal of Biotechnology*, 4(3).
- Costa, G.B., de Felix, M.R.L., Simioni, C., Ramlov, F., Oliveira, E.R., Pereira, D.T., Maraschin, M., Chow, F., Horta, P.A., Lalau, C.M., da Costa, C.H., Matias, W.G., Bouzon, Z.L. & Schmidt, E.C., 2016. Effects of copper and lead exposure on the ecophysiology of the brown seaweed *Sargassum cymosum*. *Protoplasma*, 253(1), pp.111–125.
- Costa, G.B., Simioni, C., Pereira, D.T., Ramlov, F., Maraschin, M., Chow, F., Horta, P.A., Bouzon, Z.L. & Schmidt, E.C., 2016. The brown seaweed *Sargassum cymosum*: changes in metabolism and cellular organization after long-term exposure to cadmium. *Protoplasma*.
- Davis, T., Ramirez, M., Mucci, A. & Larsen, B., 2004. Extraction, isolation and cadmium binding of alginate from *Sargassum* spp. *Journal of Applied Phycology*, 16(4), pp.275–284.
- Davis, T., Volesky, B. & Mucci, A., 2003. A review of the biochemistry of heavy metal biosorption by brown algae. *Water Research*, 37(18), pp.4311–30.
- Davis, T., Volesky, B. & Vieira, R., 2000. *Sargassum* seaweed as biosorbent for heavy metals. *Water Research*, 34(17), pp.4270–4278.
- Dawczynski, C., Schubert, R. & Jahreis, G., 2007. Amino acids, fatty acids, and dietary fibre in edible seaweed products. *Food Chemistry*, 103(3), pp.891–899.
- Decho, A.W., 1999. Imaging an alginate polymer gel matrix using atomic force microscopy. *Carbohydrate Research*, 315(3–4), pp.330–333.
- Deniaud, E., Fleurence, J. & Lahaye, M., 2003. Interactions of the mix-linked  $\beta$ -(1,3)/ $\beta$ -(1,4)-d-xylans in the cell walls of *Palmaria palmata* (rhodophyta). *Journal of phycology*, 39(1), pp.74–82.



- Deniaud, E., Quemener, B., Fleurence, J. & Lahaye, M., 2003. Structural studies of the mix-linked  $\beta$ -(1 $\rightarrow$ 3)/ $\beta$ -(1 $\rightarrow$ 4)-d-xylans from the cell wall of *Palmaria palmata* (Rhodophyta). *International Journal of Biological Macromolecules*, 33(1–3), pp.9–18.
- Dohnalkova, a, Bilskis, C. & Kennedy, D., 2006. TEM Study of Manganese Biosorption by Cyanobacterium *Synechocystis* 6803. *Microscopy and Microanalysis*, 12(S02), p.444.
- Dong, D., Nelson, Y.M., Lion, L.W., Shuler, M.L. & Ghiorse, W.C., 2000. Adsorption of Pb and Cd onto metal oxides and organic material in natural surface coatings as determined by selective extractions: new evidence for the importance of Mn and Fe oxides. *Water Research*, 34(2), pp.427–436.
- Dring, M.J., 1992. *The Biology of Marine Plants*, Cambridge University Press.
- Dunne, W.M., 2002. Bacterial adhesion: seen any good biofilms lately? *Clinical Microbiology Reviews*, 15(2), pp.155–166.
- Egan, S., Harder, T., Burke, C., Steinberg, P., Kjelleberg, S. & Thomas, T., 2012. The seaweed holobiont: understanding seaweed-bacteria interactions. *FEMS Microbiology Reviews*, pp.1–15.
- Eisler, R., 2000. Chromium. In *Handbook of Chemical Risk Assessment: Health Hazards to Humans, Plants, and Animals*. CRC Press.
- Elicityl-Oligotech, 2012. Xylan Structure. Available at: [http://www.elicityl-oligotech.com/?fond=produit&id\\_produit=409&id\\_rubrique=23](http://www.elicityl-oligotech.com/?fond=produit&id_produit=409&id_rubrique=23) [Accessed November 23, 2012].
- Engel, D.W. & Fowler, B. a, 1979. Factors influencing cadmium accumulation and its toxicity to marine organisms. *Environmental health perspectives*, 28(February), pp.81–8.
- EPA, 2015. *Water Quality in Ireland 2010 - 2012* C. Byrne & A. Fanning, eds., EPA.
- Eslick, E., Beilby, M. & Moon, A., 2014. A study of the native cell wall structures of the marine alga *Ventricaria ventricosa* (Siphonocladales, Chlorophyceae) using atomic force microscopy. *Microscopy*, pp.131–140.
- European Commission, 2015. *The Water Framework Directive and the Floods Directive: Actions towards the “good status” of EU water and to reduce flood risks*,
- Faes, V.A. & Viejo, R.M., 2003. Structure and dynamics of a population of *Palmaria palmata* (rhodophyta) in northern Spain. *Journal of Phycology*, 39, pp.1038–1049.
- Fahim, N.F., Barsoum, B.N., Eid, A.E. & Khalil, M.S., 2006. Removal of chromium(III) from tannery wastewater using activated carbon from sugar industrial waste. *Journal of Hazardous Materials*, 136(2), pp.303–9.
- Le Faucheur, S., Schildknecht, F., Behra, R. & Sigg, L., 2006. Thiols in *Scenedesmus vacuolatus* upon exposure to metals and metalloids. *Aquatic Toxicology*, 80(4), pp.355–61.
- Favero, N. & Frigo, M., 2002. Biomonitoring of metal availability in the southern basin of the Lagoon of Venice (Italy) by means of macroalgae. *Water, Air, & Soil Pollution*, 140, pp.231–246.

- Feng, D. & Aldrich, C., 2004. Adsorption of heavy metals by biomaterials derived from the marine alga *Ecklonia maxima*. *Hydrometallurgy*, 73(1–2), pp.1–10.
- Ferris, F.G., Schultze, S., Witten, T.C., Fyfe, W.S. & Beveridge, T.J., 1989. Metal Interactions with Microbial Biofilms in Acidic and Neutral pH Environments. *Applied and environmental microbiology*, 55(5), pp.1249–57.
- Figueira, M., Volesky, B., Ciminelli, V. & Roddick, F., 2000. Biosorption of metals in brown seaweed biomass. *Water Research*, 34(1), pp.196–204.
- De Filippis, L. & Pallaghy, C., 1994. Heavy metals: sources and biological effects. In L. C. Rai, J. P. Gour, & C. J. Soeder, eds. *Advances in Limnology*. Stuttgart: Schweizerbatsche Verlagsbuchhandlung.
- Flemming, H., Griebe, T. & Schaule, G., 1996. Antifouling strategies in technical systems—a short review. *Water Science and Technology*, 34(5–6), pp.517–524.
- Fleurence, J., 1999. Seaweed proteins: biochemical, nutritional aspects and potential uses. *Trends in food science and technology*, 10, pp.26–29.
- Forsberg, Å., Söderlund, S., Frank, A., Petersson, L.R. & Pedersén, M., 1988. Studies on metal content in the brown seaweed, *Fucus vesiculosus*, from the Archipelago of Stockholm. *Environmental Pollution*, 49(4), p.1988.
- Foster, P., 1976. Concentrations and concentration factors of heavy metals in brown algae. *Environmental Pollution*, 10(1), pp.45–53.
- Fourest, E. & Volesky, B., 1997. Alginate properties and heavy metal biosorption by marine algae. *Applied Biochemistry And Biotechnology*, 67, pp.215–226.
- Fourest, E. & Volesky, B., 1996. Contribution of sulfonate groups and alginate to heavy metal biosorption by the dry biomass of *Sargassum fluitans*. *Environmental Science & Technology*, 30(1), pp.277–282.
- Fritioff, A., Kautsky, L. & Greger, M., 2005. Influence of temperature and salinity on heavy metal uptake by submersed plants. *Environmental pollution*, 133(2), pp.265–74.
- Fuge, R. & James, K., 1973. Trace metal concentrations in brown seaweeds, Cardigan Bay, Wales. *Marine Chemistry*, 1(4), pp.281–293.
- Funami, T., Hiroe, M., Noda, S., Asai, I., Ikeda, S. & Nishinari, K., 2007. Influence of molecular structure imaged with atomic force microscopy on the rheological behavior of carrageenan aqueous systems in the presence or absence of cations. *Food Hydrocolloids*, 21(4), pp.617–629.
- Gaete Olivares, H., Moyano Lagos, N., Jara Gutierrez, C., Carrasco Kittelsen, R., Lobos Valenzuela, G. & Hidalgo Lillo, M.E., 2016. Assessment oxidative stress biomarkers and metal bioaccumulation in macroalgae from coastal areas with mining activities in Chile. *Environmental Monitoring and Assessment*, 188(1), pp.1–11.
- Galland-Irmouli, A. V, Fleurence, J., Lamghari, R., Luçon, M., Rouxel, C., Barbaroux, O., Bronowicki, J.P., Villaume, C. & Guéant, J.L., 1999. Nutritional value of proteins from edible seaweed *Palmaria palmata* (dulse). *The Journal of Nutritional Biochemistry*, 10(6), pp.353–9.
- García-Ríos, V., Freile-Pelegrín, Y., Robledo, D., Mendoza-Cózatl, D., Moreno-Sánchez, R. & Gold-Bouchot, G., 2007. Cell wall composition affects Cd<sup>2+</sup> accumulation and intracellular thiol peptides in marine red algae. *Aquatic*

- toxicology (Amsterdam, Netherlands)*, 81(1), pp.65–72.
- Gaudenzi, S., Furfaro, M.G., Pozzi, D., Silvestri, I. & Congiu Castellano, A., 2003. Cell-metal interaction studied by cytotoxic and FT-IR spectroscopic methods. *Environmental toxicology and pharmacology*, 14(1–2), pp.51–9.
- Geertz-Hansen, O. & Sand-Jensen, K., 1992. Growth rates and photon yield of growth in natural populations of a marine macroalga *Ulva lactuca*. *Marine Ecology Progress Series*, 81, pp.179–183.
- Gibb, D.C., 1957. The Free-Living Forms of *Ascophyllum Nodosum* (L.) Le Jol. *The Journal of Ecology*, 45(1), pp.49–83.
- Giordano, S., Adamo, P., Spagnuolo, V., Tretiach, M. & Bargagli, R., 2013. Accumulation of airborne trace elements in mosses, lichens and synthetic materials exposed at urban monitoring stations: Towards a harmonisation of the moss-bag technique. *Chemosphere*, 90(2), pp.292–299.
- Giusti, L., 2001. Heavy metal contamination of brown seaweed and sediments from the UK coastline between the Wear river and the Tees river. *Environment International*, 26(4), pp.275–86.
- Gledhill, M., Brown, M.T., Nimmo, M., Moate, R. & Hill, S.J., 1998. Comparison of techniques for the removal of particulate material from seaweed tissue. *Marine Environmental Research*, 45(3), pp.295–307.
- Gledhill, M., Nimmo, M., Hill, S.J., Brown, M.T. & Bryan, K., 1999. The release of copper-complexing ligands by the brown alga *Fucus vesiculosus* (Phaeophyceae) in response to increasing total copper levels. *Journal of Phycology*, 35, pp.501–509.
- Godlewska-Zytkiewicz, B., 2006. Microorganisms in inorganic chemical analysis. *Analytical and bioanalytical chemistry*, 384(1), pp.114–23.
- Gómez-Ordóñez, E. & Rupérez, P., 2011. FTIR-ATR spectroscopy as a tool for polysaccharide identification in edible brown and red seaweeds. *Food Hydrocolloids*, 25(6), pp.1514–1520.
- Gouveia, C., Kreusch, M., Schmidt, E.C., Felix, M.R.D.L., Osorio, L.K.P., Pereira, D.T., Dos Santos, R., Ouriques, L.C., Martins, R.D.P., Latini, A., Ramlov, F., Carvalho, T.J.G., Chow, F., Maraschin, M. & Bouzon, Z.L., 2013. The Effects of Lead and Copper on the Cellular Architecture and Metabolism of the Red Alga *Gracilaria domingensis*. *Microscopy and microanalysis*, 19(3), pp.513–524.
- Graham, L.E. & Wilcox, L.W., 2000. *Algae*, Prentice Hall.
- Green, N., Bjerkgang, B., Hylland, K., Ruus, A. & Rygg, B., 2003. *Hazardous substances in the European marine environment: Trends in metals and persistent organic pollutants*, European Environment Agency.
- Gregory, C., 2009. *An Investigation of the Possible Influence of Microorganisms on the Uptake of Trace Metals by Ulva lactuca*. University of Wollongong.
- Gunning, A., Cairns, P., Kirby, A., Round, A., Bixler, H.J. & Morris, V., 1998. Characterising semi-refined iota-carrageenan networks by atomic force microscopy. *Carbohydrate Polymers*, 36(1), pp.67–72.
- Günzler, H. & Gremlich, H.-U., 2002. *IR Spectroscopy: An Introduction*, Wiley-VCH.
- Gustavo González, A. & Ángeles Herrador, M., 2007. A practical guide to analytical

- method validation, including measurement uncertainty and accuracy profiles. *Trends in Analytical Chemistry*, 26(3), pp.227–238.
- Gutknecht, J., 1963. Zn<sup>65</sup> Uptake by Benthic Marine Algae. *Limnology and Oceanography*, 8(1), pp.31–38.
- Hashim, M. & Chu, K.H., 2004. Biosorption of cadmium by brown, green, and red seaweeds. *Chemical Engineering Journal*, 97(2–3), pp.249–255.
- Haug, A., Melsom, S. & Omang, S., 1974. Estimation of heavy metal pollution in two Norwegian fjord areas by analysis of the brown alga *Ascophyllum nodosum*. *Environmental Pollution*, 7(3), pp.179–192.
- Hayden, H., Blomster, J., Maggs, C.A., Silva, P., Stanhope, M.J. & Waaland, J., 2003. Linnaeus was right all along: *Ulva* and *Enteromorpha* are not distinct genera. *European Journal of Phycology*, 38(3), pp.277–294.
- He, J. & Chen, J.P., 2014. A comprehensive review on biosorption of heavy metals by algal biomass: materials, performances, chemistry, and modeling simulation tools. *Bioresource technology*, 160, pp.67–78.
- Heaton, B.M.G., Prater, C.B. & Kjoller, K.J., 2004. Lateral and Chemical Force Microscopy: Mapping Surface Friction and Adhesion. *Veeco Application Notes*.
- Holdt, S.L. & Kraan, S., 2011. Bioactive compounds in seaweed: functional food applications and legislation. *Journal of Applied Phycology*, 23(3), pp.543–597.
- Holtkamp, A., 2009. *Isolation, Characterisation, Modification and Application of Fucoïdan from Fucus vesiculosus*. Universitätsbibliothek Braunschweig.
- Horta-Puga, G., Cházaro-Olvera, S., Winfield, I., Avila-Romero, M. & Moreno-Ramírez, M., 2013. Cadmium, copper and lead in macroalgae from the Veracruz Reef System, Gulf of Mexico: Spatial distribution and rainy season variability. *Marine Pollution Bulletin*, 68(1–2), pp.127–133.
- Howe, P., Malcolm, H. & Dobson, S., 2004. *Manganese and its compounds: Environmental Aspects*, WHO.
- Hu, S., Tang, C.-H. & Wu, M., 1996. Cadmium accumulation by several seaweeds. *Science of The Total Environment*, 187(2), pp.65–71.
- Huerta-Diaz, M.A., de León-Chavira, F., Lucila Lares, M., Chee-Barragán, A. & Siqueiros-Valencia, A., 2007. Iron, manganese and trace metal concentrations in seaweeds from the central west coast of the Gulf of California. *Applied Geochemistry*, 22(7), pp.1380–1392.
- Hurst, D., 2006. *Marine Foresight Series No. 5: Marine functional foods and functional ingredients*, Marine Institute.
- Ibáñez, J.P. & Umetsu, Y., 2004. Uptake of trivalent chromium from aqueous solutions using protonated dry alginate beads. *Hydrometallurgy*, 72(3–4), pp.327–334.
- Iwasaki, H., 1967. Nutritional studies of the edible seaweed *Porphyra tenera*. II. Nutrition of conchocelis. *Journal of Phycology*, 3(1), pp.30–34.
- Jalili, N., 2004. A review of atomic force microscopy imaging systems: application to molecular metrology and biological sciences. *Mechatronics*, 14(8), pp.907–945.
- Jarvis, T.A. & Bielmyer-Fraser, G.K., 2015. Accumulation and effects of metal mixtures in two seaweed species. *Comparative Biochemistry and Physiology*

- Part - C: Toxicology and Pharmacology*, 171, pp.28–33.
- Jayasekera, R. & Rossbach, M., 1996. Use of seaweeds for monitoring trace elements in coastal waters. *Environmental Geochemistry and Health*, 18(2), pp.63–68.
- Jensen, A., Rystad, B. & Melsom, S., 1974. Heavy metal tolerance of marine phytoplankton. I. The tolerance of three algal species to zinc in coastal sea water. *Journal of Experimental Marine Biology and Ecology*, 15(2), pp.145–157.
- Jensen, A., Rystad, B. & Melsom, S., 1976. Heavy metal tolerance of marine phytoplankton. II. Copper tolerance of three species in dialysis and batch cultures. *Journal of Experimental Marine Biology and Ecology*, 22(3), pp.249–256.
- Jiao, G., Yu, G., Zhang, J. & Ewart, H.S., 2011. Chemical structures and bioactivities of sulfated polysaccharides from marine algae. *Marine drugs*, 9(2), pp.196–223.
- Johansen, P., Hansen, M.M., Asmund, G. & Nielsen, B.P., 1991. Marine Organisms as Indicators of Heavy Metal Pollution-Experience from 16 Years of Monitoring at a Lead Zinc Mine in Greenland. *Chemistry and Ecology*, 5(1–2), pp.35–55.
- Johnston, E.L., Marzinelli, E.M., Wood, C. a, Speranza, D. & Bishop, J.D.D., 2011. Bearing the burden of boat harbours: heavy contaminant and fouling loads in a native habitat-forming alga. *Marine pollution bulletin*, 62(10), pp.2137–44.
- Kaim, W. & Schwederski, B., 1994. *Bioinorganic Chemistry: Inorganic Elements in the Chemistry of Life*, Chichester, UK: John Wiley & Sons Ltd.
- Kaimoussi, A., Chafik, A., Mouzdahir, A. & Bakkas, S., 2002. Diagnosis on the state of healthiness, quality of the coast and biological resources “case of the Moroccan Atlantic coast” (City of El Jadida). *Comptes Rendus Biologies*, 325(3), pp.253–60.
- Kamala-Kannan, S., Prabhu Dass Batvari, B., Lee, K.J., Kannan, N., Krishnamoorthy, R., Shanthi, K. & Jayaprakash, M., 2008. Assessment of heavy metals (Cd, Cr and Pb) in water, sediment and seaweed (*Ulva lactuca*) in the Pulicat Lake, South East India. *Chemosphere*, 71(7), pp.1233–40.
- Kapoor, A. & Viraraghavan, T., 1997. Heavy metal biosorption sites in *Aspergillus niger*. *Bioresource technology*, 61, pp.221–227.
- Karez, C.S., Magalhaes, V.F., Pfeiffer, W.C. & Amado Filho, G.M., 1994. Trace metal accumulation by algae in Sepetiba Bay, Brazil. *Environmental Pollution*, 83(3), pp.351–356.
- Kearns, J. & Turner, A., 2016. An evaluation of the toxicity and bioaccumulation of bismuth in the coastal environment using three species of macroalga. *Environmental Pollution*, 208, pp.435–441.
- Khaled, A., Hessein, A., Abdel-Halim, A.M. & Morsy, F.M., 2014. Distribution of heavy metals in seaweeds collected along marsa-matrouh beaches, Egyptian mediterranean sea. *Egyptian Journal of Aquatic Research*, 40(4), pp.363–371.
- Kim, J., Gibb, H. & Howe, P., 2006. *Concise International Chemical Assessment Document 69: Cobalt and Inorganic Cobalt Compounds*,
- Klein, D. & Goldberg, E., 1970. Mercury in the marine environment. *Environmental Science & Technology*, 4(9), pp.765–768.
- Kotaś, J. & Stasicka, Z., 2000. Chromium occurrence in the environment and methods

- of its speciation. *Environmental Pollution*, 107(3), pp.263–83.
- Kováčik, J., Babula, P., Hedbavny, J., Krystofova, O. & Provaznik, I., 2015. Physiology and methodology of chromium toxicity using alga *Scenedesmus quadricauda* as model object. *Chemosphere*, 120, pp.23–30.
- Kozelka, P.B. & Bruland, K.W., 1998. Chemical speciation of dissolved Cu, Zn, Cd, Pb in Narragansett Bay, Rhode island. *Marine Chemistry*, 60, pp.267–282.
- Kratochvil, D. & Volesky, B., 1998. Advances in the biosorption of heavy metals. *Trends in Biotechnology*, 16(July), pp.291–300.
- Ksheminska, H., Fedorovych, D., Babyak, L., Yanovych, D., Kaszycki, P. & Koloczek, H., 2005. Chromium(III) and (VI) tolerance and bioaccumulation in yeast: a survey of cellular chromium content in selected strains of representative genera. *Process Biochemistry*, 40(5), pp.1565–1572.
- Kumar, R. & Goyal, D., 2008. Comparative biosorption of Pb<sup>2+</sup> by live algal consortium and immobilized dead biomass from aqueous solution. *Indian Journal of Experimental Biology*, 47(8), pp.690–694.
- Lahaye, M., Alvarez-Cabal Cimadevilla, E., Kuhlenkamp, R., Quemener, B., Lognoné, V. & Dion, P., 1999. Chemical composition and <sup>13</sup>C NMR spectroscopic characterisation of ulvans from *Ulva* (Ulvales, Chlorophyta). *Journal of Applied Phycology*, 11(1), pp.1–7.
- Lahaye, M. & Robic, A., 2007. Structure and functional properties of ulvan, a polysaccharide from green seaweeds. *Biomacromolecules*, 8(6), pp.1765–74.
- Latasa, C., Solano, C., Penadés, J.R. & Lasa, I., 2006. Biofilm-associated proteins. *Comptes rendus biologiques*, 329(11), pp.849–57.
- Leal, D., Matsuhiro, B., Rossi, M. & Caruso, F., 2008. FT-IR spectra of alginic acid block fractions in three species of brown seaweeds. *Carbohydrate research*, 343(2), pp.308–16.
- Leal, M., Vasconcelos, M. & Van den Berg, C., 1999. Copper-induced release of complexing ligands similar to thiols by *Emiliana huxleyi* in seawater cultures. *Limnology and Oceanography*, 44(7), pp.1750–1762.
- Leal, M., Vasconcelos, M., Sousa-Pinto, I. & Cabral, J., 1997. Biomonitoring with benthic macroalgae and direct assay of heavy metals in seawater of the Oporto coast (Northwest Portugal). *Marine Pollution Bulletin*, 34(12), pp.1006–1015.
- Lee, H. & Volesky, B., 1997. Interaction of light metals and protons with seaweed biosorbent. *Water Research*, 31(12), pp.3082–3088.
- Lee, T.F. & Webster, W., 1986. *The Seaweed Handbook: An Illustrated Guide to Seaweeds from North Carolina to the Arctic*, Dover Publications.
- Lee, W.-Y. & Wang, W.-X., 2001. Metal accumulation in the green macroalga *Ulva fasciata*: effects of nitrate, ammonium and phosphate. *The Science of the Total Environment*, 278(1–3), pp.11–22.
- Liao, H., Ai, W., Zhang, K., Nakauma, M., Funami, T., Fang, Y., Nishinari, K., Draget, K.I. & Phillips, G.O., 2015. Mechanisms of oligoguluronate modulating the calcium-induced gelation of alginate. *Polymer (United Kingdom)*, 74, pp.166–175.
- Lindsay, D. & Von Holy, A., 2006. Bacterial biofilms within the clinical setting: what

- healthcare professionals should know. *The Journal of Hospital Infection*, 64(4), pp.313–25.
- Lobban, C.S. & Harrison, P.J., 1996. *Seaweed Ecology and Physiology*, Cambridge University Press.
- Lucey, J., 2007. *Water Quality in Ireland 2006: Key Indicators of the Aquatic Environment*, Environmental Protection Agency.
- Lucila Lares, M., Flores, M.G. & Lara-Lara, R., 2002. Temporal variability of bioavailable Cd, Hg, Zn, Mn and Al in an upwelling regime. *Environmental pollution (Barking, Essex : 1987)*, 120(3), pp.595–608.
- Luoma, S.N., Bryan, G.W. & Langston, W.J., 1982. Scavenging of heavy metals from particulates by brown seaweed. *Marine Pollution Bulletin*, 13(11), pp.394–396.
- Mages, M., Ovári, M., von Tümpling, W. & Kröpfl, K., 2004. Biofilms as bio-indicator for polluted waters? Total reflection X-ray fluorescence analysis of biofilms of the Tisza river (Hungary). *Analytical and bioanalytical chemistry*, 378(4), pp.1095–101.
- Malec, P., Maleva, M.G., Prasad, M.N. V & Strzałka, K., 2009. Identification and characterization of Cd-induced peptides in *Egeria densa* (water weed): Putative role in Cd detoxification. *Aquatic toxicology*, 95(3), pp.213–21.
- Marine Institute, 2010. *An Assessment of Dangerous Substances in Water Framework Directive Transitional and Coastal Waters: 2007 - 2009*,
- Martin, J., Guan, D., Elbaz-Poulichet, F., Thomas, A. & Gordeev, V., 1993. Preliminary assessment of the distributions of some trace elements (As, Cd, Cu, Fe, Ni, Pb and Zn) in a pristine aquatic environment: the Lena River estuary (Russia). *Marine Chemistry*, 43(1–4), pp.185–199.
- Martin, M., Nickless, G. & Stenner, R., 1997. Concentrations of cadmium, copper, lead, nickel and zinc in the alga *Fucus Serratus* in the severn estuary from 1971 to 1995. *Chemosphere*, 34(2), pp.325–334.
- Martinez, B. & Rico, J., 2002. Seasonal variation of P content and major N pools in *Palmaria palmata* (rhodophyta). *Journal of Phycology*, 1089(July 1999), pp.1082–1089.
- Maruyama, T., Matsushita, H., Shimada, Y., Kamata, I., Hanaki, M., Sonokawa, S., Kamiya, N. & Goto, M., 2007. Proteins and protein-rich biomass as environmentally friendly adsorbents selective for precious metal ions. *Environmental science & technology*, 41(4), pp.1359–64.
- Maschek, J.A. & Baker, B.J., 2008. The Chemistry of Algal Secondary Metabolism. In C. D. Amsler, ed. *Algal Chemical Ecology*. Berlin Heidelberg: Springer-Verlag.
- Matthiessen, P., Reed, J. & Johnson, M., 1999. Sources and Potential Effects of Copper and Zinc Concentrations in the Estuarine Waters of Essex and Suffolk, United Kingdom. *Marine Pollution Bulletin*, 38(10), pp.908–920.
- McHugh, D.J., 2003a. Introduction to Commercial Seaweeds. In *A Guide to the Seaweed Industry*. Food and Agriculture Organization of the UN.
- McHugh, D.J., 2003b. Seaweeds used as a source of alginate. In *A Guide to the Seaweed Industry*. Food and Agriculture Organization of the UN.

- McHugh, D.J., 2003c. Seaweeds used as a source of carrageenan. In *A Guide to the Seaweed Industry*. Food and Agriculture Organization of the UN.
- Mehta, S. & Gaur, J., 1999. Heavy-metal-induced proline accumulation and its role in ameliorating metal toxicity in *Chlorella vulgaris*. *New Phytologist*, 143(2), pp.253–259.
- Mehta, S.K. & Gaur, J.P., 1999. Heavy-metal-induced proline accumulation and its role in ameliorating metal toxicity in *Chlorella vulgaris*. *New Phytologist*, 143(2), pp.253–259.
- Meichik, N., Popova, N., Nikolaeva, Y., Yermakov, I. & Kamnev, A., 2011. Ion-exchange properties of cell walls of red seaweed *Phyllophora crispa*. *Applied Biochemistry and Microbiology*, 47(2), pp.176–181.
- Mel Lytle, C., Lytle, F.W., Yang, N., Qian, J.-H., Hansen, D., Zayed, A. & Terry, N., 1998. Reduction of Cr(VI) to Cr(III) by Wetland Plants: Potential for In Situ Heavy Metal Detoxification. *Environmental Science & Technology*, 32(20), pp.3087–3093.
- Melhuus, A., Seip, K., Seip, H. & Myklestad, S., 1978. A preliminary study of the use of benthic algae as biological indicators of heavy metal pollution in Sjøfjorden, Norway. *Environmental Pollution*, 15(2), pp.101–107.
- Met Eireann, 2016. Marine Observations. Available at: [http://www.met.ie/marine/marine\\_map.asp](http://www.met.ie/marine/marine_map.asp) [Accessed March 6, 2012].
- Metzler, D.E., 1997. *Biochemistry: The chemical reactions of living cells*, Academic Press, Inc.
- Miller, D., Mellman, I., Lamport, D. & Miller, M., 1974. The chemical composition of the cell wall of *Chlamydomonas gymnogama* and the concept of a plant cell wall protein. *The Journal of Cell Biology*, 63(2), p.420.
- Miramand, P. & Bentley, D., 1992. Heavy metal concentrations in two biological indicators ( *Patella vulgata* and *Fucus serratus*) collected near the French nuclear fuel reprocessing plant. *Science of the Total Environment*, 111(2–3), pp.135–149.
- Misheer, N., Kindness, a & Jonnalagadda, S.B., 2006. Elemental uptake by seaweed, *Plocamium corallorhiza* along the Kwazulu-natal coast of Indian Ocean, South Africa. *Journal of environmental science and health. Part. B, Pesticides, food contaminants, and agricultural wastes*, 41(6), pp.1037–48.
- Moenne, A., González, A. & Sáez, C.A., 2016. Mechanisms of metal tolerance in marine macroalgae, with emphasis on copper tolerance in Chlorophyta and Rhodophyta. *Aquatic Toxicology*, 176, pp.30–37.
- Molloy, F.J. & Hills, J.M., 1996. Long-term changes in heavy metal loadings of *Ascophyllum nodosum* from the Firth of Clyde, UK. *Hydrobiologia*, 326–327(1), pp.305–310.
- Morris, A. & Bale, A., 1975. The accumulation of cadmium, copper, manganese and zinc by *Fucus vesiculosus* in the Bristol Channel. *Estuarine and Coastal Marine Science*, 3(2), pp.153–163.
- Morrison, L., Baumann, H. & Stengel, D., 2008. An assessment of metal contamination along the Irish coast using the seaweed *Ascophyllum nodosum* (Fucales, Phaeophyceae). *Environmental Pollution*, 152(2), pp.293–303.
- Munda, I., 1984. Salinity dependent accumulation of Zn, Co and Mn in *Scytosiphon*



- lomentaria (Lyngb.) Link and Enteromorpha intestinalis (L.) Link from the Adriatic Sea. *Botanica marina*, 27, pp.371–376.
- Munda, I., 1979. Temperature Dependence of Zinc Uptake in *Fucus virsoides* (Don.) J. Ag. and *Enteromorpha prolifera* (O. F. Müll.) J. Ag. from the Adriatic Sea. *Botanica Marina*, 22(3), pp.149–152.
- Munda, I. & Hudnik, V., 1988. The Effects of Zn, Mn, and Co Accumulation on Growth and Chemical Composition of *Fucus vesiculosus* L under Different Temperature and Salinity Conditions. *Marine Ecology*, 9(3), pp.213–225.
- Murphy, V., 2007. *An Investigation into the Mechanisms of Heavy Metal Binding by Selected Seaweed Species*. Waterford Institute of Technology.
- Murphy, V., Hughes, H. & McLoughlin, P., 2008. Comparative study of chromium biosorption by red, green and brown seaweed biomass. *Chemosphere*, 70(6), pp.1128–34.
- Murphy, V., Hughes, H. & McLoughlin, P., 2007. Cu(II) binding by dried biomass of red, green and brown macroalgae. *Water research*, 41(4), pp.731–40.
- Murphy, V., Hughes, H. & McLoughlin, P., 2009. Enhancement strategies for Cu(II), Cr(III) and Cr(VI) remediation by a variety of seaweed species. *Journal of Hazardous Materials*, 166(1), pp.318–26.
- Murphy, V., Tofail, S., Hughes, H. & McLoughlin, P., 2009. A novel study of hexavalent chromium detoxification by selected seaweed species using SEM-EDX and XPS analysis. *Chemical Engineering Journal*, 148(2–3), pp.425–433.
- Murugadas, T.L., 1995. *Bioaccumulation and Toxicity Studies of Heavy Metals in Selected Malaysian Seaweeds*. University of Malaya.
- Naja, G., Deneux-Mustin, S., Mustin, C., Rouiller, J., Munier-Lamy, C. & Bertherlin, J., 1999. Potentiometric titration: a dynamic method to study the metal binding-mechanism of microbial biomass. *Process Metallurgy*, 9, pp.201–210.
- Naja, G., Mustin, C., Volesky, B. & Berthelin, J., 2005. A high-resolution titrator: a new approach to studying binding sites of microbial biosorbents. *Water research*, 39(4), pp.579–88.
- Nakamoto, K., 1997. *Infrared and Raman Spectra of Inorganic and Coordination Compounds. Part B: Application in Coordination, Organometallic and Bioorganic Chemistry*, Wiley-Blackwell.
- Nancharaiah, Y. V., Dodge, C., Venugopalan, V.P., Narasimhan, S. V & Francis, a J., 2010. Immobilization of Cr(VI) and its reduction to Cr(III) phosphate by granular biofilms comprising a mixture of microbes. *Applied and environmental microbiology*, 76(8), pp.2433–8.
- Nassar, C.A.G., Salgado, L.T., Yoneshigue-Valentin, Y. & Amado Filho, G.M., 2003. The effect of iron-ore particles on the metal content of the brown alga *Padina gymnospora* (Espírito Santo Bay, Brazil). *Environmental Pollution*, 123(2), pp.301–305.
- National Oceanographic Data Center, 2012. Sea surface temperature. Available at: <http://www.nodc.noaa.gov/cgi-bin/OC5/WOA09F/woa09f.pl>.
- Nielsen, S.S., 2010. Protein Analysis. In *Food Analysis*. Springer, p. 550.
- NL Department of Environment and Conservation, 2013. Pulp and Paper Mills.

- Available at: [http://www.env.gov.nl.ca/env/env\\_protection/ics/pulp.html](http://www.env.gov.nl.ca/env/env_protection/ics/pulp.html).
- O'Connell, D.W., Birkinshaw, C. & O'Dwyer, T.F., 2008. Heavy metal adsorbents prepared from the modification of cellulose: a review. *Bioresource Technology*, 99(15), pp.6709–24.
- O'Leary, C. & Breen, J., 1997. Metal levels in seven species of mollusc and in seaweeds from the Shannon estuary. *Biology and Environment: Proceedings of the Royal Irish Academy*, 97B(2), pp.121–132.
- Ostapczuk, P., Burow, M., May, K., Mohl, C., Froning, M., Süßenbach, B., Waidmann, E. & Emons, H., 1997. Mussels and algae as bioindicators for long-term tendencies of element pollution in marine ecosystems. *Chemosphere*, 34(9/10), pp.2049–2058.
- Park, D., Lim, S.-R., Yun, Y.-S. & Park, J.M., 2007. Reliable evidences that the removal mechanism of hexavalent chromium by natural biomaterials is adsorption-coupled reduction. *Chemosphere*, 70(2), pp.298–305.
- Park, D., Yun, Y., Cho, H. & Park, J.M., 2004. Chromium biosorption by thermally treated biomass of the brown seaweed, *Ecklonia* sp. *Industrial & Engineering Chemistry*, 43, pp.8226–8232.
- Park, D., Yun, Y.-S. & Park, J.M., 2005. Studies on hexavalent chromium biosorption by chemically-treated biomass of *Ecklonia* sp. *Chemosphere*, 60(10), pp.1356–64.
- Paskins-Hurlburt, A., Skoryna, S., Tanaka, Y., Moore, W. & Stara, J., 1978. Fucoidan: Its binding of lead and other metals. *Botanica Marina*, 21(1).
- Patankar, M.S., Oehninger, S., Barnett, T., Williams, R.L. & Clark, G.F., 1993. A revised structure for fucoidan may explain some of its biological activities. *The Journal of biological chemistry*, 268(29), pp.21770–6.
- Pawlik-Skowrońska, B., Pirszel, J. & Brown, M.T., 2007. Concentrations of phytochelatin and glutathione found in natural assemblages of seaweeds depend on species and metal concentrations of the habitat. *Aquatic toxicology*, 83(3), pp.190–9.
- Pedersén, M., 1969. Marine Brown Algae Requiring Vitamin B12. *Physiologia Plantarum*, 22(5), pp.977–983.
- Perales-Vela, H.V., Peña-Castro, J.M. & Cañizares-Villanueva, R.O., 2006. Heavy metal detoxification in eukaryotic microalgae. *Chemosphere*, 64(1), pp.1–10.
- Pereira, L., Amado, A., Critchley, A., Van de Velde, F. & Ribeiro-Claro, P., 2009. Identification of selected seaweed polysaccharides (phycocolloids) by vibrational spectroscopy (FTIR-ATR and FT-Raman). *Food Hydrocolloids*, 23(7), pp.1903–1909.
- Persson, J.-Å., Wennerholm, M. & O'Halloran, S., 2008. *Handbook for Kjeldahl Digestion*, Foss.
- Phaneuf, D., Côté, I., Dumas, P., Ferron, L. a & LeBlanc, A., 1999. Evaluation of the contamination of marine algae (Seaweed) from the St. Lawrence River and likely to be consumed by humans. *Environmental Research*, 80(2 Pt 2), pp.S175–S182.
- Phelps, C., 1972. *Polysaccharides*, Oxford University Press.
- Pons, M.-N., Le Bonté, S. & Potier, O., 2004. Spectral analysis and fingerprinting for

- biomedia characterisation. *Journal of biotechnology*, 113(1–3), pp.211–30.
- Portlaw I.C.A., 2012. History of Portlaw. Available at:  
[http://homepage.eircom.net/~portlawns/Pages/history\\_of\\_portlaw.htm](http://homepage.eircom.net/~portlawns/Pages/history_of_portlaw.htm).
- Preston, A., Jeffries, D., Dutton, J., Harvey, B.R. & Steele, A.K., 1972. British Isles coastal waters: the concentrations of selected heavy metals in sea water, suspended matter and biological indicators—a pilot survey. *Environmental Pollution*, 3(1), pp.69–82.
- PubChem, 2012. PubChem Compound. Available at:  
<http://pubchem.ncbi.nlm.nih.gov/> [Accessed November 28, 2012].
- Punnett, T. & Derrenbacher, E.C., 1966. The amino acid composition of algal cell walls. *Journal of general microbiology*, 44(1), pp.105–14.
- Ragan, M. & Glombitza, K., 1986. Phlorotannins, brown algal polyphenols. *Progress in Phycological Research*, 4, pp.129–241.
- Rainbow, P.S., 1995. Biomonitoring of heavy metal availability in the marine environment. *Marine Pollution Bulletin*, 31(4–12), pp.183–192.
- Rainbow, P.S., Smith, B.D. & Lau, S.S.S., 2002. Biomonitoring of trace metal availabilities in the Thames estuary using a suite of littoral biomonitors. *Journal of the Marine Biological Association of the United Kingdom*, 82, pp.793–799.
- Ramesh, K., Berry, S. & Brown, M.T., 2015. Accumulation of silver by *Fucus* spp. (Phaeophyceae) and its toxicity to *Fucus ceranoides* under different salinity regimes. *Ecotoxicology*, 24(6), pp.1250–1258.
- Reeder, R.J., Schoonen, M. a. a. & Lanzirotti, a., 2006. Metal Speciation and Its Role in Bioaccessibility and Bioavailability. *Reviews in Mineralogy and Geochemistry*, 64(1), pp.59–113.
- Reis, P.A., Cassiano, J., Veiga, P., Rubal, M. & Sousa-Pinto, I., 2014. *Fucus spiralis* as monitoring tool of metal contamination in the northwest coast of Portugal under the European Water Framework Directives. *Environmental Monitoring and Assessment*, 186(9), pp.5447–5460.
- Rice, D.L. & Lapointe, B.E., 1981. Experimental outdoor studies with *ulva fasciata delile*. II. Trace metal chemistry. *Journal of Experimental Marine Biology and Ecology*, 54(1), pp.1–11.
- Riget, F., Johansen, P. & Asmund, G., 1997. Baseline levels and natural variability of elements in three seaweed species from West Greenland. *Marine Pollution Bulletin*, 34(3), pp.171–176.
- Riget, F., Johansen, P. & Asmund, G., 1995. Natural seasonal variation of cadmium, copper, lead and zinc in brown seaweed (*Fucus vesiculosus*). *Marine Pollution Bulletin*, 30(6), pp.409–413.
- Rioux, L.-E., Turgeon, S. & Beaulieu, M., 2007. Characterization of polysaccharides extracted from brown seaweeds. *Carbohydrate Polymers*, 69(3), pp.530–537.
- Robic, A., Bertrand, D., Sassi, J.-F., Lerat, Y. & Lahaye, M., 2008. Determination of the chemical composition of ulvan, a cell wall polysaccharide from *Ulva* spp. (Ulvales, Chlorophyta) by FT-IR and chemometrics. *Journal of Applied Phycology*, 21(4), pp.451–456.
- Robic, A., Gaillard, C., Sassi, J.-F., Lerat, Y. & Lahaye, M., 2009. Ultrastructure of

- ulvan: a polysaccharide from green seaweeds. *Biopolymers*, 91(8), pp.652–64.
- Rødde, R.S.H., Vårum, K.M., Larsen, B.A. & Myklestad, S.M., 2004. Seasonal and geographical variation in the chemical composition of the red alga *Palmaria palmata* (L.) Kuntze. *Botanica Marina*, 47(2), pp.125–133.
- Rodríguez-Bernaldo de Quirós, A., Lage-Yusty, M.A. & López-Hernández, J., 2010. Determination of phenolic compounds in macroalgae for human consumption. *Food Chemistry*, 121(2), pp.634–638.
- Rodríguez-Figueroa, G.M., Shumilin, E. & Sánchez-Rodríguez, I., 2009. Heavy metal pollution monitoring using the brown seaweed *Padina durvillaei* in the coastal zone of the Santa Rosalía mining region, Baja California Peninsula, Mexico. *Journal of Applied Phycology*, 21(1), pp.19–26.
- Romeril, M., 1977. Heavy metal accumulation in the vicinity of a desalination plant. *Marine Pollution Bulletin*, 8(4), pp.84–87.
- Romero-González, M., Williams, C., Gardiner, P., Gurman, S. & Habesh, S., 2003. Spectroscopic studies of the biosorption of gold(III) by dealginated seaweed waste. *Environmental science & technology*, 37(18), pp.4163–9.
- Rönnerberg, O., Adjers, K., Ruokolaihti, C. & Bondestam, M., 1990. *Fucus vesiculosus* as an Indicator of Heavy Metal Availability in a Fish Farm Recipient in the Northern Baltic Sea. *Marine Pollution Bulletin*, 21(8), pp.388–392.
- Rosell, K.-G. & Srivastava, L.M., 1985. Seasonal variations in total nitrogen, carbon and amino acids in *Macrocystis integrifolia* and *Nereocystis luetkeana* (Phaeophyta). *Journal of Phycology*, 21, pp.304–309.
- Ruelas-Inzunza, J.R. & Páez-Osuna, F., 2000. Comparative bioavailability of trace metals using three filter-feeder organisms in a subtropical coastal environment (Southeast Gulf of California). *Environmental Pollution*, 107(3), pp.437–44.
- Ryan, S., 2010. *An Investigation into the Biochemical Effects of Heavy Metal Exposure on Seaweeds*. Waterford Institute of Technology.
- Ryan, S., McLoughlin, P. & O'Donovan, O., 2012. A comprehensive study of metal distribution in three main classes of seaweed. *Environmental Pollution*, 167, pp.171–7.
- Sadiq, M., 1992. Basic concepts in marine chemistry. In *Toxic Metal Chemistry in Marine Environments*. Marcel Dekker, pp. 154–197.
- Sáez, C.A., Lobos, M.G., Macaya, E.C., Oliva, D., Quiroz, W. & Brown, M.T., 2012. Variation in Patterns of Metal Accumulation in Thallus Parts of *Lessonia trabeculata* (Laminariales; Phaeophyceae): Implications for Biomonitoring. *PloS one*, 7(11), p.e50170.
- Sáez, C.A., Roncarati, F., Moenne, A., Moody, A.J. & Brown, M.T., 2015. Copper-induced intra-specific oxidative damage and antioxidant responses in strains of the brown alga *Ectocarpus siliculosus* with different pollution histories. *Aquatic Toxicology*, 159, pp.81–89.
- Sanchez, J., Marino, N., Vaquero, M.C., Ansorena, J. & Legorburu, I., 1998. Metal pollution by old lead-zinc mines in Urumea River Valley (Basque country, Spain). Soil, biota and sediment. *Water, Air, and Soil Pollution*, 107, pp.303–319.
- Sánchez-Rodríguez, I., Huerta-Díaz, M.A., Choumiline, E., Holguín-Quiñones, O. &

- Zertuche-González, J. a, 2001. Elemental concentrations in different species of seaweeds from Loreto Bay, Baja California Sur, Mexico: implications for the geochemical control of metals in algal tissue. *Environmental Pollution*, 114(2), pp.145–60.
- Satarug, S., Baker, J., Urbenjapol, S., Haswell-Elkins, M., Reilly, P., Williams, D. & Moore, M., 2003. A global perspective on cadmium pollution and toxicity in non-occupationally exposed population. *Toxicology Letters*, 137(1–2), pp.65–83.
- Sawidis, T., Brown, M.T., Zachariadis, G. & Sratis, I., 2001. Trace metal concentrations in marine macroalgae from different biotopes in the Aegean Sea. *Environment International*, 27(1), pp.43–7.
- Schiavon, M., Moro, I., Pilon-Smits, E.A.H., Matozzo, V., Malagoli, M. & Dalla Vecchia, F., 2012. Accumulation of selenium in *Ulva* sp. and effects on morphology, ultrastructure and antioxidant enzymes and metabolites. *Aquatic Toxicology*, 122–123, pp.222–231.
- Schmidt, É.C., Marthiellen, M.R., Polo, L.K., Kreusch, M.G., Pereira, D.T., Costa, G.B., Simioni, C., de P. Martins, R., Latini, A., Chow, F., Ramlov, F., Pereira, A., Maraschin, M., Ouriques, L.C., Steiner, N. & Bouzon, Z.L., 2015. Influence of cadmium and salinity in the red alga *Pterocladia capillacea*: cell morphology, photosynthetic performance and antioxidant systems. *Revista Brasileira de Botanica*, 38(4), pp.737–749.
- Schoenwaelder, M.E.A., 2008. The biology of phenolic containing vesicles. *Algae*, 23(3), pp.163–175.
- Seeliger, U. & Edwards, P., 1977. Correlation coefficients and concentration factors of copper and lead in seawater and benthic algae. *Marine Pollution Bulletin*, 8(1), pp.16–19.
- Segel, I., 1976. *Biochemical calculations*, John Wiley & Sons Ltd.
- Semmler, T., Wang, S., McGrath, R. & Nolan, P., 2006. Regional climate ensemble simulations for Ireland: Impact of Climate Change on River Flooding. *National Hydrology Seminar 2006*.
- Serfor-Armah, Y., Nyarko, B., Osa, E., Carboo, D., Anim-Sampong, S. & Seku, F., 2001. Rhodophyta seaweed species as bioindicators for monitoring toxic element pollutants in the marine ecosystem of Ghana. *Water, Air, & Soil Pollution*, 127(1), pp.243–253.
- Serrano, J., Puupponen-Pimiä, R., Dauer, A., Aura, A.-M. & Saura-Calixto, F., 2009. Tannins: current knowledge of food sources, intake, bioavailability and biological effects. *Molecular nutrition & food research*, 53 Suppl 2, pp.S310-29.
- Sharp, G.J., Samant, H.S. & Vaidya, O.C., 1988. Selected metal levels of commercially valuable seaweeds adjacent to and distant from point sources of contamination in Nova Scotia and New Brunswick. *Bulletin of Environmental Contamination and Toxicology*, 40(5), pp.724–30.
- Sharp, W.E., 1995. *Distribution of Heavy Metals in the Brown Alga, Ascophyllum nodosum along the fjords of the Trondheim region, Norway*, Trondheim.
- Sheng, P.X., Ting, Y.-P., Chen, J.P. & Hong, L., 2004. Sorption of lead, copper, cadmium, zinc, and nickel by marine algal biomass: characterization of biosorptive capacity and investigation of mechanisms. *Journal of colloid and*

- interface science*, 275(1), pp.131–41.
- Sieburth, J. & Tootle, J.L., 1981. Seasonality of microbial fouling on *Ascophyllum nodosum* (L.) Lejol., *Fucus vesiculosus* L., *Polysiphonia lanosa* (L.) and *Chodrus crispus* Stakh. *Journal of Phycology*, 2(17), pp.57–64.
- Siegel, B. & Siegel, S., 1973. The chemical composition of algal cell walls. *CRC Critical Reviews in Microbiology*, 3(1), pp.1–26.
- Silver, G., 1991. Environmental plutonium: What is the redox potential of seawater? *Journal of radioanalytical and nuclear chemistry*, 155(3), pp.177–181.
- Singh, P. & Chowdhuri, D.K., 2016. Environmental Presence of Hexavalent but Not Trivalent Chromium Causes Neurotoxicity in Exposed *Drosophila melanogaster*. *Molecular Neurobiology*.
- Singh, R.P., Shukla, M.K., Mishra, A., Kumari, P., Reddy, C.R.K. & Jha, B., 2011. Isolation and characterization of exopolysaccharides from seaweed associated bacteria *Bacillus licheniformis*. *Carbohydrate Polymers*, 84(3), pp.1019–1026.
- Sirota, G. & Uthe, J., 1979. Heavy metal residues in dulse, an edible seaweed. *Aquaculture*, 18(1), pp.41–44.
- Skoog, D.A., Holler, F.J. & Crouch, S.R., 2007. *Principles of Instrumental Analysis*, Thomson Brooks/Cole.
- Smidsrød, O. & Draget, K., 1996. Chemistry and physical properties of alginates. *Carbohydrates in Europe*, 14, pp.6–13.
- Son, B.C., Park, K., Song, S.H. & Yoo, Y.J., 2004. Selective biosorption of mixed heavy metal ions using polysaccharides. *Korean Journal of Chemical Engineering*, 21(6), pp.1168–1172.
- Sondergaard, J., 2013. Dispersion and bioaccumulation of elements from an open-pit olivine mine in Southwest Greenland assessed using lichens, seaweeds, mussels and fish. *Environmental Monitoring and Assessment*, 185(8), pp.7025–7035.
- Spooner, G., 1949. Observations on the absorption of radioactive strontium and yttrium by marine algae. *Journal of the Marine Biological Association of the United Kingdom*, 28(3), pp.587–625.
- Steinberg, P. & De Nys, R., 2002. Chemical mediation of colonization of seaweed surfaces. *Journal of Phycology*, 38(4), pp.621–629.
- Stengel, D. & Dring, M.J., 2000. Copper and iron concentrations in *Ascophyllum nodosum* (Fucales, Phaeophyta) from different sites in Ireland and after culture experiments in relation to thallus age and epiphytism. *Journal of Experimental Marine Biology and Ecology*, 246(2), pp.145–161.
- Stengel, D., McGrath, H. & Morrison, L., 2005. Tissue Cu, Fe and Mn concentrations in different-aged and different functional thallus regions of three brown algae from western Ireland. *Estuarine, Coastal and Shelf Science*, 65(4), pp.687–696.
- Stengel, D.B. & Dring, M.J., 1997. Morphology and in situ growth rates of plants of *Ascophyllum nodosum* (Phaeophyta) from different shore levels and responses of plants to vertical transplantation. *European Journal of Phycology*, 32(2), pp.193–202.
- Stokes, P.M., 1983. Responses of freshwater algae to metals. In *Progress in Phycological Research*. pp. 87–112.

- Tako, M., Tamanaha, M., Tamashiro, Y. & Uechi, S., 2015. Structure of Ulvan Isolated from the Edible Green Seaweed, *Ulva pertusa*, (October), pp.645–655.
- Talarico, L., 2002. Fine structure and X-ray microanalysis of a red macrophyte cultured under cadmium stress. *Environmental pollution*, 120(3), pp.813–21.
- Tewari, B., 2002. Electrophoretic studies on the chelating tendency of bioactive sulphur-containing amino acids. The metal-methylcysteine-cysteine system. *Journal of Chromatography. A*, 962(1–2), pp.233–7.
- ThermoNicolet Corporation, 2001. *Introduction to Fourier Transform Infrared Spectrometry*,
- Tomlinson, D. & Wilson, J., 1980. Problems in the assessment of heavy-metal levels in estuaries and the formation of a pollution index. *Helgoländer Meeresuntersuchungen*, 33(1–4), pp.566–575.
- Toth, G. & Pavia, H., 2000. Lack of phlorotannin induction in the brown seaweed *Ascophyllum nodosum* in response to increased copper concentrations. *Marine Ecology Progress Series*, 192, pp.119–126.
- Tropin, I. & Zolotukhina, E.Y., 1994. The time course of heavy metal accumulation by brown and red macroalgae. *Russian Journal of Plant Physiology*, 41(2), pp.267–273.
- United Nations Economic Commission for Europe, 1998. *The 1998 Aarhus Protocol on Heavy Metals*,
- United Nations Economic Commission for Europe, 2012. [www.unece.org](http://www.unece.org). Available at: <http://www.unece.org/#>.
- US EPA, 1978. *Environmental Health Effects Research Series: Iron*, US Environmental Protection Agency.
- Usov, A.I., 2011. Polysaccharides of the red algae. In *Advances in Carbohydrate Chemistry and Biochemistry*. Elsevier, pp. 115–217.
- Usov, A.I., 1998. Structural analysis of red seaweed galactans of agar and carrageenan groups. *Food Hydrocolloids*, 12(3), pp.301–308.
- Vajpayee, P., Sharma, S., Tripathi, R., Rai, U. & Yunus, M., 1999. Bioaccumulation of chromium and toxicity to photosynthetic pigments, nitrate reductase activity and protein content of *Nelumbo nucifera gaertn.* *Chemosphere*, 39(12), pp.2159–2169.
- Vajpayee, P., Tripathi, R.D., Rai, U.N., Ali, M.B. & Singh, S.N., 2000. Chromium (VI) accumulation reduces chlorophyll biosynthesis, nitrate reductase activity and protein content in *Nymphaea alba* L. *Chemosphere*, 41(7), pp.1075–82.
- Vala, A.K., Anand, N., Bhatt, P.N. & Joshi, H. V, 2004. Tolerance and accumulation of hexavalent chromium by two seaweed associated aspergilli. *Marine pollution bulletin*, 48(9–10), pp.983–5.
- Varma, R., Turner, A. & Brown, M.T., 2011. Bioaccumulation of metals by *Fucus ceranoides* in estuaries of South West England. *Marine Pollution Bulletin*, 62(11), pp.2557–62.
- Varma, R., Turner, A., Brown, M.T. & Millward, G.E., 2013. Metal accumulation kinetics by the estuarine macroalga, *Fucus ceranoides*. *Estuarine, Coastal and Shelf Science*, 128, pp.33–40.

- Vasconcelos, M. & Leal, M., 2008. Exudates of different marine algae promote growth and mediate trace metal binding in *Phaeodactylum tricornutum*. *Marine Environmental Research*, 66(5), pp.499–507.
- Vasconcelos, M. & Leal, M., 2001. Seasonal variability in the kinetics of Cu, Pb, Cd and Hg accumulation by macroalgae. *Marine Chemistry*, 74(1), pp.65–85.
- Vasconcelos, M., Leal, M. & Van den Berg, C., 2002. Influence of the nature of the exudates released by different marine algae on the growth, trace metal uptake and exudation of *Emiliania huxleyi* in natural seawater. *Marine Chemistry*, 77(2–3), pp.187–210.
- Van de Velde, F., 2008. Structure and function of hybrid carrageenans. *Food Hydrocolloids*, 22(5), pp.727–734.
- Venugopal, V., 2008. *Marine Products for Healthcare: Functional and Bioactive Nutraceutical Compounds from the Ocean*, CRC Press.
- Viana, I.G., Aboal, J.R., Fernández, J. a, Real, C., Villares, R. & Carballeira, a, 2010. Use of macroalgae stored in an Environmental Specimen Bank for application of some European Framework Directives. *Water research*, 44(6), pp.1713–24.
- Vignati, D. a L., Dominik, J., Beye, M.L., Pettine, M. & Ferrari, B.J.D., 2010. Chromium(VI) is more toxic than chromium(III) to freshwater algae: A paradigm to revise? *Ecotoxicology and Environmental Safety*, 73(5), pp.743–9.
- Villares, R., Fernández-Lema, E. & López-Mosquera, E., 2013. Seasonal variations in concentrations of macro- and micronutrients in three species of brown seaweed. *Botanica Marina*, 56(1), pp.49–61.
- Villares, R., Puente, X. & Carballeira, A., 1999. Nitrogen and phosphorus in *Ulva* sp. in the Galician Rias Bajas (northwest Spain): seasonal fluctuations and influence on growth. *Boletín del Instituto Espanol de Oceanografía*, 15(1–4), pp.337–341.
- Volesky, B., 2007. Biosorption and me. *Water Research*, 41(18), pp.4017–29.
- Wahbeh, M.I., Mahasneh, D.M. & Mahasneh, I., 1985. Concentrations of zinc, manganese, copper, cadmium, magnesium and iron in ten species of algae and sea water from Aqaba, Jordan. *Marine Environmental Research*, 16(2), pp.95–102.
- Wahl, M., Goecke, F., Labes, A., Dobretsov, S. & Weinberger, F., 2012. The second skin: ecological role of epibiotic biofilms on marine organisms. *Frontiers in microbiology*, 3(August), p.292.
- Wallenstein, F.M., Torrão, D.F., Neto, A.I., Wilkinson, M. & Rodrigues, A.S., 2009. Effect of exposure time on the bioaccumulation of Cd, Mg, Mn and Zn in *Cystoseira abies-marina* samples subject to shallow water hydrothermal activity in São Miguel (Azores). *Marine Ecology*, 30, pp.118–122.
- Walsh, M. & Watson, L., 2011. *A Market Analysis towards the Further Development of Seaweed Aquaculture in Ireland*,
- Wang, W.-X., 2013. Personal Communication. , 306(2003).
- Wang, W.-X. & Dei, R., 2001. Influences of phosphate and silicate on Cr(VI) and Se(IV) accumulation in marine phytoplankton. *Aquatic toxicology*, 52(1), pp.39–47.
- Wang, W.-X. & Dei, R., 1999. Kinetic measurements of metal accumulation in two



- marine macroalgae. *Marine Biology*, 135(1), pp.11–23.
- Wang, Y.-T. & Shen, H., 1995. Bacterial reduction of hexavalent chromium. *Journal of industrial microbiology & biotechnology*, 14, pp.159–163.
- Waterford City Council, 2011. *Environmental Enforcement Plan*,
- WHO, 2001. *Environmental health criteria 221: Zinc*, Geneva.
- Williams, C. & Edyvean, R., 1997. Ion exchange in nickel biosorption by seaweed materials. *Biotechnology progress*, 13, pp.424–428.
- Williams, D. & Fleming, I., 1995. *Spectroscopic Methods in Organic Chemistry* 5th ed., McGraw-Hill Higher Education.
- Woolston, M., Breck, W. & VanLoon, G., 1982. A sampling study of the brown seaweed, *Ascophyllum nodosum* as a marine monitor for trace metals. *Water Research*, 16(5), pp.687–691.
- www.seaweed.ie, 2016. The Seaweed Site: Information on marine algae. Available at: [www.seaweed.ie](http://www.seaweed.ie).
- Xia, J.R., Li, Y.J., Lu, J. & Chen, B., 2004. Effects of copper and cadmium on growth, photosynthesis, and pigment content in *Gracilaria lemaneiformis*. *Bulletin of environmental contamination and toxicology*, 73(6), pp.979–86.
- Yoshie, Y., Wang, W., Petillo, D. & Suzuki, T., 2000. Distribution of catechins in Japanese seaweeds. *Fisheries Science*, 66, pp.998–1000.
- Yu, S., Blennow, A., Bojko, M., Madsen, F., Olsen, C.E. & Engelsen, S.B., 2002. Physico-chemical characterization of floridean starch of red algae. *Starch*, 54, pp.66–74.
- Yuan, Y., 2008. Marine Algal Constituents. In F. Shahid & C. Barrow, eds. *Marine Nutraceuticals and Functional Foods*. Boca Raton, FL: CRC Press.
- Yun, Y.S., Park, D., Park, J.M. & Volesky, B., 2001. Biosorption of trivalent chromium on the brown seaweed biomass. *Environmental science & technology*, 35(21), pp.4353–8.
- Zayed, A., Lytle, C.M., Qian, J.-H. & Terry, N., 1998. Chromium accumulation, translocation and chemical speciation in vegetable crops. *Planta*, 206(2), pp.293–299.
- Zhang, C., Qiao, Q., Piper, J.D. a & Huang, B., 2011. Assessment of heavy metal pollution from a Fe-smelting plant in urban river sediments using environmental magnetic and geochemical methods. *Environmental Pollution*, 159(10), pp.3057–70.
- Zhou, Q., Zhang, J., Fu, J., Shi, J. & Jiang, G., 2008. Biomonitoring: an appealing tool for assessment of metal pollution in the aquatic ecosystem. *Analytica chimica acta*, 606(2), pp.135–50.

# Appendix 1: Research Outputs

Murphy C, McLoughlin P, Hughes H, O' Donovan O (2009) 'The Effect of Temperature on the Bioaccumulation of Cr(VI) and Cr(III) by Live Seaweeds'. EPA Doctoral and Post-Doc Seminar 2009, The Gresham, Dublin November (12-13/11/2009).

Murphy C, McLoughlin P, Hughes H, O' Donovan O (2009) 'An Investigation into the Mechanisms of Chromium Uptake by Live Seaweed'. Environ 2009, Waterford Institute of Technology, Waterford February (18-20/02/2009).

Murphy C, McLoughlin P, Hughes H, O' Donovan O (2008) 'An Investigation into the Mechanisms of Bioaccumulation of Chromium by Seaweed'. International Seaweed Research Symposium, Marine Institute, Oranmore, Galway January (22/01/2009).

Murphy C, McLoughlin P, Hughes H, O' Donovan O (2008) 'An Investigation into the Mechanisms of Bioaccumulation of Chromium by Seaweed'. 14th ICHMET, National Taiwan University, Taipei, Taiwan November (16-22/12/2008).

### **Peer Reviewed Conference Proceedings**

#### **Abstract**

The accumulation of Cr by six species of seaweeds common to the south-east of Ireland was investigated in order to identify seaweeds with a high capacity for bioaccumulation and investigate mechanisms of bioaccumulation. Potentiometric and conductometric titrations allowed the number and type of acidic groups on the seaweed surface to be calculated, facilitating the identification of the most promising seaweeds for further study. FTIR spectroscopy of protonated and metal bound forms was used to identify the key functional groups present on the seaweed surface and their relative importance in metal binding. Preliminary studies using scanning force microscopy were carried out with significant surface morphology changes on metal binding identified.

**Key words:** Heavy metals, Cr, seaweed, bioaccumulation, FTIR, SFM, potentiometric titration.

Murphy C, McLoughlin P, Hughes H, O' Donovan O (2008) 'An Investigation into the Mechanisms of Bioaccumulation of Chromium by Seaweed'. EPA Fellowships & Scholarships Seminar, Hilton Kilmainham Hotel, Dublin November (13-14/11/2008).

Murphy C, McLoughlin P, Hughes H, O' Donovan O (2008) 'Study of the Factors Affecting the Bioaccumulation of Chromium by Seaweed'. 3rd Congress of the International Society for Applied Phycology and the 11th International Conference on Applied Phycology, NUI Galway, Galway June (21-27/06/2008).

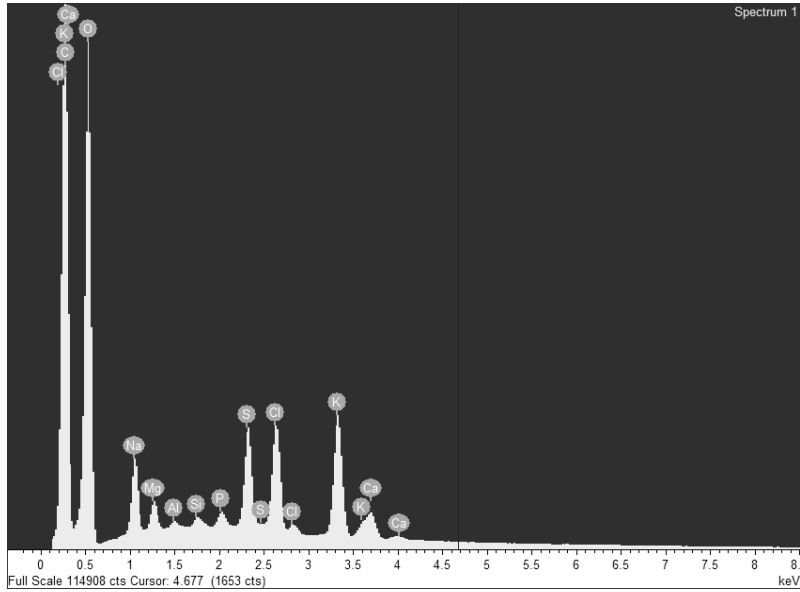
Murphy C, McLoughlin P, Hughes H, O' Donovan O, O' Mahony J (2008) 'An Investigation into the Effect of Heavy Metal Binding on Seaweeds and Seaweed Biofilms Using Scanning Force Microscopy'. 5th Biennial Conference of Analytical Sciences, Waterford Institute of Technology, Waterford May (7/05/2008).

Murphy C, McLoughlin P, Hughes H, O' Donovan O (2008) 'Study of the Factors Affecting the Biosorption of Chromium by Seaweed'. EPA Conference to Showcase Environmental Protection Research Projects, Royal Hospital Kilmainham, Dublin February (6-7 February 2008).

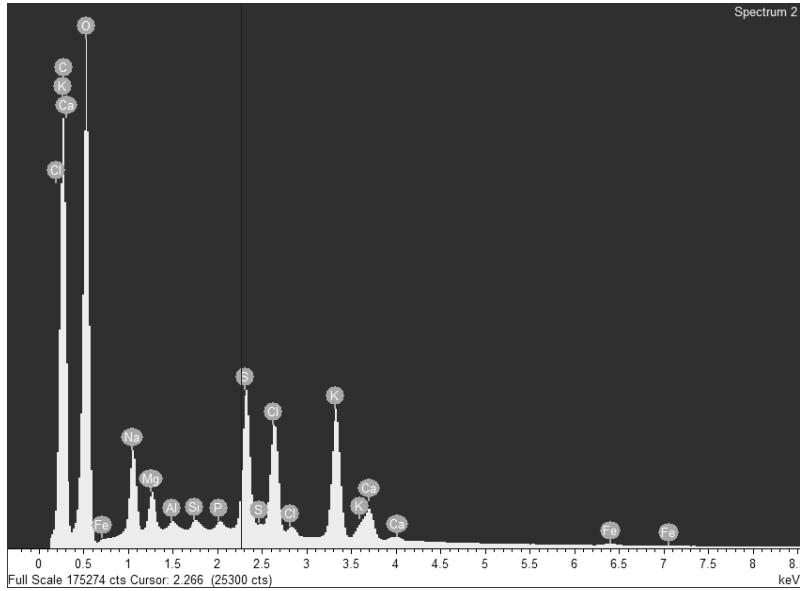
Murphy C, McLoughlin P, Hughes H, O' Donovan O (2008) 'Study of the Factors Affecting the Biosorption of Chromium by Seaweed'. Environ 2008, Dundalk Institute of Technology, Dundalk February (1-3/02/2008).

# Appendix 2: EDX Scans

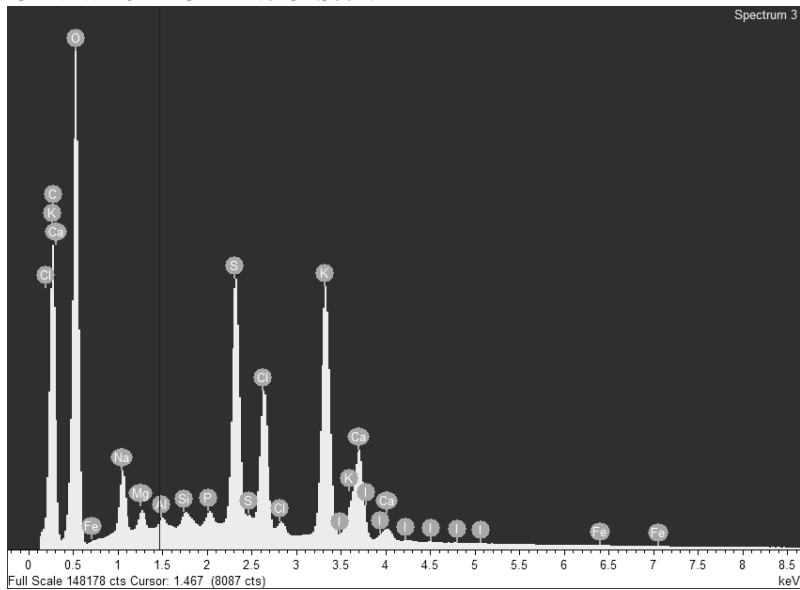
13 FV W 16 B R1 No Cr Seen.



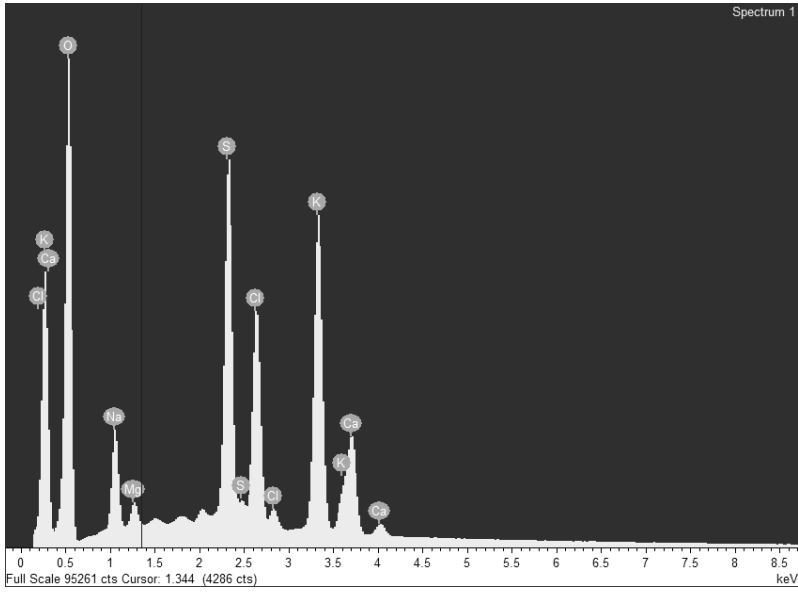
13 FV W 16 B R2 No Cr Seen.



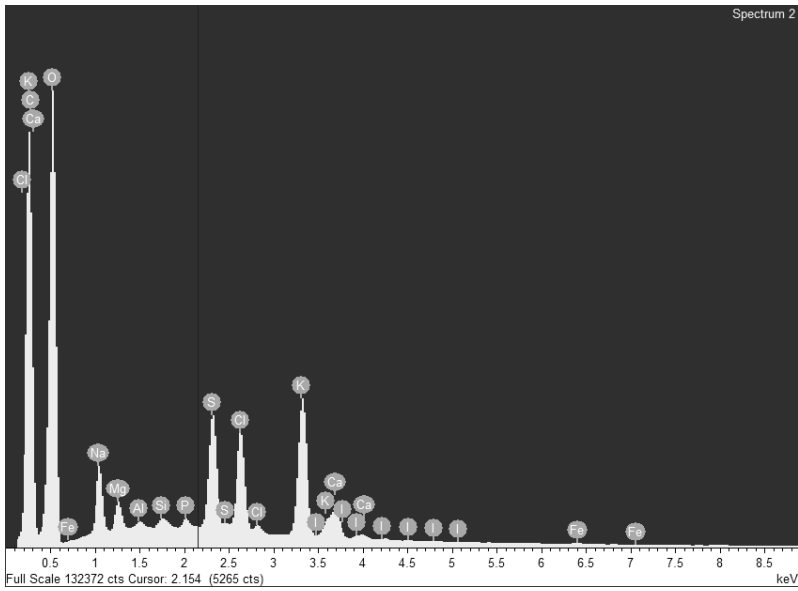
13 FV W 16 B R3 No Cr Seen.



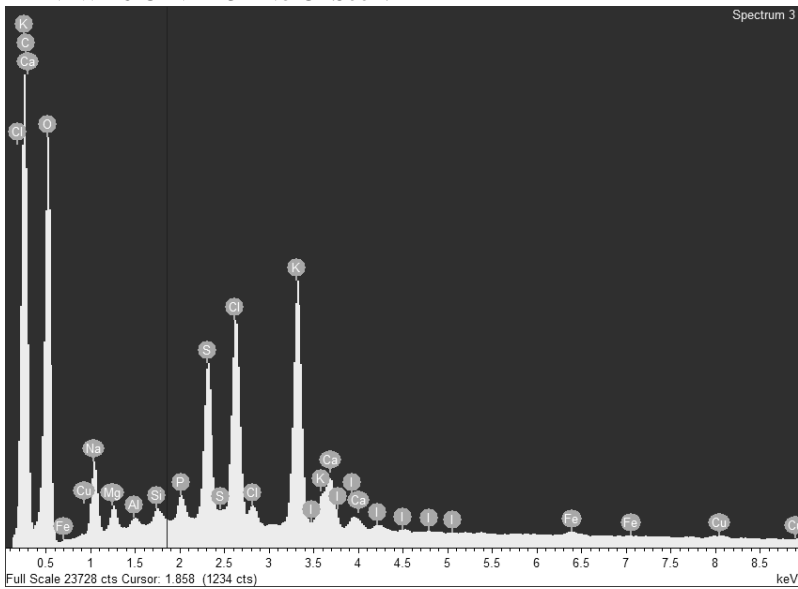
14 FV W 16 Cr VI R1 No Cr Seen.



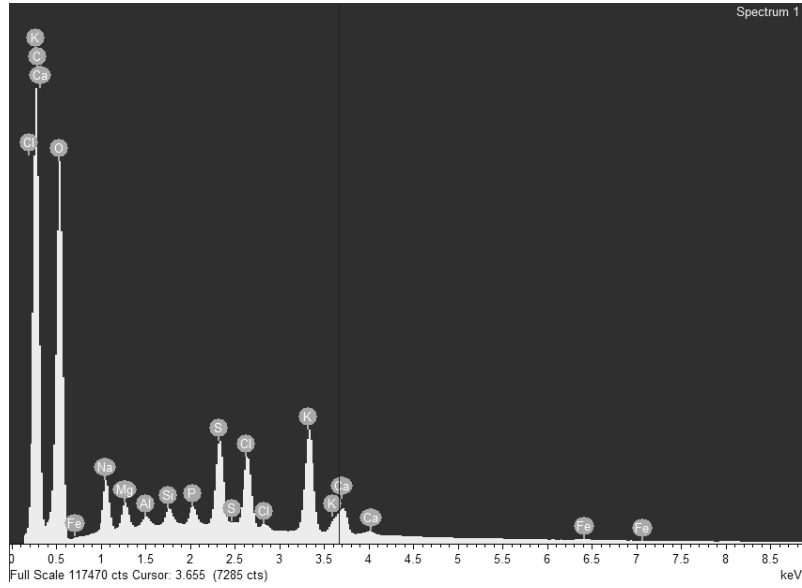
14 FV W 16 Cr VI R2 No Cr Seen.



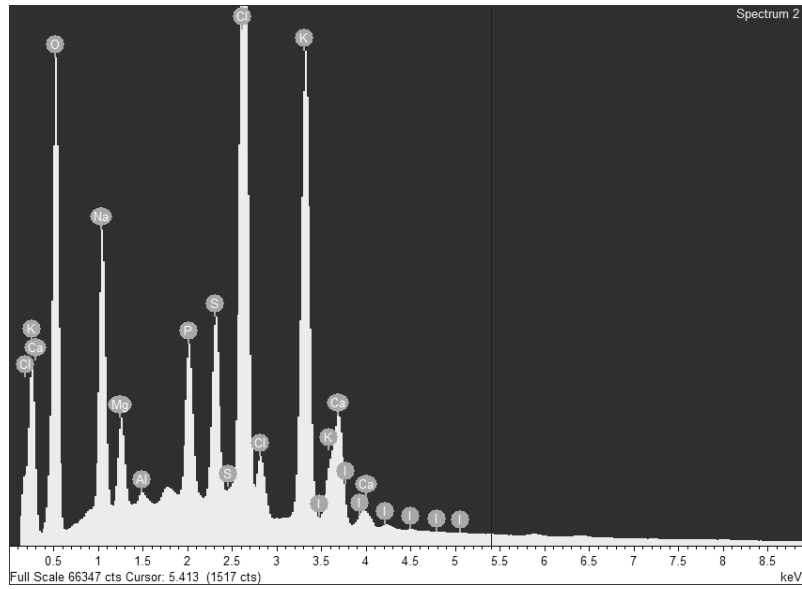
14 FV W 16 Cr VI R3 No Cr Seen.



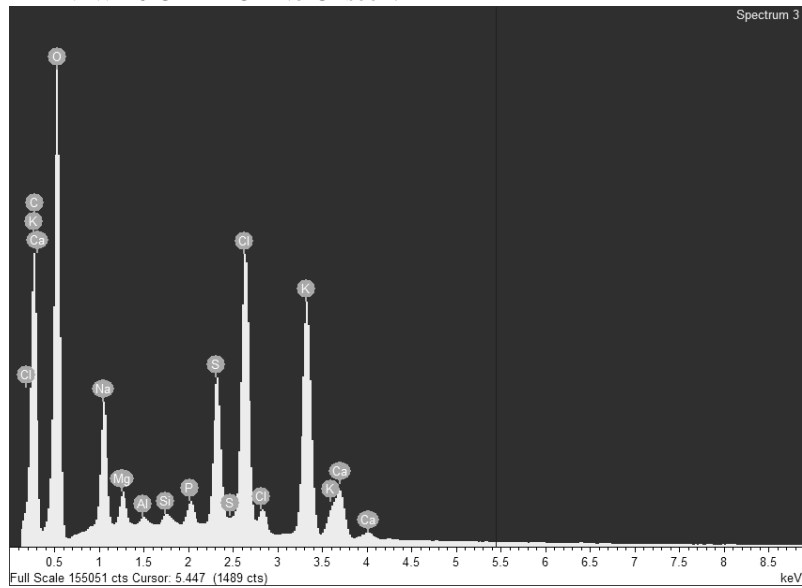
B 1 FV W 16 Cr III R1 No Cr seen.



B 1 FV W 16 Cr III R2 No Cr seen.

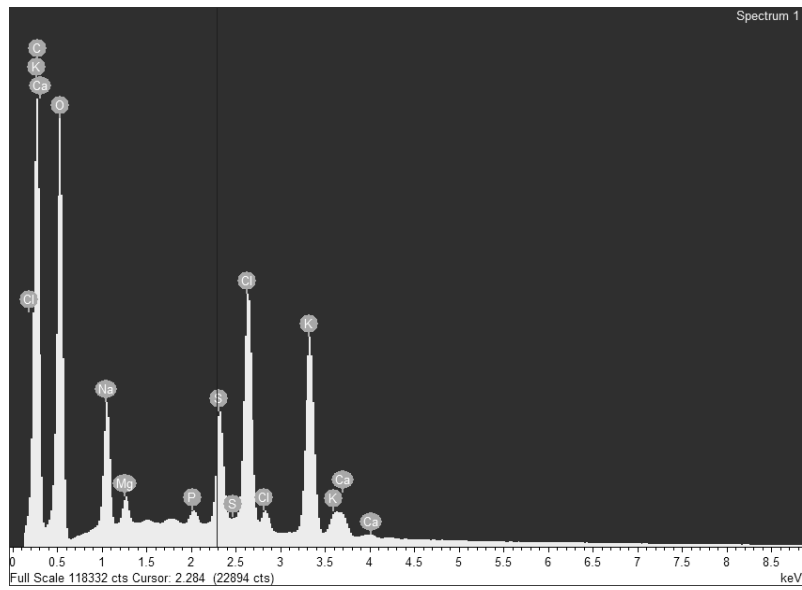


B 1 FV W 16 Cr III R3 No Cr seen.

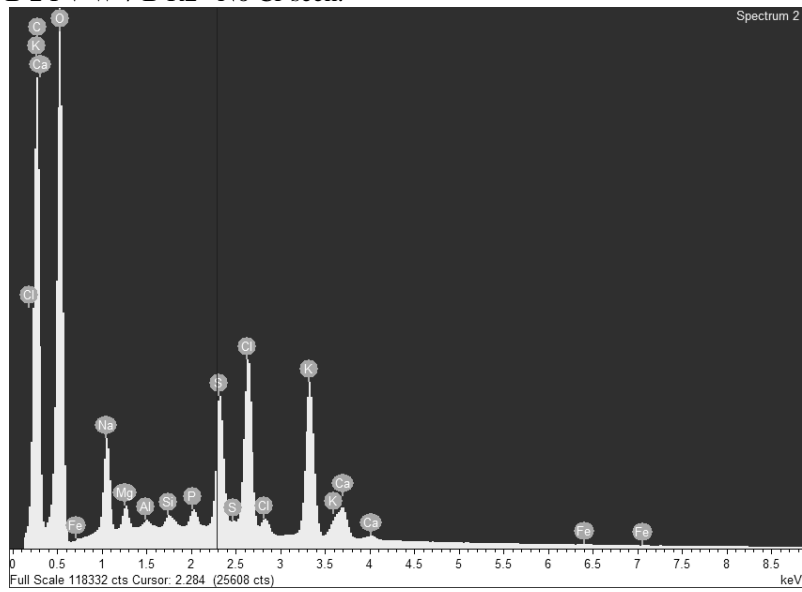


B 2 FV W 7 B R1 No Cr seen.

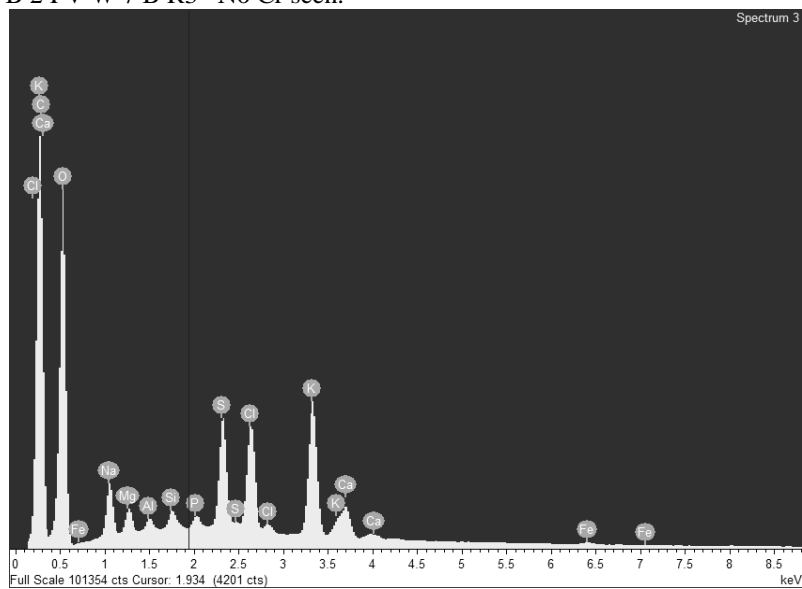




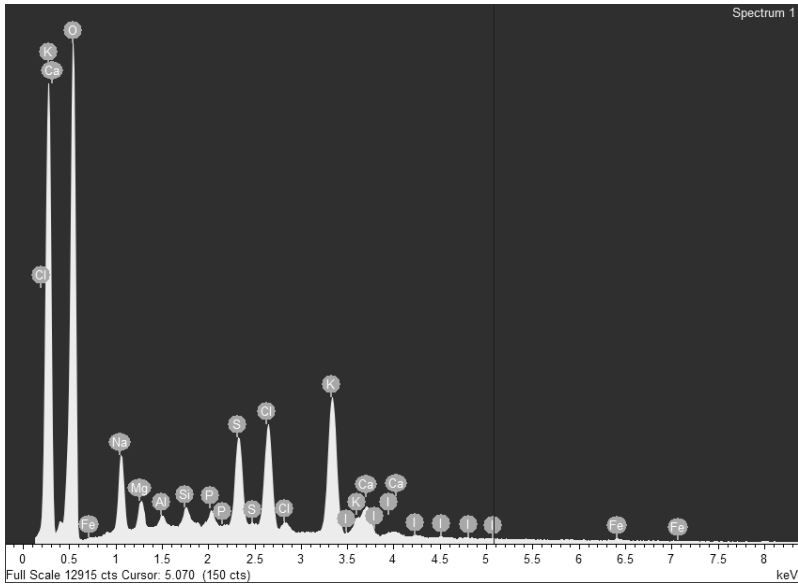
B 2 FV W 7 B R2 No Cr seen.



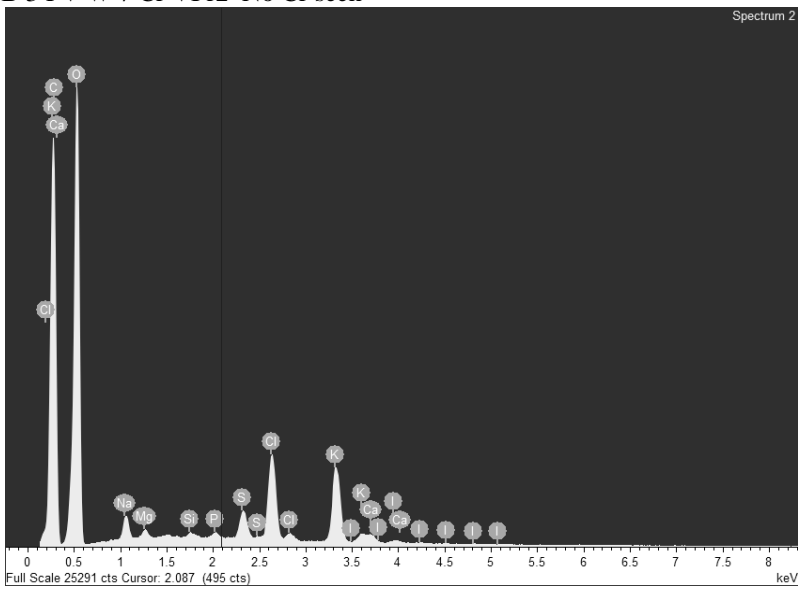
B 2 FV W 7 B R3 No Cr seen.



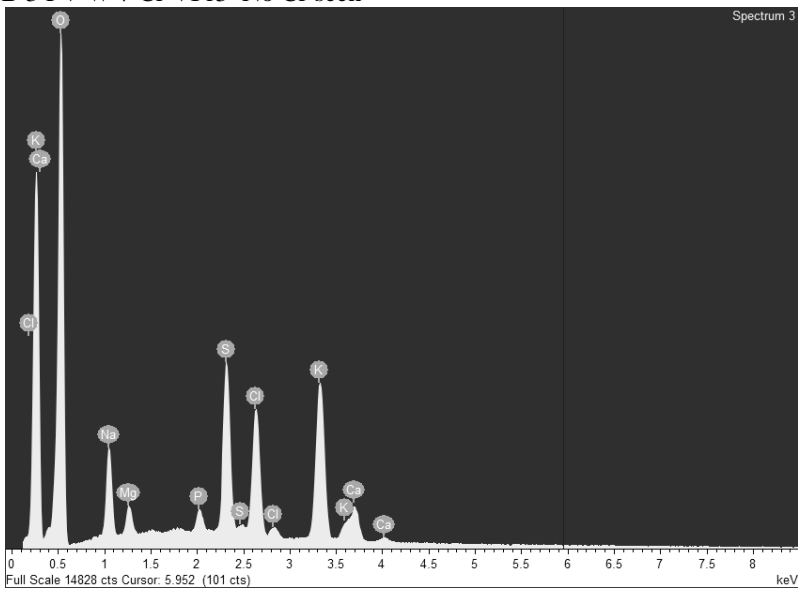
B 3 FV W 7 Cr VI No Cr seen



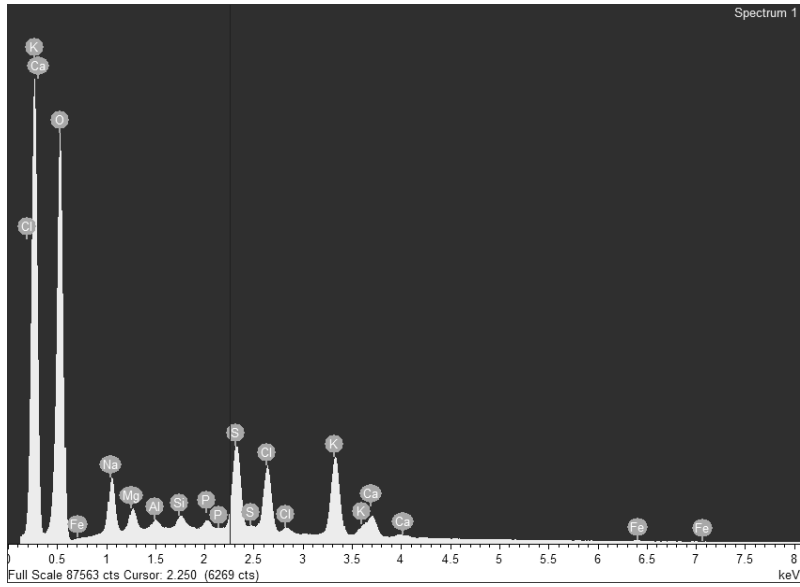
B 3 FV W 7 Cr VI r2 No Cr seen



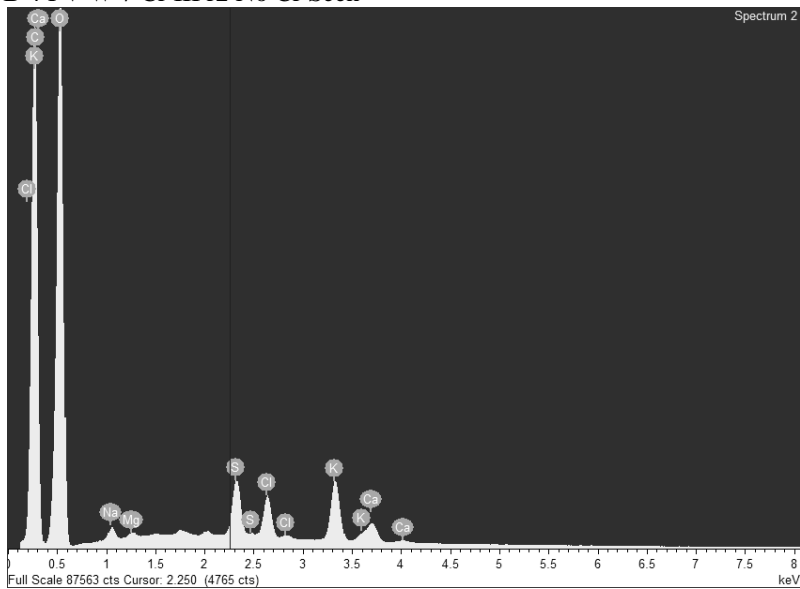
B 3 FV W 7 Cr VI r3 No Cr seen



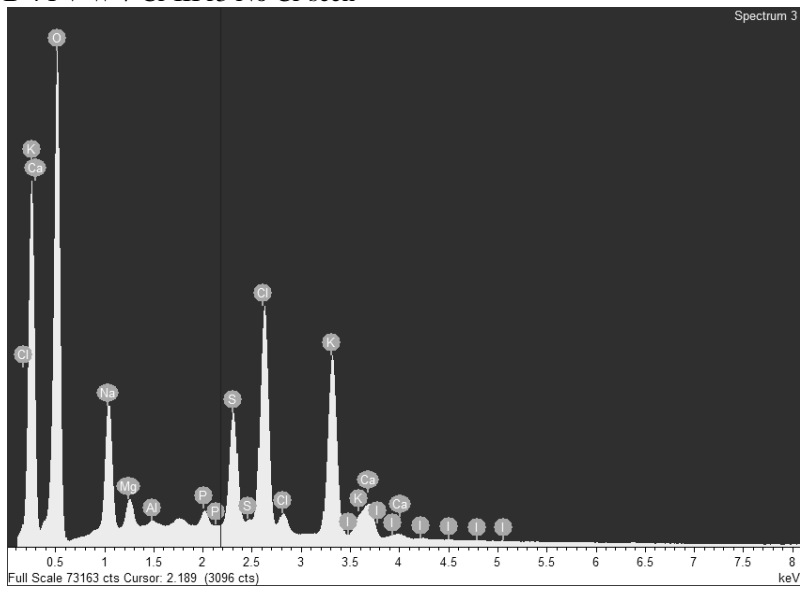
B 4 FV W 7 Cr III r1



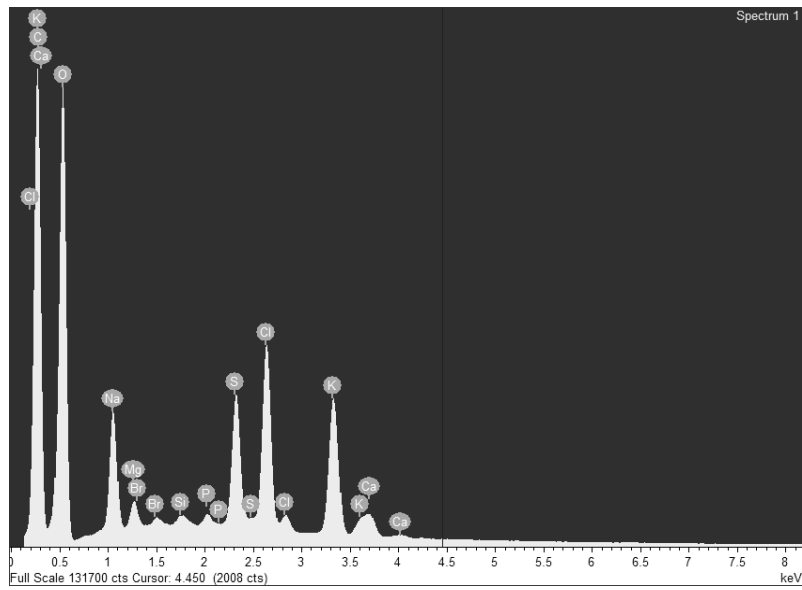
B 4 FV W 7 Cr III r2 No Cr Seen



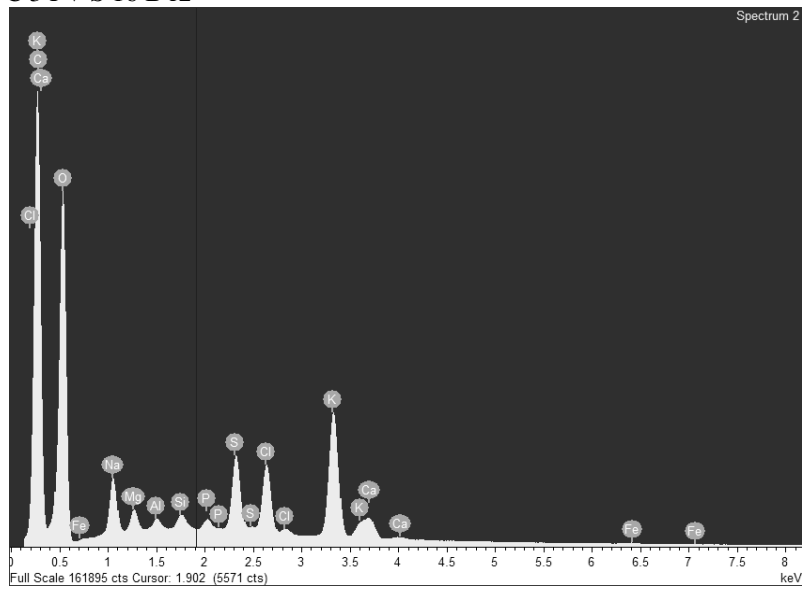
B 4 FV W 7 Cr III r3 No Cr seen



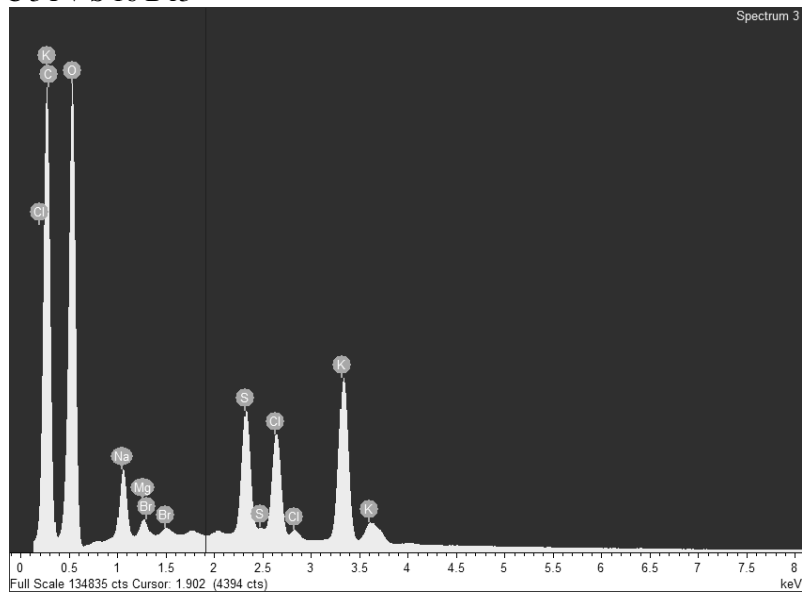
C 3 FV S 16 B r1



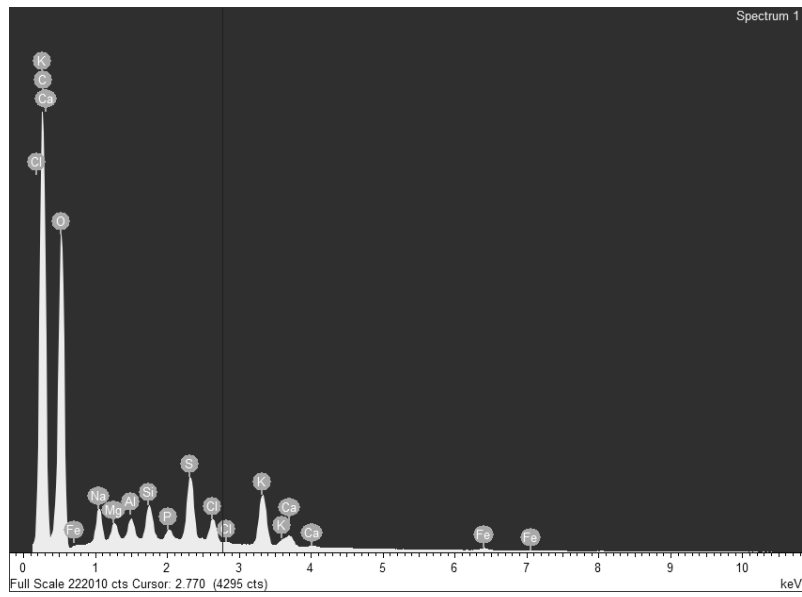
C 3 FV S 16 B r2



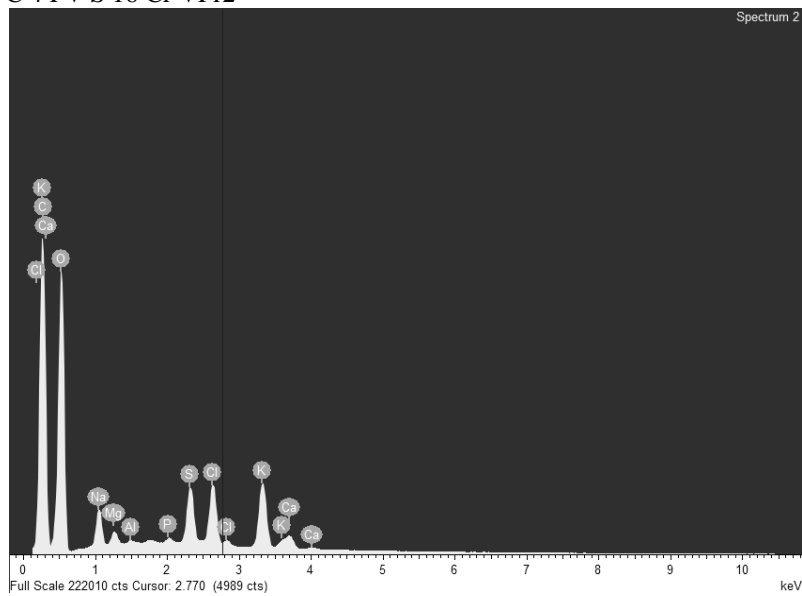
C 3 FV S 16 B r3



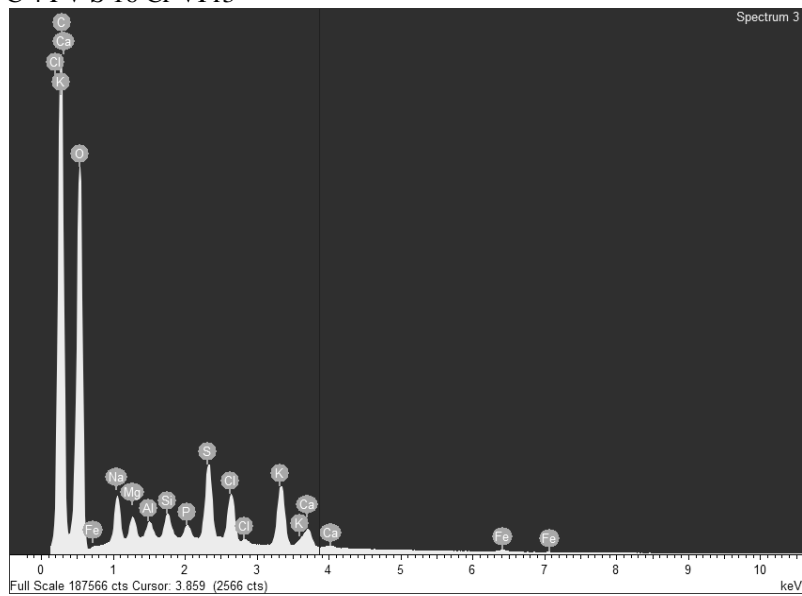
C 4 FV S 16 Cr VI r1



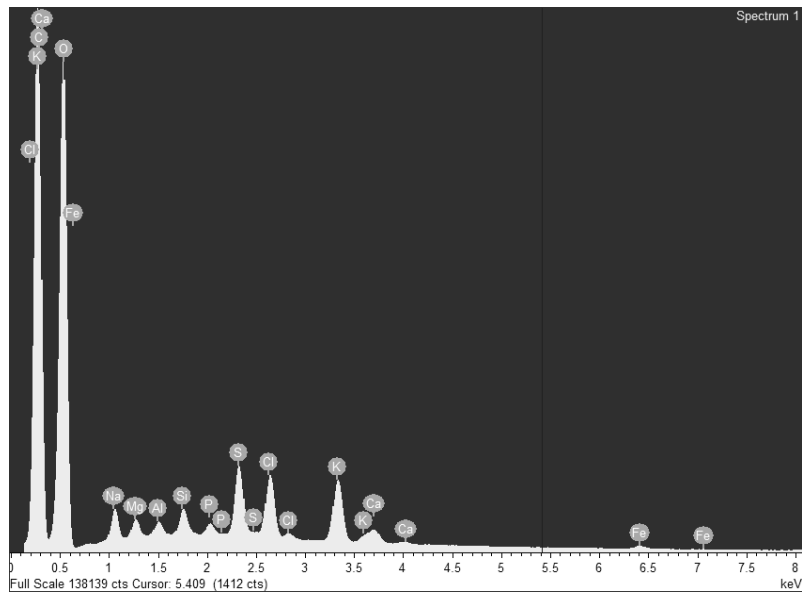
C 4 FV S 16 Cr VI r2



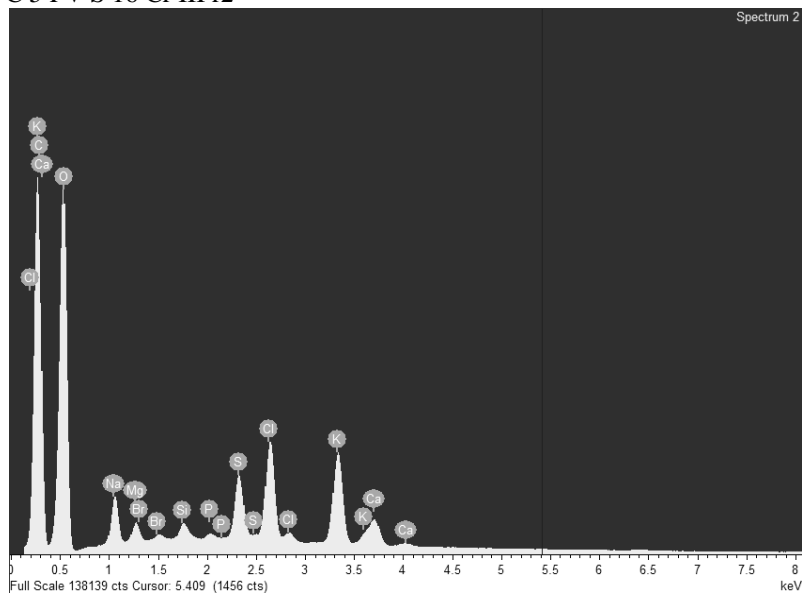
C 4 FV S 16 Cr VI r3



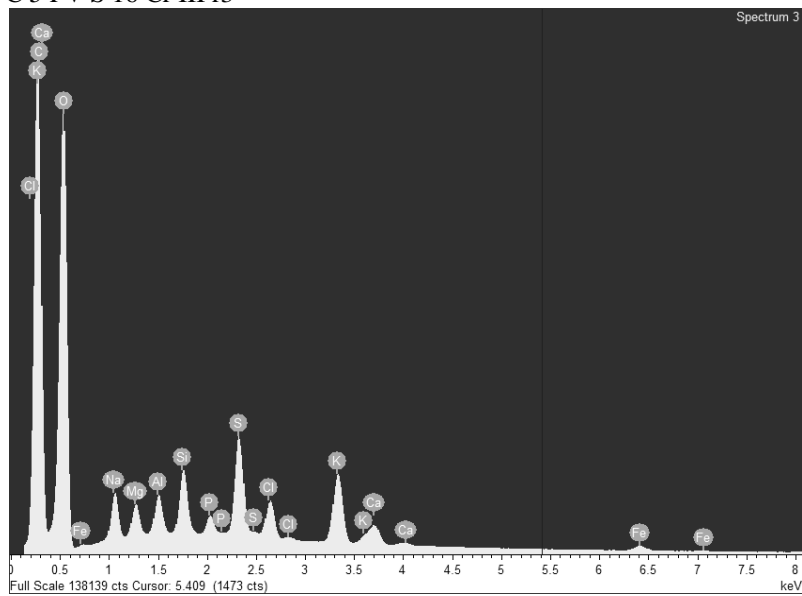
C 5 FV S 16 Cr III r1



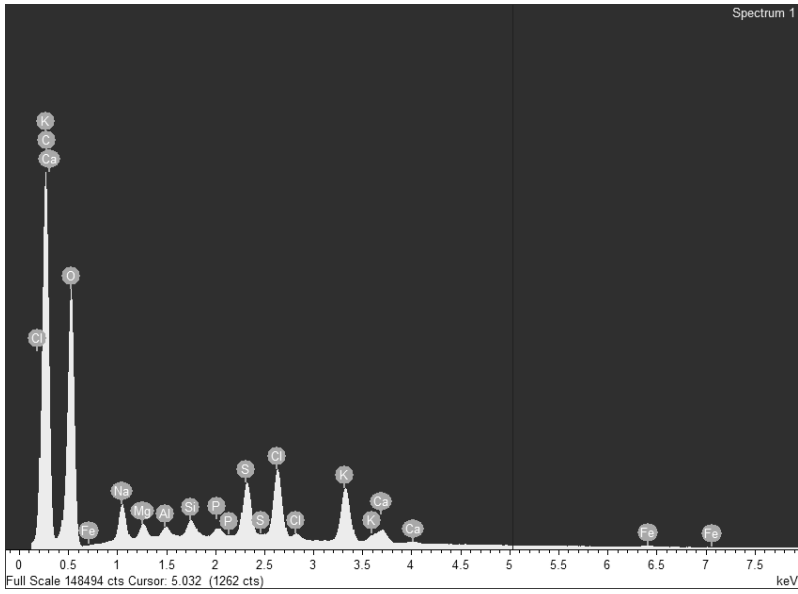
C 5 FV S 16 Cr III r2



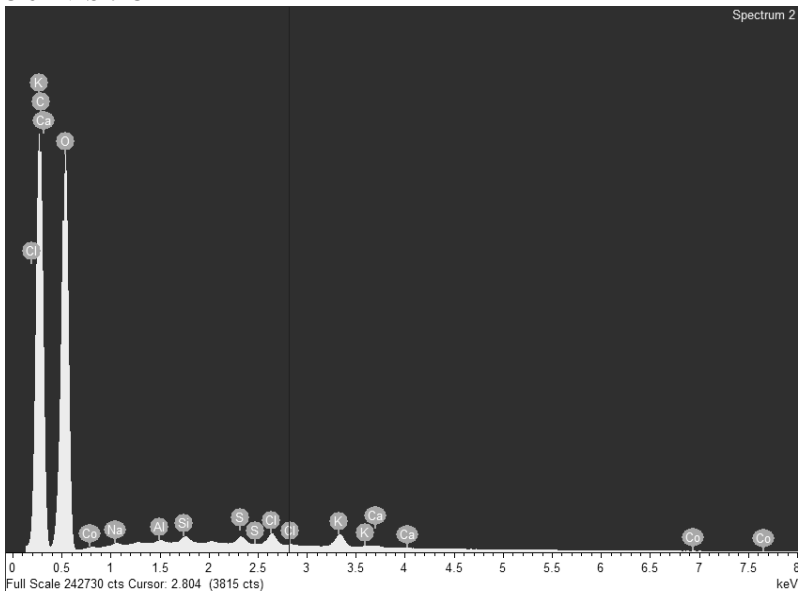
C 5 FV S 16 Cr III r3



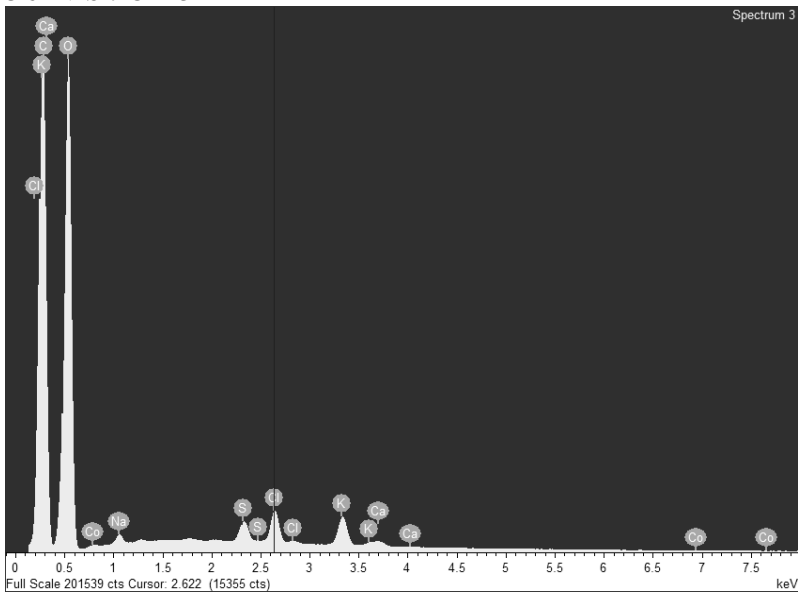
C 6 FV S 7 CB r1



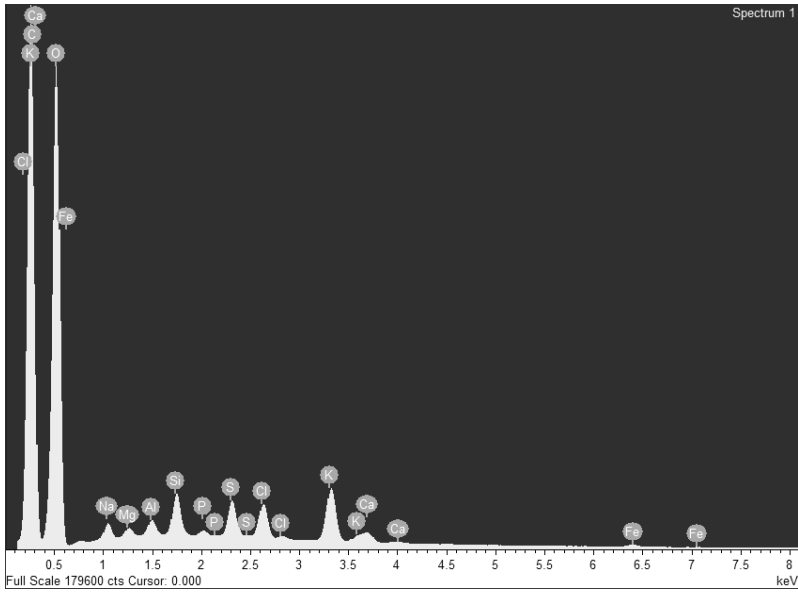
C 6 FV S 7 CB r2



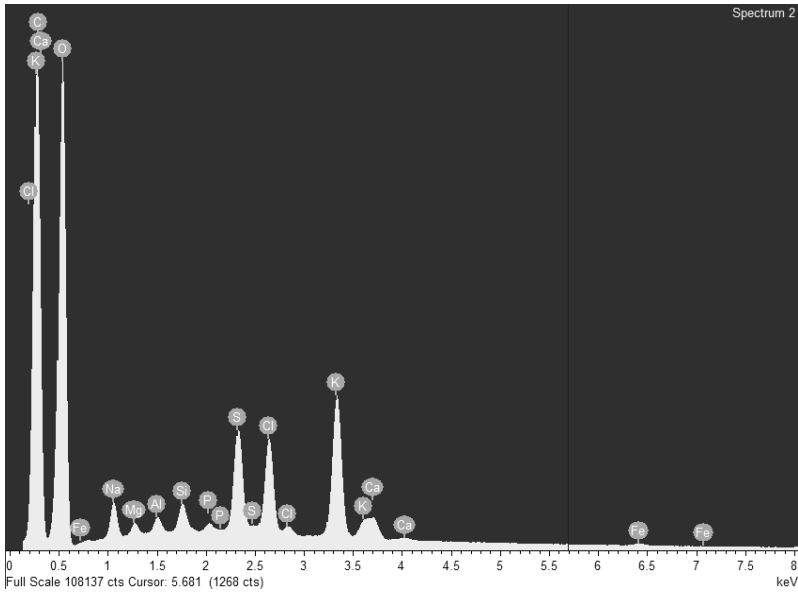
C 6 FV S 7 CB r3



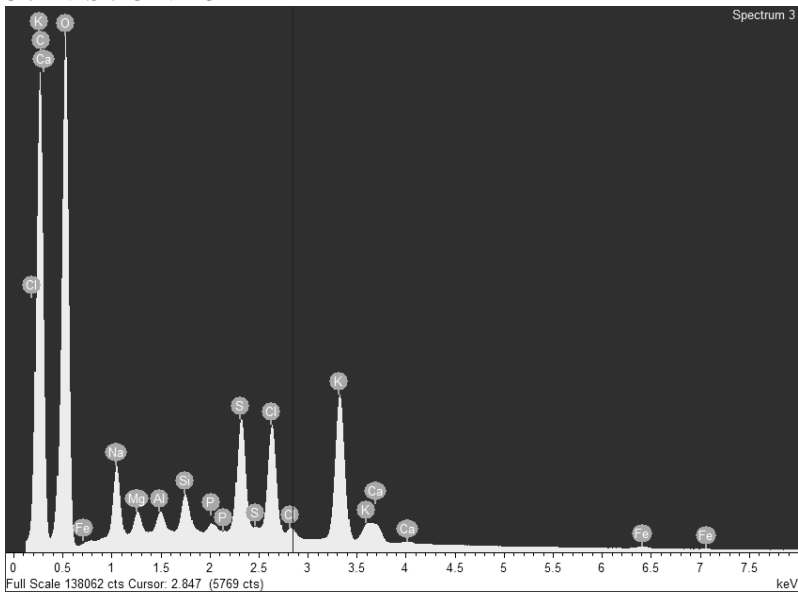
C 7 FV S 7 Cr VI r1



C 7 FV S 7 Cr VI r2

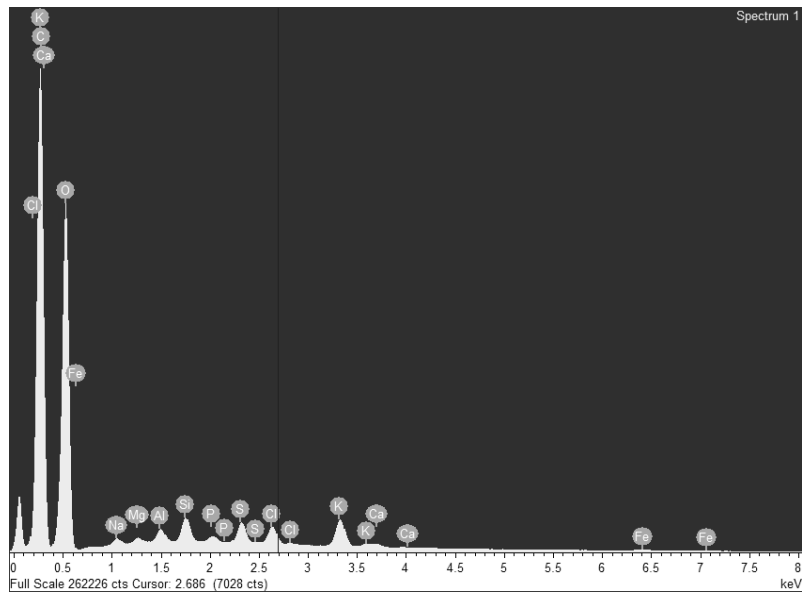


C 7 FV S 7 Cr VI r3

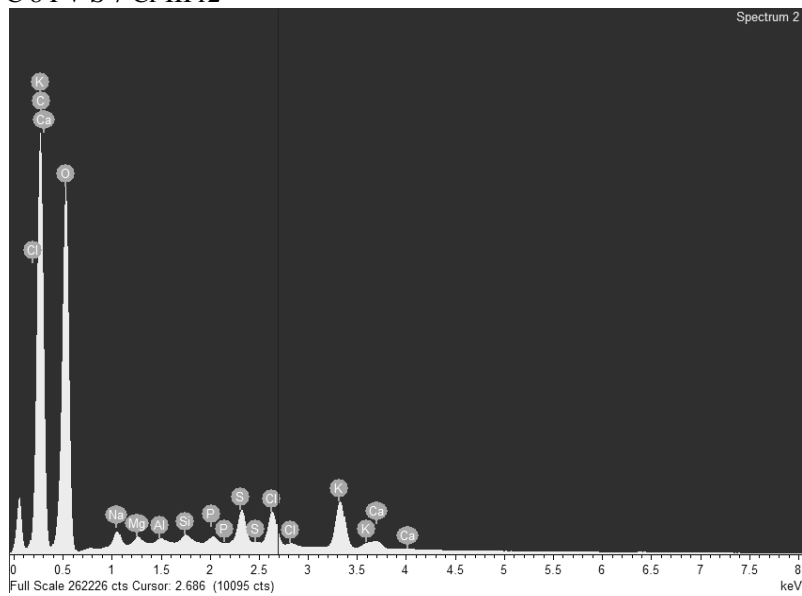


C 8 FV S 7 Cr III r1

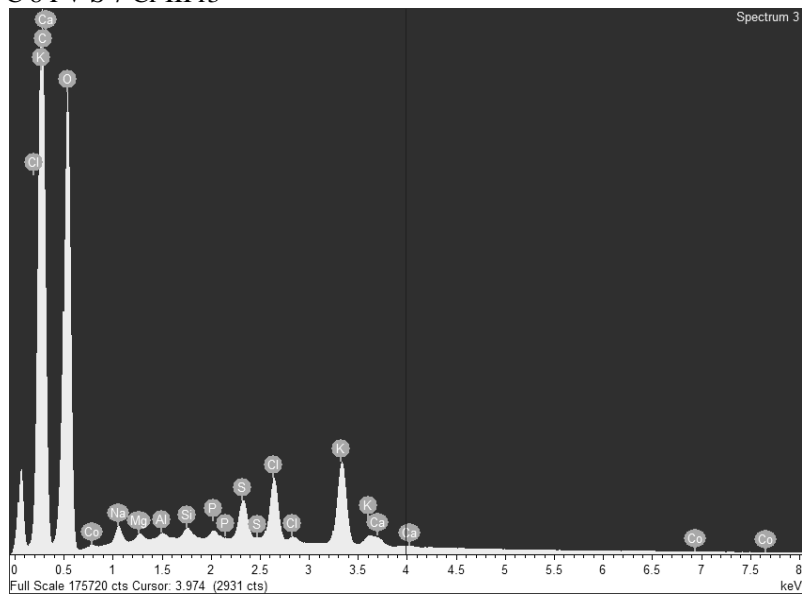




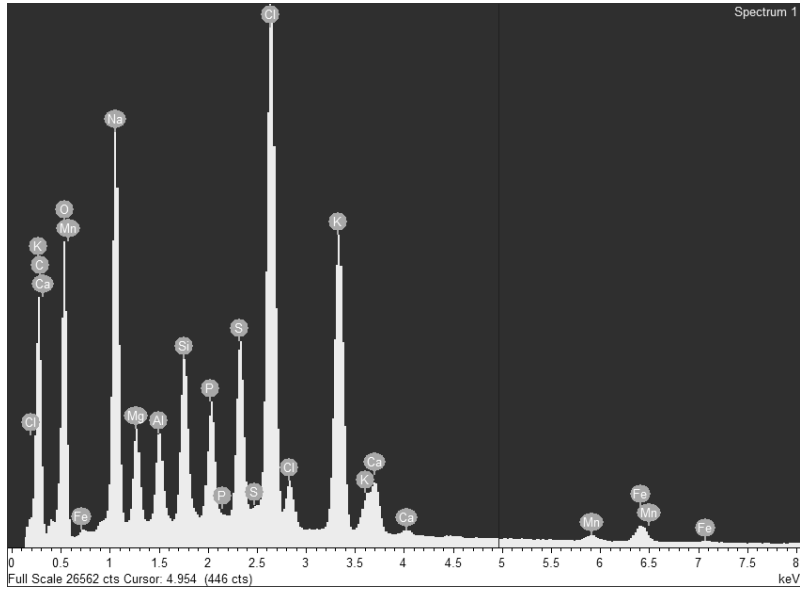
C 8 FV S 7 Cr III r2



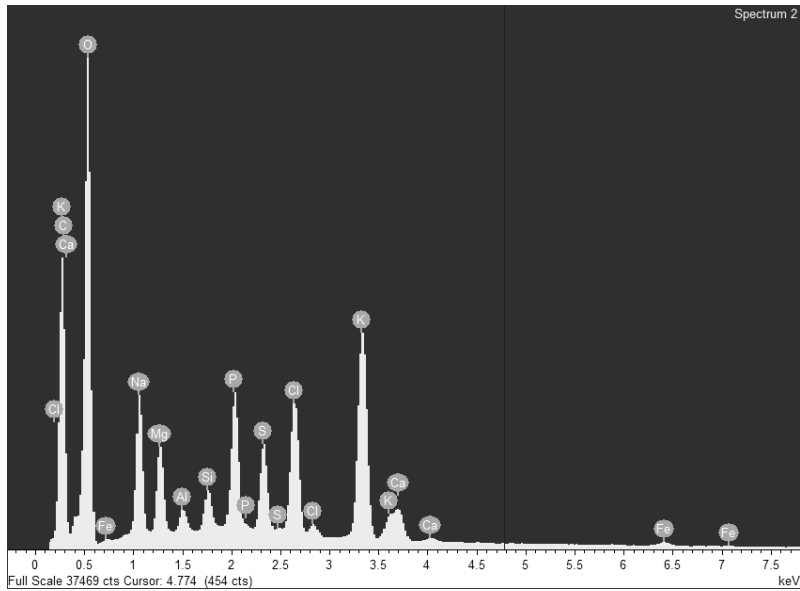
C 8 FV S 7 Cr III r3



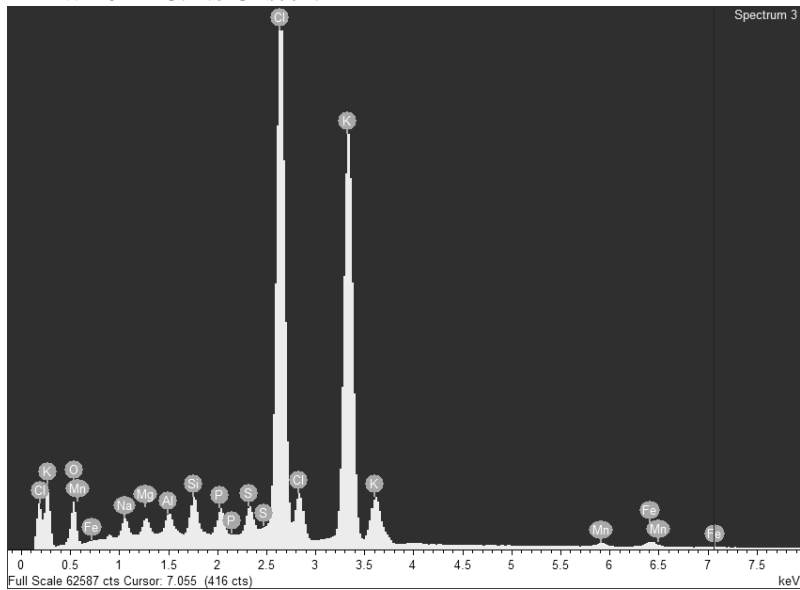
1 PP W 16 B R1. No Cr seen.



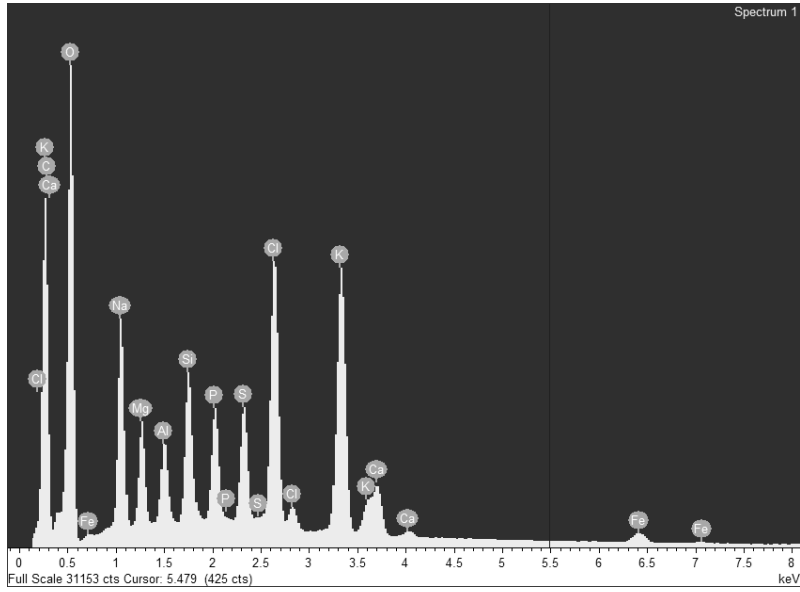
1 PP W 16 B R2. No Cr seen.



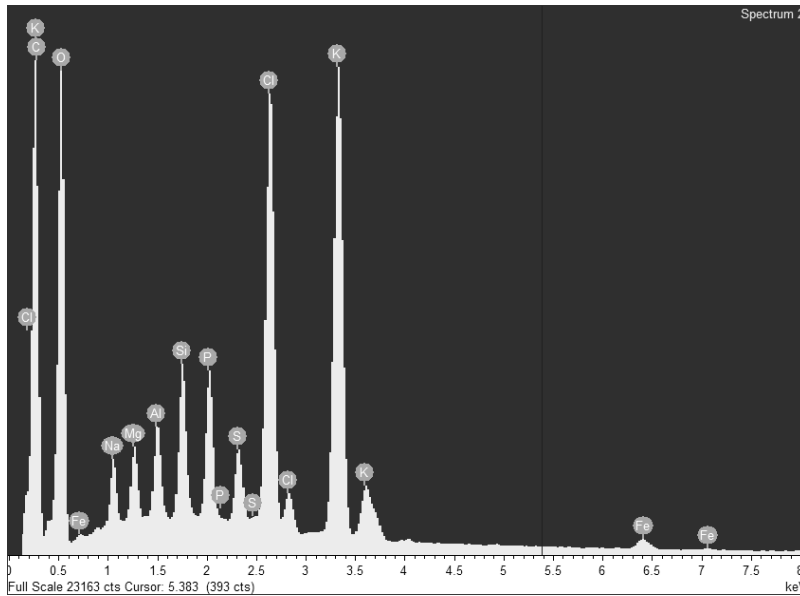
1 PP W 16 B R3. No Cr seen.



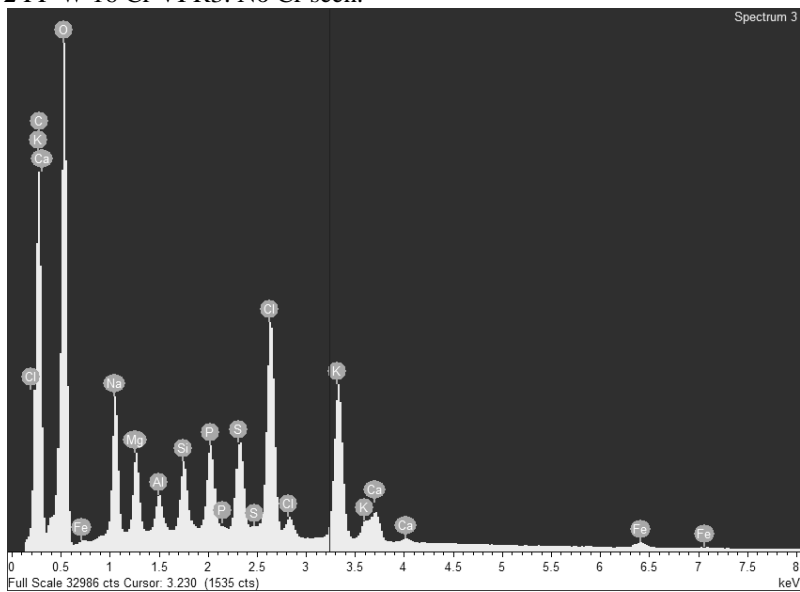
2 PP W 16 Cr VI R1



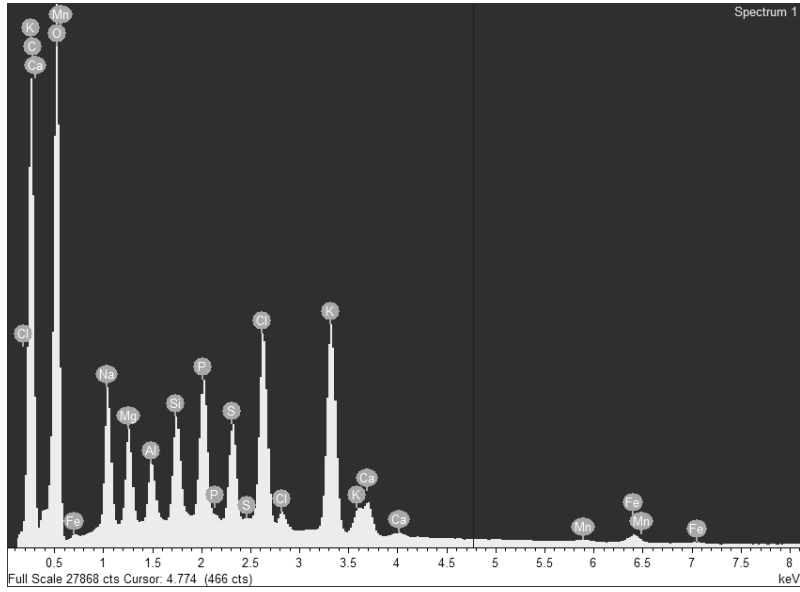
2 PP W 16 Cr VI R2. No Cr Seen.



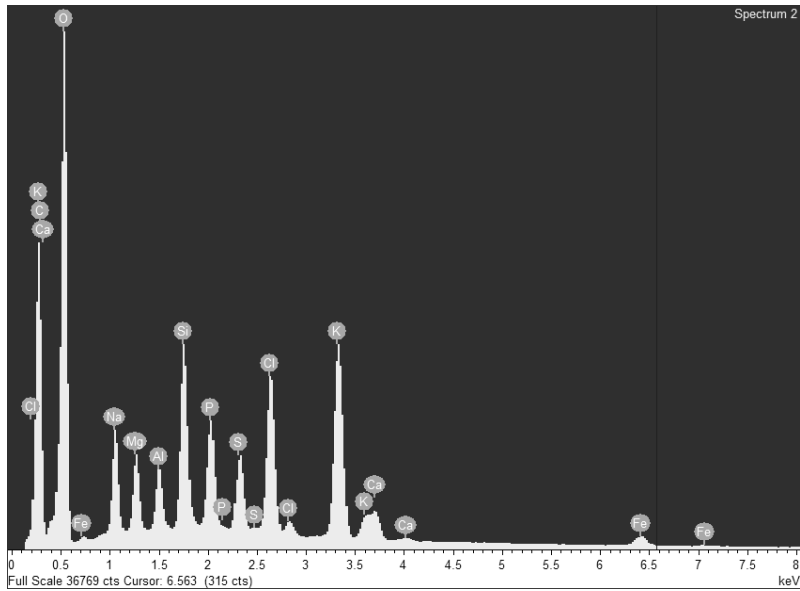
2 PP W 16 Cr VI R3. No Cr seen.



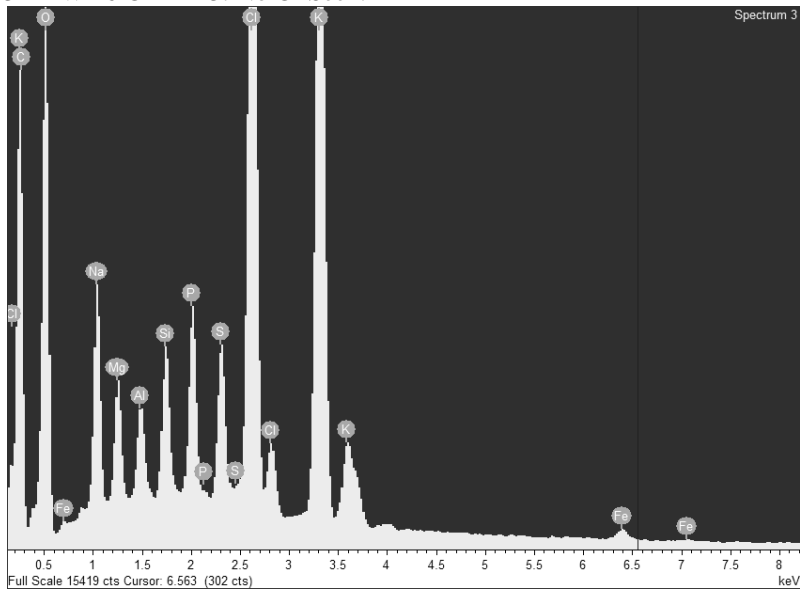
3 PP W 16 Cr III R1. No Cr Seen.



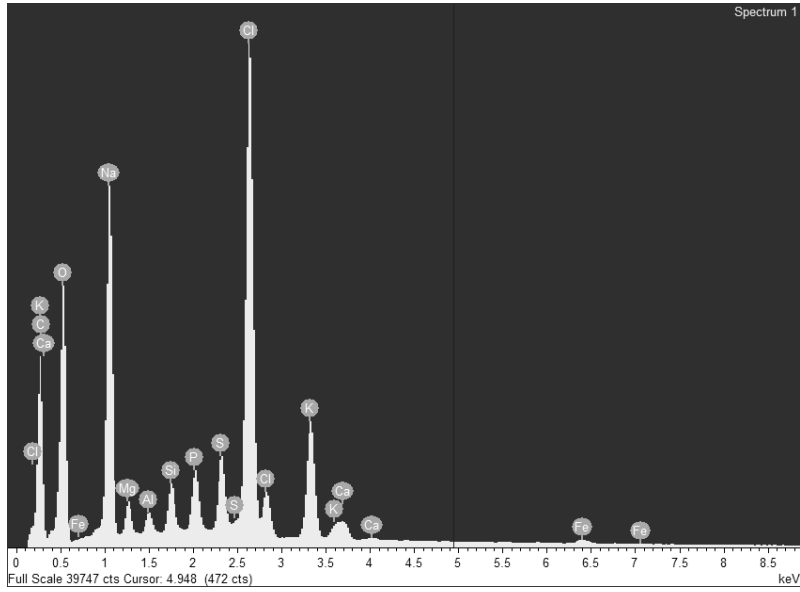
3 PP W 16 Cr III R2. No Cr Seen.



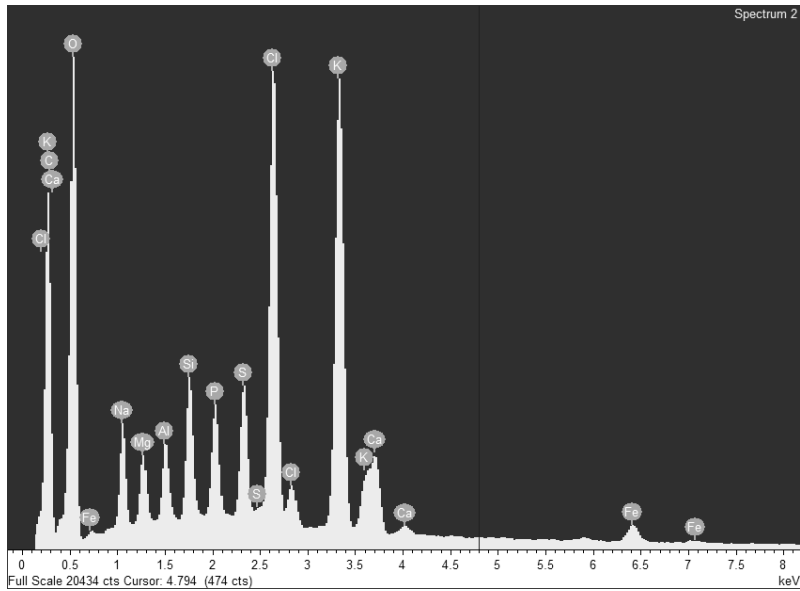
3 PP W 16 Cr III R3. No Cr Seen.



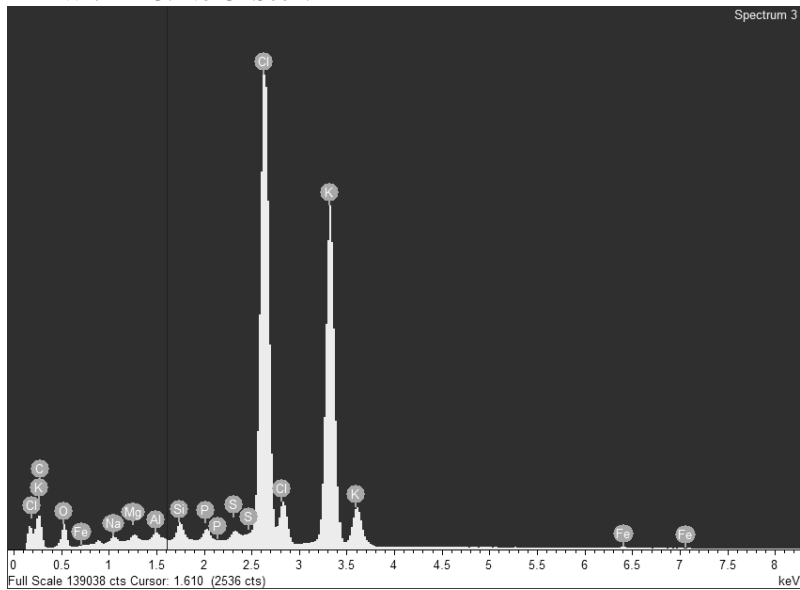
4 PP W 7 B R1. No Cr seen.



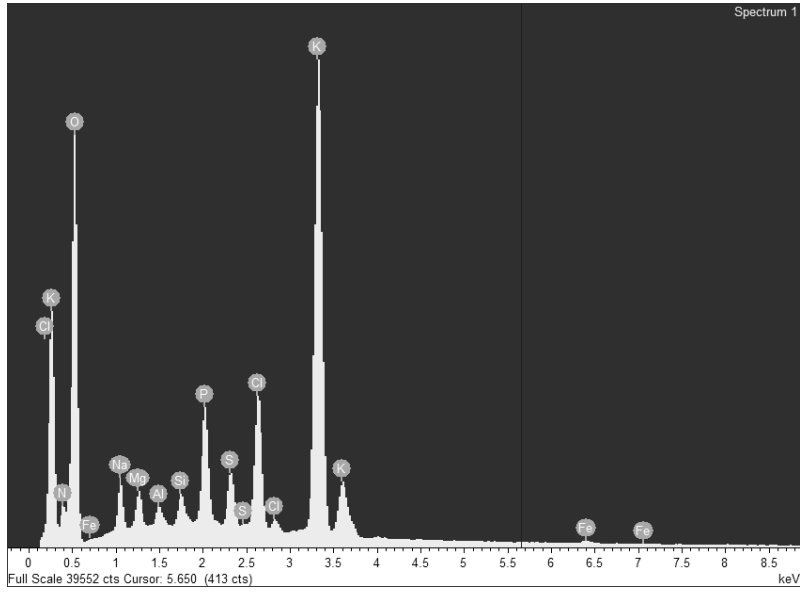
4 PP W 7 B R2. No Cr seen.



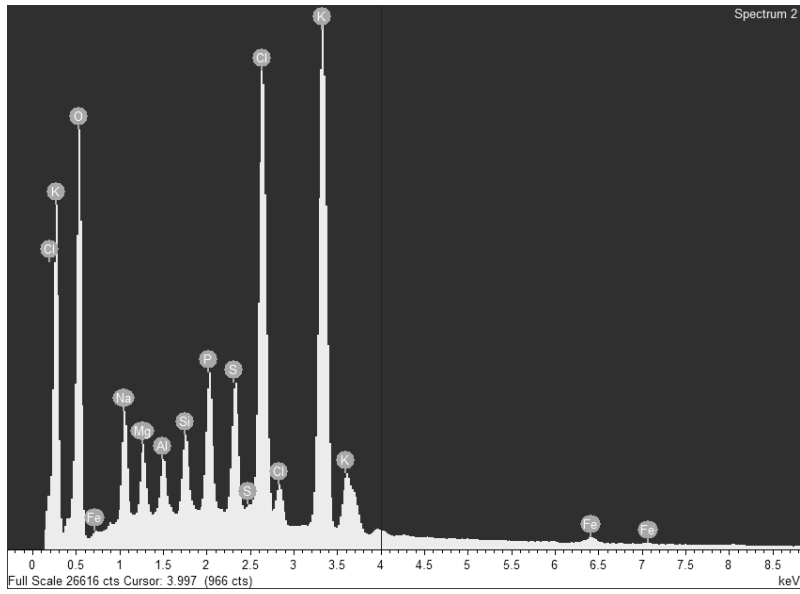
4 PP W 7 B R3. No Cr Seen.



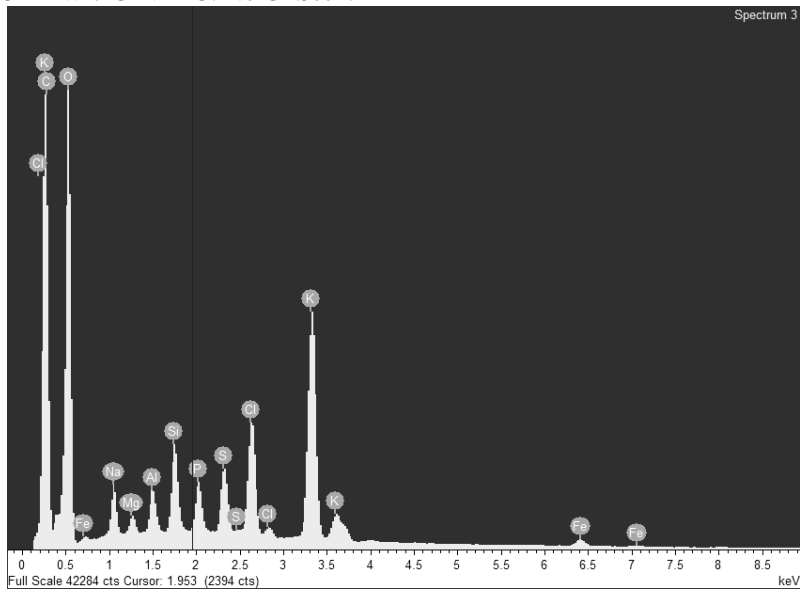
5 PP W 7 Cr VI R1. No Cr Seen.



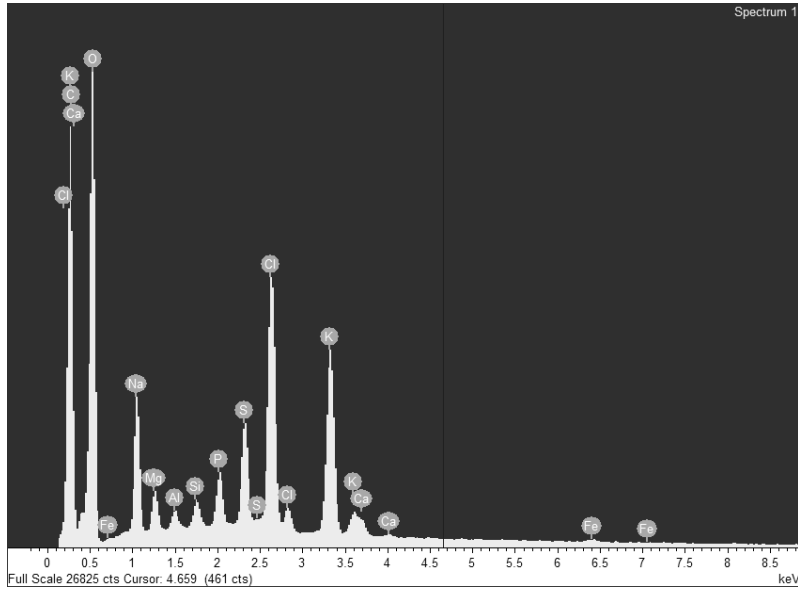
5 PP W 7 Cr VI R2. No Cr Seen.



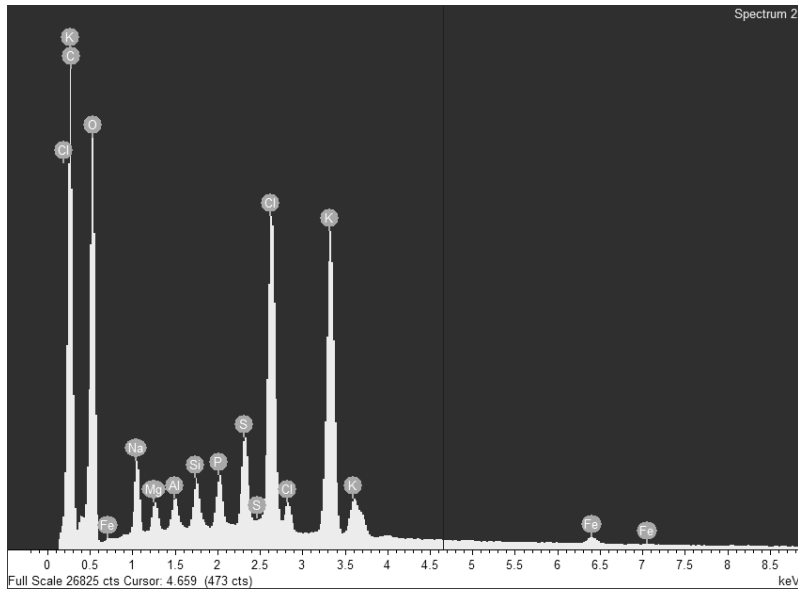
5 PP W 7 Cr VI R3. No Cr Seen.



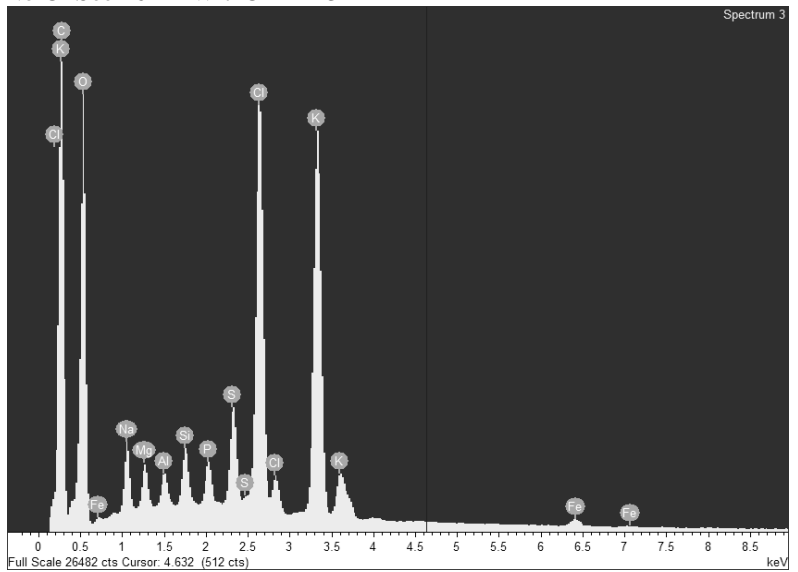
No Cr Seen 6 PP W 7 Cr III R1



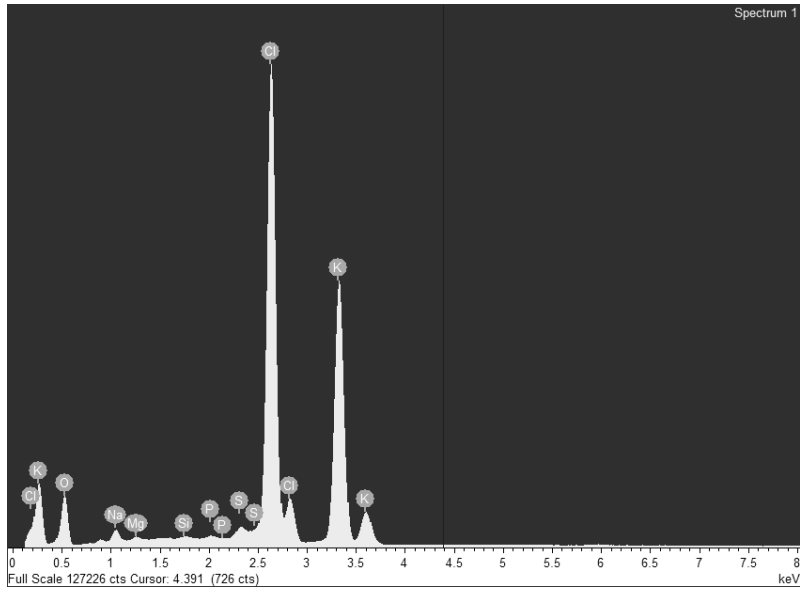
No Cr Seen 6 PP W 7 Cr III R2



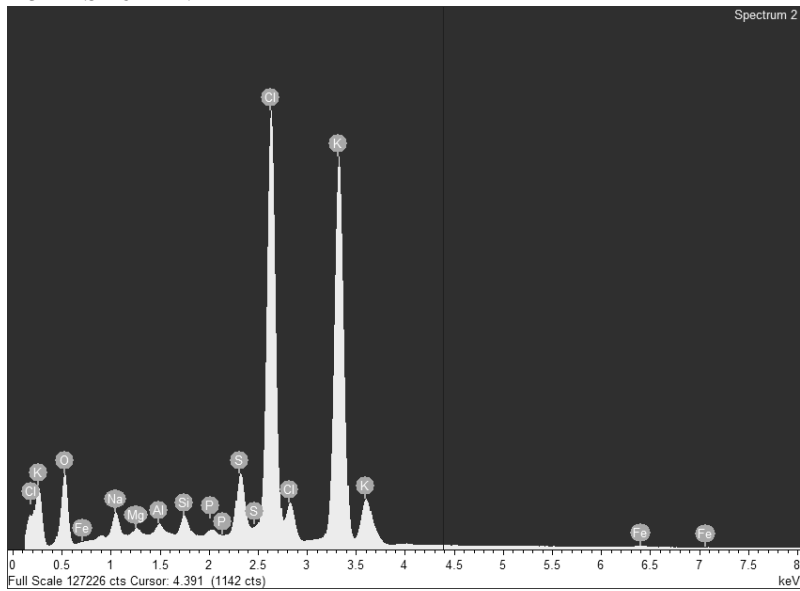
No Cr Seen 6 PP W 7 Cr III R3



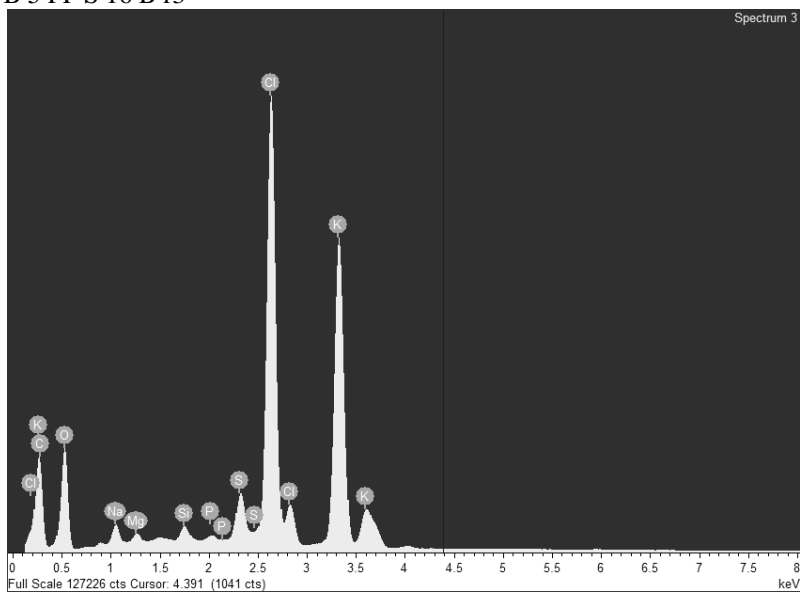
B 5 PP S 16 B r1.



B 5 PPS 16 B r2.

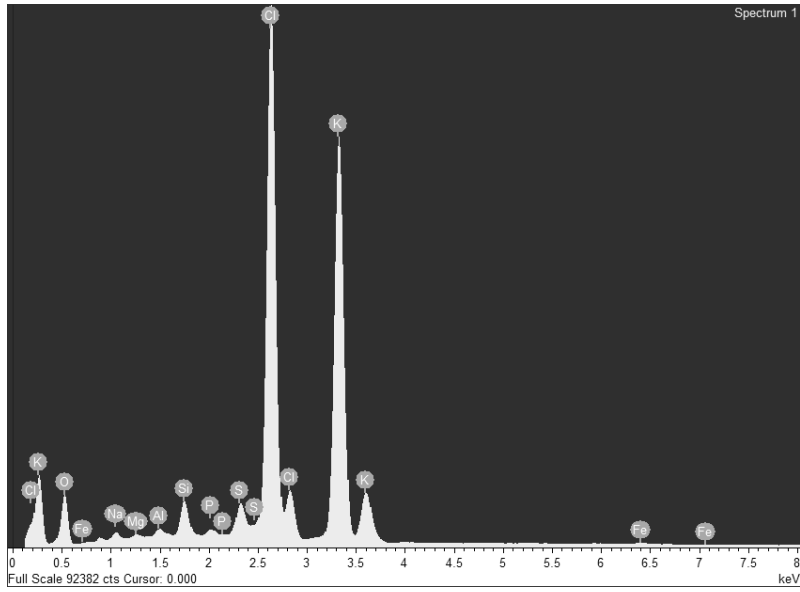


B 5 PPS 16 B r3

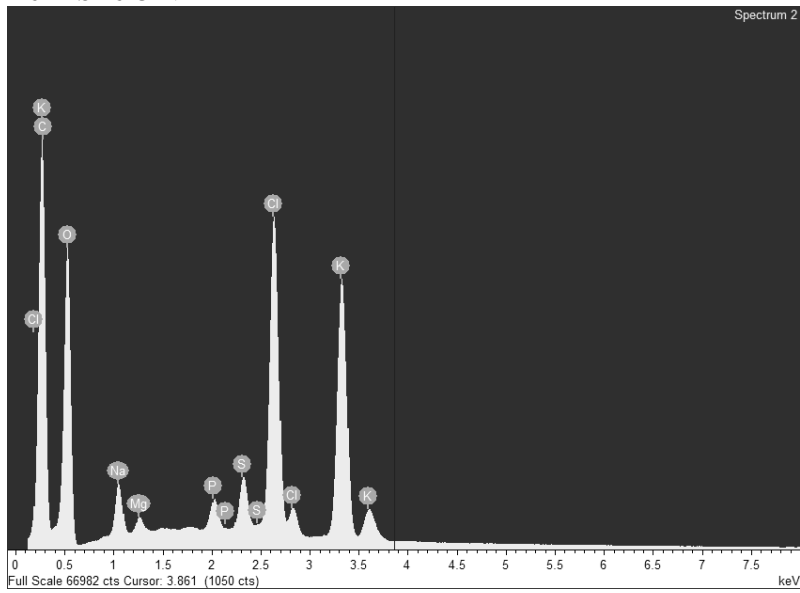


B 6 PPS 16 Cr VI r1

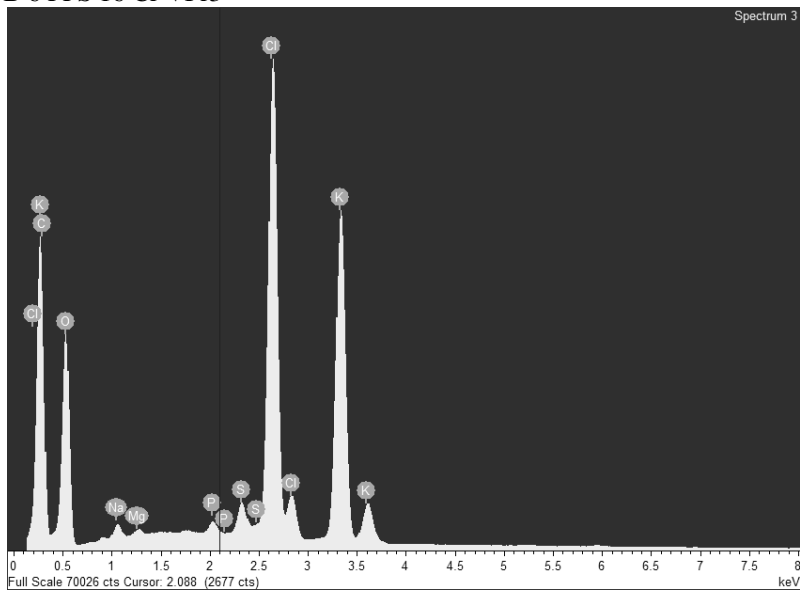




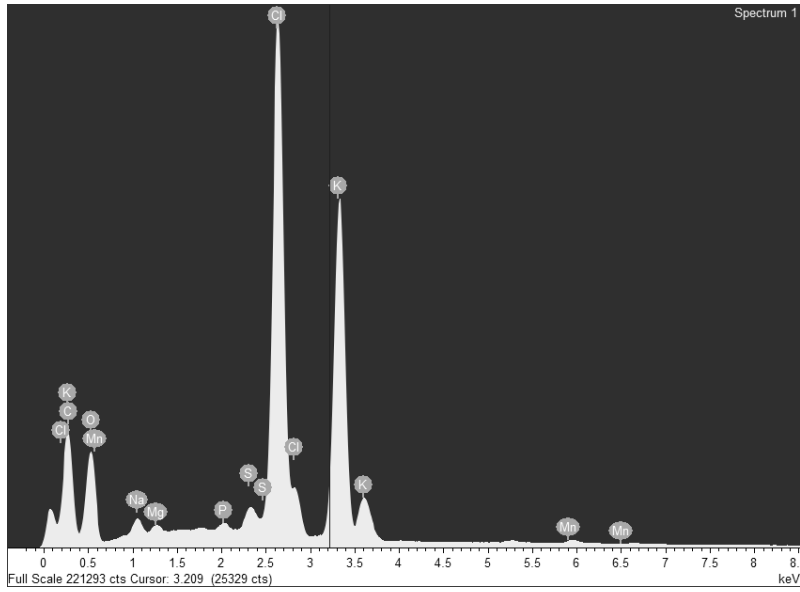
B 6 PPS 16 Cr VI r2



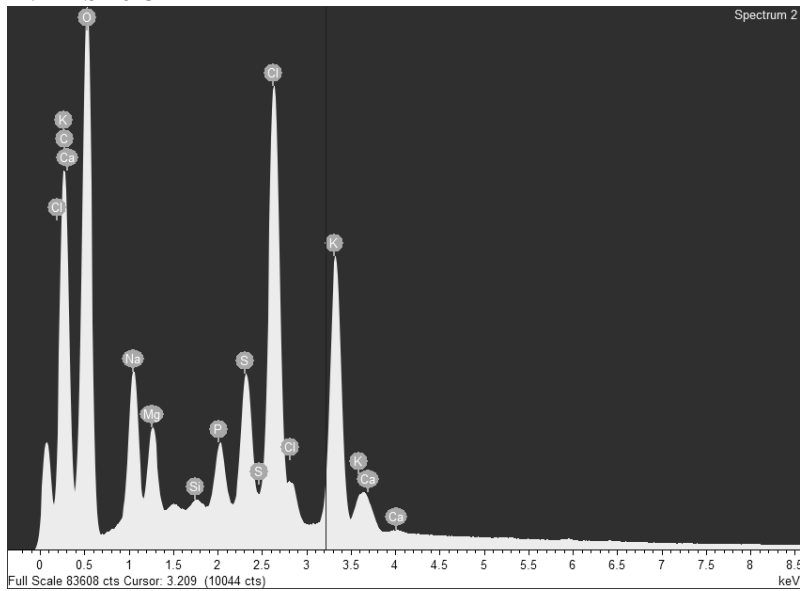
B 6 PPS 16 Cr VI r3



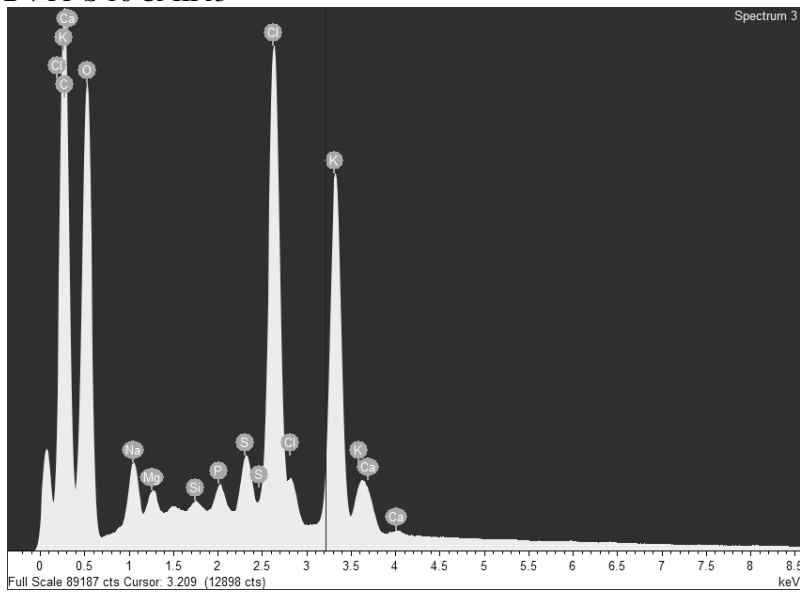
B 7 PPS 16 Cr III r1



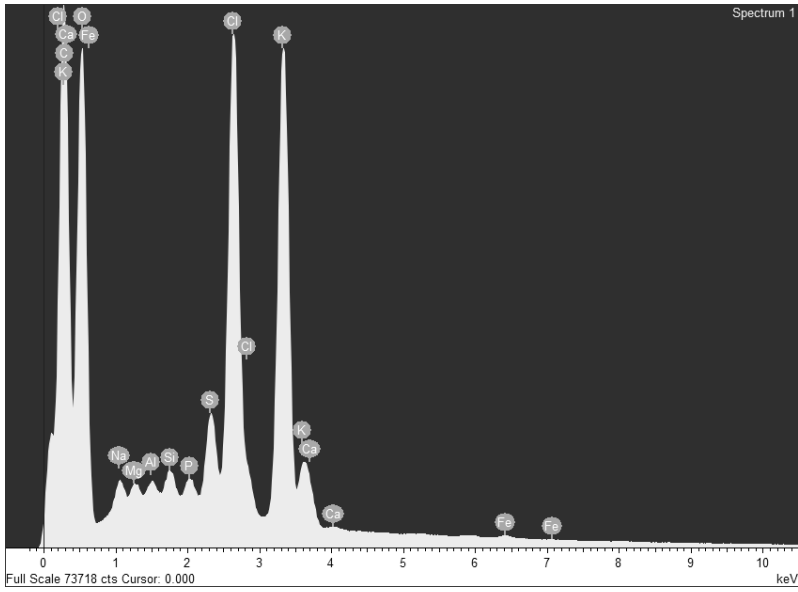
B 7 PP S 16 Cr III r2



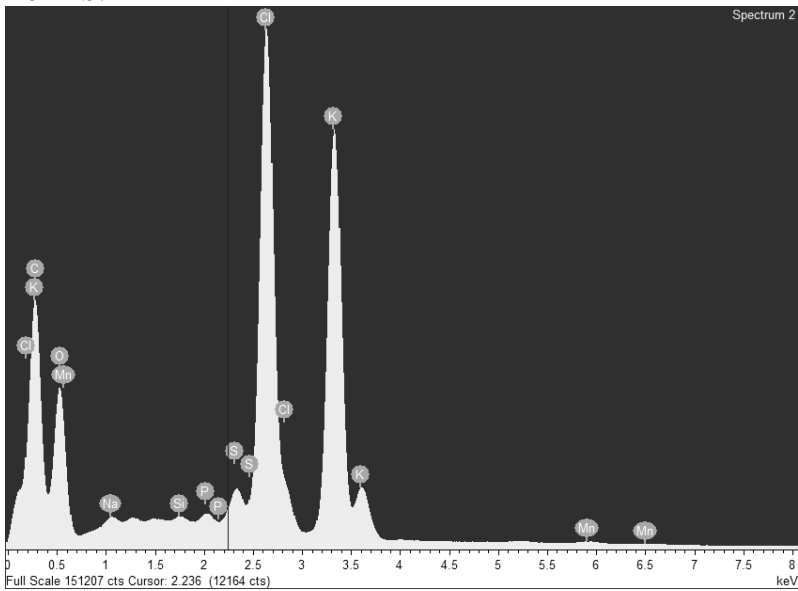
B 7 PP S 16 Cr III r3



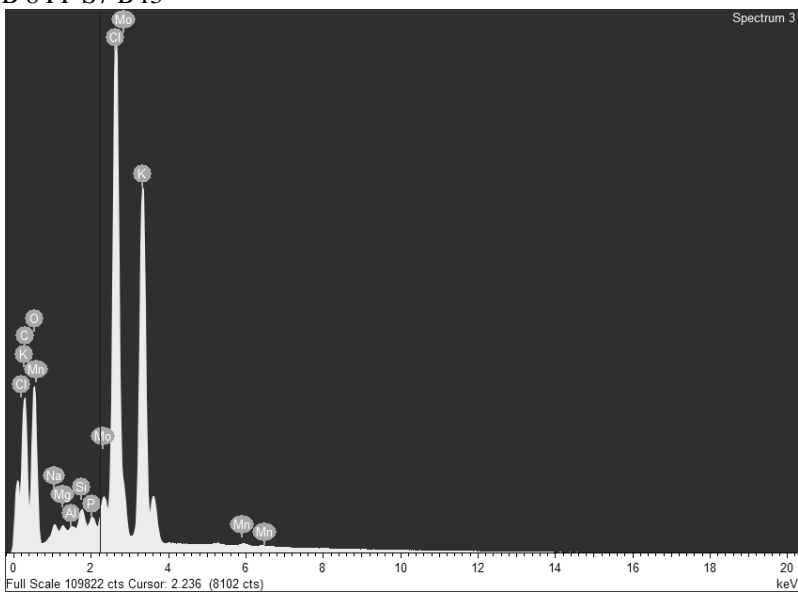
B 8 PP S7 B r1



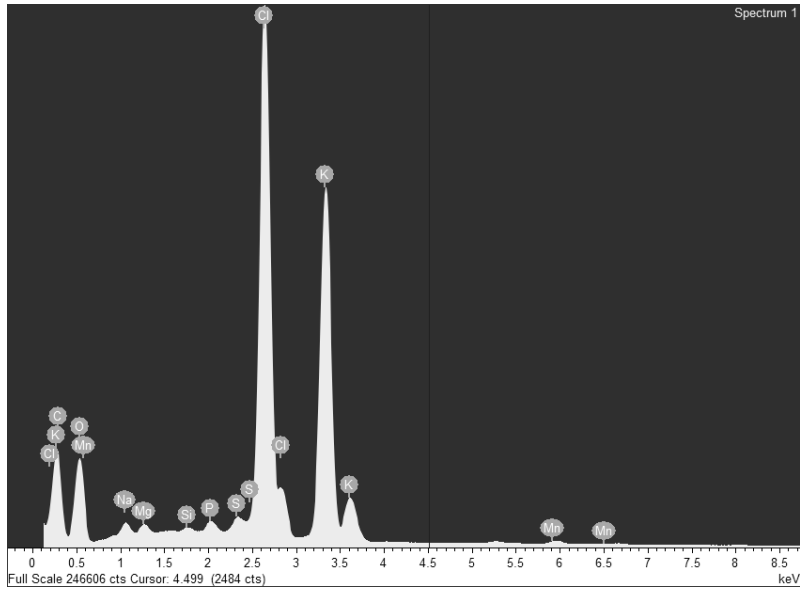
B 8 PP S7 B r2



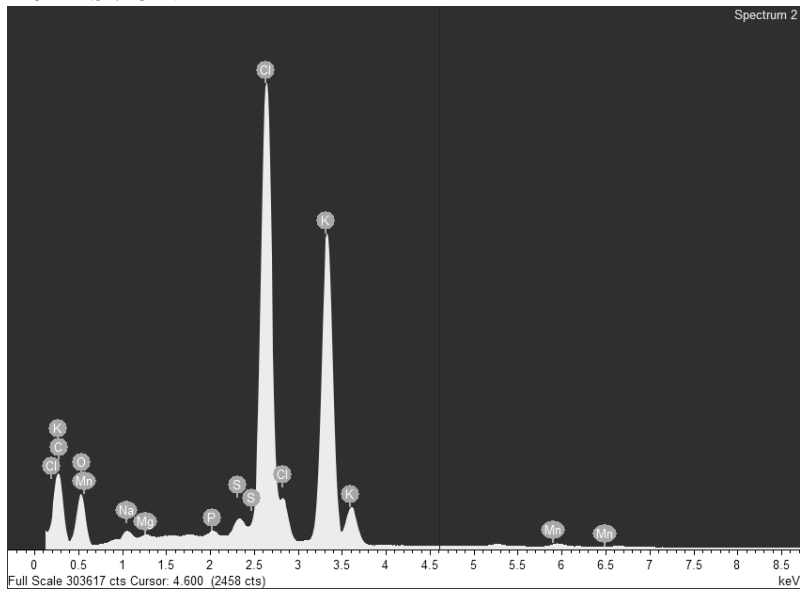
B 8 PP S7 B r3



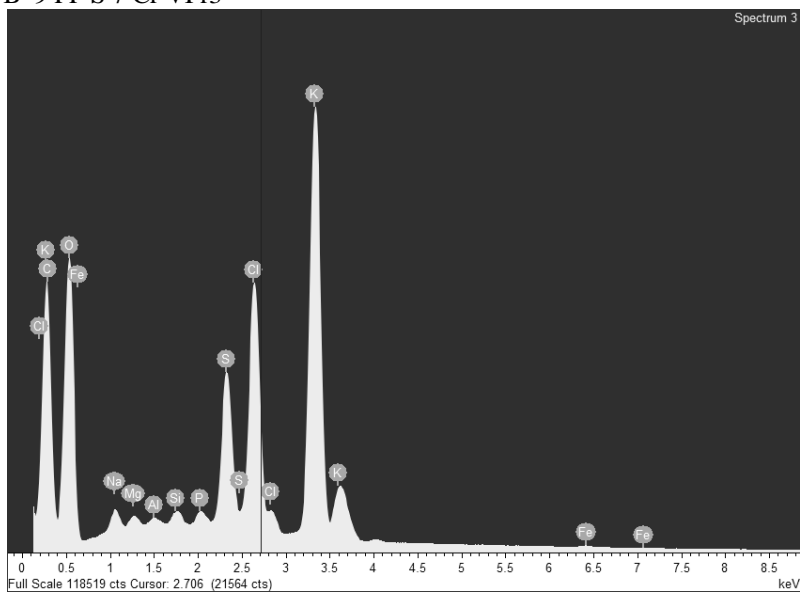
B 9 PP S7 Cr VI r1



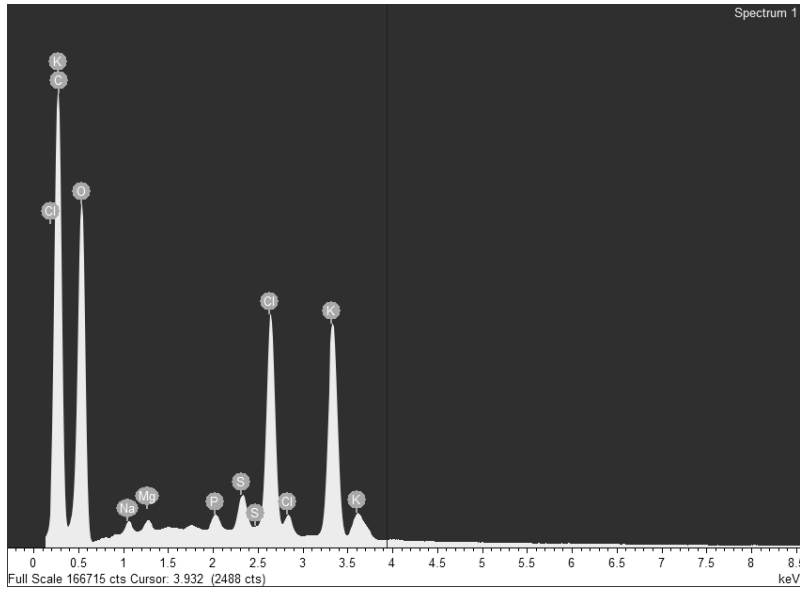
B 9 PP S 7 Cr VI r2



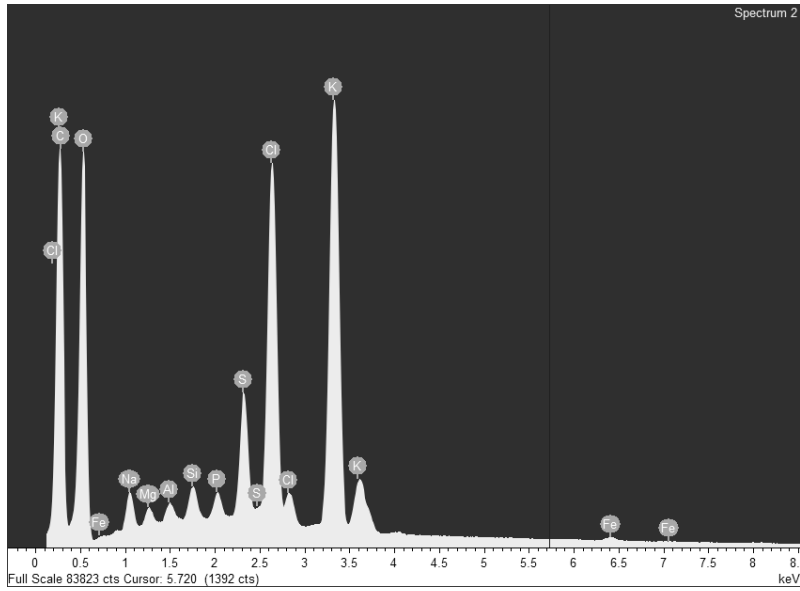
B 9 PP S 7 Cr VI r3



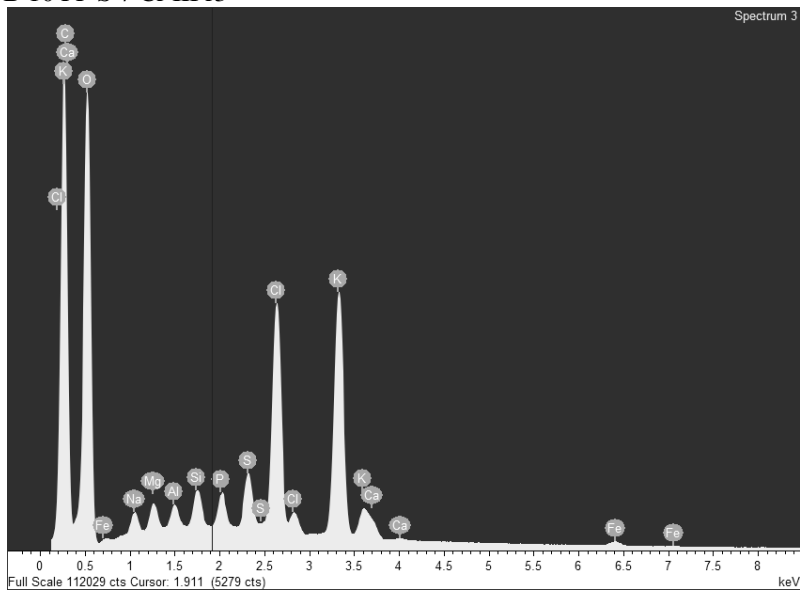
B 10 PP S 7 Cr III r1



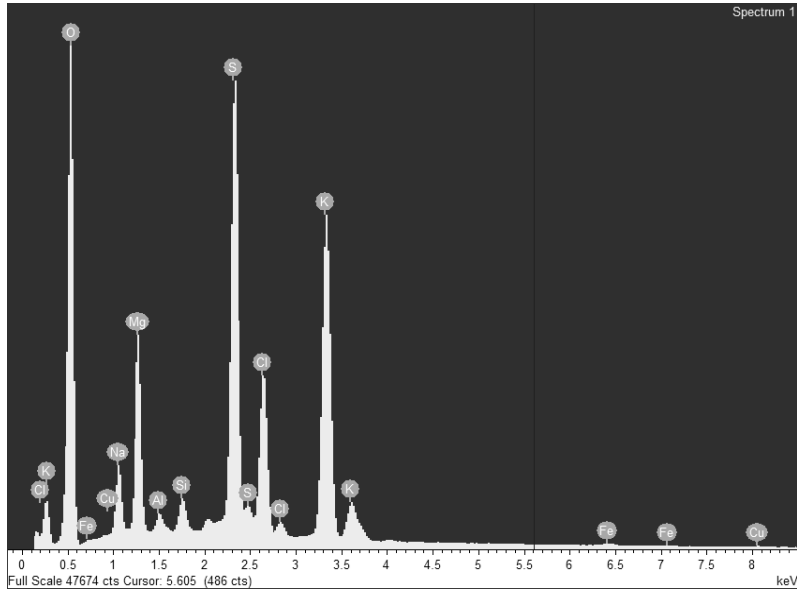
B 10 PP S 7 Cr III r2



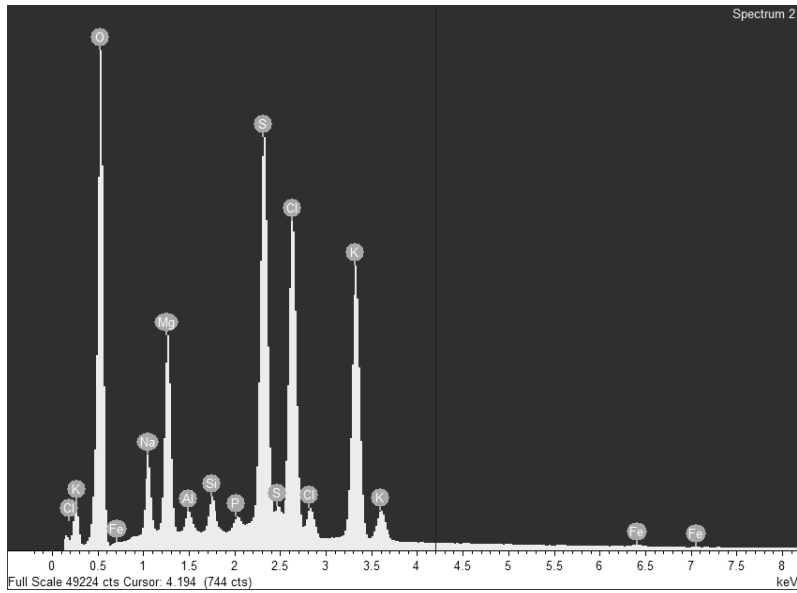
B 10 PP S 7 Cr III r3



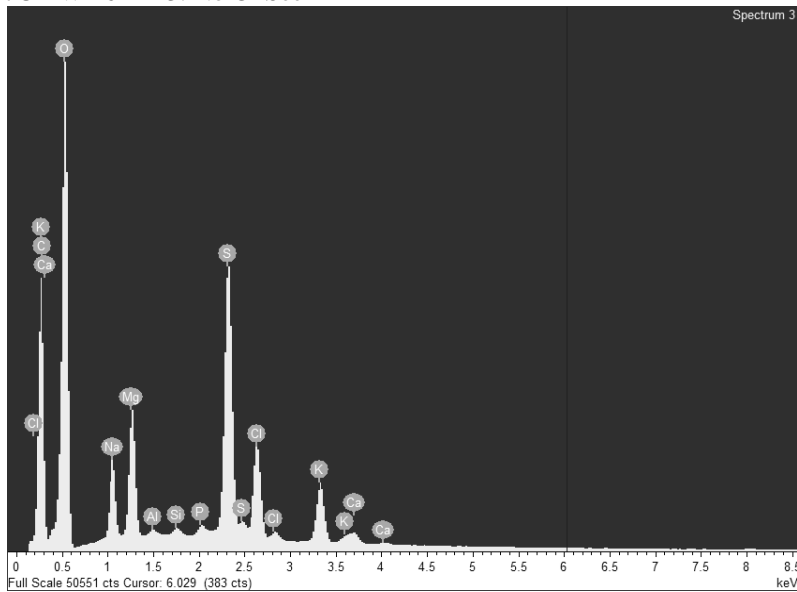
7UL W 16 B R1. No Cr Seen



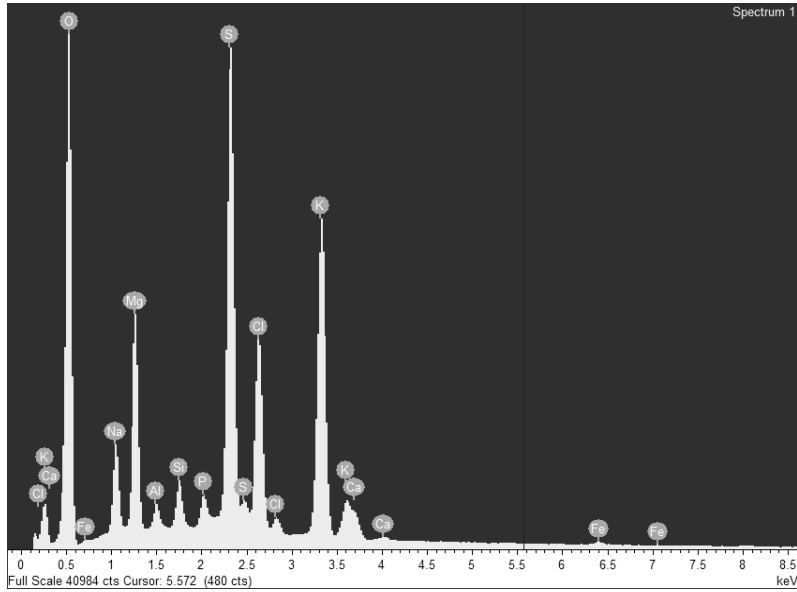
7UL W 16 B R2. No Cr Seen



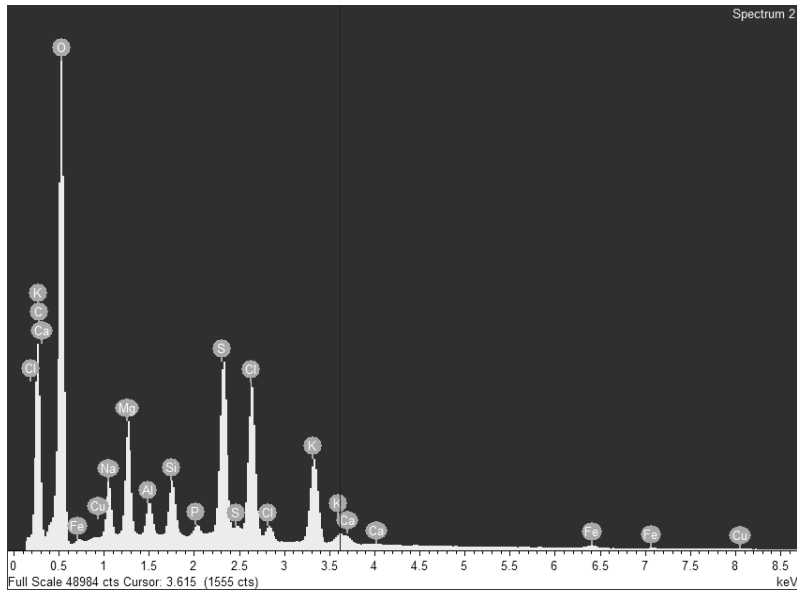
7UL W 16 B R3. No Cr Seen



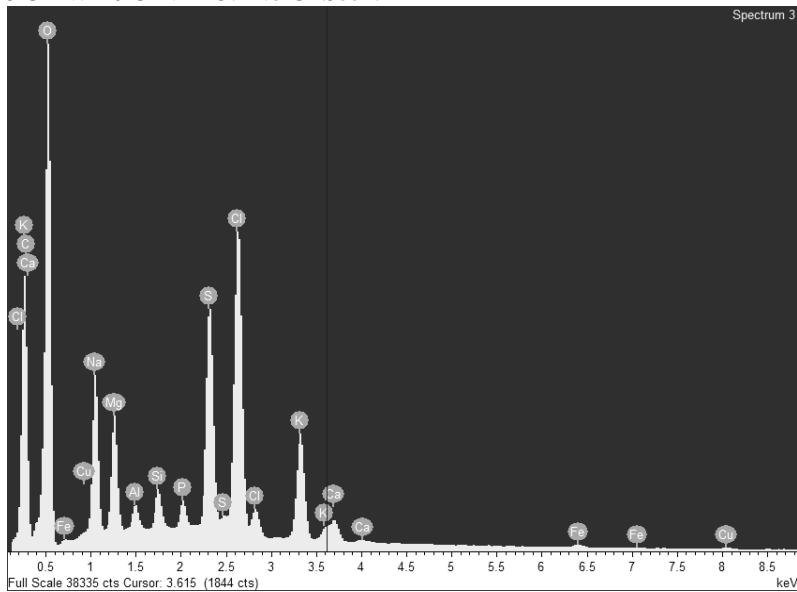
8 UL W 16 Cr VI R1. No Cr Seen.



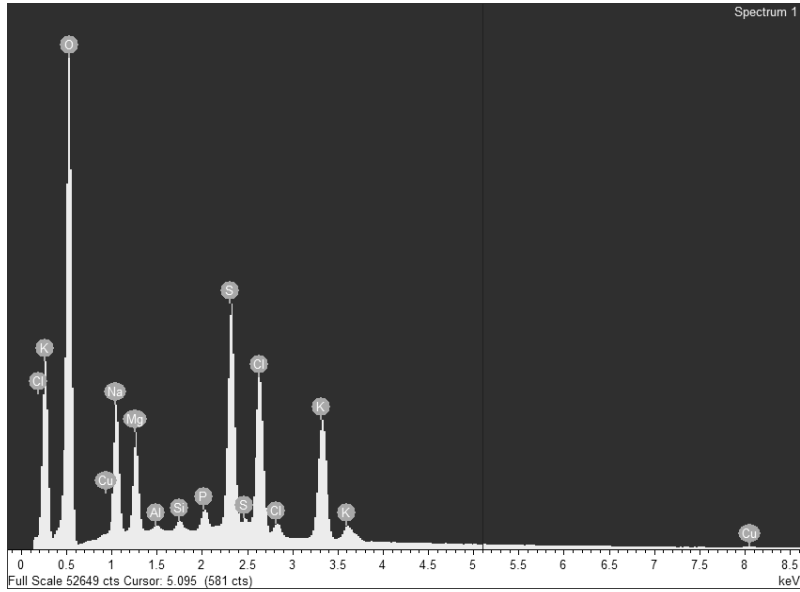
8 UL W 16 Cr VI R2. No Cr Seen.



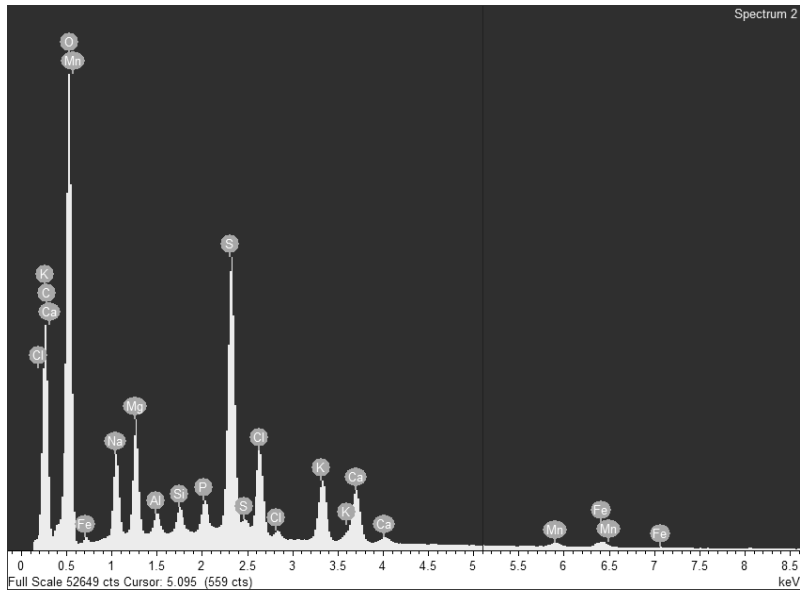
8 UL W 16 Cr VI R3. No Cr Seen.



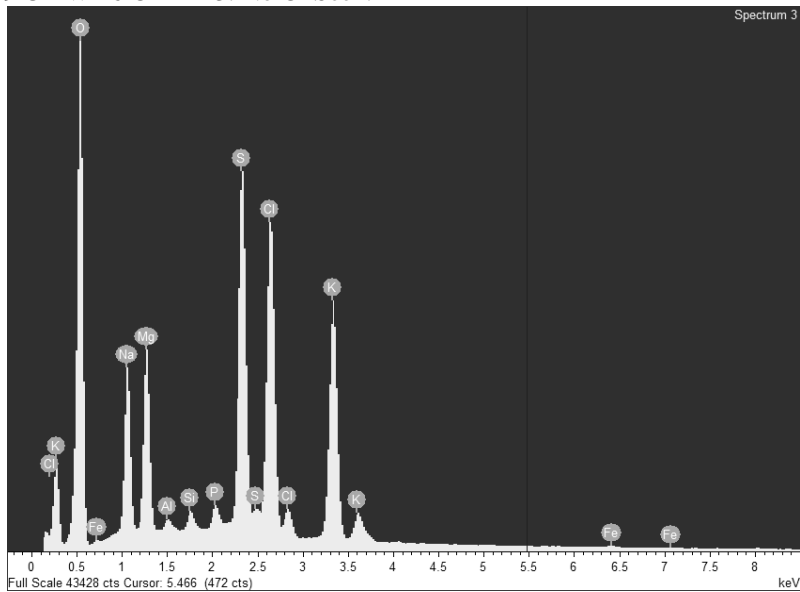
9 UL W 16 Cr III R1. No Cr Seen.



9 UL W 16 Cr III R2. No Cr Seen.

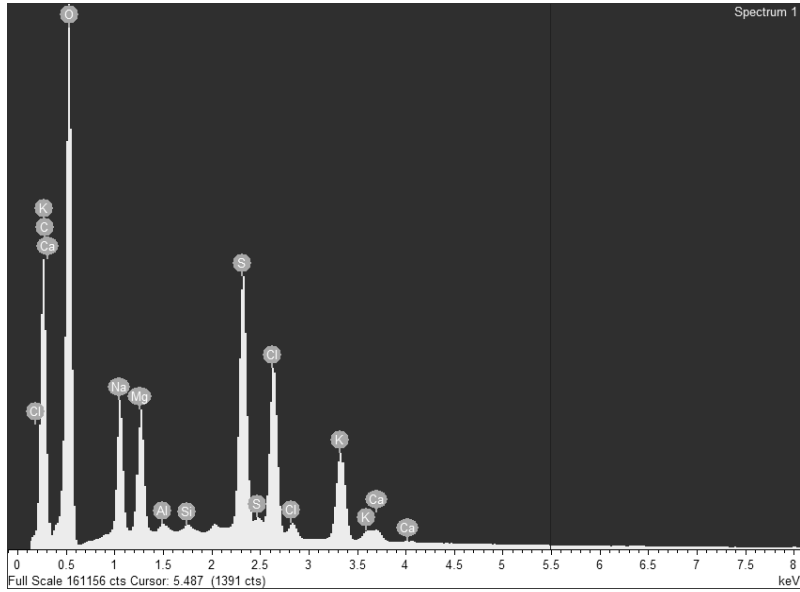


9 UL W 16 Cr III R3. No Cr Seen.

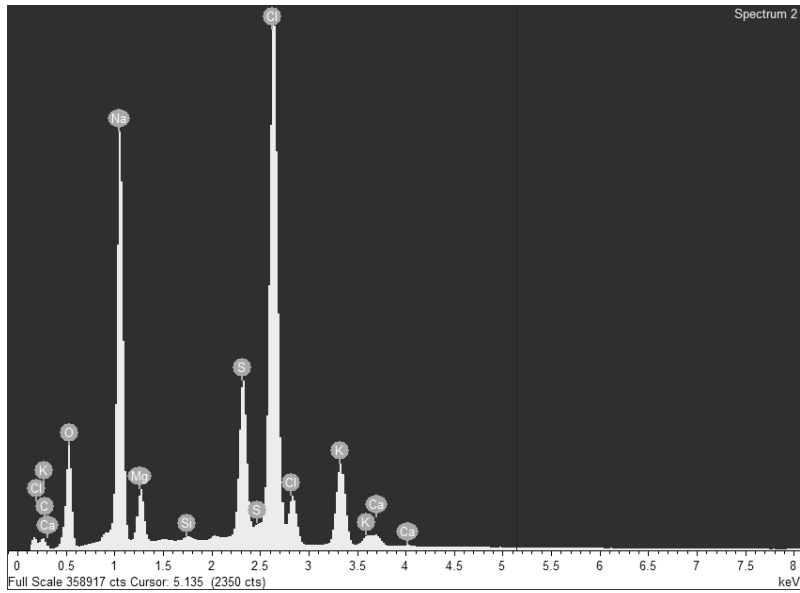




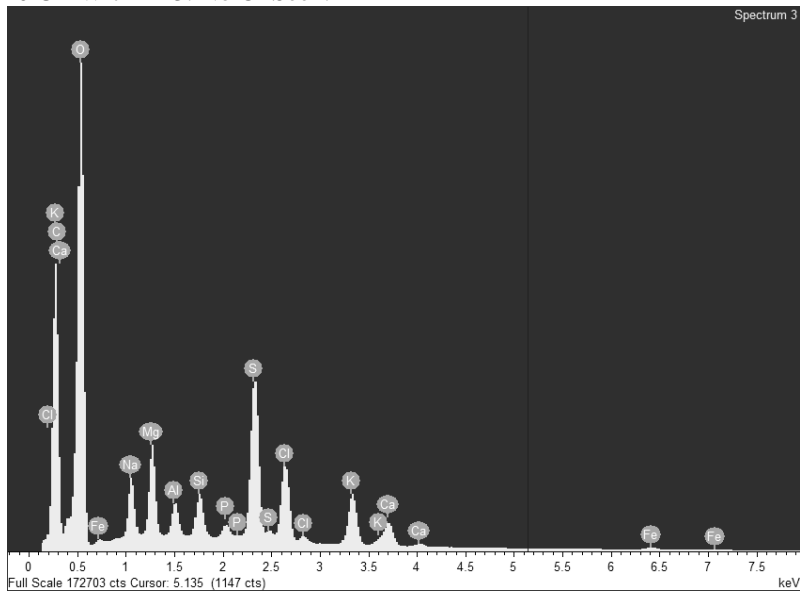
10 UL W 7 B R1. No Cr Seen.



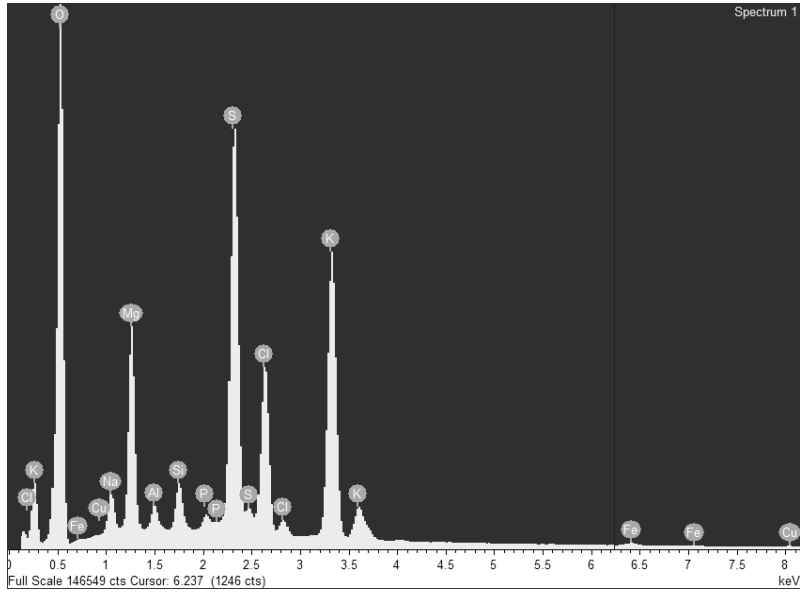
10 UL W 7 B R2. No Cr Seen.



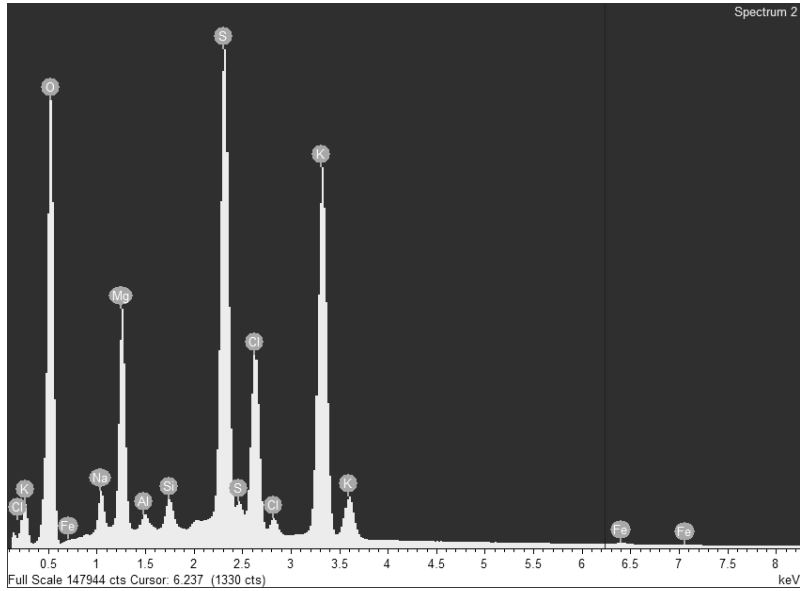
10 UL W 7 B R3. No Cr Seen.



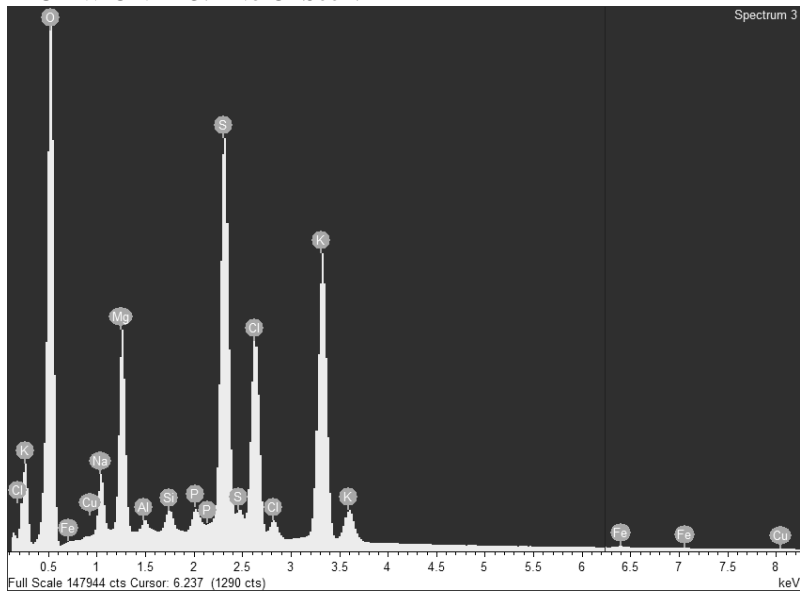
11 UL W CrVI R1. No Cr Seen.



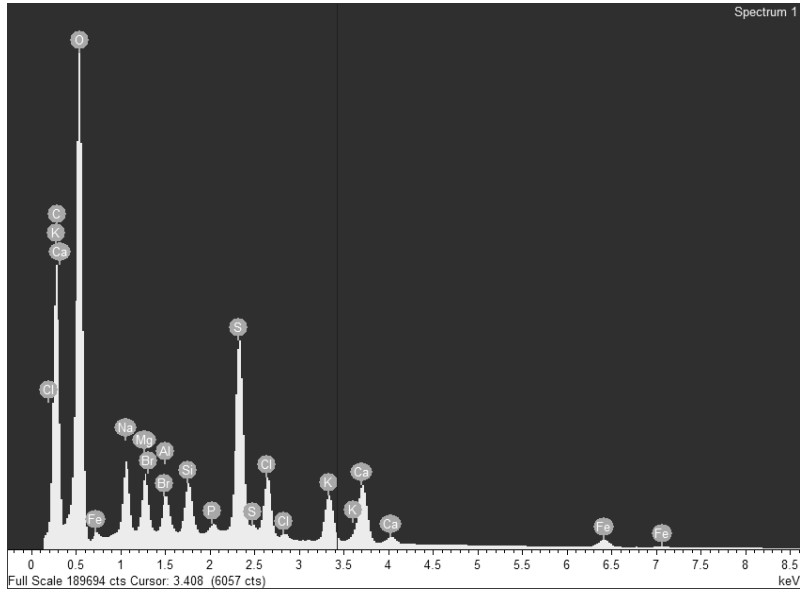
11 UL W CrVI R2. No Cr Seen.



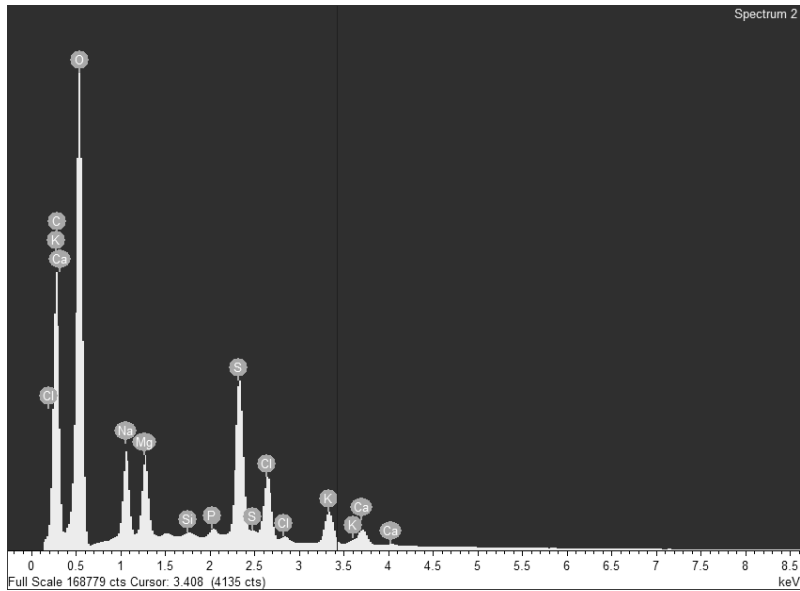
11 UL W CrVI R3. No Cr Seen.



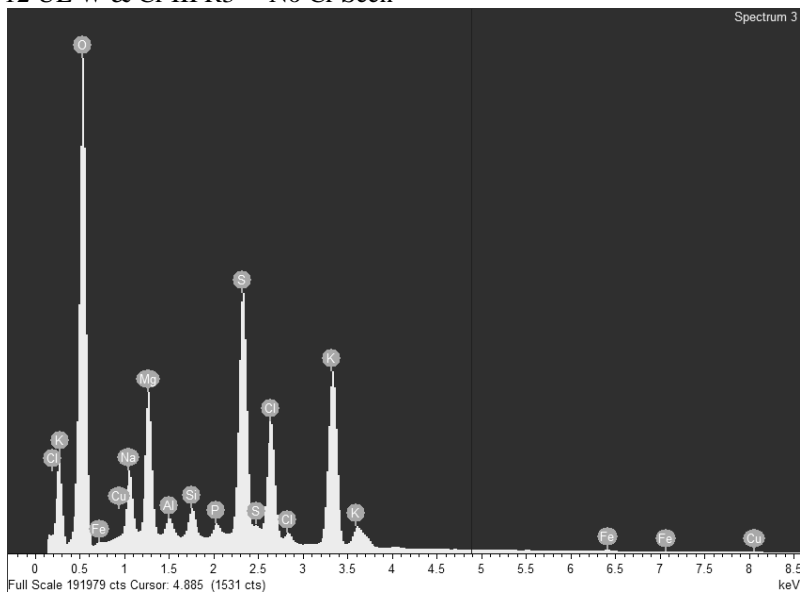
12 UL W & Cr III R1 No Cr Seen



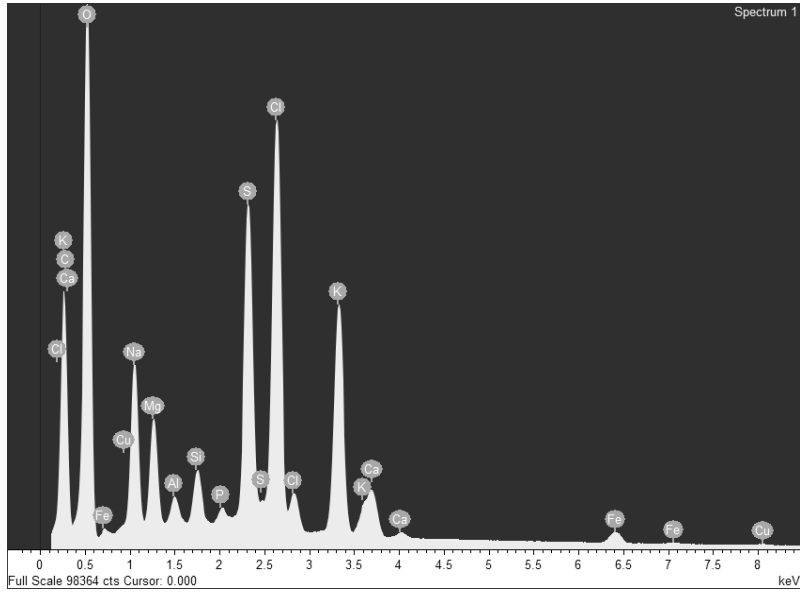
12 UL W & Cr III R2 No Cr Seen



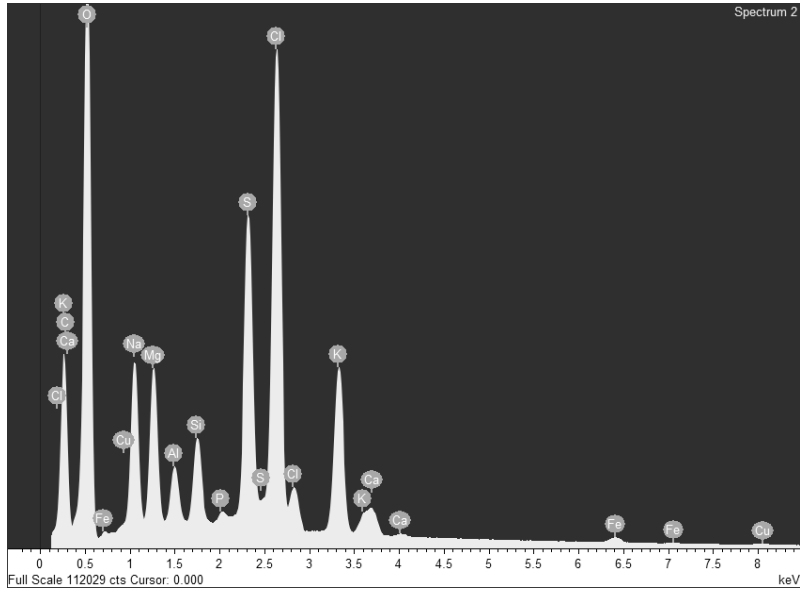
12 UL W & Cr III R3 No Cr Seen



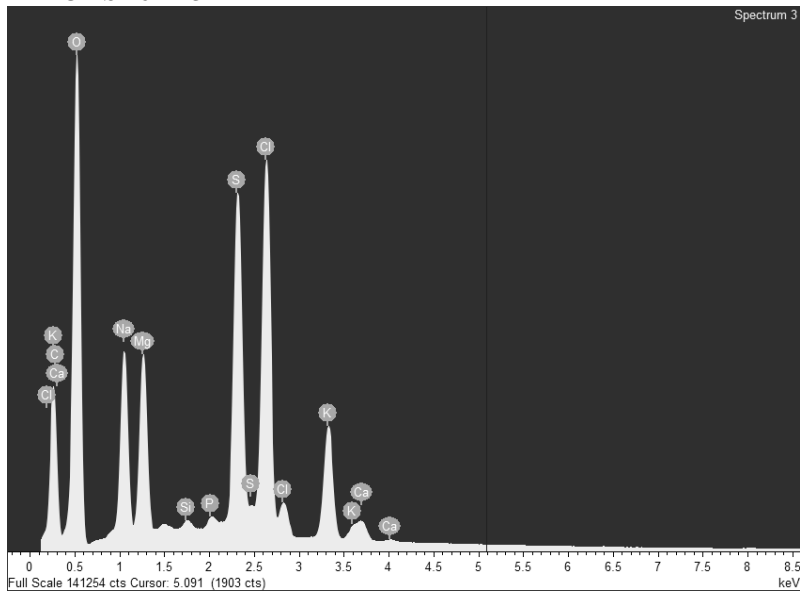
B 11 UL S 16 B r1



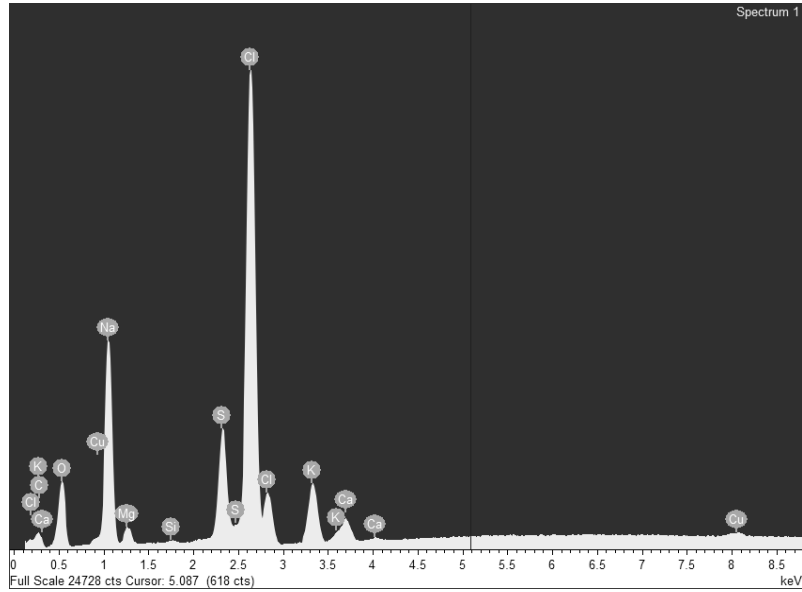
B 11 UL S 16 B r2



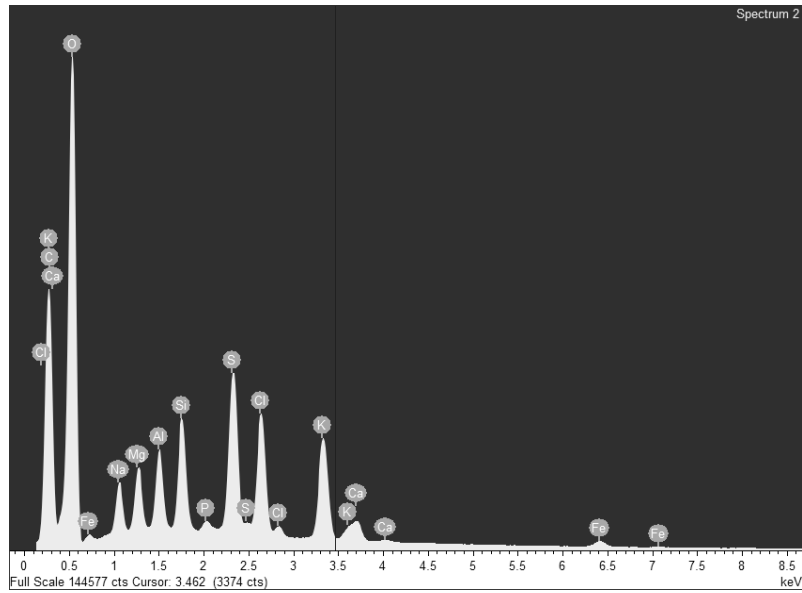
B 11 UL S 16 B r3



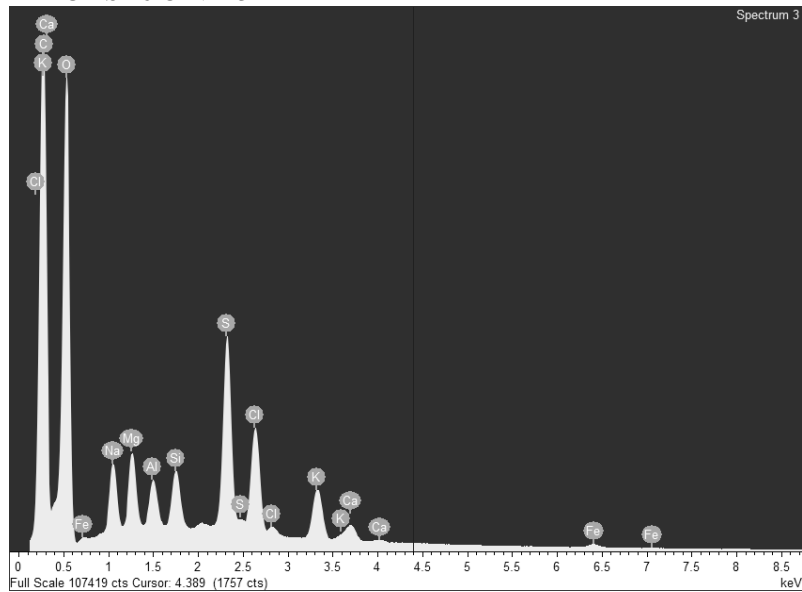
B 12 UL S 16 Cr VI r1



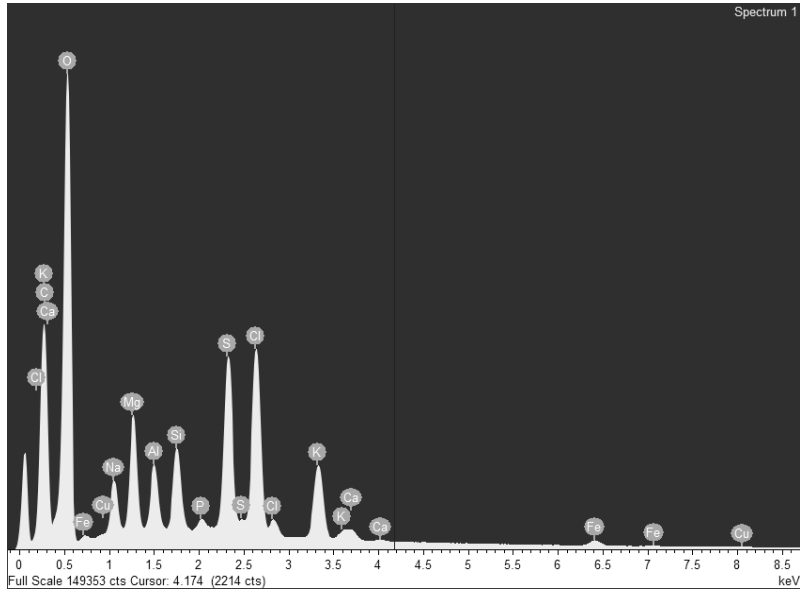
B 12 UL S 16 Cr VI r2



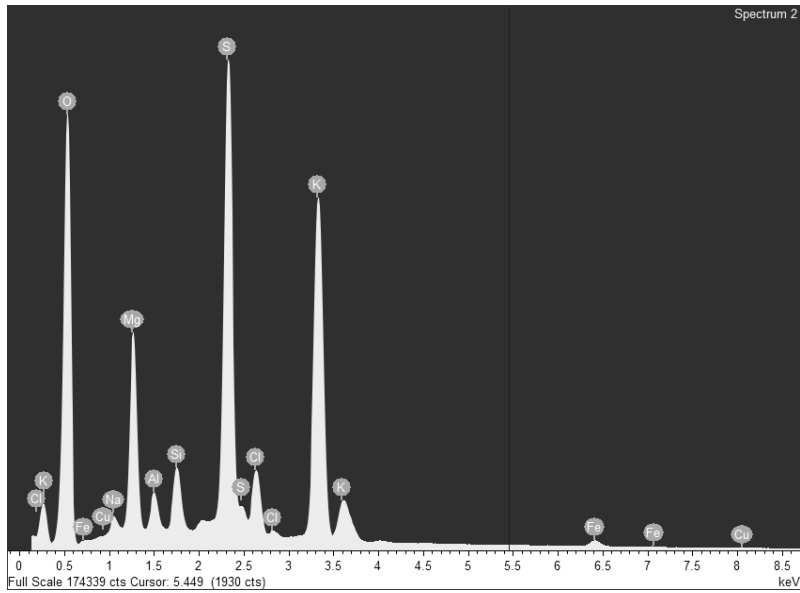
B 12 UL S 16 Cr VI r3



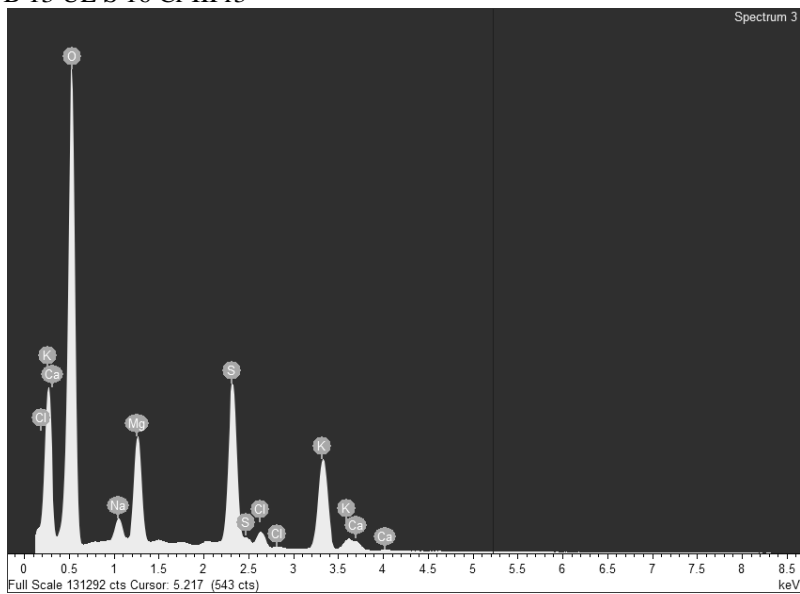
B 13 UL S 16 Cr III r1



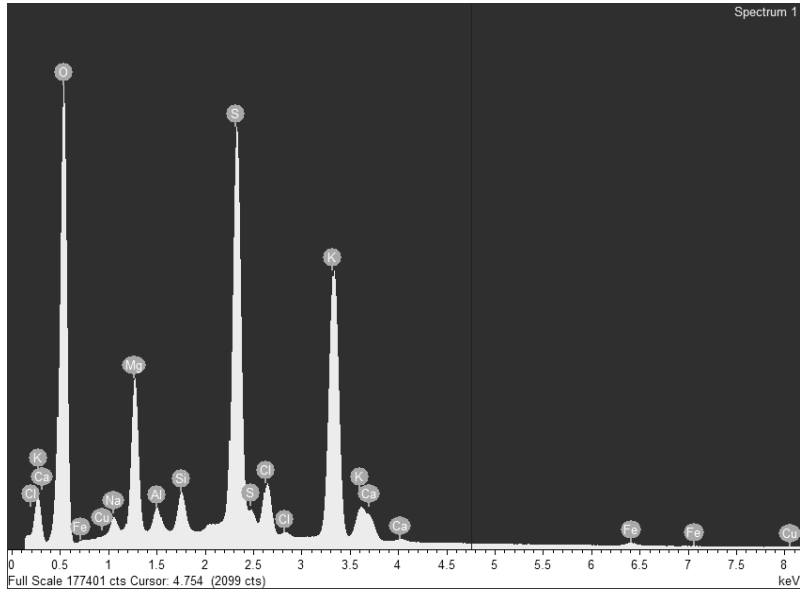
B 13 UL S 16 Cr III r2



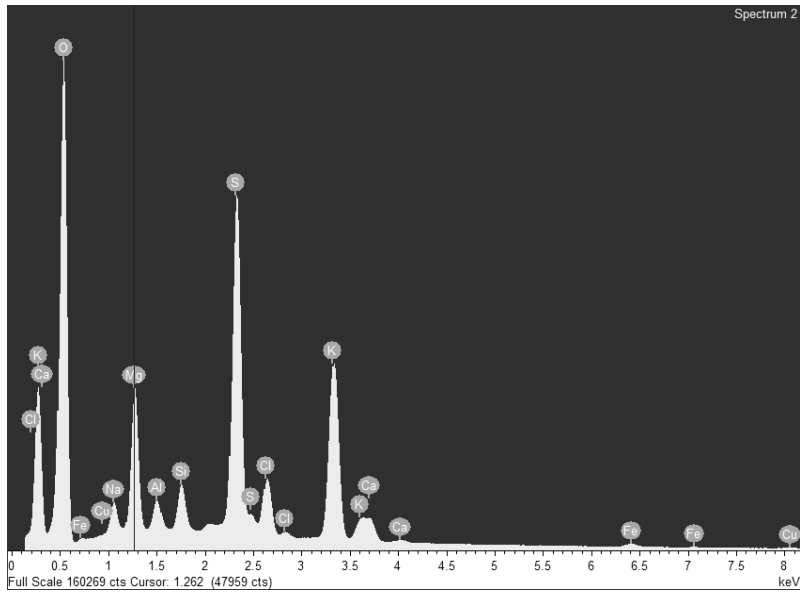
B 13 UL S 16 Cr III r3



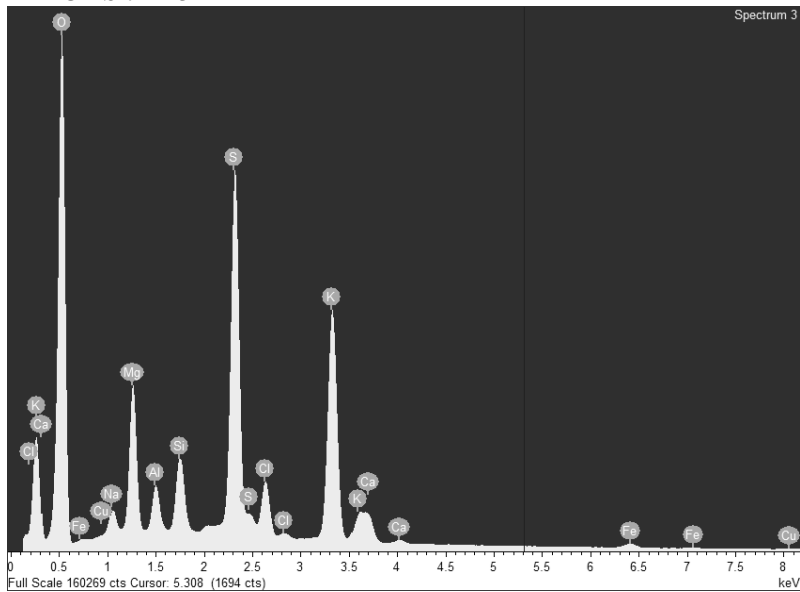
B 14 UL S 7 B r1



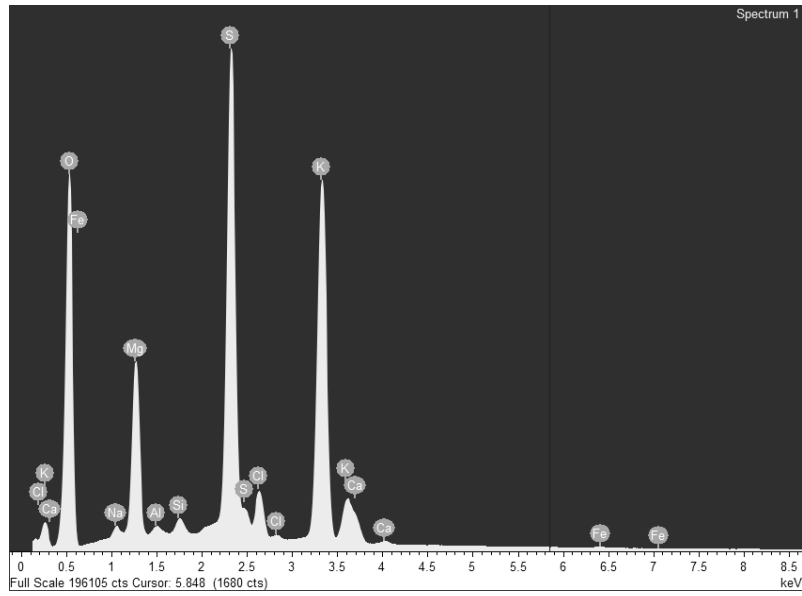
B 14 UL S 7 B r2



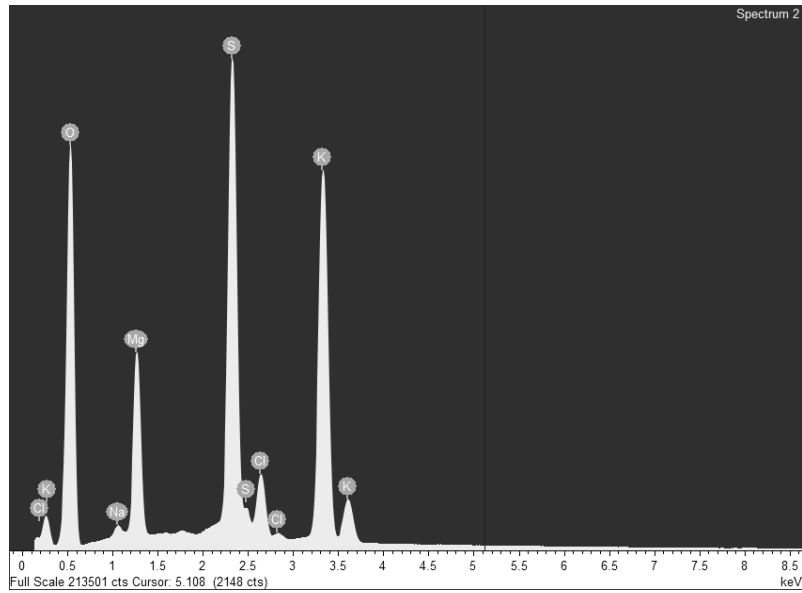
B 14 UL S 7 B r3



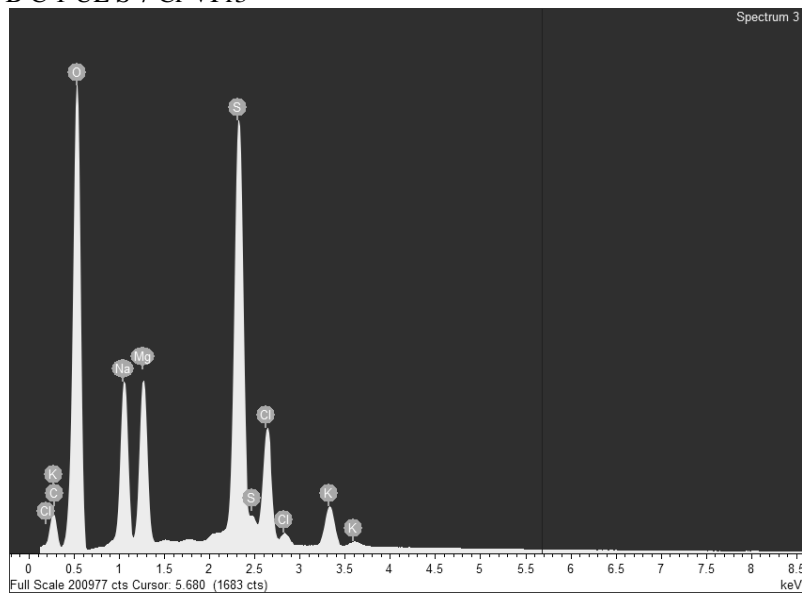
C 1 U L S 7 Cr VI r1



C 1 U L S 7 Cr VI r2

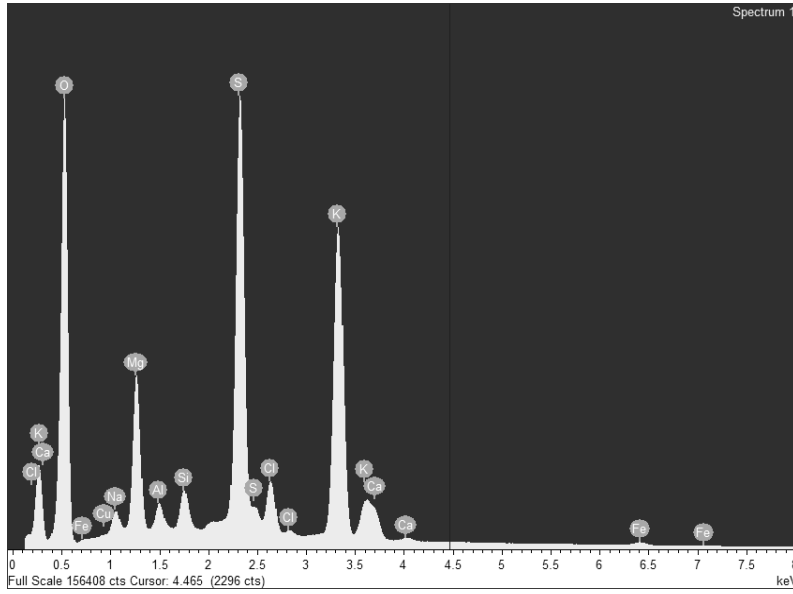


B C 1 U L S 7 Cr VI r3

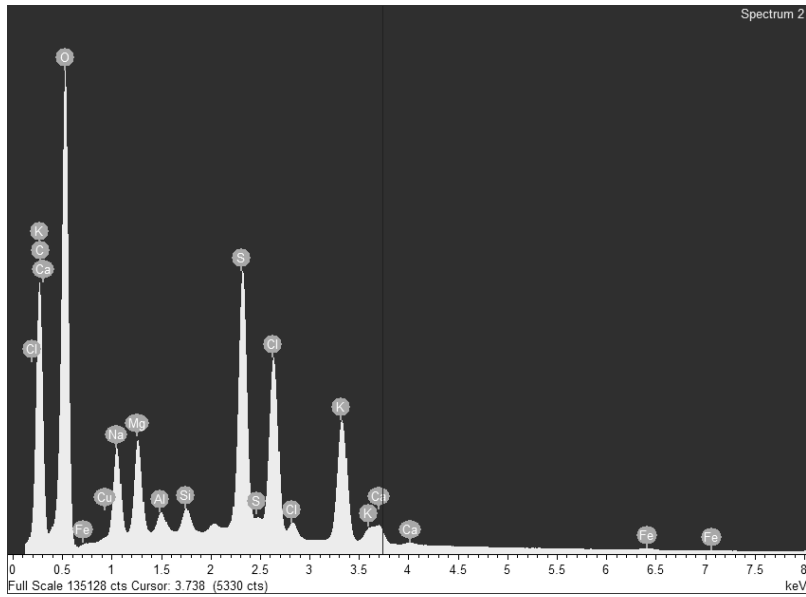




C 2 UL S 7 Cr III r1



C 2 UL S 7 Cr III r2



C 2 UL S 7 Cr III r3

